Advances in High Pressure Bioscience and Biotechnology

Horst Ludwig (Editor)

Advances in High Pressure Bioscience and Biotechnology

Proceedings of the International Conference on High Pressure Bioscience and Biotechnology, Heidelberg, August 30 - September 3, 1998

Springer

Editor
Professor Dr. Horst Ludwig
University of Heidelberg
Institute for Pharmaceutical Technology
and Biopharmacy
- Section Physical Chemistry -
Im Neuenheimer Feld 346
D - 69120 Heidelberg, Germany
e-mail: horst.ludwig@urz.uni-heidelberg.de

ISBN-13:978-3-642-64300-2 e-ISBN-13:978-3-642-60196-5
DOI: 10.1007/978-3-642-60196-5

Library of Congress Cataloging-in-Publication Data
International Conference on High Pressure Bioscience and Biotechnology
(1998 : Heidelberg, Germany)
Advances in high pressure bioscience and biotechnology : proceedings of the International Conference on High Pressure Bioscience and Biotechnology, Heidelberg, August 30 -September 3, 1998 / H. Ludwig (ed.)
Includes bibliographical references
ISBN-13:978-3-642-64300-2
1. Hydrostatic pressure--Physiological effect Congresses. 2. Biotechnology Congresses. 3. Food--Biotechnology Congresses. I. Ludwig, H. (Horst). II. Title.
QP82.2.P7I55 1998 99-28992 571.4'37--dc21

Softcover reprint of the hardcover 1st edition 1999

Coverdesign: E. Kirchner, Heidelberg
Typesetting: Camera-ready by Claudia Hölters and Ingmar Köser
SPIN:10676112 02/3020-5 4 3 2 1 0 - Printed on acid-free paper

Preface

The International Conference on High Pressure Bioscience and Biotechnology at Heidelberg continued the tradition of Japanese and European joint meetings, following the conferences at La Grand Motte, near Montpellier (1992), Kyoto (1995), and Leuven (1996). The first meeting at Montpellier, promoted by Claude Balny (INSERM, Montpellier, France) and Rikimaru Hayashi (Kyoto University, Japan) stimulated many scientists and practitioners, especially from Europe and Japan. At Heidelberg (1999), it was a pleasure to welcome 153 participants from 20 countries, among them large delegations from Japan and the USA.

This book records the contributions presented at the Heidelberg meeting and shows the great potential of high pressure technology. It covers the whole range of current high pressure bioscience, from marine microbiology and investigations on deep-sea diving to applications in food science. High pressure can be used to process foods and sterilize pharmaceutical products; moreover it is a valuable tool for fundamental research. For example, pressurized proteins exhibit intermediate states of their folding and unfolding pathways.

We hope that this publication will stimulate further developments in basic and applied research as well as foster fruitful contacts between industry and academia.

Heidelberg, June 1999 Horst Ludwig

Scientific Committee

K. Autio, Espoo; C. Balny, Montpellier; D. H. Bartlett, San Diego; J.C. Cheftel, Montpellier; P. Colman, Temse; J. Frank, Delft; R. Hayashi, Kyoto; M. Hendrickx, Leuven; K. Heremans, Leuven; C. Kato, Yokosuka; D. Knorr, Berlin; S.Kunugi, Kyoto; A. Macdonald, Aberdeen; P. Masson, La Tronche; E. Raetz, Lausanne; J. Smelt, Vlaardingen; Y. Tanigushi, Kyoto; P. Taoukis, Athens; B. Tauscher, Karlsruhe; J. Westerlund, Vaesteraas; R. Winter, Dortmund.

Local Organizing Committee

H. Ludwig (Chairman), K.-H. Loebel (Conference Secretary), R. Eicher, C. Hölters, I. Köser, N. Merkulow, M. Schauer, E. Schinko, Ch. Schreck, E. Sternberger.

The conference has been supported by:

Deutsche Forschungsgemeinschaft, Bonn, Germany

and the following companies:

ABB Pressure Systems, Västerås, Sweden; Bayer AG, Wuppertal, Germany; ANTITOXIN Dr. Helmbold GmbH, Meckesheim, Germany; Engineered Pressure Systems International N.V., Temse, Belgium; GEC ALSTHOM ACB, Nantes, France; Goedecke AG, Freiburg, Germany; Heidelberger Zement AG, Heidelberg, Germany; Hoechst Marion Roussel GmbH, Frankfurt am Main, Germany; Mannesmann Rexroth GmbH, Lohr am Main, Germany; Dr. Eduard Ritsert GmbH, Eberbach, Germany; Sitec Sieber Engeneering AG, Zürich, Schweiz; Stansted Fluid Power Ltd, Stansted, UK; Uhde Hochdrucktechnik, Hagen, Germany; Unilever Research Laboratorium, Vlaardingen, Netherlands

Acknowledgements:

We would like to express our gratitude and special appreciation to Mr. Karl-Heinz Loebel, conference secretary, for his self-sacrificing and successful work before and during the conference and to Ms Claudia Hölters and Mr. Ingmar Köser for their assistance in preparing this conference proceedings.

Table of Contents

Microorganisms from the Deep-Sea

Microorganisms

Microorganisms in Food

Membranes and Lipids

Proteins

Enzymes

Food Proteins

Nucleic Acids and Linear Polymers

High Pressure Induced Gelation of Proteins and Polysaccharides

Chemical Reactions of Food Constituents at High Pressure

High Pressure Processing of Foods and Food Related Materials

Milk and Milk Products

Freezing and Thawing Under High Pressure

New Experimental Methods, Applications and Equipment

Whole Organisms and Human Cells, Deep Diving

Microorganisms from the Deep-Sea

The Properties of Deep-Sea Piezophilic Bacteria and Their Possible Uses in Biotechnology

A.A. Yayanos

University of California San Diego, Scripps Institution of Oceanography, 9500 Gilman Drive, Dept. 0202, La Jolla, California 92093-0202, USA

Abstract. Bacteria inhabit virtually all of Earth's high pressure oceanic environments. The deep oceanic habitats are at pressures as high as ~109 MPa and at temperatures between -0.5 and ~113 °C. The study of bacteria from these environments gives an idea of how pressure, p, and temperature, T, as coordinate variables affect bacterial adaptation and evolution. The comparison of the growth kinetics of bacteria from the cold deep sea (2 °C), from the abyssal Sulu Sea (9.8 °C), and from the abyssal Mediterranean Sea (13.5 °C) shows the interplay of habitat temperature and pressure to set the response of an organism. The traditional definition of barophily is profitably replaced with one of piezophily which is operationally defined with the aid of a plot of the growth rate constant, k, as a function of T and p. Such a plot, called a pTk diagram, also provides quantitative relationships between growth characteristics of an organism and its habitat. The relationships, furthermore, allow for an otherwise difficult comparison of organisms from different pT habitats. These diagrams may also help in the selection of bacteria with properties appropriate for particular biotechnological applications.

1 Introduction

Bacteria inhabiting conditions close to those limiting the existence of life are attracting wide attention. Studies of these organisms will shed light on where to seek life in extraterrestrial settings, on the origin and dissemination of life, on how life processes work, and on new technologies to improve the pragmatic and aesthetic aspects of human welfare. Earth's oceans are inhabited at pressures from 0.1 to over 100 MPa along the 2 °C isotherm and between −1.8 and ~113 °C along the 25 MPa isopiest. Inspection of Fig. 1 reveals that there are possible habitats in terms of temperature and pressure that may not exist in the oceans. For example, there are no known hydrothermal vents at a water depth of 7,000 m. Therefore, there are no ~113 °C aqueous environments at a pressure of 70 MPa. Yet such a high pressure environment would likely be habitable and perhaps to an even greater temperature than 113 °C.

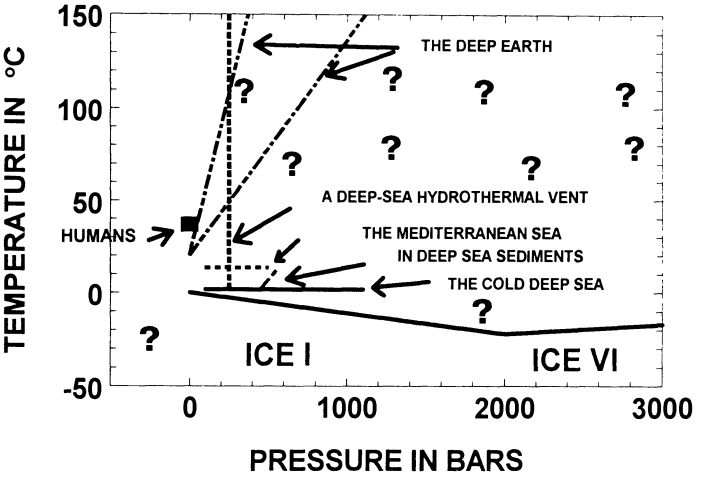

Fig. 1. We know something about the distribution and physiology of organisms on the *pT* plane, especially along the 0.1 MPa isopiest (not shown) and along a few of the indicated oceanic isopiests and isotherms. Along the geothermal gradients shown in this figure, we do not yet have convincing results. When through either analysis or experiments, the *pT* curve defining the existence of life is someday known, it will likely be a closed, concave inward, continuous curve defining the *pT* domain of life. It is also likely that all of the *pT* conditions compatible with life processes do not exist on Earth. This is especially the case at high temperatures around 100 °C with pressures greater than 70 MPa and perhaps as great as 200 to 300 MPa. The question marks are placed close to or beyond the imagined *pT* limits of life

The manifestations of adaptation of life to high pressure are a strong function of the temperature of the habitat. That is, temperature and pressure are coordinate variables defining at the molecular level biological adaptation to the environment. A difference of 4 °C in environmental temperature, as between the abyssal (5,000 m deep) Sulu and Mediterranean Seas, is sufficient to cause their bacterial inhabitants to possess substantially different responses to pressure change. The truly dramatic effect of environmental temperature in moderating the pressure response of bacteria is not readily apparent from inspection of growth curves but becomes strikingly clear and quantifiable with *pTk*-diagrams. The study of *pTk*-diagrams of bacteria from a variety of *pT* habitats leads also to the concept of piezophily. Bacteria from these diverse *pT* habitats should provide new opportunities in biotechnology but there are not yet many examples.

2 Material & Methods

Animals were collected in pressure-retaining traps and in traps providing only thermal insulation. Sediments were collected with gravity and piston corers. Samples from the Pacific and Atlantic Oceans, the Sulawesi Sea, the Sulu Sea, and the Mediterranean Sea all yielded bacteria in enrichments incubated at high

pressure. Pure cultures were obtained with a pour tube method adapted for use at high pressures. The kinetics of growth of bacteria as a function of temperature and pressure were determined with two types of high pressure apparatus. Survival of bacteria under stress was determined with a colony forming ability assay conducted at high pressure with the pour tube method. References to the above field and laboratory methods are in two recent reviews [11, 12].

The exponential growth rate constant, k, of a bacterial strain is a function of T, p and the chemical composition of the medium

$$k = k(p, T, x_1, x_2, \ldots, x_N) \,, \tag{1}$$

where the x's are the concentrations of the medium components. If we assume that these concentrations do not change significantly during exponential growth, then k is simply a function of p and T. A pTk-diagram is an empirical determination of the function in (1). Examination of these diagrams is far more conducive to the development of new hypotheses than is the study of two-dimensional plots of k versus p or T alone.

3 Results, Discussion & Conclusions

Bacteria of the cold deep sea are called piezophiles if their maximum growth rate on a pTk-diagram is at a high pressure [11, 12]. The bacteria of the cold deep sea are also psychrophilic and are thus piezopsychrophiles. An example of the pTk diagram of a piezopsychrophile is shown in Fig. 2. Bacteria such as MT41 [10], *Colwellia hadaliensis* [6], DB21MT-2, and DB21MT-5 [7] from the deepest parts

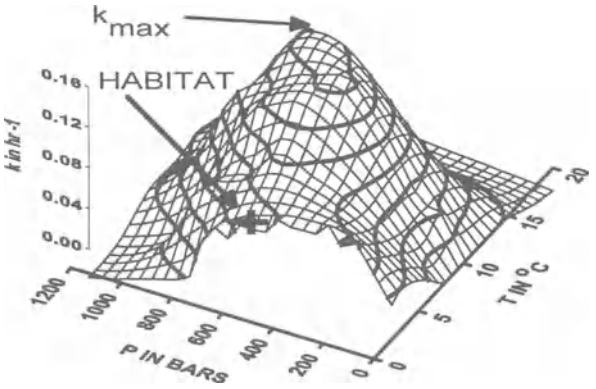

Fig. 2. A pTk diagram for bacteria isolate CNPT3[11] from a depth of 5,782 m of the central North Pacific Ocean. The pressure where the maximum growth rate is found is almost the same as the habitat pressure

of the sea are hyperpiezophilic because the maximum growth rate is at a pressure greater than 50 MPa.

Heterotrophic deep-sea bacteria from the abyssal Mediterranean Sea have growth rates which are nearly pressure invariant at their habitat temperature of 13.5 °C. A comparison of the *pTk*-diagrams of deep-sea bacteria from 5,000 m of the Mediteranean Sea, the Sulu Sea and the Pacific Ocean, leads to the hypothesis that hyperpiezomesophilic and hyperpiezothermophilic bacteria would need a warm high pressure environment which is absent on Earth.

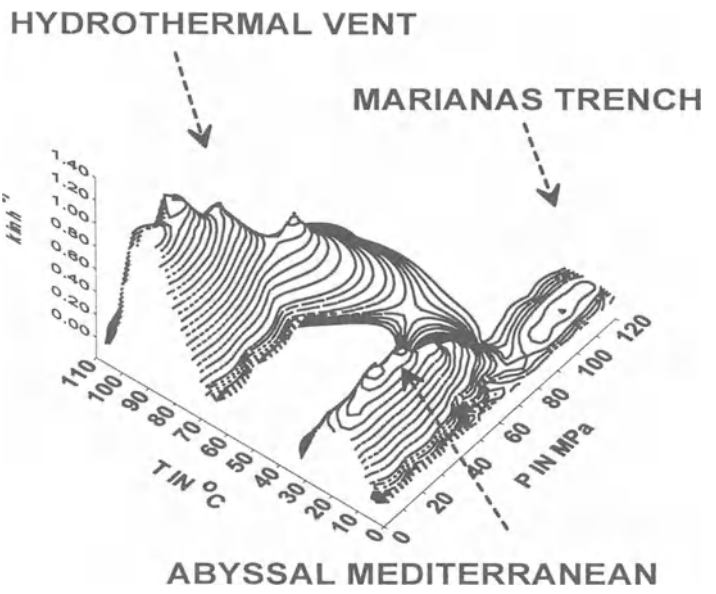

Fig. 3. *pTk* diagrams for three different bacterial isolates. The diagrams were made from data of Pledger *et al.* [9] on a hydrothermal vent isolate, Yayanos and DeLong (submitted) on the Mediterranean Sea isolate, and from Yayanos [10] on the Marianas Trench isolate. These isolates occupy 3 different *pT* domains

Bacteria from deep-sea habitats differing in temperature are profoundly different in their response to pressure (Fig. 3). The hyperthermophile ES4 is barophilic (has a pressure facilitated growth rate) at temperatures somewhat above its maximum growth rate temperature. As seen in Fig. 3, however, ES4 perhaps just qualifies as a piezophile. More experiments would be needed to tell for sure. One implication of the absence of growth facilitation by pressure is that high temperature, high pressure habitats can be most likely sampled without the use of pressure-retaining instruments for purposes of cultivating bacteria. Another consequence of the trend evident in Fig. 3 is that the pressure dependence of the growth rate constant is not a sensitive measure of pressure adaptation in organisms of high temperature, high pressure environments.

The hyperpiezopsychrophile growth rates are seen in Fig. 3 to be exceedingly small. The contours of constant growth rate shown at the lowest values are all less than 0.05. Without adding these low value isopleths of growth rate, the MT41 data would not be visible. Comparing the *pTk* diagrams of MT41 and ES4 suggests life limiting processes at high pressure limits are different from those at high temperature limits.

Isolate ES4 occupies a huge *pT* domain, isolate MED6 a smaller one, and isolate MT41 exists over a very small *pT* domain. This contrast between a hyperthermophile and a hyperpiezopsychrophile is dramatic. We often think that thermophiles among all types of bacteria have the greatest challenge in the struggle for existence. Yet this diagram shows that strain MT41 in occupying the smallest *pT* niche known will have the greatest challenges to meet if there is environmental change. The greatest threats to existence faced by isolate MT41 are the lethal effects of warming and of decompression. Isolate ES4 would most likely survive and disperse in the low temperature, high pressure regions outside of its *pT* domain. So it seems that, indeed, thermophiles have two advantages over psychrophiles.

Bacteria of the deep sea possess traits in addition to those evident in *pTk*-diagrams and some of them are:

1. Bacteria of the cold deep ocean display maximal growth rates at 8 to 10 °C [10].
2. The temperature range for growth of bacteria from the cold deep sea is roughly 15 °C [10, 13].
3. Heterotrophic piezopsychrophiles have their maximum growth rate within 5 MPa of their capture depth pressure [10].
4. Piezopsychrophiles rapidly loose viability when warmed [11].
5. Cell division is inhibited at pressures at the high and low ends of the growth pressure range and filamentous cells form. Piezopsychrophilic bacteria form large cells and abnormal cell shapes when grown at atmospheric pressure [11].
6. Deep-sea bacteria alter their membrane phospholipid fatty acid composition in response to a change in growth pressure or temperature [4, 5].
7. Some deep-sea bacteria synthesize polyunsaturated fatty acids as components of their membrane phospholipids [5].
8. Deep-sea bacteria alter the types or levels of membrane proteins in response to a pressure change [1].
9. Bacteria from the deep Pacific Ocean are extremely sensitive to UV light.
10. The pressure dependence of the growth rate is less pronounced in bacteria inhabiting warm deep seas.
11. The generation times of bacteria from the cold deep sea are between 4 and 30 h. The shortest generation times are found with bacteria from bathyal depths and the longest with those from hadal depths.
12. The generation times can be increased by several fold by changing the carbon source [6].

13. In the case of isolate PE36, its growth rate became independent of pressure between 0.1 and 40 MPa at 4 °C when grown in a minimal salts medium with glycerol as the only carbon source (Yayanos and Chastain, unpublished).
14. The *pTk*-diagram and values of the maximum growth rate constant and of the pressure and temperature where the maximum occurs can be obtained unambiguously in a given growth medium, comprise an essential part of the physiological signature of an organism, and through a comparative analysis can reveal the nature of its habitat.
15. The values of temperature and pressure where a given organism can grow are bounded on a *pT*-diagram by a closed curve. This implies that the boundary for life itself will be a similar concave inward, closed curve.

What can we say about the prospects of biotechnological applications of *pT*-adapted bacteria? The use of these bacteria in old or novel processes will be driven by human needs and curiosity [2, 8]. The needs are in many areas. Some examples are as follows. In national defense, governments are becoming increasingly occupied with finding countermeasures to microbiological warfare agents and methods of detecting them. With further increases in the world's population, there will be a greater need for food. Antibiotic resistant diseases are on the increase. Waste products of human activities are entering the oceans in large amounts. Some scientists feel that the oceans can handle even more wastes and that deep-sea bacteria can play an important part in degrading them. Research to find environmentally benign methods for the synthesis of chemicals is partly based on studies of bacterial enzymes having the capability of working at high temperature and pressure. In all of these societal problems, pressure adapted organisms may be able to offer part of the solution. There is no prescription, however. The history of science shows that significant problems are solved by those who are engaged in curiosity driven research and are prepared with a profound understanding of a discipline. This was the case for Helmholtz (before he came to the University of Heidelberg as Professor of Physiology) who came upon the idea of the ophthalmoscope while preparing a lecture for medical students on the subject of optics. His invention had an immediate and world-wide impact on medical practice and human health [3].

References

[1] Bartlett, D., Wright, M., Yayanos, A.A., and Siverman, M. (1989); Isolation of a gene regulated by hydrostatic pressure in a deep-sea bacterium; Nature, 342, 572-574.
[2] Bud, R. (1991); Biotechnology in the twentieth century; Social Studies of Science, 21, 415-457.
[3] Cahan, D. (1993); Introduction; Helmholtz at the Borders of Science; 1-13. In: Hermann von Helmholtz and the Foundations of Nineteenth-Century Science. University of California Press; Berkeley.
[4] DeLong, E.F. and Yayanos, A.A. (1985); Adaptation of the membrane lipids of a deep-sea bacterium to changes in hydrostatic pressure; Science, 228, 1101-1103.

[5] DeLong, E.F. and Yayanos, A.A. (1986); Biochemical function and ecological significance of novel bacterial lipids in deep-sea prokaryotes; Applied and Environmental Microbiology, 51, 730-737.

[6] Deming, J.W., Somers, L.K., Straube, W.L., Swartz, D.G., and MacDonell, M.T. (1988); Isolation of an obligately barophilic bacterium and description of a new genus, Colwellia gen. nov.; System. Appl. Microbiol., 10, 152-160.

[7] Kato, C., Li, L., Nakamura, Y., Tamaoka, J., and Horikoshi, K., (1998); Extremely barophilic bacteria isolated from the Mariana Trench, Challenger Deep, at a depth of 11,000 meters; Applied and Environmental Microbiology, 1510-1513.

[8] Malik, V.S. (1989); Biotechnology--the golden age; Advances in Applied Microbiology, 34, 263-306.

[9] Pledger, R.J., Crump, B.C., and Baross, J.A. (1994); A barophilic response by two hyperthermophilic, hydrothermal vent Archaea; An upward shift in the optimal temperature and acceleration of growth rate at supra-optimal temperatures by elevated pressure; FEMS Microbiology Ecology, 14, 233-241.

[10] Yayanos, A.A. (1986); Evolutional and ecological implications of the properties of deep-sea barophilic bacteria; Proc. Natl. Acad. Sci. USA, 83, 9542-9546.

[11] Yayanos, A.A. (1995); Microbiology to 10,500 meters in the deep sea; Annual Reviews of Microbiology, 49, 777-805.

[12] Yayanos, A.A. (1998); Empirical and theoretical aspects of life at high pressures in the deep sea; Horikoshi, K. and Grant, W. D. Extremophiles. John Wiley & Sons; New York.

[13] Yayanos, A.A., Van Boxtel, R., and Dietz, A.S. (1984); High-pressure-temperature gradient instrument; Use for determining the temperature and pressure limits of bacterial growth.; Applied and Environmental Microbiology, 48, 771-776.

Changes in the Microbial Community in Deep-Sea Sediment During Cultivation Without Decompression

C. Kato, M. Yanagibayashi, Y. Nogi, L. Li and K. Horikoshi

The DEEP-STAR group, Japan Marine Science and Technology Center, 2-15 Natsushima-cho, Yokosuka 237-0061, Japan.
katoc@jamstec.go.jp

Abstract. A sample of deep-sea sediment was obtained from the Japan Trench at a depth of 6,292 m using a pressure-retaining sediment sampler. Microorganisms in the sediment sample were cultivated in marine broth 2216 at ambient pressure (65 MPa) without decompression, and at atmospheric pressure (0.1 MPa) as a control experiment. The results of phylogenetic analysis based on 16S rDNA sequences indicated that: I) microbial diversity in the original sediment samples showed a wide distribution of types in the domain bacteria, whereas II) in the mixed cultures incubated at 65 MPa without decompression, bacterial strains belonging to the *Shewanella* barophiles branch and the genus *Moritella* existed together at the beginning of cultivation, and *Moritella* strains became dominant towards the end of the cultivation period, and III) in the mixed cultures incubated at atmospheric pressure, strains belonging to the genus *Pseudomonas* were dominant at all times.

1 Introduction

The DEEP-BATH system (deep-sea baro/thermophiles collecting and cultivating system) constructed by the Japan Marine Science and Technology Center is very useful for cultivating microorganisms at high pressures and high temperatures [1]. This system also contains a pressure-retaining sediment sampler which is able to obtain a sample while maintaining ambient pressure and temperature after sampling at the deep-sea bottom. In our experience, just a few hours of decompression may not have a serious effect in isolating barophilic strains, but it is possible that some pressure sensitive strains, if present in the deep-sea sediment, might die during such decompression. Therefore, it is necessary to analyze the microbial communities in the original sample and in samples cultivated without decompression using molecular phylogenetic techniques in order to understand the diversity of barophilic bacteria in the deep-sea environment. In this study, we have analyzed the changes in a microbial community of Japan Trench sediment obtained by means of the pressure-retaining sampler (SHINKAI 6500 dive #373 at a depth of 6,292 m), during cultivation without decompression (65 MPa) and at atmospheric pressure (0.1 MPa).

2 Material & Methods

A sample of deep-sea sediment (about 5 ml) was collected from the inside of a deep-sea fissure of the Japan Trench, the Mannequin Valley (39° 20.5' N. 144° 35.9' E), at a depth of 6,292 m, by means of the pressure-retaining sediment sampler of the DEEP-BATH system, using the manned submersible SHINKAI 6500 (dive #373, June, 1997). The sample obtained was carried to the sea-surface without any change in temperature or pressure (2 °C and about 65 MPa) in the sampler, and was placed in a refrigerator (2–4 °C) on the support ship M. S. Yokosuka.

The sample (5 ml) maintained at ambient pressure was diluted to 500 ml by addition of sterilized sea water at 65 MPa and 10 °C using the dilution device of the DEEP-BATH system, and then the diluted sample (10 ml) was transferred as inoculum to 1.5 l of filter-sterilized marine broth 2216 in the cultivation chamber without any change in pressure or temperature. At the same time, a similar diluted sample was transferred as inoculum to 1.5 l of the same medium at atmospheric pressure and 10 °C as a control experiment. Cultivation was repeated five times at 65 MPa without decompression, or at atmospheric pressure, using the cultivation chamber. These protocols are summarized in Fig. 1.

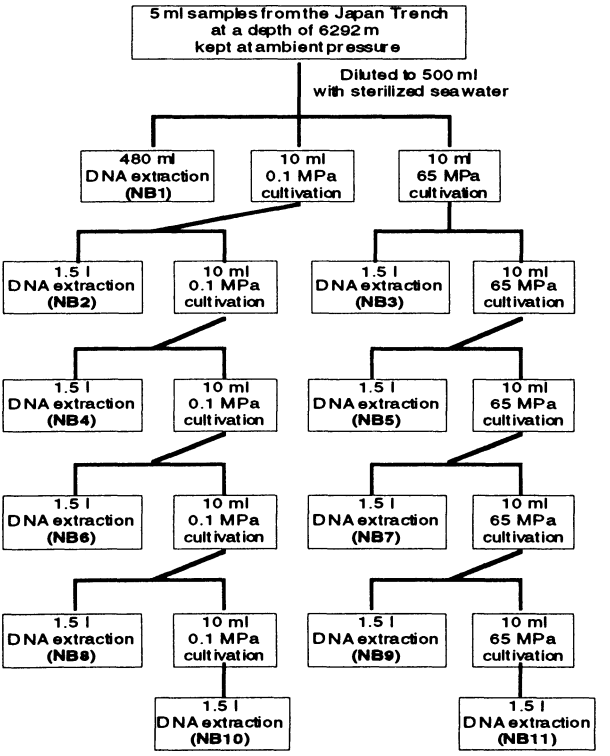

Fig. 1. Strategy for cultivation of microorganisms in a sediment sample maintained at ambient pressure using the DEEP-BATH system

Molecular phylogenetic analyses were carried out according to the procedure reported by Kato *et al.* [2].

3 Results

The results of RFLP (restriction fragment length polymorphism) analysis [3] and the patterns obtained for the original sediment (NB1) and cultivated cells (NB2–11) are shown in Tables 1 and 2, respectively. The patterns, NB1-a, b, and f from the sample NB1 were similar to those of samples NB65-A, E, and NB0.1-H, which comprised the majority of the cultivated samples. Those with patterns differing from the NB1 sample might correspond to bacterial strains that were unculturable under the growth conditions employed.

Table 1. Number of clones showing different RFLP patterns of amplified 16S rDNA gene from the DNAs extracted from the original sediment (NB1) obtained by the pressure-retaining sampler (65 MPa)

RFLP pattern	Number of the clones	RFLP pattern	Number of the clones
NB1-a	2	NB1-i	1
NB1-b	2	NB1-j	3
NB1-c	2	NB1-k	3
NB1-d	1	NB1-l	4
NB1-e	6	NB1-m	1
NB1-f	1	NB1-n	3
NB1-g	1	NB1-o	1
NB1-h	1	total	32

Table 2. Number of clones showing different RFLP patterns of amplified 16S rDNA gene from the DNAs cultivated (**a**) at high pressure (65 MPa,) and (**b**) atmospheric pressure (0.1 MPa). D* showed a fusion sequence of NB65-A and E

(**a**) RFLP pattern	NB3	NB5	NB7	NB9	NB11	Total
NB65-A	2	2	0	0	0	4
NB65-B	0	1	1	0	0	2
NB65-C	3	0	0	0	0	3
NB65-D	0	1	0	0	0	1
NB65-E	3	6	8	8	0	34
NB65-F	0	0	0	2	0	2
NB65-G	0	0	1	0	0	1
(**b**) RFLP pattern	NB2	NB4	NB6	NB8	NB10	Total
NB0.1-H	8	12	10	11	11	52
NB0.1-I	0	1	0	0	0	1
NB0.1-J	0	0	1	0	0	1

A phylogenetic tree based on 16S rDNA sequences is shown in Fig. 2. 16S rDNA sequences from the original sediment sample (NB1) were widely distributed in the domain bacteria, but the sequences found in DNA from the samples

cultivated at high pressure (65 MPa; samples NB3, 5, 7, 9, and 11) or at atmospheric pressure (0.1 MPa; samples NB2, 4, 6, 8, and 10) fell into particular genera and branches. Sequences found in DNA from samples NB65-A, B, and NB1-a belonged to the *Shewanella* barophiles branch reported previously [4], and those in samples NB65-E, F, G, and NB1-b were closely related to the genus *Moritella*. These strains are well-adapted to the deep-sea high pressure environment, and bacteria related to these branches particularly show growth properties characteristic of barophilic or barotolerant organisms [4–6]. The sequences found in DNA from samples NB0.1-H, I, J, and NB1-f, g, were closely related to the genus *Pseudomonas* which is widely distributed in the ocean environment [2].

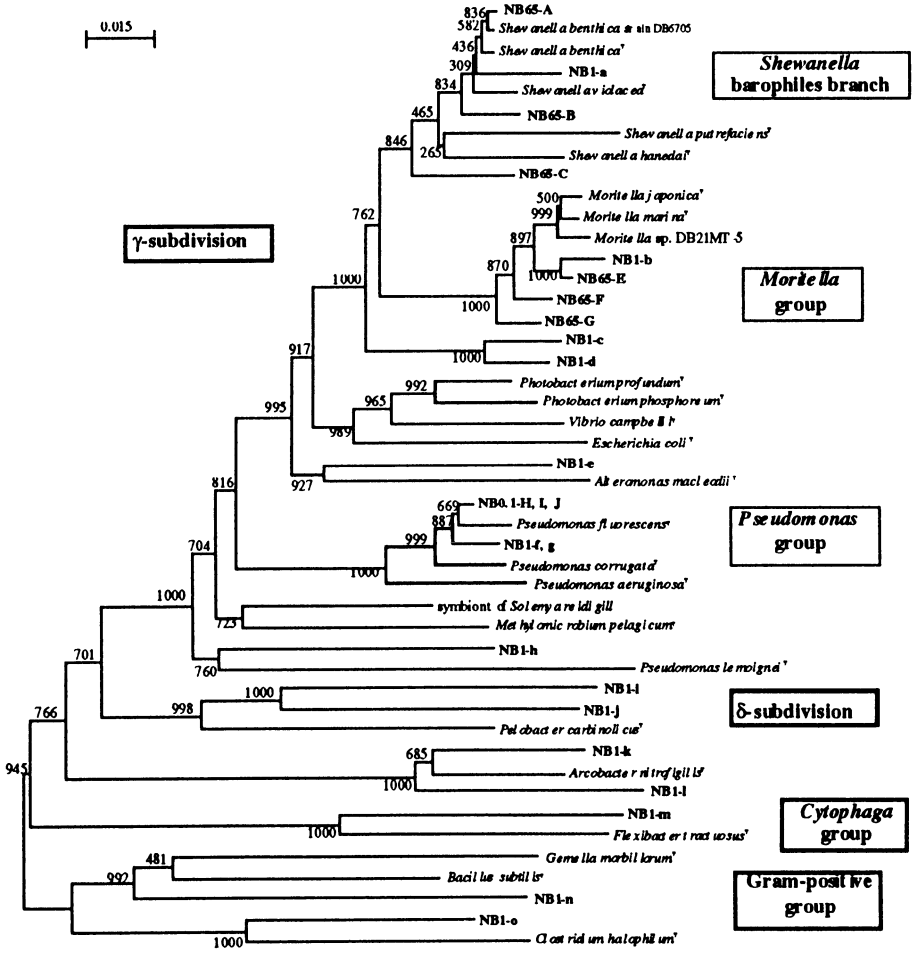

Fig. 2. Phylogenetic tree showing the relationships between the sequences determined in this study and 16S rDNA sequences of other bacteria. The scale represents the average number of nucleotide substitutions per site. Numbers denote bootstrap probabilities

4 Discussion

A microbial community from deep-sea sediment can be changed by cultivation conditions. The deep-sea adapted barophilic bacteria, like barophilic *Shewanella* and *Moritella* strains, only survived in the community under high pressure conditions, and the genus *Pseudomonas* which shows widespread distribution in the ocean environment [2] was selected in the community under atmospheric pressure conditions. The former investigations indicated that the major microorganisms adapted to the environment in the Japan Trench belong into particular phylogenetic branches, the genus *Moritella* and the barophilic *Shewanella* species [7–9]. Our present results support the findings of these previous investigations, as we have shown by means of the DEEP-BATH system that the genus *Moritella* is particularly selected from the mixed community during high pressure cultivation. Using this system, cultivation is performed under facultatively anaerobic conditions, so it appears that the genus *Moritella* is better adapted to growth under limited oxygen conditions than the barophilic *Shewanella* strains.

References

[1] Kyo, M., Tsuji, T., Usui, H. and Itoh, T. (1991): Collection, isolation and cultivation system for deep-sea microbes study: concept and design: Oceans 1, 419-423.

[2] Kato, C., Li, L., Tamaoka, J. and Horikoshi, K. (1997): Molecular analyses of the sediment of the 11000 m deep Mariana Trench: Extremophiles 1, 117-123.

[3] Yanagibayashi, M., Nogi, Y., Li, L. and Kato, C.: Changes in the microbial community in Japan Trench sediment from a depth of 6,292 m during cultivation without decompression: submitted for publication.

[4] Li, L., Kato, C., Nogi, Y. and Horikoshi, K. (1998): Distribution of the pressure-regulated operons in deep-sea bacteria: FEMS Microbiol. Lett. 159, 159-166.

[5] Kato, C., Li, L., Nogi, Y., Nakamura, Y., Tamaoka, J. and Horikoshi, K. (1998): Extremely barophilic bacteria isolated from the Mariana Trench, Challenger Deep, at a depth of 11,000 meters: Appl. Environ. Microbiol. 64, 1510-1513.

[6] DeLong, E. F., Franks, D. G. and Yayanos, A. A. (1997): Evolutionary relationships of cultivated psychrophilic and barophilic deep-sea bacteria: Appl. Environ. Microbiol. 63, 2105-2108.

[7] Kato, C., Sato, T. and Horikoshi, K. (1995): Isolation and properties of barophilic and barotolerant bacteria from deep-sea mud samples: Biodiv. Conserv. 4, 1-9.

[8] Hamamoto, T., Takata, N., Kudo, T. and Horikoshi, K. (1995): Characteristic presence of polyunsaturated fatty acids in marine psychrophilic vibrios: FEMS Microbiol. Lett., 129, 51-56

[9] Urakawa, H., Kita-Tsukamoto, K. and Ohwada, K. (1998): Restriction fragment length polymorphism analysis of 16S rRNA gene of the family Vibrionaceae isolated from cold marine environments: Proceedings of the NIPR Symposium on Polar Biology, 11, 8-21.

Microbial Communities in the World's Deepest Ocean Bottom – The Mariana Trench

L. Li, C. Kato and K. Horikoshi

The DEEP-STAR Group, Japan Marine Science and Technology Center, 2-15 Natsushima-Cho, Yokosuka, 237-0061, Japan
lil@jamstec.go.jp

Abstract. We have performed the molecular analyses of the DNA extracted from the sediment of the Mariana Trench. DNA fragments corresponding to the 16S rDNA sequences of bacteria and archaea, and the pressure-regulated operons, typically identified in deep-sea adapted bacteria, were amplified and analyzed. Two extremely barophilic bacteria, strain DB21MT-2 and DB21MT-5, were isolated from the Mariana sediment. The optimal pressure conditions for growth of the two isolates were 70 and 80 MPa, respectively. These results indicated that the microbial community of the Mariana Trench consist of particular deep-sea adapted bacteria and widely distributed microorganisms.

1 Introduction

The Mariana Trench, Challenger Deep, is an area of cold, dark remoteness and the highest pressure environment in the ocean bottom. Relatively little is known about the natural bacterial communities in the sediment there because of the need to use uncommon instruments to keep deep-sea organisms at high pressure and to develop new methods to maintain and cultivate these organisms in the laboratory. By using the unmanned submersible KAIKO developed by the Japan Marine Science and Technology Center, we have obtained sediment samples from this extreme environment. In order to understand the natural microbial communities in the sediment of the Mariana Trench, we have employed molecular phylogenetic techniques to analyze the microbial diversity in the sediment, and have isolated and characterized two extremely barophilic bacteria from the sediment.

2 Material & Methods

Sediment samples were collected from the Mariana Trench, Challenger Deep (11° 22.10' N. 142° 25.85' E), at a depth of 10,898 m, by means of sterilized mud

samplers. The samples were carried to the sea-surface without temperature changes but with pressure changes. Most of the samples obtained were apportioned into 2 ml sterilized serum tubes and placed in a liquid nitrogen tank (–150 °C). A part of each sample was pressurized at about 100 MPa in a pressure vessel and these vessels were placed in a refrigerator (2–4 °C) on the support ship M.S. YOKOSUKA. Total DNA was extracted from the sediment samples by a modification of the methods of Herrick *et al.* [1]. 16S rDNAs were PCR amplified and sequenced, and subsequently phylogenetically analyzed. Barophilic bacteria were isolated from the sediment according to the method described by Kato *et al.* [2].

3 Results & Discussion

3.1 Molecular Phylogenetic Analyses of the Sediment

3.1.1 PCR Amplification of DNA from the Mariana Trench. DNA fragments corresponding to the rRNA small-subunit sequences of bacteria and archaea, and the pressure-regulated operons (ORF1, 2 and 3) were amplified by PCR from the purified DNA extracted from the Mariana sediment, however no DNA corresponding to the eukaryal rRNA small-subunit was amplified. The amplified fragments were subsequently cloned and sequenced.

3.1.2 Phylogenetic Relationships of the Amplified Bacterial and Archaeal 16S rDNA Sequences. The amplified bacterial and archaeal 16S rDNA sequences were determined and phylogenetically analyzed. The results suggested that at least three kinds of sequences from the bacteria domain were present in DNA isolated from the sediment and belonged to the γ-subdivision of Proteobacteria. Two of the amplified sequences were closely related to the *Pseudomonas* branch, and another one belonged to the branch containing *Shewanella* and barophilic bacteria [2, 3]. At least three kinds of archaeal sequences were present in DNA from the sediment and belonged to the planktonic archaea group I reported by DeLong [4]. These planktonic archaea were unculturable strains cloned from ocean waters, and group I belongs to one of the major branches of archaea. These unculturable archaea are widely distributed in the ocean. It is still unknown whether the group I archaea have some physiological functions as a symbiont in some deep-sea animals. Our results indicate that the planktonic archaea exist at the sea-bottom of the Mariana Trench, and these archaea probably arrived from the middle ocean with planktonic particles which settled there like a marine snow.

3.1.3 Distribution of the Pressure-regulated Operons in the DNA from the Mariana Sediment. Several clones which included the amplified ORF1, 2 and 3 sequences were obtained; the similarity with other sequences was analyzed, and the

results indicated that both of the identified sequences corresponding to ORF1, 2 and 3 found in the DNA from the Mariana sediment were more similar to those of the barophilic strain DB6705 than those of the moderately barophilic strain DSS12. These results suggest that the bacteria of the Mariana sediment which display the pressure-regulated operon are more like barophilic organisms (like the strain DB6705) than moderately barophilic organisms (like the strain DSS12) [2].

3.2 Isolation and Characterization of Extremely Barophilic Bacteria from the Mariana Sediment

3.2.1 Analysis of the Barophilic Isolates. Two kinds of obligately barophilic strains which were able to grow well at 100 MPa and not able to grow at atmospheric pressure were isolated. The pressure-regulated operons particularly identified in *Shewanella* barophilic strains were amplified from the strain DB21MT-2, but were not amplified from the strain DB21MT-5. Phylogenetic analysis of the 16S rDNA suggested that strain DB21MT-2 is closely related to *Shewanella benthica* and strain DB21MT-5 is closely related to *Moritella* marinus and barotolerant strain DSK1 [2].

3.2.2 Growth Properties Under Hydrostatic Pressures. As shown in Fig.1, the optimal pressure conditions for growth of strains DB21MT-2 and DB21MT-5 were 70 and 80 MPa, respectively. Neither of these strains was able to grow at pressures below 50 MPa, but both were able to grow well at higher pressures, even at

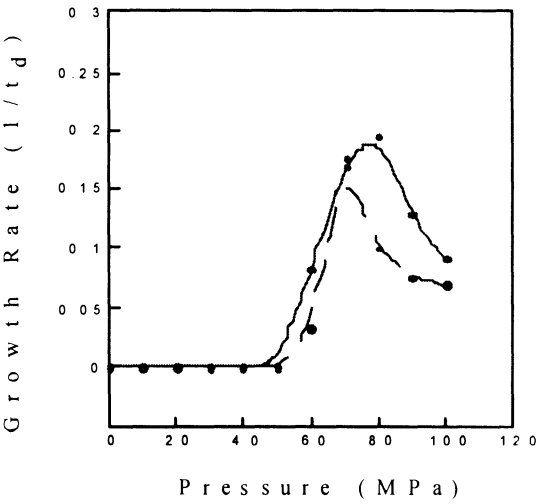

Fig. 1. Growth properties of the extreme barophiles at elevated hydrostatic pressure. DB21MT-2 (*dotted line*); DB21MT-5 (*solid line*). t_d indicates doubling time (h)

100 MPa. Therefore, strains DB21MT-2 and DB21MT-5 are defined as extremely barophilic bacteria.

3.2.3 Fatty Acids Analysis. The whole-cell fatty acid composition of the strains, DB21MT-2 and DB21MT-5, and that of selected reference strains, were analyzed. The dominant fatty acid in the isolated barophiles was hexadecenoic acid (16:1), and the long-chain polyunsaturated fatty acids (PUFAs) present in significant amounts were eicosapentaenoic acid (EPA) (20:5) in strain DB21MT-2 and docosahexaenoic acid (DHA) (22:6) in strain DB21MT-5. Around 70% of the membrane lipids in both extreme barophiles were unsaturated fatty acids, and compared with the reference strains, higher amounts of octadecenoic acid (18:1) in strain DB21MT-2 and tetradecenoic acid (14:1) in strain DB21MT-5 were evident. EPA production is one of the particular characteristics of deep-sea adapted *Photobacterium* species, such as *Photobacterium profundum* [5]. The significant amount of PUFAs in these extreme barophiles may play an important role in maintenance of membrane fluidity at low temperature and high pressure.

These results indicated that the microbial community of the Mariana Trench consist of particular deep-sea adapted bacteria (extreme barophiles), and widely distributed microorganisms (marine archaea group I and the genus of *Pseudomonas*).

References

[1] Herrick, J.B., Madsen, E.L., Batt, C.A. and Ghiorse, W.C. (1993) Polymerase chain reaction amplification of naphthalene-catabolic and 16S rRNA gene sequences from indigenous sediment bacteria; Appl. Environ. Microbiol., 59, 687-694.

[2] Kato, C., Sato, T. and Horikoshi, K. (1995) Isolation and properties of barophilic and barotolerant bacteria from deep-sea mud samples; Biodiv. Conserv., 4, 1-9.

[3] Kato, C., Masui, N. and Horikoshi, K. (1996) Properties of obligately barophilic bacteria isolated from a sample of deep-sea sediment from the Izu-Bonin trench; J. Mar. Biotechnol., 4, 96-99.

[4] DeLong, E.F. (1992) Archaea in coastal marine environments; Proc. Natl. Acad. Sci. USA, 89, 5685-5689.

[5] Nogi, Y., Masui, N. and Kato, C. (1998) *Photobacterium profundum* sp. nov., a new, moderately barophilic bacterial species isolated from a deep-sea sediment; Extremophiles, 2, 1-7.

An Expression of a Cold Shock Inducible Gene *CspA* Under Hydrostatic Pressure in Deep-Sea Barophilic Bacterium, *Shewanella* sp. Strain DSS12

S. Fujii, K. Nakasone and K. Horikoshi

The DEEP-STAR Group, Japan Marine Science & Technology Center, 2-15 Natsushima-cho, Yokosuka 237, Japan
fujiis@jamstec.go.jp

Abstract. We cloned and sequenced a cold-shock-inducible gene from the psychrophilic and moderately barophilic bacterium, *Shewanella* sp. strain DSS12 by a PCR-based approach using a pair of degenerate primers with sequences corresponding to a highly conserved region within cspA-related proteins. Following a temperature downshift, the level of the *cspA* mRNA transcript increased. The *cspA* mRNA transcript increased in logarithmic phase cells at a hydrostatic pressure of 30 or 60 MPa. These results suggest that the DSS12 cspA plays an important role as an RNA chaperone not only for cold adaptation but also for growth under elevated hydrostatic pressure.

1 Introduction

Shewanella sp. strain DSS12 is a psychrophilic and moderately barophilic bacterium which was isolated from mud of the Ryukyu Trench (5110 m depth) collected by the SHINKAI 6500 System. This bacterium displays optimal growth at a temperature of 8 °C and at a pressure of 30 MPa [1]. Pressure-regulated operon and genes have been recognized and characterized in this bacterium [2, 3].

CspA has been identified as the major cold shock protein in *E. coli*. A family of cspAs sharing highly conserved sequences (>45% identity) has been recognized in a variety of Gram-positive and Gram-negative bacteria. CspA functions as a RNA chaperone and as a transcriptional regulator for itself and for other cold shock genes in *E. coli*.

We cloned a *cspA*-like gene from DSS12 and the cloned gene, designated *cspA*, is rapidly induced upon temperature downshift like other bacterial *cspA*-like genes. Furthermore, we demonstrate that *cspA* gene expression occurs under elevated hydrostatic pressure conditions.

2 Material & Methods

2.1 Bacterial Strain and Culture Medium

Bacterial strain DSSl2 was used for all experiments and was grown in Marine Broth 2216 (Difco Laboratories, USA). Cultures were incubated in a pressurized vessel as described previously [1].

2.2 Cloning and Sequencing of the *CspA* Gene

We selected amino acid sequences from the alignment of 18 members of the cspA family of proteins. Primer F matches the *E. coli* cspA sequence from amino acid residues 7 through 13; Primer R represents amino acid residues 29 through 34. Degenerate PCR was performed and a 83-bp fragment was amplified. By using an internal portion of the amplified fragment as a probe, we screened the DSSl2 genomic DNA library. The sequences of these primers correspond to bases 356 to 376 (complementary) and bases 378 to 397 in Fig. 1.

Fig. 1. Nucleotide sequence and deduced amino acid sequence of the *cspA* gene of DSSl2. RNA binding motifs, RNPI and RNP2, are boxed. The putative –10 and –35 regions, ribosome binding site, and the sequence of a potential transcription terminator are underlined. The bent arrow indicates the transcription initiation site

3 Results & Discussion

3.1 Structure of the *CspA* Gene

As shown in Fig. 1, the *cspA* gene is 213 bp in length and encodes a protein comprising 70 amino acid residues with a molecular mass of 7,583 Da and a calculated pI of 4.48. The deduced amino acid sequence of *cspA* has RNP 1

(KGFGFL) and RNP2 (VFVFHF) motifs, and comparison with sequences in the EMBL database using the program BLAST revealed 62% identity to the major cold shock protein cspA of *E. coli*.

3.2 Induction of *CspA* mRNA Under Various Culture Conditions

To examine the level of expression of *cspA* mRNA under various culture conditions, Northern blot analysis was carried out using total RNA prepared from cells grown at 8 °C with shaking until the culture reached logarithmic phase, and from cells shifted to –1 °C and 4 °C for 30 min, 1 h or 2 h with shaking. After 1 h or 2 h cold shock transcription of *cspA* significantly increased compared with the control (data not shown).

As DSS12 is a moderately barophilic bacterium, we examined the influence of pressure on transcription of *cspA*. As a negative control, cells were cultured in plastic bags at 8 °C without bubbled air (anaerobic cultivation) until the logarithmic or stationary phase was reached. The same level of transcription in lanes 3 and 4 of Fig. 2 indicates that the increase in transcription of *cspA* that occurs under anaerobic cultivation condition is regulated in a manner independent of the growth phase. On the other hand, the level of transcription of *cspA* was greater in logarithmic-phase cells grown under elevated pressure conditions (lanes 5 and 7) than in cells grown at atmospheric pressure (lane 3).

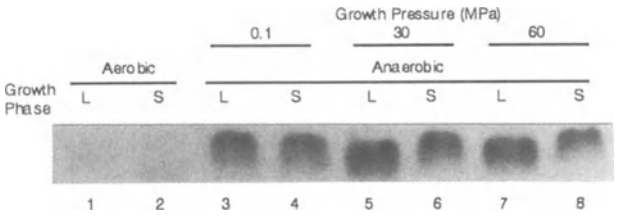

Fig. 2. The *cspA* mRNA transcript under elevated hydrostatic pressure cultivation . Total RNA prepared from cells grown at 8 °C aerobically (lanes 1 and 2) or anaerobically (lanes 3 to 8). Some of these cells were grown at 30 MPa (lanes 5 and 6) or 60 MPa (lanes 7 and 8). Samples were subjected to Northern blot hybridization with the DIG-labeled sequence of *cspA* as a probe. The letters L and S indicate logarithmic (lanes 1, 3, 5 and 7) and stationary phase (lanes 2, 4, 6 and 8) cells, respectively

3.3 Unusually Long 5' Untranslated Region of *CspA* mRNA

mRNAs of *E. coli cspA*, *cspB* and *cspG* have unusually long 5' untranslated regions (5' UTR). The 5' UTR of *cspA* has been reported to play an important role in regulation of not only the expression of cspA itself but also the expression of other cold shock proteins as well as in *cspA* mRNA stabilization at different temperatures in *E. coli*. We found that DSS12 *cspA* mRNA contains an AT-rich (73%) 5' UTR of 177 bases (Fig. 1), and this sequence can display a secondary

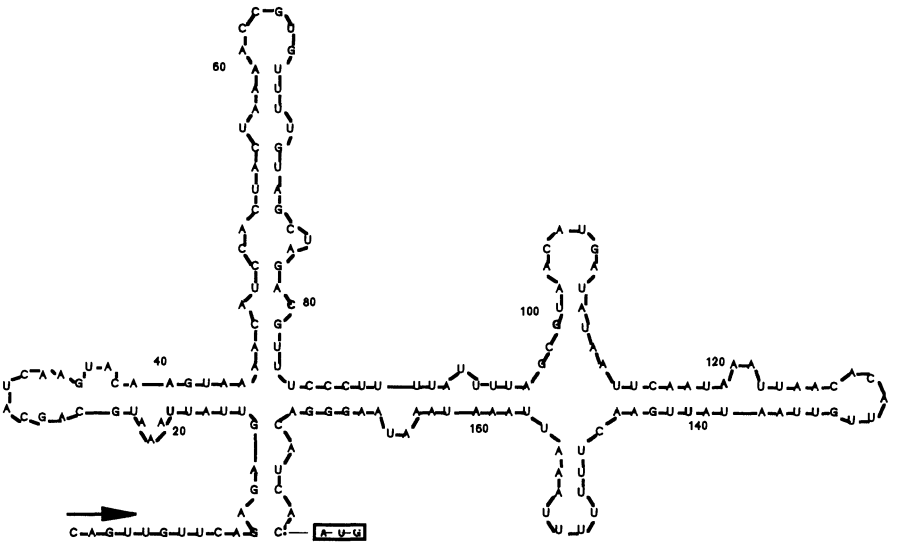

Fig. 3. Putative secondary structure of the 5' UTR of *cspA* mRNA. The initiation codon (AUG) is boxed

structure similar to *E. coli cspA* and *cspB* mRNA [4] as shown in Fig. 3. These features indicate that the 5' UTR of DSS12 *cspA* may play an important role in regulation of proteins as in the case of *E. coli cspA*.

The mRNA secondary structure or the affinity of a protein(s) for mRNA may be drastically altered under atmospheric pressure or high pressure conditions. It is thought that the affinity of ribosomes for binding to mRNA changes during temperature downshift in the proposed cold adaptation model. In addition, a recent report revealed that Csps as RNA chaperones are essential for not only cold adaptation but also for optimum growth in *Bacillus subtilis*. We speculate that DSS12 cspA might function as a RNA chaperone which facilitates the translation of mRNAs under high pressure conditions, and it might be essential for growth under low temperature and high pressure conditions such as in the deep-sea.

References

[1] Kato, C., Sato, T. and Horikoshi, K. (1995); Isolation and properties of barophilic and barotolerant bacteria from deep-sea mud samples. Biodiv. Conserv., 4, 1-9.

[2] Kato, C., Smorawinska, M., Li, L. and Horikoshi, K. (1997); Comparison of the gene expression of aspartate β-D-semialdehyde dehydrogenase at elevated hydrostatic pressure in deep-sea bacteria. J. Biochem., 121, 717-723.

[3] Kato, C., Tamegai, H., Ikegami, A., Usami, R. and Horikoshi, K. (1996); Open reading frame 3 of the barotolerant bacterium strain DSS12 is complementary with *cydD* in *Escherichia coli*: *cydD* functions are required for cell stability at high pressure. J. Biochem., 120, 301-305.

[4] Etchegaray, J.P., Jones, P.G. and Inouye, M. (1996); Differential thermoregulation of two highly homologous cold-shock genes, *cspA* and *cspB*, of *Escherichia coli*. Genes to Cells., 1, 171-178.

Microorganisms

Interaction Between Osmotic and Hydrostatic Pressure in Yeast Inactivation

J.M. Perrier-Cornet, M. Hayert, E. Saurat, C. Milesse and P. Gervais

Laboratoire de Génie des Procédés Alimentaires et Biotechnologiques
ENSBANA – Université de Bourgogne
1 esplanade Erasme, 21000 Dijon, France
Phone: +33-(0)3 80 39 68 45; Fax: +33-(0)3 80 39 66 11
jperrier@u-bourgogne.fr

Abstract. The protective effect of an osmotic perturbation on high-pressure inactivation has been investigated using a yeast strain: *Saccharomyces cerevisiae*. Osmotic shocks have been carried out with binary medium (glycerol/sorbitol and water) with or without glucose. Variations of osmotic level, osmotic shift kinetics and time between osmotic and hydrostatic treatment (350 MPa/10 min) have allowed the characterization of cell baroprotection. Two different cumulative baroprotection effects have been distinguished: one conferred by the solute on biological structures and the other related to the osmotic stress, cell volume variations and stress metabolism response (HSP, trehalose). These experiments have also exhibited a repair phase, which occurred immediately after the high-pressure treatment and required the presence of glucose.

1 Introduction

The influence of hydrostatic pressure on living organisms associated with food is now better known and has often been reviewed [1]. The water activity of the medium is one of the major parameters involved in microorganism baroprotection. Numerous authors have described important baroprotection effects on *E. coli* [2] and *Rhodotorula rubra* [3]; very high pressure level (>700 MPa) and/or higher temperature were then necessary to achieve a complete inactivation. Such osmotic baroprotection was also observed on protein structures [4] and certainly explains part of microorganisms protection. Howevera global comprehension of cell baroprotection would imply an analysis of cell osmotic response implications.

The effects of osmotic shift on microorganisms are well known: a passive transient phase with a rapid cell volume shrinkage [5], a non-specific stress response with heat shock protein (HSP) synthesis [6] and in the presence of energy, an osmoregulation phase which involves polyols synthesis and volume recovery.

The objective of this work was to understand the implications of these different osmotic mechanisms in high-pressure inactivation of microorganisms. This knowl-

edge would certainly allow a better comprehension of overall mechanisms of high-pressure inactivation.

2 Material & Methods

2.1 Microorganisms and Growth Conditions

The yeast *Saccharomyces cerevisiae* (CBS 1171) was grown in Malt Wickerham medium and harvested (48 h) at the beginning of the stationary phase. Viability measurements were done with the plate method on MW agar using appropriate dilutions.

2.2 Osmotic Treatment

Osmotic shifts were obtained by centrifuging and resuspending cells in the binary solutions (glycerol, sorbitol) at a_w 0.960 with or without glucose (10 g/l). For short delays between treatments, the mix was accomplished in the plastic bag just before or at the beginning of the pressurization.

2.3 High-Pressure Treatment

Samples were conditioned in polyethylene bags and pressurized in a 1.5 l/600 MPa apparatus (ACB, France). Pressure loading and release were done quickly (<10 s).

3 Results & Discussion

In order to characterize the baroprotection effect of low a_w medium (0.960), cell samples obtained with different conditions were compared to a reference without osmotic depressor (Fig. 1).

Whatever the conditions, yeast cells pressurized in low a_w medium were more resistant to high-pressure treatment (about 3 log). Osmotically stressed cells seem less sensitive than those adapted (about 2.5 log). Although kinetics of a_w variation was essential for cell survival at low a_w [5], no significant differences were observed between osmotic shock and slope.

The inactivation difference between low a_w culture and cells recently stressed pointed out the importance of the proximity between the two treatments. A complete study using a variable delay has been carried out with binary medium (Fig. 2A) and also in presence of glucose (Fig. 2B).

For long delays (>15 min) and whatever the medium, yeast inactivation follows cell volume variations. Osmoregulation metabolism reduced the baroprotection induced by osmotic stress. The inactivation rate 6 h after the osmotic shock in

glucose medium was similar to yeast culture at 0.960. Unlike medium with glucose where yeast protection was immediate, without glucose short delays lead to a progressive decrease of yeast protection, which was not related to the cell volume but reveals the kinetics of baroprotection setting (2 min for completion).

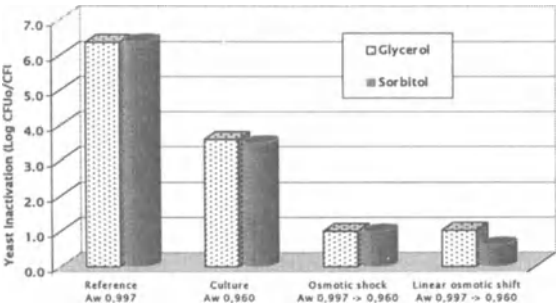

Fig. 1. Effect of osmotic change conditions on yeast inactivation (log) obtained after a high-pressure treatment (300 MPa/15 min). The delay between osmotic change and pressurization was 92 h for culture and 15 min for osmotic shock and slope

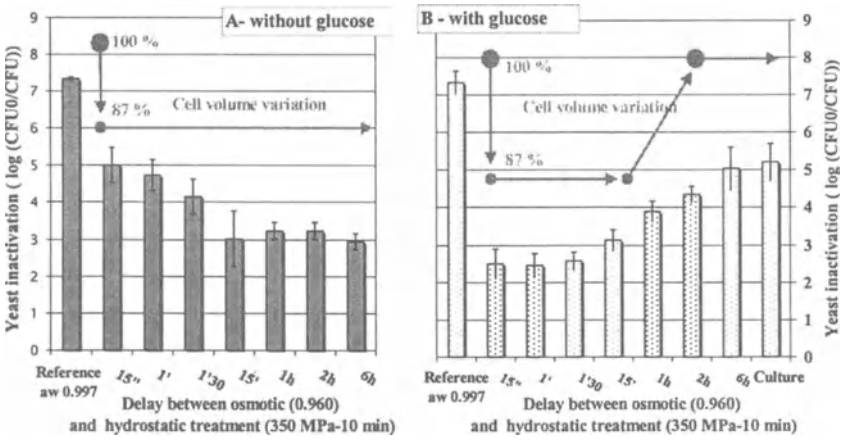

Fig. 2. Effect of variable delays between osmotic shock (a_w 0.997 to 0.960) and high-pressure treatment (350 MPa/10 min) on yeast inactivation in water-glycerol medium (**A**) or water-glycerol-glucose medium (**B**)

The addition of glucose after the hydrostatic treatment (results not given) in samples treated in binary medium leads to results similar to those obtained with glucose for short delays and was unchanged for times greater than 15 min. This specific effect of glucose was only effective for stressed cells. Then, the presence of glucose immediately after the treatment allows activation repair mechanisms induced by osmotic shift. This phenomenon masks the progressive setting of stress protection obtained without glucose.

Numerous studies have shown that osmotic stress can induce the synthesis of stress proteins which protect or repair cell structures [7] and particularly prevent protein aggregation. This osmotic response could be set in few minutes [8]. Moreover, Iwahashi *et al.* [9] have shown that thermally induced synthesis of HSP 104 and trehalose was implicated in yeast barotolerance.

Because kinetics of osmotically induced baroprotection could be related to synthesis of HSP, effect of osmotically induced protein synthesis has been investigated. The addition of cycloheximide before osmotic shock had only a slight effect on yeast baroprotection (results not given). *De novo* synthesis of HSP could not explain the whole protection induced by osmotic shift. More precise investigations have to be carried out to understand the role of osmotic stress response in baroprotection and the targets of these substances.

4 Conclusions

This work have shown that osmotic shift always induces a baroprotection phenomenon which consists of two parts:

A physicochemical part conferred by the solute on microorganisms' structures (membrane, proteins) attributed to the hydration state.

A physiological part conferred by osmotic stress response of the yeast that is set up in a few minutes after the solute addition with or without glucose and suppressed by osmoregulation mechanisms. This protection could occur immediately after hydrostatic treatment but only in the presence of glucose.

References

[1] Cheftel, J.C., (1995); Review: High pressure microbial inactivation and food preservation; Food Sci. and Technol. Int., 1, 75-90.

[2] Satomi, M., Yamagushi, T., Okuzumi, M. and Fujii, T., (1995); Effect of conditions on the barotolerance of *Escherichia coli*; J. Food Hyg. Soc. Japan, 36(1), 29-34.

[3] Oxen, P. and Knorr, D., (1993); Baroprotective effects of high solute concentrations against inactivation of *Rhodotorula rubra*; Food Sci. and Technol., 26(3), 220-223.

[4] Oliveira, A.C., Gaspar, L.P., Da Poian, A.T. and Silva, J.L., (1994); Arc repressor will not denature under pressure in the absence of water; J. Mol. Biol., 240, 184-187.

[5] Marechal, P.A. and Gervais, P., (1995); Yeast viability related to the water potential variation: influence on the transient phase; Appl. Microbiol. Biotechnol., 42, 617-622.

[6] Blomberg, A., (1995); Global changes in protein during adaptation of the yeast *Saccharomyces cerevisiae* to 0.7 M NaCl; J. Bacteriol., 12, 3563-3572.

[7] Mager, W.H. and De Kruijff, A.J.J., (1995); Stress-induced transcriptional activation; Microbiol. Rev., 59(3), 506-531.

[8] Yamamori, T. and Yura, T., (1980); Temperature-induced synthesis of specific proteins in *Escherichia coli*: evidence for transcriptional control; J. Bacteriol., 142, 843-851.

[9] Iwahashi, H., Obuchi, K., Fujii, S. and Komatsu, Y., (1997); Effect of temperature on Hsp104 and trehalose in barotolerance of *Saccharomyces cerevisiae*; FEBS Lett., 416, 1-5.

Multiple Stress Resistance in Pressure Resistant *Escherichia coli* Mutants

K. Hauben, T. Nyström, A. Farewell and C. Michiels

Laboratory of Food Microbiology, Katholieke Universiteit Leuven, Kard. Mercierlaan 92, B-3001 Leuven, Belgium
chris.michiels@agr.kuleuven.ac.be

Abstract. The *E. coli* mutants LMM1010 and LMM1030, which were previously isolated on the basis of their pressure resistance, are demonstrated here to show cross-resistance to acid, reactive oxygen and/or heat. Analysis of protein expression revealed derepression of common heat shock proteins in both mutants under non-stress conditions. Heat shock treatment of the parent strain resulted in transient induction of heat shock proteins, and enhanced its survival at moderate pressures (220 MPa). However, heat shock did not protect the parent strain from inactivation at higher pressures (500 MPa). Hence, overexpression of heat shock proteins seems not sufficient to explain the high level of pressure resistance in the mutants.

1 Introduction

We previously reported the acquisition of pressure resistance in *E. coli* by spontaneous mutation [1]. Pressure treatments up to 800 MPa (15 min at 20 °C) reduced the viability of these mutants by only 2–3 log units, while the parent strain was inactivated by ≥8 log units in excess of 500 MPa. In view of the associated food safety risk, we analysed the resistance of these mutants to other stresses relevant to food preservation, and searched for possible ways to efficiently inactivate them at pressure levels (<800 MPa) that are currently exploited for food processing.

2 Material & Methods

E. coli strains LMM1010 and LMM1030 were previously isolated as pressure resistant mutants of strain MG1655 [1]. Pressure treatments were done for 15 min at 20 °C in phosphate buffer as described [1]. 2-D analysis of protein synthesis was performed according to [2].

3 Results

3.1 Multiple Stress Resistance of Mutants

Parent strain MG1655 and pressure resistant mutants LMM1010 and LMM1030 were analysed for their resistance against heat, acid and reactive oxygen species. Decimal reduction values (D-values) for heat and acid inactivation are given in Table 1. Oxidative stress was imposed by the superoxide generator plumbagin (Fig. 1). Superoxide killing did not follow first-order kinetics, which made calculation of D-values impossible. Both mutants showed increased D-values for acid inactivation, and were more resistant to superoxide killing during the first 3 h of exposure compared to the parent strain. In addition, D-values for heat inactivation were increased for mutant LMM1030. Heat resistance of LMM1010 was comparable to the parent strain. Apparently, pressure resistance is associated with a general cross-resistance type in these mutants.

Table 1. D-values for heat or acid inactivation of *E. coli* strains

Strain	Heat		Acid	
	58 °C	60 °C	pH 2.6	pH 2.3
MG1655	1.97 min	0.83 min	131 min	94 min
LMM1010	1.65 min	0.95 min	200 min	142 min
LMM1030	6.54 min	1.71 min	194 min	208 min

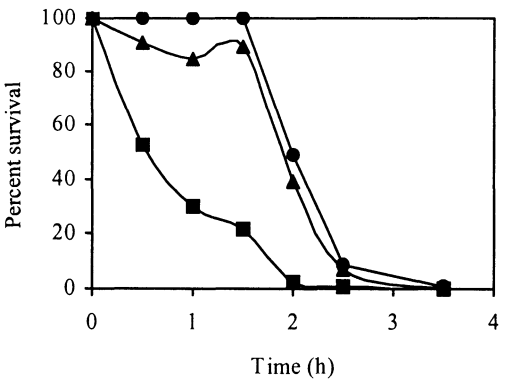

Fig. 1. Survival of *E. coli* MG1655 (■), LMM1010 (▲) and LMM1030 (●) in Hepes buffer supplemented with 0.8 mM plumbagin

3.2 Analysis of Protein Expression Profile

The global pattern of protein synthesis in the *E. coli* strains was compared in order to identify differences in protein expression that could potentially explain the enhanced stress resistance of the mutants. Two-dimensional gel electrophoresis of protein extracts from unstressed cells revealed that both mutants produced increased levels of the common heat shock proteins DnaK, GrpE, GroEL, GroES and ClpB. Overexpression of heat shock proteins was observed during exponential growth and at the onset of starvation. It is known that some of these stress proteins are involved in various types of stress resistance [3, 4], and it is possible that their overexpression also contributes to the pressure resistance of the mutants.

3.3 Heat Shock Treatment of Parent Strain

We further examined whether induction of heat shock proteins by heat shock treatment affected pressure resistance of the parent strain. Cultures of MG1655 containing *dnaK-luxCDABE* or *grpE-luxCDABE* gene fusions were shifted from 28 to 42 °C for 5 min. Transient induction of heat shock proteins after this treatment was evident from the transient increase in light production. Heat shock treatment enhanced survival of MG1655 at 220 MPa, but not at 270 and 500 MPa (Table 2). Therefore, overexpression of heat shock proteins seems not sufficient to achieve the level of pressure resistance observed in the mutants.

Table 2. Effect of heat shock treatment (5 min shift from 28 to 42 °C) on pressure resistance of parent strain MG1655

Pressure treatment for 15 min at 20 °C	Viability reduction (log N/N_0)	
	untreated	heat-shocked
220 MPa	–4.1	–1.8
270 MPa	–5.9	–5.6
500 MPa	> –6.5	> –6.5

3.4 Effect of Antimicrobial Peptides on Pressure Inactivation of Mutants

In order to increase the pressure inactivation of the mutants, nisin (100 IU/ml) or lysozyme (10 µg/ml) was added before pressure treatment (Fig. 2). Addition of these antimicrobials strongly enhanced the inactivation of the pressure resistant mutants, mostly by ≥2 log units for pressures above 300 MPa.

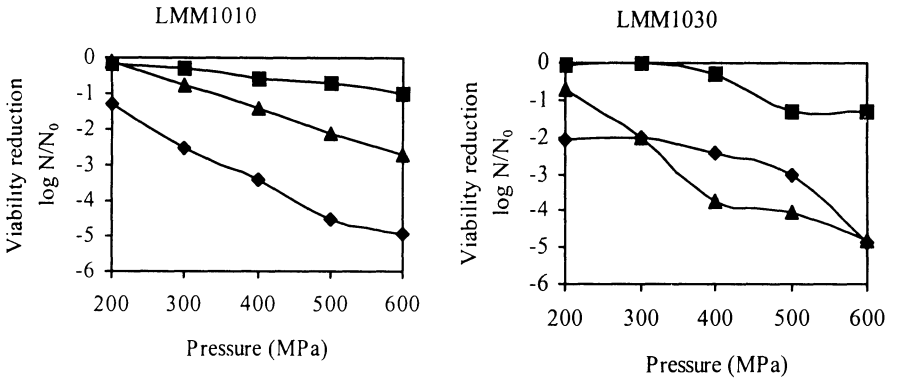

Fig. 2. Inactivation of *E. coli* LMM1010 and LMM1030 after 15 min pressure treatment at 20 °C without additions (■), with 10 µg/ml lysozyme (▲) and with 100 IU/ml nisin (◆)

4 Conclusions

Two pressure resistant mutants, which were independently isolated solely on the basis of their pressure resistance [1], both display a remarkable cross-resistance to reactive oxygen, acid and/or heat killing. Their multiple stress resistance coincided with higher levels of common heat shock proteins, and it is possible that the latter may contribute to their overall stress resistance, including pressure resistance. However, induction of heat shock proteins in the parent strain after heat shock treatment did not result in the same level of pressure resistance. Therefore, overexpression of heat shock proteins seems not sufficient for the high level of pressure resistance in the mutants.

It is relevant that pressure inactivation of the mutants was strongly enhanced in the presence of nisin or lysozyme. Combining pressure-processing with such antimicrobial peptides seems an appropriate means to increase the safety of pressure-treated foods.

References

[1] Hauben, K. *et al.* (1997); *Escherichia coli* mutants resistant to inactivation by high hydrostatic pressure; Appl. Environ. Microbiol., 63, 945-955.

[2] Nyström, T. and Neidhardt, F.C. (1992); Cloning, mapping and nucleotide sequencing of a gene encoding a universal stress protein in *Escherichia coli*; Mol. Microbiol., 6, 3187-3198.

[3] Rockabrand, D. *et al.* (1995); An essential role of the *Escherichia coli* DnaK protein in starvation-induced thermotolerance, H_2O_2 resistance, and reductive division; J. Bacteriol., 177, 3695-3703.

[4] Rockabrand, D. *et al.* (1998); Roles of DnaK and RpoS in starvation-induced thermotolerance of *Escherichia coli*; J. Bacteriol., 180, 846-854.

Strain Differences in Resistance to High Pressure and Mild Heat in Isolates of *Escherichia coli* O157

A. Benito and B. Mackey

Institute of Food Research, Earley Gate, Reading RG6 6BZ, UK
bernard.mackey@bbsrc.ac.uk

Abstract. Strains of *Escherichia coli* O157 isolated from clinical cases of food-borne illness and other sources showed wide differences in resistance to high hydrostatic pressure but the differences in pressure resistance were seen only in stationary phase cells. The two most pressure-resistant strains were also more resistant to heating at 52 °C and 57 °C. These studies emphasise the importance of including stress-resistant strains of *Escherichia coli* O157 when testing the efficacy of novel or mild food preservation treatments

1 Introduction

The initial applications of high hydrostatic pressure treatment of foods are likely to be as a replacement for thermal pasteurisation processes aimed at inactivating vegetative cells of food-borne pathogens and spoilage organisms. In this context it is clearly necessary that any pressure process be capable of inactivating *Escherichia coli* O157 since this organism has been found in a wide range of foods, has a low infective dose and causes severe illness. It is well known that resistance to pressure and other stresses varies widely between species but, more recently, it has become apparent that significant differences in resistance exist between different strains of the same species [2,3] In this work we have examined the resistance to pressure of five different strains of *Escherichia coli* O157 and a non-O157 strain. Two O157 strains that were associated with large outbreaks of food-borne illness were substantially more pressure resistant than the others and were also more resistant to mild heat.

2 Material & Methods

2.1 Bacterial Strains and Growth Conditions

The following *Escherichia coli* O157:H7 strains were used: NCTC 12079 and H1071 (clinical isolate from M. Patterson, Queen's University, Belfast); C9490 (clinical isolate from the 'Jack-in-the-box', Western States hamburger patty outbreak of 1993); 30-2C4 (clinical isolate from outbreak associated with dry cured salami), W2-2 (poultry isolate); all from M. Doyle, University of Georgia, USA. Strain NCTC 8003 (serotype 0124) was also tested. Cells in the stationary phase of growth were prepared by sub-culturing a loopful of overnight culture in tryptone soya broth (TSB) into 100 ml fresh TSB and incubating for 18 h in shaken culture at 37 °C. To obtained exponential-phase cells, 100 µl of the stationary-phase culture were introduced into 100 ml of fresh medium and incubated for 3 h to give an optical density reading of 0.2 at 680 nm.

2.2 Viable Counts

Cell suspensions were serially diluted in maximum recovery diluent (MRD, Oxoid) and plated on Tryptone Soya Agar (TSA, Oxoid) containing 0.3% yeast extract (YE). Colonies were counted after incubating the plates at 37 °C for 48 h. Survival curves are based on mean values from two or more experiments.

2.3 Pressure Treatment

Cells were centrifuged and resuspended in phosphate buffered saline (PBS) pH 7.0 to give a viable count of about 10^9 cfu·ml^{-1}. Cell suspensions (2 ml) were sealed in plastic pouches and pressure treated in a Stanstead Fluid Power, model S-FL-850-9-W pressure rig. The pressure transmitting fluid was ethanol:castor oil (80:20). The temperature increase in the pressurisation fluid caused by adiabatic heating was monitored using a thermocouple. The maximum temperature reached during pressurisation at 500 MPa was approximately 45 °C for 80 s.

2.4 Heat Resistance

Stationary-phase cultures were diluted 1:100 in TSB and 1 ml volumes sealed in glass ampoules and kept on ice. Ampoules were heated by fully submerging in a stirred waterbath at 52 °C or 57 °C. After the contents of the ampoule had reached the desired temperature ampoules were withdrawn at timed intervals and kept on ice before determining viable counts.

3 Results

The pressure resistance of stationary-phase cells of *Escherichia coli* O157 at 500 MPa is shown in Fig 1. Two strains, C9490 and 30-2C4, were substantially more resistant than the others. When the different strains were tested in exponential

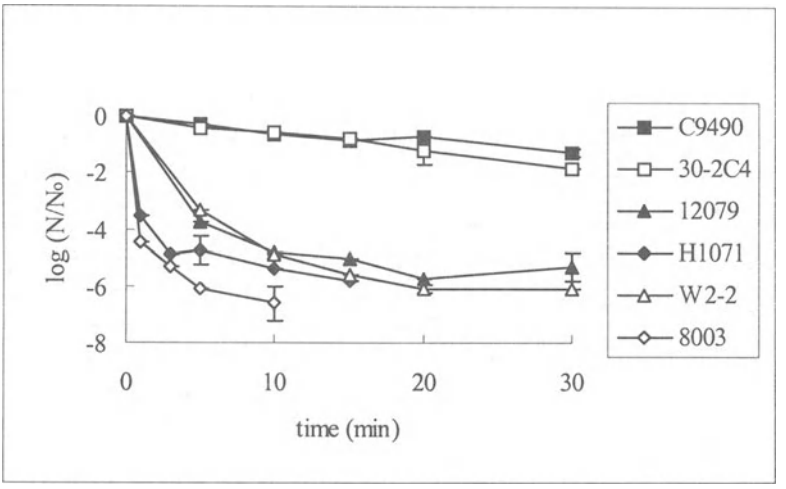

Fig. 1. Resistance of *Escherichia coli* strains to pressure treatment at 500 MPa in phosphate buffered saline

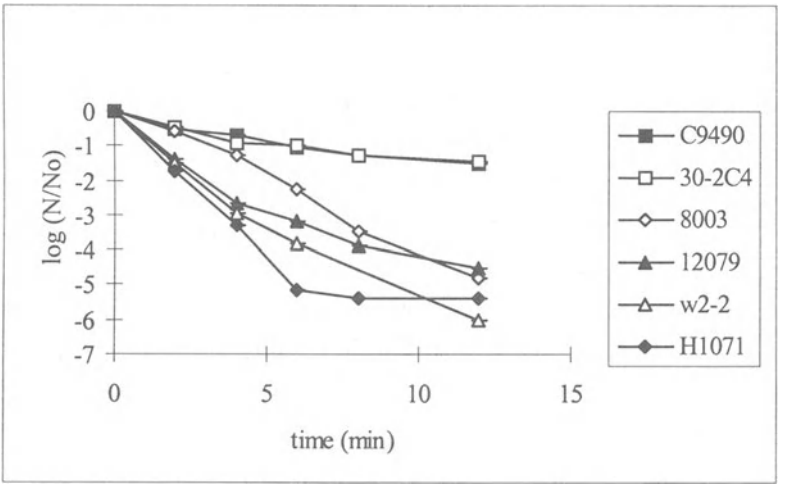

Fig. 2. Resistance of *Escherichia coli* strains to heating at 57 °C in TSB

phase no differences in pressure resistance were apparent (data not shown). The resistance to heating at 57 °C is shown in Fig. 2. The two pressure-resistant strains were also more resistant to heat than the others. Similar results were obtained at 52 °C (data not shown). The correlation between heat and pressure resistance was not absolute. Strain 8003, for example, was the most pressure-sensitive but was not the most heat sensitive.

4 Discussion

This work has shown that strains of *Escherichia coli* O157 differ widely in resistance to high pressure. Our results are in agreement with those of Patterson *et al.* [3] but are even more pronounced. Two strains isolated from food poisoning outbreaks associated with hamburgers and salami were more resistant than the most resistant strain examined by Patterson *et al.* [3]. Differences in pressure resistance were seen only in stationary-phase cells suggesting that the differences could be related to functions controlled by the stationary-phase sigma factor encoded by the *rpoS* gene. However, other factors could be involved and genetic studies will be needed to determine the basis of strain variation

Although the two most pressure-resistant strains were also the most heat-resistant the correlation did not hold within the more sensitive strains tested. Hauben *et al.* [1] reported that two out of three pressure-resistant mutants of *Escherichia coli* were also more heat resistant but the heat resistance of a third mutant was unchanged. It thus appears that some cell functions affect resistance to both heat and pressure, but other cell functions may affect resistance to each stress separately.

The inactivation of resistant strains of vegetative pathogens by pressure may depend on the application of other 'hurdles' such as low pH. A practical implication of this work is that cocktails of *Escherichia coli* O157 organisms used to validate the efficacy of novel or mild food preservation treatments should include representative resistant strains similar to those described here.

References

[1] Hauben, K.J.A., Barlett, D.H., Soontjens, C.F., Cornelis, V., Wuytack, E.Y. and Michiels, C.W. (1997); *Escherichia coli* mutants resistant to inactivation by high hydrostatic pressure; Applied and Environmental Microbiology, 63, 945-950.

[2] Humphrey, T.J., Slater, E., McAlpine, K., Rowbury, R.J. and Gilbert, R.J. (1995); *Salmonella enteritidis* phage type PT4 isolates more tolerant of heat, acid, or hydrogen peroxide also survive longer on surfaces; Applied and Environmental Microbiology, 61, 3161-3164.

[3] Patterson, M.F., Quinn, M., Simpson, R. and Gilmour, A. (1995); Sensitivity of vegetative pathogens to high hydrostatic pressure treatment in phosphate-buffered saline and foods. Journal of Food Protection, 58, 524-529.

Hsc70 Is Not Essential for Thermotolerance but for Barotolerance

H. Iwahashi, S. Nwaka, K. Obuchi and Y. Komatsu

National Institute of Bioscience and Human Technology,
Higashi 1-1, Tsukuba, Ibaraki 305, Japan
iwahashi@nibh.go.jp

Abstract. We studied the contribution of Hsc70 to barotolerance by measuring barotolerance in logarithmic phase cells of the Hsc70 (*ssb1* and *ssb2*) deletion mutant and the deletion mutant which carries the Hsc70 gene on the low copy number plasmid and high copy number plasmid. The deletion mutant strain showed higher thermotolerance and slightly lower barotolerance than that of the control strain. The mutant which has Hsc70 gene on multicopy plasmid showed more barotolerance than the strain which has the gene on low copy plasmid. These results suggest that Hsc70 contributes to barotolerance. We also compared the effect of Hsp104 and Hsc70 deletion to barotolerance at different temperatures (20–35 °C). The effect of Hsp104 deficiency was significant with increase in temperature; however, that of Hsc70 was significant at moderate temperatures. These results suggest Hsp104 contributes to barotolerance at higher temperature and Hsc70 at moderate temperature.

1 Introduction

Physically, hydrostatic pressure is considered to be analogous to temperature [1]. On the basis of this consideration, new technology which uses high pressure instead of high temperature has developed in the food industry [2]. However, from the biological aspect, basic research on the effect of hydrostatic pressure on living cells has not been accumulated. Using *Saccharomyces cerevisiae* as a model system, we have been studying the analogy between hydrostatic pressure and temperature. We have shown that the molecular chaperone, Hsp104, and non-reducing disaccharide trehalose are important factors for barotolerance [3]. Recently we found that Hsp104 and the molecular chaperon of Hsc70 are essential for the normal activities of trehalose metabolizing enzymes [4]. The effect of Hsp104 on these enzymes was significant at high temperature and that of Hsc70 was at moderate temperature [4]. This suggests that molecular chaperones of Hsp104 and Hsc70 share the functions at different temperatures. This speculation explains why Hsp104 is essential for thermotolerance and Hsc70 is not. Hsc70 may not function under the conditions used for estimating thermotolerance (thermo-

tolerance is usually measured at 40–50 °C). However, it is possible for Hsc70 to function under the conditions used for estimating barotolerance (<30 °C). In this paper, we discuss the contribution of Hsc70 to barotolerance.

2 Material & Methods

S. cerevisiae strains used in this work are listed in Table 1. Cells were grown on YPD medium at 30 °C as previously described [5]. Barotolerance and thermotolerance were measured as previously described [5].

Table 1. List of strains and plasmids

Strain or Plasmid	Genotype	Characteristic
JN54	*MATa his3,3 leu2 ura3 trp1 lys2?*	Wild type
JN212	*MATa his3,3 leu2 ura3 trp1 *ssb1-1::LEU2 *ssb2-1::HIS3*	-Hsc70
JN212-pRS316K-SSB1	*MATa his3,3 leu2 ura3 trp1 *ssb1-1::LEU2 *ssb2-1::HIS3* pRS316K-SSB1	+Hsc70
JN212-pRS426-SSB1	*MATa his3,3 leu2 ura3 trp1 *ssb1-1::LEU2 *ssb2-1::HIS3* pRS426-SSB1	++Hsc70
W303aLEU2+	*MATa can1 ade2 his3 LEU2+ trp1 ura3*	Wild type
ΔHsp104 LEU2+	*MATa can1 ade2 his3 leu2 trp1 ura3 Δhsp104::LEU2+*	-Hsp104
pRS316K	*URA3 SSB1 AmpR* (YCp-type)	Low copy
pRS426	*URA3 SSB1 AmpR* (YEp-type)	High copy

*Hsc70s are encoded on *ssb1* and *ssb2* genes.

3 Results & Discussion

We measured the time course of barotolerance (140 MPa, 25 °C) and thermotolerance (44 °C and 46 °C) in logarithmic phase cells of the Hsc70 (*ssb1* and *ssb2*) deletion mutant and the control strain (Table 2). Logarithmic phase cells were selected as Hsc70 was expressed in logarithmic phase but was repressed under the stress conditions [6]. The mutant strain which has the deletion in the genes of *ssb1* and *ssb2* showed higher thermotolerance and slightly lower barotolerance than that of the control strain (Table 2). Higher thermotolerance suggests that the deletion of *ssb1* and *ssb2* genes induced other unknown factors that cause high thermotolerance and increased basal stress tolerance.

Table 2. Time course of thermotolerance and barotolerance. Thermotolerance and barotolerance are shown as cfu relative to untreated control (0 min)

	Wild type			Hsc70⁻		
min	44 °C	46 °C	140 MPa	44 °C	46 °C	140 MPa
0	1.0	1.0	1.0	1.0	1.0	1.0
60	2.0×10^{-1}	1.0×10^{-3}	1.2×10^{-2}	4.8×10^{-1}	1.1×10^{-2}	1.0×10^{-2}
120	1.4×10^{-2}	4.8×10^{-5}	8.1×10^{-4}	1.1×10^{-1}	9.6×10^{-4}	4.0×10^{-4}
240	1.7×10^{-3}	3.7×10^{-6}	4.8×10^{-5}	2.1×10^{-2}	5.1×10^{-5}	2.0×10^{-6}

We investigated whether the barotolerance defect of Hsc70 mutant is a direct effect of Hsc70 gene. We measured the barotolerance of the strains which have *ssb1* gene on plasmids. JN212-pRS316K-SSB1 and JN212-pRS426-SSB1 have the deletion of *ssb1* and *ssb2* genes on chromosome but JN212-pRS316K-SSB1 has the *ssb1* gene on the low copy number plasmid and JN212-pRS426-SSB1 has the *ssb1* gene on the high copy number plasmid. Thus, JN212-pRS316K-SSB1 expresses lower amount of Hsc70 than JN212-pRS426-SSB1. Table 3 shows the barotolerance of the two strains. JN212-pRS426-SSB1 showed higher barotolerance than JN212-pRS316K-SSB1. This means that the amount of Hsc70 influences barotolerance, and suggests that Hsc70 contributes to barotolerance.

Table 3. Barotolerance of the strains which have Hsc70 genes on the plasmid

	Strain	
	JN212-pRS316K-SSB1 (+Hsc70)	JN212-pRS426-SSB1 (++Hsc70)
Barotolerance	1.0×10^{-3}%	2.6×10^{-3}%

To characterize the contribution of Hsc70 to barotolerance, we compared the relative barotolerance of the Hsc70 deletion strain and the Hsp104 deletion strain under different temperatures. Relative barotolerance was calculated as a ratio (barotolerance of the deletion strain / barotolerance of the wild type) because the different barotolerance between the mutant and the wild type can be considered due to the deletion of the target genes. The Hsc70 deletion strain shows lower barotolerance (around 0.50) at moderate temperatures of 25, 30 °C but the strain shows almost the same degree (0.83) at higher temperature (35 °C). On the other hand, the Hsp104 deletion decreased barotolerance at higher temperature (20 °C; 0.56, 25 °C; 0.28, 30 °C; 0.26, 35 °C; 0.15). These results strongly suggest that Hsp104 and Hsc70 share their functions at different temperature.

References

[1] Bett, K. E. and Cappi, J. B. (1965); Effect of pressure on the viscocity of water; Nature, 207, 620-621.
[2] Hayashi, R. (1989); Use of high pressure to food processing and preservation; Use of High Pressure in Food, 1-30.
[3] Iwahashi, H., Obuchi, K., Fujii, S. and Komatsu, Y. (1997); Barotolerance is dependent on both trehalose and heat shock protein 104 but is essentially different from thermotolerance in *Saccharomyces cerevisiae* ; Lett. Appl. Microbiol., 25, 43-47.
[4] in preparation
[5] Iwahashi, H., Obuchi, K., Fujii, S. and Komatsu, Y. (1997); Effect of temperature on the role of Hsp104 and trehalose in barotolerance of *Saccharomyces cerevisiae*; FEBS Letters, 416, 1-5.
[6] Iwahashi, H., Yang, W. and Tanguay, R. M. (1995); Detection and expression of the 70 kDa heat shock protein ssb1p at different temperatures in *Saccharomyces cerevisiae*; Biochem. Biophys. Res. Com., 213, 484-48.

Ribosome Analysis *In Vivo* by Differential Scanning Calorimetry: The Effects of High Pressure on *Escherichia coli*

G.W. Niven and B.M. Mackey

Institute of Food Research, Reading Laboratory, Whiteknights Road, Reading RG6 6BZ, UK
gordon.niven@bbsrc.ac.uk

Abstract. We are developing differential scanning calorimetry (DSC) as a technique for ribosome analysis *in vivo*. This enables information to be obtained about ribosome conformation without cell disruption and using minimum cell processing. Using this method, we observed a linear correlation between cell death and the decrease in ribosome-associated enthalpy in pressure treated cells. This suggested a direct relationship between cell death and ribosome damage. Initially, the surviving ribosomes in pressure treated cells adopted a less stable conformation. During subsequent incubation at 37 °C, they restabilized over a period of several hours. The presence of elevated levels of extracellular Mg^{2+} during pressure treatment reduced ribosome destabilization.

1 Introduction

Bacterial protein synthesis is inhibited by elevated hydrostatic pressure [1], which is also known to cause dissociation of purified ribosomes [2]. These observations have led to the suggestion that damage to the protein synthesis system may be a potential cause of growth inhibition in pressure treated bacterial cultures. We set out to investigate the further possibility that irreversible ribosome damage may be a primary cause of cell death after pressurization.

Most methods of ribosome analysis involve their isolation from the cells. As ribosome conformation is highly dependent on the chemical environment, observations made *in vitro* may not be easily related to events *in vivo*. This is particularly true for studies of cells during physical stress when the precise composition of the cellular environment may be unknown.

For this reason, we have embarked on the development of differential scanning calorimetry (DSC) as a method of ribosome analysis *in vivo*. Samples are heated according to a predefined temperature gradient. The energy required to maintain the gradient varies depending on the occurrence of exothermic or endothermic events in the sample. The endothermic events associated with the denaturation of ribosome components in whole cell cultures have been identified [3]. It is therefore

possible to obtain information on ribosome conformation *in vivo* from the temperatures and enthalpies of these events.

We have applied this technique to an investigation of the effects of high hydrostatic pressures on *Escherichia coli.*

2 Material & Methods

All experiments were carried out using *Escherichia coli* NCTC 8164 grown to stationary phase at 37 °C. Cell cultures were pressure treated for 20 min at the pressures stated in the text using a Stansted Mark II Enhanced Mini Food Lab pressure rig. Samples of whole cell cultures were concentrated for DSC analysis by centrifuging 1.5 ml aliquots for 4 min at 12000 *g* and resuspending the pellet in a minimum volume of supernatant (<20 µl). Thermograms were obtained using a Perkin-Elmer DSC7 and a temperature gradient of 40–100 °C at 10 °C min^{-1}.

3 Results

Two main ribosome-associated endothermic events were observed in DSC thermograms of stationary phase *E. coli* cultures (Fig. 1). The larger event, peak *m*, had a temperature maximum of 69 °C and accounted for approximately 85–90% of the total ribosome-associated enthalpy of 4 J g^{-1}. The temperature maximum of peak *n* was 80 °C.

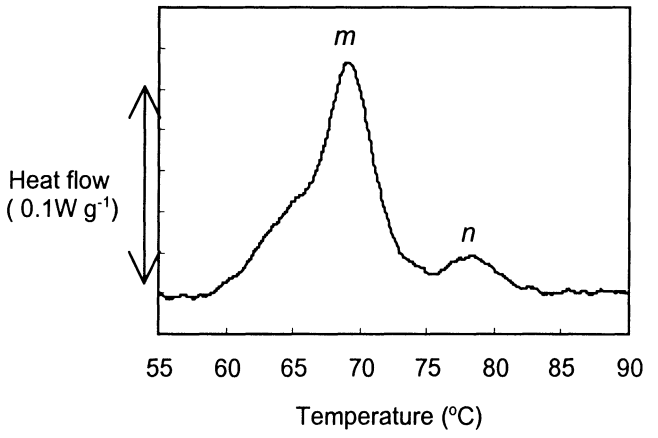

Fig. 1. The DSC thermogram of a stationary phase *E. coli* culture

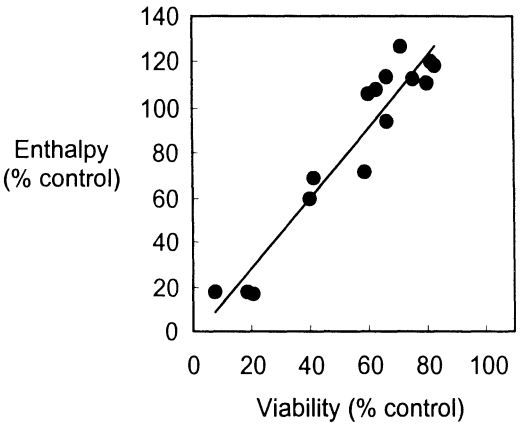

Fig. 2. The relationship between cell viability and total ribosome-associated enthalpy in stationary phase cultures of *E. coli* pressure treated at 50–250 MPa for 20 min

When cells were subjected to treatment at 50-100 MPa, the ribosome-associated enthalpy (RAE) increased approximately 20% and cell viability decreased by 20–25%.

At higher pressures (to 250 MPa), a linear relationship was observed between cell viability and the remaining RAE (Fig. 2).

When analyzed immediately following high pressure treatment at 200 MPa for 20 min, the DSC thermograms revealed changes in the conformation of surviving ribosomes. The enthalpies of peaks *m* and *n* were reduced to 56% and 31% of control values, respectively. The temperature maximum of peak *m* was reduced by 3.0 °C, and that of peak *n* by 1.4 °C, which indicated that surviving ribosomes had adopted a less stable conformation. When pressure treated cells were incubated at 37 °C, the ribosomes recovered a more stable conformation. The peak temperatures returned to control values within 4 h (peak *m*) and 2 h (peak *n*). The total RAE recovered to only 70–80% of control levels after 5 h. During this time, cell viability continued to decrease, falling from 50% immediately after pressure treatment to 6% after incubation for 5 h. Pressure treatment and incubation in the presence of 5 mM $MgCl_2$ prevented destabilization of surviving ribosomes, but had no effect on the initial loss of RAE, or on cell viability.

4 Discussion

This work has demonstrated that DSC is a potentially powerful method of *in vivo* ribosome analysis. Although the precise nature of the ribosome-associated thermogram events is not yet fully understood, this technique has enabled observations of pressure treated cultures of *E. coli* that could not have been made by conventional methods.

When analyzed immediately after pressure treatment, cell death was proportional to the loss of RAE. As cell viability continued to decrease during subsequent incubation with no further decline in RAE, ribosome damage was not an inevitable consequence of cell death. It is thus possible that it was a direct cause of death immediately following decompression.

The linearity of this relationship may give some indication of the mechanism by which high pressure resulted in cell death. It may be expected that cell death would only occur when the number of functional ribosomes fell below a critical level in an individual cell. Had pressure-induced damage been distributed throughout the ribosome population, few cells would have ribosome numbers close to the threshold and would be killed by modest reductions in RAE. As the amount of ribosome damage increased, proportionally more cells would have the ribosomes reduced to below the threshold. Eventually, when most cells had ribosome numbers below the threshold, further decreases in RAE could not result in further cell death. This model would be expected to result in a sigmoidal relationship between cell viability and RAE. The linear relationship observed suggests that cell death and ribosome damage is an "all-or-nothing" phenomenon. That is, the ribosomes in an individual cell remain relatively undamaged until they are all destroyed together in a single event.

The addition of Mg^{2+} to the culture had no effect on DSC thermograms before pressure treatment. It increased ribosome stability after pressure treatment but cell death was not reduced. A possible explanation is that high pressure resulted in membrane permeablization which enabled influx of Mg^{2+} and stabilization of surviving ribosomes. Other factors, possibly associated with membrane permeablization, may have resulted in gradual cell death during post-pressure incubation.

Further work is in progress to characterize ribosome-associated DSC thermogram events. We believe that this will make a positive contribution to the investigation of physical stresses on living cells, and to other areas requiring analysis of ribosome structure and function *in vivo*.

References

[1] Landau, J. (1967); Induction, transcription and translation in *Escherichia coli*: a hydrostatic pressure study; Biochimica et Biophysica Acta, 149, 506-512.

[2] Gross, M., Lehle, K., Jaenicke, R. & Nierhaus, K.H. (1993); Pressure-induced dissociation of ribosomes and elongation cycle intermediates. Stabilizing conditions and identification of the most sensitive functional state; European Journal of Biochemistry, 218, 463-468.

[3] Mackey, B.M., Miles, C.A., Parsons, S.E. & Seymore, D.A. (1991); Thermal denaturation of whole cells and cell components of *Escherichia coli* examined by differential scanning calorimetry; Journal of General Microbiology, 137, 2361-2374.

Measurement of Microbial Activities Under High Pressure by Calorimetry

K. Tamura, Y. Kamiki and M. Miyashita

Department of Chemical Science and Technology, Faculty of Engineering, The University of Tokushima, Minamijosanjima-cho, Tokushima 770-8506, Japan
Phone and Fax: +81-(0)886-56-7416
tamura@chem.tokushima-u.ac.jp

Abstract. Microcalorimetry is becoming an important method for study of the metabolic activities of cells and biological tissues. This method is mainly based on the fact that the heat evolved during metabolic processes is strictly proportional to the metabolic activity, so the magnitude of the calorimetric signal is an index of biological activity. This method was adopted to investigate the thermotolerance of heat- and pressure-shocked yeast and to estimate microbial activities at high pressure. The effect of the non-reducing disaccharide trehalose on the stress response of yeast was also studied by calorimetry.

1 Introduction

In all living systems, various metabolic events in cells are reactions producing heat and the heat evolved during metabolic processes is strictly proportional to metabolic activity. Accordingly, metabolic heat can be used as an index of the biological activities of living cells and tissues [1, 2]. Thus the microbial activities of multiplication and metabolic processes under high pressure can be estimated precisely by calorimetry. A high-pressure line was constructed and connected to a microcalorimeter to obtain growth thermograms of yeast under high pressures of 30 MPa.

We studied the responses of microbes to stresses such as heat, high pressure, and drugs, the thermotolerance of heat-shocked yeast, and the effect of trehalose on the thermotolerance [3]. To investigate the activities of yeast under high pressure quantitatively and in detail, we used a microcalorimeter with four high-pressure ampoules. The effect of medium containing trehalose, which protects organisms against external stress, on the thermotolerance of yeast was also studied.

2 Material & Methods

The yeast used was *Saccharomyces cerevisiae* IFO10149. After pre-cultivation for two days, the cells in logarithmic phase cultivated for 4 h were used for experiments (1.0×10^5 cells/ml).

The high-pressure microcalorimeter is shown diagrammatically in Fig.1. High pressure was produced with a screw-type hand-operated pump (Hikari Koatsukiki, KP-2A type) directly connected to a nitrogen or oxygen gas cylinder. The growth thermogram of yeast was monitored with a microcalorimeter CSC4100 manufactured by Calorimetry Science Corporation. A stainless steal high-pressure ampoule (0.4 ml) was connected to a 1/16 inch stainless steel tube with silver solder. Since it usually took 2 to 7 d of cultivation of yeast, a multi-cell calorimeter was desirable for experiments.

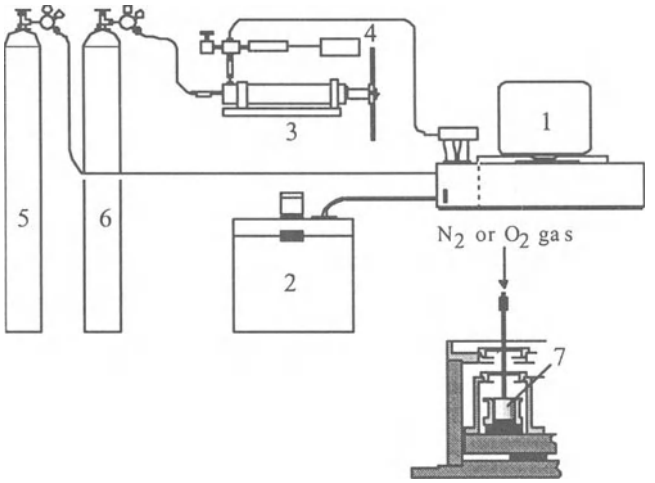

Fig. 1. High-pressure differential scanning calorimeter (DSC). 1. Microcalorimeter (CSC 4100). 2. Cooling bath. 3. High pressure pump. 4. Pressure gauge. 5. N_2 gas cylinder. 6. N_2 or O_2 gas cylinder. 7. High-pressure ampoule in DSC

3 Results

First, the growth thermograms of heat-shocked yeast were studied to confirm that calorimetry was useful for the estimation of thermotolerance of stressed yeast. A temperature of 43 °C is best for induction of thermotolerance of the yeast we used [4]. After heat shock treatment and then exposure of the yeast cells to a lethal temperature, they were cultivated at an optimum temperature according to the

following temperature program: T °C (30 min) - 51 °C (10 min) - 30 °C (about 3 d), where T is 20, 30, 43, or 46 (°C). The growth thermograms of yeast cells cultivated under these conditions are shown in Fig. 2. Clear effects of heat shock treatment and trehalose as a protectant can be observed in the thermograms.

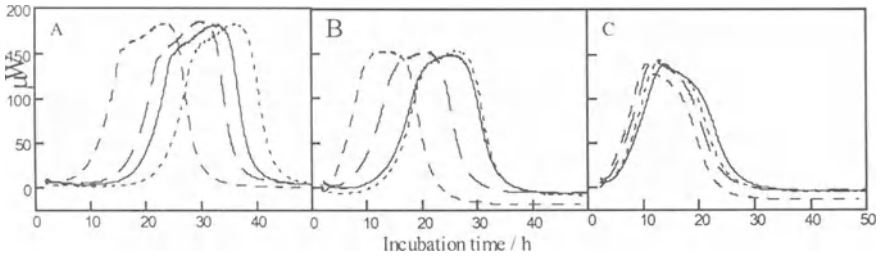

Fig. 2. Growth thermograms of yeast treated for 30 min at various temperatures and at atmospheric pressure. Logarithmic phase cells suspended in YPD medium with and without trehalose were put in ampoules of the calorimeter. Trehalose concentration: A, 0 mol/l; B, 0.5 mol/l; C, 1.0 mol/l. Temperature of treatment:
———— , 20 °C, — — , 30 °C, – – – – , 43 °C, , 46 °C

Namely, the thermotolerance was strongly dependent on the temperature of heat shock treatment before exposing the yeast cells to a temperature of 51 °C when trehalose was not added to the medium. Since the start time and peak time of growth thermograms reflect the thermotolerance of yeast cells, the results show that yeast cells treated at 43 °C acquired the highest thermotolerance. When 1 mol/l of trehalose was added to the medium, the effect of temperature (T) disappeared almost completely and the yeast cells acquired high thermotolerance. Trehalose, a non-reducing disaccharide, is known to stabilize proteins and biomembranes [5], and induces tolerance against high temperature, dryness, freezing, etc. of living cells. Trehalose usually accumulates in yeast cells exposed to higher temperatures. But, we found that it was not synthesized in cells shocked by pressures of 25 to 75 MPa for 30 to 60 min where the cells acquired high thermotolerance. Heat shock protein Hsp 104 was induced by both heat shock and pressure shock [3].

Figure 3 shows the growth thermograms of yeast cells incubated at 10 MPa. Nitrogen gas was used to induce pressure. Clear differences were observed in the thermograms for temperature effects and pressure effects. Namely, at higher temperatures of 38 or 40 °C, recovery from the high temperature effect depended on the concentration of trehalose: in medium containing a high concentration of trehalose recovery was fast [6]. On the contrary, recovery at a high pressure of 10 MPa in medium containing 0.5 mol/l of trehalose was faster than that in medium containing 1.0 mol/l of trehalose. The rate of recovery did not necessarily correspond to the concentration of trehalose. These results suggest that the effects of hydrostatic pressure and high temperature are not always linked physiologically. When oxygen gas was used to induce high pressure and microbial suspensions

were pressurized to 5 MPa, no evolution of heat was observed regardless of the presence of trehalose and the yeast cells died.

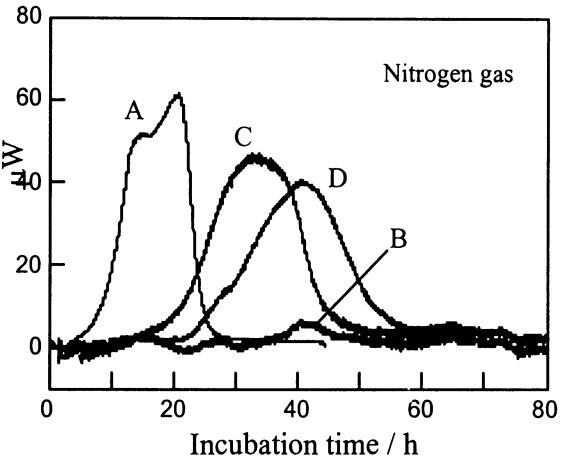

Fig. 3. Effects of pressure and trehalose on growth thermograms of yeast at 30 °C. Sample: 0.25 ml. A: 0.1 MPa, [trehalose] = 0 mol/l; B: 10 MPa, [trehalose] = 0 mol/l; C: 10 MPa, [trehalose] = 0.5 mol/l; D: 10 MPa, [trehalose] = 1.0 mol/l

References

[1] Belaich, J. P. (1980); Biological Microcalorimetry, Beezer, A. E., Ed., Academic Press, pp. 1-42.

[2] Beezer, A. E., Fujita, T., Nunomura, K., Brettel, R., Schaarschmidt, B. and Zotin, A. I. (1977); Application of Calorimetry in Life Sciences, Lamprecht, I. and Schaarschmidt, B., Eds., Walter de Gruyter, 1977, pp. 107-156.

[3] Miyashita, M., Tamura, K. and Iwahashi, H. (1996); High pressure bioscience and biotechnology, Progress in Biotechnology Vol.13, Hayashi, R. and Balny, Eds., C., Elsevier, pp.101-104.

[4] Iwahashi, H., Kaul, S. C., Obuchi, K. and Komatsu, Y. (1991); Induction of barotolerance by heat shock treatment in yeast; FEMS Microbiol. Lett., 80, 325-328.

[5] Crowe, J. H., Crowe, L. M. and Chapman, D. (1984); Preservation of membranes in anhydrobiotic organisms: the role of trehalose; Science, 223, 701-703.

[6] Tamura, K., Kamiki, Y. and Miyashita, M. (1998); High pressure biotechnology, Kunugi, S. and Hayashi, R., Eds., Sanei, in press.

Use of a Fatty Acid Auxotroph To Study the Role of Membrane Fatty Acid Composition on the Pressure Resistance of *Escherichia coli*

M.A. Casadei and B.M. Mackey

Institute of Food Research, Earley Gate, Reading RG6 6BZ, UK
Phone: +44 (0)118 9357032; Fax: +44 (0)118 9357222

Abstract. *E. coli* K1060, a mutant defective in the synthesis and degradation of unsaturated fatty acids, was used to obtain membranes of different fatty acid composition without altering other growth parameters. The pressure resistance of the cells varied according to the different fatty acid supplement used in the growth medium. Cells grown on elaidic acid were the least pressure resistant in exponential phase and the most resistant in stationary phase. The fluidity of the membrane, as measured by differential scanning calorimetry of stationary-phase cell lipids, showed a secondary peak at high temperature (51.9 °C) for cells grown on elaidic acid. Cells with a more rigid membrane were more sensitive to pressure in exponential phase and more resistant in stationary phase confirming the results previously obtained with cells grown at different temperatures.

1 Introduction

Damage to the cell membrane may play an important role in the inactivation of bacteria by high hydrostatic pressure [1, 2]. We have shown previously [3] that cells grown at different temperatures have different pressure resistance and concluded that membrane fluidity may be involved in the cell response to pressure. In this work, by using a mutant defective in synthesis and degradation of fatty acids, we obtained cells with different membrane composition without altering the growth conditions. The pressure resistance of the cells was affected by the fatty acid supplemented, corroborating the possibility of a link between membrane rigidity and pressure resistance.

2 Material & Methods

Escherichia coli K1060, a mutant defective in the synthesis and degradation of unsaturated fatty acids, was grown at 37 °C in minimum salts medium (M63)

supplemented with 0.01% linoleic acid (C18:2), oleic acid (C18:1(9)) or elaidic acid (*trans*-C18:1).

Exponential and stationary-phase cells (OD_{680} of 0.2 and 24 h incubation, respectively) were pressure treated in sealed plastic bags at 200 and 300 MPa, respectively, using a Stansted Fluid Power pressure apparatus (Stansted, Essex, UK).

Fatty acid extracts from whole cells were obtained as described by Miller and Berger [4] and then analysed by gas chromatography (GC) using a HP 6890 Series gas chromatograph (Hewlett Packard, Wilmington, USA).

Total lipids were extracted following the method of Bligh and Dyer [5]. 20 µl aliquots of the extract in chloroform were placed in aluminium pans (Perkin-Elmer, Norwalk, USA) and the excess solvent was evaporated. The pans were sealed and heated in a Perkin-Elmer DSC 7 calorimeter at a rate of 5 °C per minute from –10 to 60 °C using an empty pan as reference.

3 Results

No difference was observed in the growth of *E. coli* strain K1060 in M63 supplemented with linoleic, oleic or elaidic acid (data not shown).

Fatty acid analysis showed that the fatty acids supplied in the medium were incorporated into the cells in different proportions of the total (Table 1).

Table 1. Fatty acid composition, as a percentage of the total, of *E. coli* strain K1060 grown at 37 °C in M63 supplemented with linoleic (18:2), oleic (18:1(9)) or elaidic acid (*trans*-18:1)

	Exponential phase			Stationary phase		
Supplement	18:2	18:1(9)	*trans*-18:1	18:2	18:1(9)	trans-18:1
Fatty acid						
12:0	5.3	5.6	6.7	7.9	8.0	6.2
14:0	8.2	9.4	9.2	17.6	12.2	8.9
β-14:0-OH	11.4	11.2	11.6	13.6	16.6	17
16:1	2.2	1.6	11.8	-	-	-
16:0	31.2	24.2	13.9	39.2	24.8	14.8
17:0 Δ[a]	1.1	-	4.2	3.2	-	6.7
18:2	35.1	-	-	17.2	-	-
18:1	2.1	-	-	2.4	-	-
18:1(9)	-	46.4	-	-	35.1	-
trans-18:1	-	-	42.6	-	-	46.3
19:0 Δ[a]					3.2	

[a]cyclopropane fatty acid

Elaidic acid, a *trans*-unsaturated fatty acid, has a higher melting point than a similar chain length *cis*-unsaturated fatty acid. Thus cells containing elaidic acid would be expected to have more rigid membranes [6].

In exponential phase, pressure resistance was least in cells grown on elaidic acid and greatest in cells grown on linoleic acid, i.e cells with rigid membranes were more pressure sensitive (Fig. 1). Stationary-phase cells grown on different fatty acids had a similar pressure resistance irrespective of the supplement used. However, cells grown on elaidic acid showed a more resistant "tail" (Fig. 2).

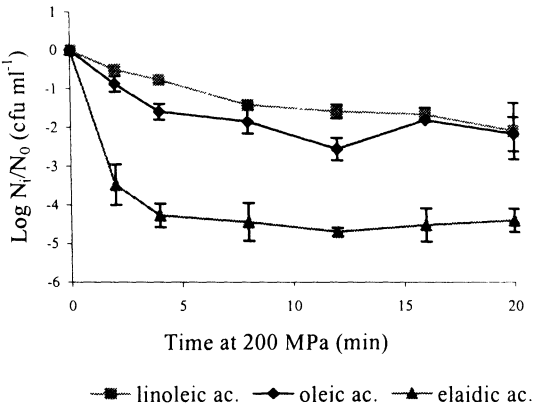

Fig. 1. Pressure resistance of *E. coli* strain K1060 grown at 37 °C to exponential phase in M63 supplemented with linoleic, oleic or elaidic acid

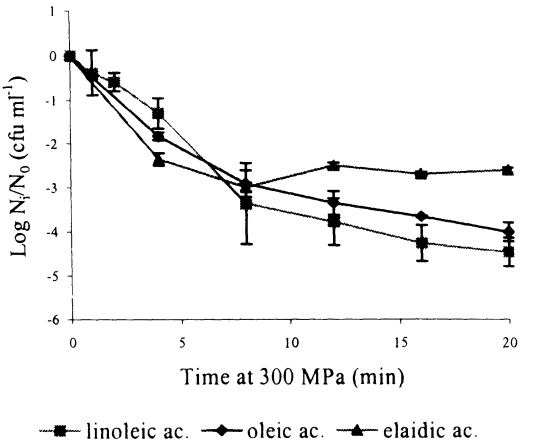

Fig. 2. Pressure resistance of *E. coli* strain K1060 grown at 37 °C to stationary phase in M63 supplemented with linoleic, oleic or elaidic acid

In stationary-phase cells the proportion of saturated fatty acid (C16:0) was higher than in exponential-phase cells and cells were more resistant than those in exponential phase.

The DSC thermograms of total lipids extracted from whole stationary-phase cells showed a major peak at similar temperature irrespective of the fatty acid supplement (average values: 39.2 °C, linoleic acid and oleic acid, 39.5 °C elaidic acid).

Stationary-phase cells grown on elaidic acid showed a second smaller peak at a higher temperature (51.9 °C) which would be expected to increase membrane rigidity and decrease resistance. In fact, the opposite was observed and a more resistant "tail" was seen in elaidic acid grown cells.

4 Conclusions

Pressure resistance was affected by membrane fatty acid composition, but the effect was different in stationary-phase and exponential-phase cells. In exponential-phase cells, increased resistance was correlated with a more fluid membrane whereas the reverse was true for stationary-phase cells. A similar behaviour has been observed previously in cells grown at different temperatures.

References

[1] Shigehisa, T., Ohmori, T., Saito, A., Taji, S. and Hayashi, R. (1991) Effects of high hydrostatic pressure on characteristics of pork slurries and inactivation of microorganisms associated with meat and meat products. *Int. J. Food Microbiol.* **12**, 207-216.

[2] Wouters, P.C., Galaasker, E. and Smelt, J.P.P.M. (1998) Effects of high pressure on inactivation kinetics and events related to proton efflux in *Lactobacillus plantarum*. *Appl. Environm. Microbiol.* **64**, 509-514.

[3] Casadei, M.A. and Mackey, B.M.M. (1997). The effect of growth temperature on pressure resistance of *Escherichia coli*. *High Pressure Research in the Biosciences and Biotechnology*, K. Heremans (Ed.) 281. Leuven, Belgium: Leuven University Press.

[4] Miller, L. and Berger, T. (1985) Bacteria identification by gas chromatography of whole cell fatty acids. *Hewlett Packard Gas Chromatography* pub. no.43-5953-1838, 1-8.

[5] Bligh, E.G. and Dyer, W.J. (1959) A rapid method of total lipid extraction and purification. *Can. J. Biochem. Physiol.* **37**, 911-917.

[6] Overath, P., Schairer, H.U. and Stoffel, W. (1970) Correlation of *in vivo* and *in vitro* phase transitions of membrane lipids in *Escherichia coli*. *Proc. Nat. Acad. Sci. USA* **67**, 606-612.

High Pressure Inactivation of Heat Activated Ascospores of the Mould *Eurotium repens*

R. Eicher and H. Ludwig

University of Heidelberg, Institute for Pharmaceutical Technology and Biopharmacy, Section Physical Chemistry, INF 366, D-69120 Heidelberg, Germany
Phone: +49-(0)6221-545235; Fax: +49-(0)6221-545475
Horst.Ludwig@urz.uni-heidelberg.de
http://www.uni-heidelberg.de/institute/fak12/PC/ludwig/ludwig.html

Abstract. Heat activation of *E. repens* ascospores was carried out in the temperature range 50-60 °C. Activation improved the inactivation result, though the inactivation rate is raised only at the beginning of the high pressure treatment. A holding time between activation and inactivation led to a partial re-stabilization of the spores.

1 Introduction

Usually fungal spores are in a rest period called dormancy. Dormant spores are very stable and can survive harmful conditions, for example, heat or pressure treatments. In case of bacterial spores it is well known that the transition to the germinating stage leads to a drastic loss of stability [1]. In order to germinate, many fungal spores need activation which is by definition any treatment, e.g. heat, leading to an increase in the number of germinating spores [2].

In this study the effect of heat activation on the following high pressure inactivation of ascospores of the mould *Eurotium repens* is examined.

2 Materials & Methods

The mould *Eurotium repens* (strain DSMZ 62631) was obtained from the Deutsche Sammlung von Mikroorganismen und Zellkulturen, Braunschweig. The ascospores were grown and harvested as previously reported [3].

For all experiments highly purified ascospores were used. Purification was done by isopycnic density centrifugation. To separate the ascospores from mycelium and conidiospores the concentrated suspension (1 ml) was placed on top of 34% (wt/wt) CsCl solution and centrifuged for 5 min with 2,600 *g* (centrifuge model Vetter 425-C). The ascospores which settled to the bottom because of their higher density could be separated by removing the upper solution. This procedure was

carried out at least three times until no conidiospores were left. Afterwards the ascospores were placed on top of a second CsCl solution, having a concentration of 38% CsCl (wt/wt), and centrifuged for 20 min with 1100 × g (centrifuge model Beckman
TJ-6) to separate viable from non-viable spores. The ascospores gained by this procedure were washed three times to remove all CsCl.

Activation and inactivation experiments were carried out in an aqueous model system consisting of 0.9% NaCl and 0.1% Tween 80.

The number of germinating spores and the number of spores surviving the pressure treatment were determined by plating the treated spores on Sabouraud agar dishes.

The maximum number of viable spores was determined using a Neubauer counting chamber. It was assumed that every spore present in the suspension was viable (unpublished data) and therefore in principle able to germinate.

The high pressure device was also described earlier [3].

3 Results

Figure 1 shows the heat activation at 55 °C. The number of germinating spores increased with the duration of heating. A plateau was reached after 20 min. In this state almost all of the spores were germinated. The sigmodial shape of the activation curve remained the same using temperatures of 60 °C or 50 °C (data not shown).

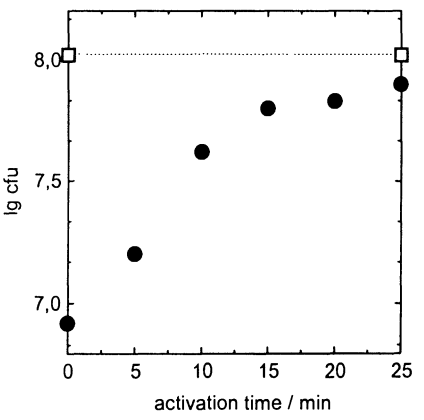

Fig. 1. Activation of ascospores at 55 °C. ● Number of germinating spores, □ □ number of spores found in the counting chamber

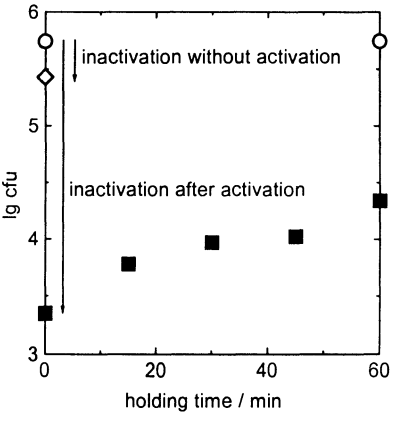

Fig. 2. Influence of time between activation and inactivation. ■ Inactivation (500 MPa, 30 min, 25 °C) after activation (60 °C, 15 min) and holding time *t*. ◇ Inactivation (500 MPa, 30 min, 25 °C) without activation. O Control without activation

Using 60 °C as activation temperature led to a quicker rise of germinating spores and to a plateau after less than 10 min. Activation at 50 °C resulted in a slower activation rate and the plateau was reached after heating the spores for more than 60 min. Application of higher temperatures, e.g. 65 °C, led to the beginning of heat inactivation after a short heating time (data not shown). Addition of nutrients to the activation medium did not improve the activation result though they are necessary for the complete germination process (unpublished data).

Figure 2 shows the combination of heat activation and high pressure inactivation. It can be seen that a previous activation treatment, 60 °C and 15 min in this case, led to a drastic improvement of the inactivation result. High pressure inactivation using 500 MPa and 25 °C for 30 min reduced the germ number by two and a half logarithmic step compared to the control. Without a previous activation treatment less than half a logarithmic step was obtained. Inactivation was most successful if carried out immediately after the activation process. A holding time between activation and inactivation led to re-establishment of the spores' stability and therefore to a worse inactivation result. This partial re-stabilisation stopped after 60 min and a plateau was reached (data not shown).

The linkage of heat activation with the inactivation improvement is given in Fig. 3. The upper plot shows the rise of germinating spores due to the time of the activation treatment, the lower plot shows the result of a pressure inactivation of 500 MPa and 25 °C for 30 min after the same activation treatment. The more spores germinated due to the activation the higher was the decrease of the germ number caused by the following high pressure treatment.

In Fig. 4 inactivation kinetics of activated and non-activated ascospores are compared. The white plot shows the inactivation at 500 MPa and 25 °C without an

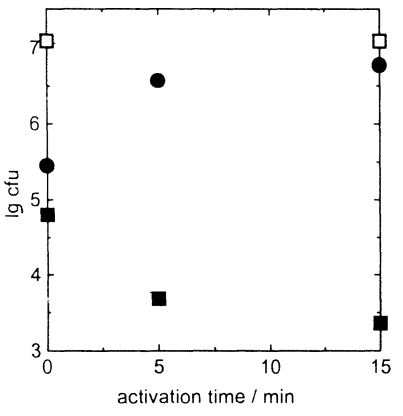

Fig. 3. ● Activation of ascospores at 60 °C. ■ Inactivation (500 MPa, 25 °C, 30 min) after activation at 60 °C. □ □ Number of spores found in the counting chamber

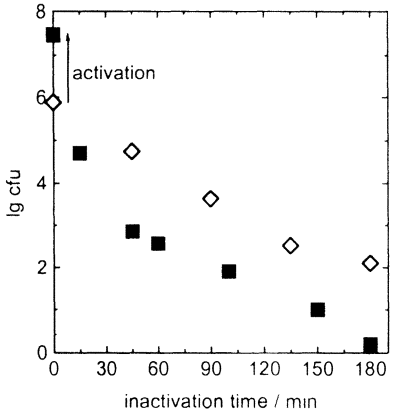

Fig. 4. ■ Inactivation (500 MPa, 25 °C) of ascospores after activation (60 °C, 15 min). ◇ Inactivation (500 MPa, 25 °C) without previous activation. Marks detection limit

activation treatment, the black plot shows the inactivation with a previous heat activation of 60 °C for 15 min. It can be seen that the inactivation of the activated spores was much faster in the beginning but the slope of both inactivation curves became the same after about 45 min.

4 Discussion

Variation of the activation temperature in the range between 50 °C and 60 °C has neither an effect on the shape of the activation curves nor on the activation degree. But the rate of activation is much faster with higher temperatures. Above a critical temperature activation is covered by temperature induced killing of the spores. All temperature treatments in this study led to spore activation only, not to a reduction of the germ numbers. The usage of low, activating temperatures in combination with inactivating high pressures is of advantage in sterilizing temperature sensitive products.

Combination of heat activation and high pressure inactivation leads to an advanced inactivation result, especially at the beginning of the high pressure treatment. Due to the linking of activation and improvement of inactivation the activation should be proceeded to its maximum level in order to obtain the best inactivation success. Moreover the inactivation should immediately follow the activation treatment. A holding time between the two processes leads to a partial re-stabilisation of the spores although the initial level of stability is not reached.

Still unanswered is the question whether activation is also possible after the inactivation treatment. Maybe the germ number can by raised after inactivation by the same amount as it increases due to activation before the high pressure treatment (Fig. 4). This would mean that there is a hidden fraction of 'super dormant' spores in high pressure treated samples becoming visible and inactivable only after activation. Future experiments will clear up this question.

Acknowledgements: This work was supported by the EU (COST D10 and FAIR-CT96-1175) and the Landesgraduiertenförderung Baden-Württemberg.

References

[1] Sojka, B. (1994) Pressure-induced germination and inactivation of *Bacillus subtilis* spores; Pharm. Ind., 57, 251-252.

[2] Sussman, A.S. (1976) Activators of fungal spore germination; in: The Fungal Spore, 2nd International Fungal Spore Symposium; 101-139; John Wiley and Sons, New York.

[3] Eicher, R.; Merkulow, N.; van Almsick, G.; Ludwig, H. (1997); in: Bennet, P.B., Demchenko, I., Marquis, R.E. (eds.) High Pressure Biology and Medicine, University of Rochester Press, Rochester, New York, pp. 65–75.

Microorganism Inactivation Using High Pressure Generation in Sealed Vessels Under Sub-Zero Temperature

K. Hayakawa, Y. Ueno, S. Kawamura, T. Kado[1], K. Kamiyama[1], Y. Tamaoka[2], M. Morishita[2], M. Matsumoto[2], S. Kawai[2] and R. Hayashi[3]

Kyoto Prefectural Comprehensive Center for Small and Medium Enterprises, 17 Chudoji Minami-machi, Shimogyo-ku, Kyoto 600-8813, Japan
[1]San Contact Lens Co., Ltd., 475 Fuyachodori, Ebisugawa-agaru, Nakagyo-ku, Kyoto 604-0983, Japan
[2]Teramecs Co., Ltd., 37 Nishi-Okenoi-cho, Fushimi-ku, Kyoto 612-8428
[3]Laboratory of Biomacromolecular Chemistry, Division of Applied Life Sciences, Graduate School of Agriculture, Kyoto University, Sakyo-ku, Kyoto 606-8502, Japan

Abstract. In order to test the possibility of utilizing high pressure in bioscience and biotechnology, a simple high pressure generation method and its use for microbial inactivation have been studied. When a pressure vessel was filled with water, sealed tightly and cooled to sub-zero temperature, high pressure was generated in the vessel. The maximum pressure generation was 206 MPa at –23 °C. The high pressure generated was effective at inactivating microorganisms: yeast (*Saccharomyces cerevisiae* and *Zygosaccharomyces rouxii*), bacteria (*Lactobacillus brevis* and *Eschericia coli*), fungi (*Aspergillus niger* and *Aspergillus oryzae*) were completely inactivated by storing the sealed vessels containing these microorganisms at –20 °C for 24 h. However, *Staphylococcus aureus* was only partly inactivated under the same conditions. This method opens up a new application of high pressure for storing, transporting, and sterilizing of foods and biological materials.

1 Introduction

High pressure has recently been exploited as a new method for sterilization and processing of food [1, 2]. In the course of our studies on the utilization of high pressure in food science and technology, we had an idea for a simple pressurization method for foods where high pressure is naturally generated without using an oil pressure pump.

This method is based on a well-known phenomenon that water filled in a sealed vessel increases the volume by freezing and generates high pressure in the vessel when it is stored at sub-zero temperatures and, therefore, food placed in the vessel would be affected by the generated pressure. The purpose of this report is to describe the extent of high pressure generated in a sealed vessel which is kept

under different sub-zero temperatures and the effects of such high pressure on the inactivation of microorganisms.

2 Material & Methods

2.1 Sample Preparation of Microorganisms and Measurement of Surviving Microorganisms

Saccharomyces cerevisiae IAM 4274 and *Zygosaccharomyces rouxii* IAM 12880 were cultivated in malt extract both containing 5% NaCl at 30 °C for 5 d and 2 d, respectively; *Aspergillus oryzae* H-3 and *Aspergillus niger* IFO 9455 in potato dextrose agar at 30 °C for 7 d; *Lactobacillus brevis* IFO 12005 in GYP medium at 30 °C for 2 d; *Escherichia coli* IFO 3972 and *Staphylococcus aureus* IFO 13276 in Mueller Hinton broth at 30 °C for 2 d. Cultivated cells and spores of two fungi were collected by centrifugation, washed two times with sterilized water, and re-suspended in deionized water. The number of microorganisms surviving the high pressure treatment was measured by counting colonies after each strain was incubated on agar plates of the medium described above.

2.2 High Pressure Generation in the Sealed Vessel

To estimate the high pressure generation, a high pressure chamber connected to a pressure gauge was used. The inner volume of the chamber was 167 ml and its resistance to pressure was 300 MPa. A rubber balloon containing 140 ml of water was set into the pressure chamber after the neck of balloon had been tightly fastened with a cotton thread. The chamber was filled with 27 ml of ethanol which was used as pressure medium (see Fig. 1). The chamber was tightly sealed and kept under sub-zero temperature in a cooling bath. To obtain a higher pressure, a modified pressure vessel (Type II) which contains the minimum pressure medium (water:ethanol=98:2) was used (Fig. 2). The generated pressure was measured by the pressure gauge.

To test microbial inactivation, a cylinder type of pressure-resistant vessel (Type III) was used. Both ends were stoppered with two plugs. The inner volume of the vessel was approximately 20 ml and its resistance pressure was 300 MPa. Microbial suspension in a polyethylene pouch was placed in the pressure vessel. The vessel was filled with distilled water and sealed tightly. Then, the sealed vessel was kept in a temperature-controlled freezer for 24 h. After the storage, the vessel was taken out from the freezer and equilibrated with room temperature. The vessel was opened and surviving cells were counted.

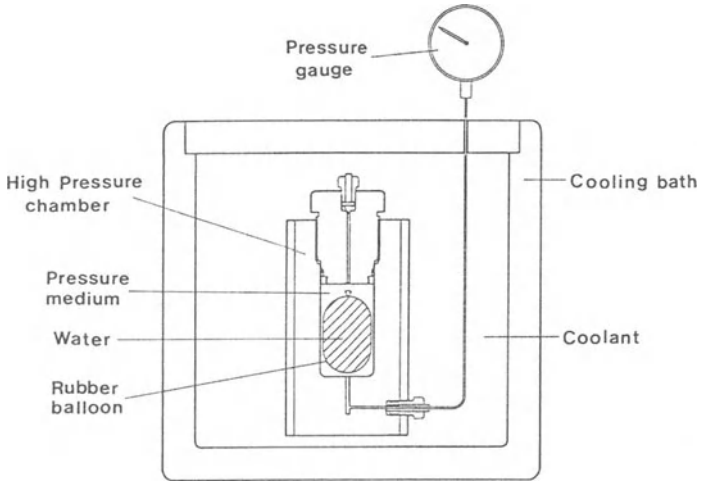

Fig. 1. Measurement of pressure generation in a high pressure chamber (Type I) which is stored under sub-zero temperatures

3 Results

3.1 High Pressure Generation

When the Type I pressure chamber had cooled to –22 °C, pressure was generated after 15 min and reached 140 MPa after 60 min without further increase with time. When the chamber was immersed in the cooling bath controlled at different temperatures for 1 h, gauge pressures of 60, 103, 140 and 140 MPa were obtained at –5, –10, –15 and –22 °C, respectively. Theoretical pressure was obtained by the Type II pressure vessel which was designed to minimize the volume of the pressure medium (80 ml of water and 1.5 ml of ethanol): maximum pressure reached 206 MPa at –23 °C (Fig. 3).

3.2 Inactivation of Microorganisms

When suspensions of *S. cerevisiae* and *Z. rouxii* in a sealed vessel (Type III) were stored in a freezer at different temperatures for 24 h, surviving yeasts were decreased with lowering temperature of the freezer and no surviving yeast was detected after storage at –10 °C. In this condition, a pressure of 100 MPa or higher was expected to be generated according to Fig. 3. On the other hand, the yeasts stored in the same conditions in an open vessel under 0.1 MPa were only slightly changed.

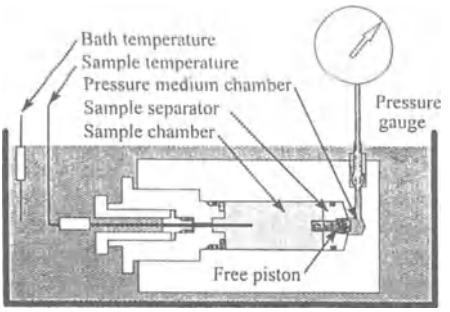

Fig. 2. Modified pressure vessel (Type II) for freeze pressurization

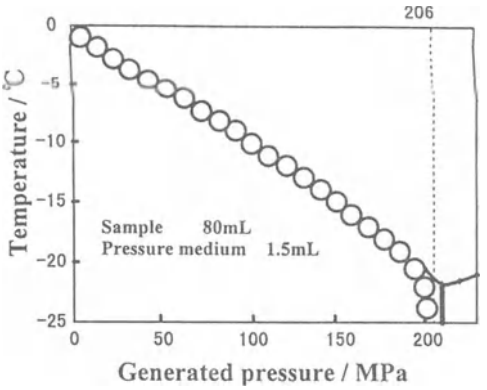

Fig. 3. Relation between temperature and pressure in the modified sealed vessel (Type II). O observed pressure; — the equilibrium curve of water and Type I ice [3]

Table 1 summarizes the inactivation effect of the present experimental method on yeasts, fungi, and bacteria. Most of them were completely inactivated by storing them in a sealed vessel (Type III) at –20 °C for 24 h without *S. aureus*.

Table 1. Inactivation of microorganisms in the sealed vessels at –20 °C

	Cells/ml		
Microorganism	Initial	Open vessel	Sealed vessel (Type III)
Saccharomyces cerevisiae	4.2×10^{7}	1.9×10^{7}	n.d.
Zygosaccharomyces rouxii	5.6×10^{7}	3.5×10^{7}	n.d.
Aspergillus oryzae	6.8×10^{5}	2.5×10^{5}	n.d.
Aspergillus niger	2.2×10^{5}	6.7×10^{4}	n.d.
Lactobacillus brevis	6.5×10^{8}	2.1×10^{8}	n.d.
Escherichia coli	3.8×10^{5}	5.2×10^{4}	n.d.
Staphylococcus aureus	9.0×10^{6}	6.9×10^{6}	7.2×10^{2}

n.d. not detected

4 Discussion

According to the phase diagram of water [3], an equilibrium of Type I ice and water changes depending on temperature and pressure as shown by the solid line in Fig. 3. When water filled in the sealed vessel is cooled down to sub-zero temperature, high pressure would naturally be generated inside the vessel along the equilibrium line to reach to 220 MPa at –22 °C as the temperature decreases. This principle was realized by the present experiments when the sealed pressure

chamber was cooled down from 0 to –23 °C. The maximum pressure was reached to 206 MPa at –23 °C.

Microorganisms are inactivated more easily by the combined use of low temperature and moderately high pressure than by pressurization at room temperature [4,5]. This is also the case of the present experiment as shown in Table 1. As the Type III sealed vessel used in the experiment of Table 1 contained only water, high pressure of 206 MPa must be attained as shown in Fig. 2. As no microorganisms used in the present experiment were inactivated only by freezing at the ambient pressure, the results clearly show the effectiveness of pressurization at moderately high pressure and sub-zero temperature. This inactivation of microorganisms is different from pressurization at room temperature which needs high pressure [6].

Freezing is widely used in transporting and storing food and biological compounds. Therefore, the present high pressure generation system may be used for transporting and storing of not only food but also unstable biological materials in medical and pharmaceutical industries. To attain the idea, large scale pressure vessels resistant to moderately high pressure must be economically developed.

References

[1] Hayashi, R. (1992); In: Balny, C., Hayashi, R., Heremans, K., Masson, P.(eds) High Pressure and Biotechnology, Colloques INSERM, vol 224, John Libbey Eurotext Ltd., pp. 185-193.

[2] Hayashi, R. (1996); In: Hayashi, R., Balny, C.(eds) High Pressure Bioscience and Biotechnology, Progress in Biotechnology 13, Elsevier, pp. 1-6.

[3] Bridgman, P.W. (1912); Proc Amer Acad Arts Sci 47: 466-558.

[4] Sonoike, K., Setoyama, T., Kuma, Y., Kobayashi, S. (1992); In: Balny, C., Hayashi, R., Heremans, K., Masson, P.(eds) High Pressure and Biotechnology. Colloques INSERM, vol 224, John Libbey Eurotext Ltd, pp. 297-301.

[5] Hashizume, C., Kimura, K., Hayashi, R. (1995); Biosci Biotech Biochem 59: 1455-1458.

[6] Ludwig, H., Almsick, G. Van, Sojka, B. (1996); In: Hayashi, R., Balny, C. (eds) High Pressure Bioscience and Biotechnology. Progress in Biotechnology 13, Elsevier, pp. 237-244.

High Pressure Inactivation of Anaerobic Spores from *Clostridium pasteurianum*

C. Hölters, G. van Almsick and H. Ludwig

Universität Heidelberg, Institut für Pharmazeutische Technologie und Biopharmazie, Gruppe Physikalische Chemie, INF 366, D-69120 Heidelberg, Germany
Horst.Ludwig@urz.uni-heidelberg.de

Abstract. The pressure induced germination and inactivation of *Clostridium pasteurianum* spores are investigated. The germination is followed by the release of dipicolinic acid (DPA). The temperature has only a minor effect on the DPA-release. At 60 °C and with pressures above 400 MPa almost complete DPA-release is obtained within 15 min. From the results of the germination experiments an effective process is derived to inactivate the spores using oscillatory pressures.

1 Introduction

The inactivation of microorganisms by hydrostatic pressure has become an intensively studied field. Nevertheless, data presenting the inactivation of anaerobic bacteria, especially anaerobic spores, are lacking [1]. It is known that spores are difficult to inactivate. Inactivation of spores by pressure is a two step process. Before killing can happen the spore has to germinate. Hydrostatic pressure is able to cause germination and killing. The germination of spores can be followed by measuring the release of dipicolinic acid (DPA), a spore specific compound, into the surrounding medium [2]. In this work, the germination and inactivation of *Clostridium pasteurianum* spores by hydrostatic pressure were studied.

2 Materials & Methods

For the handling of anaerobic bacteria the exclusion of oxygen during all working steps has to be guaranteed. Therefore, a glovebox (Mecaplex) and for the incubation on agar plates anaerobic jars (GasPak® 100; Becton Dickinson) were used. The atmosphere contains 90% nitrogen, 5% carbon dioxide and 5% hydrogen. To control the anaerobic conditions the redox indicator resazurin (1 mg/l; Fluka) and the reducing agent cysteine (0.5 g/l; Fluka) were added to all media.

Clostridium pasteurianum (strain ATCC 6013) was purchased from the Deutsche Sammlung von Mikroorganismen (Braunschweig). It was grown in a solution of glucose (20 g/l; Merck), yeast extract (10 g/l; Difco) and calcium carbonate (20 g/l; Merck). A quarter of a lyophilized pellet of *C. pasteurianum* was added to 40 ml of the culture medium and incubated at 37 °C overnight. Subsequently, the overnight culture was plated on agar plates containing the same ingredients as the culture medium with additional agar (17 g/l). Spores were harvested after 10–14 d incubation at 37 °C and suspended in physiological NaCl-solution. The amount of spores was determined by counting the survivors of a 12 min lasting treatment at 70 °C. It was about 90%. The agar plates, described above, were also used for the determination of viable counts.

The amount of released DPA was analyzed by HPLC using the counter ion method [2]. The HPLC-system was a Shimadzu liquid chromatograph type LC10 connected with an UV-detector (Latek). Pressurized suspensions of spores were centrifuged at 5000×g and 20 µl of the supernatant fluid were injected onto a 120×4 mm Superspher 100 RP-18, 4 µm (encapped) column (Knauer). After an isocratic elution with a phospate buffer pH 7.3 containing tetrabutylammoniumhydrogensulfate (2.3 g/l; Sigma) and 15% methanol DPA was detected at 270 nm. The total DPA content in the spores was determined after autoclavation for 30 min at 121 °C. These conditions were suited to achieve complete DPA-release. All DPA values were related to the maximal DPA exudation.

The high pressure device consisted of 10 small pressure vessels arranged in 2 groups of 5 each that could be thermostated separately. For kinetic studies, the series connection of the pressure vessels allows the separate opening of each autoclave. The pressure transmitting medium was water.

For inactivation experiments 1–2 ml of the spore suspension were filled into polyethylene tubes (Ratiolab) that were plugged with silicone stoppers.

Germination experiments were performed in 400 µl Beckman type reaction vials made of polyethylene filled with the spore suspension. These vials were enclosed additionally in polyethylene tubes that were filled completely with physiological NaCl-solution and sealed with silicone stoppers.

3 Results & Discussion

In imitation of the procedure used succesfully in the case of *Bacillus subtilis* spores a two step process was applied using moderate pressures as pretreatment to induce germination and higher ones for inactivation of germinated spores. Spores of *C. pasteurianum* were treated at 55 °C three times with pressures of 100 MPa for 60 min followed by 10 min with 300 MPa (Fig. 1). In contrast to all the following experiments which were done in physiological NaCl-solution the results of Fig. 1 were obtained in culturing medium to offer the spores nutritive substances for germination. After the first cycle 98% of the spores are killed but then no further inactivation occurs. It seems clear that these are not the optimal conditions for

spores of *C. pasteurianum*. Therefore, before further inactivation experiments were done, germination was studied via the release of DPA. It is a rapid indicator for the germination progress. Optimization of germination would be helpful for effective inactivation. Figure 2 shows the DPA-release after 15 min treatment at 30, 40, 50 and 60 °C with pressures from 50–500 MPa. It is striking that there is only a small influence of temperature on the DPA-release. Pressures below 200 MPa cause no DPA exudation. Between 200 and 350 MPa it increases strongly up to 90%. With higher pressures a plateau is reached. The temperature has only an influence on the maximal amount of DPA released. At 30 °C it is 90%, at 40, 50 and 60 °C it is nearly 100%. The germination is the more complete the higher the pressure is. This is similar to germination experiments with *B. stearothermophilus* spores [2]. The kinetics of DPA-release was followed at 60 °C and different pressures of 250, 300 and 350 MPa (Fig. 3). It occurs very fast. After 5 min almost the maximal amount of DPA at each pressure is released. Further treatment gives only a slight increase in DPA exudation.

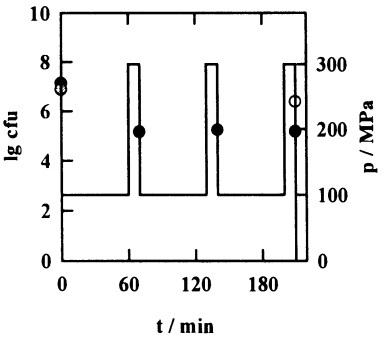

Fig. 1. ● Inactivation of *C. pasteurianum* spores at 55 °C by an oscillatory pressure treatment with 60 min at 100 MPa and 10 min at 300 MPa; open symbol is control; ● amount of spores; — course of pressure

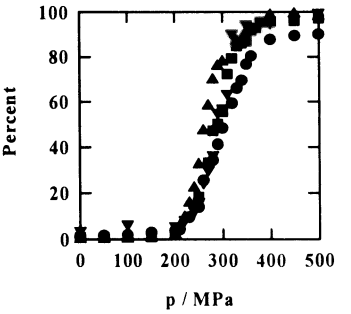

Fig. 2. Pressure dependence of DPA-release from *C. pasteurianum* spores after 15 min treatment at different temperatures of ● 30, ■ 40, ▲ 50 and ▼ 60 °C

Refering to the results of the germination experiments an oscillatory pressure treatment for spore inactivation was carried out. In Fig. 4 spores were pressurized at 60 °C with 5 cycles each consisting of 10 min treatment with 420 MPa and 5 min with ambient pressure. The pressure cycling leads to a strong decline in viable counts with a reduction by 2 log-steps during the first cycle and a 4 times slower inactivation rate for the following cycles. Compared to a treatment with constant 420 MPa it is much more effective. This leads to the conclusion that building up the pressure is an important factor for inducing germination. The kinetics of DPA-release supports this hypothesis. Most of the DPA had already been released after the pressure had been built up in about 30 s. Temperature rise

due to adiabatic compression has a minor influence (data not shown). For *C. pasteurianum* spores it is difficult to separate germination from inactivation. The germination occurs best with higher pressures that also effect the inactivation.

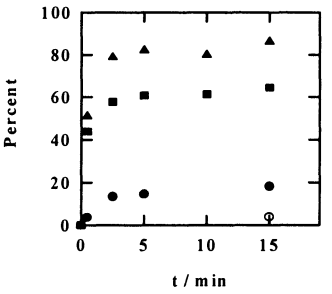

Fig. 3. Kinetics of DPA-release from *C. pasteurianum* spores at 60 °C and different pressures of ● 250, ■ 300 and ▲ 350 MPa; open symbol is control (DPA-release after 15 min at 60 °C and ambient pressure)

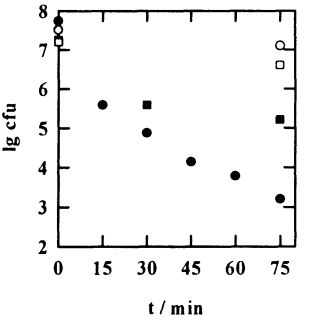

Fig. 4. Pressure inactivation of *C. pasteurianum* spores at 60 °C by ● oscillatory pressure cycling (one cycle consists of 10 min treatment with 420 MPa followed by 5 min at ambient pressure. The picture shows 5 cycles) and by ■ constant 420 MPa; open symbols are controls; ●, ■ amount of spores

4 Conclusions

The DPA-release from *C. pasteurianum* spores increases with rising pressures and the temperature has only a minor effect on the maximal amount released.

For inactivation of spores a process using changes between high and low pressures is more effective than a treatment with constant pressure. For further studies oscillatory pressures seem to be suitable to achieve complete inactivation of *C. pasteurianum* spores.

References

[1] Van Almsick, G., and Ludwig, H. (1997). High pressure inactivation of vegetative anaerobic bacteria. In: High Pressure Research in the Biosciences and Biotechnology, K. Heremans (Ed.), Leuven University Press, Leuven, Belgium, pp. 253-256.

[2] Hölters, C., Sojka, B., and Ludwig, H. (1997). Pressure-induced germination of bacterial spores from *Bacillus subtilis* and *Bacillus stearothermophilus*. In: High Pressure Research in the Biosciences and Biotechnology, K. Heremans (Ed.), Leuven University Press, Leuven, Belgium, pp. 257-260.

Neutral Trehalases Contribute to Barotolerance in *Saccharomyces cerevisiae*

H. Iwahashi, S. Nwaka, K. Obuchi and Y. Komatsu

National Institute of Bioscience and Human Technology,
Higashi 1-1, Tsukuba, Ibaraki 305, Japan
iwahashi@nibh.go.jp

Abstract. To estimate the contribution of neutral trehalases to barotolerance, we measured barotolerance of neutral trehalase I and/or neutral trehalase II deficient strains. Under 180 MPa for 2 h, the neutral trehalase I deficient strain showed lower barotolerance than the wild type strain. The neutral trehalase II deficient strain did not show lower barotolerance than the wild type strain. However, the neutral trehalase I and neutral trehalase II double mutant showed much lower barotolerance than the neutral trehalase II deficient strain. These results suggest that neutral trehalase I directly contributes to barotolerance and that neutral trehalase II may indirectly contribute to barotolerance. To confirm the direct contribution of neutral trehalase I, we transformed the neutral trehalase I deficient strain with the plasmid which contained neutral trehalase I gene. This transformant showed higher barotolerance than the control strain which carried the plasmid without neutral trehalase I gene. Our data suggest that neutral trehalase I has a direct role in barotolerance.

1 Introduction

We have studied the analogy between hydrostatic pressure and temperature using *S. cerevisiae* as a model system. We have shown that barotolerance and thermotolerance are based on a similar mechanism but are essentially different [1] and that the molecular chaperones Hsp104 and Hsp70, as well as the nonreducing disaccharide trehalose, are important factors for barotolerance [1, 2]. Hsp104 [3] and trehalose [4] were suggested to be important factors in thermotolerance. Recently, it was suggested that neutral trehalase I and neutral trehalase II contribute to thermotolerance [5–7]. Neutral trehalase I is the enzyme which is responsible for breaking trehalose in cells and neutral trehalase II is encoded by a gene, which is a homologue of neutral trehalase I gene [8]. As the factors which contribute to thermotolerance may also contribute to barotolerance, we investigated the contribution of neutral trehalases to barotolerance.

2 Materials & Methods

The strains used in this paper were derived from YS18 (*7Mata his3 leu2 ura3 CanR gal-*) and are shown in Table 1 [7]. The plasmids used are also listed in Table 1. Barotolerance of stationary phase cells were measured as % colony forming unit (CFU) of high pressure treated cells, relative to untreated control. Trehalose contents were measured as described previously [9].

Table 1. Strains and plasmids used

Strain	Genotype	Characteristic
YS18	*Mata his3 leu2 ura3 CanR gal-*	Wild type
YSN1	*Mata his3 leu2 ura3 CanR gal- nth1::LEU2*	-NTH1
YSN01	*Mata his3 leu2 ura3 CanR gal- nth2::URA3*	-NTH2
YSN1-01	*Mata his3 leu2 ura3 CanR gal- nth1::LEU2 nth2::URA3*	-NTH1,2
YSN1-pSEY8	*Mata his3 leu2 ura3 CanR gal- nth1::LEU2 URA3*	Control
YSN1-pNTH2	*Mata his3 leu2 ura3 CanR gal- nth1::LEU2 URA3 NTH1*	++NTH1
Plasmid		
pSEY8	*Ap^r URA3 ori*(2μ DNA)	Control
pNTH2	*Ap^r URA3 ori*(2μ DNA) *NTH1*	+NTH1

3 Results & Discussion

To estimate the contribution of neutral trehalases to barotolerance, we measured barotolerance of stationary phase cells of neutral trehalase I and/or neutral trehalase II deficient strains. Stationary phase cells were selected as we could not estimate barotolerance in logarithmic phase cells and heat shocked cells with high reproducability. This is possibly because of the amount of trehalose accumulated in the cells. It had been shown that trehalose content of the cells affect barotolerance and thus trehalose may decrease the apparent contribution of neutral trehalase to barotolerance.

Under 140 MPa for 2 h, we could not detect the contribution of these factors. However, when pressure was increased to 180 MPa, the neutral trehalase I deficient strain showed lower barotolerance than the wild type strain. The neutral trehalase II deficient strain did not show lower barotolerance than the wild type

strain. However, the neutral trehalase I and neutral trehalase II double mutant showed much lower barotolerance than the neutral trehalase II deficient strain. These results suggest that neutral trehalase I directly contributes to barotolerance and that neutral trehalase II may indirectly contribute to barotolerance.

To confirm the direct contribution of neutral trehalase I, we transformed the neutral trehalase I deficient strain with the plasmid which contained the neutral trehalase I gene. This transformant showed higher barotolerance than the control strain which carried the plasmid without the neutral trehalase I gene (data not shown). Our data suggest that neutral trehalase I has a direct role in barotolerance.

Trehalose had been shown to contribute to barotolerance and considered as a macromolecule stabilizer under high hydrostatic pressure conditions. Neutral trehalase is responsible for breaking trehalose in cells and the deletion of neutral trehalase caused higher accumulation of trehalose in the cells [8] (Table 2). However, the deletion of neutral trehalase decreases barotolerance. These observations suggest that trehalose is not only a macromolecule stabilizer but the degradation of trehalose is also important for yeast cells to survive higher hydrostatic pressure conditions. In the aspect of thermotolerance it was suggested that glucose from trehalose degradation is important as an energy source to rescue the stressed cells [8], and that trehalose inhibits the disaggregation of denatured proteins [10]. Similar mechanisms could be understood with barotolerance.

Table 2. Barotolerance (140 MPa, 25 °C, 2 h and 180 MPa, 25 °C, 2 h) and trehalose levels (μg/mg protein) of neutral trehalase deficient mutants

Conditions	Wild type	ΔNTH1	ΔNTH2	ΔNTH1 ΔNTH2
140 MPa, 25 °C, 2 h	0.27	0.29	53	44
180 MPa, 25 °C, 2 h	0.0017	0.00056	6.7	0.0082
Trehalose level	12.4	21.5	17.9	20.4

References

[1] Iwahashi, H., Obuchi, K., Fujii, S., and Komatsu, Y. (1997); Barotolerance is dependent on both trehalose and heat shock protein 104 but is essentially different from thermotolerance in *Saccharomyces cerevisiae*; Lett. Appl. Microbiol., 25, 43-47.

[2] Iwahashi, H., Nwaka, S., Obuchi, K., and Komatsu Y. (1999); Hsc70 is not essential for thermotolerance but for barotolerance (in these proceedings).

[3] Sanchez, Y. E. and Lindquist, S. (1990); Hsp104 required for induced thermotolerance; Science, 248, 1112-1115.

[4] Hottiger, T., Boller, T. and Wiemken, A. (1987); Rapid changes of heat and desiccation tolerance correlated with changes of trehalose content in *Saccharomyces cerevisiae* cells subjected to temperature shift; FEBS Letters, 220, 113-115.

[5] Nwaka, S., Kopp, M., Burgert, M., Deuchler, I., and Holzer, H. (1994); Is thermotolerance of yeast dependent on trehalose accumulation; FEBS Lett., 344, 225-228.

[6] Nwaka, S., Mechlen, B., Destruelle, M., and Holzer, H. (1995); Phenotypic features of trehalase mutants in *Saccharomyces cerevisiae*; FEBS Lett., 360, 286-290.

[7] Nwaka, S., Kopp, M., and Holzer, H. (1995); Expression and function of the trehalase genes NTH1 and YBR0106 in *Saccharomyces cerevisiae*; J. Biol. Chem., 270, 10193-10198.

[8] Nwaka, S., and Holzer, H. (1998); Molecular biology of trehalose and trehalases in the yeast *Saccharomyces cerevisiae*; Prog. Nuc. Acid Res. Mol. Biol., 58, 197-237.

[9] Iwahashi, H., Obuchi, K., Fujii, S., and Komatsu, Y. (1995); The correlative evidence suggesting that trehalose stabilizes membrane structure in the yeast *Saccharomyces cerevisiae*; Cel. Mol. Biol., 41, 763-769.

[10] Singer, M.A., and Lindquist, S. (1998); Multiple effects of trehalose on protein folding in vitro and in vivo; Mol Cell., 1, 639-648.

Ultra High Pressure Treatment of *Streptomyces* sp. R61

W. Kurzatkowski, J. Solecka, B. Rozbicka, J. Filipek, A. Laudy,
M. Fonberg-Broczek[1] and S. Porowski[1]

Laboratory of Actinomycetes and Fungi Imperfecti, National Institute of Hygiene, Chocimska 24, 00-791 Warsaw, Poland
[1]High Pressure Research Centre, Polish Academy of Sciences, Sokolowska 29/37, 01-142 Warsaw, Poland
eg@medstat.waw.pl

Abstract. At present, ultra high pressure (UHP) is proposed to be used for food preservation. For the experiments the strain *Streptomyces* sp. R61 was used. The purpose of the work was to test: ultrastructural changes of UHP treated cells, UHP killing pressure, UHP mode of killing, mutagenic effect of UHP. The hyphal cells were treated separately at 100, 200, 300, 400, 500 MPa, (exponential phase) for 10 min. The ultrathin sections were examined under a transmission electron microscope. A *Prokaryote* ultrastructure was observed. In comparison with not UHP treated cells in the cells after 100 MPa treatment no ultrastructural changes could be seen. After UHP treatment some of the cells (about 20%, i.e. young cells and senescent cells) were disrupted showing a lack of cytoplasm. Other cells did not show ultrastructural changes. At 300–500 MPa in the not disrupted cells the ribosomes were crushed. Only a few colonies were grown on solid medium after 300 MPa. The colonies after 300 MPa did not show morphological changes. The second generation did not show a genetically diversified population. Ultra high killing pressure for the tested strain is 400 MPa. UHP mode of killing: disruption of young and senescent cells at 200–300 MPa, crushing of ribosomes of mature cells, disturbing the protein biosynthesis. No mutagenic effect of UHP was observed.

1 Introduction

At present, ultra high pressure is proposed to be used for food preservation and processing [3]. UHP inactivation of anaerobic bacteria was examined previously [1]. Influences of UHP treatment on behaviour of bacteria in foods is at present a purpose of experimentation [2, 7, 11, 12, 14, 15]. Inactivation of microorganisms by UHP was described [13]. The inactivation of vegetative bacteria by pressure was tested [10].

The purpose of the work was to test the influences of UHP treatment on the ultrastructure and behaviour of *Streptomyces* sp. R61, i.e.:

1. Influences of UHP treatment on the ultrastructure of cells.
2. Ultra high killing pressure.
3. UHP mode of killing.
4. Mutagenic effect of UHP.

Previously the strain *Streptomyces* sp. R61 has been the subject of numerous experimentations. The morphology, ultrastructure, physiology, exocellular enzyme production such as xylan degrading enzymes, DD-carboxypeptidases/transpeptidases, β-lactamases were tested [4–6, 8].

2 Materials & Methods

2.1 Microorganisms

For the experiments the strain *Streptomyces* sp. R61 was used (Culture Collection of the National Institute of Hygiene in Warsaw).

2.2 Cultivation

The strain was maintained on yeast extract-malt extract agar (ISP-2) composed of (g/dm^3): yeast extract (Difco) 4, malt extract (Difco) 10, glucose (Difco) 4 , agar (Difco) 20, distilled water; pH was adjusted to 7.3. The inoculated slopes of the sporulation medium were incubated for 10 d at 28 °C.

Spores harvested from two slopes were used to inoculate 30 cm^3 of medium GZ-5 composed of (g/dm^3): soya meal 20, peptone (Difco) 4, yeast extract (Difco) 5, corn steep liquor 10, $MgSO_4 \cdot 7H_2O$ 0.5, KH_2PO_4 4, $CaCO_3$ 3, Soya oil 0.3 cm^3, 20% solution of glucose 3 cm^3, tap water; pH was adjusted to 7.5. Culture was shacked at 220 rpm for 24 h at 28 °C.

2.3 Phase-Contrast Microscopy

The growth of mycelium was observed under a phase-contrast microscope Docuval (Carl Zeiss, Jena, Germany).

2.4 Preparation of Samples for UHP Treatment

Cultures were centrifuged for 15 min at 4500×g. The mycelium was washed twice with 0.05 M phosphate buffer, pH 7.0 and centrifuged for 15 min. The mycelium harvested from two fermentation flasks was suspended in 25 cm^3 0.2 M phosphate buffer, pH 7.0. Samples of 2.0 cm^3 of mycelial suspension in special vials were UHP treated at 100, 200, 300, 400, 500 MPa for 15 min at room temperature.

2.5 Cultivation of UHP Treated Mycelium

Yeast extract-malt extract agar (ISP-2) in Petri dishes were inoculated with 0.5 cm^3 suspension of UHP treated mycelium. Cultures were incubated at 28 °C for 10 d.

2.6 Electron Microscopy

The mycelium after UHP treatment was centrifuged 8 min at 3500×g, washed carefully with distilled water and again centrifuged under the same conditions. The mycelium was suspended in 2% solution of glutaraldehyde and stored over night at room temperature. The samples were centrifuged for 10 min at 3500×g and the mycelium was prepared for electron microscopy as described previously and the procedure for immunolocalisation was omitted [9]. Ultrathin sections were observed under a transmission electron microscope JEM 100C (JEOL, Tokyo, Japan).

3 Results

The effect of UHP treatment on survival of *Streptomyces* sp. R61 was examined by the use of yeast malt-extract agar (ISP-2). In comparison with the control samples (not UHP treated mycelium), after UHP treatment of mycelium at 100 MPa and 200 MPa an essentially reduced growth of colonies was observed. Mycelium after 300 MPa treatment showed the growth of a few colonies (2–3 colonies). No growth of colonies was observed after 500 MPa treatment.

The ultrastructure of UHP treated mycelium was observed under electron microscopy. The cells showed a *Prokaryote* ultrastructure. In ultrathin sections of mycelial control samples the following subunits were observed: cell wall, cross wall, plasma membrane, nucleoid, cytoplasm densely packed with ribosomes.

The mycelium treated at 300 MPa showed essential ultrastructural changes. About 80% of cells of the population, most likely young cells at the tips of hyphae and senescent cells, were disrupted showing cell wall without cytoplasm. On the other hand, the cytoplasm of mature cells was electron dense showing areas of amorphous material packed with crushed ribosomes.

The UHP treated cells did not show genetically diversified population. Further experiments should be done to test if UHP is a mutagenic agent. For this reason the characteristics obtained in previous experiments for *Streptomyces* sp. R61 should be helpful.

4 Conclusions

1. At 300 MPa treated population of cells showed disrupted, most likely young and senescent cells and mature not disrupted cells with crushed ribosomes.

2. The ultra high killing pressure for the tested strain is 400 MPa.
3. UHP mode of killing: disruption of young and senescent cells at 300 MPa, crushing of ribosomes of mature cells, disturbing the protein biosynthesis.
4. After UHP treatment no genetically diversified population was observed.
5. Further experiments should be done especially to compare the physiological properties of untreated and UHP treated cultures.

References

[1] van Almsick, G. and Ludwig, H. (1997); *in* High pressure research in the biosciences and biotechnology (K. Heremans, ed.), pp. 253-256, Leuven University Press, Belgium.
[2] Chi, Y., Ma, X., Jin, Z., Luo, W., Liu, L. and Liu, B. (1997); *in* High pressure research in the biosciences and biotechnology (K. Heremans, ed.), pp. 283-286, Leuven University Press, Belgium.
[3] De Cordt, S., Denys, S., Ludikhuyze, L., Van den Broeck, I., Van Loey, A., Weemaes, C., Hendrickx, M., Heremans, K. and Tobback, B. (1997); *in* High pressure research in the biosciences and biotechnology (K. Heremans, ed.), pp. 311-314, Leuven University Press, Belgium.
[4] Frére, J.-M., Duez, C., Ghuysen, J.-M. and Vandekerkhove, J. (1976). FEBS Letters. 70, 257-260.
[5] Georgopapadakou, N.H., Liu, F.Y., Ryono, D.E., Neubeck, R. and Ondetti, M.A. (1981). Eur. J. Biochem. 115, 53-57.
[6] Georgopapadakou, N.H., Smith, S.A. and Cimarusti, Ch.M. (1982). Eur. J. Biochem. 124, 507-512.
[7] Gervilla, R., Felipe, X., Ferragut, V. and Guamis B. (1997); *in* High pressure research in the biosciences and biotechnology (K. Heremans, ed.), pp. 287-290, Leuven University Press, Belgium.
[8] Ghuysen, J.-M. (1994). Trends in Microbiol. 2, 372-380.
[9] Kurzatkowski, W., Palissa H., Van Liempt, H., von Döhren, H. Kleinkauf, H., Wolf, W.P. and Kurylowicz, W. (1991). Appl. Microbiol. Biotechnol. 35, 517-520.
[10] Ludwig, H. and Schreck, Ch. (1997); *in* High pressure research in the biosciences and biotechnology (K. Heremans, ed.), pp. 221-224, Leuven University Press, Belgium.
[11] Ponce, E., Pla, R., Sendra, E., Yuste, J. and Guamis, B. (1997); *in* High pressure research in the biosciences and biotechnology (K. Heremans, ed.), pp. 299-302, Leuven University Press, Belgium.
[12] Rademacher, B. and Kessler, H.G. (1997); *in* High pressure research in the biosciences and biotechnology (K. Heremans, ed.), pp. 291-293, Leuven University Press, Belgium.
[13] Smelt, J.P.P.M., Courrier, W., Cuppers, H.G.A.M., Wouters, P.C. and Rijke, A.G.F. (1997); *in* High pressure research in the biosciences and biotechnology (K. Heremans, ed.), pp. 273-276, Leuven University Press, Belgium.
[14] Szczawinski, J., Szczawinska, M., Stanczak, B., Fonberg-Broczek, M., Arabas, J. and Szczepek, J. (1997); *in* High pressure research in the biosciences and biotechnology (K. Heremans, ed.), pp. 295-298, Leuven University Press, Belgium.
[15] Yuste, J., Mor-Mur, M., Ponce, E., Pla, R. and Guamis, B. (1997); *in* High pressure research in the biosciences and biotechnology (K. Heremans, ed.), pp. 303-306, Leuven University Press, Belgium.

The Effects of Sub-Lethal Pressure Treatment on *Escherichia coli* O157:H7

M. Linton, G.J. M^{c}Cann and M.F. Patterson

Food Science Division, Department of Agriculture for Northern Ireland, Newforge Lane, Belfast BT9 5PX, Northern Ireland, UK
Margaret.patterson@dani.gov.uk

Abstract. The resistance of Escherichia coli O157:H7 to high pressure varies between strains. In the first experiment a pressure resistant strain, NCTC 12079, was used to investigate the effect of sub-lethal pressure treatment on the heat resistance of E. coli O157:H7. UHT skimmed milk was inoculated with a stationary phase culture, pressure treated at 200 MPa for 30 min and heat treated at 55, 58 and 60 °C. Pressure treatment caused an increase in the heat sensitivity of E. coli O157:H7 at all three temperatures. This has important implications for the safety of pressure treated foods which are intended for subsequent heat treatment. In the second experiment the effect of sub-lethal pressure treatment on verotoxin production was investigated. Samples were first pressure treated at 400 MPa or held at ambient pressure as a control. Verotoxin production was assayed at various stages during storage at 25 °C in laboratory medium. Pressure treatment caused an increase in the time to detection of verotoxin activity. This effect may be explained in terms of cell numbers rather than any effect on the production or the activity of verotoxins, as pressure treatment caused an increase in the lag period during subsequent storage. This would indicate that although injured, pressure treated E. coli O157:H7, which are allowed to proliferate, are still capable of producing toxins and therefore likely to be capable of causing illness.

1 The Effect of High Pressure on the Heat Sensitivity of *E. coli* O157:H7 in Skimmed Milk

E. coli O157:H7 is of growing concern to the food industry and has been isolated from a wide variety of foods including various meats, water and unpasteurised milk and apple juice [1,2]. Patterson *et al.* found *E. coli* O157:H7 strain NCTC 12079 to be particularly resistant to high pressure [3]. Previous studies have shown that this strain of *E. coli* O157:H7 in laboratory medium is more sensitive to heat inactivation following a sub-lethal pressure treatment [4]. This effect was investigated in skimmed milk, a foodstuff which is suitable for high pressure processing.

1.1 Materials & Methods

E. coli O157:H7 NCTC 12079 was grown for 18 h at 37 °C in tryptone soya broth with 0.6% yeast extract added (TSBYE). Cells were harvested by centrifugation at 2400×g for 20 min, washed in phosphate-buffered saline and resuspended in UHT skimmed milk to give approximately 10^8 cfu ml^{-1}. This cell suspension was held at 3 °C for 18 h before pressure treatment at 200 MPa for 30 min at 10 °C, using a Stansted Foodlab 9000 high pressure isostat. The pressurising fluid was 90% distilled water: 10% ethanol and the come-up time was approximately 1 min. The temperature increase due to adiabatic heating was approximately 3 °C per 100 MPa and the pressure release time was 2 min. Pressure treated samples were held at 3 °C for a maximum of 2 h before heat treatment at 55, 58 and 60 °C. Surviving cells were enumerated on tryptone soya agar containing 0.6% yeast extract incubated at 37 °C for 24 h.

1.2 Results & Discussion

A pressure treatment of 200 MPa for 30 min at 10 °C had little effect on the numbers of *E. coli* O157:H7 in skimmed milk, resulting in only a mean $\log_{10}$ decrease of 0.25. However this pressure treatment did have a significant effect on the heat sensitivity of the organism, as can be seen in Table 1.

Table 1. Time (min) to achieve a 4-log10 inactivation of pressure treated E. coli O157:H7

55 °C		58 °C		60 °C	
Control	200 MPa	Control	200 MPa	Control	200 MPa
74.0	55.0	30.0	20.0	11.9	5.3

At all three temperatures tested the time required to achieve a 4-$\log_{10}$ reduction in numbers was significantly decreased following pressure treatment (p=0.034, 0.058 and 0.024 at 55, 58 and 60 °C, respectively). The reduced heat tolerance of *E. coli* O157:H7 after a comparatively mild high pressure treatment has important implications for foodstuffs which are to be heated after high pressure processing.

2 The Effect of High Pressure on Verotoxin Production by *E. coli* O157:H7

Verotoxins (VT) are cytotoxins which are regarded as important virulence factors in *E.coli* strains causing human disease such as haemorraghic colitis and the uraemic syndrome [5]. The activity of VT-1 produced by *E. coli* O157:H7 can be reduced by exposure to extreme conditions such as low pH and high temperature [6]. Little is known of the effects of sub-lethal pressure on verotoxin production by *E. coli* O157:H7. In this study the effect of high pressure on the production of verotoxins was investigated.

2.1 Materials & Methods

The same pressure resistant strain of *E. coli* O157:H7, described above, was used for this study. The organism was grown for 18 h at 37 °C in TSBYE. Polyethylene pouches containing 5 ml of this stationary phase culture were prepared and subjected to a pressure treatment of 400 MPa for 30 min at 30 °C. Pressure treatment of samples was carried out using a Haskel high pressure generating system (Haskel Energy Systems Ltd., Sunderland, England), capable of operating at 400 MPa. The pressure transmission fluid was distilled water containing 10% Dromus oil B (Shell UK, London, England) and temperature was controlled by an electrical heating device which surrounded the pressure chamber. At this pressure treatment the adiabatic heating effect caused a 5 °C increase in temperature. The come-up time and pressure release times were instantaneous. TSBYE broth (100 ml) was inoculated with *E. coli* O157:H7, in duplicate, to a level of approximately 1×10^3 cfu/ml and incubated at 25 °C until stationary phase was attained . Growth curves were generated and regular sub-samples (1 ml) taken for bioassay. The verocell cytotoxicity test [7] was used to test verotoxin production and toxicity.

2.2 Results

The detection of verotoxin using this technique could not be achieved until cell numbers reached approximately 1×10^6 cfu/ml. Fig. 1 shows that a pressure treatment of 400 MPa for 30 min at 30 °C leads to an increase in the time to detection of toxin from 11 h to 24 h.

The time to detection would appear to be a function of cell numbers. There is nothing to suggest toxin synthesis is inhibited following pressure treatment, as similar results were obtained for control and pressure treated cells when verocell cytotoxicity was tested at the stationary phase of growth.

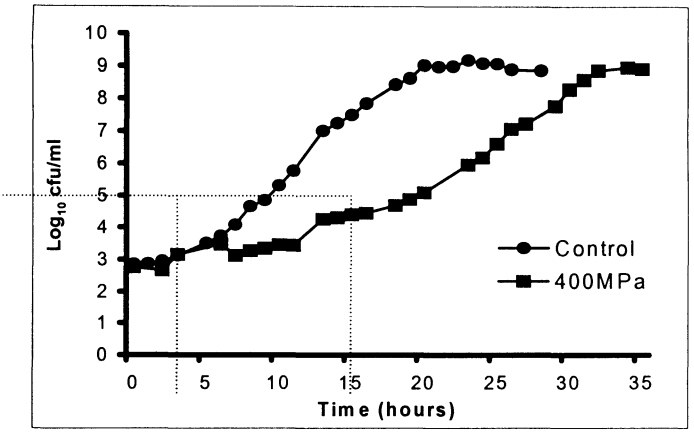

Fig. 1. The effect of high pressure (400 MPa/30 min/30 °C) on *E. coli* O157:H7 growth and verotoxin production; --- Limit of VT detection

References

[1] Doyle, M.P. (1991) *Escherichia coli* O157:H7 and its significance in foods. Int. J. Food Microbiol. **12**:289-302.

[2] Besser, R.E., Lett, S.M., Weber, J.T., Doyle, M.P., Barrett, T.J., Wells, J.G. and Griffin, P.M. (1993) An outbreak of diarrhea and hemolytic uremic syndrome from *Escherichia coli* O157:H7 in fresh-pressed apple cider. J. Am. Med. Assoc. **269**:2217-2220.

[3] Patterson, M.F., Quinn, M., Simpson, R. and Gilmour, A. (1995) Sensitivity of vegetative pathogens to high hydrostatic pressure treatment in phosphate-buffered saline and foods. J. Food Prot. **58**:524-529.

[4] Patterson, M.F., Linton, M. and McClements, J.M.J. (1998) Pathogen inactivation by high pressure treatment of foods. These Proceedings.

[5] O'Brien, A.D., Tesh, V.L., Donohue-Rolfe, A., Jackson, M. P., Olsnes, S., Sandvig, K., Lindberg, A.A. and Keusch, G.T. (1992) Shiga toxin: biochemistry, genetics, mode of action and role in pathogenesis. Current Topics in Microbiology and Immunology. **180**:65-94.

[6] Kittell, F.B., Padhye, V.V. and Doyle M.P. (1991) Characterization and inactivation of Verotoxin 1 produced by *Escherichia coli* O157:H7. J. Agric. Food Chem. **39**:141-145.

[7] Ball, H.J., Finlay, D., Burns, L. and Mackie, D.P. (1994). Application of monoclonal antibody-based sandwich ELISAs to detect verotoxins in cattle faeces. Res. Vet. Sci. **57**:225-232.

Inactivation Kinetics of Fungal Conidiospores

N. Merkulow and H. Ludwig

Universität Heidelberg, Institut für Pharmazeutische Technologie und Biopharmazie,
INF 366, D-69120 Heidelberg, Germany
Phone: +49-(0)6221-545235; Fax: +49-(0)6221-545475
Horst.Ludwig@urz.uni-heidelberg.de

Abstract. Fungal conidiospores can be inactivated by high hydrostatic pressure. The pressure resistance depends on the species. Simple first order inactivation is only found at low temperatures. At high temperatures the inactivation is not complete, a pressure stable fraction remains.

1 Introduction

Some moulds are known to cause diseases in human beings and many others to cause spoilage of food [1]. The majority of these fungi belong to the class *Deuteromycetes* (*fungi imperfecti*). Their reproduction follows an asexual cycle and results in the building of conidiospores. These spores are much more resistant to high hydrostatic pressure than the vegetative cells [2].

High pressure treatment may offer an alternative to high temperature sterilisation of food and heat sensitive drugs. Accordingly experiments were done with the moulds *Penicillium expansum* which attacks mature fruits and produces the mycotoxin Patulin [3], with *Botrytis cinerea* that spoils fruits and cereals with grey rot, and with *Aspergillus fumigatus*.

2 Materials & Methods

P. expansum (strain DSM 1994), *B. cinerea* (DSM 877) and *A. fumigatus* (DSM 790) were obtained from the Deutsche Sammlung von Mikroorganismen (DSM), Braunschweig. *P. expansum* and *B. cinerea* were grown on Potato Dextrose Agar (PDA) at 24 °C, *A. fumigatus* on PDA at 37 °C. The spores were harvested after 10–14 d. For pressure treatments the spores were freshly prepared and suspended in isotonic NaCl-solution containing 0.1% Polysorbate 80. The number of surviving microorganisms was determined by counting colony forming units (cfu) on agar plates after 3–5 d at 24 °C. The surviving cells of *P. expansum* were counted on Malt Extract Agar (MEA), of *B. cinerea* on MEA containing 1 g of ox bile/l and those of *A. fumigatus* on MEA with 0.05 g Bengal Rose/l. All experiments were repeated at least once.

3 Results

3.1 *Penicillium expansum*

Figure 1 shows the barotolerance of conidiospores from *P. expansum* at 25 °C. Their inactivation needs a minimum pressure of 250 MPa. The inactivation rate accelerates with rising pressure. As shown in Fig. 2 the inactivation of spores at 4 °C and 350 MPa follows a first order reaction with a "Decimal Reduction Value" (D-value) of one minute. At 25 °C a two phase inactivation kinetics is

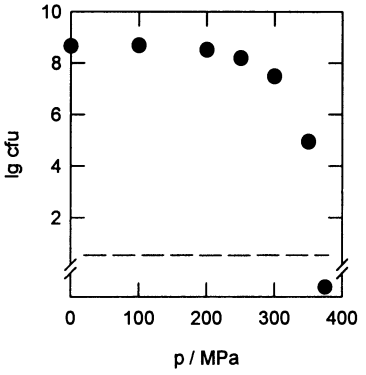

Fig. 1. Pressure dependence of conidiospores of *P. expansum*, 30 min at 25 °C; – – – detection limit

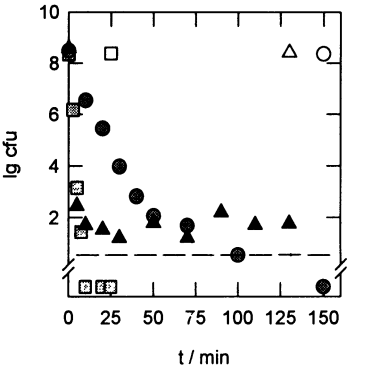

Fig. 2. Inactivation of conidiospores of *P. expansum* at 350 MPa and 4 °C, ● 25 °C and ▲ 40 °C; open symbols are controls; – – – detection limit

found. The D-values are ≈ 7 min (D1) for the more sensitive fraction, and ≈ 30 min (D2) for the more resistant one. At 40 °C a fast inactivation (D1 < 1 min) stops after some minutes so that a stable fraction remains. If the temperature of this fraction is lowered to 25 °C the stability against pressure is lost immediately.

3.2 *Botrytis cinerea*

The inactivation of spores from *B. cinerea* starts at 150 MPa, at 300 MPa no viable cells are detectable after 30 min at 25 °C (Fig. 3). Experiments at 4 °C and 200 MPa result in a bent curve (Fig. 4); the first fraction is inactivated with D1 ≈ 7 min, the second with D2 ≈ 30 min. 25 and 40 °C give similar results, a fast inactivation in the first minutes with D-values (D1) of about 6 and 3 min and remaining stable fractions.

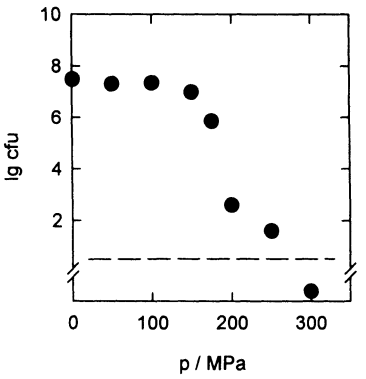

Fig. 3. Pressure dependence of conidiospores of *B. cinerea*, 30 min at 25 °C; – – – detection limit

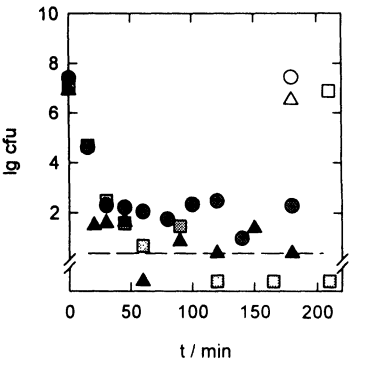

Fig. 4. Inactivation of conidiospores of *B. cinerea* at 200 MPa and 4 °C, ● 25 °C and ▲ 40°C; open symbols are controls; – – – detection limit

3.3 *Aspergillus fumigatus*

The conidiospores of *A. fumigatus* are the most pressure resistant ones of the investigated moulds. The inactivation starts at 300 MPa and accelerates with rising pressure (Fig. 5). The inactivation kinetics at 4 °C and 400 MPa seems to be a first order reaction with a D-value of ≈ 3 min (Fig. 6). But under these conditions it is impossible to obtain sterile samples even after pressure treatments of 5 h. At 25 °C a two phase inactivation is found with D-values of ≈ 10 min (D1) and ≈ 80 min (D2). Results at 40 °C were similar to those at 4 °C (data not shown). At 55 °C there remains a pressure stable fraction with an average of 1000 cells/ml after the first fraction is inactivated with a D-value of ≈ 7 min.

4 Conclusions

In most cases the kinetics of inactivation runs in two phases. A fast reaction in the first minutes is followed by a slower one, both reactions being first order. A single first order reaction (one phase inactivation) seems to occur at low temperatures only. Temperature induced changes from one to two phase inactivation has also been found in case of bacteria. For them, the bent curves could be explained by two bacterial fractions with different resistance against pressure [4].

At high temperatures there remain pressure resistant fractions of conidiospores. It seems that this phenomenon occurs in pressure inactivation above the optimal growth temperature. More detailed studies are planned to reveal the underlying mechanisms.

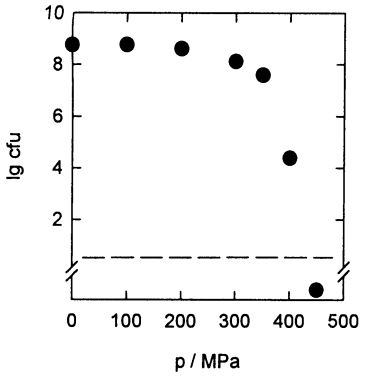

Fig. 5. Pressure dependence of conidiospores of *A. fumigatus*, 30 min at 25 °C; – – – detection limit

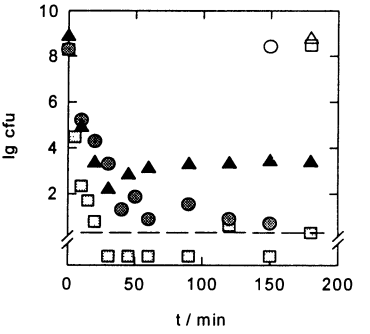

Fig. 6. Inactivation of conidiospores of *A. fumigatus* at 400 MPa and 4 °C, ● 25 °C and ▲ 55 °C; open symbols are controls; – – – detection limit

References

[1] Filtenborg, O. et al. (1996). International Journal of Food Microbiology, **33**, 85-102.

[2] Eicher, R., Merkulow, N., van Almsick, G., Ludwig, H. (1997). High Pressure Biology and Medicine, Bennett, P. B., Demchenko, I., Marquis, R. E. (Eds.), University of Rochester Press, Rochester, USA, pp. 65-75.

[3] Sommer, N. F., Buchanan, J. R., Fortlage, R. J. (1974). Applied Microbiology, **28** (4), 589-593.

[4] Ludwig, H., Schreck, C. (1997). High Pressure Research in the Biosciences and Biotechnol., Heremans, K. (Ed.), University Press Leuven,Leuven, Belgium, pp. 221-224.

Acquired Barotolerance and Thermal Stability of Cellular Components at High Pressure in *Saccharomyces cerevisiae* Cells

K. Obuchi, H. Iwahashi and Y. Komatsu

National Institute of Bioscience and Human Technology, AIST, Higashi-1, Tsukuba, Ibaraki 305-8566, Japan
Kaoru@nibh.go.jp

Abstract. Whole cell DSC profiles of *Saccharomyces cerevisiae* cells were obtained at 0.1 to 150 MPa and C_p-T-p profiles were obtained. Prominent endothermic transition occurred around 60 °C over the pressure range. The profiles of the cells before and after heat shock response revealed that the response protect some cellular components against destabilization above 75 MPa and these components may include critical targets of cell killing.

1 Introduction

Heat shock response confers barotolerance as well as thermotolerance transiently in *Saccharomyces cerevisiae* cells [1]. The critical target model predicts that the thermotolerance is associated with stabilization of critical targets in the yeast cells [2] and whole cell differential scanning calorimetry (DSC) analyses of *E. coli* [3] and Chinese hamster lung V79 cells [4] showed that heat shock response stabilized cellular components thermally. As the whole cell DSC analyses at ambient pressure show the thermal stability of the components at ambient pressure relating with thermotolerance, the analysis at high pressure will show the stability at high pressure relating with barotolerance of the cells. We developed a high pressure sample applicator for an MC-2 scanning calorimeter (MicroCal Inc. MA) and found some cellular components in *S. cerevisiae* Hansen IFO-0224 cells became labile at above 75 MPa [5]. In this paper, we present stabilization of cellular components after heat shock response.

2 Materials & Methods

S. cerevisiae Hansen IFO-0224 cells were cultured at 30 °C and harvested in exponentially growing phase and subjected to heat shock treatment at 43 °C for 60 min as described previously [1]. The cells were suspended in distilled water

(~ 10^{10} cells/ml) and 10 µl of the suspension and distilled water were injected in one-terminal shielded SUS capillaries separately.

The sample and reference capillaries were connected to the applicator and pressurized. DSC scans were repeated twice from 5 to 90 °C at the rate of 1 °C/min and the trace of the second scan was subtracted from the first one. A cubic polynomial baseline was generated to the subtracted profile and subtracted again. The baseline correction provided a corrected profile comprising irreversible transition of cellular components [4]. The corrected profiles obtained at every 25 MPa from 0.1 to 150 MPa were normalized by the maximum height of each profile and contour profiles were obtained.

3 Results & Discussion

The corrected profile of exponentially growing IFO-0224 cells at ambient pressure had peak maximum at 60.2 °C (T_m) and several shoulders and minor peaks appeared from 48 to 80 °C (Fig. 1). In the profiles, positive deflection of C_p implies endothermic transition resulting from thermal denaturation of biopolymers [4].

The contour profiles of the cells before and after the heat shock response are illustrated in Fig. 2. At around 75 MPa in the profile of the cells before heat shock, the skirt of the prominent endothermic peak expanded to 40 or 45 °C, implying the pressurization even below 100 MPa destabilized some minor components as reported previously [2]. In the case of the heat shocked cells, the expansion appeared above 125 MPa. Therefore, the heat shock response stabilized the components.

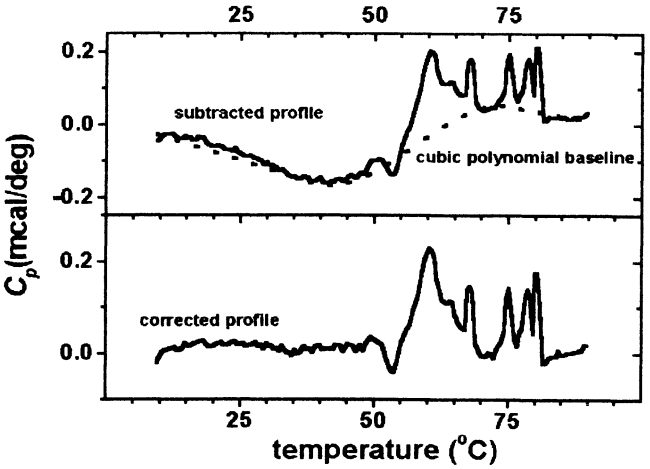

Fig. 1. Whole cell DSC profiles of exponentially growing cells at 0.1 MPa. Subtraction of the trace of the second scan from the first one provided a subtracted profile from which a cubic polynomial baseline was subtracted again and the corrected profile was obtained

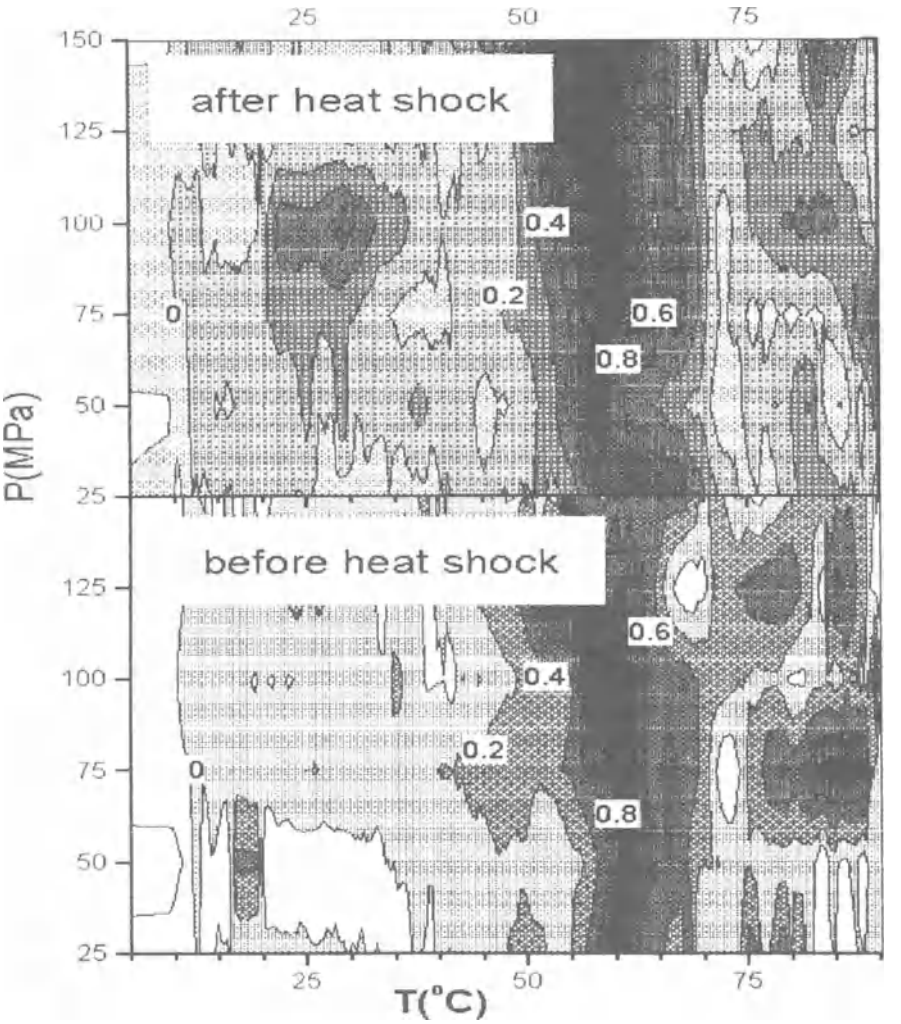

Fig. 2. C_p contour profiles on the p-T plane before and after the heat shock response

For the cells before the heat shock response, T_m of prominent peaks was held below 100 MPa and fell by 5 to 7 °C above the pressure. On the other hand, for the heat shocked cells, T_m was conserved up to 150 MPa and swell of the prominent peak appeared on the lower temperature edge above 100 MPa (Fig. 2). Therefore, over the pressure range of 0.1 to 150 MPa, major components in lFO-0224 cells lose the native conformations at around 60 °C, and heat shock response stabilized them over the range of 100 to 150 MPa. Temperature rising cell killing at ambient pressure occurs over the temperature range corresponding to the early stage of the prominent endothermic transition [2].

It is concluded that some cellular components become labile above 75 MPa and the heat shock response stabilizes some fraction of them. Stabilization of the cellular components which unfold over the corresponding temperature range may result in thermotolerance at above 100 MPa, which is a barotolerance.

References

[1] Iwahashi, H., Kaul, S.C., Obuchi, K. and Komatsu, Y. (1991); Induction of barotolerance by heat shock response in yeast; *FEMS Microbiol. Lett.* **80**, 325-328.

[2] Obuchi, K., Lepock, J.R, Iwahashi, H. and Komatsu, Y.; Stabilization of two families of critical targets for hyperthermic cell killing and acquired thermotolerance of yeast cells; *Yeast. in press.*

[3] Macckey, B.M., Miles, C.A., Seymour, D.A. and Parsons, S.E. (1993); Thermal denaturation and loss of viability in *Escherichia coli* and *Bacillus stearothermophilus*; *Lett. Appl. Microbiol.* **16**, 56-58.

[4] Lepock, J. R., Frey, H.E., Rodhal, M. and Kruuv, J. (1988); Thermal analysis of CHL V79 cells using differential scanning calorimetry: implication for hyperthermic cell killing and heat shock response; *J. Cell. Physiol.* **137**, 17-24.

[5] Obuchi, K., Kawai, S., Iwahashi, H. and Komatsu, Y. ; High pressure differential scanning calorimetry of yeast cells. in High pressure biotechnology (Kunugi, S. ed.). San-ei Syuppan Co. Kyoto. *in press.*

Role of Oxidative Stress in the Inactivation of *Escherichia coli* by High Hydrostatic Pressure

M. Robey, S.F. Park and B.M. Mackey

Institute of Food Research, Earley Gate Reading, RG6 6BZ, UK
robeym@bbsrc.ac.uk

Abstract. The role of oxidative stress in pressure-induced inactivation of *Escherichia coli* was investigated. Mutations in the genes encoding superoxide dismutase (SOD), *sodA* and *sodB*, were found to render *E. coli* more sensitive to high hydrostatic pressure at 550 MPa. The addition of catalase to the recovery medium was found to aid the recovery of pressure-damaged SOD mutants. Microbial inactivation by high hydrostatic pressure may be due to damage caused by the production of hydroxyl free radicals via a Fenton-type reaction.

1 Introduction

The ability of high hydrostatic pressure to cause bacterial inactivation is currently being exploited as a novel means of food preservation. Hydrostatic pressure degrades enzymes, ribosomes and causes membrane damage, but despite growing awareness of changes occurring in bacteria during high hydrostatic pressure treatments, the exact sequence of events leading to cell death is not yet well characterised. The aim of this work was to investigate whether genes responsible for protecting the cell against other stresses, such as oxidative stress, were involved in helping cells overcome the effects of pressure, either by rendering them more barotolerant or by aiding their recovery. Reported here are our investigations into the effects of high hydrostatic pressure on a mutant devoid of superoxide dismutase (SOD); SOD catalyses the removal of harmful superoxide (O_2^-) radicals (Fig. 1a).

a) $O_2^- + O_2^- + 2H^+ \xrightarrow{\text{SOD}} H_2O_2 + O_2$

b) $2H_2O_2 \xrightarrow{\text{catalase}} 2H_2O + O_2$

Fig. 1. The oxidation reactions catalysed by (a) SOD and (b) catalase

2 Materials & Methods

The SOD mutant and its wild type parent were grown to stationary phase then pressurised in phosphate-buffered saline (PBS) in sealed plastic sachets at 550 MPa using a Stansted Fluid Power pressure rig. Viability was assessed by counting colonies obtained following plating of the pressurised bacterial suspension on tryptone soya agar supplemented with yeast extract (TSAYE) and 48 h incubation at 37 °C. The effect of the presence of catalase during recovery was also assessed through the addition of catalase (1760 units) to TSAYE plates.

3 Results & Discussion

The SOD mutant was 1–2 logs more pressure sensitive than its wild type parent (Fig. 2), suggesting that SOD may protect the cell from pressure-induced inactivation or aid the recovery of sublethally-injured organisms. The presence of catalase during recovery on TSAYE plates increased the recovery of the SOD mutant by 1–2 logs (Fig. 2). The substrate for catalase is hydrogen peroxide (H_2O_2; Fig. 1b), therefore, H_2O_2 may be involved in the killing of pressure-damaged SOD mutants during recovery on agar plates.

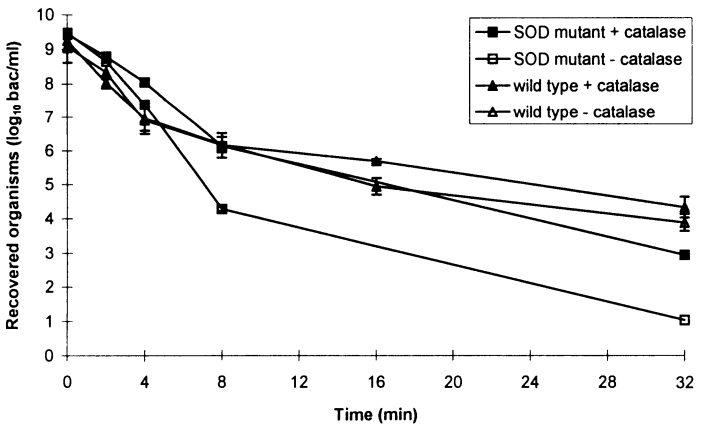

Fig. 2. Pressure resistance of SOD mutant and wild type parent at 550 MPa pressurised in PBS and plated on TSAYE plates (*open symbols*) or TSAYE plates supplemented with catalase (*closed symbols*)

The substrate for SOD is O_2^-, whereas the substrate for catalase is H_2O_2, so why should a mutant devoid of SOD be affected by the presence of H_2O_2 (Fig. 1)? One explanation is that the damage to the SOD mutant may be being mediated via a Fenton-type reaction [1]. One of the main targets for O_2^- is believed to be iron-sulphur (Fe-S) clusters at the active sites of certain enzymes. Superoxide is

thought to attack these active sites releasing Fe^{2+} into the cell. The Fe^{2+} is then free to react with H_2O_2 with the concomitant production of the highly damaging hydroxyl free radical (OH^-) in a Fenton reaction (Fig. 3).

$$O_2^- + \text{Fe-S clusters} \rightarrow Fe^{2+}$$

(Fenton reaction)

$$H_2O_2 + Fe^{2+} \rightarrow OH^- + Fe^{3+} + H_2O$$

Fig. 3. The action of O_2^- on Fe-S clusters of certain enzymes makes ferric iron available to participate in a Fenton reaction

In unpressurised SOD mutants, the Fenton reaction does not appear to affect the viability of the parent and the SOD mutant (see Fig. 2, time = 0 min). However, when the SOD mutant and the parent are exposed to high hydrostatic pressure the SOD mutant appears to be much more sensitive to H_2O_2. It is possible that high pressure accentuates the Fenton reaction by, for example, (a) increasing the availability of one of the components, e.g. Fe^{2+}, or (b) damaging enzymes which repair the DNA damage caused by OH^- radicals.

We are currently investigating whether Fenton-mediated damage is occurring and whether high pressure is exacerbating its effects. However, preliminary investigations using the iron-chelating agent, 2,2'-dipyridyl, have had no effect on the recovery of the pressure-damaged SOD mutants.

Acknowledgements: We are grateful to the UK Ministry of Agriculture for financial support of this work.

References

[1] Keyer, K.; Strohmeier Gort, A.; Imlay, J. A. (1995); Superoxide and the production of oxidative DNA damage; Journal of Bacteriology, 177, 6782-6790.

Effects of Heat and Pressure Shock on Growth Thermograms of Yeast

M. Miyashita and K. Tamura

Department of Chemical Science and Technology, Faculty of Engineering, The University of Tokushima, Minamijosanjima-cho, Tokushima 770-8506, Japan
Phone and fax: +81-(0)886-56-7416
tamura@chem.tokushima-u.ac.jp

Abstract. Using a differential scanning calorimeter, we estimated the thermotolerance of heat- and pressure-shocked yeast and compared the results with those obtained by the colony count method. The growth thermograms of yeast showed clear acquisition of thermotolerance in the following orders of temperature treatments, 43, 30, 20, and 46 °C, and shock pressures of 50, 75, 100, 25 and 0.1 MPa. On the other hand, survival of yeast cells determined by colony counts increased in the order of shock pressures of 50, 75, 25, 100, and 0.1 MPa. Thus the orders obtained by different methods were not always consistent. Pressure shock treatment seems to give yeast cells not only thermotolerance but also enhanced microbial activity. The addition of trehalose to the medium increased the thermotolerance of yeast cells. High hydrostatic pressures also induced thermotolerance, but reduced the influence of trehalose on high temperature stress.

1 Introduction

All cells from microbes to mammals synthesize heat shock proteins (hsps) in response to various stresses such as heat, pressure, and chemicals, and acquire resistance to various subsequent stresses that would normally be lethal. For example, yeast cells exposed to a slightly higher temperature than that for optimum growth, immediately respond by induction of hsps and trehalose, with increase in tolerance against lethal stress. This phenomenon is called acquired stress tolerance. It is known that in the yeast *Saccharomyces cerevisiae*, the induction of hsp104 and the accumulation of trehalose contribute to their acquisition of thermotolerance [1]. The addition of trehalose to the cell suspensions also enhances the stress tolerance of yeast cells [2].

The metabolic heat of microbes can be measured precisely using a microcalorimeter and can be used to study microbial activities under various conditions quantitatively. We measured the heats produced by heat- and pressure-

shocked yeast cells in media with or without trehalose, from thermograms of the cells and compared the results with those on colony counts [3].

2 Materials & Methods

The yeast *Saccharomyces cerevisiae* IFO 10149 was grown at 30 °C in YPD medium containing (in g/l) glucose, 20; polypeptone, 20; and yeast extract, 10. Cultures were used in the logarithmic phase of growth. Exponentially growing cells in YPD medium (cell density, 1.0×10^5 cells/ml for thermograms, 1.0×10^7 cells/ml for survival) with or without trehalose were subjected to pressures of 0.1 to 100 MPa or to temperatures of 20 to 46 °C, and then exposed to a lethal temperature (51 °C, 10 min). The number of viable cells was determined by counting colonies on YPD agar medium.

Growth thermograms of yeast were obtained using a multi-cell microcalorimeter (CSC4100). Yeast cells were subjected to heat shock in a calorimeter, and to pressure shock in a high-pressure vessel before measurement of heat.

3 Results

Heat shock treatment of yeast cells and the estimation of their thermotolerance were carried out according to the following temperature programs in a microcalorimeter: T °C (30 min) - 51 °C (10 min) - 30 °C (about 2 d), where T is 20, 30, 43, or 46 (°C). The optimum temperature for growth of the yeast cells used in this experiment is 30 °C. To compare the effects of the preconditioning temperatures on the thermotolerance of yeast cells, the relative start time of growth (ΔT) was determined from the thermograms. The values of ΔT were determined by subtracting the start time of the thermogram obtained at 30 °C without trehalose (control) from those obtained at other temperatures.

Figure 1 shows the relative start time (ΔT) for yeast cells exposed to a lethal temperature (51 °C, 10 min) after heat shock or pressure shock treatment. The multiplication rate of surviving yeast cells in medium without trehalose increased in the following order on temperature treated: 46, 20, 30, and 43 °C (Fig. 1A). The thermotolerance of yeast cells treated at 43 °C was highest, consistent with results obtained previously by the colony count method [3]. The addition of trehalose at 0.5 mol/l to the medium enhanced the thermotolerance, showing a similar temperature pattern. However, in suspensions with 1.0 mol/l trehalose, the effect of temperature disappeared almost completely, although the tolerance was still higher. Pressure shock treatment also induced thermotolerance of yeast cells (Fig. 1B). The thermotolerance of pressure-shocked yeast was highest when treated at 50 MPa at all trehalose concentrations.

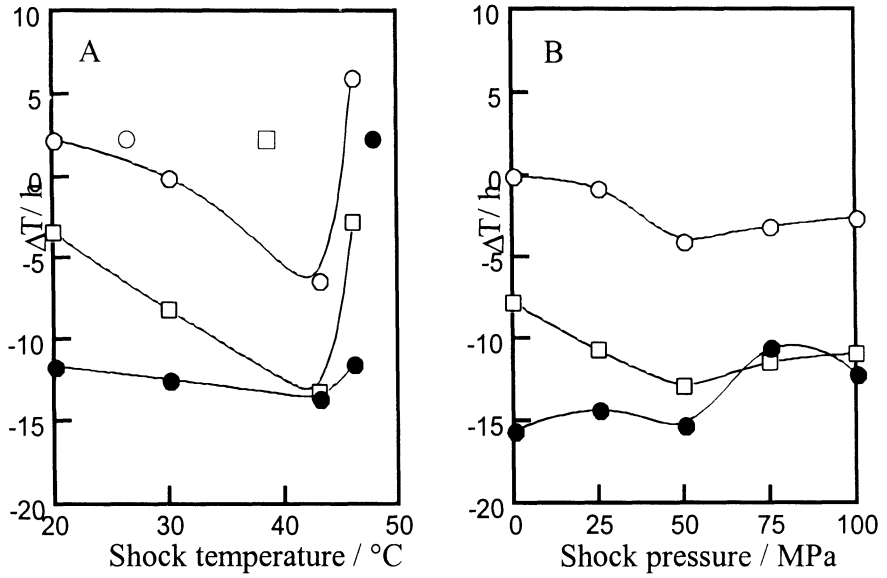

Fig. 1. Relative start time of growth of yeast cells. Yeast cells were subjected to high temperature (51 °C, 10 min) (**A**) after temperature shock treatment at 20 to 46 °C at atmospheric pressure or (**B**) to pressure shock at 0.1 to 100 MPa at 30 °C in medium without trehalose 0 (○), with 0.5 (□) or 1.0 (●) mol/l of trehalose. ΔT indicates the relative start time of the growth thermogram (control: 0.1 MPa, 30 °C)

Figure 2 shows the survival curve of pressure-shocked yeast cells determined by the colony count method. The survival of yeast cells treated at 100 MPa was almost the same as that at atmospheric pressure, and from the thermograms the thermotolerance of yeast cells subjected to 100 MPa was higher than that of cells at atmospheric pressure. This suggests that pressure shock treatment increases the biological activities of yeast cells. The survival of yeast cells treated at 50 MPa was 37 times that of those treated at 0.1 MPa. Figure 3 shows results on SDS-PAGE electrophoresis of pressure-shocked yeast. Pressure shock treatment induced heat shock proteins (hsps) of 106, 104, 87, and 70 in the cells. Data on cells heat shocked at 43 °C are shown for comparison. Pressure shock treatment (25 to 70 MPa, 1 h) induced more hsp 106 than heat shock treatment at 43 °C (30 min), although the amounts of hsps 104, 87, and 70 obtained by pressure shock were apparently less than those induced by heat shock. On the other hand, as reported before, trehalose was not induced at all by pressure shock treatment [3]. These results suggest that both heat shock and pressure shock treatments are inducers of thermotolerance, but that their effects on yeast cells are physiologically different.

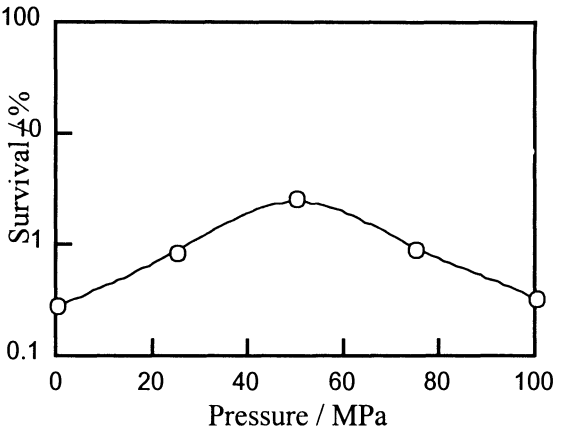

Fig. 2. Survival curve of pressure-shocked yeast cells. The cells were subjected to heat treatment at 51 °C for 10 min after being shocked at various pressures for 1 h. The medium did not contain trehalose

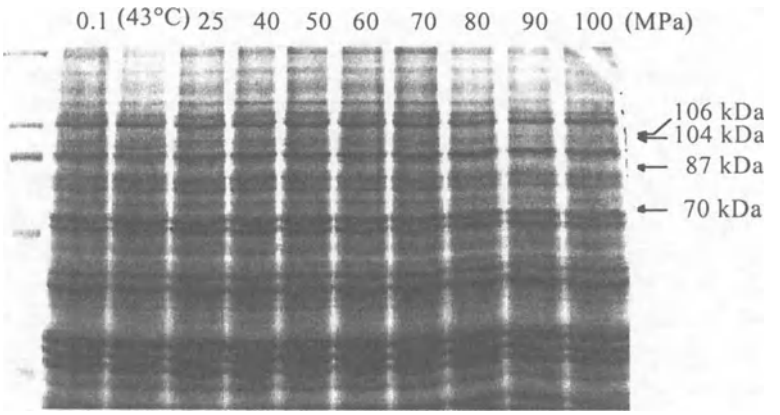

Fig. 3. SDS-PAGE electrophoresis of pressure-shocked yeast. Arrows show the heat-shocked proteins induced by pressure shock treatment

References

[1] Piper, P.W. (1993); Molecular events associated with acquisition of heat tolerance by the yeast *Saccharomyces cerevisiae*; FEMS Microbio. Rev. 11, 339-356.

[2] Fujii, S., Obuchi, K., Iwahashi, H., Fujii, T. and Komatsu, Y. (1996); Saccharides that protect yeast against hydrostatic pressure stress correlated to the mean number of equatorial OH groups; Biosci. Biotech. Biochem. 60 (3), 476-478.

[3] Miyashita, M., Tamura, K. and Iwahashi, H. (1996); Acquisition of stress tolerance by pressure shock treatment in yeast; High Pressure Bioscience and Biotechnology, Progress in Biotechnology, 13, 101-104.

Description of *Listeria* Behaviour Under Various Pressurization Strategies

R.F. Vogel, V. Herdegen and P. Klostermaier

Technische Universität München, Lehrstuhl für Technische Mikrobiologie, 85350 Freising, Germany
Rudi.Vogel@lrz.tu-muenchen.de

Abstract. The effect of high pressure on *Listeria innocua* was (partly) quantified and also mathematically described to estimate the contribution of dynamic and structural parameters. With increasing pressure times *Listeria* were increasingly inactivated following sigmoidal isobars. The lethal effect was referred to pressure build up rate and holding time only when a threshold pressure was surpassed. Selected experimental data were fitted to an adopted Gompertz equation forming a model sufficiently describing the inactivation of the *Listeria*.

1 Introduction

Listeria are food spoiling pathogens which are problematic in foods which cannot be pasteurized prior to consumption, e. g. fermented sausages or raw milk cheeses. For these desirable products it is tempting to develop novel preservation technologies including high pressure treatments [1–4]. The effective use of high pressure to inactivate food spoiling and pathogenic microorganisms requires a thorough knowledge of the influence of pressure dynamics on their inactivation. The relevant parameters include pressure height, holding time and possibly the velocity of pressure up- and downshifts [5]. Furthermore, repeated pressure treatments may have a different effect as compared to single pressurization. Such external technical parameters can be easily varied as compared to internal parameters such as pH, water activity or even the intrinsic microorganisms' properties and status. To assist the evaluation of results obtained preferably after variation of external parameters in pressurization mathematical models are valuable [6]. Internal parameters may be included in the model or just added as a qualitative or semiquantitative information. Such models are available for the description of microbial growth which can be adapted for their use in the description of pressure inactivation. We have chosen *Listeria innocua* which is closely related to the food pathogen *L. monocytogenes* to investigate parameters which affect the lethal action of high pressure on these bacteria.

2 Materials & Methods

2.1 Influence of the Growth Phase

To investigate the influence of the growth phase on the inactivation of *L. innocua* WSLC2012 samples of cultures were taken adjusted to a cell density of 6.5×10^9 colony forming units (CFU). After pressurization at 400 MPa for 5, 10, and 15 min, respectively, the CFU were determined on plate count agar. For all other experiments cells of the late exponential growth phase were used. Pressurization was performed in an 1.2 l autoclave. Selected experimental data were fitted to an adopted Gompertz equation with a constraint simplex routine.

3 Results & Discussion

3.1 Influence of the Growth Phase

The growth phase strongly affected the inactivation of *L. innocua* upon pressurization. Figure 1 shows that exponentially growing cells were much more sensitive to pressurization than stationary phase cells. An 8 h old culture was most pressure sensitive. Because of the high pressure resistance a 24 h old culture was chosen for all subsequent experiments.

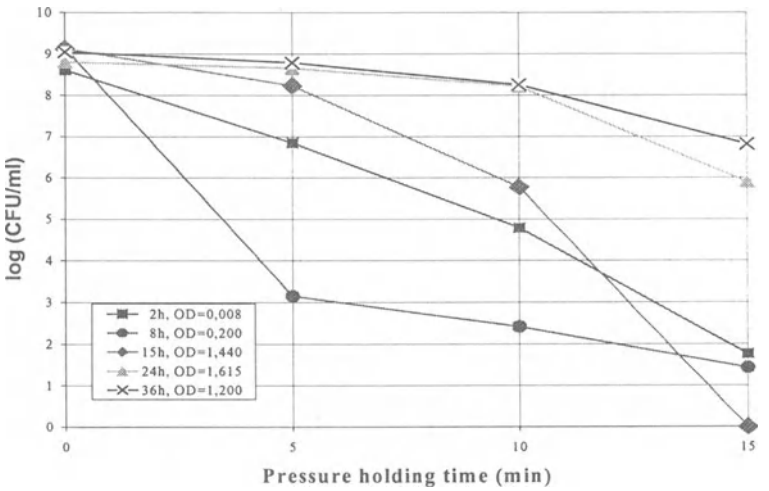

Fig. 1. Influence of the growth phase on pressure inactivation of *L. innocua*

3.2 Influence of Holding Time and Pressure Height

The dependence of the inactivation of *L. innocua* on the holding time at different pressure heights is shown in Fig. 2. The difference in inactivation at 15 min as compared to Fig. 1 may be due to a variation in the growth phase of the cells. All experiments were performed twice, and a modeled curve calculated by the Gompertz equation was introduced. It is clearly demonstrated that the inactivation follows a sigmoidal curve rather than a linear decline. The calculated coefficients *A*, *B*, *C* and *M* are summarized in Table 1.

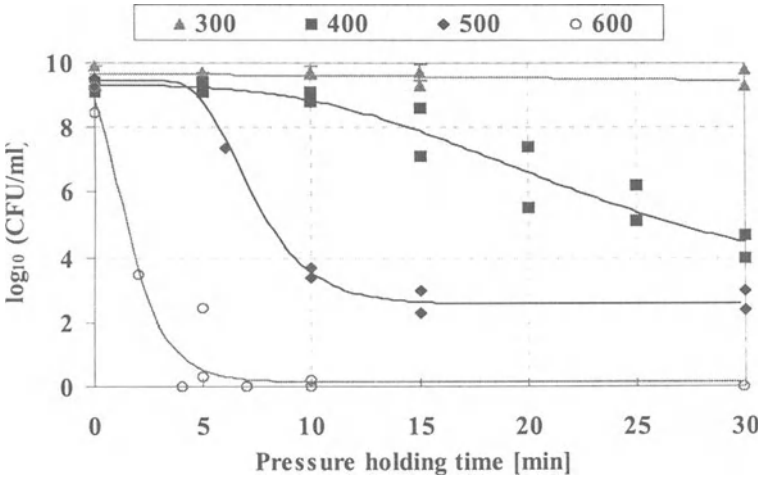

Fig. 2. Dependence of the inactivation of *L. innocua* on the holding time at different pressure heights (given in MPa)

Table 1. Coefficients calculated from the Gompertz equation

Pressure [MPa]	A [ml^{-1}]	B [min^{-1}]	C	M [min]
300	9.776	0.0058	–0.3616	23.817
400	9.310	0.1010	–4.8000	18.900
500	9.452	0.5502	–6.8840	6.5540
600	9.722	0.8308	–9.5730	1.0466

Correlation of the calculated coefficients for *L. innocua* to the various pressure heights results in Fig. 3. Coefficients calculated from this dependence are given in Table 2. With the calculated coefficients it was possible to calculate a theoretical

value for each variable A, B, C and M in a pressure range between 300 and 600 MPa.

Table 2. Coefficients calculated from the measurements and used in the modified Gompertz equation

Coefficient	B	C	M
curve	Polynom 2. degree	linear	linear
equation	$y = dx^2+ex+f$	$y = dx+e$	$y = dx+e$
d	$5 \cdot 10^{-6}$	–0.0297	–0.0807
e	–0.0012	7.9685	48.875
f	–0.0633	-	-
coefficient of determination: R^2	0.9696	0.9735	0.9694

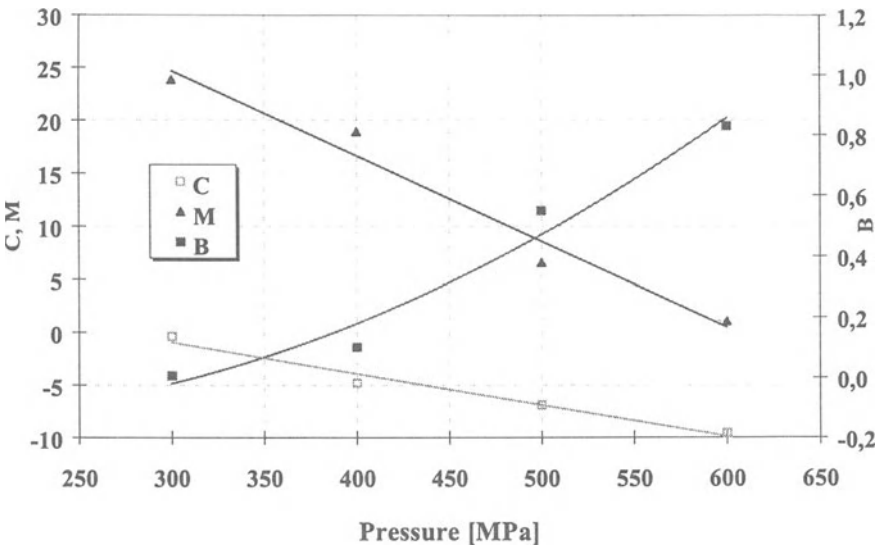

Fig. 3. Correlation of the calculated coefficients for *L. innocua* to the various pressure heights

Combination of the equations depicted in Table 2 with the Gompertz equation resulted in a modified Gompertz equation (1).

$$N = \sum_{n}^{1}(A/n) + C\mathrm{e}^{(-\mathrm{e}^{-B(t-M)})} \quad (1)$$

With N and A being the $\log_{10}$ of the current and initial cell counts, respectively, and $\sum_{n}^{1}(A/n)$ being the average of the As of all (n) experiments performed. The lag time [min] for a certain pressure can be calculated as $M-(1/B)$.

From this calculation data can be interpolated to estimate the inactivation at any pressure height/holding time combination in this range (Fig. 4).

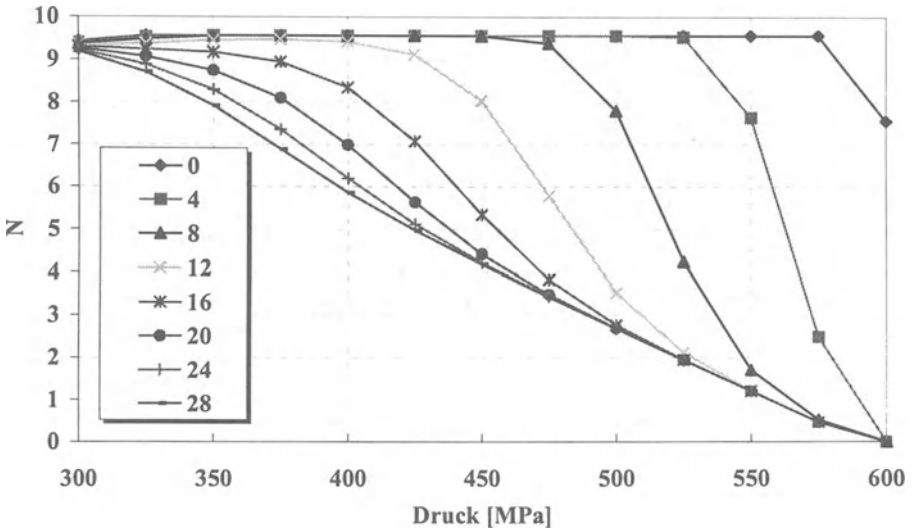

Fig. 4. Calculation of *Listeria innocua* inactivation by the modified Gompertz equation (1) with $N = \log_{10}$(CFU/ml) at various holding times (given in min)

Figure 4 demonstrates that pressure up- and downshift without holding time did not result in inactivation up to a pressure of 575 MPa.

At low pressures no inactivation was observed at all while the curves followed a plateau. At a certain threshold pressure a sharp bend is observed which at longer holding times is smoothed and shifted to lower pressures.

4 Conclusions

With increasing pressure times *L. innocua* was increasingly inactivated following sigmoidal isobars. In analogy to growth curves an inactivation lag-phase was observed which was correlated to the pressure height. The lethal effect could be referred to pressure build up rate and holding time rather than pressure release. The velocity of pressure up- and downshift did not per se alter lethality. However, this

velocity determines the time the bacteria are over the threshold pressure. Thus, at the same maximal pressure, the lethal effect is increased at slow pressure shifts. Further experiments indicated that the presence of a matrix had a protective effect. The data obtained at the various pressure/time combinations were used to establish a mathematical model on the lethal effects which sufficiently described the inactivation of *L. innocua*. This approach can be transferred to other *Listeria* [7] and microorganisms which exhibit a sigmoidal inactivation characteristic.

References

[1] Chilton, P., Isaacs, N.S., Mackey, B. and Stenning, R. (1997); The effects of high hydrostatic pressure on bacteria, In: High Pressure Research in the Biosciences and Biotechnology, K. Heremans (Ed.); Leuven University Press, Leuven, Belgium, pp. 225-228.

[2] Cheftel, J.C. (1995); Review: High-pressure, microbial inactivation and food preservation; Food Sci. Technol. Int. 1, 75-90.

[3] Kalchayanand, N., Sikes, T., Dunne, C.P. and Ray, B. (1994); Hydrostatic pressure and electroporation have increased bactericidal efficiency in combination with bacteriocins; Appl. and Environ. Microbiol. 60, 4174-4177.

[4] Ludwig, H., Gross, P., Scigalla, W. and Sojka, B. (1994); Pressure inactivation of microorganisms; High Pressure Research, 12, 193-197.

[5] Herdegen, V. (1998) Hochdruckinaktivierung von Mikroorganismen in Lebensmitteln und Lebensmittelreststoffen. PhD Thesis, Technische Universität München.

[6] Whiting, R.C. and Buchanan, R.L. (1994); Scientific Status Summary: Microbial modeling; Food Technol. 48, 113-120.

[7] Simpson, R.K. and Gilmour, A. (1997); The resistance of *Listeria monocytogenes* to high hydrostatic pressure in foods; Food Microbiol. 14, 567-573.

Microorganisms in Food

Pathogen Inactivation by High Pressure Treatment of Foods

M.F. Patterson, M. Linton and J.M.J. McClements

Food Science Division, Department of Agriculture for Northern Ireland, Newforge Lane, Belfast BT9 5PX, Northern Ireland, UK
Margaret.patterson@dani.gov.uk

Abstract. There is increasing commercial interest in using high pressure processing to produce a range of high quality foods including fruit, dairy and meat products. However, the microbiological safety of such products is of concern and processors need to choose appropriate treatment conditions to achieve known, satisfactory levels of inactivation.

Different species of pathogens, and even strains of the same species, are known to vary in their resistance to pressure. The substrate can also affect the level of kill. For example, certain strains of *Escherichia coli* O157:H7 have been found to be resistant to pressure. A pressure treatment of 600 MPa for 30 min at 20 °C resulted in $<2\text{-log}_{10}$ inactivation in milk and $<3\text{-log}_{10}$ inactivation in poultry meat. Therefore, pressure alone would not be sufficient to guarantee the microbiological safety of such products. This problem could be overcome by using pressure in combination with other preservation techniques such as mild heating or use of acidic environments. This paper illustrates how these combination treatments have been successfully applied to improve the microbiological safety of a range of products.

1 The Simultaneous Application of Pressure and Heat for the Inactivation of Pathogens in Milk and Poultry Meat

The aim of this study was to produce simple models that could predict the pressure/temperature conditions required to achieve a known level of kill of pathogens in milk and poultry meat.

1.1 Materials & Methods

Two vegetative pathogens which were known to be relatively resistant to pressure (*Escherichia coli* O157:H7 NCTC 12079 and *Staphylococus aureus)* were used in this study. Inocula of cells in the late log to early stationary phases of growth were prepared and the substrates (poultry meat which had been sterilised by irradiation and UHT milk) were

inoculated to a level of approximately 1×10^9/g or ml as described by Patterson and Kilpatrick [1]. Pressurisation of samples was carried out using a Stansted Food Lab 9000 high-pressure isostat. The pressure transmission fluid was distilled water containing 10% Dromus oil B (Shell UK Oil, London, England). The come-up rate was approximately 200 MPa/min and pressure release time was 2 min. The treatment time was 15 min, excluding come-up and release times. Pressure studies were carried out from 20 – 60 °C (temperature at start of the experiment). The temperature was controlled by an electrical heating device which surrounded the pressure chamber. The temperature increase from adiabatic heating effects during pressure increase was approximately 2 °C/100 MPa.

1.2 Results & Discussion

The simultaneous application of high pressure and heat was more lethal than either treatment alone. The substrate was found to have a significant effect on the survival of the pathogens. The pressure-temperature inactivation curves for each organism, in each substrate, were fitted using the Gompertz equation. Polynomial expressions derived from the Gompertz variables were used to devise simple models that predicted the inactivation of each pathogen at various pressure-temperature combinations. An example of the predictions obtained is given in Table 1. The use of such models will provide flexibility in selecting optimum processing conditions without compromising microbiological safety.

Table 1. Predicted pressure treatment (15 min) required at various temperatures for a 6-$\log_{10}$ inactivation of *Escherichia coli* O157:H7 NCTC 12079 and *Staphylococcus aureus* NCTC 10652 in poultry meat and milk

Temperature during pressure treatment (°C)	Estimated pressure (MPa) required for 6-$\log_{10}$ reduction in pathogens in substrate			
	Escherichia coli		*Staphylococcus aureus*	
	Poultry meat	UHT milk	Poultry meat	UHT milk
30	717*	862*	768*	621
35	659	762*	760*	621
40	594	651	725*	613
45	517	532	658	583
50	422	405	549	517

*predicted values outside experimental range.

2 Effect of Pressure Followed by Mild Heat on the Inactivation of *Escherichia coli* O157:H7

Previous studies have shown that, although certain strains of *E. coli* O157:H7 could survive relatively high pressures, they were sub-lethally injured [1]. The aim of this study was to test the hypothesis that pressure-injured cells would be more sensitive to subsequent heating than non-injured cells.

2.1 Materials & Methods

E. coli O157:H7 NCTC 12079 was grown for 18 h in methionine assay medium (MAM) at 30 °C. For each 100 ml of sample required 1 ml of this broth was added to 100 ml of MAM and incubated for 18 h at 30 °C to give 10^6 cells/ml. Samples were pressurised at 100, 200 and 300 MPa for 30 min at 30 °C, as described above. The samples were then heated for various time intervals at 55, 58 and 60 °C and heat D_{10} values calculated.

2.2 Results & Discussion

Pressure injury was found to sensitise cells to subsequent heating at temperatures of 55–60 °C. For example, the heat $D_{55\,°C}$ value in non-pressurised cells treated in MAM was 25 min, while cells that were pressurised at 300 MPa for 30 min at 30 °C had a heat $D_{55\,°C}$ value of 0.9 min. Other studies have shown that this sensitising effect was also found when the treatment was carried out in milk [2]. These findings are of relevance as many pressure treated foods will be stored and then cooked/reheated prior to consumption.

3 Effect of Pressure and pH on the Inactivation of *Escherichia coli* O157:H7 in Orange Juice

High pressure treatment of fruit products has the benefits of giving microbial kill without the loss of quality attributes, such as flavour, colour and vitamins, and without the use of preservatives. However, there have been several cases of food poisoning associated with *E. coli* O157:H7 found in unpasteurised apple juice [3]. This has raised doubts about the microbiological safety of other unpasteurised fruit juices. This experiment investigated the effect of high pressure on the survival of a pressure resistant strain of *E. coli* O157:H7 in orange juice over a pH range of 3.4–5.0. The overall aim was to achieve at least a 6-$\log_{10}$ inactivation of the pathogen, equivalent to a conventional heat pasteurisation.

3.1 Materials & Methods

Locally purchased pasteurised orange juice (initial pH 3.68–3.76) was adjusted to the required pH (3.4, 3.6, 3.9, 4.5 and 5.0) using 10 M NaOH or 37% HCl. *E. coli* O157:H7 NCTC 12079 was grown in tryptone soya broth containing 0.6% yeast extract, for 18 h at 37 °C. The resulting culture was centrifuged at 2400 × g for 20 min, washed in PBS and resuspended in the juice samples to give approximately 10^8 cells/ml. The samples were packaged in polythene pouches and left overnight at 3 °C. The next day the pouches were pressurised at 400, 500 or 550 MPa for up to 5 min at 20 °C (as described above) or were held at ambient pressure (controls). Duplicate samples from each treatment were taken and the numbers of surviving

organisms were enumerated on tryptone soya agar containing 0.6% yeast extract (TSAYE). Plates were incubated at 37 °C for 24 h. The whole experiment was carried out on three separate occasions.

3.2 Results & Discussion

Pressure, pH and treatment time interacted to affect the survival of the pathogen. For example, a pressure treatment of 550 MPa for 5 min at 20 °C was sufficient to give a 6-$\log_{10}$ inactivation at pH 3.4, 3.6 and 3.9, but not at pH 4.5 and 5.0 (Table 2). A pressure treatment at 400 MPa was not sufficient to achieve a 6- $\log_{10}$ kill, irrespective of the pH or treatment times used in this study. It was concluded that processing conditions for pressure treatment of fruit juices should be considered carefully to ensure they are microbiologically safe.

Table 2. Effect of pressure (MPa), pH and treatment time on the inactivation of *Escherichia coli* O157:H7 in orange juice

Pressure treatment	Log_{10} inactivation achieved in orange juice (SEM = 0.22)				
	pH 3.4	pH 3.6	pH 3.9	pH 4.5	pH 5.0
400 MPa					
1 min	1.9	1.1	0.9	0.8	0.4
2 min	3.3	1.8	1.4	1.1	0.8
4 min	5.9	3.1	2.5	2.6	1.6
500 MPa					
1 min	5.4	3.5	1.9	3.2	2.0
2 min	>6.0	4.4	3.1	4.2	3.1
5 min	>6.0	>6.0	5.6	5.2	3.9
550 MPa					
1 min	>6.0	4.1	4.1	3.5	2.8
2 min	>6.0	5.9	4.0	3.9	3.5
5 min	>6.0	>6.0	>6.0	5.9	5.5

References

[1] Patterson, M.F. and Kilpatrick, D.J. (1998) The combined effect of high hydrostatic pressure and mild heat on inactivation of pathogens in milk and poultry. *J. Food Prot.* **61**: 432-436.

[2] Linton, M., McCann, G.J. and Patterson, M.F. (1998) The effects of sub-lethal pressure treatment on *E. coli* O157:H7. These Proceedings.

[3] McCarthy, M. (1996) *E. coli* O157:H7 outbreak in USA traced to apple juice. *Lancet* **348**: 1299.

Building Fail-Safe Models To Describe the Effect of Temperature and Pressure on the Kinetics of Inactivation of Infectious Pathogens in Foods

J.C. Hellemons and J.P.P.M. Smelt

Unilever Research Vlaardingen Dept Microbiology and Preservation Olivier van Noortlaan 120, 3133 AT Vlaardingen/ PO Box 3130 AC Vlaardingen The Netherlands Phone: +314605028; Fax: +314605188
Johan.Hellemons@Unilever.com

Abstract. When building models to describe inactivation of pathogens several aspects have to be addressed: the choice of the strain, type of substrate to be pressurised, cultivation conditions of the strain, the choice of the mathematical model to describe the inactivation and finally validation in real food situations. With high pressure treatments, temperature effects play an important role caused by adiabatic heating. A model must describe effects in dynamic situations and thus should describe inactivation due to the combined effect of pressure and temperature. Here a distribution model is presented that describes the combined effect of heat and pressure on the inactivation kinetics satisfactorily.

1 Introduction

High pressure is an interesting alternative to heat pasteurization as it can kill microorganisms and leave small molecules such as flavours and vitamins intact. The primary goal of industrial preservation processes is to achieve a safe product. This means that the number of viable pathogenic microorganisms has to be reduced to an acceptable low level. As temperature always plays an important role in pressure treatments, the combined effects of pressure and temperature need to be built into an appropriate model. To build a fail-safe model several factors have to be taken into account. Factors that affect apparent resistance include (1) the variation of 'intrinsic' resistance between strains of one species, (2) the physiological state of the microorganisms, (3) the composition of the pressure menstruum, and (4) the recovery conditions. Finally an appropriate mathematical model has to be chosen that adequately predicts the combined effects of heat and pressure on inactivation of the investigated microorganisms. Here the various phases of model building will be illustrated with *Listeria monocytogenes*.

2 Materials & Methods

Strains of *Listeria monocytogenes* were grown in BHI-broth pH 7 at 30 °C and left in the stationary phase for 48 h. The culture was 100 fold diluted in 50 mM ACES (Merck A-9758) pH 7.0. Heat treatments were carried out according to the method of Kooiman and Geers [3]. After treatment the samples were stored for 2 h on ice and a serial dilution was made in peptone physiological saline. Pour plates, made by mixing 1 ml samples in PCA-agar supplemented with 0.5% pyruvate, were incubated for 5 d at 30 °C. For the inactivation kinetics a 96 h stationary culture of *Listeria monocytogenes* VBLLi 01-105 was used. Before the treatment at different temperature and pressure combinations the culture was washed twice with 50 mM ACES pH 7.0 by centrifugation at 2000×g for 15 min.

3 Results & Discussion

3.1 Intra Species Variation of Pressure and Heat Resistance

To build a fail-safe model it is necessary to choose a strain that is the most resistant for the inactivation process. A specific problem when describing inactivation by high pressure is the generation of adiabatic heat. Therefore a model is needed that combines the effect of pressure and temperature. Ideally, the strain that will be used to build the model is the one most resistant to heat and pressure. To select the most appropriate strain, 100 strains of *Listeria monocytogenes* were compared with respect to heat and pressure resistance. Results showed that there was a weak positive correlation between heat resistance and pressure resistance. Strain VBLLi 01-105 was selected to build the model.

3.2 Effect of Physiological State on Pressure Resistance

Microorganisms in the stationary phase are much more resistant towards high pressure than those in exponential phase [1]. In Fig. 1 the effect of prolonging the stationary phase is shown. The resistance of the strain increased during prolonged incubation times.

3.3 Effect of Substrate During Pressure Treatment

It is well known that due to pressure or temperature there is a change in pH. It is expected that a shift to lower pH will cause more inactivation. Besides, it is important to distinguish the pH effect and the pressure effect in order to increase the predictive power of inactivation models. Apart from the purely physical properties of the buffers, the physiological effects are different. E.g. the pH of Tris

buffer is pressure stable but this buffer is slightly toxic to the bacterial cell. We have selected 10 organic buffers that have a relatively small reaction volume and hence remain pH stable [2]. Phosphate buffer has been used as a reference buffer because of its general use in resistance studies of microorganisms. Pressure treatment was carried out at 350 MPa at 21 °C for 5, 15 and 45 min or a heat treatment for 5, 10 and 20 min at 59 °C. In both cases *L. monocytogenes* was most resistant in ACES buffer.

3.4 Effect of Recovery Conditions After High Pressure Treatments

As with heat, there could be an effect of recovery conditions. Several combinations of media (PCA, BHI and TSA) and several additives (pyruvate and catalase) were tested. Pyruvate and/or catalase in the media did not improve the recovery of *L. monocytogenes*.

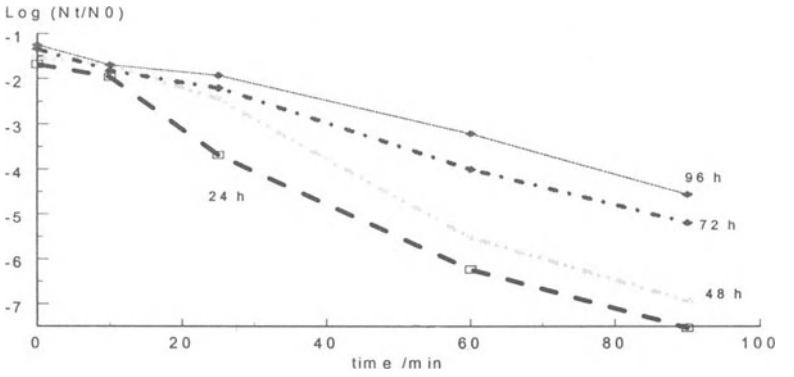

Fig. 1. Effect of duration of stationary phase towards pressure resistance

4 Effect of Temperature/Pressure Combinations

After having optimized the culture conditions, buffer, recovery conditions and having selected the most appropriate strain, kinetic data were gathered in a matrix ranging from 50 to 600 MPa and −15 to 60 °C. The data were modeled with distribution models according to Smelt *et al.* [4]. The relation of the distribution parameters with temperature and pressure was fitted by a linear regression as a quadratic model. An example of the prediction is given in Fig 2. At 35 °C the inactivation of *L. monocytogenes* reached a minimum. At higher and lower temperature the inactivation increased. These results were similar to results found with enzyme inactivation.

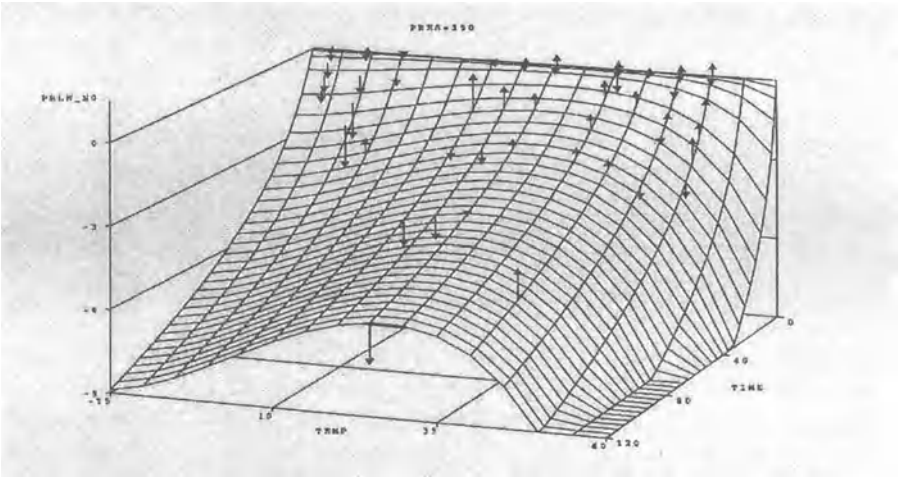

Fig. 2. The relation of pressure and temperature of inactivation of *L. monocytogenes* at different times. Predicted (*surface*) and observed values (*arrows*)

5 Conclusions and Future Work

A prototype model describing the combined effect of pressure and temperature has been build for *L.monocytogenes* in neutral buffer. This model will be extended with the effect of pH. The model will be tested in real food systems and validated with some other strains.

References

[1] B.M. Mackey, K. Forestiere and N. Isaacs. 1995. Factors affecting the resistance of *Listeria monocytogenes* to high hydrostatic pressure. Food Biotechnology, 9, 1-11.

[2] Y. Kitamura and T. Itoh. 1987. Reaction volume of protonic ionization for buffering Agents. Prediction of pressure dependence of pH and pOH. Journal of Solution Chemistry, Vol. 16, 9, 715-725.

[3] W.J. Kooiman and J.M. Geers 1975. Simple and accurate technique for the determination of heat resistance of bacterial spores. Journal of Applied Bacteriology, 38, 185-189.

[4] J.P.P.M. Smelt, M.F. Patterson, H.G.A.N. Cuppers, R.K. Simpson, J.C. Hellemons and A. Gilmour. 1998. The use of distribution models to described physical inactivation of bacteria. Applied Environmental Microbiology. Submitted for publication.

Advances in Bacterial Spores Inactivation in Thermal Treatments Under Pressure

P. Rovere[1], N.G. Lonnerborg[2], S. Gola, L. Miglioli, N. Scaramuzza and N. Squarcina

[1]ABB Industria, via Edison, 50 Sesto San Giovanni, Milan, Italy
[2]ABB Pressure Systems AB, Vasteras, Sweden
Stazione Sperimentale per l'Industria delle Conserve Alimentari, Parma, Italy
rovere.pierpaolo@ntt.it
<SecondoGola> ssicapr@rsadvnet.it

Abstract. The effect of heat treatments coupled with high pressure on *Clostridium sporogenes* putrefactive anaerobe spores in a model system was studied. A meat broth used as model system was sterilised and inoculated with spores of *Clostridium sporogenes* putrefactive anaerobe 3679 ATCC 7955 (2×10^6 spores/ml). The inoculated meat broth (2.5 ml) was packaged in sterilised PE vials. The vials were kept at 0 °C until processed. The packages were subjected to pressures from 600 to 800 MPa and the processing time was up to 20 min using an experimental press (the ABB QFP 15000 high pressure food processor). The temperatures of the samples (from 90 to 110 °C) were kept constant during the process using an internal control system placed into the press vessel. The processed samples were aseptically opened and the surviving spores were counted using TSC Agar Base (OXOID). The plates were incubated at 30 °C for 7 d under anaerobic conditions. "*D*" and "*z*" values were calculated for various processing pressures (600, 700 and 800 MPa). The "*D*" values decreased from 1.28 to 0.69 min as the processing pressure increased from 600 to 800 MPa. The "*z*" values increased from 16 to 17.9 °C as the processing pressure increased from 600 to 800 MPa. The heat treatment in combination with high pressure appears to be as effective or better than thermal processing alone (D_{120}=1.9', z=11.8 °C at ambient pressure). From these results it has been possible to establish a relation between time, temperature and pressure. This relation is able to calculate the *D* value at known pressure and temperature in a predictive way. This relation seems to have a good correlation with reality. Its use will allow the calculation and prediction of the effect of any processing at high pressure conditions for *Clostridium sporogenes* putrefactive anaerobe 3679 ATCC 7955. Further studies are performed to verify and optimise the relation founded.

1 Introduction

Various tests have confirmed the efficacy of the use of pressure [1] in stabilising preserves when combined with other interventions on the product [2], such as acidification, a reduction in water activity and refrigerated storage [3]. At the same time it has already been shown [4] that the problem of inactivating bacterial spores can be solved by using "under-pressure heat treatment" exploiting the principle that an increase in pressure causes a uniform and immediate practically adiabatic heating of the alimentary matrix. Therefore, by means of appropriate preheating of the product, immediately followed by baric treatment, inactivation of both spores and enzymes can be achieved. It has practically been proved that under high pressure conditions a greater efficacy in heat treatment can be obtained which results in shorter treatment times or the possibility to apply lower operating temperatures to obtain the same effect [5, 6]. These possibilities are of even greater interest when we consider that the increase in temperature is conditioned neither by the geometry or dimensions of the system nor by factors connected with the problems of heat exchange. At the same time it is important to note that in these conditions heat damage phenomena can be greatly limited not only because of what has been said, but also thanks to the capacity of pressure to slow down the kinetics of the reactions from heat damage [7, 8].

From data already collected, it has been demonstrated that the common rules inherent in the calculation of sterilisation treatments are also applicable in these extreme operating conditions [9, 10]. A kinetic interpretation of the phenomenon, capable of evaluating the effects of modifications to each of the parameters (pressure, p, time and temperature, T), has been founded for analogies arising with traditional heat treatment.

The aim of our work was therefore to use the data collected to develop a method to evaluate the effect of HPP during its application.

2 Materials & Methods

2.1 Microbial Stock

A stock of *Clostridium sporogenes* PA-3679, ATCC 7955 was used. The spores were prepared in the following way: the cultures were activated in TSP medium [11], inoculated in meat broth and incubated anaerobically at 30 °C for three weeks. The spores were then collected by means of centrifugation from the culture medium, resuspended in sterile water, treated at 80 °C for 30 min and kept at 1 °C until used. The meat broth used in the tests was composed of the following (g/100g): meat extract 5, yeast extract 1, peptone 2, distilled water 92. The mixture obtained was treated at 121 °C for 15 min, inoculated with *C. sporogenes* spores (the inoculation varied from 1×10^6 to 3×10^6 spores/ml) and then subdivided and placed into sterile glass tubes (2.5 ml/tube) for the heat resistance tests at

atmospheric pressure and in sterile polythene tubes (4.5 ml/tube) for heat treatment under pressure. The heat resistance was determined of the *C. sporogenes* PA 3679 spores suspended in the meat broth we used; the value of $D_{0.1}$ (at atmospheric pressure =0.1 MPa) was calculated at 110, 115 and 121 °C in order to obtain the value of $z_{0.1}$. The tests were carried out by immersing the tubes containing the spore suspension in an oil bath thermostated at the three different temperatures. To calculate the duration of the treatment, the starting point was taken as being the moment when the required temperature was reached in the tube. Immediately after their extraction from the bath, the tubes were cooled by immersion in melting ice. The tests were conducted using an experimental isostatic press (QFP-15, ABB Pressure Systems) capable of reaching a pressure of 1500 MPa. The temperatures considered were those reached by the sample under pressure, inside the sample loading container; here, thanks to a system of measurement and control, the temperature was kept constant throughout the treatment [12].

To obtain the desired treatment combinations, after a series of preliminary tests carried out with the intention of standardising the procedure, the individual loads were pre-heated to the required temperature (60–95 °C) in an external water bath. Two tubes were introduced into each load and treated simultaneously; after the hyperbaric treatment, they were cooled rapidly in melting ice and kept at a temperature of 1 °C until microbial analysis was carried out. The number of spores surviving the different treatments were counted in M5 medium [13] shown by inclusion and then incubated in anaerobiosis at 30 °C for 7 d. Table 1 shows the D_T^P values calculated from the preceding tests conducted using the same method.

Table 1. *D* values obtained during the various tests

Pressure (MPa)	Temperature (°C)	*D* (min)
0.1	0	nd
0.1	110	13.3
0.1	115	6.5
0.1	120	1.9
400	90	76.9
400	100	28.7
400	110	6.1
500	100	7.75
600	90	16.7
600	100	3.5
600	108	1.3
700	93	6.7
700	100	3.2
700	108	0.9
800	90	5.3
800	93	5.3
800	98	2.8
800	108	0.7
1000	90	5.35
1200	90	4.38

3 From the Algorithm to a Mathematical Model

Table 2 presents the algorithm we constructed by means of the application of conventional sterilisation rules to the data collected taking into consideration their modification due to the continuous pressure variation. This table allows the calculation, at a given temperature (°C) and pressure (MPa), of the D_T^P value in minutes. From the development of the same algorithm for p values from 0 to 1500 MPa and for temperature values from 60 to 120 °C, a matrix was obtained which was then put into an electronic sheet for the calculation of the three-dimensional regressions at two independent variables (Fig. 1). The simplest equation among those of the lowest grade capable of describing the behaviour of the points calculated is (1), where a, b and c (see Table 3) are given coefficients, $z=D_T^P$, $x=T$ and $y=p$.

Thus:

$$\ln D_T^p = 22.9025 - 0.1835 \times T - 0.0085 \times p, \tag{1}$$

from which we get:

$$\log D_T^p = \frac{22.9025 - 0.1835 \times T - 0.0085 \times p}{2.30259}, \tag{2}$$

thus:

$$D_T^p = 10^{\frac{22.9025 - 0.1835 \times T - 0.0085 \times P}{2.30259}} \tag{3}$$

or generalising:

$$D_T^p = 10^{-(AT+BP-C)}, \tag{4}$$

where A, B and C are given constants. From (4) and from Fig. 2, relating to the study of function (1), it is evident that the pressure and temperature during treatment can influence the inactivating capacity. Indeed, from (4) it can be seen

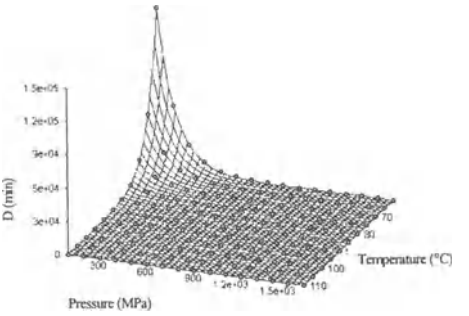

Fig. 1. Regression analysis on algorithm

Table 2. Development of the algorithm of D_T^P

Pressure	Temperature (°C)										
(MPa)	121	120	115	110	105	100	95	90	85	80	75
0.1	1.73037	2.084189	5.283573	13.39425	33.95541	86.07946	218.2178	553.1982	1402.398	3555.183	9012.651
100	1.297968	1.547781	3.731959	8.998377	21.69659	52.31411	126.1381	304.14	733.3324	1768.187	4263.395
200	0.973339	1.150266	2.651359	6.111377	14.08671	32.46983	74.84287	172.5126	397.6412	916.5621	2112.673
300	0.729901	0.855594	1.893586	4.190853	9.275127	20.52756	45.43126	100.5477	222.5306	492.5011	1089.995
400	0.547349	0.63689	1.358526	2.897818	6.181221	13.18492	28.12423	59.9907	127.9638	272.9546	582.2286
500	0.410454	0.474401	0.978488	2.018205	4.162698	8.585874	17.709	36.52614	75.33789	155.39	320.5035
600	0.307797	0.35357	0.707181	1.414447	2.829061	5.658458	11.31759	22.63652	45.27572	90.5568	181.1243
700	0.230815	0.263646	0.512639	0.996786	1.93817	3.768616	7.327771	14.24826	27.7046	53.86936	104.7446
800	0.173087	0.19668	0.372602	0.705879	1.337256	2.533373	4.799365	9.092186	17.22475	32.63153	61.81901
900	0.129797	0.146781	0.271457	0.502033	0.92846	1.717094	3.175594	5.872946	10.86143	20.08713	37.14915
1000	0.097334	0.10958	0.198184	0.35843	0.648247	1.172403	2.120378	3.834862	6.935633	12.54361	22.68605
1100	0.07299	0.081833	0.14496	0.256785	0.454874	0.805773	1.427361	2.528453	4.478947	7.934088	14.05459
1200	0.054735	0.061129	0.106209	0.184535	0.320624	0.557072	0.967894	1.681681	2.921863	5.076635	8.820476
1300	0.041045	0.045675	0.077936	0.132984	0.226914	0.387188	0.660668	1.127314	1.923562	3.28222	5.600529
1400	0.03078	0.034135	0.057268	0.096076	0.161183	0.270411	0.453658	0.761086	1.276845	2.142116	3.593749
1500	0.023081	0.025517	0.042133	0.06957	0.114875	0.189681	0.313202	0.51716	0.853936	1.410021	2.32823

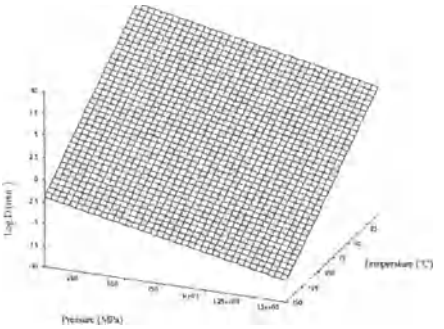

Fig. 2. Study of the function (2)

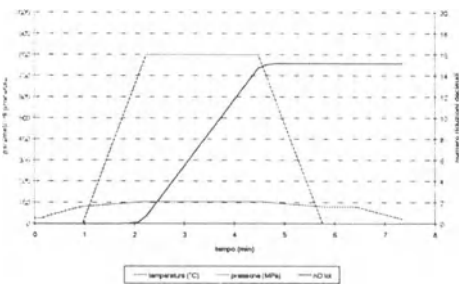

Fig. 3. Evaluation of the sterilising effect

that even slight pressure variations, and yet more so temperature variations, to which the former are in any case always linked, are able to generate sizeable differences in the kinetics of inactivation by modifying the decimal reduction time. Figure 2, where, by means of the logarithmic expression, spatial compression of the z axis can be exerted, clearly shows the variation in the velocity of the process as a function of pressure and temperature variation. From (4) it can be seen that it is possible to calculate, at any time in the course of HP treatment, the value of D_T^P. Thus, hypothesising finite time intervals under constant conditions, their effect in terms of decimal reductions is equal to:

$$nD = \frac{t}{D_{T_1}^{P_1}} \cdot$$

Thus, by supposing we operate in infinitesimals of time, or else by taking temperature and pressure measurements at very frequent intervals during the process, we can theoretically know the contribution of every infinitesimal t_i at the value of nD obtained. In fact, by generalising and then simplifying:

$$\int_0^t \frac{1}{D_p^T} \mathrm{d}t = \sum_0^t \frac{t}{D_p^T} \cdot$$

Thus, from the operative viewpoint, given the frequency f of measurements effected by the control systems (Hz) and having measured p (MPa) and T (°C), it is possible at any given moment to determine dynamically the nD obtained for the microbial form under consideration (Fig. 3). As regards the PA spores considered by us:

$$nD = \sum_0^t \left(\frac{10^{9.9464 - 0.7969 \times Tt_i - 0.0037 \times pt_i}}{f \times 60} \right) \tag{5}$$

Table 3. Results of regression analysis on algorithm. Statistical parameters in equation (1)

	$\ln z=a+bx+cy$
a	22.9025 (±0.0376)
b	–0.1835 (±0.0006)
c	–0.0085 (±0.0000)
r (correlation coef.)	1
r^2	0.99954
adjusted r^2	0.99953
statistical F	225353

4 Conclusions

In view of what has been observed from the experiments we carried out here on PA3679 *C. sporogenes* spores, we can confirm not only that it is possible to achieve sterilisation by the use of heat treatments under high pressure conditions, but also that this type of process is technically manageable. The model proposed by us, (1), although needing to be backed up by further and more detailed studies on other microbial forms, is surprising as much for its simplicity as for its capability to describe the effects of treatments under both conventional and high pressure conditions. In the light of the experiments conducted by us on non-spore bacterial forms [14, 15], it is highly probable that a model similar to this one – that is, one based on the combined effect of p and T – may also be able to describe the kinetics of the inactivation of vegetative microbial forms. The presence of a precise relationship between process parameters applied and effect obtained is such as to allow, as shown, for the calculation of the latter also during treatment, by means of appropriate monitoring of the parameters; this condition renders the technique an applicable technology in that it is measurable. Knowledge of the kinetic parameters of this process and of the relationships which exist between them will pave the way for a detailed study of the technique of high pressure heat treatment leading to the optimisation necessary for its future application. Although convinced that much remains to be done, we consider that a further step has been taken towards the understanding and application of HPP, the most promising of the new food technologies.

References

[1] P. Rovere, D. Tosoratti, A. Maggi, *Industrie Alimentari, 35*, 1062, 1996.
[2] G. Carpi, E. Vicini, A. Maggi, P. Rovere, M. Previdi e, G. Dall'Aglio, in "*L'impiego dell'alta pressione nell'Industria limentare*" Eds. G. Dall'Aglio, C. Lerici e, A. Zamorani, p. 77, RAISA-CNR, 5 maggio 1995 Parma.
[3] G. Carpi, S. Gola, A. Maggi, P. Rovere, M. Buzzoni, *Ind. Cons., 70*, 386, 1995.
[4] P. Rovere, G. Carpi, A. Maggi e, G. Dall'Aglio, in "*Ricerche ed innovazioni nell'industria alimentare*" Ed. S. Porretta, p. 455, Chiriotti, Pinerolo, 1994.
[5] S. Gola, C. Fornari, G. Carpi, A. Maggi, A. Cassarà e, P. Rovere, in "*High Pressure Bioscience and Biotechnology*" Eds. R. R Hayashi and C. Balny, p. 253, Elsevier, Tokyo 1996.
[6] L. Miglioli, S. Gola, A. Maggi, P. Rovere, G. Carpi, N. Scaramuzza e, G. Dall'Aglio in "*High Pressure Research in the Biosciences and Biotechnology*" Ed. K. Heremans, p. 227, Leuven University Press, 1997.
[7] E. Kowalski, H. Ludwig, and B. Tauscher, in "*High Pressure Bioscience and Biotechnology*" Eds. R. R Hayashi and C. Balny, p. 473, Elsevier, Tokyo, 1996.
[8] N.S. Isaacs, M. Coulson, in "*High Pressure Bioscience and Biotechnology*" Eds. R. R Hayashi and C. Balny, p. 479, Elsevier, Tokyo, 1996.
[9] P. Rovere, A. Maggi, N.Scaramuzza, S. Gola L. Miglioli, G. Carpi, G. Dall'Aglio, *Ind. Cons. 71,* 473, 1996.
[10] P. Rovere, S. Gola, in "*Proceedings of Fresh Novel Foods by High Pressure*", 21-22 September Helsinki, Finland, in press.
[11] S.M. Zoha, H.L. Sadoff, *J. Bacteriol., 76*, 203, 1958.
[12] A. Maggi, S. Gola P. Rovere, L. Miglioli, G. Dall'Aglio, N.G. Lonneborg, *Ind. Cons. 71,* 8, 1996.
[13] A. Casolari, in "Proceedings of the 4th International Congress of Science and Technology", vol.3, p. 86, Valencia (Spain) 1974.
[14] A. Maggi, S. Gola, E. Spotti, P. Rovere, P. Mutti, *Ind. Cons.,69*, 26, 1994.
[15] A. Maggi, N. Squarcina, P. Rovere, S. Gola, *Ind. Cons., 72,* 48,1997.

Effect of Supercritical Carbon Dioxide on Some Bacteria and Yeasts of Interest in the Food Industry

F. Dellaglio[1], V. Dallacasa[1], A. Venturi[1], A. Bertucco[2] and P. Pallado[3]

[1]University of Verona, Istituto Policattedra, Facoltà di Scienze MM.FF.NN., Ca' Vignal, strada Le Grazie, 37134 Verona, Italy
[2]University of Padova, Istituto di Impianti Chimici, v. Marzolo, 9, 35131 Padova, Italy
[3]Exenia Group S.r.l., v. L. Da Zara, 13 – 35020 Albignasego (PD), Italy

Abstract. The sterilisation with supercritical carbon dioxide of some microorganisms of interest in food technology is considered as a first step for the application of this technique to complex media on a large scale. A sourdough yeast strain and several bacterial species (*Enterococcus faecium*, *Escherichia coli* and *Lactobacillus casei*) are treated with supercritical carbon dioxide in a static system. Experiments are performed at a temperature of 313 K, at different pH values (6.4 and 7.4), different pressures (10 and 20 MPa) and several times of exposition at the operating conditions (20, 40, 60, 80 min). It is found that *E. coli* and *E. faecium* are more sensitive to the treatment than *L. casei* and sourdough yeast. The effect is enhanced at a pH value of 6.4 for each pressure/time combination and stronger inactivation is obtained by increasing the exposition time and pressure. Nevertheless, a similar inactivation can be achieved with both 20 MPa+60 min and 10 MPa+80 min in buffer at pH=6.4; the latter are relatively mild conditions in view of possible industrial applications.

1 Introduction

The sterilisation of microorganisms with supercritical carbon dioxide (SC-CO_2) has received more and more interest as an alternate technique for protecting foods from undesirable microbial activities [1]. This technique may become a simple, effective and rather inexpensive method to preserve heat-sensitive materials. For example, it is reported that the *Escherichia coli* decay after 15 min CO_2 processing at p=150 bar is similar to that obtained at p=3,000 bar by a hydrostatic method [2].

The lethal effect of SC-CO_2 on microorganisms has been considered by several authors with good results. Among others, Kamihira *et al.* [3] treated *Escherichia coli*, *Staphylococcus aureus*, baker's yeast and conidia of *Aspergillus niger* at pressure p=200 bar and temperature T=35 °C for 2 h obtaining strong inactivation. Wei *et al.* [4] successfully applied SC-CO_2 for controlling pathogenic microorganisms (*Listeria* and *Salmonella*) in model food systems. The inactivation effect could be markedly enhanced when using the so-called micro-bubble method, as shown by Ishikawa *et al.* [5] with *Lactobacillus brevis* and *Saccharomyces cerevisiae*: in this way, Ishikawa *et al.* [6] could obtain inactivation of *Bacillus*

spores as well. The SC-CO_2 treatment was also employed together with explosive decompression: Enomoto *et al.* [7] examined this way of operation at different decompression rates for *Saccharomyces cerevisiae* and *Bacillus* spores.

As reported by Haas *et al.* [1], parameters like treatment time and operating pressure and temperature are very important in SC-CO_2 sterilisation processes. The presence of water is essential, since experiments on dry materials showed no killing action due to CO_2: so, the pH also plays a relevant role. However, both the high pressure involved and the reduction of pH caused by CO_2 cannot explain alone the resulting strong sterilisation effect. This probably depends also on the interactions between the cell and CO_2 dissolved in the liquid. Recently, Kumagai *et al.* [8] measured the CO_2 sorption by microbial cells under high pressure and correlated it to the sterilisation rate constant. In spite of all of these efforts, the mechanism for inactivation by SC-CO_2 has not yet been clarified.

The aim of this work is to test the effect of SC-CO_2 on different microorganisms at well defined process conditions (pH, pressure, exposition time) and to study and compare the sensitivity of several strains belonging to different taxonomic groups (gram+, gram– and yeasts). At this stage, a batch process is considered; the application of a continuous flow system is in progress, in view of the development of a continuous countercurrent process on the industrial scale.

2 Materials & Methods

Three bacterial strains and a sourdough yeast strain were grown in their optimal growth conditions for 24 h, as detailed in Table 1. Compositions of media used are reported in Table 2. The cultures were suspended in PBS buffer and diluted to reach about 10^7 CFU/ml for bacteria and 10^5 CFU/ml for yeast.

Table 1. Growth conditions in liquid medium for bacterial and sourdough yeast strains

Microorganisms	Source	Medium	Conditions
YEAST			
Saccharomyces spp.	Sourdough	YPD Broth	30 °C
GRAM POSITIVE BACTERIA			
Enterococcus faecium	Cheese	MRS Broth (Oxoid)	37 °C
Lactobacillus casei	Cheese	MRS Broth (Oxoid)	30 °C anaerobiosis
GRAM NEGATIVE BACTERIA			
Escherichia coli	Sausage	LB Broth	37 °C, shaking

Test tubes containing 10 ml of cell suspension in PBS were employed. They were equipped with a perforated cap filled with hydrophobic cotton to avoid the dragging and leakage of the suspension; in this way, the contact between CO_2 and the liquid phase occurs by diffusion only. The tubes were placed in a thermostated autoclave and then pressurized with SC-CO_2. The process requires three steps: the loading of the vessel with CO_2 up to the selected p and T, the exposition at these

conditions, the discharge of CO_2 before collecting the tubes. Linear pressure profiles were ensured during the pressurization and depressurization steps. Both of them required 10 min each and were always accurately reproduced. All experimental runs were performed twice or three times.

After treatment, viable microorganisms were counted using the spread plate method of the serially diluted samples in a 0.9% NaCl solution according to conditions summarized in Table 3. The values found were compared with those counted in the control samples, which were exposed to the same temperature for the same time at atmospheric pressure.

Table 2. Composition of buffer, LB broth and YPD broth. All concentrations in g/l

PBS Buffer	pH 6.4	pH 7.4	LB Agar		YPD Broth	
NaCl	8.0	8.0	Yeast extract (Oxoid)	5	Yeast extract (Oxoid)	10
KCl	0.2	0.2	Tryptone (Oxoid)	10	Peptone (Oxoid)	20
KH_2PO_4	1.4	0.6	NaCl	10	Dextrose	20
Na_2HPO_4	0.25	1.0	Agar	15		

Table 3. Microorganisms selective growth conditions in solid medium

Microorganism	Medium	Conditions
YEAST		
Saccharomyces spp.	Rose Bengal chloramphenicol agar (Oxoid)	30 °C, 48 h
GRAM POSITIVE BACTERIA		
Enterococcus faecium	Kanamicine azide agar (Oxoid)	37 °C, 24 h
Lactobacillus casei	MRS pH 5.4 (Oxoid)	30 °C, 48 h anaerobiosis
GRAM NEGATIVE BACTERIA		
Escherichia coli	LB agar	37 °C, 24 h

3 Results

Preliminary experiments showed that the microorganisms were partially deactivated if exposed to T=323 K and room pressure for more than 40 min; therefore, T=313 K was always used. The other variables investigated were: pH (6.4 and 7.4), pressure (10 and 20 MPa) and time of exposition at the operating conditions (20, 40, 60, 80 min). It was checked that the pressurization and depressurization steps had negligible influence on bacteria deactivation: at 20 min of exposition time no appreciable reduction of the population was usually observed. For all the conditions investigated and the microorganisms considered the process showed a lag (activation) time of about 40 min.

As is clearly shown in Table 4, a complete sterilisation could be obtained in all cases, at suitable values of pressure, pH and exposition time; also, *E. coli* is the most influenced by SC-CO_2 while *L. casei* and *Saccharomyces* strains are the most resistant. However, bacteria behave differently with respect to process variables. In general, larger deactivation is reached at high pressure and lower pH values

(20 MPa and 6.4); at these conditions, $\log(N_0/N)$ profiles along with exposition time become asymptotic. At intermediate conditions, i.e. at high (or low) values of *both* pressure and pH, these profiles are linear for stronger microorganism (yeasts and *L. casei*) and asymptotic for weaker bacteria (*E. coli* and *E. faecium*). At mild operating conditions (low pressure and high pH, i.e. 10 MPa and 7.4), the curve of $\log(N_0/N)$ is upward concave for the stronger microorganisms and linear for the weaker ones.

Table 4. Microorganisms reduction, $\log(N_0/N)$, as a function of pH, pressure and time of exposition. Data marked with symbol «>» means no CFU detected at those conditions

		Saccharomyces		*L. casei*		*E. faecium*		*E. coli*	
p, MPa	*t*, min	pH 6.4	pH 7.4	pH 6.4	pH 7.4	pH 6.4	pH 7.4	pH 6.4	pH 7.4
10	40	0.44	0.21	1.00	0.45	1.06	0.65	1.87	1.44
10	60	2.35	1.30	3.02	1.96	>6.09	2.59	>6.94	2.72
10	80	>4.74	>4.49	>5.67	>4.99	>6.44	5.42	>7.12	4.49
20	20			2.04	0.95	2.74	1.23	2.20	1.81
20	40	0.79	0.30	1.52	1.49	3.38	1.60	3.45	2.10
20	60	>5.30	>5.18	>6.66	>5.44	>6.26	4.01	>7.19	5.12
20	80	>5.77	>5.58	>6.74	>6.35	>6.69	>6.51	>7.55	>6.98

4 Conclusions

Experiments to study the effect of SC-CO_2 on different microorganisms were carried out in a batch system. Both bacteria and yeasts could be completely killed at relatively mild process conditions. The pressure effect was similar for all the microorganisms considered, while *E. faecium* and *E. coli* were more affected by a pH decrease. *E. faecium* and *L. casei* behaved similarly except for the activation time, which was larger for *L. casei*. It was confirmed that bacteria having a weaker cell wall structure (in comparison with gram+) are more sensitive to SC-CO_2.

References

[1] G.J.Haas *et al. J. Food Safety*, **1989**, *9*, 253-265.
[2] J.P.P.M.Smelt, G.G.F.Rijke. In: *High Pressure Biotechnology,* C.Balny, R.Hayashi, K.Heremans, P.Masson Eds., **1992**, John Libbey Ltd., London, 361-364.
[3] M.Kamihira *et al. Agric.Biol. Chem.*, **1987**, *51*, 407-412.
[4] C.I.Wei *et al. J. Food Protection*, **1991**, *53*, 189-193.
[5] H.Ishikawa *et al. Biosci. Biotech. Biochem.*, **1995**, *59*, 1949-1950.
[6] H.Ishikawa *et al. Biosci. Biotech. Biochem.*, **1997**, *61*, 1022-1023.
[7] A.Enomoto *et al. Biosci. Biotech. Biochem.*, **1997**, *61*, 1133-1137.
[8] H.Kumagai *et al. Biosci.Biotech.Biochem.*, **1997**, *61*, 931-935.

The Effect of High Pressure on the Microbial Quality of Apple Juices

A. Boyd[1], M.F. Patterson[1,2], A. McCracken[2] and B. Mackey[3]

[1]Department of Food Science (Food Microbiology), The Queens University of Belfast, Belfast, N. Ireland
[2]Department of Agriculture for Northern Ireland, Newforge Lane, Belfast BT9 5PX, N. Ireland
[3]Institute of Food Research, Earley Gate, Whiteknights Road, Reading RG6 2EF, UK
a.boyd@qub.ac.uk

Abstract. Six fresh apple juice samples were exposed to high pressure treatments, ranging from 250 to 400 MPa for 5 min at 20 °C. All the juices exhibited a significant reduction in total viable counts immediately post pressurisation. The pressurised samples were stored at 4 °C and sampled monthly. Counts from juices pressurised up to 350 MPa increased after 1 months storage, whereas 400 MPa treated juice did not increase in counts until 2 months storage. The surviving microbial population of the juices was found to be predominately yeasts, e.g. *S. cerevisiae, Candida* species, *Zygosaccharomyces* spp. and *Rhodotorula* spp., and moulds, e.g. *Penicillium* spp.

1 Introduction

It has taken the 100 years since Hite provided the first report on the high pressure treatment of food [1] for a range of high pressure products to become commercially available. The renewed interest in high pressure processing has resulted from the consumer demanding alternatives to traditionally heat treated foods which avoid thermal damage and the subsequent reduction in flavour. High pressure, being a non-thermal, isostatic process mainly affecting non-covalent bonds, results in a food which retains the properties of flavour, taste and texture associated with the fresh produce [2]. The first products on the market in 1990 were fruit preserves, dressings and sauces [3] with the current consensus being that fruit based products will initially provide the major opportunities for high pressure treatment. The recognised microflora of apple juice is primarily yeasts and moulds. Yeasts have been isolated from the genera *Candida, Saccharomyces, Zygosaccharomyces, Rhodotorula, Pichia, Torulopsis* and *Klockera* [4]. Moulds identified in apple juice are from the genera *Penicillium, Cladosporium, Aspergillius, Botrytis* and *Fusarium* [5]. Yeast species of *Candida* and *Saccharomyces* genera are inactivated by relatively low pressures [6,7]. The aim of

this investigation was to study the effect of pressure on the microbial quality of fresh apple juice, derived where possible from single apple varieties, and any subsequent microbial growth under refrigerated storage.

2 Materials & Methods

2.1 Samples

Six freshly squeezed apple juice samples were collected from a local processor. Four originated from single apple varieties, one each from Cox and Golden Delicious and two from Bramley. The remaining two samples constituted a mixture of apple varieties. Each sample was refrigerated overnight and pressurised the following day. Samples for pressurisation were poured into narrow mouthed 8 ml plastic bottles [Nalgene]. The bottles were filled to the brim to exclude air and the lids tightly secured before being packed in two polyethylene vacuum pouches and vacuum sealed twice [Multivac, Haggenmulle, Germany].

2.2 High Pressure Treatment

Samples were pressurised using a Stansted Food Lab. 9000 high pressure isostat capable of operating at 900 MPa [Stansted Fluid Power Ltd., Stansted, England] with a cylinder 7 cm in diameter and 20.3 cm in length. Pressurising medium consisted of distilled water containing 10% Shell Dromas oil B [Shell UK Oil, London, England]. The come-up rate was approximately 200 MPa/min and the pressure release time 2 min. The sample treatment time did not include come-up or pressure release times. The adiabatic heating was approximately 2 °C per 100 MPa. Juice samples were exposed to pressures of 250, 300, 350 and 400 MPa for 5 min, at 20 °C.

2.3 Sampling Protocol and Identification Procedure

For each sample, an unpressurised sample was used as a control to give an initial count. Appropriate dilutions were prepared in peptone saline diluent [Oxoid CM733]. Duplicate 0.1 ml volumes were spread plated on yeast mould agar [Oxoid CM920] and the number of colonies counted after incubation at 25 °C for 72 h. Pressurised samples were subsequently stored at 4 °C and sampled monthly for 3 months. Statistical analysis involved calculation of least significant differences, $p>0.05$. Where colonies numbered less than 20, all were isolated for identification. However, if colony numbers exceeded 20, random selection for identification involved use of a Harrison disk. Selected colonies were repeatedly streaked onto malt extract agar [Oxoid CM59] until pure. Yeasts were identified using API ID32C identification strips [API System, 1987]. The pure colonies were examined weekly for a month and their morphological and microscopic characteristics observed and compared with those described by Kregar van Rij [8]. Moulds were identified by comparing the growth characteristics on specified agars at varying temperatures with those published by Pitt [9].

3 Results & Discussion

It can be seen from the experimental results that high pressure treatment could be effective in preserving apple juice. Pressure treatments of 250 MPa and 400 MPa produced $3\log_{10}$ and $6\log_{10}$ reductions, respectively, from an initial count of $7\log_{10}$ cfu/ml, both significantly lower, $p>0.05$ (Fig. 1). However, after storage at 4 °C for one month, only juice pressurised at 400 MPa did not show significant increases in microbial counts. When juice treated at 400 MPa was stored for 2 months, a significant increase in counts, $p>0.05$, occurred to approximately $6\log_{10}$ cfu/ml, with the count remaining at this level after 3 months storage.

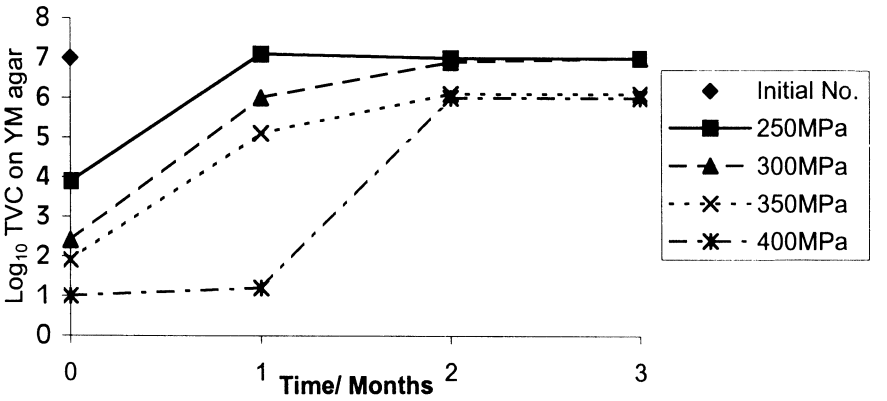

Fig. 1. The effect of pressure, 5 min, 20 °C, and storage at 4 °C on the microbial quality of fresh apple juice

The microorganisms which composed the microbial population were primarily yeasts and moulds as expected. API identified yeasts as *S. cerevisiae, Cryptococcus laurentii, Zygosaccharomyces* spp., *Pichia* spp., *Klockera* spp., *Rhodotorula* spp. and a range of *Candida* spp. The majority of moulds were initially identified as *Penicillium* spp., with one species of *Cladosporium* and *Aspergillius* also present. *Penicillium* species identified included *P. italicum, P. roquefortii* and *P. citrinium*, but not *P. expansum*. Table 1 shows that juice exposed to 250 MPa had a more diverse microbial population than juice pressurised at 400 MPa, where the population consisted only of *Candida* spp, *Penicillium* spp. and *Crypto. laurentii*. During refrigerated storage, juice treated at 250 MPa retained its varied microbial population. Juice treated at 400 MPa showed an increase in population diversity, but *Candida* and *Penicillium* spp. still dominated. Concerning specific juice varieties, Golden Delicious had the lowest pH, of 3, and it was found that *Candida* spp. were the only microorganisms able to survive 400 MPa at this pH. The other juices had pH values in the range 3.4–3.5 enabling *Penicillium* spp. and *Crypto. laurentii* to survive treatment at 400 MPa, along with *Candida* spp. Where *Penicillium* spp. survived pressurisation in large

numbers, they dominated the microbial population to such an extent other microorganisms could not compete.

Table 1. The relative number of each species out of the total isolates identified from the juice samples [*blank*: species not identified from sample]

Pressure, MPa	250				400			
Months	0	1	2	3	0	1	2	3
Species								
Candida	70	75	79	87	2	32	70	38
S.cerevisiae	18	22	20	23			9	16
Zygosacch.	16	15	21	22				12
Rhodotorula	12	10	17	24			6	
Pichia	10	8	3	2				
Klockera			2	1				
Crypto. laurentii				1	2		3	
Pencillium	1				4	30	38	34
Total isolates identified	126	130	142	160	8	62	126	100

Under the conditions investigated, apple juice pressurised at 400 MPa for 5 min at 20 °C could have a shelf life of one month at 4 °C storage. However to extend this, higher pressures, increased exposure time or other stresses such as heat, water activity or pH, combined with pressure may need to be introduced.

References

[1] Hite, B.H., 1899. The effects of pressure on the preservation of milk. W. Virginia Agricultural Experiment Station Bulletin, 58, p 5.

[2] Galazka, V.B., Ledward, D.A., 1995. Developments in high pressure food processing. Food Technology International Europe, 123-125.

[3] Earnshaw, R.G., 1992. High pressure technology and its potential use. Food Technology International Europe, 85-88.

[4] Doores, S.C., 1983. The microbiology of apples and apple products. Critical reviews in Food Science and Nutrition, 133-149.

[5] Beech, F.W., 1958. The yeast flora of apples and ciders. Journal of Applied Bacteriology, 527-266.

[6] Korobi, H., Sato, M., Tameike, A., Hamada, K., Shimada, S., Osumi, M., 1995. Ultrastructural effects of pressure stress on the nucleus in *Saccharomyces cerevisiae* a study by immunoelectron microscopy using frozen thin sections. FEMS Microbiology Letters, 253-258.

[7] Sato, M.,Korobi, H., Shimada, S., Osumi, M., 1995. Pressure effects on the ultrastructure of cells of the dimorphic yeast *Candida tropicalis*. FEMS Microbiology Letters, 11-15.

[8] Kregar van Rij, N.J.W., 1984. The yeast A taxonomic study. 3rd Edition., Amsterdam, Elsevier Science Publishers.

[9] Pitt, J.I., 1979. The genus *Penicillium* and its teleomorphic state *Eupenicillium* and *Talormyces*., Academic Press.

Thermal Effect Before High Pressure Treatment on the Reduction of *Enterococcus faecalis* in Duck Fatty Liver

P. Ballestra, C. Cruz, M. Antoine, A. Largeteau[1], G. Demazeau[1], D. Le Ba[2], F. Zuber[2] and A. El Moueffak

Equipe de Recherche Agroalimentaire Périgourdine, IUT de Périgueux
39, rue P. Mazy, 24019 Périgueux cedex, France
moueffak@montesquieu.u-bordeaux.fr
[1]Interface Haute Pression, ENSCPB, Université Bordeaux I, Talence, France
[2]Centre Technique de la Conservation des Produits Agricoles, Dury, France

Abstract. The results of this study show that a preheating associated with slight HP treatments can enhance the reduction of inoculated *E. faecalis* flora and TMAF in duck fatty liver. Moreover, the inoculated *E. faecalis* flora seems to be much more sensitive to this preheating than the TMAF.

1 Introduction

High hydrostatic pressure processing can be used as a « soft » alternative technique to food stabilization thermal treatments [1]. Pressurization allows a reduction in the time and temperature usually required for sterilization or pasteurization. However, high pressure (HP) technology for food treatment is still expensive and application can be found for high added value, thermally fragile, foods. Duck fatty liver naturally appears as one of the first products to be processed through this technology. Previous studies have shown that HP treatments are efficient to stabilize duck fatty liver with good organoleptic qualities ("half cooked" traditional duck fatty liver characteristics) [2,3]. Nevertheless, potential synergy between pressure and other parameters such as preheating could be investigated as means for operating at lower pressures and/or temperatures or for shorter times, to further improve the organoleptic properties of this product.

The main objective of our work was to study the effect of a "moderate" preheating before pressurization on the reduction of inoculated *Enterococcus faecalis* flora and total mesophilic aerobic flora (TMAF) in duck fatty liver. *E. faecalis* is a good indicator microorganism for its thermoresistance and baroresistance.

2 Materials & Methods

Samples. The fatty livers used were taken from 4 mulard type ducks for each experiment, provided by the Lycee Agricole et Agro-alimentaire (Périgueux, France); they were immediately disembowelled and refrigerated at 4 °C. Livers of optimum and homogeneous quality were selected by weight (400 to 500 g) and appearance, and five 30 g cubes (30×30×30 mm) were cut off the main lobe, then cut in 10x10x10 mm small cubes. Samples inoculated with *Enterococcus faecalis* (107/g) were vacuum conditioned in a polyethylene/polyamide/polyethylene (PE/PA/PE) film before treatment. Untreated fatty liver sample was packaged with the same film and also held at 4 °C before analysis.

For a better understanding, samples were identified as: T (thermal treatment), HP (high pressure treatment without preheating) and T+HP (high pressure treatment with preheating).

Thermal Treatment (T). Samples were submitted to immersion in water at 45 °C for 20 min, followed by cooling to 4 °C by immersion in cold water and stored for 2 d at 4 °C.

Microbiological contamination was measured and compared with untreated sample.

High Pressure Treatment (HP). Samples were pressurized at the Interface Hautes Pressions (Université Bordeaux I), cooled immediately and stored at 4 °C for 2 d.

Selection of two temperatures (55 or 65 °C) and two pressures (350 or 550 MPa) was based on published literature, and on results about the efficiency of these treatments.

The 4 treatments used were:

HPa: 350 MPa for 20 min at 55 °C HPb: 350 MPa for 20 min at 65 °C
HPc: 550 MPa for 20 min at 55 °C HPd: 550 MPa for 20 min at 65 °C

Microbiological contamination was measured and compared with untreated and thermally treated samples.

High Pressure Treatment Combined with a Preheating Phase (T+HP). All samples were preheated at 45 °C for 20 min in a water bath before pressurization as cited in the "High pressure treatment" section.

After treatments, samples were stored at 4 °C for 2 d. Then, microbiological contamination was measured and compared with untreated sample, thermally treated sample and pressurized without preheating treated samples.

Microbiological Analysis of Samples. Analyses were performed on 2 d after treatments counting (CFU/g) for total mesophilic aerobic flora (TMAF) on Plate Count Agar medium (PCA), after incubation at 30 °C for 72 h and *Enterococcus faecalis* on KF-Streptococcus medium supplemented with TTC (triphenyl 2,3,5-tetrazolium chloride) after incubation at 37 °C for 48 h. For commodity, log CFU_0/CFU was calculated with CFU_0 the initial bacterial charge of untreated sample.

3 Results & Discussion

All results concerning T, HP and T+HP treatments on *E. faecalis* flora and TMAF are shown in Fig. 1.

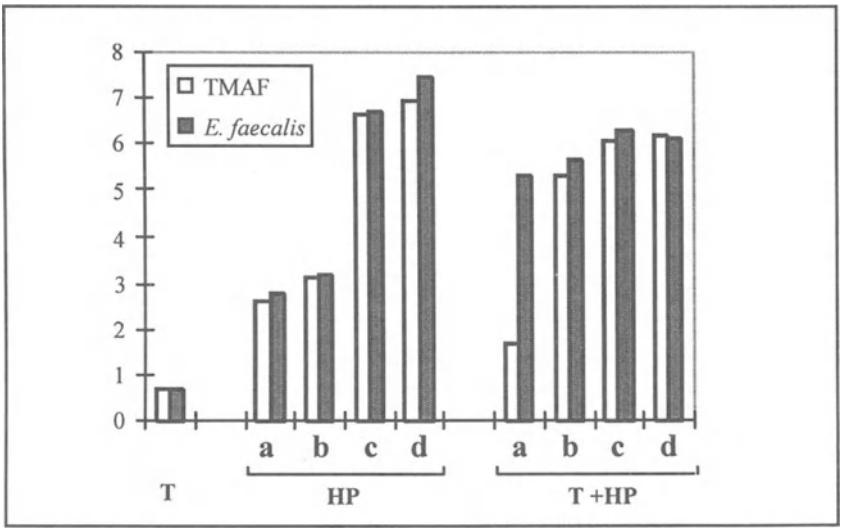

Fig. 1. Thermal (T), high pressure (HP), high pressure with preheating (T+HP) treatments effect on the TMAF and *Enterococcus faecalis* flora reduction in duck fatty liver. T treatment: 45 °C/20 min; HP treatments: a: 350 MPa/20 min/55 °C; b: 350 MPa/20 min/ 65 °C, c: 550 MPa/ 20 min/55 °C, d: 50 MPa/20 min/65 °C; T+HP treatments: HP treatments (a, b, c or d) with preheating 45 °C/20 min

T Treatment Effect on TMAF. As expected, T treatment has no significant effect on TMAF (<1log of reduction). Indeed, 45 °C is much lower than the traditional pasteurization temperature.

HP Treatment Effect on TMAF. At 350 MPa, treatments allowed slight reduction of TMAF whatever the temperature used, 55 or 65 °C (2.5 and 3log of destruction, respectively). However at 550 MPa, for both temperatures, the bacterial reduction was almost complete (6.5–7log of reduction). Increasing pressure from 350 to 550 MPa enhances the TMAF reduction while increasing temperature from 55 to 65 °C has no significant effect. So, in our experimental conditions, the pressure effect appears to be predominant compared with that of the temperature.

T+HP Treatment Effect on TMAF. Preheating was shown to influence differentially the efficiency of high pressure proceeding. In fact, it has no additional effect on the reduction when it is applied before the strongest HP treatments (550 MPa/55 or 65 °C) and before the lowest HP treatment (350 MPa/55 °C) but increases significantly the 350 MPa/65 °C treatment decontamination. This phenomenon could be explained by the additional effect, at

a low pressure intensity, of the two succesive temperatures used, 45 and 65 °C, this last temperature is very close to the usual pasteurization one.

Treatments Effect on *E. faecalis* Compared with TMAF. *E. faecalis* flora and TMAF reductions were quite similar after T, HP or strongest T+HP applications (Fig. 1). Moreover, the synergic thermal effect of the T+HP treatment at 350 MPa/65 °C can be observed for *E. faecalis* flora as for TMAF. However, in our experimental conditions, the preheating phase of the lowest T+HP treatment (350 MPa/55 °C) enhanced significantly *E. faecalis* flora reduction while it did not modify TMAF decontamination. So, the inoculated *E. faecalis* flora seems to be much more sensitive to a heating phase applied before pressurization than the total mesophilic contamination. This observation could be explained by a better adaptation of the natural flora to the environmental medium [4]. Moreover, a varying proportion of *E. faecalis* may be stressed, but not inactivated, by T+HP treatments and are able to grow on the selective medium KF-TTC [5].

4 Conclusions

Our study points out that:

- a preheating phase associated with slight HP treatments can enhance the reduction of inoculated *E. faecalis* flora and TMAF in duck fatty liver.
- in our experimental conditions, the inoculated *E. faecalis* flora seems to be more sensitive to this preheating phase than the TMAF.

So, the preheating use interest depends on the nature of contamination, the HP-treatment conditions and probably on the nature of food or suspending medium.

References

[1] J.C. Cheftel, 1992. Effect of high hydrostatic pressure on food constituents: an overview. In: *High Pressure and Biotechnology, Colloques INSERM*, (edited by C. Balny, R. Hayashi, K. Heremans and P. Masson), pp. 195-209. London: John Libbey Eurotext Ltd.

[2] A. El Moueffak, C. Cruz, M. Antoine and M. Montury (EURIA), G. Demazeau and A Largeteau (IHP), D. Le Ba, B. Roy and F. Zuber (CTCPA). 1994. Stabilisation of fatty duck liver by high pressure treatment. *High Pressure Research,* 12, 248-250.

[3] A. El Moueffak, C. Cruz, M. Antoine, M. Montury, G. Demazeau, A. Largeteau, B. Roy and F. Zuber. 1995. High pressure and pasteurisation effect on duck foie gras. *International Journal of Food Science and Technology*, 30, 6, 737-743.

[4] A. Carlez, J.P. Rosec, N. Richard and J.C. Cheftel. 1994. Bacterial Growth During Chilled Storage of Pressure-Treated Minced Meat. *Lebensmittel-Wissenschaft und Technologie*, 27, 48-54.

[5] A. Hurst. 1977. Bacterial injury: a review. *Canadian Journal of Microbiology*, 23, 8, 935-944.

High Pressure Inactivation and Survival of Pressure-Resistant *Escherichia coli* Mutants in Milk

C. García-Graells, B. Masschalck, N. Moonjai and C. Michiels

Laboratory of Food Microbiology, Katholieke Universiteit Leuven, Kardinaal Mercierlaan 92, B-3001 Heverlee, Belgium
Phone: +32/16/32.15.78; Fax:+32/16/32.19
chris.michiels@agr.kuleuven.ac.be

1 Introduction

Liquid milk is usually pasteurized or sterilized by heat treatment before it is consumed or used for other applications. Recently, high pressure has been proposed as an alternative to thermal treatment that allows an increase in the shelf-life of milk, while maintaining most of its raw qualities. Information on the response of microorganisms to pressure is necessary to further evaluate and optimize the process. In this respect, the development of high levels of pressure resistance in some strains of *E. coli* [2] causes serious concern about the safety and stability of pressure-processed foods. In the current work, we studied the inactivation of these *E. coli* strains in milk by high pressure treatment alone, and in combination with lysozyme and/or nisin.

2 Materials & Methods

Three types of commercial UHT milk (whole, half-whole and skim) have been used in this study. Milk was inoculated with stationary-phase cell suspensions of *E. coli* MG1655 and its three pressure-resistant mutants (LMM1010, LMM1020, LMM1030) at approximately 10^8 cells/ml. Pressure treatments were done in polythylene bags at up to 700 MPa and 50 °C. Survivors were counted after serial dilution and plating on tryptic soy agar.

3 Results

3.1 Pressure Sensitivity of *E. coli* in Milk

The study clearly showed that the *E. coli* parent strain was much more resistant when treated in milk than in buffer (Table 1). Even at 700 MPa, it could not be efficiently inactivated in 15 min at room temperature. The mutants had

approximately the same level of resistance in milk and in buffer, and were still slightly more resistant than the parent strain in milk. This dramatic increase in baroresistance is probably due to the physicochemical composition of the substrate that can act as a protective compound. These data confirm the results obtained by others [3–5]. Pressure treatments in milk with different fat concentrations revealed that resistance increased with increasing fat content (Table 2). Treatments conducted in skim milk show that the combined used of mild heating (50 °C) with high pressure (600 MPa) proved an effective method of reducing the parent strain, >8-log, but only 3.5–4.5 log was achieved for the mutants.

Table 1. Logarithmic viability reduction of *E. coli* parent strain MG1655 and the mutant LMM1010 in UHT whole milk and in buffer for 15 min pressure treatment at 20 °C

	Whole Milk		Phosphate Buffer pH 7.0	
Pressure	MG1655	LMM1010	MG1655	LMM1010
300 MPa	0.49	0.28	4.96	0.35
400 MPa	0.74	0.27	6.99	0.62
500 MPa	1.40	0.28	7.29	0.44
600 MPa	1.60	0.60	8.32	0.67
700 MPa	2.33	0.40	9.80	0.90

Table 2. Logarithmic viability reduction of *E. coli* in milks with different fat content: whole (3.6%), half-whole (1.55%) and skim (0.05%) at 600 MPa for 15 min at 20 °C

E. coli strains	Whole	Half-whole	Skim
MG1655	1.60	2.34	2.96
LMM1010	0.11	0.27	0.29
LMM1020	0.45	1.61	1.42
LMM1030	0.85	1.26	1.39

3.2 Combined High Pressure and Antimicrobial Treatments

A slight increase in lethality was achieved in the presence of lysozyme (400 μg/ml) and/or nisin (400 μg/ml) (Fig. 1) but the effect of both antimicrobials was much less than in buffer (see Hauben *et al.* in this volume) and not enough to assure safety of the pressurised milk. The sensitivity of *E. coli* to nisin and lysozyme in milk was dependent on the milk fat concentration. For instance, inactivation in skim milk in the presence of nisin was 4-log units for the parent strain and 1.2–3.2-log units for the mutants compared to 1.7 and 0.22–1.19-log reduction respectively in whole milk.

Upon storage of the pressurised milk at refrigerated temperature (8 °C), the number of survivors did not decline as we previously observed in fruit juices [1]. For at least 30 d at 8 °C and in the presence of the antimicrobials, the surviving population remained stable and no improvement in the shelf-life of the pressurised milk could be achieved. Upon storage at 20 °C, the population increased

significantly after 72 h. These results indicated that cells are only sensitise to the bactericidal activity of lysozyme and nisin during pressure treatment and no further reduction of injured cells occurs after treatment upon storage.

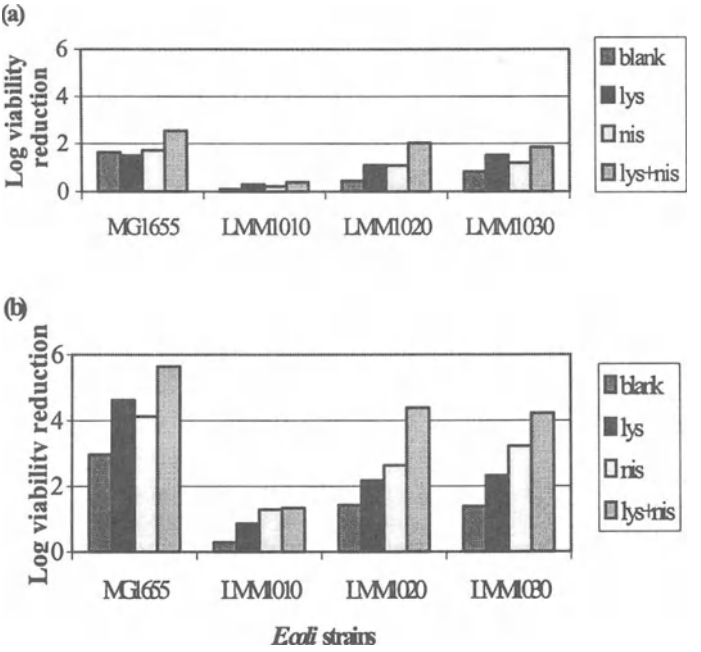

Fig. 1. Effect of lysozyme and nisin and their combination during pressure treatment (600 MPa) at 20 °C for 15 min in (**a**) whole milk and (**b**) skim milk

3.3 Pressure Cycling Treatments

To achieve higher inactivation levels without further increasing pressure, we tested cyclic pressure treatments and found these to be considerably more effective than single continuous treatment for the same total treatment time.With three 10 min pressure cycles at 550 MPa at 20 °C in the presence of lysozyme, a 8-log reduction in viable *E.coli* MG1655 and 5-log reduction in viable *E.coli* LMM1010 was achieved, whereas only 4-log and <1-log reductions were achieved in 30 min continuous treatment. As can be seen from Fig. 2, cycling enhanced both the high pressure inactivation in the absence of additives, as well as the sensitivity of the cells to lysozyme and nisin.

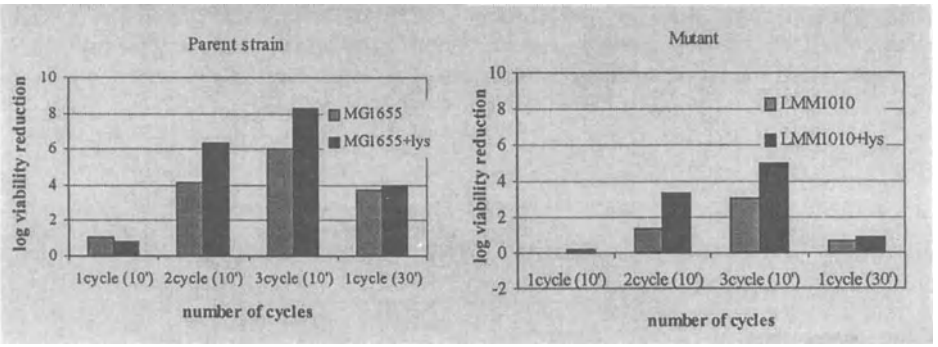

Fig. 2. Effect of cycled high pressure treatments at 550 MPa and 20 °C in skim milk inoculated with *E.coli* parent strain MG1655 and the mutant LMM1010 in the presence of lysozyme

4 Conclusions

The pressure resistance of *E. coli* can be affected by many intrinsic and environmental parameters. Their ability to survive high pressure is greatly increased when they are treated in nutritionally rich media (milk) containing substances which may provide protection against damage or nutrients essential for repair.

The effect of the antimicrobials lysozyme and nisin is strongly reduced in milk, even at high concentration. The fat content also affects the effectiveness of these antimicrobials against *E.coli*.

Cycled short high pressure treatments combined with low concentrations of lysozyme and nisin were more effective in the inactivation of *E.coli* than continuous treatments for the same treatment time.

References

[1] García-Graells *et al.*, (1998), Appl. Environ. Microbiol 64, 1566-1568.
[2] Hauben *et al.*, (1997), Appl. Environ. Microbiol. 63, 945-950.
[3] Patterson *et al.*, (1995), J. Food Prot. 58, 524-529.
[4] Raffalli *et al.*, (1994), Sci. Aliments 14, 349-358.
[5] Styles *et al.*, (1991), J. Food Sc. 56, 1404-1407.

Membranes and Lipids

Some Preliminary Measurements of the Effect of High Hydrostatic Pressure on the Porin Omp C from *E. coli*

A.G. Macdonald[1] and B. Martinac[2]

[1]Department of Biomedical Sciences, Zoology Building, University of Aberdeen, Aberdeen AB24 2TZ, Scotland, UK
[2]Department of Pharmacology, University of Western Australia, Nedlands, WA6907, Australia
[1]a.macdonald@abdn.ac.uk
[2]b.martinac@receptor.pharm.uwa.edu.au

Abstract. The bacterial Omp C, extracted from *E. coli*, has been reconstituted in liposomes and then subjected to patch-clamp analysis at high hydrostatic pressure. The results demonstrate the feasability of the technique and that pressure favours transient channel openings.

1 Introduction

Porins are trimeric membrane proteins. They function as channels in the outer membrane of Gram-negative bacteria, providing a permeability path for small molecules, generally less than 600 Daltons [1]. Porins may be extracted and reconstituted in planar bilayers or liposome bilayers, either of which enable their permeability and gating characteristics to be studied. Thus far neither of these properties has been investigated as a function of high hydrostatic pressure, unlike eukaryote ion channels which have attracted a number of studies [2, 3], based on classical voltage clamp and patch-clamp techniques. Bacteria are subjected to high pressure in the deep sea, and in various industrial processes. The latter are generally intent on killing whilst the deep sea environment is one to which bacteria are specifically adapted (barophiles). In the latter category *Photobacterium profundum* SS9 manifests an inverse pressure regulation of the expression of two genes, Omp H and Omp L [4]. Expression of the corresponding porin in the latter case predominates at normal atmospheric pressure whilst expression of Omp H predominates when the bacteria are grown at 28 MPa. This strongly suggests that specific porins are required to function at high pressure, consistent with the idea that in bacterial-killing processes, porins could be targets of interest.

Porin subunits are constructed of antiparallel β-strands traversing the supporting bilayer many times, 16 in the case of the porin from *Rhodobacter capsulatus* [5]. Typically three subunits form a coherent trimer. Single channel (porin) conductance refers to the current passing through a monomer; often the gating of

monomers appears cooperative and the high conductance of porins is a notable feature [6].

The present study is based on the Omp C porin whose structure and kinetic properties have been extensively studied [7]. The channel favours cations rather than anions, and has a single unit conductance of 56 pS determined in patch-clamped liposome membranes, in symmetrical 150 mM KCl. Two unit conductances most frequently occur (i.e. 2 monomers open), giving a 100–116 pS conductance channel. Gating is voltage-dependent. Inside-out patches (inside referring to the interior of the liposome vesicle) show an increase in the probability of channels opening as the potential on the pipette side is made more positive, over the range –100 to +100 mV.

The experiments described here are exploratory in nature and have concentrated on gating. They show that 30 MPa hydrostatic pressures favour the porins' opening reaction.

2 Materials & Methods

E. coli was grown using the procedure of Delcour *et al.* [8], harvested, and cell membrane vesicles were prepared by passing the cells through a French press. Outer membrane fractions were prepared and stored at –80 °C for up to several months before use. Liposomes composed of L-α-phosphatidylcholine, prepared from soybeans, and cholesterol (both Sigma) in the ratio of 9:1 by weight, were prepared by the method of Bangham *et al.* [9], sonicated to transparency and centrifuged at 100,000 g to form a concentrated pellet. Outer membrane fraction protein was mixed with the dried liposome suspension (ratio 1: 600–1000, protein:lipid) to provide material for use within 5 d. Rehydration of the dried liposome suspension at 5 °C took place the day before use. Approximately 20 µl of the rehydrated liposomes, incorporating porins which spontaneously adopt a common outside-out orientation in the bilayer, were transferred to a dish containing the recording solution. [200 mM KCl, 40 mM $MgCl_2$, 5 mM Bis-Tris (bis[2-hydroxyethyl]imino-tris[hydroxymethyl]methane (Sigma) to pH 6.1, room temperature]. Subsequent osmotic swelling produced favourable "blisters" which readily formed giga-ohm seals with patch pipettes. Usually the best seals formed spontaneously when the pipette tip touched a "blister". Inside-out patches were readily formed with symmetrical solutions at room temperature, and then generally lasted an hour or so.

An Axon patch-clamp amplifier was used and the output low pass filtered at 1 kHz and recorded by a Vetter PCM Recorder, Model 200. Patch pipettes were made of borosilicate glass containing a filament (e.g. Clark Electromedical, 1.5 × 0.86 mm I.D.), the tips were unpolished, and their resistance was typically 10 MΩ. All experiments were conducted at room temperature (21–24 °C) using the inside-out patch configuration, and symmetrical solutions. Control experiments comprised a series of recordings of the patch's electrical activity with the

membrane potential held at + and –100 mV, or at selected voltages within the range. The recordings were of 20–30 s duration at approximately 5–10 min intervals through a time span of 40–120 min.

High pressure experiments required the pipette supporting the inside-out patch to be transferred to a high pressure vessel. This was accomplished by means of a "transfer dish" [10]. The tip of the patch pipette was then immersed in an aqueous solution of 7 ml volume which, in turn, was immersed in liquid paraffin which transmitted high pressure within the pressure vessel. A hand-powered pump generated hydrostatic pressure, creating within the pressure vessel a heat transient such that the patch experienced +3 °C on compression to 90 MPa, which dissipated within 30 min. In practice lesser pressure was applied in steps so the temperature excursion experienced by the patch was much less than this. Decompression produced a mirror-image transient cooling.

As some of the first experiments using various solutions revealed infrequent but significant channel openings at high pressure, a single channel style of recording protocol was adopted rather than a whole cell recording program, which measures the current flowing through a population of open channels.

3 Results

The experiments were based on a protocol comprising an initial pre-compression control phase at room pressure, followed by a step increase to 30 MPa, which was held for many minutes. Control experiments were also carried out in parallel, in which patch activity was recorded at intervals over a similar time, at normal atmospheric, room pressure.

Irrespective of the recording solution which was used, the normal background activity of a patch consisted of a steady "baseline" current, whose magnitude was determined by the applied potential and the number of open porins in the patch. Typically more than 10 porins would probably be present. Superimposed on the steady baseline current there occurred transient reductions in current, typically 10 pA for less than 20 ms at a frequency of approximately 1 s^{-1}.

At V_H = +100 mV the pulses were negative and at –100 mV they were positive, i.e. corresponding to channel closures. On rare occasions such background activity was interrupted either by larger (100–500 pA) and apparently spontaneous currents ("bursting" behaviour) corresponding to channel openings or by a channel closure which lasted for several seconds. The application of 30 MPa had no immediate effect on baseline current or background activity but it increased the probability of bursting. The results are summarised in Table 1. Of the three batches of liposomes used, A, B, E, no bursting behaviour took place in control experiments (mean of 100 mins). High pressure (30 MPa) experiments using the same batch of liposomes produced bursting behaviour after a mean of 13 mins at pressure.

Table 1. Effect of 30 MPa on Omp C gating. Symmetrical solutions were used; the data relate to + 100 mV

Experiment	Porin batch	Baseline current pA	Micro-activity s^{-1}	Time 30 MPa applied, min after start	Time bursts started, min	Total length of experiment min
HIGH PRESSURE						
1	A	260	0.8	8	9.24	40
2	A	300	1.2	26	43	55
3	B	120	2.3	21	43	55
4	E	negligible	negligible	16	28	37
CONTROL						
1	A	570	0.8	–	–	120
2	A	1400	discernible not measureable	–	–	41
3	B	negligible	negigible	–	–	123
4	E	740	1.8	–	–	115

4 Discussion & Conclusions

Hydrostatic pressure increases the probability of the porin Omp C undergoing an opening transition but it has no obvious effect on conductance. It has not been possible to quantify the increased probability of opening. The responses of Omp C to high pressure are only manifest after a delay, which presents the experiments with a considerable difficulty. The molecular mechanism for this effect of pressure is going to be impractical to investigate until a tighter coupling between cause and effect (pressure and porin opening) can be contrived. Generally however it is worth noting that an open ion channel is likely to be more hydrated than a closed one, and hydration is generally associated with a $-\Delta V$, often a quantitatively significant one. The delay between the application of pressure and opening is consistent with the $p\Delta V$ term in the ΔG of the opening transition being a minor component, and/or a number of steps being required for opening to take place. The response of other types of porin to high pressure would provide an interesting comparison, especially those porins which are expressed at high pressure in barophiles.

References

[1] Jap, B.K. and Walian, P.J. (1996); Structure and functional mechanism of porins; Physiol. Rev. 76, 1073–1088.

[2] Kendig, J.J., Grossman, Y and Heinemann, S.H. (1993); Ion channels and nerve cell function. In Effects of High Pressure on Biological Systems. edited Macdonald A.G. Springer-Verlag, Heidelberg.

[3] Meyer, R and Heinemann, S.H. (1997); Temperature and pressure dependence of Shaker K^+ channel N- and C- type inactivation; European Biophysics J. 26, 433–445.

[4] Bartlett, D.H., Kato, C. and Horikoshi, K. (1995); High pressure influences on gene and protein expression; Res. in Microbiology. 146, 697–706.

[5] Schiltz, E., Kreusch, A., Nestel, U. and Schulz, G.E. (1991); Primary structure of porin from *Rhodobacter capsulatus;* European J. Biochem. 199, 587–594.

[6] Delcour, A.H. (1997); Function and modulation of bacterial porins: insights from electrophysiology; FEMS Microbiology Letters. 151, 115–123.

[7] Delcour, A.H., Adler, J. and Kung, C. (1991); A single amino acid substitution alters conductance and gating of Omp C porin of *Escherischia coli;* J. Membrane Biol 119, 267–275.

[8] Delcour A.H., Martinac, B., Adler, J. and Kung, C. (1989); Voltage-sensitive ion channel of *Escherichia coli;* J. Membrane Biol. 112, 267- 275.

[9] Bangham, A.D., Standish, M.M. and Watkins, J.C. (1965); Diffusion of univalent ions across the lamellae of swollen phospholipids; J. Mol. Biol. 13, 238–252

[10] Macdonald, A.G. (1997); Effects of high hydrostatic pressure on the BK channel in bovine chromaffin cells; Biophys. J. 73, 1866–1873.

New Transition of Dioleoylphosphatidylcholine Bilayer Membrane Under High Pressure

S. Kaneshina, H. Ichimori[1], T. Hata and H. Matsuki

Department of Biological Science & Technology, Faculty of Engineering,
The University of Tokushima, Minamijosanjima, Tokushima 770-8506, Japan
kanesina@bio.tokushima-u.ac.jp
[1]Anan College of Technology, Minobayashi, Anan, Tokushima, 774-0017, Japan

Abstract. The phase transitions of 1,2-dioleoyl-*sn*-glycero-3-phosphocholine (DOPC) bilayer membranes were observed by high-pressure optical methods. The so-called main transition between the liquid crystalline (L_α) and the lamellar gel (L_β) phases was observed in water at above 0 °C under high pressure, in addition to the transition between the L_α and the lamellar crystalline (L_c) phases in 50% aqueous ethylene glycol. The pressure of the main transition increased linearly with an increase in temperature. Extrapolation of temperature (T) – pressure (p) phase boundary to ambient pressure suggests the temperature of the main transition to be –40.3 °C, which has never been found by DSC methods. On the other hand, the temperature of the L_c/L_α phase transition in 50% aqueous ethylene glycol was found to be –12.0 °C at ambient pressure. The values of dT/dp were 0.233 K MPa^{-1} for the L_β/L_α phase transition and 0.147 K MPa^{-1} for the L_c/L_α phase transition, respectively.

1 Introduction

High pressure study of lipid bilayer membranes is of particular interest to the studies of pressure reversal of anesthesia, pressure adaptation in deep sea organisms and high-pressure sterilization in food processing. Although bilayer membranes of saturated diacylphosphatidylcholines have been most thoroughly studied under high pressure, there have been few studies on the phase properties of unsaturated phosphatidylcholine bilayer membranes under high pressure [1–3]. The phospholipids of most biological membranes contain a high percentage of unsaturated fatty acyl chains. The biological importance of unsaturated fatty acids is believed to be related to the fact that their melting points are much lower than those of saturated fatty acids, with the result that membrane lipids containing unsaturated acyl chains tend to have lower temperatures of transition from the gel phase to the liquid crystalline phase. Since the phase transition of dioleoylphosphatidylcholine (DOPC) bilayer membrane at ambient pressure has been observed at temperatures below 0 °C [4–9], information on phase behavior has been difficult to obtain by conventional techniques, but such information is readily

accessible from high-pressure experiments. The present study demonstrates the pressure effect on the phase behavior of DOPC bilayer membranes.

2 Materials & Methods

Synthetic DOPC, 1,2-dioleoyl-*sn*-glycero-3-phosphocholine, was obtained from Sigma and used without further purification. The multilamellar vesicle was prepared by suspending DOPC in water or aqueous ethylene glycol at 1.0×10^{-3} mol kg^{-1}. The suspension was sonicated for a short time (ca. 3 min) in order to prepare a multilamellar vesicle suitable for the optical measurements of the phase transition. The average size of vesicles was 320±90 nm, which was determined by the light scattering method. The phase transition of DOPC bilayer vesicles under ambient pressure was observed by differential scanning calorimetry (DSC) using a Seiko SSC 560U calorimeter. The heating rate was 0.75 K min^{-1} The phase transitions of DOPC bilayer membrane under high pressures were observed by two kinds of optical methods. One is the observation of the isothermal barotropic phase transition and the other is the isobaric thermotropic phase transition. The general arrangement of the high pressure apparatus has been described previously [10].

3 Results & Discussion

A typical measurement of isothermal barotropic phase transition for DOPC bilayer membrane is shown in Fig. 1A. The light transmittance of vesicle suspensions at 560 nm was measured at 0 °C and depicted as a function of pressure. The phase transition pressure, which was determined from the transmittance–pressure profiles as a midpoint in transmittance change, increased linearly with an increase in temperature. This situation is depicted on the temperature (T) – pressure (p) phase diagram shown in Fig. 2. Extrapolation of this T–p line to ambient pressure suggests the temperature of the phase transition to be –40.3 °C, which has never been found in the literature.

The phase transition of DOPC bilayer membrane at ambient pressure has been observed at temperatures below 0 °C by DSC. Many workers have used aqueous ethylene glycol as an antifreeze solvent [4–6]. Lewis *et al.* [4] have described that DOPC bilayer membrane can form more stable lamellar crystalline (L_c) phases in aqueous ethylene glycol than in water. Therefore, the transition temperatures found at between –11.8 °C and –21.0 °C can be regarded as the transition from the L_c phase to the liquid crystalline (L_α) phase, namely the L_c/L_α phase transition. Although the presence of 50% ethylene glycol did not influence the main transition temperature [9], the temperature of the L_c/L_α phase transition is dependent upon the ethylene glycol content. The hydrated state at the membrane surface is likely to be important for stability of the L_c phase.

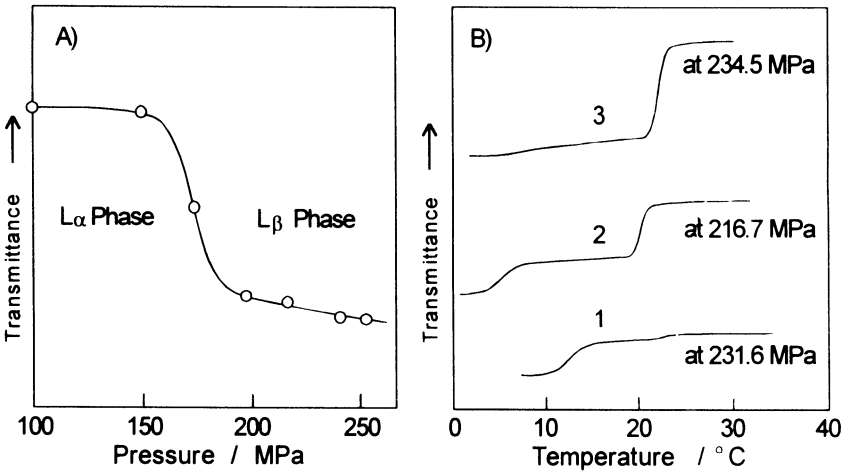

Fig. 1. Phase transitions of DOPC bilayer membrane. (**A**) A typical pressure-induced phase transition at 0 °C from the L_α phase to the L_β phase. (**B**) Two kinds of phase transitions in 50% aqueous ethylene glycol. DOPC suspension was pressurized first to about 200 MPa at 0 °C and then heated after being allowed to stand for (1) 0.1 h; (2) 2 h; and (3) 4 h

The L_c/L_α phase transition under high pressure was observed by the isobaric thermotropic change of transmittance in aqueous ethylene glycol. DOPC suspension prepared in 50% aqueous ethylene glycol was pressurized to a desired pressure at ca. 0 °C and was heated slowly (0.65 K min^{-1}) after the vesicle suspension was allowed to stand for a definite period of time. The transmittance–temperature profiles under high pressures are shown in Fig. 1B, which shows the existence of two kinds of transitions. When the vesicle suspension was immediately after it was pressurized, a lower temperature transition was observed (curve 1 in Fig. 1B). Curve 2 shows clearly the two step increase in transmittance, which was obtained in the case of the solution standing for a relatively short time (ca. 2 h) at 0 °C and ca. 220 MPa. In the case of the solution standing for a relatively long time (ca. 4 h) at 0 °C, only one transition was observed (curve 3 in Fig. 1B), which is consistent with higher temperature transition. As is seen from Fig. 2, the higher temperature transition in 50% aqueous ethylene glycol refers to the L_c/L_α phase transition, since extrapolation of this T–p line to ambient pressure suggests the temperature of transition to be –12.0 °C, which is obtained by DSC. This higher temperature transition could not be observed in the cooling scan or in the pressurizing scan, because the formation of the lamellar crystalline phase is extremely slow. On the other hand, lower temperature transition in 50% aqueous ethylene glycol was consistent with the transition in water, which can be regarded as the so-called main transition between the lamellar gel (L_β) phase and the L_α phase. This L_β/L_α phase transition could be observed by not only heating but also pressurizing scans in the range of temperature above 0 °C. At ambient pressure, however, the transition at about –40 °C has never been observed by DSC. From these facts it may be concluded that the L_β phase is a metastable phase in the pressure range studied.

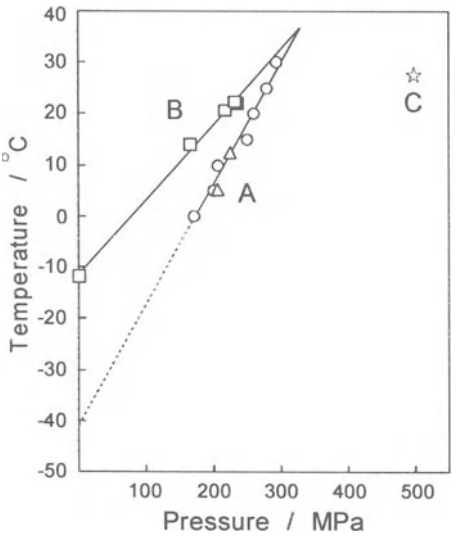

Fig. 2. Phase diagram of DOPC bilayer membrane. The concentration of DOPC was 1.0×10^{-3} mol kg^{-1}. A: The L_β/L_α main transition in water (O) and in 50% aqueous ethylene glycol (Δ). B: The L_c/L_α transition in 50% aqueous ethylene glycol (□). C: The transition observed by Wong and Mantsch (☆)

Wong and Mantsch [2] observed a phase transition at 28 °C and 500 MPa from a disordered liquid crystalline phase to highly ordered gel phase. In the present study, the L_c/L_α phase transition at 28 °C has to be observed at around 275 MPa, which differs from the observation at 500 MPa by Wong and Mantsch. As mentioned before, the phase transition from the L_α phase to the L_c phase is difficult to observe in the pressurizing scan because the transformation into the L_c phase is extremely slow. Therefore, the superpressing to transform into the L_c phase may be responsible for the pressure difference in the L_c/L_α phase transition. Alternatively, the observation by Wong and Mantsch may be a new pressure-induced phase transition. As is seen from Fig. 2, it is unlikely that the phase transition at 500 MPa and 28 °C is the same kind of transition as the L_c/L_α phase transition at –12 °C and ambient pressure.

References

[1] D.J. Siminovitch *et al.* (1987) Biochemistry, 26, 3277–3287.
[2] P.T.T. Wong and H.H. Mantsch (1988) Biophys. J., 54, 781–790.
[3] D.J. Siminovitch *et al.* (1988) Chem. Phys. Lipids, 46, 79–87.
[4] R.N.A.H. Lewis *et al.* (1988) Biochemistry, 27, 880–887.
[5] P.W.N. van Dijck *et al.* (1976) Biochim. Biophys. Acta, 455, 576–587.
[6] J.R. Silvius and R.N. McElhaney (1979) Chem. Phys. Lipids, 25, 125–134.
[7] P.G. Barton and F.D. Gunstone (1975) J. Biol. Chem., 250, 4470–4476.
[8] P.J. Davis and K.M.W. Keough (1983) Biochemistry, 22, 6334–6340.
[9] J.F. Santarem *et al.* (1982) Biochem. Biophys. Acta, 687, 231–237.
[10] H. Ichimori *et al.* (1997) Chem. Phys. Lipids 89, 97–105.

Effect of Pressure on the Phase Transitions of Dimyristoylphosphatidylethanolamine and Dimyristoylphosphatidylcholine Bilayers

H. Ichimori[1], S. Endo, T. Hata, H. Matsuki and S. Kaneshina

[1]Anan College of Technology, Minobayashi, Anan, Tokushima 774-0017, Japan
Department of Biological Science & Technology, Faculty of Engineering,
The University of Tokushima, Minamijosanjima, Tokushima 770-8506, Japan
kanesina@bio.tokushima-u.ac.jp

Abstract. The temperature (T) – pressure (p) phase diagrams of the dimyristoylphosphatidylcholine (DMPC) and dimyristoylphosphatidylethanolamine (DMPE) multilamellar vesicles were constructed by the method of high-pressure light transmittance. DMPC bilayer membrane undergoes pretransition at 13.9 °C from the lamellar gel ($L_{\beta'}$) phase to the ripple gel ($P_{\beta'}$) phase, and succeedingly the main transition at 23.9 °C from the $P_{\beta'}$ phase to the liquid crystalline (L_{α}) phase. The slopes of phase boundary, dT/dP, were 0.212 K MPa^{-1} for the main transition and 0.13 K MPa^{-1} for the pretransition, respectively. On the other hand, DMPE bilayer membrane undergoes transition at 56.8 °C from the highly ordered subgel (L_c) phase to the L_{α} phase. The value of dT/dp for this transition was 0.195 K MPa^{-1}. The main transition of DMPE bilayer membrane was observed at 49.6 °C and the value of dT/dp was 0.222 K MPa^{-1}.

1 Introduction

The phase behavior of diacylphosphatidylcholine bilayer membranes has been most extensively studied by various physical techniques [1–4]. We showed the pressure effect on the bilayer phase transitions of a series of diacylphosphatidylcholines containing linear saturated acyl chains [1], and extend these measurements and thermodynamic analysis to another major phospholipid group, i.e., the phosphatidylethanolamines (PE). The main transition of PE bilayer membrane has been studied [5–10], and only one research group reported on the relationship between pressure and main transition temperature by the method of adiabatic compression [5]. Recently the highly ordered subgel phase has been studied in detail by differential scanning calorimetry (DSC). However, there is no observation of subgel phase under high pressure.

The present study demonstrates the pressure effect on the phase transitions of dimyristoylphosphatidylethanolamine (DMPE) bilayer membrane and reveals the

difference in phase behavior between DMPE and dimyristoylphosphatidylcholine (DMPC) bilayer membranes.

2 Materials & Methods

Synthetic DMPE, 1,2-ditetradecanoyl-*sn*-glycero-3-phosphoethanolamine, and DMPC, 1,2-ditetradecanoyl-*sn*-glycero-3-phosphocholine, were obtained from Sigma. Water was distilled twice from dilute alkaline permanganate solution. The multilamellar vesicle was prepared by suspending DMPE or DMPC in water, using a Branson model 185 sonifier at a temperature several degrees above the main phase transition. The phase transitions under high pressures were observed by two kinds of optical methods. One is the observation of isothermal barotropic phase transitions and the other is the isobaric thermotropic phase transitions. The general arrangement of the high-pressure apparatus has been described in detail previously [2]. The sudden change in transmittance accompanying the phase transition was followed at 560 nm. In addition to the optical observation, the phase transitions of DMPE and DMPC bilayer membranes under ambient pressure were observed by DSC using a Micro Cal MCS calorimeter (Northampton, Mass, USA). The heating rate was 0.75 K min^{-1}.

3 Results & Discussion

The heating DSC thermogram of DMPC bilayer membrane at ambient pressure showed two kinds of endothermic transitions. Higher-temperature transition can be assigned as the main transition from the ripple gel (P_β') phase to the liquid crystalline (L_α) phase. On the other hand, lower-temperature transition can be assigned as the pretransition from the lamellar gel (L_β') phase to the P_β' phase. The light transmittance also changed clearly at two transition temperatures. The two transition temperatures by both methods were in good agreement with each other. The temperatures of the main transition and pretransition of DMPC bilayer membrane were 23.9 °C and 13.9 °C, respectively.

The temperature (T) – pressure (p) phase diagram of DMPC bilayer membrane is shown in Fig. 1. The temperatures of the main transition and pretransition increase with an increase in pressure. The T–p curves for the main transition and pretransition are slightly convex upward. The slopes of the phase boundary at ambient pressure were 0.212 K MPa^{-1} for the main transition and 0.13 K MPa^{-1} for the pretransition.

The volume changes (ΔV) associated with the transitions were calculated from the Clapeyron–Clausius equation,

$$dT/dp = T\Delta V/\Delta H, \quad (1)$$

where the enthalpy changes (ΔH) of transitions were determined by DSC.

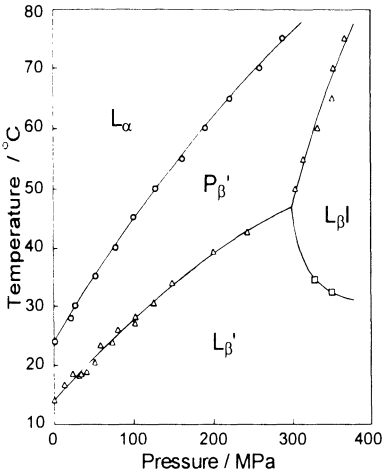

Fig. 1. Temperature–pressure phase diagram of DMPC bilayer membrane. The concentration of DMPC was 2.0 mmol kg^{-1}. Phase transitions: (O) $P_{\beta}' \rightarrow L_{\alpha}$, (Δ) $L_{\beta}' \rightarrow P_{\beta}'$ or $L_{\beta}I \rightarrow P_{\beta}'$, (□) $L_{\beta}' \rightarrow L_{\beta}I$

All the thermodynamic quantities for the phase transitions of DMPC bilayer membrane are summarized in Table 1. As is seen from Fig. 1, a pressure-induced interdigitated gel phase, in which the hydrocarbon chains from apposing monolayers become interdigitated with the chains, was observed at pressures above 300 MPa. A triple point on the phase diagram among P_{β}', L_{β}' and $L_{\beta}I$ phases was found at 300 MPa and 47 °C.

Table 1. Thermodynamic properties of phase transitions for bilayer membranes of DMPE and DMPC

Lipid	T (K)	dT/dp (K MPa^{-1})	ΔH (kJ mol^{-1})	ΔS (J $K^{-1}mol^{-1}$)	ΔV ($cm^3 mol^{-1}$)
DMPE ($L_{\beta} \rightarrow L_{\alpha}$)	322.8	0.222	24.1	75	16.7
($L_c \rightarrow L_{\alpha}$)	330.0	0.195	68.2	207	40.4
DMPC ($P_{\beta}' \rightarrow L_{\alpha}$)	297.1	0.212	24.7	83	17.6
($L_{\beta}' \rightarrow P_{\beta}'$)	287.1	0.13	4.0	14	1.8

On the other hand, the DSC thermogram of DMPE at ambient pressure showed two kinds of endothermic transitions. Higher-temperature transition can be assigned as the L_c/L_{α} transition from the highly ordered subgel (L_c) phase to the L_{α} phase, which is the transition between stable phases. Lower-temperature transition can be assigned as the main transition from the lamellar gel (L_{β}) phase to the L_{α} phase, which is the transition between metastable phases. The light transmittance also changed clearly at two transition temperatures. The temperatures of the L_c/L_{α} transition and main transition of DMPE bilayer membrane were 56.8 °C and 49.6 °C, respectively, which are in good agreement with previously published data [6, 8, 10].

The values of dT/dP were 0.195 K MPa^{-1} for the L_c/L_{α} transition and 0.222 K MPa^{-1} for the main transition. The previous value of dT/dP for the main transition was 0.258 K MPa^{-1} which is comparable with the present result. Regarding the effect of pressure on the L_c/L_{α} transition temperature, no research has been reported. The enthalpy and entropy changes associated with phase

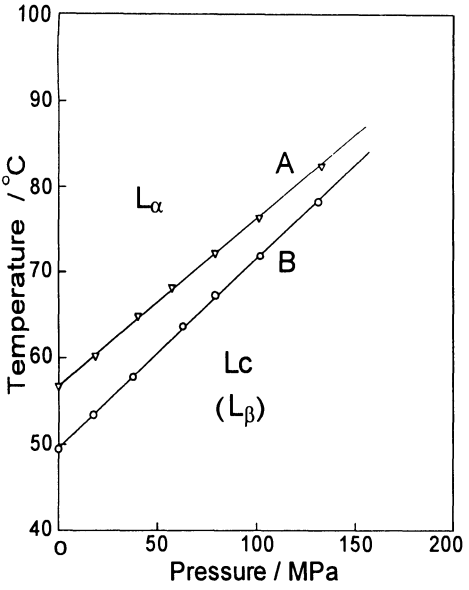

Fig. 2. Temperature–pressure phase diagram of DMPE bilayer membranes. The concentration of DMPE was 1.0 mmol kg^{-1}. A) L_c/L_α phase transition, B) L_β/L_α main phase transition

transitions of DMPE bilayer membrane are listed in Table 1 together with the volume changes calculated from Eq. (1).

As is seen from the comparison between Figs. 1 and 2, the P_β' and $L_\beta I$ phases were not observed in the DMPE membrane. There is a difference of 25.7 °C in the main-transition temperature between DMPE and DMPC bilayers. DMPC and DMPE molecules differ only in the polar head groups. Difference in the phase behavior can be attributed to the difference in size, specifically area per headgroup, between the two types of molecules. The larger PC headgroup prevents chains that are perpendicular to the bilayer from coming close enough together to minimize their van der Waals interactions. As a result of tilting, the distance between chains is reduced and the van der Waals interactions are minimized. In the L_β and/or L_c phase of DMPE, the hydrocarbon chains are perpendicular to the bilayer and not tilting.

References

[1] H. Ichimori *et al.* (1997) Chem. Phys. Lipids, 89, 97–105.
[2] H. Ichimori *et al.* (1998) Chem. Lett., 75–76.
[3] R. Koynova *et al.* (1996) Biochim. Biophys. Acta, 1285, 101–108.
[4] L. Finegold and M.A. Singer (1986) Biochim. Biophys. Acta, 855, 417–420.
[5] N.D. Russell and P.J. Collings (1982) J. Chem. Phys., 77, 5766.
[6] R. Koynova and M. Caffrey, (1994) Chem. Phys. Lipids, 69, 1–34.
[7] H. Chang and R.M. Epand, (1983) Biochim. Biophys. Acta, 728, 319–324.
[8] H.H. Mantsch *et al.* (1983) Biochim. Biophys. Acta, 728, 325–330.
[9] S. Mulukutla and G.G. Shipley (1984) Biochemistry, 23, 2514–2519.
[10] D.A. Wilkinson and J.F. Nagle (1984) Biochemistry, 23, 1538–1541.

Solidification and Melting of Some Edible Fats and Model Lipid Systems Under Pressure

W. Buchheim, E. Frede, M. Wolf and P. Baldenegger

Federal Dairy Research Centre, Hermann-Weigmann-Str. 1, D-24103 Kiel, Germany
buchheim@bafm.de

Abstract. Different edible fats and oils (milkfat, lard, coconut fat, cocoa butter, rapeseed oil), food emulsifiers (acetic esters (ACETEM) and propylene glycol esters (PGMS) of monoglycerides) and model systems (stearic and oleic acid, tristearin, triolein) were pressure-treated between 100 and 400 MPa. The temperature-time curves obtained after rather instantaneous compression or subsequent decompression showed characteristic courses depending on whether endothermic or exothermic phase transitions had been induced. The maximal temperature change occurred approx. 30 s after compression/decompression and varied between 6 and 16 K per 100 MPa depending on experimental conditions (pressure, temperature) and type of lipid. The pressure-induced shifts of major phase transition temperatures as derived from linear heating or cooling regimes at isobaric conditions amounted to approx. 16 K/100 MPa for milkfat, coconut fat and lard but 21 K/100 MPa for ACETEM.

1 Introduction

Edible fats and oils represent mixtures of a large number of triglyceride species. Whereas chemically pure triglycerides exhibit defined phase transition temperatures and often show polymorphic crystal forms (α, β', β), complex triglyceride mixtures gradually melt within a broad temperature range. Milkfat, for example, begins to melt at –40 °C and is completely liquid at 37 °C [1]. At ambient pressure, melting and solidification processes are usually followed by thermal analysis, i. e. DTA, DSC or related methods. The solid fat content can be directly measured by low resolution NMR, even if the fat is present in an emulsified state and this technique has been applied for studying the effects of high pressure treatments on milkfat emulsions like cream [2, 3]. By continuous temperature registration within a fat sample during selected pressure–temperature regimes it is possible to demonstrate the pressure-induced shift of phase transition temperatures [4].

2 Materials & Methods

Different edible fats (milkfat, lard, coconut fat, cocoa butter, rapeseed oil), food emulsifiers (acetic esters of monoglycerides: Grindsted™ ACETEM 70-00, m. p. approx. 40 °C; propylene glycol esters of monoglycerides: Grindsted™ PGMS-SPV, m. p. approx. 40 °C) and model lipids (stearic and oleic acid, tristearin, triolein) were investigated. A 20 ml temperature-controlled high pressure autoclave (inner diameter 16 mm) with hydraulic oil as pressure-transfer medium was used, the different lipid systems (4.5 ml) being within a plastic tube. By a thermocouple being permanently inserted in the lipid phase, the temperature-time curves obtained after rather instantaneous compression (up to 400 MPa at various temperatures) or decompression were measured. Furthermore, programmed linear cooling and heating (0.5 K per min) were applied (for milkfat, coconut fat, lard and ACETEM only) at isobaric conditions in order to identify major endo- and exothermic transitions and their shift under pressure.

3 Results

Figure 1 shows two typical series of directly measured temperature vs. time curves obtained after rapid compression or decompression of tristearin and oleic acid at 40 °C and pressures of 100, 200, 300 and 400 MPa. Although the build-up of maximum pressure as well as decompression to ambient pressure were completed within a few seconds, the resulting, largely adiabatic temperature increases/decreases were highest after approx. 30 s followed by a slow approach to the original temperature within 10 to 15 min.

Lipid systems which retain either a completely solid state like tristearin under the pressure-temperature conditions chosen or a completely liquid state (not shown) exhibit highly symmetric heating/cooling curves after compression/decompression. If such pressure treatment results in partial solidification of the lipid phase which is followed by re-melting after subsequent decompression, the corresponding heating/cooling curves become increasingly asymmetric like for oleic acid. Its 400 MPa compression curve in particular shows two pronounced exothermic reactions indicating major crystallization processes.

Table 1 summarizes the maximal temperature changes observed in all lipid systems under study at four temperature–pressure combinations (20 and 40 °C; 100 and 300 MPa) both after compression and decompression. There is wide variation in maximum (adiabatic) heating or cooling, e. g., between 6.0 and 16.1 K for the 100 MPa experiments and 14.5 and 34.2 K for 300 MPa experiments depending on initial temperature and, particularly, on the type of lipid.

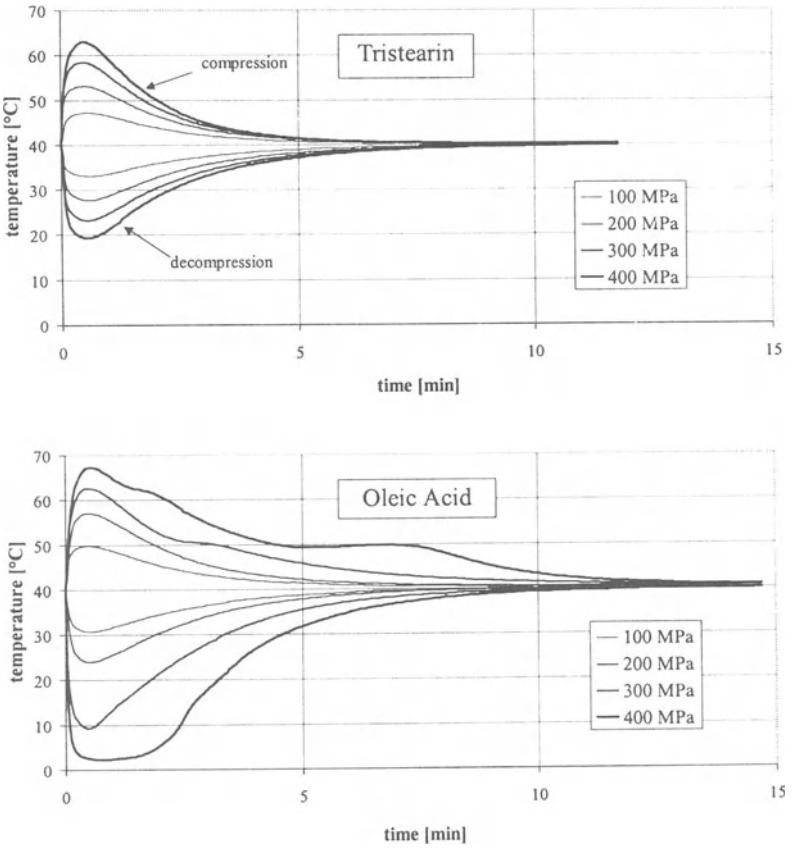

Fig. 1. Temperature courses after rapid compression/decompression

Table 1. Maximal temperature changes in lipid systems after rapid compression (C) and decompression (D)

	20 °C				40 °C			
	100 MPa		300 MPa		100 MPa		300 MPa	
	C	D	C	D	C	D	C	D
Stearic acid	6.4	6.0	18.0	14.5	7.0	6.3	17.0	15.5
Oleic acid	8.7	11.4	28.2	21.6	9.6	9.4	22.3	31.7
Tristearin	6.7	6.2	17.2	15.6	7.3	7.0	18.5	16.9
Triolein	8.4	8.1	21.0	19.6	8.7	8.6	21.1	20.3
Rapseed oil	8.5	8.2	21.1	20.1	8.9	8.6	21.5	20.6
Lard	7.9	9.0	21.3	21.0	8.9	12.6	21.8	22.7
Coconut fat	10.8	9.0	23.3	16.3	8.9	8.6	21.5	28.5
Cocoa butter	8.2	8.0	20.6	18.1	8.9	8.5	22.9	28.2
Milkfat	9.2	10.7	26.4	24.2	9.3	9.0	22.7	29.8
PGMS	10.0	11.4	29.4	18.6	12.9	11.7	37.7	25.5
ACETEM	7.9	8.9	24.0	22.1	16.1	9.6	34.2	25.2

The pressure-induced shifts of major phase transition temperatures as derived from linear heating and cooling at isobaric conditions were approx. 16 K per 100 MPa for milkfat, coconut fat and lard but 21 K for ACETEM.

4 Discussion

From the measurements described above it follows that despite the adiabatic temperature rise any pressure treatment of food lipids corresponds to a substantial cooling at ambient pressure. However, at least 15 min will pass before the heat which has been generated during the pressure build-up is abducted and the positive shift of the melting profile (approx.16 K/100 MPa) will be fully effective. During decompression to ambient pressure the melting profile is shifted downward in connection with an adiabatic temperature drop followed by slow temperature compensation. The maximal temperature changes after compression and decompression should be equal in the absence of additional structural changes of the lipid phase as, e. g., crystallization/melting or transitions from one polymorphic form to another. This is observed at least for most of the 100 MPa experiments. Major deviations between the maximal temperature rise and its corresponding drop are apparently due to exothermic (crystallization) and endothermic (melting) processes which may either occur at the beginning of the compression/decompression or be delayed. It should be possible to optimize the pressure-induced crystallization of edible fats by taking into account these phenomena. This could be relevant, e. g., for modifying crystal size and shape in fat products like shortenings.

References

[1] Timms, R.E. (1994); Physical chemistry of fats; in: Fats in Food Products (Moran, D.P.J., Rajah, K.K., eds.) Blackie Academic & Professional, London, 1–28.

[2] Buchheim, W. and Abou El-Nour, A. (1992); Induction of milkfat crystallization in the emulsified state by high hydrostatic pressure; Fat-Science, Technology, 94, 369–373.

[3] Buchheim, W., Schütt, M. and Frede, E. (1996); High pressure effects on emulsified fats; in: High Pressure Bioscience and Biotechnology (Hayashi, R., Balny, C., eds.) Elsevier Science, Amsterdam, 347–350.

[4] Yasuda, A. and Mochizuki, K. (1992); The behaviour of triglycerides under high pressure; in: High Pressure and Biotechnology (Balny, C., Hayashi, R., Heremans, K., Masson, P., eds.) John Libbey Eurotext, Montrouge (F); 255–259.

The Effects of High Pressure on Signal Transducing Systems of Cultural Endothelial Cells

L.B. Buravkova

State Scientific Centre of Russian Federation – Institute for Biomedical Problems,
Khoroshevskoye shosse 76a, 123007 Moscow, Russia
Phone: +7(095)-1956329; Fax: +7(095)-1952063
buravkova@mmcc.ibmp.rssi.ru

Abstract. To investigate the involvement of Ca-mobilizing signal transduction in cell modifications at high pressure we used well known Ca-agonists – histamine, serotonin and bradikinine. Besides human umbilical EC, cultured smooth muscle cells (SMC) and bull pulmonary artery endothelial cells (BPAEC) were used. It was shown that neither histamine (10^{-5} M), nor serotonin (10^{-6} M) stimulated PI-turnover after 30 min exposure to 6 MPa high hydrostatic pressure (HHP). The basal level of IPn did not differ from control cells. Similar results were obtained in cultured SMC (disappearance of serotonin stimulation) and in cultured BPAEC (disappearance of bradikinine stimulation). Thus, this pressure had no influence on basal PI-turnover but inhibited membrane signal transduction. 10 MPa HHP increased the all fraction of IPn (IP_1, IP_2, IP_3) up to 135%, but histamine did not activate the Ca-mobilising system in human EC after decompression in concentration more than 10 times higher than that usually used for activation control cells. To compare the effects of HHP and high partial pressure of nitrogen and helium we studied PI-turnover in EC after fast decompression. In case of human EC, HHP and high partial pressure of N_2 and He did not have an effect on IPn basal level, but signal transduction trough PI-turnover was inhibited. Activation «R - G-pr. - PL C» complex was observed only after slow decompression or after 30–60 min incubation at normal pressure. These results suggest the desensitisation of EC during HHP exposure.

1 Introduction

It is known the Ca-influx and intracellular Ca-exchange are modified under high pressure [1]. To understand the possibility of involving the PI-turnover in these processes we have studied the intensity of accumulation inositol phosphates (IPn) in cultured endothelial cells (EC) and the changes of lipids and free fatty acid membrane composition after exposure to high hydrostatic pressure (HHP) [2, 3]. Phosphoinositides (PIs) are minor membrane phospholipids, resident in all eucariotic cells. Activation of phospholipase C (PL C) results in increased 1,2-

diacylglycerol (DG) and inositolphosphates (IP, IP_2, IP_3) in cytoplasme. The products of PI-turnover regulate the different metabolic reactions.

Inositol-1,4,5-trisphosphate (IP_3) acts as an intracellular messenger mobilizing Ca from intracellular compartments, for instance, from endoplasmic reticulum; 1,2-diacylglycerol activates protein kinase C – an enzyme that phosphorilises many proteins. Arachidonic acid is metabolised in other mediators including prostaglandins, thromboxanes and leucotrienes that are tissue regional hormones. Thus, a multicomponent phosphoinositide turnover system consists of a number of protein molecules incorporated into a membrane which functionally bind with each other and regulate many cell biochemical reactions. It is a system, along with other multienzyme systems such as adenylatecyclase, ATP-ase etc., which is very sensitive to the influence of HHP and high partial pressure of inert gases.

2 Materials & Methods

2.1 Isolation and Culture of Endothelial Cells

Human EC were isolated from the umbilical cord of newborns (HUVEC) by enzymatic disaggregation (0.1% collagenase) as described earlier [4, 5]. Growth medium was medium 199 containing Earle's balanced salts, 20% heat inactivated human serum, penicillin-streptomycin (each 100 U/ml), 20 mM HEPES (pH 7.3), 2 mM glutamine, human brain growth factor (200 μg/ml) and heparin (100 μg/ml). EC were passaged using 0.05% trypsin / 0.1% EDTA and cells were seeded at a minimum density of 10^5 cells/cm^2. Prior to all experimental protocols, cultures of EC were rinsed free of growth medium incubations at 37 °C in medium 199.

2.2 Modelling of Hyperbaric Conditions

In order to simulate hyperbaric conditions confluent cultures (in medium MMH) of EC in multi-well plates were placed in a pressure chamber KON&KM at 30 °C, and pressure was increased to 5–10 MPa. Temperature during isopressure was 37 °C. For HHP conditions special syringes were used. After the selected period(s) of hyperbaria, pressure was normalized, plates withdrawn from the pressure chamber and all subsequent manipulations conducted under normobaric conditions.

2.3 Measurement of Phosphoinositide Catabolism

PI-turnover was assayed in EC monolayers as described previously [5]. Sub-confluent EC were cultured for 48 h in growth medium containing myo-2-[^{3}H]-inositol (5 μCi/ml). After removal of radiolabelled growth medium and rinsing of EC monolayers, cells were incubated for 30 min at 37 °C in medium 199

containing 20 mM HEPES (pH 7.3) and 20 mM LiCl, prior to addition of agonists. Incubations were terminated by addition of boiling 1% sodium dodecyl sulphate/ 3 mM EDTA, and inositol phosphates (IP, IP_2, IP_3) resolved by anion exchange chromatography on Dowex [6].

3 Results & Discussion

Preliminary experiments of dose- and time-dependence of Ca-agonist effects on PI-turnover in cultured cells under normal athmospheric pressure showed that maximum of IPn release was revealed after 5 min incubation with hormones. The optimal concentrations were: for histamine –10 μM, for serotonin –1 μM, for bradikinin –10 nm. It was shown that histamine was more active for HUVEC, serotonin – for smooth muscle cells (SMC) and bradikinin – for bull pulmonary artery endothelial cells (BPAEC).

At the first stage of the experiments we studied summary inositolphosphates (IPn) in cells. It was shown that PI-turnover was not activated by Ca-mobolizing agonist after 30 min exposure of SMS and HUVEC under HHP 6 MPa (Fig. 1). HHP resulted in reduction of histamine- or serotonin-stimulated levels of IPn when compared with control cells. Similar results were obtained in cultured BPAEC. In control cells PI-turnover was activated up to 240% and HHP resulted in desensitization of the transducing system.

Measurement of IP fractions showed that HHP (6–10 MPa) slightly increased the amount of all fractions and especially IP_2 and IP_3. The total level of IPn in HUVEC was increased up to 120% after HHP exposure. It is important that histamine did not activate EC after decompression either in a concentration 10 μM (this concentration doubled the activity of PI-turnover in control cells), or in a concentration 100 μM. These results suggest cell desensitization.

To compare the effects of HHP and high pressure of inert gases (nitrogen and helium) we studied PI-turnover in EC after fast decompression (about 1 min). HHP and high pressure of nitrogen insignificantly increased the basal level of PI-turnover in HUVEC but completely terminated transmission of hormone signals. After slow decompression (0.15 MPa/min, 30 min), the basal level of all IP fractions was unchanged but histamine-stimulated levels were the same as in control cells. This indicates that the sensitivity of cultured cells was completely recovered when slow decompression was used. Similar results were obtained for BPAEC.

Thus, the rate of decompression influenced cell sensitivity to hormones. Fast decompression resulted in desensitization caused by pressure *per se*. However, «receptor - G-protein - phospholipase C» complex transfer signals from agonist to intracellular processes after slow decompression.

To examine the recovery of the sensitivity of cells to Ca-mobilizing hormones, BPAEC were incubated for 35 min under normal pressure after 30 min exposure at 6 MPa and fast decompression. In this case, the recovery period was equal to the time of slow decompression. We ascertained that the bradikinin-stimulated level of

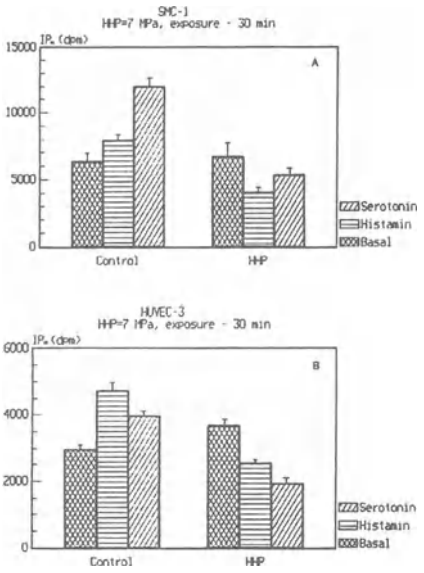

Fig. 1. The total level of IPn without (basal level) and after stimulation by Ca-mobilizing agonists (histamine and serotonin) in control cells and after 30 min HHP exposure (7 MPa). (**A**) SMC, (**B**) HUVEC

IPn did not significantly differ from control cells after the recovery period. The results suggest that high pressure could result in cell desensitization. However this effect disappears after recovery or when the decompression period is increased.

References

[1] Grossman Y., Golan H. Synaptic transmission under hyperbaric condition. (1990); Proc. II-nd Intern. Meeting on High Pressure Biology, Toulon, France paper N16.

[2] Buravkova L.B., Rudakovsky M.L. (1990); Effects of high hydrostatic pressure on Ca mobilizing in cultured cells. Proc. II-nd Intern. Meeting on High Pressure Biology, Toulon, France, paper N4.

[3] Buravkova L., Naydina V. (1997); Cellular membrane lipids and fatty acid composition after high pressure exposure. Undersea&Hyperbaric Med., v.27. Suppl., p53.

[4] Allikmets E.Yu., Danilov S.M. (1986); Mitogen-induced disorganization of capillary-like structures formed by human large-vessel endothelial cells in vitro. Tissue and Cell, 18, 481–489.

[5] Resink T.J., Grigorian G.Y., Moldabaeva A.K., Danilov S.M., Buhler F.R. (1987); Histamine-inducted phosphoinositide metabolism in cultured human umbilical vein endothelial cells. Association with thromboxane production and prostacyclin release. Biochem. Biophys. Res. Commun., 44, 438–446.

[6] Resink T.J., Buravkova L.B., Mirzapoyazova T., Kohler E., Erne P., Tkachuk V. (1996); Involvement of protein kinase C in hypoxia-induced desensitization of the β-adrenergic system in human endothelial cells. Biochem. Biophys. Res. Commun., 222, 753–758.

Thermotropic and Barotropic Phase Behavior of 1-Hexadecyl-2-Palmitoylphosphatidylcholine Bilayer Membrane

H. Ichimori[1], H. Matsuki, T. Hata and S. Kaneshina

[1]Anan College of Technology, Minobayashi, Anan, Tokushima 774-0017, Japan
Department of Biological Science & Technology, Faculty of Engineering,
The University of Tokushima, Minamijosanjima, Tokushima 770-8506, Japan
kanesina@bio.tokushima-u.ac.jp

Abstract. The temperature (T) – pressure (p) phase diagram of the ether-ester-linked 1-hexadecyl-2-palmitoylphosphatidylcholine (HPPC) multilamellar vesicles was constructed by the method of high-pressure light transmittance. The HPPC bilayer membrane at ambient pressure undergoes pretransition (at 33.8 °C) from the lamellar gel ($L_{\beta'}$) phase to the ripple gel ($P_{\beta'}$) phase, and succeedingly the main transition (at 42.4 °C) from the $P_{\beta'}$ phase to the liquid crystal (L_{α}) phase. The slopes of the T–p diagram were 0.242 K MPa^{-1} for the main transition and 0.184 K MPa^{-1} for the pretransition, respectively. Pressure-induced interdigitated gel ($L_{\beta}I$) phase of HPPC bilayer membrane was observed at the high pressure beyond 50 MPa. A triple point among $L_{\beta'}$, $L_{\beta}I$ and $P_{\beta'}$ phases was found at 50 MPa and 41 °C.

1 Introduction

Phospholipid membranes undergo thermotropic phase transition, the temperature of which depends strongly on the nature of the phospholipid polar head groups and the hydrophobic chains. Dialkylphospholipids or alkylacylphospholipids, as well as diacylphospholipids, have been widely found in mammalian cells and organelle membranes [1]. Although dipalmitoylphosphatidylcholine (DPPC) is one of the most extensively studied ester-linked phospholipids with regard to structural and thermodynamic properties, relatively few studies have been reported on the properties of the ether-linked phospholipid, dihexadecylphosphatidylcholine (DHPC) [2–6] and the mixed ether-ester-linked phospholipid, hexadecyl-palmitoylphosphatidylcholine (HPPC) [7, 8]. We demonstrated previously the pressure effect on the phase behavior of DHPC bilayer membrane and revealed the difference in the phase diagrams between the ether-linked DHPC and the ester-linked DPPC [2]. In the present study, we focus our attention on the structure and properties of ether-ester-linked HPPC, a chemical "intermediate" between DPPC and DHPC, and reveal the pressure effect on the phase behavior of the HPPC bilayer membrane.

2 Materials & Methods

Synthetic HPPC, 1-*O*-hexadecyl-2-palmitoyl-*rac*-glycero-3-phosphocholine, was obtained from Sigma. Water was distilled twice from dilute alkaline permanganate solution. The multilamellar vesicle was prepared by suspending HPPC in water at 1 mmol kg^{-1}, using a Branson model 185 sonifier at a temperature several degrees above the main phase transition. The phase transitions of HPPC multilamellar vesicle under ambient pressure were observed by a Micro Cal MCS high-sensitivity differential scanning calorimeter (DSC) (Northampton, Mass, USA). The heating rate was 0.75 K min^{-1}. The enthalpy changes of phase transitions were determined as an average value for several vesicle solutions. The phase transitions under high pressures were observed by two kinds of optical methods. One is the observation of isothermal barotropic phase transitions and the other is the isobaric thermotropic phase transitions. The general arrangement of the high-pressure apparatus has been described in detail previously [2, 9]. The sudden change in transmittance accompanying the phase transition was followed at 560 nm.

3 Results & Discussion

An example of the thermotropic phase-transition measurements for HPPC bilayer membrane is shown in Fig. 1. The DSC thermogram of heating scan at ambient pressure showed two kinds of endothermic transitions. Higher-temperature transition refers to the main transition from the P_{β}' phase to the L_{α} phase. On the other hand, lower-temperature transition refers to the pretransition from the L_{β}' phase to the P_{β}' phase. The light transmittance also changed clearly at two transition temperatures (Fig. 1A). The two transition temperatures by both methods were in good agreement with each other. The pretransition and main transition were accompanied by an increase in transmittance. This agrees with the previous observation [2, 9]. The temperatures of the pretransition (T_p) and the main transition (T_m) of HPPC bilayer membrane were at 33.8 °C and 42.4 °C, respectively. The enthalpy changes (ΔH) associated with the main transition and the pretransition were 34.5 and 1.7 kJ mol^{-1}, respectively. Figure 1 includes the isobaric thermotropic phase transitions at various high pressures by the optical method. Both temperatures of the main transition and the pretransition increased with an increase in pressure. The difference in temperature between the two transitions became wide as the pressure increased (Fig. 1A). A new pressure-induced gel phase between L_{β}' and P_{β}' phases was observed beyond 50 MPa (Fig. 1B), which can be assigned as the $L_{\beta}I$ phase from the analogy to DPPC and DHPC bilayer membranes [2]. The temperature range in which the $L_{\beta}I$ phase appears was extended as the pressure increased.

The temperature (T) – pressure (p) phase diagram of the HPPC bilayer membrane is shown in Fig. 2. Both results of the isobaric and isothermal phase transitions are in good agreement with each other. The T–p curves for the main

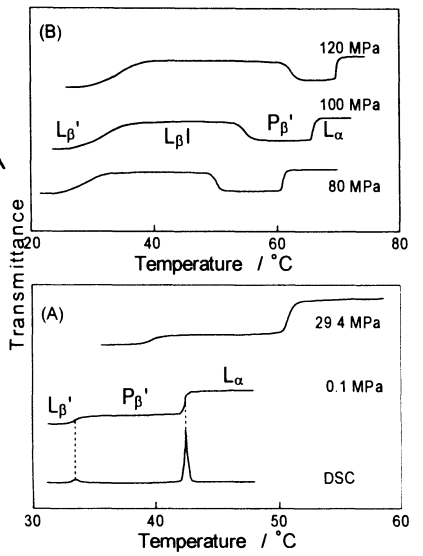

Fig. 1. Isobaric thermotropic phase transitions of HPPC bilayer membrane. (**A**) Main transition and pretransition observed by DSC and an optical method at 0.1 MPa and at 29.4 MPa. (**B**) Pressure-induced interdigitation in the HPPC bilayer membrane

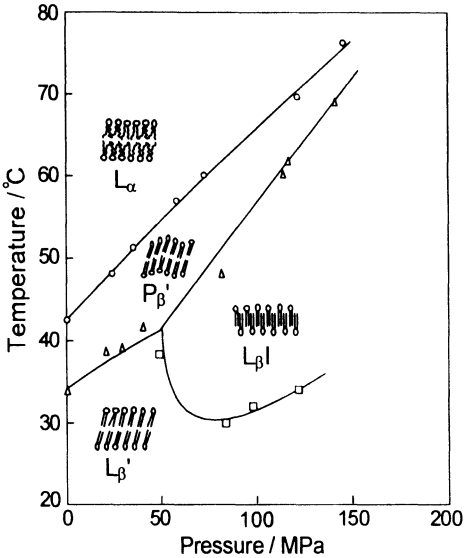

Fig. 2. Temperature–pressure phase diagram of ether-ester-linked HPPC bilayer membrane. The concentration of HPPC was 1.0 mmol kg^{-1}. Phase transitions: (○) $P_{\beta}' \rightarrow L_{\alpha}$, (△) $L_{\beta}' \rightarrow P_{\beta}'$ or $L_{\beta}I \rightarrow P_{\beta}'$, (□) $L_{\beta}' \rightarrow L_{\beta}I$

transition and pretransition are slightly convex upward. The slopes of the phase boundary, dT/dP, for the main transition and the pretransition at ambient pressure were 0.242 and 0.184 K MPa^{-1}, respectively, which are listed in Table 1 together with the thermodynamic properties for the phase transition of HPPC bilayer membrane.

The volume changes (ΔV) associated with the transitions were calculated from the Clapeyron–Clausius equation,

$$dT/dp = \Delta V/\Delta S, \quad (1)$$

and are also listed in Table 1. The values of ΔV were estimated to be 26.5 cm^3mol^{-1} for the main transition and 1.0 cm^3 mol^{-1} for the pretransition. The reported values of ΔV were 28.2 cm^3 mol^{-1} for DPPC bilayer membrane, and 25.7 cm^3 mol^{-1} for DHPC bilayer membrane [2]. There was no significant difference in the thermodynamic properties (i.e. the transition temperature, enthalpy and volume) among HPPC, DPPC and DHPC bilayer membranes.

As is seen from Fig. 2, a pressure-induced interdigitated gel phase, in which the hydrocarbon chains from apposing monolayers become interdigitated with the chains, was observed beyond 50 MPa. A triple point among L_{β}', $L_{\beta}I$ and P_{β}' phases was found at 50 MPa and 41 °C. Because the slope of the phase boundary between P_{β}' and $L_{\beta}I$ phases is larger than that of the main transition, two phase boundaries intersect each other at 200 MPa and 87 °C: we may find another triple point among L_{α}, P_{β}' and $L_{\beta}I$ phases.

Table 1. Thermodynamic properties for the phase transitions of HPPC bilayer membrane

Transition	T (K)	dT/dp ($K\,MPa^{-1}$)	ΔH ($kJ\ mol^{-1}$)	ΔS ($J\,K^{-1}\,mol^{-1}$)	ΔV ($cm^3\ mol^{-1}$)
Main($P_\beta' \rightarrow L_\alpha$)	315.6	0.242	34.5	109	26.5
Pre ($L_\beta' \rightarrow P_\beta'$)	307.0	0.184	1.7	6	1.0

HPPC, DHPC and DPPC molecules differ only in the ester and ether linkage between the polar head group and the hydrocarbon chains. In order to make clear the effect of ether or ester linkage on the phase behavior of bilayer membranes, the T–p phase diagram for HPPC membrane was compared with those for DPPC and DHPC membranes. Regarding the ester-linked DPPC bilayer membrane, a pressure-induced $L_\beta I$ phase was observed beyond 100 MPa. A triple point among L_β', $L_\beta I$ and P_β' phases was found at 100 MPa and 45 °C [2]. On the other hand, the ether-linked DHPC bilayer membrane exists in the $L_\beta I$ phase at lower temperature than pretransition under ambient pressure [2–4]. The substitution of an ether linkage for an ester linkage of DPPC brings about the appearance of the $L_\beta I$ phase at ambient pressure. Therefore the shape of the T–p diagram of DHPC bilayer membrane corresponds to that of the DPPC bilayer membrane in the regions of elevated pressures. The T–p diagram of HPPC bilayer membrane is at an intermediate location between the DPPC and the DHPC, because HPPC is a chemical intermediate between DPPC and DHPC.

Haas *et al.* [7] have reported only one phase transition of HPPC bilayer membrane which was observed at 40 °C and assigned as the transition from the $L_\beta I$ phase to the L_α phase by DSC and X-ray diffraction, although a low enthalpy shoulder on the main transition was observed by the DSC method. There are some disagreements between theirs and present results. We could not observe the $L_\beta I$ phase at ambient pressure. We used racemic mixtures of HPPC, whereas Haas *et al.* used the L conformer. Therefore, it may be concluded that the enantiomer affects the molecular packing of the hydrophobic chain in the interdigitated phase.

References

[1] L.A. Horrocks and M. Sharma (1982) in: J.N. Hawthorne and G.B. Snesell (Eds.), Phospholipids, Elsevier, Amsterdam, 51–93.
[2] S. Maruyama, H. Matsuki, H. Ichimori and S. Kaneshina (1996) Chem. Phys. Lipids, 82, 125–132.
[3] J.T. Kim, J. Mattai and G.G. Shipley (1987) Biochemistry, 26, 6592–6598.
[4] P. Laggner, K. Lohner, G. Degovics, K. Muller and A. Schuster (1987) Chem. Phys. Lipids, 44, 31–60.
[5] M.J. Ruocco, D.J. Siminovitch and G. Griffin (1985) Biochemistry, 24, 2406–2411.
[6] J.T. Kim, J. Mattai and G.G. Shipley (1987) Biochemistry, 26, 6599–6603.
[7] N.S. Haas, P.K. Sripada and G.G. Shipley (1990) Biophys. J., 57, 117–124.
[8] R.N.A.H. Lewis, R.N. McElhaney, W. Pohle and H.H. Mantsch (1994) Biophys. J., 67, 2367–2375.
[9] H. Ichimori, H. Matsuki and S. Kaneshina, (1998) Chem. Lett., 75–76.

Effect of Pressure and Local Anesthetics on the Phase Transitions of Ether-Linked Dihexadecylphosphatidylcholine Bilayer Membrane

S. Kaneshina, H. Endo, T. Hata and H. Matsuki

Department of Biological Science & Technology, Faculty of Engineering,
The University of Tokushima, Minamijosanjima, Tokushima 770-8506, Japan
kanesina@bio.tokushima-u.ac.jp

Abstract. The temperature–pressure phase diagram of ether-linked dihexadecylphosphatidylcholine (DHPC) multilamellar vesicles was constructed by the method of high-pressure transmittance in the presence of the local anesthetics, lidocaine and tetracaine hydrochlorides. While the temperature of the main transition from the ripple gel phase to the liquid crystalline phase was depressed by the addition of anesthetics and elevated by the pressure, the temperature of the pretransition from the interdigitated gel phase to the ripple gel phase was elevated by both the addition of anesthetics and pressure. The pressure-anesthetic antagonism was confirmed for only the main phase transition and a synergistic effect of pressure and anesthetic was observed for the pretransition of DHPC bilayer membrane.

1 Introduction

Pressure antagonizes the action of anesthetics [1–3]. Pressure reversal of anesthesia both *in vivo* and *in vitro* is of physiologic interest. Anesthetics are generally considered to act directly on the biomembranes, although the mechanism of the anesthetic action is still uncertain. In this respect, the study of pressure-anesthetic antagonism has been regarded as a possible key to elucidating the mechanism of anesthetic action. Phospholipid model membranes are often used to probe the mechanisms of pressure-anesthetic antagonism [4–10]. It is established that the main transition temperature of bilayer membranes of phospholipids such as dipalmitoylphosphatidylcholine (DPPC) is elevated by high pressures and is depressed by the addition of anesthetics [7, 9, 10]. Bilayer membranes of the ether-linked phospholipid, dihexadecylphosphatidylcholine (DHPC), as well as the ester-linked DPPC have been studied as model biomembranes and undergo two phase transitions with increasing temperature at ambient pressure [11–14]; one is the main transition from the ripple gel (P_{β}') phase to the liquid crystalline (L_{α}) phase and the other is the pretransition from the interdigitated gel ($L_{\beta}I$) phase to the P_{β}' phase, in contrast to the pretransition of a DPPC bilayer membrane from the lamellar gel (L_{β}') phase to the P_{β}' phase. The interdigitation of the DHPC bilayer

under ambient pressure has been confirmed by structural and thermodynamic techniques on the DHPC-water system covering a wide range of hydrations [12, 13].

In this study, we examined the phase behavior of ether-linked DHPC bilayer membrane in the absence and presence of local anesthetics with different hydrophobicity, lidocaine hydrochloride and tetracaine hydrochloride, under various pressures in order to elucidate the effects of pressure and anesthetics on the phase transitions of a model biomembrane system.

2 Materials & Methods

Synthetic DHPC, 1,2-di-*O*-hexadecyl-*rac*-glycero-3-phosphocholine, was obtained from Sigma Chemicals (St. Louis, MO, USA). Local anesthetics, lidocaine hydrochloride (LC•HCl) [2-diethylamino-*N*-(2,6-dimethylphenyl)acetamide hydrochloride] and tetracaine hydrochloride (TC•HCl) [2-dimethylaminoethyl-4-butylaminobenzoate hydrochloride] were also obtained from Sigma Chemicals and recrystallized several times from ethanol. The phospholipid multilamellar vesicles were prepared by suspending DHPC (2.0 mmol kg^{-1}) in water or anesthetic solution using a vortex mixer at a temperature several degrees above the main phase transition. The sample was incubated at 5 °C for at least 10 h before measurements in the high-pressure vessel. The phase transitions of the DHPC bilayer membrane under ambient pressure were observed using a Microcal MCS high-sensitivity differential scanning calorimeter (DSC) (Northampton, MA, USA). The heating rate was 0.75 K min^{-1}.

The phase transitions under high pressures were observed by an optical method of the isobaric thermotropic transitions. The general arrangement of the high-pressure apparatus has been described in detail previously [14]. The sudden change in transmittance accompanying the phase transition was followed at 540 nm. The heating rate at a given pressure was 0.67 K min^{-1}.

3 Results & Discussion

The DSC thermograms in the absence of local anesthetics showed two kinds of endothermic transitions of DHPC bilayer. The higher-temperature transition at 44.6 °C can be assigned to the P_β'/L_α main transition. On the other hand, the lower-temperature transition at 33.6 °C can be assigned to the $L_\beta I/ P_\beta'$ pretransition [12–14]. Both transition temperatures varied with the addition of local anesthetics in a dose-dependent manner.

Figure 1 shows the phase-transition temperatures of DHPC bilayer membrane as a function of anesthetic concentration up to 50 mmol kg^{-1}. The main transition temperature was depressed by the addition of local anesthetics; the magnitude of

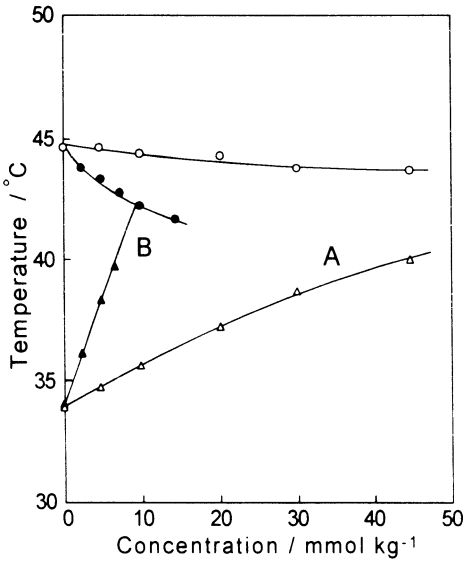

Fig. 1. Effect of local anesthetic on the phase transition temperatures of DHPC bilayer membrane. Local anesthetics: (A) LC•HCl and (B) TC•HCl. DHPC concentration was 2.0 mmol kg^{-1}. Phase transition: (○) and (●), $P_{\beta}' \rightarrow L_{\alpha}$ or $L_{\beta}I \rightarrow L_{\alpha}$; (△) and (▲), $L_{\beta}I \rightarrow P_{\beta}'$

transition-temperature depression by TC•HCl is much stronger than that by LC•HCl. In contrast, the pretransition temperature was elevated by the addition of anesthetics. The elevation of the pretransition temperature indicates that local anesthetics interact preferentially with the $L_{\beta}I$ phase relative to the P_{β}' phase [15], so that the addition of the local anesthetic shifts the phase equilibrium toward the $L_{\beta}I$ phase. At concentrations of TC•HCl above 10.0 mmol kg^{-1}, the P_{β}' phase disappeared and only a transition from the $L_{\beta}I$ phase to the L_{α} phase was observed.

The temperature (T) – pressure (p) phase diagram of DHPC bilayer membrane in the absence of local anesthetic is shown in Fig. 2A. The T–p curve for the main transition is slightly convex upward, whereas the pretransition temperature increases linearly with an increase in pressure. Since the slope of the phase

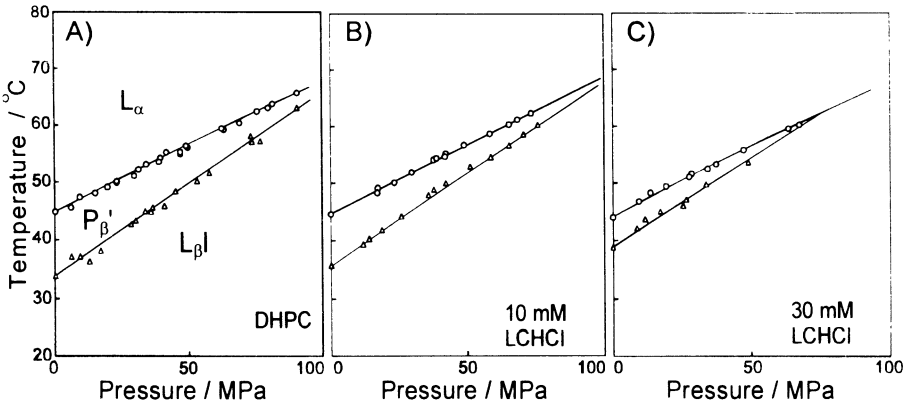

Fig. 2. Temperature–pressure phase diagrams of DHPC bilayer membrane (**A**) in the absence of LC•HCl (**B**) in the presence of 10 mmol kg^{-1} LC•HCl, and (**C**) in the presence of 30 mmol kg^{-1} LC•HCl. Phase transition: (○), $P_{\beta}' \rightarrow L_{\alpha}$ or $L_{\beta}I \rightarrow L_{\alpha}$, (△), $L_{\beta}I \rightarrow P_{\beta}'$

boundary for the pretransition is larger than that for the main transition, the two *T–p* curves intersect each other at 130 MPa and 74.5 °C, which is a triple point among the $L_{\beta}I$, P_{β}' and L_{α} phases [14]. Figures 2B and 2C show the phase diagrams of DHPC bilayer membrane in the presence of 10.0 mmol kg^{-1} and 30.0 mmol kg^{-1} LC•HCl, respectively. The temperature of the main transition was slightly depressed by the addition of LC•HCl at constant pressure, whereas the temperature of the pretransition was raised, but both transition temperatures increased almost linearly with pressure. As is seen from Fig. 2, the region of the P_{β}' phase on the phase diagram diminished as the local anesthetic LC•HCl was added. Triple point among $L_{\beta}I$, P_{β}', and L_{α} phases was shifted toward lower temperature and pressure as the LC•HCl concentration increased; 110 MPa and 71 °C in the presence of 10.0 mmol kg^{-1}, and 70 MPa and 61 °C in the presence of 30.0 mmol kg^{-1}, respectively. Consequently, the region of the $L_{\beta}I$ phase on the phase diagrams was extended to lower pressure ranges by the addition of LC•HCl in a dose-dependent manner, in comparison with the DHPC bilayer phase diagram in the absence of local anesthetics.

The effect of TC•HCl on the DHPC bilayer phase diagram is similar to that of LC•HCl. The magnitude of anesthetic effect by TC•HCl is much stronger than that by LC•HCl.

In conclusion, as regards the phase transitions of DHPC bilayer membrane, pressure antagonizes the anesthetic effect on the main transition temperature, while the pretransition temperature is influenced cooperatively by pressure and anesthetics. Since anesthesia is antagonized by applying pressure, we may say that the interdigitation of bilayer membranes is out of the anesthesia mechanism.

References

[1] F.H. Johnson and E.A. Flagler (1950) Science, 111, 91–92.
[2] M.T. Lever *et al.*, (1971) Nature, 231, 368–371.
[3] M.J. Halsey and B. Wardley-Smith (1975) Nature, 257, 811–813.
[4] J.R. Trudell *et al.*, (1975) Proc. Natl. Acad. Sci. USA, 72, 210–213.
[5] A.G. Macdonald (1978) Biochim. Biophys. Acta, 509, 26–37.
[6] D.B. Mountcastle *et al.*, (1978) Proc. Natl. Acad. Sci. USA, 75, 4906–4910.
[7] H. Kamaya *et al.*, (1979) Biochim. Biophys. Acta, 550, 131–137.
[8] W. MacNaughtan and A.G. Macdonald (1980) Biochim. Biophys. Acta, 597, 193–198.
[9] S. Kaneshina *et al.*, (1983) J. Colloid Interface Sci., 93, 215–224.
[10] S. Maruyama et al, (1997) Biochim. Biophys. Acta, 1325, 272–280.
[11] M.J. Ruocco *et al.*, (1985) Biochemistry, 24, 2406–2411.
[12] J.T. Kim *et al.*, (1987) Biochemistry, 26, 6592–6598.
[13] P. Laggner *et al.*, (1987) Chem. Phys. Lipids, 44, 31–60.
[14] S. Maruyama *et al.*, (1996) Chem. Phys. Lipids, 82, 125–132.
[15] H. Kamaya *et al.*, (1984) J. Phys. Chem., 88, 797–800.

Proteins

Pressure-Induced Thermostabilization of Glutamate Dehydrogenase from the Hyperthermophiles *Pyrococcus furiosus* and *Thermococcus litoralis*

M.M. Sun[1], N. Tolliday[2], C. Vetriani[2], F.T. Robb[2] and D.S. Clark[1]

[1]Dept. of Chemical Engineering, University of California, Berkeley, California 94720; USA
[2]Center of Marine Biotechnology, University of Maryland Biotechnology Institute, Baltimore, Maryland 21202, USA
clark@cchem.berkeley.edu

Abstract. The thermostabilities of glutamate dehydrogenases (GDH) from the hyperthermophiles *Pyrococcus furiosus* and *Thermococcus litoralis* were studied at pressures up to 500 atm. At 109 °C, *P. furiosus* GDH was stabilized 18-fold at 500 atm, one of the largest degrees of pressure stabilization reported to date. Addition of glycerol also stabilized *P. furiosus*, albeit to a lesser extent. Based on the known effects of glycerol on protein structure, two possible mechanisms of pressure stabilization of GDH were proposed. Thermoinactivation studies with the highly homologous GDH from *T. litoralis* indicated that it is less thermostable than the *P. furiosus* GDH. However, application of 500 atm stabilized the enzyme to a degree similar to that of the *P. furiosus* GDH.

1 Introduction

High pressure (>3000 atm) is typically viewed as a denaturant and has thus been mainly used in studies of enzyme denaturation [1–3]. However, there is increasing evidence that moderately high pressures (≤1500 atm) below those normally needed for pressure-induced denaturation can cause subtle, but important, changes in protein structure and dynamics [4–7]. Moreover, recent studies have shown that moderately high pressures can stabilize proteins against thermoinactivation [8–11].

In this paper, we describe an unusually large pressure stabilization of *P. furiosus* GDH against thermoinactivation. Studies of this enzyme in the presence of glycerol led us to hypothesize possible mechanisms of pressure stabilization. In addition, the highly homologous *T. litoralis* GDH displayed a similar degree of pressure stabilization to the *P. furiosus* GDH.

2 Materials & Methods

2.1 Purification of GDH

Native GDH from *P. furiosus* was kindly supplied by M.W.W. Adams (University of Georgia). Recombinant *P. furiosus* GDH was purified essentially as described previously [12], with modifications to the size and running conditions of both the anion-exchange and affinity columns. Further details of the purification procedure will appear in an upcoming manuscript.

2.2 Determination of Thermal Half-Lives

Thermoinactivation experiments were performed using a high-pressure, high-temperature bioreactor described previously [8]. Experiments were initiated by injecting 7.0 ml of a solution of the enzyme in incubation buffer (20–50 μg/ml) into the bioreactor. The incubation buffer was 100 mM EPPS (pH 8.0 at room temperature) with the appropriate concentrations of glycerol when called for. The bioreactor was immediately pressurized hyperbarically (with helium) to the appropriate pressure by opening it to the gas reservoir and then sealing the reactor; enzyme injection and pressurization were usually complete within 30 s. Samples were withdrawn from the bioreactor at various times (e.g., 10, 30, 75, 120, and 180 min) and assayed at ambient pressure to determine residual enzyme activity.

3 Results & Discussion

3.1 Pressure Studies with *Pyrococcus furiosus* GDH

The effect of pressure on the thermoinactivation of *P. furiosus* GDH is summarized in Table 1. Half-lives measured as a function of temperature at 5 and 500 atm indicate that the application of high pressure substantially stabilizes *P. furiosus* GDH against thermoinactivation.

Table 1. Half-lives of *P. furiosus* GDH as a function of temperature at 5 and 500 atm

Temp (°C)	$t_{1/2}$ (5 atm)	$t_{1/2}$ (500 atm)
103	550	1700
106	115	460
109	12	215

For example, at 109 °C, pressure stabilizes *P. furiosus* GDH 18-fold based on the ratio of half-lives at 500 and 5 atm ($t_{1/2}$ [500 atm]/ $t_{1/2}$ [5 atm]). This is one of the largest degrees of pressure-induced stabilization reported to date. Insights into

the mechanism of this large pressure stabilization may be gained by examining the effect of glycerol on protein stability and structure.

3.2 Effect of Glycerol on *P. furiosus* GDH Stability

Figure 1 shows thermoinactivation trajectories of a *P. furiosus* GDH mutant in the presence of glycerol. The mutant contains an extra tetrapeptide at the C-terminus which destabilizes the enzyme.[1] As shown in Fig. 1, all concentrations of glycerol stabilized the mutant GDH against thermoinactivation. At the optimum glycerol concentration of 25%, glycerol stabilized the enzyme 14-fold based on the ratio of half-lives in the presence and absence of glycerol ($t_{1/2}$ [glycerol]/ $t_{1/2}$). Similar results were obtained for the native GDH from *P. furiosus*; in this case, addition of 25% (v/v) glycerol stabilized the enzyme 11-fold. Although less than the 18-fold pressure-induced stabilization of the native GDH, these results nonetheless show that glycerol has a large stabilizing effect on both the native and mutant *P. furiosus* GDHs.

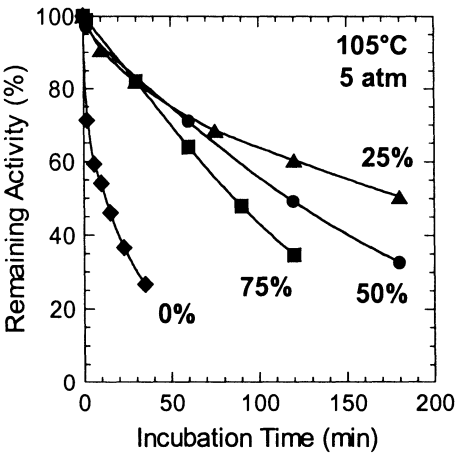

Fig. 1. Thermoinactivation trajectories of mutant *P. furiosus* GDH at 105 °C, 5 atm, and 0, 25, 50, and 75% (v/v) glycerol

3.3 Mechanism of *P. furiosus* GDH Pressure Stabilization

Glycerol has been shown to reduce protein flexibility and decrease thermal backbone fluctuations [13,14]. Furthermore, previous investigators have found that glycerol decreases the volume and compressibility of protein interiors, possibly

[1] Further properties of the *P. furiosus* GDH tetrapeptide mutant will be discussed in a separate paper.

through the compression of collapsible voids [15]. These findings suggest possible mechanisms by which glycerol stabilizes proteins against thermoinactivation.

Previous studies of the molecular effects of pressure on protein structure led to the observation that pressures in the range of 250–2750 bar reduced the flexibility of the protein interior at relatively high temperatures [5]. The same effect on flexibility was found upon addition of glycerol at atmospheric pressure. Based on this observation and the large degrees of GDH stabilization induced by both pressure and glycerol, we hypothesize that pressure and glycerol stabilize GDH by similar mechanisms. Two mechanisms can be proposed: (1) pressure and glycerol rigidify the structure and diminish thermal fluctuations away from the folded state, and (2) pressure and glycerol create a compact protein containing more stabilizing intra- and/or intersubunit contacts. Either or both mechanisms may be in effect.

To test this hypothesis, we examined the combined effect of pressure and glycerol on the thermostability of *P. furiosus* GDH. Thermal half-lives of the *P. furiosus* GDH mutant were determined under four different conditions: (1) 5 atm, no glycerol; (2) 5 atm, 25% glycerol; (3) 750 atm, no glycerol; and (4) 750 atm, 25% glycerol. In the absence of glycerol and pressure (condition 1), the enzyme inactivated quickly with a half-life of 12 min. Independently, glycerol (condition 2) and high pressure (condition 3) extended the half-life of the enzyme to 175 and 470 min, respectively. However, the combination of both (condition 4) gave nearly the same half-life, 460 min, as for 750 atm alone. This result is consistent with the hypothesis that pressure and glycerol stabilize *P. furiosus* GDH by similar mechanism(s).

3.4 Thermostability and Pressure Studies of *T. litoralis* GDH

Despite the fact that the GDHs from *T. litoralis* and *P. furiosus* are highly homologous (sharing 87% sequence identity), their thermostabilities are substantially different. At 103 °C, the half-life of *P. furiosus* GDH is 550 min, whereas that of *T. litoralis* GDH is less than 10 min (data not shown). However, as shown by the ratio of half-lives (last column) in Table 2, pressure stabilized both enzymes to a similar degree.

Table 2. Thermal half-lives and half-life ratios of *P. furiosus* and *T. litoralis* GDHs at 5 and 500 atm

	Half-life [5 atm] (min)	Half-life [500 atm] (min)	$t_{1/2}$ [500 atm] / $t_{1/2}$ [5 atm]
P. furiosus (109 °C)	12	215	18
T. litoralis (101.4 °C)	12	190	16

At different temperatures (109 °C and 101.4 °C for *P. furiosus* and *T. litoralis* GDHs, respectively) that gave low pressure half-lives of 12 min, application of 500 atm yielded 18- and 16-fold pressure stabilizations for the *P. furiosus* and *T. litoralis* GDHs, respectively. These results indicate that the degree of pressure

stabilization is not necessarily correlated with thermostability, and suggest that pressure stabilizes both enzymes through a common mechanism(s). Furthermore, the X-ray crystal structures of both *P. furiosus* and *T. litoralis* GDHs have recently become available. Inspection of both structures indicate that these enzymes have high structural homology. Further structural analysis might point to a common structural element(s) that is responsible for the large degrees of pressure stabilization of both *P. furiosus* and *T. litoralis* GDH.

4 Conclusions

In the present work, we examined the effect of pressure on the thermostability of both *P. furiosus* and *T. litoralis* GDH. Application of 500 atm stabilized both enzymes to a large extent. These results suggest that the highly homologous *P. furiosus* and *T. litoralis* GDHs follow the same mechanism of pressure stabilization. In the case of *P. furiosus* GDH, comparison of pressure and glycerol effects on GDH thermostability point to two possible mechanisms of pressure stabilization involving the reduction of thermal fluctuations and the compression of protein structure.

Acknowledgements: We are grateful to Dr. David King (Howard Hughes Medical Institute, U. C. Berkeley) and the College of Chemistry Mass Spectrometry Facility (U. C. Berkeley) for performing mass spectrometry of GDH and for helpful suggestions. We also thank Michael W. W. Adams (University of Georgia) for providing us with *P. furiosus* GDH, Alex Matschiner for purification of recombinant GDH, Mikyung Lee for purification of *T. litoralis* GDH, and Dennis Maeder for helpful discussions. This work was supported by the National Science Foundation (BES-9604561 and BES-9410687), by the Schlumberger Fellowship of D.S.C., and by Kyowa Hakko Kogyo Co. Ltd.

References

[1] Weber, G. and Drickamer, H.G. (1983); The effect of high pressure upon proteins and other biomolecules; Quart. Rev. Biophys., 16, 89–112.

[2] Samarasighe, S.D., Campbell, D.M., Jonas, A. and Jonas, J. (1992); High resolution NMR study of the pressure-induced unfolding of lysozyme; Biochemistry, 31, 7773–7778.

[3] Jaenicke, R. (1991); Protein stability and molecular adaption to extreme conditions; Eur. J. Biochem., 202, 715–728.

[4] Frauenfelder, H., Alberding, N. A., Ansari, A., Braunstein, D., Cowen, B. R. *et al.* (1990); Protein and pressures; J. Phys. Chem., 94, 1024–1037.

[5] Cioni, P. and Strambini, G. B. (1994); Pressure effects on protein flexibility of monomeric proteins; J. Mol. Biol., 242, 291–301.

[6] Heremans, L. and Heremans, K. (1989); Raman spectroscopy study of the changes in secondary structure of chymotrypsin: effect of pH and pressure on the salt bridge; Biochim. Biophys. Acta, 999, 192–197.
[7] Gross, M., Auerbach, G. and Jaenicke, R. (1993); The catalytic activities of monomeric enzymes show complex pressure dependence; FEBS Lett., 321, 256–260.
[8] Hei, D. J. and Clark, D. S. (1994); Pressure stabilization of proteins from extreme thermophiles; Appl. Environ. Microbiol., 60, 932–939.
[9] Michels, P. C. and Clark, D. S. (1997); Pressure-enhanced activity and stability of a hyperthermophilic protease from a deep-sea methanogen; Appl. Environ. Microbiol., 63, 3985–3991.
[10] Mozhaev, V. V., Lange, R., Kudryashova, E. V. and Balny, C. (1996); Application of high hydrostatic pressure for increasing activity and stability of enzymes; Biotechnol. Bioeng., 52, 320–331.
[11] Michels, P. C., Hei, D. and Clark, D. S. (1996); Pressure effects on enzyme activity and stability at high temperatures; Adv. Protein Chem., 48, 341–376.
[12] DiRuggiero, J. and Robb, F. T. (1995); Expression and in vitro assembly of recombinant glutamate dehydrogenase from the hyperthermophilic archaeon *Pyrococcus furiosus*; Appl. Environ. Microbiol., 61, 159–164.
[13] Gregory, R. B. (1988); The influence of glycerol on hydrogen isotope exchange in lysozyme; Biopolymers, 27, 1699–1709.
[14] Butler, S. L. and Falke, J. J. (1996); Effects of protein stabilizing agents on thermal backbone motions: a disulfide trapping study; Biochemistry, 35, 10595–10600.
[15] Priev, A., Almagor, A., Yedgar, S. and Gavish, B. (1996); Glycerol decreases the volume and compressibility of protein interior; Biochemistry, 35, 2061–2066.

High-Resolution NMR Studies of Proteins Under High Pressure

J. Jonas

University of Illinois, Beckman Institute for Advanced Science and Technology,
405 N. Mathews Avenue, Urbana, IL 61801, USA
Phone: (217) 244-1176; Fax: (217) 244-0987
j-jonas@uiuc.edu

Abstract. Advanced high-resolution NMR spectroscopy, including two-dimensional NMR techniques, combined with the high-pressure capability represents a powerful new tool in studies of proteins. Selected results taken from recent studies illustrate the high information content and the range of problems that can be investigated. This lecture is organized in the following way. First, the specialized instrumentation needed for high-pressure NMR experiments is discussed. Design features and performance characteristics of high-sensitivity, high-resolution, variable temperature NMR operating at 500 MHz and at pressures up to 900 MPa will be described. The main part of this lecture deals with an overview of several recent studies or studies in progress from our laboratory using 1D and 2D high-resolution, high-pressure NMR spectroscopy to investigate the pressure-induced reversible unfolding and cold denaturation of proteins. The following proteins were studied: lysozyme, apomyoglobin, α-lactalbumin, and ubiquitin. The experimental evidence for the relationship between the residual secondary structure of pressure-assisted cold-denatured states and the structure of early folding intermediates is given. The use of pressure as a tool for generating intermediate folding states is discussed.

1 Introduction

Increasing attention has recently been focused on denatured and partially folded states of proteins [1–3], since determination of their structure and stability may provide novel information on the mechanisms of protein folding. The native conformations of hundreds of proteins are known in great detail from structural determinations by X-ray crystallography and, more recently, NMR spectroscopy. However, a detailed knowledge of the conformations of denatured and partially folded states is lacking, and represents a serious shortcoming in current studies of protein stability and protein folding pathways.

From the results so far in our laboratory [4] and elsewhere [5], it is clear that pressure denaturation is more easily controlled and represents a less drastic perturbation of protein structure than thermal or chemical denaturation. Indeed, the main conclusions from our work can be summarized as follows:

- Pressure and pressure-assisted cold-denaturated states exhibit significant residual secondary structure.
- Cold-denaturated state is different from thermally denaturated state.
- Pressure allows stabilization of intermediate states.
- Pressure-assisted cold-denaturated states have residual secondary structures resembling those of early folding intermediates.
- Mutations in the core of proteins affect their pressure stability differently than their thermal stability or resistance to chemical denaturation.

The combination of advanced high-resolution NMR techniques with high-pressure capability represents a powerful new experimental tool in studies of protein folding. Our laboratory was the first to develop high-pressure NMR probes suitable for high-resolution and high-sensitivity experiments on biochemical systems. A general review of high-pressure NMR spectroscopy [6] has recently been published and high-pressure NMR studies of proteins and membranes were reviewed by us in 1994 [4].

2 Results & Discussion

2.1 High-Resolution NMR Probes for Experiments at High Pressures

Our recent instrumentation efforts have focused on several issues: pressure range, sensitivity, resolution, amount of sample, and feasibility of experiments at a high frequency of 500 MHz.

The previous pressure limit of our 300 MHz, high-resolution, high-sensitivity NMR equipment was around 5 kbar (500 MPa). While this pressure range is adequate for many studies, we have recently become interested in developing NMR probes capable of attaining even higher pressures, as complete unfolding of many proteins often requires pressures well in excess of 5 kbar [7].

Recently we designed a new high-pressure, high-resolution NMR probe [8] which has been tested to 925 MPa at a proton frequency of 300 MHz using an 8 mm diameter sample. It is important to point out that, in contrast to our earlier designs, the tuning capacitor is located inside the high-pressure environment. This facilitates high-frequency tuning to frequencies as high as 500 MHz.

Since NMR is inherently a low-sensitivity technique, work with dilute biochemical samples can be problematic. Apart from increasing the concentration of the samples, methods available for improving sensitivity include improving the electronic circuit, increasing the sample coil filling factor, and increasing the spectrometer frequency. To meet this challenge, we have been focusing our efforts on an alternative RF coil design which has increased the sensitivity, power, and tuning range of our double tuned ($^1H/^2H$) NMR probes [9]. The materials and experimental conditions for the various NMR experiments were discussed in detail in the original studies [10–12].

2.2 Cold-Denatured States

Earlier work [4] on pressure and cold denaturation suggested that these specific denaturation processes can leave appreciable structure in proteins, particularly when compared to other processes such as thermal or urea denaturation. The main motivation of our recent work [10–12] was to characterize several proteins by cold denaturation and compare them to known species observed during folding.

We chose lysozyme for these studies because its structure and folding has been studied extensively, but information about its cold denaturation was lacking. From our hydrogen exchange rate data on lysozyme in the cold-denatured state, it is clear that many regions of lysozyme are significantly protected from exchange with P factors exceeding 10. P factors ranged from 1.19 for F3 to 71.0 for R114.

In a useful variant of conventional pulsed-labeling hydrogen exchange studies, Gladwin and Evans [13] observed relatively early stages in the folding of lysozyme by confining the exchange to the dead time of their instrumentation (~3.5 ms). Slowing of exchange measured during this time can be quantified by comparing the measured exchange rate to that for a random coil, as in other hydrogen exchange studies. The resulting quantity, though similar to a protection factor, is determined from a rate that changes considerably as the protein refolds; as a result, it is best referred to as a "dead time inhibition factor" (I_D) rather than a true protection factor [13]. Nevertheless, I_D values provide information similar to that provided by P values in equilibrium-denatured states. The early stages of lysozyme refolding show a marked resemblance to our cold-denatured state. We have thus observed a strong parallel between a stable, denatured form of lysozyme and the transient species observed during folding.

The strong similarity of the cold-denatured state of lysozyme to species observed during lysozyme folding suggested the possibility of a more general phenomenon. To investigate this idea in more detail, our previous data on ribonuclease A (RNase A) [10] were reexamined. The range of protection factors observed in cold-denatured RNase A (2.8 to 78) is similar to that present in cold-denatured lysozyme. Both the extent and the stability of residual structure in cold-denatured lysozyme and RNase A are similar to those found in early folding ($t < 10$ ms) species of these proteins.

To test this idea, we investigated ubiquitin, which has markedly different folding kinetics from either RNase A or lysozyme. In particular, ubiquitin shows much less evidence of early structure formation than lysozyme [13]. For ubiquitin, the dead time inhibition study showed no evidence for protection from exchange, with the largest dead time inhibition factors being approximately 2. In the case of ubiquitin, the folding reaction appears to proceed in one highly cooperative step [13], with little of the multiphasic behavior observed in lysozyme or RNase A [14]. Our results for the cold-denatured state of ubiquitin show that there is no partially folded state that is stable enough to be characterized by hydrogen exchange methods when ubiquitin is cold-denatured.

2.3 Pressure-Denatured States

Since high pressure has been shown to produce states with significant residual structure, the high-pressure denaturation process can be explored as a technique for generating partially stable protein-folding intermediate states. For our studies, we have chosen apomyoglobin and α-lactalbumin for which intermediates have been detected [15–17].

The folding of apomyoglobin is very well characterized, and the structure of the native state has been solved by NMR. Stopped-flow hydrogen exchange experiments used to follow apomyoglobin refolding from urea have shown that the helices form in the order that the AGH core is protected from exchange within the first 5 ms. A generalized charge effect causes the unfolding of I_1 to U as the pH is further reduced. Because apomyoglobin is known to form both kinetic and equilibrium intermediates [18], it is a promising candidate to form a partially folded structure under high pressure as well.

We used high-pressure NMR techniques to show that apomyoglobin reversibly pressure denatures in the presence of TCA to form a pressure-denatured state that still retains an intact AGH core. The elements of structure remaining stable in the high pressure-denatured state are also stable in the pH denaturation intermediate, I_1, and an early kinetic folding intermediate. High-pressure NOESY spectra clearly show residual structure at 200 MPa. A few weak cross-peaks belonging to a cluster of aromatics were present at 200 MPa, and the W14 – V17 cross-peaks indicate the A helix is involved in a conformational change that is slow on the NMR time scale. Based on the aggregation properties, the fluorescence, the 2D NMR data, and the small ΔG for pressure denaturation compared to urea denaturation, we propose that the high-pressure intermediate has some characteristics similar to the pH-induced intermediate, I_1, and possibly the earliest kinetic folding intermediate. No native cross-peaks were observed upon further increasing the pressure to 500 MPa, indicating that the pressure intermediate is denatured. Although residual structure in the pressure-denatured state has previously been shown to resemble early folding intermediates, this is the first instance where the structure of both states is resolved enough for a more detailed comparison. The presence of a similar intermediate for several methods of denaturation indicates that the intrinsic stability of the AGH core is responsible for its early folding.

Since α-lactalbumin is very well known for ist formation of a molten globule [17], we decided to study the protein to find if we could isolate any other intermediate apart from the molten globule, and also to gain more insight into the structure of the molten globule itself. Our results from the study of bovine α-lactalbumin in acetate buffer at a pH of 4.2 and temperature of 25 °C in the pressure range of 0.1 to 500 MPa show that the protein unfolds completely at 500 MPa and forms two distinct intermediates in the process, the well-known molten globule (M6) exists from 300 to 400 MPa, while another intermediate with a modified hydrophobic core exists in the range of 150 to 200 MPa. This can be seen from the denaturation curve of some residues which shows two distinct slopes and also from the 2D-NOESY spectra. The MG state was identified mainly by the

chemical exchange cross-peaks between the native and the MG conformation of the residues W26, F31 and Y103. This spectrum compares very well with the molten globule obtained by thermal denaturation of the protein. Also, a residual structure, especially in the 101–110 residues region, could be clearly seen. The new intermediate of 150 MPa was confirmed by the presence of some new cross-peaks – that of W104 with F31, W60 and W118, and a relative chemical shift change of F53 and F31 and indicating a structural rearrangement of the hydrophobic core of the protein to accommodate the increase in pressure.

Our 2D-NOESY experiments show that there is some structural reorganization prior to the formation of the molten globule. The structure at 150–200 MPa can be identified as a pre-molten globule structure which is different from the molten globule and the native structure, but is more "native-like" than the molten globule in that it retains most of the native cross-peaks and has only a few non-native interactions.

References

[1] Dill, K. and Shortle, D. (1991); Denatured states of proteins; Annu. Rev. Biochem., 60, 795–825.

[2] Shortle, D. (1996); Structural analysis of non-native states of proteins by NMR methods; Current Opinion in Structural Biology, 6, 24–30.

[3] Shortle, D. (1996); The denatured state (the other half of the folding equation) and its role in protein stability; FASEB J., 10, 27–34.

[4] Jonas, J. and Jonas, A. (1994); High pressure NMR spectroscopy of proteins and membranes; Annu. Rev. Biophys. Biomol. Struct., 23, 287–318.

[5] Mozhaev, V., Heremans, K., Frank, J., Masson, P. and Balny, C. (1996); High pressure effects on protein structure and function; Proteins: Structure, Function and Genetics, 24, 81–91.

[6] Ballard, L. and Jonas, J. (1997); High pressure NMR; Annu. Rep. NMR Spectrosc., 33, 115–150.

[7] Samarasinghe, S., Campbell, D., Jonas, A. and Jonas, J. (1992); High resolution NMR study of the pressure induced unfolding of lysozyme; Biochemistry, 31, 7773–7778.

[8] Ballard, L., Reiner, C. and Jonas, J. (1996); High resolution NMR probe for experiments at high pressures; J. Magn. Reson., 123, 81–86.

[9] Ballard, L., Yu, A., Reiner, C. and Jonas, J. (1998); A high pressure, high resolution NMR probe for experiments at 500 MHz; J. Magn. Reson., 133, 190–193.

[10] Nash, D., Lee, B.-S. and Jonas J. (1996); Hydrogen exchange kinetics in the cold-denatured state of ribonuclease A; Biochim. Biophys. Acta, 1297, 40–48.

[11] Nash, D. and Jonas, J. (1997); Structure of pressure-assisted cold denatured lysozyme and comparison with lysozyme folding intermediates; Biochemistry, 36, 14375–14383.

[12] Nash, D. and Jonas, J. (1997); Structure of the pressure-assisted cold denatured state of ubiquitin; Biochem. and Biophys. Res. Comm., 238, 289–291.

[13] Gladwin, S. and Evans, P. (1996); Structure of very early protein folding intermediates – new insights through a variant of hydrogen exchange labeling; Folding and Design, 1, 407–417.

[14] Houry, W. and Scheraga, H. (1996); Structure of a hydrophobically collapsed intermediate on the conformational folding pathway of ribonuclease A probed by hydrogen – deuterium exchange; Biochemistry, 35, 11734–11746.

[15] Hughson, F., Wright, P. and Baldwin, R. (1990); Structural characteristics of a partly folded apomyoglobin intermediate; Science, 249, 1544–1548.

[16] Kay, M. and Baldwin, R. (1996); Packing interactions in the apomyoglobin folding intermediate; Nature and Structural Biology, 3, 439–445.

[17] Kuwajima, K. (1996); The molten globule state of α-lactalbumin; FASEB J., 10, 102–109.

[18] Eliezer, D., Yao, J., Dyson, H. and Wright, P. (1998); Structural and dynamic characterization of partially folded states of apomyoglobin and implications for protein folding; Nat. Struct. Biol., 5, 148–155.

Pressure–Temperature Induced Unfolding and Aggregation of Proteins

K. Heremans

Department of Chemistry, Katholieke Universiteit Leuven, B-3001 Leuven, Belgium
Karel.Heremans@fys.kuleuven.ac.be

Abstract. The effect of pressure and temperature on protein unfolding and aggregation as detected by infrared spectroscopy is discussed with a number of examples. At 45–50 °C the spectra of pressure denatured myoglobin and lipoxygenase show bands, but only *after* pressure release, that are typical for temperature induced protein aggregation.

1 Introduction

Proteins can be unfolded by high hydrostatic pressure as well as by low or high temperature. This gives rise to an elliptic phase diagram in the temperature-pressure plane which describes the conditions under which the protein is in the native or the unfolded state at a given temperature and pressure with a specified solution composition. For the interpretation of the elliptic shape of the phase boundaries we favour a thermodynamic model that assumes that the changes in entropy, ΔS, and in volume, ΔV, of the unfolding are temperature and pressure dependent. Within this physical model, the diagram gives also unique information on the difference in heat capacity, ΔC_p, compressibility, $\Delta\beta$, and thermal expansion, $\Delta\alpha$, between the unfolded and the folded state of the protein. The latter quantities can be related to the differences in dynamics of the protein conformations. Direct information on these quantities is difficult to obtain otherwise [1].

In many, if not almost all, cases the diagrams are obtained from kinetic rather than from equilibrium data. The first diagram that was obtained by Suzuki [2] on the denaturation of ovalbumin and hemoglobin was of such a kind. Many kinetic diagrams have been published since then. The inactivation kinetics of microorganisms gives similar diagrams strongly suggesting that the inactivation of proteins and/or enzymes is the main factor controlling these events [3, 4]. Similar diagrams are observed for the survival conditions of deep sea bacteria. Yayanos has proposed calling these *pTk* diagrams [5]. In all these instances it is still possible to interpret the data in terms of a thermodynamic model as is done in the formulation of rate processes. The denaturation process is usually interpreted in terms of a preequilibrium between the native (N) and the unfolded (U) state followed by an irreversible step which leads to the inactivated enzyme or the aggregated protein (A):

$$N \leftrightarrow U \rightarrow A .$$

The *negative* activation energies that are obtained for the denaturation of proteins at high pressure [2] strongly supports the model that the kinetic data largely reflect the thermodynamics of the unfolding of the protein from the N to the U state.

The pressure- and temperature-induced conformational transitions and unfolding can be studied with a number of spectroscopic techniques. Although NMR spectroscopy is expected to give potentially the most details on the mechanism of unfolding [6], Fourier transform infrared (FTIR) spectroscopy in combination with the diamond anvil cell makes it possible to follow the changes in the secondary structure. For the temperature unfolded proteins an extensive intermolecular hydrogen bond network develops which is absent in the pressure unfolded proteins. This leads us to use pressure as a rather unique tool to unravel the mechanism of protein aggregation.

2 Pressure–Assisted Cold Denaturation

Cold denaturation of proteins is a natural consequence of the elliptic phase diagrams of protein stability [1]. Pressure assisted cold denaturation of ribonuclease was first observed with NMR techniques by Jonas [6]. The approach makes use of the fact that the freezing point of ice I is about –20 °C at 200 MPa. When the infrared spectra of the cold, heat and pressure denaturated horse heart metmyoglobin are compared at pD 4, interesting differences are noted [7]. The spectrum of the heat denatured protein shows the typical bands of the intermolecular hydrogen bonded interactions visible in many proteins. The spectrum of the pressure denatured protein and the pressure assisted cold denatured protein are very similar but not identical. In both instances there is no indication of intermolecular hydrogen bonding. The helical content of the protein is strongly reduced in favour of the formation of sheet structures. The effect of pressure on the temperature induced aggregation of this protein is discussed in Sect. 4 [8].

3 Hydrogen/Deuterium Exchange and Enzyme Inactivation

When a protein is dissolved in D_2O, the protons exchange for deuterons. The solvent exposed protons exchange rather quickly but the internal ones do so very slowly unless the protein unfolds. The rate of exchange can be measured by either NMR or infrared spectroscopy. Again the observed rate contains the equilibrium of the unfolding and it should be possible to obtain *pTk* diagrams for the H/D exchange. This has been done in detail for lipoxygenase and there is a good correlation with the kinetics of inactivation of the enzyme activity [9].

Less systematic investigations have been performed on the correlation between the effect of temperature and pressure on β-galactosidases from different biological sources. The experiments essentially confirm the idea that the stability of enzymes and proteins can be correlated with the rate of H/D exchange [10].

According to the infrared spectra, the pressure induced denaturation of lipoxygenase takes place at 6 kbar. Nevertheless changes in the protein fluorescence spectrum take place well below this pressure. The largest changes are observed when the experiment is performed at 25 °C. A slight tendency for the formation of aggregates is observed, a tendency which disappears in the presence of the fluorescent dye ANS. This suggests that hydrophobic sites are involved in the pressure induced aggregation [11]. This aggregation is not visible in the infrared spectrum.

During the course of the stability studies on lipoxygenase, it was noticed that when the pressure induced denaturation was performed at 45–50 °C, bands appeared in the infrared spectrum that are typical for the temperature denatured protein. The important point is that these bands only appear *after* pressure release. The bands disappear upon pressure increase. This interesting effect was investigated more systematically in metmyoglobin as discussed in the next section.

4 Pressure Effect on Protein Aggregation

When metmyoglobin from horse heart is heat denatured, bands appear in the infrared spectrum that are typical for the formation of an intermolecular hydrogen bonded network between the unfolded protein molecules. As is the case for most proteins, these bands do not appear in the spectrum of the pressure denatured spectrum. However, when the pressure induced denaturation is performed at about 45 °C, well below the denaturation temperature, the bands appear *after* pressure release [8]. The effect is absent at lower temperatures. The experiments suggest that pressure is able to induce conformational changes that are different from those induced by temperature. In addition they show that the intermolecular hydrogen bonded structures that are formed upon denaturation by heat can be reversed by pressure provided the temperature is not too high. Whether the effects that have been observed on myoglobin are similar in nature to the ones observed on lipoxygenase, as discussed in the previous section, remains to be investigated.

5 Conclusions

Protein aggregation has been considered for a long time as a nuisance especially for a thermodynamic analysis of protein unfolding. Recent work show however, that the biological implications of protein aggregation may be very profound and may lead to fatal diseases. Work on lysozyme shows that naturally occurring variants show pronounced differences in their tendency to aggregate [12]. The work reviewed in this paper shows the interplay between temperature, pressure and time on the aggregation of proteins.

The differences between pressure and temperature induced gel formation point to stronger *inter*molecular interactions in the temperature induced in contrast to the pressure induced gels. This correlates with rheological and structural data for some food proteins [13].

A final question relates to the molecular origin of the elliptic *pTk* diagrams in proteins. In many literature reports this is assumed to be related to hydrophobic interactions which are assumed to dominate the stability of proteins. However, the simple observation that starch can be gelatinised not only by temperature but also by pressure [14], suggests that these forces are not the primary source of the unique behaviour of proteins.

Acknowledgements: Research in our laboratory is supported by grants from the EU (FAIR CT-97-1175), FWO Flanders (Belgium) (G.0339.98) and KU Leuven (OT 97/20).

References

[1] Heremans, K. & Smeller, L. (1998); Protein structure and dynamics at high pressure; Biochim. Biophys. Acta, 1386, 353–370.

[2] Suzuki, K. (1960) Studies on the kinetics of protein denaturation under high pressure; Rev. Phys. Chem Japan, 29, 91–98

[3] Ludwig, H., Scigalla, W. & Sojka, B. (1996) Pressure- and temperature-induced inactivation of microorganisms, in J. L. Markley, C. Royer & D. Northrup (Eds.) High Pressure Effects in Molecular Biophysics and Enzymology, Oxford University Press, 346–363.

[4] Hashizume, C., Kimura, K. & Hayashi, R. (1995) Kinetic analysis of yeast inactivation by high pressure treatment at low temperatures, Biosci. Biotech. Comm. 59, 1455–1458.

[5] Yayanos, A.A. (1998); Empirical and theoretical aspects of life at high pressure in the deep sea, K. Horikoshi and W.D. Grant (Eds.), Extremophiles, John Wiley & Sons, NY, 47–92.

[6] Jonas, J. (1998) High resolution NMR studies of proteins under high pressure, These proceedings.

[7] Meersman, F., Smeller, L. & Heremans, K. (1998) Cold, heat and pressure denaturation of horse heart metmyoglobin: a FTIR study, These proceedings.

[8] Smeller, L., Rubens, P. & Heremans, K. (1998) Pressure effect on the temperature-unfolding and gelation of myoglobin, These proceedings.

[9] Rubens, P., Frank, J. & Heremans, K. (1998) Hydrogen-deuterium exchange of lipoxygenase at high pressure and temperature, These proceedings.

[10] Rubens, P., Degraeve, P., Lemay, P. & Heremans, K. (1998) Pressure and temperature stability of β-galactosidases: a structural and functional study, These proceedings.

[11] Rubens, P., Bec, N., Lange, R., Balny, C., Frank, J. & Heremans, K. (1998) Conformational changes of lipoxygenase at elevated pressure and temperature, These proceedings.

[12] Booth, D. R., Sunde, M. *et al.* (1998) Instability, unfolding and aggregation of human lysozyme variants underlying amyloid fibrillogenesis, Nature 385, 787–793.

[13] Heremans, K., Van Camp, J. & Huyghebaert, A. (1997) High Pressure Effects on Proteins. In Food Proteins and their Applications, S. Damodaran & A. Paraf, Eds. M. Dekker, NY, 473–502.

[14] Snauwaert, J. & Heremans, K. (1998) Pressure induced swelling kinetics of starch granules, These proceedings.

Comparison of the Pressure–Temperature Behavior of Neutral Proteases from Thermophilic and Psychrophilic Bacteria

S. Kunugi[1], H. Ikeuchi[1] and K. Oda[2]

[1]Department of Polymer Science and Engineering, and [2]Department of Applied Biology, Kyoto Institute of Technology, Matsugasaki, Sakyo, Kyoto 606-8585, Japan
kunugi@ipc.kit.ac.jp

Abstract. Thermolysin (TLN) and vimelysin (VLN) are neutral metalloproteinases from thermophilic and psychrophilic bacteria, respectively. The $k_{cat}/K_{m(app)}$ of TLN increased up to 200–250 MPa and showed a maximum activity at 45 °C and 200 MPa, for an acyl-dipeptide amide substrate, where the apparent catalytic activity became more than 100-fold of that at ambient pressure. VLN also showed a pressure-induced activation and the apparent catalytic optimum for VLN was found to be 15 °C and 150 MPa, but the activation was smaller than TLN. The activation volumes for $k_{cat}/K_{m(app)}$ were about –60 ml/mol for TLN and about –30 ml/mol for VLN; the latter is comparable to a mesophilic metalloproteinase from *B. subtilis* (BSNP). Pressure and temperature dependence of the fluorescence intensity of the intrinsic Trp shows that TLN undergoes a structural change above 300 MPa with a negative expansibility (–0.45 ml/mol/K) and that VLN shows a transition in fluorescence above 250 MPa at 30 °C; the transition pressure becoming lower on both higher and lower temperature sides.

1 Introduction

Several metalloproteinases have been found in various microorganisms. Thermolysin (TLN) (E.C. 3.4.24.4) is the most widely known and it is a thermostable neutral proteinase purified from a thermophilic bacteria *B. thermoproteolyticus* [1]. Some homologous enzymes from *Bacillus* spp. have been studied for their catalytic properties and structures including their pressure response, and a dramatic pressure activation was found for TLN [2–4].

Vimelysin (VLN) is another neutral proteinase from a psychrophilic bacteria *Vibrio* sp. [5, 6], which has high activity at low temperatures [7] and has no homology with TLN in the primary structure [5].

We have studied these two types of metalloproteinase, one from a thermophilic bacterium and one from a psychrophilic bacterium, over a wide range of pressure and temperature; the catalytic activity and the fluorescence intensity of these

enzymes were investigated, and the effects of the pressure and temperature on the enzymatic reactions and structure are mainly discussed.

2 Materials & Methods

Thermolysin was obtained from Daiwa Kasei (Osaka, Japan). Vimelysin was isolated and purified as previously reported [1]. Their activities were determined by a kinetic assay under our standard conditions against a dipeptide substrate, furylacryloyl(Fua)-Gly-LeuNH$_2$ (Bachem).

The ultraviolet/visible absorbance was measured by a spectrophotometer PRAS-5000 (Otsuka Electric Co.) attached to a two-window high pressure cell (Teramecs). Fluorescence was measured using a fluorospectrometer RF-5000 (Shimadzu) by attaching a three-window high pressure cell (Teramecs).

3 Results & Discussion

Figure 1 shows the pressure and temperature dependence of the apparent second-order rate constant by VLN (a) and TLN (b) for the hydrolysis of Fua-Gly-LeuNH$_2$ at pH 6.0 for VLN and 6.5 for TLN. At each temperature the $k_{cat}/K_{m(app)}$ of TLN increased up to 200–250 MPa and the highest activity was obtained at 45 °C and 200 MPa; where the $k_{cat}/K_{m(app)}$ became more than 100-fold of that at ambient pressure. The apparent activation volume ($\Delta V^{\#}$) was roughly calculated as -110 ml/mol.

On the other hand VLN showed the highest activity at 15 °C and 150 MPa, where the $k_{cat}/K_{m(app)}$ became around 5-fold of that at ambient pressure and $\Delta V^{\#}$ was roughly estimated as –30 ml/mol. For both enzymes, however, further increase in pressure resulted in inactivation. This $\Delta V^{\#}$ value for VLN was similar to the values obtained for another neutral proteinase from mesophilic bacteria, *B. subtilis amyloliquifaciens* (BSNP). In our previous study [3] a significant pressure and temperature dependence was observed for both k_{cat} and K_m parameters in the case of TLN, but BSNP showed distinct pressure dependence only for the k_{cat} parameter. Similar tendencies were reported for the temperature dependence of VLN [6] and the pressure dependence of the kinetic parameters for VLN was studied here is in the same line (Table 1). The k_{cat} for VLN increased with increasing pressure, while the K_m parameter showed only a small pressure dependence. Under high pressure, the optimum temperature was shifted 5 °C→15 °C (150 MPa) for VLN and 60 °C→45 °C (250 MPa) for TLN. It is notable that the increase in pressure shifted the respective extermephilicity (under ambient pressure) towards more or less mesophilic.

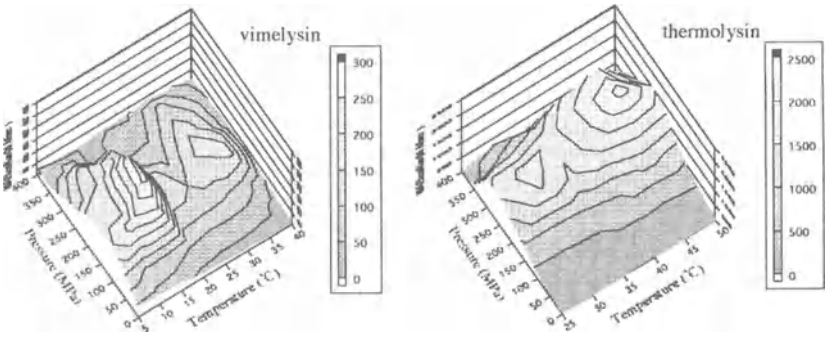

Fig. 1. Pressure and temperature dependence of the apparent second-order rate constant of the hydrolysis of Fua-GIy-LeuNH$_2$ by vimelysin (left) and thermolysin (right).
Left, vimelysin: [E]= 5–10 nm, [S]= 0.2 mM, 50 mM MES/NaOH (pH 6.0), 10 mM $CaCl_2$, 2% DMSO
Right, thermolysin: [E]= 0.6–12 nm, [S]= 0.2 mM, 50 mM MES/NaOH (pH 6.5), 10 mM $CaCl_2$, 2% DMSO

Table 1. k_{cat} and K_m values for the hydrolysis of Fua-Gly-LeuNH$_2$ by vimelysin at various pressures. Values were measured at pH 4.8 and 25 °C

Pressure (MPa)	k_{cat} (s^{-1})	K_m (mM)
0.1	11±2	0.72±0.26
25	23±2	0.67±0.11
50	27±6	0.51±0.13
100	64±11	0.67±0.38

Figure 2 shows the pressure and temperature dependence of the relative fluorescence intensity of TLN and VLN. TLN is known to show irreversible changes in several spectroscopic properties with pressure-induced catalytic loss [4]; essentially similar changes in the fluorescence spectrum were observed for VLN under high pressure, as well as the irreversible change in the CD spectrum after the incubation at high pressure. These results suggest that some structural changes occurred in VLN under very high pressure.

TLN undergoes a structural change above 300 MPa with a negative expansibility (–0.45 ml/mol/K). VLN showed a transition above 250 MPa at 30 °C. However the change in the fluorescence intensity for both TLN and VLN did not always correspond to the change in the activity. A strong fluorescence intensity region in which the structure of VLN will be stable was observed on the low temperature and high pressure side. On the contrary, the stable structure region was observed for TLN on the high temperature and low pressure side. For the latter the less stable structure was also seen on the low temperature side.

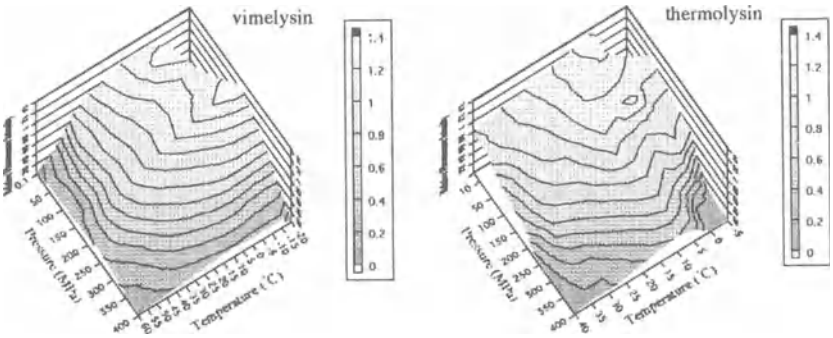

Fig. 2. Pressure and temperature dependence of the relative fluorescence intensity of vimelysin (left) and thermolysin (right).
Left, vimelysin: 1~0.4 μM VLN, 50 mM MES-NaOH (pH 6.0) and 10 mM $CaCl_2$
Right, thermolysin: 8 μM TLN, 50 mM HEPES-NaOH (pH 6.5) and 10 mM $CaCl_2$
λ ex. = 280 nm

References

[1] Endo, S. (1962); Studies on protease produced by thermophilic bacteria; J. Ferment. Technol. 40, 346–353.
[2] Kunugi, S., Hirohara, H. & Ise, N. (1982); pH and temperature dependencies of thermolysin catalysis. Catalytic role of zinc-coordinated water; Eur. J. Biochem. 124, 157–163.
[3] Fukuda, M. & Kunugi, S. (1984); Pressure dependence of thermolysin catalysis; Eur. J. Biochem. 142, 565–570.
[4] Kunugi, S., Kitayaki, M., Yanagi, Y., Tanaka, N., Lange, R. & Balny, C. (1997); The effect of high pressure on thermolysin; Eur. J. Biochem. 248, 567–574.
[5] Oda, K., Okayama, K., Okutomi, K., Shimada, M., Sato, R. & Takahashi, S. (1996); A novel alcohol resistant metalloproteinase, vimelysin, from *Vibrio* sp. T1800: Purification and characterization; Biosci. Biotech. Biochem. 60 (3), 463– 467.
[6] Takahashi, S., Okayama, K., Kunugi, S. & Oda, S. (1996); Substrate specificity of a novel alcohol resistant metalloproteinase, vimelysin from *Vibrio* sp. T 1800; Biosci. Biotech. Biochem. 60, 1651–1654.
[7] Kunugi, S., Koyasu, A., Kitayaki, M., Takahashi, S. & Oda, K. (1996); Kinetic characterization of the neutral protease vimelysin from *Vibrio* sp. T1800; Eur. J. Biochem. 241, 368–373.

Cold Denaturation of Proteins Under Pressure Studied by Time-Resolved Fluorescence. Application to Ribonuclease P2 from *S. sofataricus*

P. Tauc, P. Fusi[1], P. Tortora[1], R. Lange[2] and J.C. Brochon

LBPA, Ecole Normale Supérieure de Cachan, IGR, CNRS UMR1772, CACHAN, France
Phone: +33(0)47 40 27 17; Fax: +33(0)47 40 24 79
brochon@lbpa.ens-cachan.fr
[1]Universita degli di Milano, via Celoria 26, 20133 Milano, Italy.
[2]INSERM U128, BP5051, 34033 Montpellier, France.

Abstract. The ribonuclease P2 and the F31A one point mutation form of the hydrophobic core of the enzyme have been studied in term of heterogenity of conformational states. A cold denaturation under pressure of the F31A mutant takes place below 0 °C since the wild-type form is more resistant and changes are quite reversible.

1 Introduction

Thermophilic enzymes have been widely investigated because of their high resistance to denaturating agents compared to their mesophilic analogues. Ribonuclease P2, from *Sulfolobus sofataricus* [1], a thermoacidophilic archaebacterium living at 87 °C and acidic pH in hot springs, is a model of choice for an exploration of the capability of time-resolved spectroscopy to investigate the resistance to denaturation of native protein structures under extreme conditions. This small protein (7 kDa) exhibits a "melting" temperature close to the boiling temperature at neutral pH [3]. The structure, determined by NMR [2], shows a triple-stranded β-sheet which is orthogonal to a double-stranded β-sheet. A strongly hydrophobic core consists mainly of three aromatic residues, Phe5, Phe31, Tyr7 and eight other residues, Val3, Val14, Ile19, Val22, Ile29, Val45, Ala50 and Leu54. A hydrophilic mantle that contains many basic residues (2 arginines and 13 lysines) surrounds this hydrophobic cluster. The substitution of Phe31 was assayed to investigate the role of the hydrophobic cluster in protein stability.

The time-resolved fluorescence (TRF) measurements provide two types of information. First the fluorescence decay gives insight into the local environment of the fluorescent probe which may be linked to a structural heterogeneity. The anisotropy decay yields the rotational correlation time which depends on the volume of the hydrated molecular assembly. In addition local flexibility, ranging from lateral chain to peptide segment motion, can also be evidenced.

The unique tryptophanyl residue (W26) of ribonuclease P2 is the intrinsic probe used for the TRF study of structural changes in the wild-type and mutant proteins under extreme conditions.

2 Materials & Methods

Fluorescence decay and fluorescence anisotropy decays under pressure were recorded with a high-pressure optical cell mounted in a time-correlated single photon counting fluorometer as described elsewhere [4,5]. The excitation light pulse source was a Ti:sapphire subpicosecond laser (Spectra Physics) associated with a third harmonic generator tuned at 300 nm. Fluorescence emission was measured through a monochromator set at 350 nm ($\Delta\lambda$=8 nm). The stability of the laser intensity, over several hours, was routinely better than 5% and the excitation peak position better than 10 ps. Analysis of the data was performed using the quantified maximum entropy method [6] which yields a distribution of lifetimes and distribution of rotational correlation times. The recombinant WT protein [7] and the F31A mutant [8] were dissolved in a pyrophosphate buffer pH=3.

3 Results

The study was carried out below 0 °C without addition of any cryosolvent; the sample was first pressurised to 2000 bar at 20 °C and then the temperature was decreased until a strong denaturation was observed.

3.1 Wild-Type Enzyme (data not shown)

At 1 bar, 20 °C, the fluorescence lifetime distribution of the single tryptophan residue displays three peaks indicating a heterogeneity in the environment of the fluorescent probe. As the decay of the fluorescence anisotropy indicates that the indole moiety of this residue is rather immobile, the heterogeneity is not due to local rapid dynamics of the tryptophan side chain. The simplest explanation is to assume several conformations of the structure. The molecule rotates as a rigid sphere. At 2 kbar the molecule is slightly more compact and the fluorescence decay pattern is also changed indicating a change in one of the three conformational structures. There is practically no change in decreasing the temperature from 20 °C to 0 °C since the centre of each peak in the distribution is slightly shifted to a higher value as expected for a thermal effect on the lifetime of the probe. At -10 °C a fourth component appears in the fluorescence decay. Return to 1 bar at 20 °C indicates that the process is reversible for the WT protein. The resistance of the wild-type enzyme to denaturation is also shown by the rotational dynamics of the molecule. From 20 °C to –5 °C, the protein appears as a rigid globular molecule.

At –10 °C and –14 °C a small peak appears in the correlation time distribution (~1 ns) which seems to indicate an internal flexibility of small amplitude.

3.2 Mutant F31A (Figs. 1 and 2)

At normal pressure and 20 °C, this mutant also displays three lifetime classes. The distribution pattern is very similar to those of the WT protein. A fourth lifetime class appears under pressure of 2 kbar. At 10 °C, a fifth component around 6 ns appears indicating the early stage of a larger conformational heterogeneity. The relative contribution of this long component increases regularly with the decrease

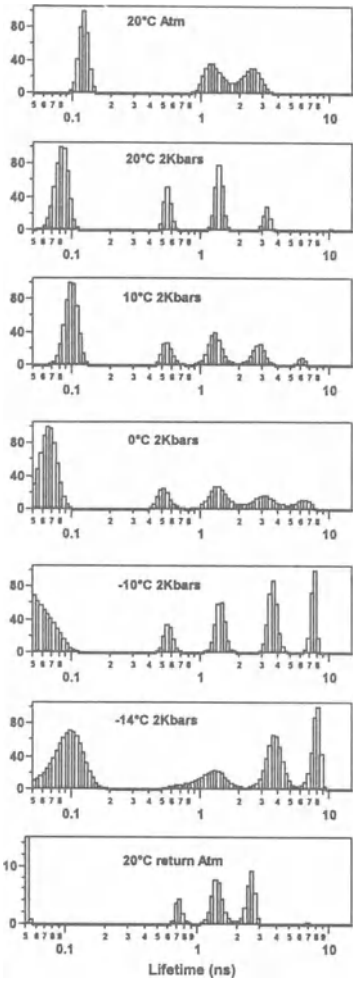

Fig. 1. Lifetime distributions of F31A mutant ribonuclease P2

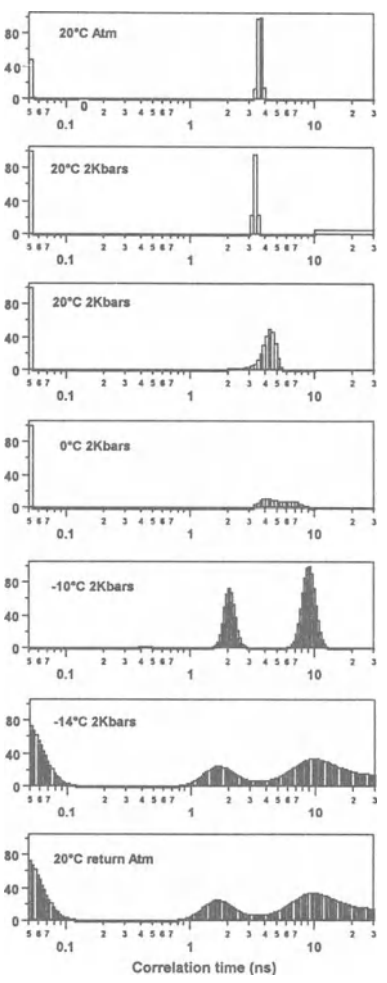

Fig. 2. Rotational correlation time distributions of F31A mutant ribonuclease P2

of temperature. The return at 20 °C and at 1 bar indicates a rather limited reversibility of the structural changes. The mutant F31A is a rigid globular molecule at 20 °C and the pressurisation to 2 kbar affects the hydrated volume of the molecule. The rotational correlation time decreases from 3.8 ns to 3.4 ns. The most striking effect of cooling below 0 °C is the broadening of the peaks in the correlation time distribution, i.e. volume distribution. The broadness of the peaks evidences a dramatic heterogeneity of the structure and some partial state of aggregation takes place at –14 °C. From 0 °C to –14 °C an internal motion of large amplitude appears indicating the beginning of an unfolding process. The immediate return to 20 °C (10 min) and 1 bar does reverse this conformational dynamics situation.

4 Conclusions

The cold and pressure denaturation of a modified hydrophobic domain of a thermophilic protein was evidenced from the loss of the conformational compactness and the broadening of the fluorescence lifetime distribution. The time-resolved fluorescence technique is a very sensitive tool for the study of the structural homogeneity of proteins and of the state of protein oligomerisation as well. Further kinetics experiments are needed for a better understanding of sequence transitions.

References

[1] Choli, T., Wittmann-Liebold, B. and Reihardt, R. (1988) J. Biol. Chem. 263, 7087.
[2] Baumann, H., Knapp, S., Lunback, T., Ladenstein, R., Hard, T. (1994) Nat. Struct. Biol. 1, 808–819.
[3] Monbelli, E., Afshar, M., Fusi, P., Mariani, M., Tortora, P., Connelly, J.P. and Lange, R. (1997) Biochemistry 36, 8733–8742.
[4] Brochon, J. C., Tauc, P., Merola, F. and Schoot, B.M.. (1993) Anal. Chem. 65, 1028–1034.
[5] Tauc, P., Mateo, C. R.and Brochon, J. C. (1998) Biophys. J .74, 1864–1870.
[6] Brochon, J.C. (1994) Methods in Enzymology 240:262–311.
[7] Consonni, R., Fusi, O., Goossens, K., Grisa, M., Heremans, K., Puricelli, P., Tortora, P., Vanoni, M. and Zetta, L. (1996) in High Pressure Bioscience and Biotechnology (Heremans K. ed.) pp 31–34, Leuven University Press, Leuven, Belgium.
[8] Fusi, P., Grisa, M., Mimbelli, E., Consonni, R., Tortora, P. and Vanoni, M. (1995) Gene 154, 97–102.

High Pressure Fluorescence Studies of Porphyrins and Hemoproteins

L. Smeller, K. Kis-Petik, A.D. Kaposi and J. Fidy

Institute of Biophysics, Semmelweis University of Medicine Budapest
Budapest VIII. Puskin u. 9. Pf. 263, H-1444 Hungary
smeller@puskin.sote.hu

Abstract. Fluorescence line narrowing in combination with high pressure was used to obtain information on the Mg-mesoporphyrin molecule incorporated into a protein mimetic matrix (DMSO). Two distinct conformers were found, their population was changed when pressure was applied. ΔV between the conformers, and the excited state vibrational levels of the chormophore, were determined. When the chromophore was embedded into horseradish peroxidase, there was only one dominant conformer in the inhomogeneous distribution function.

1 Introduction

Heme proteins have basic importance in living organisms. They play an essential role in biochemical processes like O_2 transport and storage, electron transfer and catalysis of peroxidative reactions. They have been studied extensively by several spectroscopic methods. The secondary structure of the polypeptide backbone, and changes in this structure, were detected by infrared spectroscopy [1, 2], while other methods (like resonance Raman and fluorescence spectroscopy etc.) can provide information about the prosthetic group (porphyrin) of the protein.

Fluorescence line narrowing (FLN) spectroscopy is a sophisticated technique to monitor the environment of a chromophore. This technique was combined here with the application of high pressure. One of the special features of the FLN technique is that it needs cryogenic temperatures of ca. 10 K. The chromophore molecules are not vibrationally excited by the thermal energy at this temperature. The illumination is by a laser light that excites selectively a certain subpopulation of the chromophores (site selective spectroscopy). Because of the selective excitation, the emission spectra are resolved, containing several lines resulting from the resonant excitation, while the wide background shows the emission after nonresonant excitations [3, 4]. Analysis of the spectra allows the determination of the vibrational levels of the electronically excited state, and the inhomogeneous distribution function (IDF) [5]. This function represents the true (0,0) band, and thus reveals the perturbation of the electronic level by environmental effects.

Therefore important information can be obtained from this function about the structural organisation of the chromophore in the matrix.

The native heme group in hemoproteins is not suitable for fluorescence spectroscopy, because the emission of Fe-protoporphyrin is of very short lifetime. Replacement by Mg-containing fluorescent porphyrin although reducing the association constant of substrate molecules binding in the heme pocket, does not abolish the property required for biological functioning. Thus the substituted form can be considered as a model of the native conformation.

2 Experimental

The high resolution optical spectroscopic (FLN) technique was applied in combination with variable hydrostatic pressure. The exciting light source was a CW ring dye laser (Coherent 899-01) pumped by an Ar ion laser (Coherent Innova 307). The sample was pressurized in a special low-temperature diamond anvil cell (DAC) (Diacell Products). This cell allows us to apply pressures in the range of 0–20 kbar. The DAC was mounted on the cold finger of a closed cycle helium cryostat (Cryophysics) that cooled the sample to 10 K. The temperature was measured by silicon diodes on the body of the DAC, and the ruby chip used for the pressure determination [6] also made it possible to check the temperaure [7]. The spectra were recorded by a Jobin-Yvon monochromator equipped with a cooled photomultipier operating in photon counting mode (Hamamatsu).

We studied Mg-mesoporphyrin (MgMP) dissolved in DMSO matrix and horseradish peroxidase (HRP) substituted with MgMP.

3 Results & Discussion

FLN emission spectra of MgMP in DMSO were measured over the pressure range of 0–20 kbar. By scanning the excitation one can calculate the inhomogeneous distribution function which characterises the effect of the environment on the chromophore.

The inhomogenous distribution function (IDF) of purely electronic (0,0) transitions of MgMP was determined at various pressures up to 20 kbar. It was shown earlier that this band is identical to the lowest energy absorption band of the chromophore at low temperature [8]. Two spectral components were found. The two peaks appearing in the IDF indicate that there are two distinct conformations of the chromophore–matrix complex in this system.

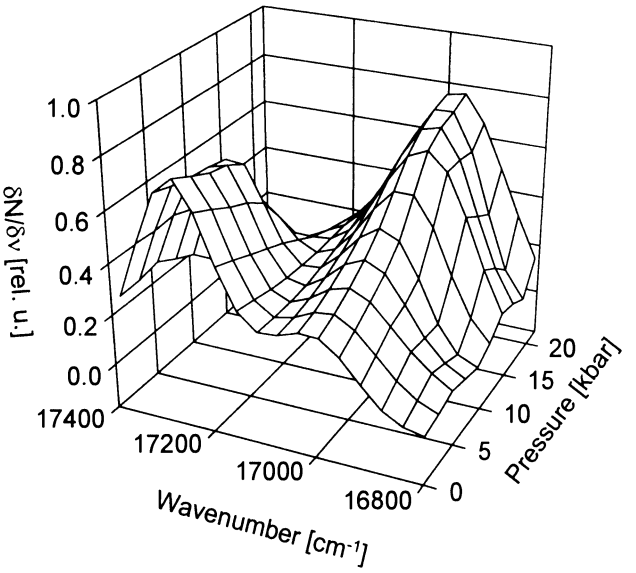

Fig. 1. The effect of pressure on the inhomogenous distribution function of MgMP in DMSO matrix at 10 K

Figure 1 shows the change of the IDF as a function of the applied pressure. One can observe that, when the applied pressure was varied, the population of these peaks was affected and the maximum position was shifted to lower energies by increasing pressure. The change in the population was interpreted on the basis of the different volumes occupied by the distinct species and the volume difference could be determined; it was found to be ΔV=0.18 cm^3/mol=0.3 Å^3/molecule, which corresponds approximately to the volume of a hydrogen atom. It was found that the one with greater volume has its electronic transition at higher energy as expected.

Table 1. Vibrational levels of the first electronically excited level (ν_{exc}) of MgMP

ν_{exc} [cm^{-1}]	483	593	672	733	904	966
Intensity	vw	w	w	vs	w	s
ν_{exc} [cm^{-1}]	988	1064	1087	1145	1241	1345
Intensity	s	vs	vs	s	s	vs

The FLN technique also allows the determination of the vibrational levels of the excited state. In the range of the 590–1200 cm^{-1} region the vibrational energies of 12 vibrational levels were measured. These are listed in the Table 1 with the determined absorption intensities to the corresponding vibronic levels. The pressure dependence was determined for a few of the excited state vibrations and the $\delta\nu/\delta p$ values found to be 0.3 cm^{-1}/kbar which are in the same order of

magnitude as the shifts of the ground state vibrational levels determined in the Raman and infrared measurements.

The IDF of MgMP in HRP reveals mostly one component at ambient pressure in the protein matrix. Unfortunately pressure studies have not been performed yet on the protein sample. A comparison with the model DMSO system suggests that the protein defines the structure of the porphyrin more definitely than the glassy matrix.

4 Conclusions

The high resolution fluorescence line narrowing method combined with high pressure is capable of unravelling important information concerning the coupling of a porphyrin and the surrounding matrix. High pressure is able to change this conformation into another specific configuration predetermined by the matrix. The structural change is in the range of one atomic displacement. However, the spectral consequences are well measurable by the FLN method. The vibrational energies determined by the FLN technique show pressure dependence as found in Raman or IR studies.

References

[1] Byler, D. M. & Susy, H., (1986); Biopolymers, 25, 469–487.
[2] Heremans, K., Goossens, K. & Smeller, L. (1996); in: High pressure effects in molecular biophysics, Markley, J. L. Northrop, D.B.. Royer C. A. (Eds.), Oxford University Press, N.Y. pp. 44–61.
[3] Personov, R. I. (1983); in: Spectroscopy and excitations dynamics of condensed molecular systems. Agranovich, V. M., Hochstrasser, R. M (Eds.), North-Holland Amstrerdam. pp. 555–619.
[4] Fidy, J., Laberge, M., Kaposi, A.D. & Vanderkooi, J.M. (1998); Biochim. Biophys. Acta, 1386, 331–351.
[5] Kaposi, A. D. & Vanderkooi, J.M (1992); Proc Natl Acad Sci USA, 89, 11371–11375.
[6] Forman, R. A., Piermarini, G. J., Barnett, J. D. & Block S. (1972); Science, 176, 284–286.
[7] Weinstein, B. A. (1986); Rev. Sci. Instrum., 57, 910–913.
[8] Balog, E., Kis-Petik, K, Fidy, J, Köhler, M & Friedrich, J. (1997); Interpretation of multiple (0,0) bands in the absorption spectrum of Mg mesoporphyrin embedded in horseradish peroxidase. Biophys. J., 73, 397–405.

Pressure-Induced Rearrangement of Aryl-Iron Complexes in Cytochrome P-450cam: Application to Topological Mapping of the Compressed Active Site

G. Hui Bon Hoa[1], R.A. Tschirret-Guth[2] and P.R. Ortiz de Montellano[2]

[1]INSERM U310, Institut de Biologie Physico-Chimique, 13 rue Pierre et Marie Curie, 75005 Paris, France
[2]Department of Pharmaceutical Chemistry, University of California, 513 Parnassus, San Francisco, 94143-0446 California, USA
Phone: 33 (1) 43298127; Fax: 33 (1) 43298088
huibonho@ibpc.fr

Abstract. The reactions of cytochrome P-450cam with phenyldiazene result in the formation of phenyl-iron complexes. Oxidation of such complexes at 1 bar causes regioselective migration of the phenyl group from the iron to the porphyrin nitrogens. The four N-arylprotoporphyrin IX regioisomers formed indicate that the active site is open above pyrrole ring D and to a small extent above pyrrole ring C. The iron-aryl complexes decompose at pressures above 1500 bar for Fe-phenyl or 2500 bar for Fe-(2-naphthyl and Fe-(p-biphenyl) complexes. The kinetics of the decomposition processes exhibit negative activation volumes. Decompression of the solutions shows that the loss of the Fe-aryl complexes is associated with the formation of new distributions of the N-arylprotoporphyrin IX regioisomers. Thus the rearrangement of aryl-iron complexes can be induced by high pressure in the absence of any exogenous oxidizing agent. These results are interpreted in term of differential distortion of the P-450cam active site stucture induced by high pressure.

1 Introduction

During the past decade, the studies of substrate activation by cytochrome P-450 have shown the formation of unusual σ-iron(III)-aryl (or alkyl) P-450 complexes. For example the reaction of cytochrome P-450 with phenyldiazene produces phenyl-iron complexes with absorption maxima between 472 and 480 nm [1]. Treatment of the cytochrome phenyl-iron complex with ferricyanide results in phenyl migration from the iron to the nitrogens of the heme prosthetic group within the intact P-450 active site. Use of model compounds such as metalloporphyrins has permitted the elucidation of the mechanism of the shift [2], showing that the iron-to-nitrogen migration involves one-electron oxidation of the Fe(III)-aryl complex to an Fe(IV)-aryl complex followed by migration of the aryl group to the nitrogen to give the Fe(II)-N-aryl complex. The oxidation-induced shift of aryl-P-450 complexes yields different patterns of N-arylprotoporphyrin IX regioisomers

(N_B:N_A:N_C:N_D) which are shown to be controlled by the residues above the heme group. The determination of the N-arylporphyrin ratios has been used to obtain information on the active site topology of several bacterial as well as mammalian cytochrome P-450s [3]. High pressure is a reversible tool to perturb protein structures and their reactions. Its effect depends on reaction volume of equilibria and activation volume of reaction rates [4]. We have applied such a technique to induce shift of the aryl-iron complexes and to explore the pressure-induced active site topology deformations at different heights above the heme plane by using three aryl probes [5].

2 Materials & Methods

Cytochrome P-450 was expressed in *Escherichia coli* and was purified as previously reported [6]. Methylphenyldiazenecarboxylate azo ester was obtained from Research Organics (Cleveland, OH). Methyl 2-naphthyldiazene carboxylate azo ester and methyl *p*-biphenyldiazenecarboxylate azo ester were prepared from the corresponding hydrazines according to the method of Huang and Kosower [7]. UV-VIS spectra were recorded with a Cary 3E spectrophotometer mounted with a pressure chamber as described elsewhere [8]. Formation of the Fe-aryl complex was followed by the increase in the absorbance at 480 nm. Kinetic measurements of the decomposition of the iron-aryl complexes were followed at 478–480 nm, initiated by a pressure jump from 1.8 bar to the desired final pressure. The curves were fitted by the following expression: $OD_t = (OD_0 - OD_f) \exp(-kt) - OD_f$ where OD_0 and OD_f are the initial and final optical densities, respectively. The rate constant k of the reaction is related to the activation energy ($\Delta G^{\ddagger}$) and activation volume ($\Delta V^{\ddagger}$) by (1) and (2):

$$k(p,T) = (k_B\, T/h) \exp\left[-\Delta G^{\ddagger}(p,T) / RT\right], \quad (1)$$

where k_B is Boltzmann's constant, h Planck's constant, R the gas constant and T the absolute temperature.

$$\ln k = -p\Delta V^{\ddagger} / RT + \ln k_0 . \quad (2)$$

$\Delta V^{\ddagger}$ is the activation volume which is equal to the difference in the volumes of the activated ($V^{\ddagger}$) and initial (V_i) states. k and k_0 are respectively the rate constants of the reaction at pressure p and at the initial pressure. HPLC analysis were carried out on a Hewlett-Packard 1090 system using a Partisil ODS-3 colum (5 μm× 4.6×250 mm) (Alltech, San Jose, CA). The samples were first added to a solution of 5% aqueous H_2SO_4 and allowed to stand at 4 °C for ~16 h before they were extracted with $CHCl_3$. The residue obtained after evaporation of the $CHCl_3$ was redissolved in 40 μl of 6:4:1 methanol/water/acetic acid for HPLC analysis.

3 Results

The complexes were first formed at 1 bar by adding 1–2 μl of diazene probes (phenyl-, p-phenyl- and 2-naphthyl-) to 500 μl of cytochrome P450cam in phosphate buffer (50 mM, pH 7.4). A typical spectrum with maximum absorption at 478–480 nm was obtained as is shown in Fig. 1. The complexes are stable up to 2 kbar for Fe-phenyl and approximately 3 kbar for Fe-(p-biphenyl) and Fe-(2-naphthyl). Then the maximum of the Fe-aryl complexes decreases as the pressure

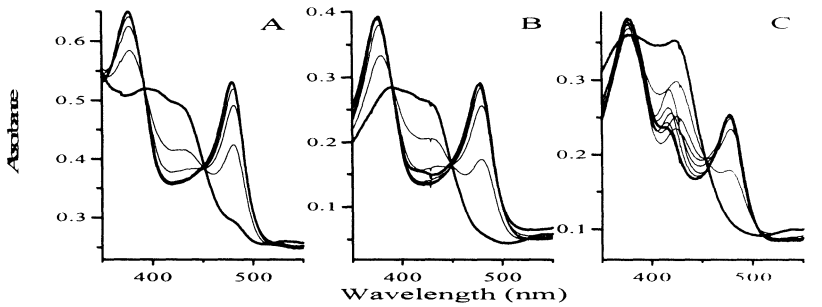

Fig. 1. Pressure-induced decomposition of P-450cam Fe-aryl complexes. Spectra changes of (**A**) Fe-phenyl, (**B**) Fe-(p-biphenyl) and (**C**) Fe-(2-naphtyl) complexes which absorbe at 375 and 480 nm, as a function of pressures from 1 to 4 kbar

is further increased with the formation of a new spectrum (Fig. 1). There is no concomittant recovery of the normal ferric Soret absorbance and/or formation of the inactive P-420 form.

Decompression of the solutions, followed by extraction with $CHCl_3$, shows that the loss of 480 nm absorbance is associated with the formation of products with characteristic absorbance at 416 nm in chloroform solution. Further analysis using HPLC confirms the formation of N-arylprotoporphyrin regioisomers. The distributions of the patterns are quite different from those obtained by oxidation at normal pressure as shown in Table 1.

Ferricyanide oxidation at 1 bar favors principally migration of the phenyl group to the N_D isomer and to a lesser extent to the N_C isomer. There is a complete shift of the 2-naphthyl group to pyrrole ring C with no isomers on the other pyrrole rings. p-Biphenyl groups shift to ring D and C but less so than for the phenyl probe; however, the proportion of the N_A isomer is higher. High pressure-induced shifts differ much from the oxidation case: the N_D isomer remains favored when the phenyl probe is used, but less so than in the oxidative rearrangement. The decrease in the N_D isomer is compensated by increases of 10% in the N_A and N_B isomers. There are dramatic shifts of the 2-naphthyl group to give isomers in all the pyrrole rings as compared to the oxidative case. Similar shifts in all the pyrrole rings are obtained for the p-biphenyl probe, but the decrease of N_D and N_C isomers are compensated for by an increase in the N_B isomer. The decomposition of the Fe-phenyl complex to the N-phenyl complex is in fact pressure dependent. *p*-Jump experiments from 1.8 kbar to different final pressures showed that the rates of de composition are accelerated by high pressure (Fig. 2a). All the kinetics exhibited

Table 1. Distributions of N-arylprotoporphyrin IX isomer ratios N_B:N_A:N_C:N_D obtained by oxidation with ferricyanide or exposition to 4 kbar of pressure from the P-450cam Fe-aryl complexes. N_A, N_B, N_C and N_D are the regioisomers with the aryl group on the nitrogens of pyrrole rings A, B, C and D, respectively. The error in the individual measurements is ±1

Aryl probes	$K_3Fe(CN)_6$	4 kbar of pressure
phenyl	00:05:25:70	10:14:33:43
2-naphthyl	00:00:100:00	12:13:37:38
p-biphenyl	00:14:40:46	15:15:33:37

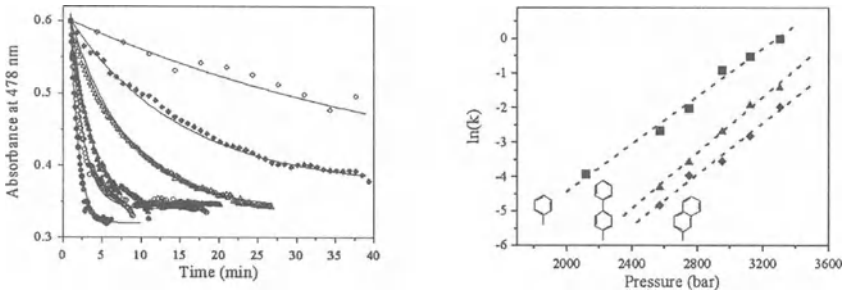

Fig. 2. (**a**) Kinetics of Fe-phenyl complex decompositions followed at 478 nm after a *p*-jump from 1.8 kbar to 2.18 (*open squares*), 2.57 (*closed squares*), 2.75 (*open triangles*), 2.95 (*closed triangles*), 3.12 (*open circles*), 3.3 kbar (*closed circles*). (**b**) Plots of ln *k* versus final pressures for the rates of Fe-phenyl, Fe-(p-biphenyl) and Fe-(2-naphthyl) decompositions

exponential decay patterns. The same experiments are repeated for the other probes. Activation volumes are deduced from Eq. (2) and Fig. 2b. $\Delta V^{\ddagger}$ obtained are –84.3, –91.7 and –98.7 ml/mol, respectively, for phenyl, p-biphenyl and 2-naphthyl migrations.

4 Conclusions

The crystal structure of P450cam shows that pyrrole ring C is partially masked by Leu 244 and pyrrole ring D is open above the heme plane but is occluded at some distance by Phe 87. Oxidation results are in agreement with crystal structure data and show that the active site is open above ring D and to a small extent above ring C. Pressure data show that the active site is compressed above rings C and D and pressure-induced compression causes an outward displacement of the I-helix which may involve dislocation of the mobile residues associated in reversible dynamics of the substrate access channel. The Fe-aryl shifts promoted by high pressure are a novel phenomenon. The transition states of the reactions are formed with huge contraction in volumes. These phenomena are compatible with local solvent and internal redox potential rearrangements induced by high pressure. The exact mechanism is now under study in our laboratories.

References

[1] Jonen, H.G *et al.* (1982); J. Biol. Chem., 257, 4404–4411.
[2] Lançon, D *et al.* (1984); J.Am.Chem.Soc., 106, 4472–4478.
[3] Ortiz de Montellano, P.R., (1995); Biochimie, 77, 581–593.
[4] Morild, E., (1981); Adv. Protein Chem., 34, 93–167.
[5] Tschirret-Guth, R.A. *et al.* (1998); J.Am.Chem.Soc., 120, 3590–3596.
[6] De Voss, J.J. *et al.* (1997), J.Am.Chem.Soc., 119, 5489–5498.
[7] Huang, P.C., Kosower, E.M., (1968); J.Am.Chem.Soc., 90, 2354–2362.
[8] Hui Bon Hoa, G. *et al.* (1982); Anal. Biochem., 120, 125–135.

The Dynamics of Protein-Bound Water in the Heme Domain of P450BM3 as Compared with P450cam and P450 2B4

D.R. Davydov, G. Hui Bon Hoa[1] and J.A. Peterson[2]

Institute of Biomedical Chemistry, 10 Pogodinskaya, 119832, Moscow, Russia
[1]Institut de Biologie Physico-Chimique, INSERM Unité 310, Paris, France
[2]Department of Biochemistry, UT Southwestern Medical Center, Dallas, TX, USA

Abstract. Pressure-induced transitions in the heme domain of cytochrome P450 BM3 (P450BMP) and P450cam were studied versus the concentration of their substrates (palmitic acid and camphor). The barotropic behavior of these bacterial proteins are compared with that of rabbit liver microsomal P450 2B4. General regularities and differencies in the dynamics of protein-bound water in these hemoproteins are discussed.

1 Introduction

In the present work, we describe pressure effects on the heme domain of P450BM3 (P450BMP), the bacterial hemeprotein having the highest homology with microsomal P450s. The effect of hydrostatic pressure on cytochrome P450cam was also re-examined at variable concentrations of camphor. The barotropic parameters of substrate binding and spin transitions in P450BMP are compared with those obtained for P450cam and rabbit liver microsomal P450 2B4. These data are interpreted in terms of the dynamics of protein-bound water in these hemoproteins.

2 Materials & Methods

The hemeprotein domain of P450BM3 (P450BMP) and cytochrome P450cam were purified by published procedures [1, 2]. An optical pressure system, capable of generating a pressure of 7000 bar [3], was used in our experiments. After each pressure adjustment, the system was allowed to stabilize for 3 min. All experiments with P450BMP were carried out at 25 °C in 100 mM Na-HEPES buffer, pH 7.4 containing 1 mM dithiothreitol and 1 mM EDTA. The experiments with P450cam were done in 100 mM Tris-HCl buffer (pH 7), in the presence of 240 mM KCl at 4 °C. The techniques of spectral analysis and data fitting were described earlier [4].

3 Results & Discussion

Exposure of P450BMP to high pressures induces a high- to low-spin shift and a subsequent transition of P450 into the inactive P420 form of the hemoprotein. The whole pool of substrate-free P450BMP undergoes this transition in contrast to that shown for P450 2B4 where only about 2/3 of the hemeprotein could be converted to the P420 state by high pressure [4].

The molar volume change for the conversion of P450 to P420 in the absence of substrate was –99 ml/mol. The ΔV° of such large proportions that suggests some important hydration of the protein accompanies this transition. This hydration is difficult to explain only by the water flux into the heme moiety. A ΔV° this large can only result from an increase of the water-accessible surface of the protein.

To perform an analysis of the pressure-induced changes in P450BMP substrate-binding and spin equilibria, we have used a four-state model of the transitions:

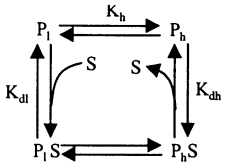

$$K_h = [P_h] / [P_l] ; \quad K_h^s = [P_hS] / [P_lS] ;$$

$$K_{dl} = [P_l][S] / [P_lS] ; \quad K_{dh} = [P_h][S] / [P_hS]$$

Here "P" and "PS" correspond to P450 and its complex with the substrate, respectively. The subscripts "l" and "h" designate respectively the low- and high-spin states of the hemeprotein. Being combined with the classical equation for the pressure dependence of chemical equilibrium, this model precisely fits the whole set of data on pressure-induced changes in the low-spin form content in P450 BMP and in P450cam versus concentration of substrates.

The values of the constants of the elementary transitions and the corresponding ΔV° values are compared with those found for P450 2B4 [4] and P450cam in Table 1. The high- to low-spin conversion of both substrate-free and substrate-bound P450BMP is accompanied by a volume decrease (–23 and –16 ml/mol, respectively). The volume change in the dissociation of the substrate complex of both low- and high-spin P450BMP is negative as well (–20 and –13 ml/mol).

Dissociation of the substrate complex of P450cam was assumed to be accompanied by a negative volume change because of water penetration into the vicinity of the heme moiety and the substrate pocket. Despite these expectations, our analysis shows that the volume change in the dissociation of the low-spin form of the camphor-bound hemeprotein is positive. The volume changes upon the interactions of the hemeprotein with the substrate are composed of the changes in the partial volume of the protein as well as the volume change due to penetration of the substrate molecule into the substrate pocket. Therefore, interpretation of the values of ΔV°_{diss} requires the partial volume (V°) of the substrate to be taken into account. As the ΔV_{diss} of the low-spin P450cam-camphor complex was estimated to be –42 ml/mol (Table 1) and the partial volume of camphor is about –148 ml/mol,

the changes in partial volume of the protein on camphor binding can be estimated to be +106 ml/mol. A subsequent transition of the low-spin P450cam complex with camphor into the high-spin form is characterized by a volume change of 90.6 ml/mol (Table 1). The sum of this value with the above estimate of +106 ml/mol gives a value of about 197 ml/mol for the total volume change in the transition of low-spin substrate-free P450cam into the high-spin camphor-bound form. If this change in the partial volume of P450cam results solely from the hydration of empty cavities in the molecule of protein, then this transition has to be accompanied by expulsion of at least 11 water molecules. This estimate is not too far from the maximal changes in the hydration of the active site of P450cam from theoretical considerations (6–9 molecules). However, we cannot exclude the possibility that the formation of the complex of P450cam with substrates involves dehydration of some loci outside of the active site.

Table 1. Equilibrium constants and reaction volumes of substrate binding and spin transitions of P450BMP (with palmitic acid as substrate), P450cam (with camphor as substrate) and P450 2B4 (with benzphetamine as substrate)

Transition	Equilibrium	Constant at	Zero pressure	$\Delta V°$, ml/mol		
	BMP	P450cam	2B4	BMP	P450cam	2B4
$P_l \leftrightarrow P_h$ (K_h)	0.19	0.013	0.32	23	20	21
$P_lS \leftrightarrow P_hS$ (K_h^S)	1.2	62	8.3	16	91	49
$PS \leftrightarrow P+S$ (K_s)	2.1 μM	4.4 μM	130 μM	–25	–48	8.1
$P_lS \leftrightarrow P_l+S$($K_{dl}$)	3.9 μM	280 μM	930 μM	–20	42	5.3
$P_hS \leftrightarrow P_h+S$($K_h$)	0.61 μM	0.047 μM	36 μM	–13	–29	–23

The sign of the reaction volume corresponds to the low- to high-spin and substrate complex dissociation reactions.

The $\Delta V°$ for dissociation of the benzphetamine complex of low-spin P450 2B4 is positive and differs from the value found for P450cam by 37 ml/mol (Table 1). The volume change on dissociation of the low-spin P450BMP–palmitic acid complex is negative and its difference from the value found for the P450cam complex with camphor is 62.3 ml/mol. Taking into account the volumes of benzphetamine (263 ml/mol) and palmitate (268 ml/mol) we estimated the changes in the partial volume of the proteins on their interactions with substrates to be about 267 ml/mol for the P450 2B4-benzphetamine pair and 248 ml/mol for P450BMP interactions with palmitic acid. These changes are considerably larger than the value of 106 ml/mol calculated above for P450cam with camphor. These results suggest that the interactions of P450BMP and P450 2B4 with their substrates induce important dehydration of sites other than the heme moiety and the substrate pocket. Structural rearrangements in both P450 2B4 and P450BMP on substrate binding appear to be more profound than in the case of P450cam.

All three hemeproteins have similar values for $\Delta V°$ of the spin transition of the substrate-free enzyme (20–23 ml/mol). This volume change is consistent with expulsion of 1 water molecule (18.1 ml/mol) from the protein. This result appears

to be reasonable, as the low- to high-spin transition requires dissociation of the 6th water ligand from the heme iron [5].

In a recent study of the interactions of P450cam with a series of analogs of camphor, a linear relationship between $\Delta V°$ and ΔG_0 for the spin-state transition was demonstrated [6]. Comparing our results with those reported in [6], we have found that the whole series of $\Delta V°/\Delta G_0$ data pairs for the spin-state transition obey the same linear dependence. The points obtained in both studies fall around the same straight line (Fig. 1). Therefore, the linear relationship between $\Delta V°$ and ΔG_0 for the spin-state transition appears to be a general feature of P450 hemeproteins and suggests a common mechanism of the shift of spin equilibrium by substrate binding for the three hemeproteins studied here. ΔG_0 of the spin shift may be thought of as linearly connected with the number of water molecules required to enter the heme moiety for the transition of the substrate-bound hemeprotein into the low-spin form.

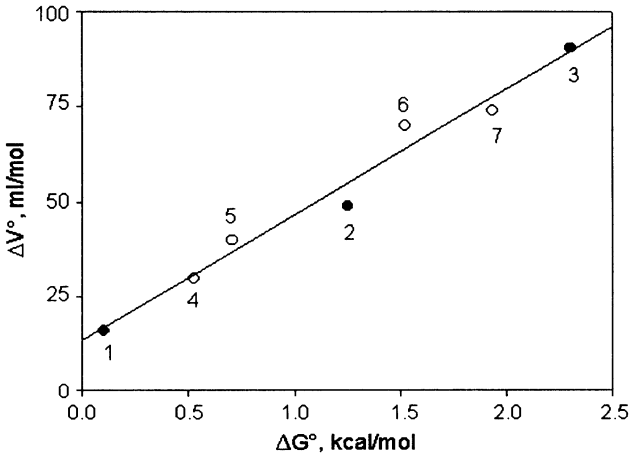

Fig. 1. Correlation between molar volume change ($\Delta V°$) and the change in Gibbs free energy (ΔG_0) in the low-to-high spin transition of substrate-bound cytochromes P450. Filled circles represent the results obtained in the present study for P450BMP/palmitic acid (1), P450 2B4/benzphetamine (2) and P450cam/camphor (3) pairs. Data shown in open circles are taken from [6] and represent the results for P450cam complexed with camphor (7) and its *endo*-borneol ethers: *O*-methyl - (4), *O*-propyl- (5), and *O*-allyl (6)

References

[1] Boddupalli, S.S., Oster, T., Estabrook, R.W., Peterson, J.A. (1992) *J. Biol. Chem. 267*,10375–80.

[2] Gunsalus, I.C., Wagner, G.C. (1978) *Meth. Enzymol. 52*, 166–88.

[3] Hui Bon Hoa, G., Marden, M.C. (1982) *Eur. J. Biochem. 124*, 311–15.

[4] Davydov D, Deprez E, Hui Bon Hoa G *et al.* (1995) *Arch.Biochem.Biophys.320*, 330–44.

[5] Griffin BW, Peterson, J.A. (1975) *J.Biol.Chem. 250*, 6445–51.

[6] Helms V, Deprez E, Gill E *et al.* (1996) *Biochemistry 35*, 1485–99.

Use of High Pressure To Investigate the Role of Carbohydrate Moiety in the Conformational Stability of Carboxypeptidase Y

M. Dumoulin, H. Ueno, R. Hayashi and C. Balny[1]

Division of Applied Life Sciences, Graduate School of Agriculture, Kyoto University, 606-8502 Kyoto, Japan
Phone: +81-75-753-6111; Fax: +81-75-753-6128
[1]INSERM, Unité 128, IFR 24, CNRS 1919, Route de Mende, 34 293 Montpellier, France

Abstract. In this work the incidence of the carbohydrate moiety of carboxypeptidase Y (CPY) on the stability of this enzyme was investigated using high pressure combined with low temperature as denaturant. We found that the carbohydrate moiety protects the native state of CPY from pressure-induced denaturation and affects the extent of reversibility.

1 Introduction

Carboxypeptidase Y is a vacuolar glycoprotein from *Saccharomyces cerevisae*. The role of the carbohydrate moiety in the structure and function of this enzyme has yet to be cleared. CPY is very stable against cold denaturation, *i.e*, several freezing-thawing cycles at atmospheric pressure do not inactivate it. In our opinion, this unique property of CPY may be related to its relatively high sugar content (about 16% of the MW).

Here we report the effects of high pressure combined with low temperature on the intrinsic and ANS-binding fluorescence, and on the activity of wild type CPY and unglycosylated CPY.

2 Materials & Methods

Unglycosylated CPY (ΔglyCPY) which was obtained by site directed mutagenesis and wild type CPY (WtCPY) were purified as described elsewhere [2]. *In situ* fluorescence emission spectra were measured in a thermostated high-pressure cell adapted in a AB2 fluorospectrophotometer (SLM Co.) with excitation at 280 nm for intrinsic fluorescence and 350 nm for ANS-binding fluorescence. Results of intrinsic fluorescence were characterized by changes in the center of the spectral mass and those of ANS-binding fluorescence by the changes in fluorescence intensity at 475 nm. *In situ* activity measurements were done using a high-pressure

optical cell made by Teramecs (Kyoto, Japan) set inside a Shimidzu UV-2500 spectrophotometer [3].

3 Results

3.1 Role of the Carbohydrate Moiety on the Native State of CPY

Effects of pressurization at 25 °C on the intrinsic fluorescence, ANS-binding fluorescence and activity of WtCPY are shown in Fig. 1. Unfolding of WtCPY occurred through at least three transitions each of them being characterized by a pressure of half transition Pm_1, Pm_2 and Pm_3.

Pressures below 150 MPa induced a slight decrease in the center of the spectral mass; however, in this pressure range no ANS-binding fluorescence was observed and about 80% of the activity remained suggesting that in this pressure range conformational changes are rather slight.

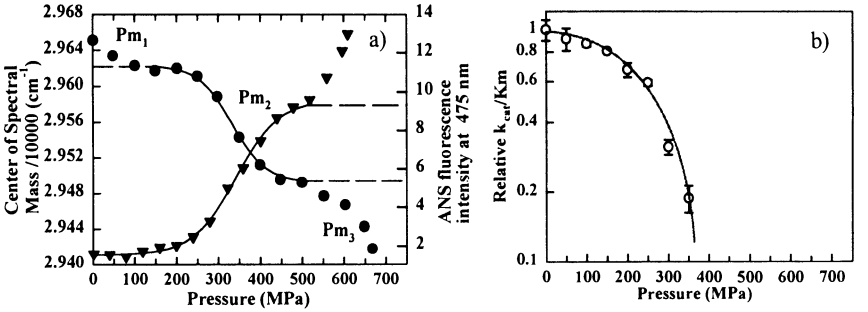

Fig. 1. Pressure-induced changes at 25 °C on (**a**) the center of the spectral mass of WtCPY intrinsic fluorescence (●), [Enz]= 0.1 mg/ml in 50 mM Tris•HCl pH 7, λ_{exc} = 280 nm, λ_{em}= 300–400 nm; and the ANS-binding fluorescence (▼), [Enz]= 0.1 mg/ml in 50 mM Tris•HCl pH 7, ANS/Enz= ~ 55–60, λ_{exc} = 350 nm, λ_{em}= 420–600 nm; (**b**) the relative k_{cat}/K_m towards the hydrolysis 0.2 mM ATEE in 50 mM Tris•HCl pH 7. [Enz]= 20–60 nm depending on the activity

Pressures between 200 and 500 MPa induced a further decrease in the center of the spectral mass with a concomitant increase in the ANS-binding fluorescence, and WtCPY was almost fully inactivated. This transition displayed a clear sigmoidal shape, which allowed the precise determination of the pressure of half transition, Pm_2. This parameter was used to compare the pressure sensibility of Wt CPY and ΔglyCPY.

Pressures higher than 550 MPa induced further structural changes characterized by a further decrease in the center of the spectral mass and increase in ANS-binding fluorescence. ANS-binding fluorescence is one of the properties of a

molten globule state and therefore we assumed that the second and third pressure-induced states are molten globule-like states.

A same three-transitions process was observed for ΔglyCPY; however, the two first transitions occurred at clearly lower pressure than that for WtCPY. Although the difference was slight it was observed at all the temperatures investigated (Table 1), clearly indicating that the carbohydrate moiety protects native CPY from pressure-induced cold denaturation.

Table 1. Temperature dependence of Pm_2 determined from the intrinsic fluorescence measurements

	Pm_2 (MPa)	
Temp. (°C)	WtCPY	ΔglyCPY
25	334	282
−5	229	190
−12.5	165	135

3.2. Role of the Carbohydrate Moiety on the Reversibility of Pressure Effects

In view of the protecting effects of the carbohydrate moiety on the native state, it was of interest to investigate if the carbohydrate moiety also affects CPY in its unfolded state and if it influences the reversibility. For this purpose, enzymes (0.6 mg/ml) were first pressurized and then activity was measured at atmospheric pressure immediately after pressure release. Pressurization was done for 30 min under 100–400 MPa at temperatures ranging from −22 to 25 °C. At a given pressure, the remaining activity decreases with the temperature of pressurization (Table 2). *In situ*, WtCPY is almost fully inactivated under 25 °C and 400 MPa (Fig. 1), therefore, partial renaturation almost instantaneously occurs upon pressure release. The extent of reversibility also decreases with the temperature of pressurization. No significant difference in the remaining activity was observed between WtCPY and ΔglyCPY except when pressurization was carried out at 200 MPa for temperatures below −10 °C (Table 2). In these latter conditions, the remaining activity of ΔglyCPY was significantly lower than that of WtCPY

Table 2. Remaining activity (%) measured immediately after pressure release from a 30 min treatment at 400 and 200 MPa as a function of the temperature of pressurization. The activity was measured towards 1 mM ATEE in 50 mM Tris•HCl buffer pH 7.5 at 25 °C

	400 MPa		200 MPa	
Temp. (°C)	WtCPY	ΔglyCPY	WtCPY	ΔglyCPY
25	78	74	86	97
10	61	71	96	110
0	55	56	88	82
−10	4.2	7.6	77	77
−15	nd	nd	68	44
−22	3.5	6.5	42	14

suggesting that the carbohydrate moiety affects the unfolded state of the CPY and/or participates in the process of renaturation. Carbohydrate moiety often protects partially denatured protein from aggregation [4]; however, native PAGE showed that no aggregation occurred either with WtCPY or with ΔglyCPY. In turn, for both enzymes, a new band with a higher apparent molecular weight was observed after pressure treatment.

4 Conclusions & Perspectives

Results showed that the carbohydrate moiety protects the native state of CPY from pressure-induced denaturation. They also showed that reversibility is higher in the presence of the carbohydrate moiety. Based on the tertiary structure of CPY and results obtained with others proteins [5, 6], we postulate that protection may arise from hydrogen bond formation between protein and carbohydrate moieties [1]. Reduced solvent accessibility due to the steric hindrance between the oligosaccharide and the protein may also contribute to the protective effects as well as local effects of sugar on the water structure. Structural properties of the pressure-induced slow-migrating protein and experiments combined with chemical modifications are under investigation with the expectation of gaining additional information about how carbohydrate affects the reversibility.

Acknowledgements: Supported by grants from the JSPS/INSERM collaboration program and the Japanese Ministry of Education, Culture and Sport.

References

[1] P.W. Bridgman (1912) Proc. Amer. Acad. Arts Sci. 47,441–558.
[2] M. Dumoulin, H. Shimidzu, H. Ueno, R. Hayashi, and C. Balny. (1998) (Submitted).
[3] M. Morishita, T. Tanaka, and S. Kawai. (1997) In High Pressure Bioscience and Technology (Suzuki A., and Hayashi R., Eds) pp. 187–194, San-ei Shuppan Co., Kyoto, Japan (in Japanese).
[4] C. Wang, M. Eufemi, C. Turano, and A. Giartosio (1996) Biochemistry, 35, 7299–7307.
[5] A. R. Dwek (1995) Science, 39, 1234–1235
[6] G. Mer, H. Hietter, and J.F. Lefèvre (1996) Nature Structural Biology, 3, 45–53

Complex Unfolding Events of Sso7d from *S. solfataricus* at High Temperature and High Pressure

R. Lange[1], E. Mombelli[1], J. Connelly[1], M. Afshar[1], P. Fusi[2], C. Balny[1] and P. Tortora[2]

[1]INSERM U128, IFR24, 1919 route de Mende, 34293 Montpellier Cedex 5, France;
[2]Università degli Studi, Dipt. di Fisiologia e Biochimica Generali, Sezione di Chimica Biologica, Via Celoria 26, 20133 Milano, Italy
Phone: +33-(0)4 67 61 33 65; Fax: +33-(0)4 67 52 36 81
lange@xerxes.cnrs-mop.fr

Abstract. We have studied the unfolding events of the archaebacterial Sso7d and some of its mutant forms at high temperature and high pressure by a combination of UV absorbance spectroscopy in the 4th derivative mode, ANS binding and molecular dynamics simulation. UV absorbance probed the changes in polarity of Tyr33, ANS binding (fluorescence increase) the exposure of the hydrophobic core to water, and the simulation helped to understand structural changes in the outer sphere protein segments. Our results suggest that unfolding is not a concerted process but affects different protein domains sequentially. The adaptation of the protein to high temperature appears to result from an increased flexibility of outer residues, whereas the hydrophobic core remains stable.

1 Introduction

Sso7d is a ribonuclease and DNA binding protein from the thermophilic archaebacteria *S. solfataricus*. It is a very small protein (7 kDa), mutant forms are available, its NMR structure is known [1] and it is one of the most thermo- and barostable proteins [2]. It appears therefore to be a suitable model to study the mechanism of heat and pressure induced protein unfolding. FTIR, CD, calorimetry and UV absorbance investigations of wild type and mutant forms led to the conclusion that its stability is due to an aromatic cluster in a very stable hydrophobic core. This core is surrounded by a mantle of mostly positively charged residues. This outer zone appeared to be less thermostable than the core [2, 3]. If this picture is true, the unfolding process of Sso7d can be expected to be a stepwise reaction. In order to confirm or infirm this hypothesis, we analyzed here the pressure and heat induced structural changes of Sso7d and several of its mutant forms by three different techniques: a) UV absorbance spectroscopy in the 4th derivative mode. This technique informs about the polarity of Tyr33, a residue completely buried in the hydrophobic core. There is another tyrosine and also a tryptophan, but these

residues are largely exposed to the solvent. b) ANS fluorescence enhancement. This technique informs about the exposure of larger hydrophobic domains to the solvent. c) Molecular dynamics simulation. The latter technique should give hints about the very first unfolding events.

2 Materials & Methods

F31A, F31Y and Y33A mutants of Sso7d were expressed as described [2, 3]. The UV absorbance spectra were recorded in a high pressure cell placed inside a Cary 3 spectrophotometer. The original spectra were then converted to their 4th derivatives as described [3]. ANS binding was determined from its fluorescence increase between 430 and 580 nm in a high pressure cell placed inside an SLM Bowman 2 spectrofluorimeter. The onset of the fluorescence increase was determined from the second derivative of the amplitude changes. The spectra were corrected for the fluorescence decrease of ANS as a function of pressure. The molecular dynamics simulation will be described elsewhere.

3 Results & Discussion

4th Derivative UV absorbance. The spectrum of the wild type did not change under high pressure (below 500 MPa). However, as shown in Fig. 1, significant changes were observed with mutant forms which had a lowered stability of their hydrophobic core. Taking as an example the F31A mutant, it is obvious that the

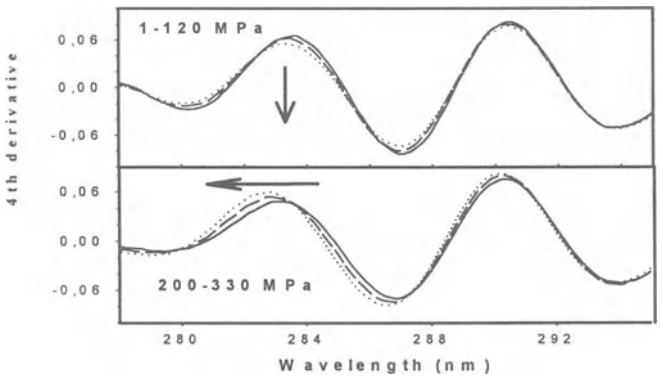

Fig. 1. Effect of pressure on the 4th derivative UV absorbance spectrum of the F31A mutant. The arrows indicate the shift of the tyrosine band (283 nm) at increasing pressure

changes of the 4th derivative spectra take place in two steps: between 100 and 120 MPa, the tyrosine band (283 nm) is decreased, and between 200 and 330 MPa, it is blue-shifted. These changes reflect a stepwise increase of polarity of the Tyr33 environment. As this amino acid is located in the center of the hydrophobic core, the increased polarity probably means a pressure induced leakage of water into the inside of the core.

ANS binding. The pressure induced binding of ANS to Sso7d was reflected by a strong fluorescence increase around 490 nm. In contrast to the changes observed by UV absorbance, the increase of fluorescence occurred at much higher pressures (> 500 MPa). The onset of the sigmoidal amplitude changes were shifted to higher pressure in the mutant forms. F31A was the least stable mutant. As shown in Fig. 2, lowering temperature resulted in ANS binding at lower pressure, suggesting that hydrophobic residues become exposed to the solvent. Binding of ANS characterizes generally the molten globule state, that is, an unfolding intermediate where larger hydrophobic domains are exposed to the solvent, but which still retains a significant amount of secondary structure.

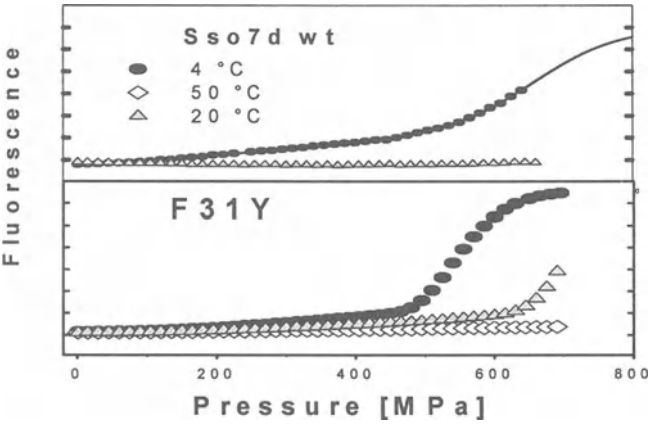

Fig. 2. Pressure induced ANS binding reflected by its fluorescence increase

Molecular dynamics simulation. The simulations were carried out for 450 ps for the wild type and the F31A mutant between 300 and 400 K. The results were consistent with a hydrophobic core structure maintained under these conditions. However, the structure of the outer part of the protein began to unfold at high temperature. This phenomenon was particularly marked for the F31A mutant. As shown in Fig. 3, the most spectacular process was the unwinding of the small

alpha-helix. Other parts of the protein – especially some loops – also showed an increased flexibility. However, the essential SH3 structure of the hydrophobic core was maintained.

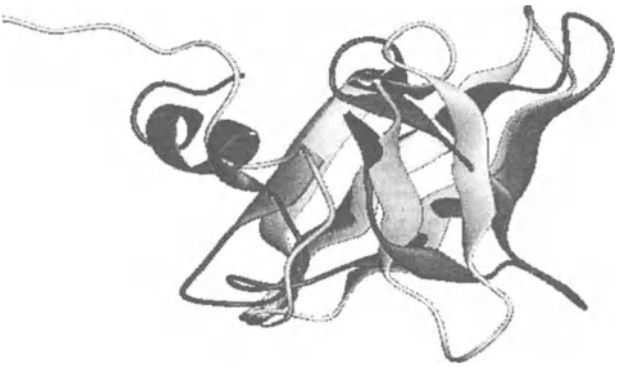

Fig. 3. Simulated structures of wild type at 300 K (black) and F31A at 400 K (grey)

4 Conclusions

The combination of different techniques, probing different structural motifs of the protein, together with the use of mutant forms, showed that this protein unfolds in distinct steps. The reason for the extreme thermo- and barostability of Sso7d might be that the structural constrain on the hydrophobic core, exerted by the adverse conditions, is compensated by the flexibility – and perhaps even partial unfolding – of its outer part structure.

Acknowledgements: This work was supported in part by COST D10.

References

[1] Baumann, H., Knapp, S., Lundback, T., Ladenstein, R., Hard, T. *Nat.Struct.Biol.* 1994, *1*, 808–819.

[2] Fusi, P., Goossens, K., Consonni, R., Grisa, M., Puricelli, P., Vecchio, G., Vanoni, M., Zetta, L., Heremans, K., Tortora, P. *Proteins* 1997, *29*, 381–390.

[3] Mombelli, E., Afshar, M., Fusi, P., Mariani, M., Tortora, P., Connelly, J.P., Lange, R. *Biochemistry* 1997, *36*, 8733–8742.

Influence of Pressure on the Reactivity of Antigens and Antibodies. Application to the Follow-up of Conformational Changes

P. Lemay, L. Estevez, S. Espeillac and P. Degraeve

Institut National des Sciences Appliquées de Toulouse,
CNRS UMR 5504, Laboratoire Associé INRA,
Complexe Scientifique de Rangueil, F-31077 Toulouse Cédex 4, France
Phone: +33 5 61 55 94 31; Fax: +33 5 61 55 94 00
Pierre.Lemay@insa-tlse.fr

Abstract. A method based on the modulation of the antigenic reactivity of β-galactosidases with corresponding antibodies to follow the denaturation of these enzymes is proposed.

1 Introduction

In a previous study [1], baro-immunodesorption was shown to be a promising and clean method to purify biological products. Further studies of the antibodies developed for this purpose showed they will be of interest in the appreciation of baro-, thermo- or chemical-induced conformational changes of their corresponding antigens. A method based on the modification of the antigenic reactivity of anti-β-galactosidase antibodies to follow the denaturation or the relationship between corresponding related antigens (*i.e.* β-galactosidases from various origins) is proposed.

2 Materials & Methods

β-Galactosidases were obtained or purified as described in [2]. Corresponding polyclonal antibodies were raised in rabbits. A serum directed against the *Escherichia coli* β-galactosidase active site was obtained as follows: a peptide corresponding to the residues Thr(496)-Gln(510) surrounding the crucial Tyr(503) residue of the bacterial enzyme was synthesized, purified and coupled to bovine thyroglobulin as a carrier; the complex was then injected into rabbits. The reactivity of the sera was checked by ELISA tests. Enzymatic activities were determined as in [2]. Protein denaturation was also screened by polyacrylamide gel electrophoresis. Pressurization methods and apparatuses have already been described [2].

3 Results

3.1 Stability of Antibodies

First a study was made of the stability of the antibodies following their exposure to pressure; no alterations seemed to occur up to 400 MPa (not shown).

3.2 Urea and Pressure Induced Changes of Antigenic Reactivity of β-Galactosidases

The results are presented in Fig. 1.

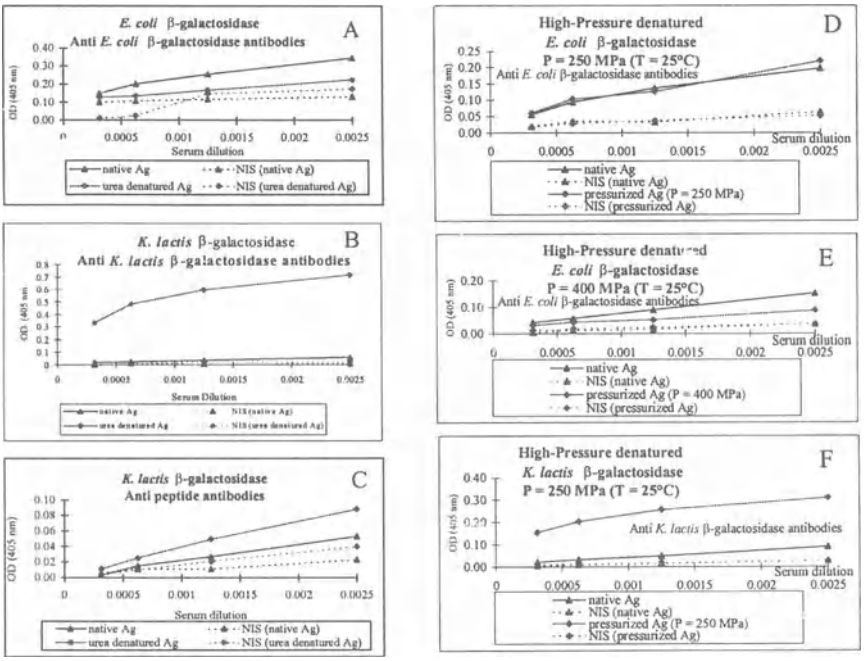

Fig. 1. Effect of urea (*left*) or pressure (*right*) on the reactivity of *E. coli* and *K. lactis* β-galactosidases with related sera. (NIS and Ag stand for non-immune serum and antigen, respectively)

3.2.1 Urea Treatment. The reactivity of anti-*E. coli* β-galactosidase antibodies was seen to decrease following the exposure of the corresponding antigen to 8 M urea. A similar treatment of the *K. lactis* enzyme resulted in an increase of the immunological reaction (Figs. 1A, B). Such a treatment led to an augmentation of the immunological signal obtained when the *K. lactis* enzyme was in contact with antibodies directed against the *E. coli* β-galactosidase active site (Fig. 1C).

3.2.2 Exposure to Pressure. As pressure increased, the reactivity of *E. coli* β-galactosidase with the corresponding antibodies decreased (Figs. 1D & E). This seems to be correlated to the pressure-dissociation of the enzyme into subunits following pressurization. In contrast, an increase in the reactivity of the *K. lactis* enzyme with its related antibodies was observed following the exposure of the antigen to 250 MPa for 1 h. (Fig. 1F)

3.3 Effects of Various Modes of Denaturation on the Reactivity of Antibodies Directed Against the *E. coli* β-Galactosidase Active Site

More interesting were the observations made with the antibodies directed against a peptide correponding to the active site of the *E. coli* enzyme. The reactivity of the antibodies varied with the mode of denaturation of the antigen: urea and pressure led to an increase of the immune response whereas the exposure to high temperature resulted in a decrease of the immunological reactivity (Fig. 2).

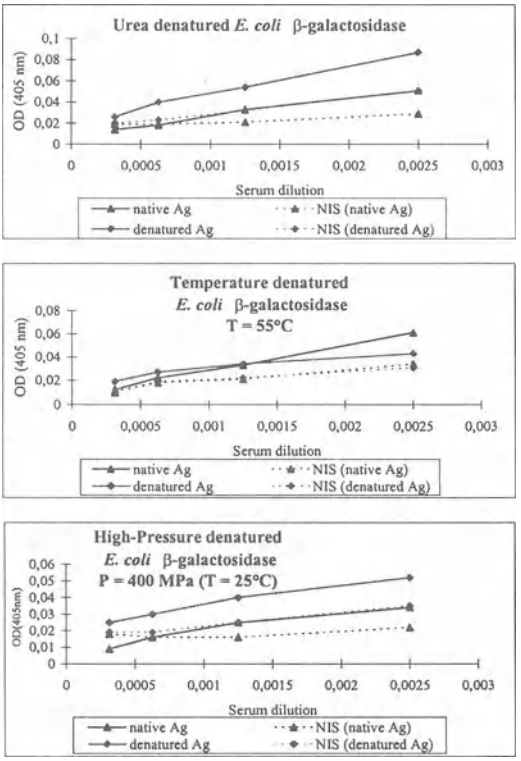

Fig. 2. Influence of the mode of denaturation on the reactivity of *E. coli* β-galactosidase with an antiserum raised against a peptide mimicking the active site of the enzyme

4 Discussion

The reactivity of polyclonal antibodies with their corresponding antigens was shown to depend on the way of denaturation of these later. Comparisons with the modulation of the activity of the model enzymes as a result of physical and chemical treatments as well as preliminary results of electrophoretic *ex situ* analyses of the denatured lactases indicate the usability of the variation of an immunological response as a way to follow protein conformational changes.

Acknowledgements: Part of this work was supported by the CNRS/PIRGP-Bio Program. The expert aid of Honoré Mazarguil and Marc Pawlowski in the design of the peptide and its corresponding antibodies as well as the fine ELISA analyses performed by Françoise Lemay, Stéphane Disselers and Anthony Fonseca are gratefully acknowledged.

References

[1] Degraeve, P., Lemay, P. (1997) *in* High Pressure Research in the Biosciences and Biotechnology, K. Heremans Ed., Leuven University Press, Leuven, Belgium, pp. 115–118.

[2] Athès, V., Degraeve, P., Cavaillé-Lefebvre, D., Espeillac, S., Lemay, P., Combes, D. (1997). *Biotechnol. Letters*, 19, 273–276.

Cold, Heat and Pressure Denaturation of Horse Heart Metmyoglobin: A FTIR Study

F. Meersman, L. Smeller[1] and K. Heremans

Department of Chemistry, Katholieke Universiteit Leuven, B-3001 Leuven, Belgium
Karel.Heremans@fys.kuleuven.ac.be
[1]Institute of Biophysics, Semmelweis University of Medicine, Budapest, Hungary

Abstract. We studied the denaturation of horse heart metmyoglobin in the diamond anvil cell (DAC) with Fourier transform infrared (FTIR) spectroscopy. The courses of both the cold and the pressure denaturation are very similar. This could indicate that the mechanisms of both processes are quite alike. Furthermore, it seems that the denatured state retains a significant amount of secondary structure. Heat denaturation distinguishes itself from the former two processes by the formation of two new bands at 1615 and 1683 cm^{-1}. These two peaks are characteristic for intermolecular β-sheet aggregation. This also explains why a gel can be observed at the end of the experiment. A gel, however, can also be observed in the case of a pressure denaturation. This could point to the existence of different interactions leading to gel formation dependent on the denaturation mechanism.

1 Introduction

Cold, heat and pressure denaturation of proteins has been extensively studied using a variety of methods such as NMR [1], UV spectroscopy [2] and DSC [3]. We studied the denaturation of horse heart metmyoglobin in the diamond anvil cell (DAC) with Fourier transform infrared (FTIR) spectroscopy. FTIR spectroscopy enables us to follow and assess, both qualitatively and quantitatively, the changes in the secondary structure upon denaturation. In combination with the DAC we can investigate the denaturation *in situ* in a broad pressure-temperature range (pressures up to 2 GPa and temperatures between –200 and 100 °C). To our knowledge this is the first report of cold denaturation studied by this technique.

2 Materials & Methods

Horse heart metmyoglobin was purchased from Sigma and used without further purification. The aqueous buffer was 25 mM deuterated acetate buffer, pD 4.

Metmyoglobin was dissolved in the deuterated buffer and the sample was stored overnight to ensure a sufficient H/D-exchange. For the cold denaturation the solution was then pipetted into the well of a stainless steel gasket which was mounted in the DAC (Diacell Products, Leicester, UK). A small amount of $BaSO_4$ was added to determine the pressure, which is obtained from the position of the sulphate peak near 983 cm^{-1} in the deconvoluted spectrum. In the next step the DAC was placed into the cryocell and the pressure was built up by a helium driven membrane up to about 200 MPa. In the final step the temperature was gradually lowered by means of solid carbon dioxide in combination with acetone. In the case of the pressure denaturation, the DAC was also used, but pressure was built up by means of a screw mechanism. For the heat experiment a CaF_2 cell and a Graseby Specac automatic temperature controller were used. The infrared spectra were obtained with a Bruker IFS66 FTIR spectrometer equipped with a liquid nitrogen cooled broad band MCT solid state detector. A total 250 interferograms were coadded after registration at a resolution of 2 cm^{-1}.

3 Discussion

The study of the cold denaturation of proteins in an aqueous solvent is limited by the formation of ice. It has been suggested that the protein might adsorb to the growing ice particles and consequently it might undergo a mechanical denaturation [4]. FTIR spectroscopy, however, shows no spectral changes in the general shape of the amide I' band upon ice formation. What can be observed is a change of background. In order to avoid this possible effect, several experimental setups have been described [5]. In this work we performed a pressure-assisted cold denaturation. The reason for this pressure assistance becomes clear when one takes the phase diagram of water into account [6]. The phase diagram of liquid water has a minimum at about 200 MPa meaning that at that pressure water still remains in the liquid phase up to –20 °C. On top of that we used an acetate buffer to assure a complete denaturation of the metmyoglobin before ice formation. The acetate buffer has the additional advantage that its pD does not change as a function of temperature.

In Fig. 1 the course of the cold denaturation is shown. Comparison of this course with the one of the pressure denaturation shows that both the cold denaturation and the pressure denaturation course are very similar. As a consequence the secondary structures of the denatured states are very much alike. Figure 2 shows the native and the heat denatured state of metmyoglobin. In the denatured state two new absorption bands at 1615 and 1683 cm^{-1} have arisen as the temperature increased. These two bands are characteristic for intermolecular β-sheet aggregation [7]. This aggregation is probably the reason why heat denaturation is irreversible in most cases. This also explains why a gel can be observed at the end of the experiment.

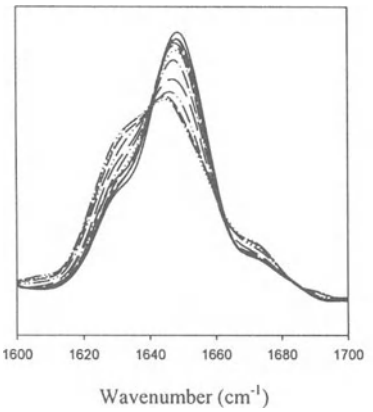

Fig. 1. The course of the cold denaturation of metmyoglobin. Remark the remaining secondary structure in the denatured state

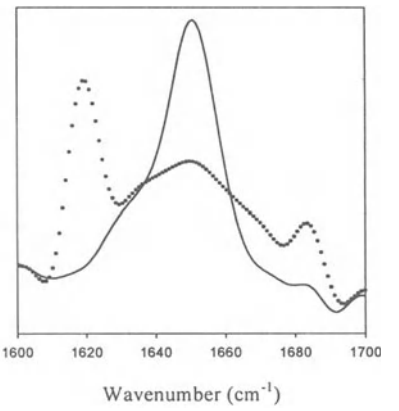

Fig. 2. Heat denaturation of metmyoglobin. Full line: native state, dotted line: denatured state

4 Conclusions

The similarity in the course of pressure and cold denaturation could indicate that the mechanisms of these processes are quite alike. Furthermore, it seems that a significant amount of secondary structure is retained in the denatured state. This is in agreement with the NMR observations on ribonuclease [1] where a partially folded structure is still present in the denatured state. Heat denaturation, on the contrary, distinguishes itself from the former two processes by the formation and increase of two new bands at 1683 and 1615 cm^{-1} as the temperature increases. As pointed out above the formation of a gel can be explained by the presence of these two bands. A gel, however, can also be observed in the case of a pressure denaturation where no such bands can be seen. This could point to the existence of different interactions leading to gel formation dependent on the mechanism of denaturation. These differences between pressure- and heat-induced gels have also been observed by rheological measurements for some proteins [8].

Acknowledgements: This research is supported by grant OT 97/20 from the Katholieke Universiteit Leuven.

References

[1] Zhang, J., Peng, X., Jonas, A. & Jonas, J. (1995), NMR Study of the Cold, Heat, and Pressure Unfolding of Ribonuclease A; Biochemistry, 34, 8631–8641.

[2] Mombelli, E., Afshar, M., Fusi, P., Mariani, M., Tortora, P., Connelly, J.P. & Lange,R. (1997), The role of Phe31 in maintaining the conformational stability of ribonuclease P2 from *Sulfolobus solfactarius* under extreme conditions of temperature and pressure; Biochemistry, 36, 8733–8742.

[3] Privalov, P.L., Griko, Yu.V. & Venyaminov, S.Yu. (1986), Cold denaturation of myoglobin; J. Mol. Biol., 190, 487–498.

[4] Strambini, G.E. & Gabellieri, E. (1996), Proteins in frozen solutions: Evidence of ice-induced partial unfolding; Biophys. J., 70, 971–976.

[5] Franks, F. (1995), Protein destabilization at low temperatures; Adv. Prot. Chem., 46, 105–139.

[6] Bridgman, P.W. (1935), J. Chem. Phys., 3, 597-605.

[7] Ismail, A.A., Mantsch, H.H. & Wong, P.T.T. (1992), Aggregation of chymotrypsinogen: portrait by infrared spectroscopy; Biochim. Biophys. Acta, 1121, 183–188.

[8] Heremans, K., Van Camp, J. & Huyghebaert, A. (1997), High pressure effects on proteins, in Food Proteins and Their Applications (Eds. Damodaran, S. & Paraf, A.), 473–502.

Hydrogen-Deuterium Exchange Versus Conformational Changes in Proteins. A Two-Dimensional FTIR Approach

L. Smeller and K. Heremans[1]

Institute of Biophysics, Semmelweis University of Medicine, Budapest, Puskin u. 9. PO Box 263, H-1444 Hungary
Smeller@puskin.sote.hu
[1]Department of Chemistry, Katholieke Universiteit Leuven, Celestijnenlaan 200D Leuven, B-3001 Belgium
Karel.Heremans@fys.kuleuven.ac.be

Abstract. Since infrared spectroscopy when applied to proteins must be performed in D_2O, the pressure induced conformational changes and hydrogen-deuterium exchanges are not easy to separate. We demonstrate that the application of two-dimensional spectroscopy makes it possible to separate these effects, and the sequence of the spectral alterations responsible for the exchange and deformation of the protein backbone can also be determined. The method is applied to the bovine pancreatic trypsin inhibitor (BPTI) where only slight deformations of the protein secondary structure take place in the range of 0–1 GPa, without the complete unfolding of the molecule.

1 Introduction

Infrared spectroscopy is used in high pressure protein research for the study of changes in the protein secondary structure [1]. The structural information can be obtained using the amide I region of the spectrum (1700–1600 cm^{-1}). In order to avoid the overlap with the strong water band at 1640 cm^{-1}, these experiments have to be performed in D_2O. However, the simultaneous occurrence of hydrogen-deuterium (H/D) exchange and conformational alterations introduce uncertainties. Since the conformational changes and the H/D exchange are not independent, the complete separation of these effects is impossible.

The use of the recently developed 2D Fourier transform infrared (FTIR) spectroscopy can improve the quality and amount of the information obtained about the spectral changes, and makes it therefore also possible to separate the above mentioned effects.

The two-dimensional (2D) infrared analysis was originally proposed by Noda [2]. The method was initially developed to study behaviour of polymers exposed to periodic elastic perturbation, but later the method was generalized for any kind of

nonperiodic perturbations [3]. It was used for the study of the temperature-induced dissociation of hydrogen-bonded *N*-methylacetamide [4] and for pH-induced changes in hydroxyapatites [5]. Changes in the structure of β-lactoglobulin were studied by varying the concentration of bromoethanol [6]. The kinetics of the H/D exchange were also investigated by using the new possibilities provided by the 2D visualization of the spectra [7]. In this paper, for the first time, *high pressure* is used as a perturbation method in 2D FTIR spectroscopy.

The application of the 2D analysis has the advantage of spreading the spectral peaks over the second dimension. As a result the visualization is simplified, the resolution is enhanced and the sequence of different phenomena can be determined.

2 Materials & Methods

BPTI was purchased from Sigma. It was dissolved in Tris/DCl buffer pD 8.6 at a concentration of 100 mg/ml and left overnight at room temperature to facilitate H/D exchange of the fast exchangeable protons. High pressure (0–1 GPa) was generated by a diamond anvil cell (Diacell Products, UK). Pressure was measured using $BaSO_4$ as internal calibrant [8]. FTIR spectra were measured with a Bruker IFS66 FTIR spectrometer. Sixteen successive spectra recorded at increasing pressures were used for the calculation of 2D spectra. They were calculated using a program developed in our laboratory according to the definitions of Noda [2, 3].

3 Results & Discussion

BPTI was selected for this study, because its unusually high pressure stability has been demonstrated earlier [9]. This allows us to use a quite wide pressure range to study the relation of the H/D exchange and elastic effects on the protein [10].

Figure 1 shows the correlation region ot the amide I and amide II spectral ranges of the infrared spectra during the initial pressurizing to 0.3 GPa. According to the standard representation of the 2D spectra suggested by Noda [2], the gray surfaces represent the negative area, the white parts show the area where the 2D spectrum is positive. The so-called synchronous part of the spectrum can be seen in Fig. 1a. The following bands give remarkable cross peaks on the synchronous plot: 1645 and 1630 cm^{-1} in the amide I region, 1540 and 1500 cm^{-1} in the amide II, 1460 and 1425 cm^{-1} in the amide II' region of the deuterated protein. All of these bands seem to change with a positive correlation, except the 1540 cm^{-1} one, which changes to the opposite direction.

The analysis of the asynchronous spectrum (Fig. 1b) makes it possible to determine the sequence of the changes of the above mentioned bands during the pressurization from atmospheric to 0.3 GPa pressure. A detailed examination of the asynchronous spectrum shows that the first changes take place in the amide I band

(1645cm^{-1}) which are followed by changes of several peaks in the amide II and amide II' bands (peaks at 1540, 1500 cm^{-1} and 1460, 1425 cm^{-1}, respectively). The last peak to change is again in the amide I region (1630 cm^{-1}). The amide I spectral changes indicate alterations in the conformation of the protein, the amide II and amide II' regions reflect the H/D exchange. We can conclude from the above sequence that the first effect of pressure is the increase in the unordered structure content in the protein, which makes the increased H/D exchange possible. The exchange is followed by further structural changes, which are observed in the infrared spectrum as the increase of the 1630 cm^{-1} band, characteristic for the β-structure.

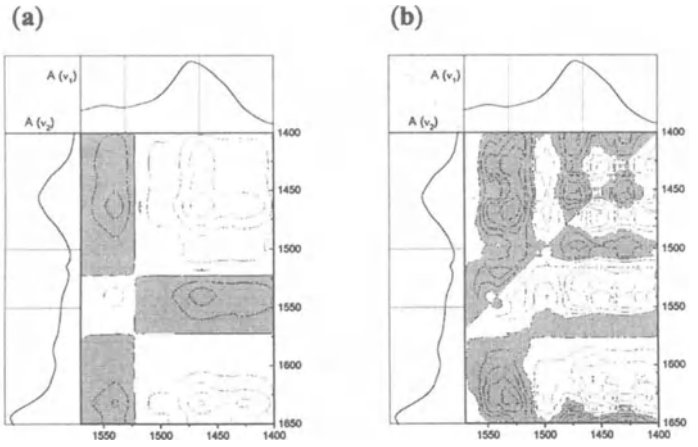

Fig. 1. 2D spectra of the bovine pancreatic trypsin inhibitor (BPTI) during the pressurising from atmospheric to 0.3 GPa pressure. (a) synchronous spectrum, (b) asynchronous spectrum. The gray area indicates that the corresponding values are negative

After reaching 0.4 GPa, the pressure was released, in order to further separate the elastic deformational effects of the protein from the exchange. A second pressurizing cycle was then performed. The 2D spectra during the second cycle were similar to the first one except for the less pronounced initial changes in the protein secondary structures (data not shown). This result indicates that the rate of exchange is not only enhanced by the pressure induced unfolding of the protein structure, but that pressure can also have a direct effect on the exchange process. A negative activation volume has indeed been observed for the uncatalyzed hydrogen exchange reaction between *N*-methylacetamide and water [11].

Since the protein does not denature in the 0–1 GPa pressure range, we could increase the pressure, up to 0.9 GPa, to introduce more elastic distortions in the protein without causing drastic conformational changes. The synchronous spectrum (data not shown) is dominated by a strong autocorrelation peak in the amide I band (at 1625 cm^{-1}) characteristic for the β-structure. This change is correlated with the amide II' band peaks (1470 and 1420 cm^{-1}). The cross correlation between the amide II and II' peaks indicates that the exchange is not

significant. In the higher pressure region, the major spectral changes in the spectrum can therefore be attributed to conformational changes in the protein.

4 Conclusions

We applied 2D correlation spectroscopy to analyze pressure-induced changes of proteins. It is shown that 2D spectroscopy makes it possible to separate the spectral features arising from H/D exchange and conformational changes. The asynchronous spectrum allows one to determine the sequence of the changes during the pressurisation. The present approach is now being extended to the comparative study of temperature- and pressure-induced changes in proteins and other biological macromolecules.

Applying the technique to BPTI, two regions could be distinguished; in the low pressure region (0–0.3 GPa) both conformational and exchange effects take place, while above 0.5 GPa (up to 0.9 GPa) the exchange is completed, and one can only observe conformational changes of the protein backbone.

Acknowledgements: This work was partially supported by FWO Flanders (Belgium). L. S. thanks the Hungarian Academy of Science for travel grant.

References

[1] Heremans, K., Goossens, K., Smeller, L. (1996); in: High-Pressure Effects in Molecular Biophysics and Enzymology. Eds: Markley, J.L., Northrop, D.B., Royer, C.A. pp. 44-61. Oxford University Press NY, Oxford.
[2] Noda I. (1990); Appl. Spectrosc., 44, 550.
[3] Noda, I. (1993); Appl. Spectrosc., 47, 1329.
[4] Liu, Y., Ozaki, Y., and Noda, I., (1996); J. Phys. Chem., 100, 7326.
[5] Gadaleta, S.J., Gericke, A., Boskey, A.L., and Mendelsohn, R., (1996); Biospectroscopy, 2, 353.
[6] Sefara, N.L., Magtoto, N.P, and Richardson, H. (1997); Appl. Spectrosc., 51, 563.
[7] Nabet, A., and Pezolet, M., (1997); Appl. Spectrosc., 51, 466.
[8] Wong, P.T.T., and Moffat, D.J., (1989); Appl. Spectrosc, 43, 1279.
[9] Goossens, K., Smeller, L., Heremans, K. (1996); Eur. J. Biochem., 236, 254.
[10] Heremans, K., and Smeller, L. (1998); Biochim. Biophys Acta, 1386, 353.
[11] Mabry, S.A., Lee, B.S., Zheng, T., and Jonas, J. (1996); J. Am. Chem. Soc., 118, 8887.

Pressure and Temperature Stability of β-Galactosidases: A Structural and Functional Study

P. Rubens[1], P. Degraeve, P. Lemay and K. Heremans[1]

INSA, Centre de BioIngénierie Gilbert Durand, CNRS UMR 5504, LA INRA, Toulouse, France
[1]Department of Chemistry, Katholieke Universiteit Leuven, Leuven, Belgium
Karel.Heremans@fys.kuleuven.ac.be

1 Introduction

There is a growing interest in exploiting the catalytic power of enzymes to produce fine chemicals. However, proteins are only stable under restricted physical and chemical conditions. High hydrostatic pressure and temperature have, for example, been shown to induce the denaturation of proteins. Both these parameters exert antagonistic effects on the weak interactions maintaining the three-dimensional structure of proteins (hydrogen bonds, ionic and hydrophobic interactions). As a consequence, their stability is affected in a different way by pressure and temperature. When plotted in a pressure-temperature plane, the structural stability diagram of many proteins has been shown to present an elliptical outline.

It has recently been reported that many enzymes are stabilized against thermal inactivation by pressures ranging from 1 to 4 kbar [1–6]. However, this protective effect is not general [1, 7, 8]. This difference of behaviour might be related to the difference of position of the elliptical outline of the structural stability domain of these proteins in a pressure-temperature plane. In previous studies [5, 6], a marked protective effect of pressures comprised between 0.5 kbar and 3 kbar against the thermal inactivation of the *E. coli* and *A. oryzae* β-galactosidases was observed. The present work combines the use of infrared spectroscopy and enzyme activity to check whether this functional stabilization is correlated with a structural stabilization of these proteins.

2 Materials & Methods

Pressure inactivation experiments: Pressurization protocols are described in detail in [6]. Purified *A. oryzae* and *E. coli* β-galactosidase preparations respectively diluted to 0.2 mg ml^{-1} and 0.25 mg ml^{-1} in 1 mM $MgCl_2$, Tris-HCl, 50 mM pH 7.5 buffer were incubated for 30 min in the thermostated high pressure vessel. After pressure release and/or after cooling, 0.5 ml of 0.013 M *p*-nitrophenyl-galactopyranoside in Tris-HCl 50 mM, pH 7.5 buffer and 0.5 ml of a β-galactosidase solution were mixed and held at 28 °C. The initial velocity was

determined by recording the absorbance at 420 nm for 2 min. The irreversibility of deactivation during the storage time periods after both temperature and pressure treatment was ascertained.

FTIR spectroscopy measurements: The proteins were dissolved in 1 mM $MgCl_2$, Tris/DCl buffer pD 7.5 at a concentration of about 100 mg ml^{-1} and left overnight at room temperature to facilitate hydrogen-deuterium exchange. The solution was mounted in the stainless steel gasket of a thermostated diamond anvil cell obtained from Diacell Products (Leicester, UK). The initial gasket thickness was 0.05 mm and the hole diameter 0.6 mm. Pressure was obtained from the sulfate stretching mode of $BaSO_4$ at 983 cm^{-1} [9]. Infrared spectra were obtained with the use of a Bruker IFS66 FTIR spectrometer equipped with a liquid-nitrogen-cooled mercury-cadmium-telluride detector. The temperature was linearly increased at a rate of 0.2 °C min^{-1} while recording 250 interferograms per 1 °C change in temperature. This avoided differences in the transition pressure or temperature from one experiment to another, since the conformational changes observed here are time dependent.

3 Results

In order to provide some insight into the mechanisms protecting β-galactosidase against thermal inactivation at 2.5 kbar, the conformational changes occurring during thermal denaturation of the two proteins have been followed by FTIR spectroscopy at different pressure values. Pressure was first increased up to the desired non-denaturing value at 25 °C in the diamond anvil cell. Temperature was then linearly increased. This increase of temperature led to a concomitant increase of pressure resulting from thermal expansion of the pressurized solution and dilatation of the gasket and the elements constituting the diamond anvil cell.

The backbone amide protons involved in α-helices and β-sheets in native proteins are strongly protected against exchange with solvent deuterons [10]. Therefore, the native proteins are only partially deuterated after one night of incubation. Under conditions favoring the denatured state, the dominant mechanism of exchange involves global unfolding. The conversion of NH groups (band at about 1550 cm^{-1} in the amide II mode) to ND moieties induces a lowering of the frequency by approximately 100 cm^{-1}. A convenient empirical parameter reflecting H-D exchange is thus to monitor the difference between the absorbances at 1450 and 1550 cm^{-1}.

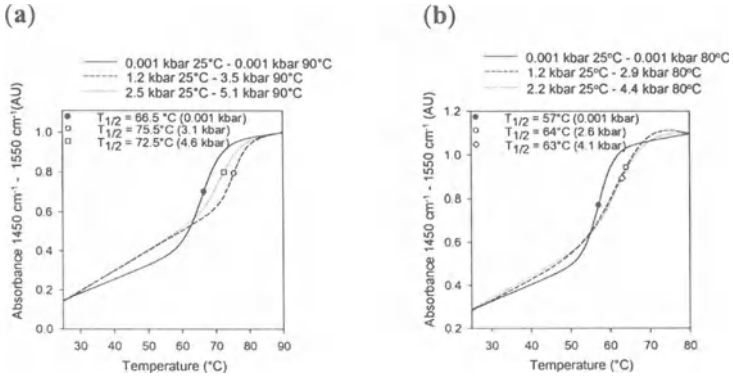

Fig. 1. Influence of pressure on H-D exchange as a function of temperature. Plots of the differences between the absorbances at 1450 and 1550 cm^{-1} of the self-deconvoluted spectra of the (**a**) *A. oryzae* and (**b**) *E. coli* β-galactosidases for different pressures as a function of temperature upon increasing temperature from 25 °C to 90 °C and 80 °C respectively

The observation that a dramatic increase of H-D exchange rate occurred in the same temperature range as the conformational changes observed in the amide I' vibrational mode (data not shown) for both proteins indicates that the rate of H-D exchange is closely related to the state of denaturation. For both proteins, when thermal denaturation was conducted at 2–3 kbar, the temperature at which the H-D exchange rate was dramatically accelerated shifted to higher temperatures (Fig. 1).

Table 1. Influence of pressure on the thermal inactivation and the temperature of H-D exchange acceleration followed by FTIR spectroscopy of *A. oryzae* and *E. coli* β-galactosidases temperature

A. oryzae β-galactosidase				*E. coli* β-galactosidase			
Pressure (kbar)	$T_{1/2}$* (°C)	Pressure (kbar)	T** (°C)	Pressure (kbar)	$T_{1/2}$* (°C)	Pressure (kbar)	T** (°C)
0.001	56.5	0.001	55	0.001	49.3	0.001	49
2.5	63	2.85	65	2.5	52.3	2.3	52
4	54	4.3	60	4	-	4.1	51

(*) $T_{½}$ is the temperature for which a 50% irreversible activity loss was observed following 30 min incubation at the pressure indicated.

(-) 30 min incubation under 4 kbar always led to an irreversible activity loss superior to 50% whatever the temperature of incubation was.

(**) T is the temperature above which the acceleration of H-D exchange was observed by FTIR spectroscopy at the indicated pressure.

Whereas the FTIR spectroscopy measurements were carried out *in situ* and the enzymatic activity measurements were performed after 30 min, incubation being thus affected by the kinetics of denaturation of the protein on one hand and the kinetics of irreversible inactivation on the other hand, the correlation between the temperature at which the dramatic acceleration of H-D exchange rate begins and the functional stability is quite good for both proteins studied (Table 1).

4 Conclusions

- ⇨ Enzyme inactivation and beginning of denaturation of the protein, as observed from infrared spectra, are concomitant phenomena.
- ⇨ The protective effects of pressure against thermal denaturation and inactivation both appeared to be maximal in the 2–3 kbar pressure range for the two proteins. The marked functional stabilization observed might then be attributed to a stabilization of the native conformation of the protein.
- ⇨ Considering H-D exchange acceleration as an empirical criterion, FTIR spectroscopy might constitute an interesting tool for the determination of the stability domain of proteins. This might be of great interest since pressure stabilization of enzymes against thermal denaturation might be used to carry out reactions at higher temperatures.

Acknowledgements: P. D. is grateful to COST-D6 Action for the financial support during his stay in the Department of Chemistry of the Katholieke Universiteit Leuven.

References

[1] Hei, D.J. & Clark, D.S. (1994) Appl. Environ. Microbiol., 60, 932–939.
[2] Mozhaev, V.V., Lange, R., Kudryashova, E.V. & Balny, C. (1996) Biotechnol. Bioeng., 52, 320–331.
[3] Bec, N., Villa, A., Tortora, P., Mozhaev, V.V., Balny, C. & Lange, R. (1996) Biotechnol. Letters, 18, 483–488.
[4] Weingand-Ziadé, A., Renault, F. & Masson, P. (1997) Biochim. Biophys. Acta, 1340, 245–252.
[5] Athès, V., Degraeve, P., Cavaillé-Lefebvre, D., Espeillac, S., Lemay, P. & Combes, D. (1997) Biotechnol. Letters, 19, 273–276.
[6] Degraeve, P. & Lemay, P. (1997) Enzyme Microb. Technol., 20, 550–557.
[7] Konisky, J., Michels, P.C. & Clark, D.S. (1995) Appl. Environ. Microbiol., 61, 2762–2764.
[8] Rubens, P., Goossens, K., Heremans, K., Weemaes, C., Hendrickx, M. & Tobback, P. (1997) High Pressure Research in the Biosciences and Biotechnology, K. Heremans (Ed.), Leuven University Press, Leuven, Belgium.
[9] Wong, P.T.T. & Moffat, D.J. (1989) Appl. Spectrosc., 43, 1279–1281.
[10] Robertson, A.D., Purisima, E.O., Eastman, M.A. & Scheraga, H.A. (1989) Biochemistry, 28, 5930–5938.

Conformational Changes of Lipoxygenase at Elevated Pressure and Temperature

P. Rubens[1], N. Bec[2], R. Lange[2], C. Balny[2], J. Frank[3] and K. Heremans[1]

[1]Department of Chemistry, Katholieke Universiteit Leuven, Leuven, Belgium
[2]INSERM U128, Montpellier Cedex 1, France
[3]Kluyver Instituut voor Biotechnologie, Technische Universiteit Delft, Delft, The Netherlands
Karel.Heremans@fys.kuleuven.ac.be

Abstract. The effect of high pressure and temperature on soybean lipoxygenase has been investigated previously using infrared spectroscopy. At high pressure or temperature, denaturation of the protein takes place, leading to cooperative changes in the infrared spectrum. Minor changes were observed at lower pressures and temperatures. The aim of this study was to characterize these changes by using fluorescence and UV absorbance techniques. The results of the present study indicate that increasing pressure induces significant conformational changes in lipoxygenase well before cooperative unfolding takes place as observed by infrared spectroscopy at 7 kbar.

1 Introduction

It has been shown that proteins are only marginally stable structures. Application of high pressure and temperature can change the three dimensional structure involving changes in activity and properties of the protein [1]. Changes in secondary structure were followed by Fourier transformed infrared (FTIR) spectroscopy. Application of high pressure had a different influence on protein conformation than high temperature [2]. The former gave a broad band at high pressures with a maximum around 1645 cm^{-1}. This can be interpreted as an increased amount of unordered structure. The latter induced a broad band at 1645 cm^{-1}, accompanied by two sidebands at 1618 and 1685 cm^{-1}. These side bands are characteristic for the formation of intermolecular hydrogen bonds [3, 4].

A more detailed examination of the pressure induced changes showed that before the major transition, smaller conformational changes occured. The aim of this study was to characterize these changes at intermediate pressures.

2 Materials & Methods

Highly purified lipoxygenase from soybean was dissolved in a 10 mM Tris buffer at a concentration of 1 mg/ml. ANS was purchased from Molecular Probe Co.

Fluorescence measurements. All fluorescence measurements were carried out with an Aminco Bowman series 2 fluorospectrophotometer (SLM Co.) which had been modified in the INSERM laboratory to measure fluorescence in a pressure range from 1 bar to 7 kbar. Fluorescence of trypsin was quantified by specifying the center of spectral mass (CSM). The excitation wavelength was 295 nm which only excites selectively the tryptophan residues.

Absorption measurements. Absorption was measured using a spectrophotometer Cary 3E (Varian) which had been modified to measure absorption under pressure from 1 bar to 4.5 kbar. The position of the fourth derivative absorption bands was then used to evaluate the polarity of the tyrosine and tryptophan environments.

For both techniques, a high pressure cell was built into a stainless steel thermostated jacket. Optical windows of the cell were made of synthetic sapphire from RSA Le Rubis (Jarrie, France). The reaction mixture was filled into a 2 ml quartz cuvette closed at the top by a flexible membrane. Distilled water was used as a pressure vector. Pressure was generated by a manually driven pump and controlled by a strain gauge.

3 Results

Fluorescence spectra of lipoxygenase at increasing pressure show a decrease in intensity of the emission band at 325 nm. This decrease in intensity is accompanied

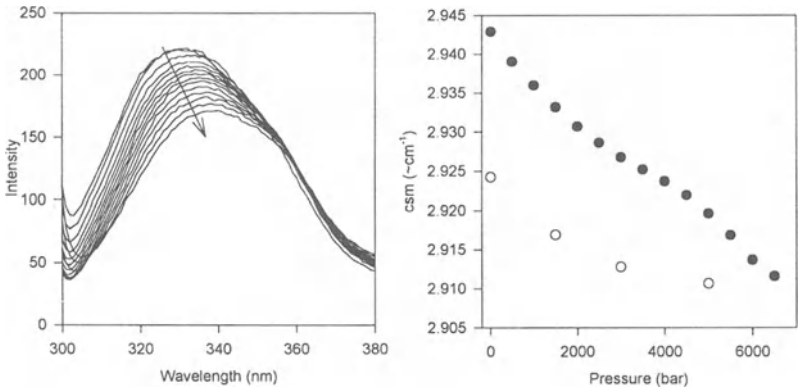

Fig. 1. Fluorescence spectra of lipoxygenase of soybean at 25 °C. 1 mg/ml in 10 mM Tris buffer. The arrow on the left indicates spectral changes at increasing pressure. Closed circles in the right plot show the shift of CSM at increasing pressures. Open circles show changes at decreasing pressure

by a shift to longer wavelengths (Fig. 1). These findings can be interpreted as a transition of the tryptophans to a more polar environment. In addition, at high pressures one also observes a narrowing of the 325 nm band.

Similar changes are found with increasing temperature. Small changes at 50 °C precede the main transition. This is in good agreement with the results obtained by infrared spectroscopy.

Aggregate formation was followed by analyzing the scattering of the excitation band at 295 nm. Remarkably, aggregation results from both high pressure and high temperature treatments.

Pressure/fluorescence experiments were performed at 5 °C, 25 °C and 40 °C up to 6.5 kbar. The changes in the fluorescence spectra are more important at 25 °C. At all three temperatures, aggregation was observed at high pressure. In the presence of ANS elevated pressures lead to an increase in the fluorescence intensity at 480 nm, indicating that at high pressure the hydrophobic sites become more accessible for ANS (Fig. 2). Moreover, ANS seems to inhibit aggregate formation which might indicate that aggregates, formed under high pressure, are caused by hydrophobic interactions. This is different for temperature induced aggregation were aggregates are formed by intermolecular hydrogen bondings [3].

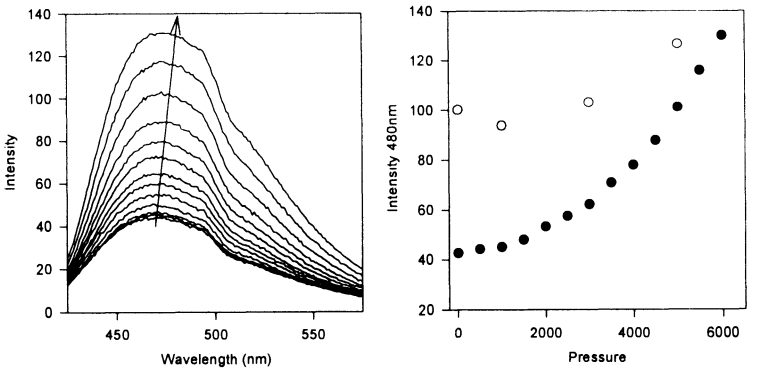

Fig. 2. Fluorescence spectra of ANS in presence of lipoxygenase at 25°C. Protein solution is 1 mg/ml in 10 mM Tris buffer. The arrow indicates changes at increasing pressure. Closed circles show intensity changes at increasing pressure. Open circles show changes at decreasing pressure

The 4th derivative UV absorption spectrum (spectra not shown) reveals gradual changes when pressure is increased up to 4 kbar. Due to the limited size of these changes, they are associated with physicochemical changes of the solution rather than conformational changes of the protein. Above 4 kbar the absorbance increases rapidly due to aggregate formation.

When the temperature is decreased to −15 °C (at 2 kbar to prevent ice formation) only very small changes in the UV spectrum and fluorescence spectrum are observed, suggesting that no important conformational transitions occur at lower temperatures. It would be interesting to see whether these results can be

correlated with the inactivation data observed from lipoxygenase of green beans [5].

4 Conclusions

Although infrared spectroscopy revealed major conformational changes at 6.6 kbar (at room temperature) and at 70 °C (at atmospheric pressure), it is shown by fluorescence and absorption measurements that smaller conformational changes occur before the main transitions.

>pressure scans at 5, 25 and 40 °C followed by fluorescence revealed gradual changes in the spectra and formation of aggregates between 4 and 5 kbar.

>temperature scans at 2 kbar at lower temperatures (–20 °C), followed by fluorescence and UV absorption, showed no significant changes in the spectrum.

>ANS inhibits the formation of pressure induced aggregation.

Acknowledgements: This research was supported in part by an INSERM/MVG travel grant and European grant FAIR CT 96-1175.

References

[1] Mozhaev, V.V., Heremans, K., Frank, J., Masson, P. & Balny, C. (1996); High pressure effects on protein structure and function; Proteins: Structure, Function and genetics 24, 81–91.

[2] Heinish, O., Kowalski, E., Goossens, K., Frank, J., Heremans, K., Ludwig, H. & Tausher, B. (1995); Pressure effects on the stability of lipoxygenase: Fourier transform infrared spectroscopy (FTIR) and enzyme activity studies; Z. Lebensm. Unters. Forsch. 201, 562–565.

[3] Ismail, A.A., Mantsch, H.H. & Wong, P.T.T. (1992); Aggregation of chymotrypsinogen: portrait by infrared spectroscopy; Biochim. Biophys. Acta 1121, 183–188.

[4] Rubens, P., Frank, J. & Heremans, K. (1998); Hydrogen-deuterium exchange of lipoxygenase at high pressure and temperature; these proceedings.

[5] Indrawati, I. (1998); Pressure stability of lipoxygenase from green beans (Phaesolus vulgaris L.) at subzero and elevated temperatures; these proceedings.

Hydrogen-Deuterium Exchange of Lipoxygenase at High Pressure and Temperature

P. Rubens[1], J. Frank[2] and K. Heremans[1]

[1]Department of Chemistry, Katholieke Universiteit Leuven, B-3001 Leuven, Belgium
[2]Kluyverlaboratorium for Biotechnology, Delft University of Technology,
2628 BC Delft, The Netherlands
Karel.Heremans@fys.kuleuven.ac.be

Abstract. One of the most characteristic properties of proteins is the elliptical outline in the stability diagram. Hereby, it is not only possible to denature the protein by application of high temperature but also by using high pressure or a combination of both. The elliptical outline of the phase diagram can be found by following either the rate of inactivation of the protein under different conditions or by plotting the transition pressure and temperatures of denaturation. In this study, we followed the rate of hydrogen- deuterium exchange in lipoxygenase. The aim was to establish a correlation in the phase diagram with previous measurements based on inactivation and denaturation. It is shown that by following kinetic parameters, one can estimate the stability of the protein under different conditions.

1 Introduction

Protein stability is one of the main topics for many research groups. After decades of investigations on the influence of temperature and solvent conditions, it has become clear that pressure also can play an important role on the protein stability. Screening protein stability under different physical conditions can be of interest in industrial application where food is treated under high pressure.

After Bridgman showed in 1914 that it was possible to denature proteins of egg white [2], pressure has gained the interest of many researchers. It was shown that proteins denature under high pressure but in a different way than at high temperature. Moreover, combinations of temperature and pressure revealed a typical behaviour of proteins in a phase diagram. The outline of the stability diagram was mentioned by Suzuki *et al.* [1, 3]. It was found that in some cases, low pressure can stabilize proteins against temperature denaturation while application of low temperatures can increase the pressure stability. Hawley described in 1971 a theoretical model which permits a fit to the pressure-temperature transition surface. It was shown that the surface can be fit to a

relatively simple equation of state which elicits approximately elliptical contours of constant free energy difference on the pressure-temperature plane [4, 5].

Lipoxygenases catalyze the formation of fatty acid hydroperoxides, products used in further biochemical reactions leading to normal and pathological cell functions [6]. The stability against pressure and temperature denaturation have been investigated previously [7, 8]. It was shown that protein denaturation was different in both cases. The major difference was the formation of intermolecular hydrogen bonds at high temperature. In recent work, Ludikhuyze [9] reported results of activity measurements at different pressures and temperatures. Temperatures up to 35 °C stabilized the protein against pressure denaturation. On the other hand, low pressures did not stabilize the protein against temperature denaturation. In this study, we will try to find a correlation between the inactivation data and the stability diagram that can be found when following the kinetics of hydrogen-deuterium exchange by using FTIR. Therefore, a thermostated diamond anvil cell (DAC) was used which allows measurements over a broad temperature (–20 °C – 90 °C) and pressure (1 bar – 30 kbar) range.

2 Materials & Methods

We used highly purified lipoxygenase from soybean that was dissolved in a 10 mM Tris-DCl buffer at pD=8.6 at a concentration of 100 mg/ml. The sample was stored overnight to ensure that exchange of the accessible protons had reached a static regime. The sample was mounted in the stainless steel gasket of a thermostated diamond anvil cell obtained from Diacell Products (Leicester, UK). The initial gasket thickness was 0.05 mm and the hole diameter 0.6 mm. The cell was placed in a Bruker IFS66 infrared spectrometer equipped with a liquid-nitrogen-cooled MCT detector. The sample compartment was continuously purged with dry air in order to avoid interference of atmospheric vapour. $BaSO_4$ was added to determine the pressure. The time for each measurement started when the thermostated sample was brought to the appropriate pressure.

3 Results

The rate of hydrogen-deuterium exchange of the interior labile protons on the amide groups is dramatically increased by external pressure and is closely associated with the global conformational structure of the protein. Figure 1 shows a stack plot of the infrared spectra of lipoxygenase at 25 °C and 5.9 kbar as a function of time. The band at ~1550 cm^{-1} is due to the amide II mode which is a mixed vibration involving N-H in plane bending and the C-N stretching. This band shifts to ~1455 cm^{-1} as a result of deuteration of labile protons on the amide

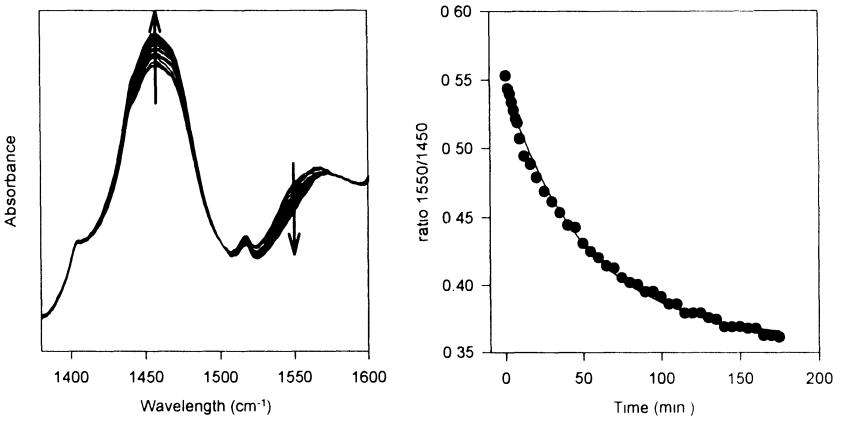

Fig. 1. Stack plot of the infrared spectra of lipoxygenase at 25 °C and 5.9 kbar as a function of time. The changes at 1450 and 1550 cm^{-1}, indicating the H-D exchange, are plotted as a function of time

group. By using a deuterated buffer, we were able to follow in situ the rate of exchange of the hydrogen atoms buried in the protein interior against deuterium atoms of the solvent. The ratio of intensities at 1550 and 1450 cm^{-1} was plotted as a function of time. For each experiment, the exchange rate was followed during 3 h. This resulted in an exponential decrease of the H-D ratio in the protein. First order kinetics were assumed and rate constants of the exchange processes were determined. This was done for a wide range of temperatures and pressures. Iso-rate

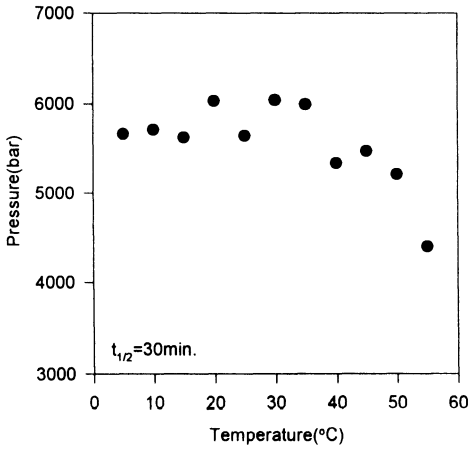

Fig. 2. Influence of pressure and temperature on H-D exchange of lipoxygenase. Half life time of 30 min for H-D exchange was plotted at different conditions

constant lines were plotted in a p,T-diagram (Fig. 2). For temperatures up to 35 °C, a small stabilizing effect can be observed. Higher temperatures destabilize the protein and thereby accelerate the exchange process. These results are in good agreement with previously performed inactivation experiments [9].

4 Conclusions

It is shown that the iso-rate constant line that is obtained by following the exchange rate in a protein under different conditions presents the same outline as those from an inactivation experiment. The combination of FTIR with a thermostated DAC has the major advantage that it allows in situ observation of the sample at different physical conditions.

Acknowledgements: This research is supported by European grant FAIR CT 96-1175.

References

[1] K. Heremans and L. Smeller, (1998); Protein structure and dynamics at high pressure; Biochim. Biophys. Acta., 1386, 353–370.
[2] Bridgman, P.W. (1914); The coagulation of albumen by pressure; J. Biol. Chem., 19, 511–512.
[3] Suzuki, K. (1960); Studies on the kinetics of protein denaturation under high pressure; Rev. Phys. Chem. Jpn, 29, 49–55.
[4] Hei, D.J. & Clark, D.S. (1994); Pressure stabilization of proteins from extreme thermophiles; Appl. Env.Micr., 60, 932–939.
[5] Hawley, S.A., (1971); Reversible pressure-temperature denaturation of chymotrypsinogen; Biochemistry, 13, 2436–2442.
[6] Gaffney, B.J. (1996); Lipoxygenases: Structural principles and spectroscopy; Annu. Rev. Biophys. Biomol. Struct., 25, 431–459.
[7] Heinish, O., Kowalski, E., Goossens, K., Frank, J., Heremans, K., Ludwig, H. & Tausher, B. (1995); Pressure effects on the stability of lipoxygenase: Fourier transform infrared spectroscopy (FTIR) and enzyme activity studies; Z. Lebensm. Unters. Forsch., 201, 562–565.
[8] Mozhaev, V.V., Heremans, K., Frank, J., Masson, P. & Balny, C. (1996); High pressure effects on protein structure and function; Proteins, 24, 81–91.
[9] Ludikhuyze, L., PhD thesis Leuven, High pressure technology in food processing and preservation: a kinetic case study on the combined effect of pressure and temperature on enzymes.

High Hydrostatic Pressure Effect on Activity of Circulating Immune Complex Formation in Blood Serum

N.V. Shishkova, L.I. Donchenko[1], B.I. Barbashova and E.V. Ulyanova

Donetsk Physics & Technology Institute of National Ukrainian Academy of Sciences,
72, R.Luxemburg St., 340114 Donetsk, Ukraine
[1]Donetsk Institute of Traumatology & Orthopedics, Donetsk State Medicine University
Phone: +380-(622)-557462, Fax: +380 (622)-557462
shishkov@host.dipt.donetsk.ua; shishkov@kinetic.ac.donetsk.ua

Abstract. High hydrostatic pressure effect on peculiarities of the immune complex formation process in a blood serum obtained from patients with a mechanical trauma is discussed. It is shown that activity of complex formation has been determined by applied pressure level and physico-chemical properties of biological fluids. Peculiarities of changes taking place in studied objects after high pressure action were studied with the help of the precipitation reaction method, ^{1}H NMR spectroscopy and by determination of pH-solution. It has been found that the higher activity serum reaction takes place in the pressure range about 150 MPa.

1 Introduction

Pressure has become an important and interesting parameter to understand structure, phase behaviour and dynamics of processes in biological systems. In addition, the studies connected with such biological fluids as human blood and its constituents, plasma and serum, are especially actual. These investigations allow an understanding of the new aspects of pathogenesis of diseases connected with autoimmune processes in an organism. The important problem of scientific and applied character is a study of serum reactions. In this respect the demonstrative model is a process of circulating immune complex (CIC) formation. Interaction of antigen- antibody (AG-AB) develops in vivo and in vitro depending on such physico-chemical properties of antigens as particle size, physical state, number of valency as well as on class and species of antibodies and experimental conditions: consistency of medium, pH, salt concentrations, temperature. For the last year the significant effect of high pressure on AG-AB interaction, also the forces included in AG-AB interaction, have shown a sensibility to the pressure [1–4].

In this work the results of study of high hydrostatic pressure (HHP) effects on antigen-antibody formation reaction (immune complexes) in blood serum with

different initial pH, obtained from invalids with a mechanical trauma of motofacient organs at the critical period of disease, are discussed.

2 Materials & Methods

The blood sera were obtained from peripheral blood directly before experiments by centrifugation. The serum pH was various (8.1...8.5) depending on individual peculiarities of homeostasis.

All biological fluids were subjected to pressures of 150 and 500 MPa at room temperature, at constant rate of loading and exposure for 10 min (see Table 1). The assays were packed in shell envelopes before high pressure treatment and placed inside a high pressure vessel of 20 mm diameter.

The study of changes in biological assays induced by pressure were carried out both by diagnostic test-detection of the CIC and physicochemical methods: ^{1}H NMR spectroscopy and pH-solution determination for initial state and after pressure treatment.

The used antigen-specific method for the detection of the CIC in the studied assays was based on polyethyleneglycol precipitation in polymerization buffer followed by photometry of precipitate density at 450 nm [5, 6].

An experimental installation used for NMR studies is a broad-band ^{1}H NMR spectrometer. The permanent magnet provides a field strength of 4600 Oe with a nonuniformity of about $2 \cdot 10^{-6}$ Oe/cm, the resonance frequency is 19.5 MHz. The described spectrometer is designed to record the absorption signals. The derivative of NMR-adsorption spectrum is monitored and the width of spectrum line ΔH determined (Fig. 1) [6, 7].

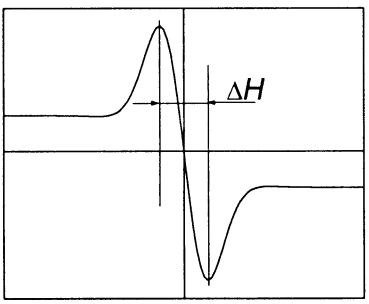

Fig. 1. NMR adsorption spectrum derivative (schematically): ΔH-the line width

3 Results & Discussion

The obtained experimental results (see Tables 1 and 2) indicate that the HHP has rendered significant effects on the properties of the biological fluids under investigation.

The increase of precipitate density values (activation of serum reaction) is observed for all pressurized samples in comparison with the initial state (Table 1). However, the level of such an increase depended on the applied high pressure level. It was revealed that pressure action at 150 MPa leads to a 2–5 times increase of serum optical density depending on the condition of metabolic processes in human organism. At a pressure of 500 MPa the density of precipitate in serum was lower than after pressure treatment at 150 MPa, but 1.5...2 times higher than in initial state.

Table 1. Precipitate density values (I, arb.unit) in the studied biofluids depending on hydrostatic pressure level

Assays	I, 10^{-3}		
	0.1 MPa	150 MPa	500 MPa
Serum N1	130	250	180
Serum N2	20	115	30
Serum N3	50	170	100

In Table 2 the values of ^{1}H NMR spectrum line widths (ΔH) for the studied assays are presented. The width of spectrum line ΔH characterizes the hydrogen mobility in the biosystem. As we can see from Table 2, the HHP application to biological fluids is accompanied by the ΔH increasing for all investigated samples. The wider line corresponds to lower mobility of hydrogen atom, and, consequently, the hydrogen bonds in the system are stronger. The appearance of a new more narrow line (see the point marked by * in Table 2) indicates that the hydrogen occupies two nonequivalent positions in the studied system, i.e. new bonds are formed. All these processes can attest to formation of macromolecular complexes of antigen-antibody.

Table 2. Changes of the line width of NMR spectra (ΔH) for different sera depending on hydrostatic pressure level

Assays	$\Delta H \cdot 10^{-2}$,Oe		
	0.1 MPa	150 MPa	500 MPa
Serum N1	1.59	5.7 (*1.27)	4.1
Serum N2	1.27	3.18	3.0
Serum N3	2.54	3.18	3.18

The results of the pH determination of studied fluids have shown some dependence of pH on pressure treatment as well. In pressurized samples we have observed the decrease of pH-index and stronger pH changes (ΔpH from 0.4 to 1.0) have taken place in the range of 150 MPa as well.

4 Conclusions

Thus, at all the investigated pressures we have observed the increasing of the activity of CIC reaction in blood serum that was caused, apparently, by formation processes of new antigen-antibody complexes from proteins of various natures contained in serum. The dynamics of these processes were determined by the HHP level. The higher activity of CIC process formation in our experiments was observed at the pressure about 150 MPa.

The different characters of high hydrostatic pressure effect on studied biofluids were caused by different biochemical processes which are responsible for the formation process of new AG-AB complexes.

References

[1] Mozhaev, V.V., Heremans, K., Frank, J, Masson P. & Balny, C. (1994), Trends Biotechnol. 12, 493.

[2] Balny, C. Progress in biotechnology «High pressure bioscience and biotechnology», R.Hayashi & C.Balny (Eds). Elsever (1996), p. 7.

[3] Degraeve, D. & Lemay, P. High pressure research in the biosciences and biotechnology, K. Heremans (Ed). Leuven University Press, Leuven, Belgium. (1997), p. 115.

[4] Olson, W.S., Leung, S.K.& Yarmush, M. L. (1989); Bio/Technology, 7, 369.

[5] Osipov, S.G., Eremeev, V.V., Rudenko, V.I. & Titov, V.N. (1983); Methods for detection of circulating immune complexes (review of literature); Laboratornoye delo V.11, Moscow, Medicina, 3, (rus).

[6] Shishkova, N.V., Donchenko, L.I, Barbashov, V.I. & Ulyanova E.V. (1998); High pressure physics and techniques, N4 (in press), (rus).

[7] Slonim, I.Y. & Lyubimov A.N. Nuclear Magnetic Resonance for Polymers. M.: Chemistry, (1966), p. 339.

Pressure Effect on the Temperature Unfolding and Gelation of Myoglobin

L. Smeller, P. Rubens[1] and K. Heremans[1]

Institute of Biophysics, Semmelweis University of Medicine,
Budapest, Puskin u. 9. PO Box 263, 1444 Hungary
[1]Department of Chemistry, Katholieke Universiteit Leuven,
Celestijnenlaan 200D Leuven, B-3001 Belgium

Abstract. Horse heart myoglobin was pressure unfolded at different temperatures. The spectrum shows specific bands characteristic for a gel stabilised by a network of intermolecular hydrogen bonds. This gel is usually found for temperature denaturation at ambient pressure. However, we found a similar network appearing after the pressure treatment already at 45 °C. This network could be partially disrupted by slight pressurisation. The protein that was pressure unfolded at room temperature did not show side bands, but when it was heated after the pressure treatment, it started to form a gel at a significantly lower temperature compared to the non-pressure treated sample.

1 Introduction

It has been known for a long time that proteins can be denatured either by temperature or by high pressure [1]. However, the difference between the pressure and the heat induced gel of denatured proteins has not yet been completely clarified. A consistent thermodynamic description of the protein unfolding is given by the so called elliptic phase diagram [2–4]. The differences found recently by Fourier transformed infrared (FTIR) spectroscopy between the secondary structure of pressure and heat denatured proteins could not be explained within this equilibrium theory [5]. In the present study we investigated the combined effect of pressure and temperature, by studying the effect of pressure on the formation of the temperature gel.

2 Materials & Methods

Myoglobin from horse heart was purchased from Sigma and was dissolved in 10 mM Tris buffer at pD=7.6 using a protein concentration of 75 mg/ml. The solution was left overnight at room temperature to allow the hydrogen/deuterium exchange of the amide group protons. The spectra were recorded by a Bruker

IFS66 FTIR spectrometer. Spectral resolution enhancement was applied to emphasise the spectral features of the overlapping amide I band. The details of this procedure are given elsewhere [6]. The resolution enhancement factor reached was 1.5. Pressure was generated by a diamond anvil cell (DAC) (Diacell Products, UK) and the temperature was measured by a thermocouple.

3 Results & Discussion

Figure 1 shows the amide I region of the infrared spectra of horse heart myoglobin recorded at 45 °C. The sample was first pressurised to 10 kbar which resulted in a broad featureless band indicating the loss of the secondary structure of the molecule. The release of the pressure did not lead to the refolding of the protein. Specific side bands of the main amide band did develop in the infrared spectrum of the depressurised protein, with a characteristic time of ca. 30 min. These side bands appearing at 1616 and 1685 cm^{-1} were observed earlier in the case of heat denatured proteins under ambient pressure conditions. They were assigned to the

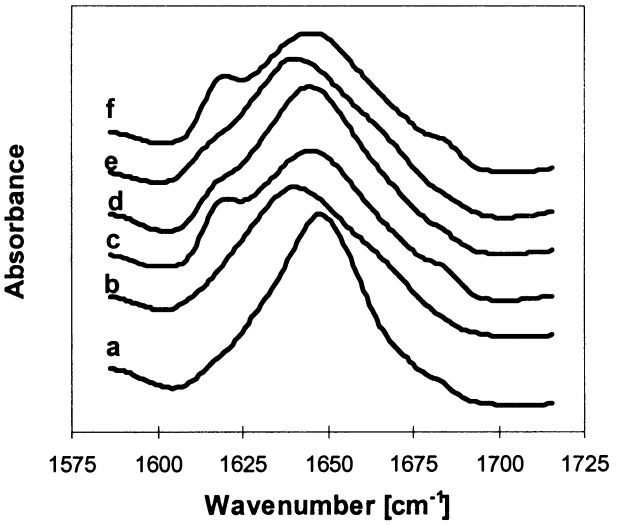

Fig. 1. Amide I region of the infrared spectra of horse heart myoglobin recorded at 45 °C. a: ambient pressure; b: 10 kbar; c: released to <0.5 kbar; d: repressurised to 2 kbar; e: further pressurised to 10 kbar; f: released to <0.5 kbar

intermolecular antiparallel beta structure [7], which stabilises the heat induced gel, preventing the protein from refolding. In this case however the bands were observed below the heat-denaturation temperature. The intermolecular hydrogen bonds appeared here after the pressure denaturation. The only explanation is that in the pressure unfolded protein the intramolecular hydrogen bonds were broken, and this allowed the formation of the intermolecular bonds. It must be noted, however,

that this gel did not form in the pressure measurements at room temperature which explains the fact why this phenomenon was not discovered earlier.

In the second pressurising cycle, moderate pressure did partially suppress the side bands. This suggests that the network formation has at least two steps, and the first step(s) can be reversed by the pressure. Pressures of typically 2 kbar could suppress the side bands, and no further significant suppression was achieved by further pressurisation to 10 kbar. After the pressure release the side bands appeared again with the same intensity as before.

The experiment was repeated at 60 °C, with very similar results, only the amplitudes of the side bands were different.

At 90 °C a special experiment was carried out in order to avoid the heat induced gelation during the heating of the sample to 90 °C. Therefore the sample was pressurised to 10 kbar at 30 °C and the pressure unfolded sample was heated to 90 °C. No side bands were observed. The side bands appeared after the pressure release (still at 90 °C). Repeated pressurisation of the sample led to the partial disappearance of the specific side bands like in the 45 °C and 60 °C experiments. The intensity of the side bands was increased after releasing the pressure. The bands remained unchanged when the sample was cooled to room temperature.

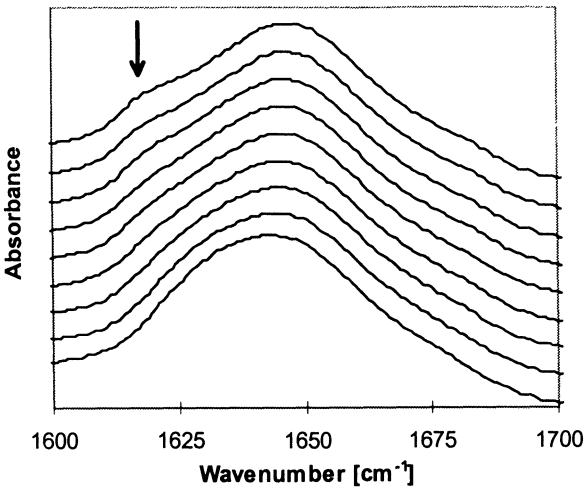

Fig. 2. Infrared spectra recorded during the heat denaturation of the horse heart myoglobin after a pressure treatment at 5 °C. The temperatures are from bottom to top: 5, 23, 32, 37, 40, 44, 48, 57, 67 °C. The arrow shows the developing side band at 1615 cm^{-1}

As already mentioned, no side bands were detected when the protein was pressure unfolded at room temperature or at lower temperatures. It was however observed that the pressure denatured protein formed a gel, similar to the heat denatured one but at significantly lower temperature. Figure 2 shows the spectra recorded during the heat denaturation of the horse heart myoglobin after a pressure treatment at 5 °C. The specific side bands of the amide I region appeared at 38 °C

after the pressure denaturation of the protein at 5 °C. The denaturation temperature for the non-pressure treated protein is 74 °C.

The above experimental results can be explained by assuming that the formation of the intermolecular hydrogen bond network needs an unfolded protein and a certain temperature. The results indicate that the formation of the structure stabilised by intermolecular antiparallel hydrogen bonds is also disfavoured by the pressure. In the case of the usual heat denaturation, the unfolding is immediately followed by the gel formation, while in the case of pressure unfolding at room temperature, the formation of the hydrogen bonds is probably too slow to be observed. The fact that the unfolded protein forms a intermolecular network already at 38 °C, suggests that the native structure of the protein is metastable above this temperature. The decrease of the side band amplitudes under the pressure shows that the aggregation process has several steps and that the loosely bounded aggregate can be disaggregated, while at the end of this process a stable, pressure insensitive gel form appears.

4 Conclusions

It was shown that the pressure unfolded horse heart myoglobin forms a gel structure which is similar to that which is found earlier in the heat treatment, if the pressure treatment was performed at 45 °C or at higher temperatures. The pressure sensitivity of the first steps of this gel formation suggests that the gelation process has several steps. Another finding that the pressure treatment at room (or lower) temperature results in a significantly decreased gelation temperature (from 74 to 38 °C) has a special interest in the case of food application. The results suggest that pressure treatment followed by a moderate heating can result in a similar gel to the high temperature treatment. The advantage of the lower temperature applied is obvious from the point of view of energy saving and also in better conservation of vitamins and other essential food components.

Acknowledgements: L.S. and K.H. thank HAS and FWO Flanders for support.

References

[1] Bridgman, P.W. (1914); J. Biol. Chem., 19, 511–512.
[2] Hawley, S.A. (1971); Biochemistry, 10, 2436–2442.
[3] Suzuki, K. (1960); Rev. Phys. Chem. Japan, 29, 91–98.
[4] Smeller, L. and Heremans, K. (1997); in: High Pressure Research in Bioscience and Biotechnology, K. Heremans (Ed), Leuven University Press, pp. 55–58.
[5] Heremans, K. and Smeller, L.(1998); Biochim. Biophys. Acta, 1386, 353–370.
[6] Smeller, L. *et al.* (1995); Applied Spectrosc., 49, 1538–1542.
[7] Clark, A.H., Saundson, D.H. and Suggett, A. (1981); Int. J. Pept. Protein Res., 17, 353 364.

The Influence of High Pressure Treatment on the Spectroscopic Properties of Ovalbumin

D.D.S. Smith[1], V.B. Galazka[2] and I.G. Sumner[1]

[1]Institute of Food Research, Earley Gate, Whiteknights Road, Reading RG6 6BZ, UK
[2]Department of Food Science and Technology, University of Reading, Whiteknights, Reading RG6 6AP, UK
drummond.smith@bbsrc.ac.uk

Abstract. Ovalbumin is the major protein found in egg white and is used extensively in the food industry. We have investigated the effect of high pressure processing on the properties of ovalbumin. High pressure treatment causes some change in the far UV circular dichroism spectrum of the protein, however pressure does not cause extensive denaturation of ovalbumin. After pressure treatment the intensity of the ovalbumin fluorescence spectrum is reduced with no change in the wavelength of maximum emission. Pressure treatment also causes an increase in binding of the probe molecule ANS to ovalbumin. These results indicate that pressure treatment causes formation of a molten globule form of ovalbumin.

1 Introduction

Ovalbumin is the major protein found in egg white and has found use in the food industry because of its foaming ability and the formation of gels on heating. The folding of ovalbumin following chemical and heat denaturation and from low pH has been studied extensively. There has been much less work addressing the response of the protein to high pressure [1, 2]. Folding studies [3, 4] have shown that an intermediate on the ovalbumin folding pathway can be trapped as a low pH molten globule. We focus here on the effect of pressure treatment of the protein on the absorption and fluorescence properties of the protein.

2 Materials & Methods

Ovalbumin was subjected to high pressure treatment at pH 6.5 for 10 min at the pressures indicated in figure legends prior to spectroscopic measurements. Intrinsic fluorescence spectra were measured using an excitation wavelength of 280 nm and ANS probe fluorimetry using an excitation wavelength of 350 nm.

3 Results

3.1 Circular Dichroism Spectroscopy

The effect of pressure treatment on the secondary structure of ovalbumin was investigated by CD spectroscopy (Fig. 1).

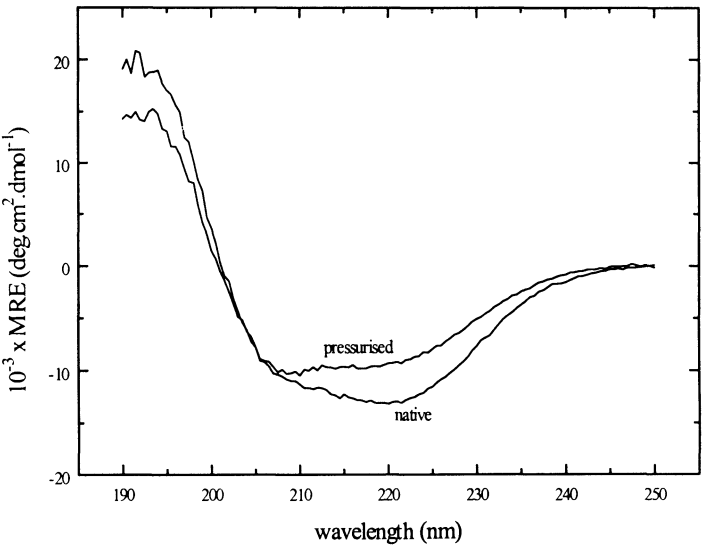

Fig. 1. Far UV circular dichroism spectroscopy of native ovalbumin and of protein after treatment at 800 MPa

Pressure treatment causes some loss of ellipticity in the 220 nm region of the spectrum indicating some change in secondary structure. It is nonetheless clear from these spectra that the secondary structural change caused by pressure treatment is limited and it does not cause extensive protein denaturation.

3.2 Fluorescence Spectroscopy

The environment of aromatic, primarily tryptophan, residues in proteins can be investigated by measuring the intrinsic fluorescence spectrum of the protein. The effect of pressure treatment on the fluorescence emission spectrum of ovalbumin was investigated (Fig. 2). The intensity of the protein fluorescence was found to diminish on pressure treatment, however there was no change in the wavelength of maximum emission. This contrasts with the results of chemical denaturation of the protein in which the fluorescence intensity and the fluorescence wavelength are changed. The lack of any change in λ_{max} on pressure treatment indicates that aromatic residues do not become fully exposed to solvent.

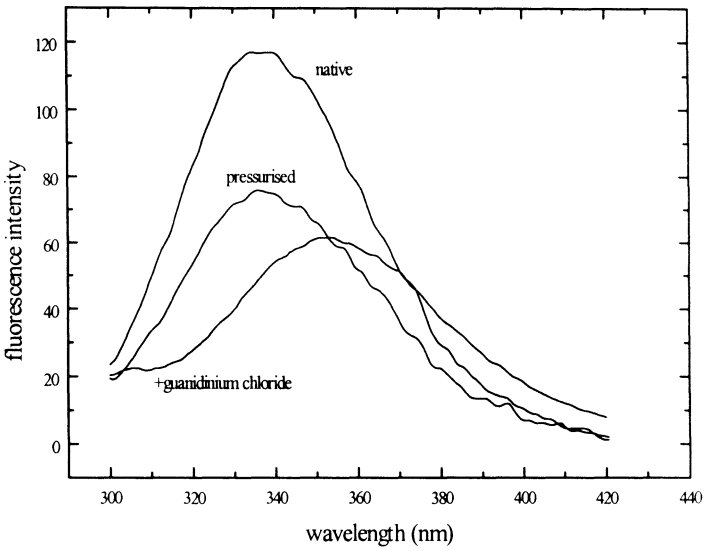

Fig. 2. Fluorescence spectroscopy of native ovalbumin and of protein after pressure treatment at 800 MPa and after chemical denaturation

At low pH a molten globule form of ovalbumin has been observed which may also be an intermediate in the folding pathway of this protein [3, 4]. In order to investigate the possible formation of an ovalbumin molten globule induced by pressure treatment at near neutral pH the binding of the probe molecule ANS was compared for native and for pressure treated protein (Fig. 3). ANS binds to pressure treated ovalbumin as indicated by the increased intensity of the fluorescence spectrum.

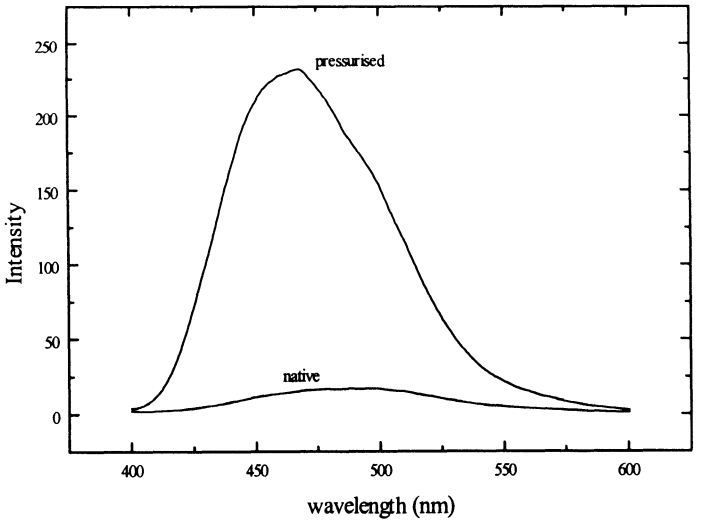

Fig. 3. Fluorescence spectroscopy of ANS in the presence of native ovalbumin or ovalbumin pressurised at 800 MPa

4 Conclusions

The decreased intensity of the protein intrinsic fluorescence after pressure treatment, accompanied by increased binding of ANS, suggests that the hydrophobic core of the protein is more solvent accessible after pressure treatment, but not fully solvent exposed. CD spectra indicate only limited change in secondary structure. These characteristics suggest that pressure may cause the formation of a molten globule form of ovalbumin.

Acknowledgements: This work was supported by the BBSRC of the UK.

References

[1] Hayakawa, I., Kajihara, J., Morikawa, K., Oda, M. & Fujio, Y. (1992) J. Food Sci., 57, 288–292.
[2] Hayakawa, I., Linko,Y. & Linko, P. (1996) Lebensm.-Wiss. u.-Technol., 29, 756–762.
[3] Tatsumi, E. & Hirose, M. (1997) J. Biochem., 122, 300–308.
[4] Onda, M., Tatsumi, E., Takahashi, N. & Hirose, M. (1997) J. Biol. Chem., 272, 3973–3979.

Contribution of Hydrophobic Residues to the Stability of Ribonuclease A Chain Folding Initiation Site Mutants. A Comparison of Pressure and Temperature Induced Unfolding

J. Torrent[1], J.P. Connelly[2], M.G. Coll[1], M. Ribó[1], R. Lange[2] and M. Vilanova[1]

[1]University of Girona, Faculty of Sciences, Department of Biology, Protein Engineering Laboratory. Campus de Montilivi, E-17071 Girona, Spain
dbjtm@fc.udg.es
[2]INSERM U128, IFR 24, 1919 Route de Mende, F-34293 Montpellier, France

Abstract. A set of ribonuclease A (RNase A) variants has been constructed within a postulated chain folding initiation site (CFIS) extending from residue 106 to 118 (of 124), in order to study the contributions of the hydrophobic residues to the stability of the protein. The free energy of unfolding of wild-type and mutants has been measured following the pressure and temperature induced equilibrium unfolding by fourth derivative absorption spectroscopy. The results obtained lay the foundations for future kinetic and structural studies of the CFIS and reinforce the potential of pressure as a denaturating agent for characterizing amino acid replacements.

1 Introduction

There is evidence that one of the primary initiation sites for the folding of RNase A is located in the hydrophobic hairpin-like structure consisting of residues 106–118 [1]. We have characterized pressure and thermally induced unfolding of RNase A and a series of mutants in which the degree of hydrophobicity of this CFIS has been changed. In order to minimize structural rearrangements, the mutations involved a reduction side-chain volume leaving a nominal cavity but avoiding steric effects. The only exception was the Ile→Leu mutation. In addition, replacement of Tyr 115 by Trp has been tested for its potential as a minimally destabilizing fluorescence probe local to the CFIS.

2 Materials & Methods

Bovine pancreatic ribonuclease A (type I-A, Sigma) was further purified as previously described [2]. The gene coding for RNase A [3] was used as a template for the mutagenesis by PCR following the method of Juncosa *et al.* [4]. Mutant and

wild-type genes were expressed in *E. coli* strain BL21(DE3) using the T7 expression system and the encoded proteins were purified as described in [5], with some modifications. By this means, the following mutant proteins were prepared, I106A/L/V, I107A/L/V, V108A/G, A109G, Y115W, V116A/G, V118A/G. Absorption spectra between 250 and 310 nm were recorded as a function of temperature at room pressure and under pressures up to 450 MPa at 40 °C, all at pH 5.0, using a modified absorption spectrometer and the methodology described elsewhere [6]. Fluorescence measurements of Y115W were made using a modified Aminco-Bowmann SLM spectrofluorimeter.

3 Results

Typical 4th derivative spectra following the effect of pressure and temperature are shown in Fig. 1 (a and b, respectively). Unfolding transitions are calculated by integrating 4th derivative difference spectra between 275 and 290 nm, resulting in an improvement in signal to noise ratio.

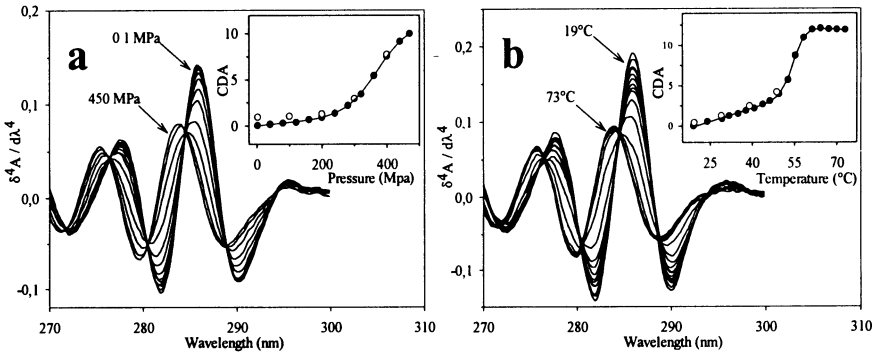

Fig. 1. (**a**) 4th derivative UV spectra of V116A as a function of pressure between room pressure and 450 MPa. (**b**) 4th derivative UV spectra of V116A as a function of temperature between 19 °C and 73 °C. The insets show the pressure (T=40 °C) (**a**) and temperature (p=1 MPa) (**b**) unfolding curves for V116A at pH 5.0. (CDA – cumulative difference amplitude absorbance)

The 4th derivative spectral progressions with pressure and temperature for all RNase A mutants show an isosbestic point. The corresponding CDA transitions are sigmoidal, preceded and followed by near linear curves. Unfolding transition curves were fitted to a two state thermodynamic model combined with sloping linear functions for the native and denatured states as described in [6]. The fitted parameters for pressure and temperature induced unfolding transitions are listed in Table 1. All unfolding transitions were observed to be reversible.

In the case of Y115W mutant, fluorescence as well as 4th derivative absorption was measured. The parameters obtained by fitting the fluorescence data were not significantly different from those of absorption, as can be seen in Table 1.

Table 1. Changes in stability between wild-type RNase A and the variants calculated at 40 °C, room pressure and pH 5.0

	Pressure denaturation			Thermal denaturation		
	ΔG (KJ/mol)	$P_{1/2}$ (MPa)	$\Delta\Delta G$ (KJ/mol)	ΔG (KJ/mol)	$T_{1/2}$ (°K)	$\Delta\Delta G$ (KJ/mol)
WT com	23.24	499.46		24.39	332.09	
WT rec	24.66	529.25		23.56	331.11	
Y115W abs	18.08	419.49	6.58	12.03	327.82	11.53
Y115W fl	19.66	413.03	5.00	13.67	328.57	8.89
I106A	2.62	41.50	22.04	2.72	316.36	20.84
I106L	12.14	278.06	12.52	12.76	324.87	10.80
I106V	17.42	329.80	7.24	12.42	327.15	11.14
I107A	13.36	217.20	11.3	8.67	321.24	14.89
I107L	12.66	247.85	12.00	11.79	322.55	11.77
I107V	23.75	520.26	0.91	21.62	331.63	1.94
V108A	3.13	56.06	21.53	3.54	316.56	20.02
V108G	-	-	-	–9.20	302.99	32.76
A109G	23.69	446.06	0.97	19.08	328.46	4.48
V116A	20.04	373.88	4.62	18.32	328.03	5.48
V116G	19.16	320.40	5.50	9.74	325.53	13.82
V118A	16.25	317.38	8.41	8.67	323.83	14.89
V118G	11.90	216.17	12.76	5.44	319.39	18.12

Changes in free energy of unfolding together with the $T_{1/2}$ or $P_{1/2}$ (Table 1) give a consistent idea of the relative stabilities both among the mutant sites and also amongst different mutants at the same site. I107V, A109G and Y115W are only slightly destabilized. The I106 mutants are less stable than their I107 analogues. Of the Val mutants the V108 mutants are the most unstable with V118 slightly less stable than V116. Generally, within each series, the stability follows the order I>V>L>A>G although the relative stabilities within each series varies a little.

4 Discussion

The 4th derivative absorption spectrum represents the average over six tirosines in a mixture of conformations with different Pro isomers. Local information is provided by fluorescence changes. Since the Y115W amino acid replacement does not substantially perturb the stability, this suggests that it can serve as a reporter group for the Pro 114 isomerization kinetics and for local effects in the CFIS.

The energetics of the hydrophobic interactions are found to be quite variable and context-dependent. In a similar manner to other studies [7–9], statistical

correlations were sought between the values of $\Delta\Delta G$ and various parameters, which are indicators of the environment surrounding a residue. Other significant correlations were found between $\Delta\Delta G$ and 1) the hydrophobicity changes, expected for each substitution made, based on free energies of transfer from n-octanol to water [7] and 2) the change in the volume occupied by residues in the protein interior [10]. These correlations underline the importance of the region to the hydrophobic stability of the protein and reinforce its presumed crucial role in directing the folding process. Having determined the critical residues we have the foundations for future kinetic and structural studies of the CFIS using the local probe provided by the mutation Y115W.

Acknowledgements: The authors thank COST (JT collaboration costs) and acknowledge grants PB96-1172-CO2-02 from DGES, MEC, Spain, ACI-96-49 and ACI-97–20 from CIRIT, Generalitat de Catalunya, and "Fundació M. F. de Roviralta" (Spain) for equipment purchasing grants. Also, JT acknowledges a short-term fellowship from CIRIT and JPC thanks INSERM for a Post Verte fellowship.

References

[1] Matheson, R.R. & Scheraga, H.A. (1978) Macromolecules, 11, 819–829.
[2] Alonso, J., Nogués, M.V. & Cuchillo, C.M. (1986) Arch. Biochem. Biophys., 246, 681–689.
[3] delCardayré, S.B., Ribó, M., Yokel, E.M., Quirk, D.J., Ruter, W.J. & Raines, R.T. (1995) Prot. Engineering, 8, 261–273.
[4] Juncosa-Ginesta, M., Pons, J., Planas, A. & Querol, E. (1994) Biothecniques, 16, 820–824.
[5] Kim, J.S., Soucek, J., Matousek, J. & Raines, R.T. (1995) J. Biol. Chem:, 270, 10525–10530.
[6] Lange, R., Frank, J., Saldana, J.L. & Balny, C. (1996) Europ. Biophys. J., 24, 284–292.
[7] Pace, C. N. (1992) J. Mol. Biol. 226, 29–35.
[8] Serrano, L., Kellis, J.T., Jr., Cann, P., Matouscheck, A. & Fersht, A.R. (1992) J. Mol. Biol., 224, 783–804.
[9] Jackson, S.E., Moracci, M., elMasry, N., Johnson, C.M. & Fersht, A.R. (1993) Biochemistry, 32, 11259–11269.
[10] Harpaz, Y., Gerstein, M., & Clothia, C. (1994) Structure, 2, 641–649.

Pressure Effect on Hydration of Biomolecules

T. Ooi

Kyoto University, Institute for Chemical Research, Uji 611, Japan
Phone & Fax: +81-(0)774-32-5158 (home)
ooi@kuicr.kyoto-u.ac.jp

Abstract. A protein molecule in aqueous solution usually unfolds under pressures of approximately a few hundred MPa as shown experimentally. The denaturation may be described in terms of thermodynamic quantities, Gibbs free energy, enthalpy, entropy as functions of temperature and pressure. The process of unfolding taking hydration into account is described as transfer of a native molecule to the gas phase, unfolding of the molecule, and transfer of the unfolded molecule into aqueous solution. The factor favorable for folding is the chain enthalpy originating from interatomic interactions, while the chain entropy and the difference in hydration upon unfolding are favorable factors for unfolding. Since the quantities associated with the chain are independent of pressure, the change in hydration is the major factor for unfolding under pressure.

1 Introduction

A protein molecule in aqueous solution usually unfolds under a pressure of approximately a few hundreds MPa as shown experimentally. The pressure denaturation, however, has not been well understood in detail; for instance, most of the experiments reported on pressure denaturation have been done on irreversible denaturaton of protein molecules, i. e., application of high pressure on a protein solution gives rise to inactivation of active enzymes. In view of the history, to understand heat denaturation of protein molecules, the process of reversible unfolding of a protein chain caused by raising temperature is the heat denaturation, this was pointed out first in the article entitled "unboiling an egg" published in 1940. The molecular process of pressure denaturation may be very similar to the heat denaturation, that is, "unpressuring an egg" would be possible. Here, we will examine what is the major factor for the pressure denaturation.

2 Methods

Reversible folding and unfolding of a protein molecule in aqueous solution may be described in terms of thermodynamic quantities; molar Gibbs free energy ($G(p,$

T)), enthalpy ($H(p, T)$), entropy ($S(p, T)$) as functions of temperature and pressure. The unfolding quantities are expressed as a difference from the native state (N) to denatured state (D);

$$\Delta G^{u}(p, T) = G_{D}(p, T) - G_{N}(p, T) = \Delta H^{u}(p, T) - T\Delta S^{u}(p, T) . \quad (1)$$

The process of unfolding taking hydration into account is described [1, 2] as follows; 1. Transfer of a folded native molecule in aqueous solution to the gas phase accompanied by dehydration about the molecule. 2. Unfolding of the molecule in the gas phase with a loss in interatomic interactions and an increase in entropy about the chain ($\Delta G^{u}_{c}(p, T)$). 3. Transfer of the unfolded molecule into aqueous environment with the creation of hydration layers around the unfolded molecule.

$$\Delta G^{u}(p, T) = \Delta G^{u}_{c}(p, T) + \Delta G^{u}_{h}(p, T) , \quad (2)$$

where $\Delta G^{u}_{h}(p, T)$ is the molar free energy difference caused by steps (1) and (2), or the difference in hydration between the native and denatured state. The dependence of $\Delta G^{u}(p, T)$ on variables, p and T, is expressed as a change from the standard state, p_0 and T_0, as follows;

$$\begin{aligned}\Delta G = {} & \Delta G^{u}(p, T) - \Delta G^{u}(p_0, T_0) = \Delta C_p^{u}(T - T_0 + T\ln(T/T_0)) + \Delta V^{u}(p - p_0) \\ & + \Delta S^{u}(p_0, T_0)(T - T_0) - (\kappa^{u}/2)(p - p_0)^2 + \alpha^{u}(p - p_0)(T - T_0) ,\end{aligned} \quad (3)$$

where ΔC_p^{u}, ΔV^{u}, κ^{u}, and α^{u} are changes in molar heat capacity, molar volume, molar isothermal compressibility, and molar thermal expansion from the native state to denatured state, respectively.

3 Results & Discussion

The factor favorable for folding is the chain enthalpy originating from mutual atomic interactions among constituent atomic groups ($\Delta H^{u}_{c}(p, T)$) in the molecule, while factors favorable for unfolding are chain entropy originating from random conformations in the unfolded state ($\Delta S^{u}_{c}(p, T)$), and differences in hydration between the folded and unfolded states ($\Delta G^{u}_{h}(p, T)$). In these factors, chain enthalpy and entropy are associated with the character of the protein molecule which is determined by its amino acid sequence, and these are independent of environmental conditions. Thus, the contributions from the chain quantities to the unfolding free energy are the chain entropy term, $T\Delta S^{u}_{c}$, for temperature, and the virial term for pressure, $p\Delta V^{u}$, both being favorable for unfolding. That is, chain entropy increases and molar volume decreases upon unfolding in the gas phase.

The hydration in the folded and unfolded states changes depending on environmental conditions, and this factor is very critical for the stability of the molecule. The physicochemical quantities of hydration about biomolecules, such as, hydration free energy, enthalpy, and heat capacity, are useful for

characterization of hydration layers around the biomolecules [2]. The hydration free energy upon denaturation, for instance, may be calculated as the change in accessible surface area of a protein molecule in the folded and unfolded states. Since the molecule in the unfolded state has more contact area with surrounding water than in the native folded state, interactions from water molecules to the protein chain become greater in the denatured state, while some structural changes occur in the hydration layer with the loss in the free energy.

The quantitative evaluation of ΔG^{u}_{c} and ΔG^{u}_{h} for globular proteins, whose three dimensional structures are known, shows that the values are approximately linear to the number of constituent atoms, N, at 25 °C [2]:

$$\Delta G^{u}_{c}\,(\text{kcal/mol}) = 9.8 + 0.2803N \tag{4}$$

$$\Delta G^{u}_{h}\,(\text{kcal/mol}) = -11.1 - 0.2722N. \tag{5}$$

For example, ΔG^{u}_{c} and ΔG^{u}_{h} for hen egg white lysozyme (2LYZ), which has 129 amino acid residues or 1001 heavy atoms, are 294 and −284 kcal/mol, respectively. These results show that the hydrophobic interaction usually emphasized in folding of a protein molecule is not the major factor to fold a protein molecule into the native conformation. In contrast, the increase in hydration favors denaturation as quantitatively shown by Eq. (5).

The importance of hydration effects in the protein stability is illustrated by cold denaturation, or the unfolding of the native protein with lowering temperature. This phenomenon has been identified experimentally, and has been recognized by a loss in enzymatic activity at a low temperature. If the major factor of denaturation is assumed to be only chain entropy, it is difficult to explain the cold denaturation, since there is no factor favoring the unfolded state with lowering temperature. The denaturation occurs with a delicate balance between ΔG^{u}_{c} and ΔG^{u}_{h}, that is, molar chain and hydration free energies compensate each other, giving rise to a small difference in the total unfolding free energy, a few kcal/mol.

As for pressure denaturation, the major factor is ΔG^{u}_{h} as mentioned already. Equation (3) shows possible factors in the system; the changes in molar volume and compressibility, ΔV^{u} and κ^{u}. In ΔG^{u}_{c}, the virial term in ΔH^{u}_{c}, $p\Delta V^{u}_{c}$, is estimated to be negative, since the molar volume of the folded molecule has a greater volume than the random chain with no void volume in gas state. However, the hydration effect has to be taken into account to estimate the molar volume in aqueous solution. Since hydrated water layers around the molecule contribute to the molar volume, the contribution may be calculated on small molecules such as alkane molecules, alcohols, acids, etc., whose experimental data on molar volumes in aqueous solution are available [3, 4]. The hydration volume thus obtained is smaller than the normal water as expected qualitatively as formation of a rigid hydration layer. In contrast to thermal denaturation, the evaluation of ΔV^{u} is quite difficult. Since an experimental value of ΔV^{u} is around several tens ml (volume change of 12.4 ml under 300 MPa corresponds to an energy of 1 kcal/mol), which is less than a thousandth of the molar volume. the calculation of ΔV^{u} should be done with an accuracy less than 0.1% in error. Furthermore, the secondary effect

originating from compressibility will become effective when the pressure becomes more than one hundred MPa.

Nevertheless, it is apparent that the pressure affects the conformation of a protein molecule through water molecules interacting with constituent atoms. Recently, experimental approaches to explore the details of interactions under pressure, e.g. using NMR, have been in progress [5, 6], and other techniques may be applicable to the measurement of physicochemical properties under pressure. The results obtained through these experiments may explore the molecular mechanism of pressure denaturation in the near future.

References

[1] Ooi, T. Adv. Biophys. (1994), Thermodynamics of protein folding: effects of hydration and electrostatic interactions, 30, 105–154.

[2] Oobatake, M., and Ooi, T. Prog. Biophys. Mol. Biol. (1992), Hydration and heat stability effects on protein unfolding, 59, 237–284.

[3] Ooi, T. High Pressure and Biotechnology. Eds. C. Balny, R. Hayashi, K. Hermans and P. Masson. Colloque INSERM/John Libbey Eurotext Ltd. (1992), Thermodynamic aspects of pressure denaturation of proteins in aqueous solution, 222, 101–104.

[4] Holland, H. Thermodynamic Data for Biochemistry and Biotechnology, Ed. H-J Hinz, Springer-Verlag, Berlin, Heidelberg, New York, Tokyo. (1986), Partial molar volumes of biochemical model compounds in aqueous solution, pp. 17–44.

[5] Akasaka, K., Tezuka, T., and Yamada, H.J. Mol. Biol. (1997), Pressure-induced changes in the folded structure of lysozyme. 271, 671–678.

[6] Li, H., Yamada, H. and Akasaka, K. Biochemistry (1998), Effect of pressure on individual hydrogen bonds in proteins, basic pancreatic trypsin inhibitor. 37, 1167–1173.

Enzymes

High Pressure Enzyme Kinetics

C. Balny

INSERM U 128, IFR 24, CNRS, 1919, route de Mende, 34293 Montpellier Cedex 5, France
balny@crbm.cnrs-mop.fr

Abstract. The elucidation of the mechanism of enzyme reaction generally requires knowledge of the maximum values of the thermodynamic parameters. High hydrostatic pressure associated with temperature can lead to such data. A description of these approaches is given together with applications where data treatment can be achieved using the general "induced-fit" theory which implies that the binding of substrate to enzyme is a two-step process.

1 Introduction

In its simplest expression, an enzyme reaction is initiated by the binding of a substrate to the enzyme, this process being followed by a series of elementary reactions leading to the release of product(s). For a full understanding of an enzyme reaction pathway, one must identify the reaction intermediates and obtain their kinetics of interconversion. Ideally, one should obtain the structure and the thermodynamic properties of each intermediate which may mean that different conditions have to be found to allow for accumulation of each intermediate in turn.

A more traditional approach is to use the Michaelis-Menten equation for the reaction rate. Using this formulation, after Laidler, Morild published, some years ago, an excellent overview of the pressure effect on enzyme kinetics [1]. This is yet a convenient starting point for interpretation of pressure effects on enzymes.

In both cases, the transition state theory (TST) of Eyring and co-workers is still used in spite of the fact that this theory is applied in its most stringent sense only to simple homogeneous gas reactions [2]. As pointed out by Morild [1], the treatment of simple reactions in solution requires additional knowledge of the properties of liquids, and the theory becomes less rigorous and less fundamental. For example, the viscosity of the medium can be important and certain experiments carried out with model systems show that the transition state theory is an oversimplification. A treatment which may approach the real situation more closely is provided by Kramer's equations [3] where the classical formalism of the Arrhenius law is retained but where a pre-exponential term is taken in function of the viscosity of the medium. This situation could be found using rather high viscous solvents (mixtures of polyols with water) under high pressure.

In other words, it means that in applying the transition state theory to enzyme kinetics, one should be careful with the interpretations of the activation quantities found (for complete developments, see [4–8]).

2 Importance of Fast Kinetics Approaches

Even if the steady state kinetics give interesting information about the thermodynamic of enzyme reactions, few are obtained regarding the structural analysis of intermediates in a reaction pathway. However, under ambient conditions, most enzyme-catalyzed reactions are rapid with k_{cat} values above 50 s^{-1}. Enzyme reaction pathways must therefore be studied in a time range less than the millisecond range. To decrease this time scale, and to obtain more, one method is available: cryoenzymology which was at its origin a way of slowing down elementary reactions, making the time of transformation of one intermediate into another so long that each intermediate is essentially 'frozen" in time, thus becoming stable species [9]. This was, for example, the case for the bacterial luciferase reaction [9]. Cryoenzymology means experimenting with enzymes at subzero temperatures and, to ensure fluidity, antifreezes (cryosolvents, salts, lipid micelles) must be added, which also have the role of one perturbant. It is another way to get information usually difficult to obtain under normal experimental conditions: to aid we perturb (by changing the experimental conditions) and then observe [10]. However, for many reactions, the low temperature is not low enough, the reaction rates remain rapid, and their study requires special equipment working under subzero conditions for rapid mixing (stopped-flow and rapid-flow quench apparatuses when no optical signal is present. It is a sampling technique which has been adapted to subzero temperature conditions. For full details concerning these apparatuses working both at low temperatures and under pressure, see [11–13]).

3 Role of the Pressure Parameter

We have seen that cosolvents and temperature are "pace-breakers" providing tools to undertake single-step kinetic studies. Varying the pressure over a broad range (up to several MPa) gives another interesting thermodynamic parameter, namely the activation volume which is, for enzyme (or chemical) reactions, the overall molar volume change which occurs when an intermediate complex is activated to the transition state. It can be computed from the slope of a plot of logarithm of the rate constant against pressure.

Using the pressure parameter together with the temperature parameter, it becomes possible to have complete estimates of the thermodynamic quantities relating to the activated complexes, namely $\Delta H^{\ddagger}$, $\Delta S^{\ddagger}$, $\Delta V^{\ddagger}$ (variation of enthalpy, entropy, and volume, respectively).

Moreover, by combining cryoenzymology with baroenzymology, one can obtain not only a "stop-action picture" of the intermediates in an enzyme reaction pathway, but their structural and energetic features ("motion features") [5].

4 High Pressure Kinetics as a Tool To Study the Flexibility and the Solvation of Proteins

As shown above, pressure studies are a way of determining the thermodynamic parameter $\Delta V^{\ddagger}$ (or ΔV in the case of equilibrium reactions). Therefore, in opposition to simple chemical reactions, it is very difficult to give a precise physical description of these quantities which must be considered as thermodynamic parameters associated with the reacting species and the solvent environment. $\Delta V^{\ddagger}_{app}$ can be considered as the sum of several components:

$$\Delta V^{\ddagger}_{app} = \Delta V^{\ddagger}_{conf} + \Delta V^{\ddagger}_{int} + \Delta V^{\ddagger}_{sol} . \quad (1)$$

$\Delta V^{\ddagger}_{conf}$ is the protein conformation term (flexibility), $\Delta V^{\ddagger}_{int}$: intramolecular interaction (or chemical reaction) term, $\Delta V^{\ddagger}_{sol}$: solvation term, i.e. interaction with the medium.

This is illustrated using the two following examples: A) the reduction of the quinoprotein glucose dehydrogenase (GDH) by D-xylose [14], and B) the two step formation of horseradish peroxidase (HRP) compound I where ethyl peroxide was substrate [6]. For both reactions, it is possible to use the classical scheme:

$$E + S \overset{K_1}{\rightleftharpoons} ES \overset{k_2}{\rightleftharpoons} E^*S \quad (2)$$

Where E and S are the enzyme and the substrate, respectively, and ES the collision complex. K_1 is an association constant which describes a rapid equilibrium for the formation of the collision complex ES which is then transformed by a slower process to E*S.

For both examples, in water, the reactions were too fast: K_1 too small and k_2 too large to be measured, here $k_+ = K_1 \cdot k_2$ was obtained. However, using organic solvent (50 or 60% dimethyl sulfoxide: DMSO) and low temperatures, saturation curves were obtained as a function of substrates concentration, permitting the determination of K_1 and k_2 as a function of pressure and the corresponding activation volumes. At these low temperatures, the volume profiles for these two reactions were given (see Fig. 1). At higher temperature, only the activation volumes related to k_+ were measurable. For the HRP reaction, $\Delta V^{\ddagger}_{conf}$ is highly temperature sensitive, which can be related to a modification of the conformation of the protein (structural flexibility due to isomerization) which is also very sensitive to the solvent ($\Delta V^{\ddagger}_{sol}$ term). Similar results were obtained with the GDH reaction where the data obtained at elevated pressure also reveal a dynamic structural flexibility of the enzyme, largely controlled by the nature of the medium.

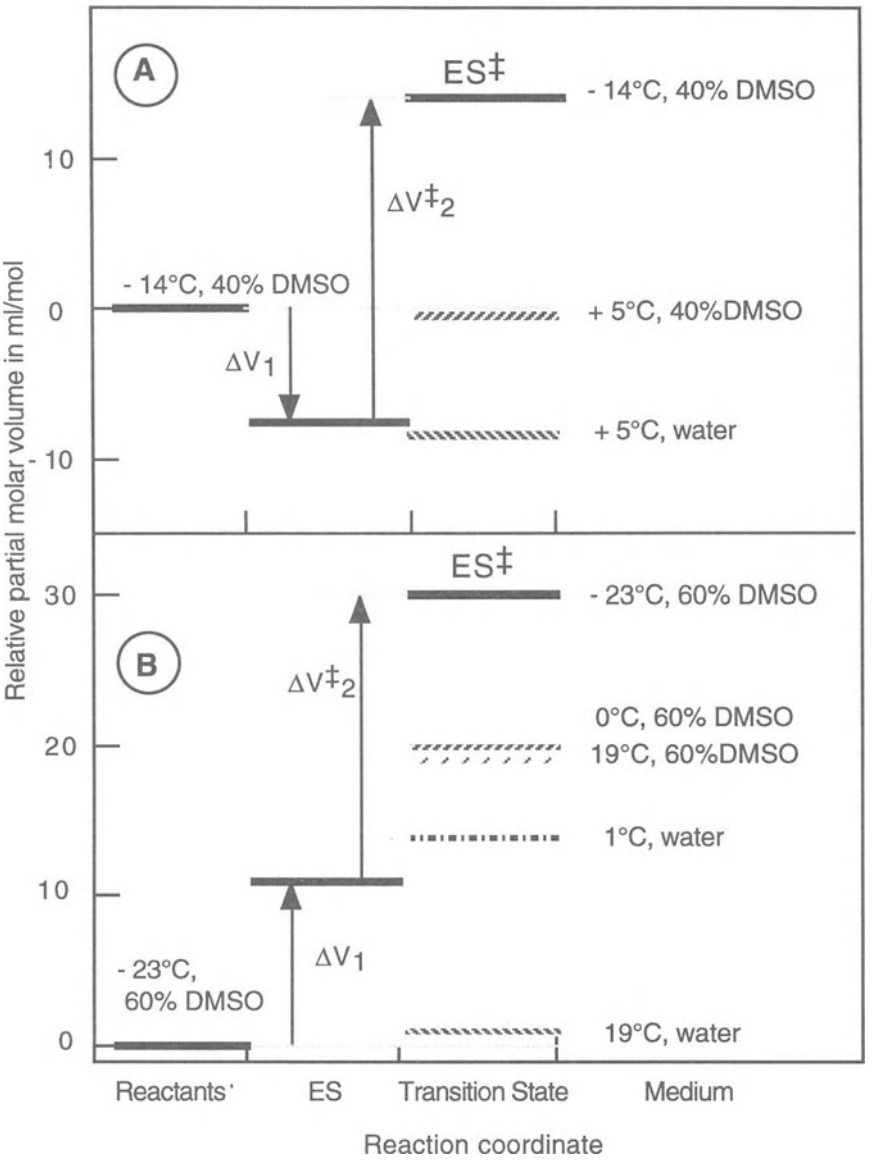

Fig. 1. Variation of the transition state volume for: (A) the reduction of GDH by D-xylose, and (B) the formation of HRP compound I, in various media and at different temperatures

This solvent modulation (regulation) is clearly shown in Fig. 1 for both reactions. For example, concerning the HRP compound I formation, the energy of the transition state can vary in a range of nearly 30 ml mol^{-1}, depending on the experimental conditions. This indicates also that it is very difficult to give a precise physical meaning of the activation volume quantities which are considered as

thermodynamic parameters associated with the reacting species and the solvent environment.

5 Conclusions

Although the above described effects of pressure on enzymes are rather complex, the potential applications of high pressures in the field of biotechnology look promising [15, 16]. However, even if numerous issues remain to be solved, pressure, temperature and non-aqueous media may be used in combination to modulate enzymatic reaction rates [17]. It is, for example, the case for micellar enzymology where the thermobarostability of some proteases in reversed micelles of Aerosol OT in apolar solvents has recently been demonstrated [18].

Acknowledgements: The author thanks Drs F. Travers, T. Barman, J. Frank, R. Lange for fruitful discussions and Mr. J-L. Saldana for technical assistance. This work is partly supported by COST D10 and INSERM/NWO grants.

References

[1] Morild, E. (1981); The theory of pressure effects on enzymes; Adv. Prot. Chem., 34, 93–166.

[2] Glasstone, S., Laidler, K.J. and Eyring, H. (1941); The theory of rate processes; McGraw-Hill, New York.

[3] Kramers, H.A. (1940); Brownian motion in a field of force and the diffusion model of chemical reaction; Physica, 7, 284–304.

[4] Balny, C., Travers, F., Barman, T. and Douzou, P. (1985); Cryoenzymic studies as a tool for investigating activated complexes: creatine kinase.ADP.Mg.nitrate.creatine as a model; Proc. Natl. Acad. Sci. USA, 82, 7495–7499.

[5] Barman, T., Travers, F., Balny, C., Hui Bon Hoa, G. and Douzou, P. (1986); New trends in cryoenzymology: probing the functional role of protein dynamics by single-step kinetics; Biochimie, 68, 1041–1051.

[6] Balny, C., Travers, F., Barman, T. and Douzou, P. (1987); Thermodynamics of the two step formation of horseradish peroxidase compound I; Eur. Biophys. J., 14, 375–383.

[7] Balny, C., Masson, P. and Travers, F. (1989); Some recent aspects of the use of high-pressure for protein investigations in solution; High Pres. Res., 2, 1–28.

[8] Balny, C. (1996); Transient enzyme kinetics at high pressure; in High Pressure Effects in Molecular Biophysics and Enzymology, Eds J.L. Markley *et al.*, Oxford Univ. Press

[9] Douzou, P. (1977) Cryobiochemistry (Academic Press, London).

[10] Travers, F. and Barman, T. (1995); Cryoenzymology: how to practice kinetic and structural studies; Biochimie, 77, 937–948.

[11] Balny, C., Saldana, J.L. and Dahan, N. (1984); High pressure stopped-flow spectrometry at low temperatures; Anal. Biochem., 139, 178–189.

[12] Balny, C., Saldana, J.L. and Dahan, N. (1987); High pressure stopped-flow fluorometry at subzero temperatures; Anal. Biochem., 163, 309–315.

[13] Hui Bon Hoa, G., Hamel, G., Else, A., Weill, G. and Herve, G. (1990); A reactor permitting injection and sampling for steady state studies of enzymatic reactions at high pressure: tests with aspartate transcarbamylase; Anal. Biochem., 187, 258–261.

[14] Frank, J., Duine, J.A. and Balny, C. (1991); Preliminary studies on quinoprotein glucose dehydrogenase under extreme conditions of temperature and pressure; Biochimie, 73, 611–613.

[15] Balny, C., Hayashi, R., Heremans, K. and Masson, P. (Eds), (1992); High Pressure and Biotechnology, Colloque INSERM, Vol. 224, John Libbey, London.

[16] Mozhaev, V.V., Heremans, K., Frank, J., Masson, P. and Balny, C.(1994); Exploiting the effects of high hydrostatic pressure in biotechnological applications; 12, 493–501.

[17] Mozhaev, V.V., Heremans, K., Frank, J., Masson, P. and Balny, C. (1996); High pressure effects on protein structure and function; Proteins: Struct. Func. Gene., 24, 81–91.

[18] Rariy, R.V., Bec, N., Klyachko, N.L., Levashov, A.V. and Balny, C. (1998); Thermobarostability of α-chymotrypsin in reversed micelles of Aerosol OT in octane solvated by water-glycerol mixtures; Biotech. Bioeng., 57, 552–556.

The Single Cysteinyl Residue (Cys341) of Carboxypeptidase Y for Cavity Control in the S1 Substrate Binding Pocket

G. Jung, H. Ueno and R. Hayashi

Division of Applied Life Sciences, Graduate School of Agriculture, Kyoto University, Kyoto 606-8502, Japan
hayashi@kais.kyoto-u.ac.jp

Abstract. Role of a single sulfhydryl group (Cys341) in carboxypeptidase Y (CPY) was investigated by combining site-directed mutagenesis and high-pressure techniques. $\Delta V^{\neq}$ in the CPY catalyzed hydrolysis of Fua-Phe-Phe and Fua-Ala-Phe and a computer simulation of the orientation of mutated residues led to an idea that Cys341 moves from inside to outside when the phenyl group in substrate P_1 site forms a transition state. Cys341 would play a role in controlling the size of the S1 substrate binding pocket so as to accept a large hydrophobic substrate by altering the cavity size of the pocket. Thus, the evaluation of the volume change by analyzing reaction kinetics under high pressure offers a useful method for microconformational change in protein.

1 Introduction

Some serine endopeptidases like subtilisin and serine carboxypeptidases contain a single cysteinyl residue, which is insensitive to chemical modifications. This cysteinyl residue is situated in the vicinity of the essential histidyl residue. Since subtilisin and serine carboxypeptidase families are genetically unrelated, the presence of the single cysteinyl residue in the two groups of enzymes suggests a specific role either in the catalytic mechanism or substrate binding [1]. However, the actual role still remains unanswered.

In the study of enzyme function, the volume change, which is obtained from the pressure dependence of the k_{cat} or K_m values, is a useful parameter to describe the detailed differences in the reaction mechanisms of enzymes [2, 3].

We have studied the high pressure effects on kinetics and conformation of carboxypeptidase Y (CPY) in which Cys341 is a single cysteinyl residue located in the S1 substrate binding pocket, within 5 Å of the catalytic residues [4, 5]. In this study, we have tried to understand the roles of Cys341 in CPY by combining site-directed mutation and high-pressure techniques.

2 Materials & Methods

The mutations were performed with the double-primer method on the PRC1 gene, which codes the CPY gene. Mutant enzymes (C341G, C341S, C341V, C341F, C341H, C341D) were expressed in the CPY-deficient strain, *Saccharomyces cerevisiae* SEY 2202. All mutant enzymes were purified to a single band on SDS-PAGE.

Secondary structure at room temperature and thermal stability of the enzyme were measured by circular dichroism (CD) in the far-UV region. The thermal stability was determined by change in [θ] at 222 nm while temperature was changed from 25 to 80 °C at pH 6.5 and expressed as a T_m-value. Enzymatic hydrolysis of Fua-Phe-Phe and Fua-Ala-Phe was performed at 25 °C in 0.05 M Mes buffer containing 1 mM EDTA, pH 6.5. Reaction kinetics was measured by an absorbance change at 332–348 nm due to the scission of the peptide bond on an ultraviolet/visible spectrophotometer. Kinetic parameters, the k_{cat} and K_m values, were calculated from Eadie-type plots.

A spectrophotometer equipped a Drickamer-type high-pressure cell [6] was used to measure the enzyme activity under the pressure. High pressure below 100 MPa was employed because the activity changes of all mutants were reversible in this pressure range. Activation volume ($\Delta V^{\neq}$) and reaction volume (ΔV) were determined from the pressure dependency of kinetic parameters, and calculated by using the following equations:

$$\Delta V^{\neq} = -RT(\mathrm{d} \ln k_{cat})/\mathrm{d}P, \quad (1)$$

$$\Delta V = -RT(\mathrm{d} \ln K_m^{-1})/\mathrm{d}P. \quad (2)$$

Computer simulation was performed with Quanta97 of Silicon Graphics to predict the conformational change in mutant enzymes and the cavity volume of the S1 substrate binding pocket.

3 Results & Discussion

3.1 Structural Properties of Cys341 Mutant Enzymes

The CD spectra of the Cys341 mutants, C341G, C341S, C341V, and C341F, and wild type CPY were almost identical at 25 °C, showing that Cys341 mutants were correctly expressed and folded in the host cell. However, C341H revealed a significantly different CD spectrum and no activity. The activity of C341D was too low to analyze ist kinetic constant under the present conditions. Thus, C341H and C341D were omitted from further studies.

The denaturation temperatures, T_m, of Cys341 mutants were 3 to 12 °C lower than that of the wild type CPY. This indicates that mutation introduced at Cys 341

significantly influences the structural stability. Therefore, Cys 341 plays a role in maintaining the structure of CPY.

3.2 Kinetic Properties of Cys341 Mutant Enzymes at Ambient Pressure

At 0.1 MPa, the k_{cat}/K_m values of mutant enzymes toward Fua-Phe-Phe were decreased more than 10-fold in all mutants, while those of C341G and C341V toward Fua-Ala-Phe were almost identical with those of the wild type enzyme but those of C341S and C341F were significantly low. In spite of the large changes in k_{cat}/K_m, K_m values toward each substrate were almost the same among wild type and mutant enzymes (Table 1). These results indicate that Cys341 mainly affects the catalytic reaction but not the affinity with the substrate, independent of the size of P1 residue.

Table 1. Kinetic parameters of Cys341 mutant CPY in the hydrolysis of Fua-Phe-Phe and Fua-Ala-Phe at ambient pressure (0.1 MPa)

Enzyme	Fua-Phe-Phe			Fua-Ala-Phe		
	k_{cat} (min^{-1})	K_m (mM)	k_{cat}/K_m ($min^{-1}\cdot mM^{-1}$)	k_{cat} (min^{-1})	K_m (mM)	k_{cat}/K_m ($min^{-1}\cdot mM^{-1}$)
Wild type	4,300	0.05	96,000	2,400	0.9	2,700
C341G	890	0.1	7,300	1,300	0.5	2,700
C341S	550	0.1	6,800	600	0.8	790
C341V	1,100	0.1	9,200	1,300	0.6	2,100
C341F	110	0.1	2,000	49	0.6	89

3.3 ΔV and $\Delta V^{\neq}$ of Cys341 Mutant Enzymes

The reaction volume (ΔV) and activation volume ($\Delta V^{\neq}$) are summarized in Table 2. Large positive ΔV values seen in the hydrolysis of Fua-Phe-Phe and Fua-Ala-Phe by wild type and mutant CPY show that the binding reaction of CPY is a volume-increasing reaction and this property is not affected by the mutation of Cys341.

Table 2. $\Delta V^{\neq}$ and ΔV of wild type and Cys341 mutant CPY toward Fua-Phe-Phe and Fua-Ala-Phe

Fua-Phe-Phe			Fua-Ala-Phe		
Enzyme	$\Delta V^{\neq}$ ml/mol	ΔV	Enzyme	$\Delta V^{\neq}$ ml/mol	ΔV
Wild type	8.4	27	Wild type	21	16
C341G	8.0	24	C341G	20	24
C341S	6.0	36	C341S	18	30
C341V	−19	22	C341V	29	10
C341F	9.8	23	C341F	16	27

Except C341V, all Cys341 mutant and wild type enzymes showed positive and almost identical $\Delta V^{\neq}$ values toward each substrate (Table 2). That is, in these enzymes, the volume of the transition intermediate in a hydrolytic reaction is greater than the volume of the ground state in spite of a different amino acid residue at 341. This probably means that amino acid residues at 341 are independent of the production of the transition state of enzymatic reactions.

C341V showed a positive $\Delta V^{\neq}$ value toward Fua-Ala-Phe, but large negative $\Delta V^{\neq}$ value toward Fua-Phe-Phe. This means that, in the hydrolysis of Fua-Ala-Phe by C341V, the normal transition intermediate is formed but, in the hydrolysis of Fua-Phe-Phe, an abnormally smaller transition intermediate is formed.

Interestingly, the difference in $\Delta V^{\neq}$ values between wild type and C341V, 27.4 ml/mol, in the hydrolysis of Fua-Phe-Phe corresponds to the volume difference of a fixed phenyl group and a freely rotating phenyl group.

Computer simulation based on the crystallographic structure of CPY could well explain the conformation of Cys341 and its mutated residues and substrate binding manner [5]. That is, the side chain of Cys341 directs to the inside of the S1 binding pocket, while most of the substituted side chains, Gly341, Ser341, and Phe341, direct to the outside of the S1 binding pocket. Only Val341 directs the same orientation with the Cys341.

4 Conclusions

Computer simulation indicates that cysteine and valine residues at the 341 position direct inside the S1 pocket and glycine, serine and phenylalanine residues at the 341 position direct outside the S1 pocket. $\Delta V^{\neq}$ values of C341G, C341S, C341F, and wild type enzyme are almost identical, but the $\Delta V^{\neq}$ value of C341V toward Fua-Phe-Phe is much smaller than that of wild type enzyme. Summarizing these results, we considered that the side chain of Cys341 moves from inside to outside on the side wall of the S1 pocket in the transition state of Fua-Phe-Phe hydrolysis reaction to easily accept the substrate phenylalanine residue at the P1 position.

Thus, applying high pressure as a perturbant to the amino acid replaced mutant enzymes, we could evaluate the dynamic conformational change in a protein.

References

[1] Winther, J.R. and Breddam, K. (1987) *Carlsberg Res. Commun.* **52,** 263–273.
[2] Morild, E. (1981) *Adv. Protein Chem.* **34,** 93–166.
[3] Laidler, K.J. and Bunting, P.S. (1973) The chemical kinetics of enzyme action, 2nd edn, ch. 7, Clarendon Press, Oxford.
[4] Hayashi, R., Moore, S. and Stein,W.H. (1975) *J. Biol. Chem.* **248,** 8366–8369.
[5] Endrizzi, J.A., Breddam, K. and Remington, S. J. (1994) *Biochemistry* **33,** 11106–11120.
[6] Fishman, E. and Drickamer, H.G. (1956) *Anal. Chem.* **28,** 804–806.

Effects of Hydrostatic and Osmotic Pressures on Dealkylation (Aging) of Phosphylcholinesterase Adducts

C. Cléry, P. Guerra, A. Redslob and P. Masson

Centre de recherches du Service de Santé des Armées, Unité d'enzymologie, BP 87, 38702 La Tronche cédex, France
101511.3606@compuserve.com

Abstract. Organophosphate adducts of serine esterase can undergo a dealkylation reaction which converts phosphylated enzymes into "aged" species which can not be reactivated. The molecular basis for the resistance to reactivation of aged enzymes is still unclear. In the present work, we focused on the importance of water in the mechanism of dealkylation. For this, we investigated the effects of hydrostatic and osmotic pressures on the rate of aging of diisopropyl-phosphorylated wild-type and mutants of human butyrylcholinesterase (DIP-wtBuChE, E197D and D70G mutants). Hydrostatic pressure strongly increased the rate of aging of wt-BuChE but had little effect on the aging of DIP-mutants. Unlike hydrostatic pressure, osmotic pressure decreased the rate of aging of both wild-type and mutant enzymes, giving large positive $\Delta v_{\pi}^{\neq}$. Our results showed that water is needed for stabilization of the transition state and that residues E197 and D70 control the water/H bond network in the active site gorge.

1 Introduction

Cholinesterases (EC 3.1.1.7/8) are inhibited by organophosphorus compounds through phosphylation of their active site serine. Phosphylated enzymes can be reactivated by nucleophilic agents like 2-PAM, an oxime used as an antidote against organophosphorus poisoning. However, phosphylated enzymes can undergo a dealkylation reaction which converts inhibited enzymes into enzymes which can not be reactivated. This process is called aging (Fig. 1). Previous results have shown that aging is accompanied by a conformational change and an increase in enzyme stability. In particular, the presence of a salt bridge between the negatively charged oxygen atom attached to the phosphorus atom and the protonated active site His 438 may contribute to the resistance to reactivation of aged BuChE [1].

In attempting to determine the importance of water in the dealkylation reaction, we investigated the effects of hydrostatic and osmotic pressures on the rate of aging of diisopropyl-phosphorylated wild-type and mutants of human butyryl-

cholinesterase (DIP-wtBuChE, E197D and D70G mutants). Residues E197 and D70 were selected because they play a part in the aging process [2].

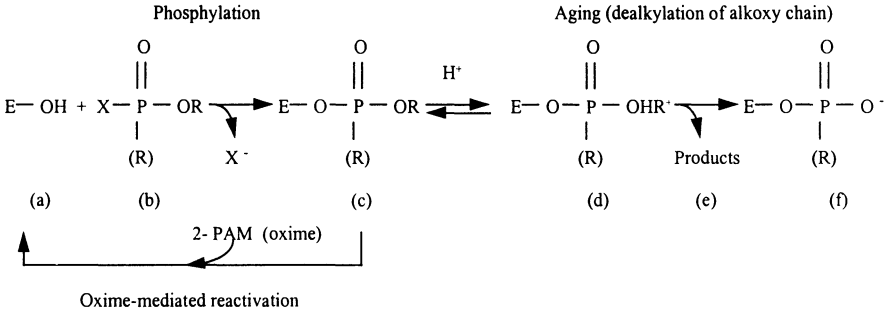

Fig. 1. Phosphylation and aging of cholinesterases: a, free enzyme; b, organophosphate; c, phosphylated enzyme; d, carbocationic intermediate; e, dealkylation products; f, aged enzyme

2 Materials & Methods

2.1 Inhibition, Aging and Reactivation

Human wild-type BuChE, purified from a plasma pool, and the E197D and D70G mutants expressed in stably transfected human embryonal kidney 293 cells, were inhibited to 90–95% by diisopropylfluorophosphate (DFP) in 50 mM phosphate buffer, pH 8.0 at 25 °C. The aging was immediately allowed to proceed for different times, t_{aging}, from 10 min to 15 h after the beginning of the inhibition plateau at atmospheric pressure and under hydrostatic pressure or osmotic pressure. Then, aliquots of DFP-phosphorylated enzymes were reactivated in several hours by 1 mM 2-pyridine aldoxime (2-PAM) at pH 8.0 at all different t_{aging}. The rate constant of aging (k_a) was calculated by the Eq. (1):

$$\ln\left[\frac{(E_r - E_i)}{(E_0 - E_i)}\right] \times 100 = k_a \times t_{aging}, \quad (1)$$

where E_0 is the activity of the native enzyme, E_i is the residual activity after inhibition by DFP, E_r is the activity of the reactivated enzyme.

2.2 Aging of DFP-Phosphorylated BuChE Under Hydrostatic Pressure

Since the pH of the phosphate buffer decreased with pressure (–0.44 units per kbar), the observed rate constant of aging had to be corrected because aging is accelerated when pH is decreased (2):

$$k_a = \frac{k_{a,obs}}{\left(1 + \frac{\Delta[H^+]}{K}\right)}, \quad (2)$$

where $\Delta[H^+]$ is the increase in H^+ concentration with pressure and K is the ionization constant of His 438 (pK ≈ 7.35).

The pressure dependence of k_a allowed the activation volumes ($\Delta V_h^{\neq}$) to be determined for the dealkylation reaction.

2.3 Aging of DFP-Phosphorylated BuChE Under Osmotic Pressure

Osmotic pressure was generated by osmolytes (fructose and sucrose) added to the phosphorylated enzyme solution at the beginning of the inhibition plateau and, thus, provided information on participation of water in the reaction. In osmotic stress experiments, the hydration layer of the protein may be regarded as a dialysis membrane. However, as Timasheff pointed out, this is an oversimplified assumption [3]. As for hydrostatic pressure, the osmotic pressure dependence of the rate constant of aging allowed the determination of the osmotic activation volume. Theoretically, from the osmotic activation volume we can estimate the change in the number of water molecules in the solute-inaccessible space: $n_w = \Delta v_\pi^{\neq}/v_w$, where v_w is the molecular volume of water (30 Å).

3 Results & Discussion

3.1 Kinetics of Aging Under Hydrostatic Pressure

Hydrostatic pressure strongly increased the rate of aging of phosphorylated wt-BuChE, giving a highly negative value ($\Delta V^{\neq} = -150$ ml mol^{-1}), suggesting that the transition state was associated with an extended conformation/hydration change and that several water molecules are involved in its stabilization. The effect of hydrostatic pressure on the aging rate of two mutants was much less important than on the aging rate of wt-BuChE ($\Delta V^{\neq} = -2.6$ ml mol^{-1} for E197D and – 2 ml mol^{-1} for D70G). Mutants are resistant to penetration of water into their active site.

3.2 Kinetics of Aging Under Osmotic Pressure

Unlike hydrostatic pressure, osmotic pressure strongly decreased the rate of aging of wt-BuChE (with sucrose as osmolyte: $\Delta V\pi^{\neq}$ = +1300 ml mol^{-1}) and both mutants ($\Delta V\pi^{\neq}$ = +5600 ml mol^{-1} for E197D and +6100 ml mol^{-1} for D70G). Thus, the highly positive values of osmotic activation volumes indicate an extended release of water both from the active site and the protein surface. However, mutants are more sensitive to osmotic pressure than wt-BuChE, suggesting that the water network in the gorge of mutants is less structured than in wt-BuChE. The calculated numbers of water molecules were too high to correspond to the number of water molecules strictly involved in stabilization of the transition state (n_w = 70 for wt-BuChE with sucrose and 310 and 340 for E197D and D70G, respectively). However, osmotic stress experiments provided evidence that water is needed for the aging process to occur. The fact that more molecules of water were released from phosphorylated mutant enzymes than from phosphorylated wt-BuChE indicates that residues E197 and D70 are important for the conformational stability of BuChE and that mutations E197D and D70G indirectly affect the solvent exposed surface of the mutant enzymes.

To relate kinetic data to conformational and hydration changes in the active site gorge accompanying the aging process, molecular dynamics simulations were undertaken; they showed that the isopropyl chain to be dealkylated was highly solvated, corroborating the result that water is important for stabilization of the dealkylation transition state.

Acknowledgements: This work was supported by DRET n° 97/12 (08) to PM and COST action D10.

References

[1] Masson,P., Rey, S, Cléry, C., Fontaine, N., Velan, B. and Shafferman, A. (1996) Stability of aged phosphylated cholinesterases and chymotrypsin. Proceedings of the 1996 Medical Bioscience Review, pp 43–52.

[2] Masson,P., Fortier, P-L, Albaret, C., Froment, M-T., Bartels, C. and Lockridge, O. (1997) Aging of diisopropyl-phosphorylated human butyrylcholinesterase, Biochem. J., 327, 601–607.

[3] Timasheff, S. (1998) In disperse solution, "osmotic stress" is a restricted case of preferential interactions, Proc. Natl. Acad. Sci. USA, 95, 7363–7367.

Post-Inactivation of Butyrylcholinesterase Following Heat and/or Pressure Treatment

F. Ribes, A. Weingand-Ziadé, F. Renault and P. Masson

Centre de Recherches du Service de Santé des Armées, Unité d'Enzymologie,
24, avenue des Maquis du Grésivaudan, BP 87, 38702 La Tronche Cedex, France
101511.3606@compuserve.com

Abstract. Inactivation of human butyrylcholinesterase (BuChE) during and after pressure and/or temperature treatment was investigated. When BuChE was subjected to the combined action of heat and pressure, an intermediate active state was irreversibly formed. Both the native and the intermediate active state were in equilibrium with two unstable active states which were inactivated after treatment interruption (post-inactivation). Inactivation kinetics followed a biexponential first-order model, whereas post-inactivation kinetics followed a simple first-order model. Post-inactivation of BuChE is a one-step transition between unstable active states and inactive states. This instability may result from hydration changes and/or subtle conformational changes occurring in the active site gorge of the enzyme.

1 Introduction

The active site of cholinesterases is located at the bottom of a deep and narrow gorge [1]. Several studies pointed out the high sensitivity of the active site gorge of butyrylcholinesterase (BuChE; EC.3.1.1.8) to environmental parameters, and its key role in the conformational stability and plasticity of the enzyme [2]. Moderate pressures (1–2 kbar) were found to induce a molten globule state, higher pressures caused irreversible inactivation/denaturation [3]. The inactivation process of BuChE induced by the combined action of pressure and/or temperature was found to continue after pressure release and cessation of heating. This process was termed post-inactivation. Our goal was to study the kinetics of inactivation and post-inactivation processes and to probe the underlying enzyme structural changes.

2 Materials & Methods

2.1 Enzyme Preparations

Human BuChE was highly purified from plasma and stored at 4 °C in 10 mM phosphate pH 7.0 as previously described [4]. The preparation showed a single band corresponding to the tetramer on both activity- and silver-stained non-denaturing acrylamide gels. The enzyme concentration was 20 μg ml^{-1}; its specific activity was 170 Units mg^{-1} (One unit corresponds to one μmol of substrate hydrolyzed per minute). Before pressurization, the enzyme was diluted 2-fold in 20 mM bis-tris buffer, pH 7.0. The pH of the buffer was checked by monitoring the molar extinction coefficient of p-nitrophenol as a function of pressure. Enzyme samples were submitted to pressure up to 5 kbar between 50 and 65 °C.

2.2 Kinetic Measurements

To study the inactivation process, the residual activity of BuChE was measured 5 min after interrupting the temperature/pressure treatment. To study the post-inactivation process, the residual activity of BuChE was measured as a function of time from 5 min to 48 h after *p/T* release. During the relaxation time, samples were stored at 4 °C. BuChE activity was determined according to the method of Ellman using butyrylthiocholine iodide as substrate at 7.0 and 25 °C [5].

2.3 Detection of Conformational Changes

To detect enzyme conformational changes and the presence of intermediate states during the denaturation and post-inactivation processes, non-denaturing polyacrylamide gel electrophoresis was carried out after different times following interruption of heating and/or pressurizing from several hours to 48 h. Gels were silver- and/or activity-stained. Activity was revealed by using a chromogenic substrate, according to the method of Karnovsky and Roots [6].

3 Results & Discussion

3.1 Characterization of an Irreversible Intermediate and a Denatured State

When native BuChE (N) was subjected to the combined action of heat and pressure, an intermediary active state (I*) was seen both on activity- and silver-stained gels. The denaturation induced by temperature led to I* and an inactive state (D). The electrophoretic mobility (μ) of these forms increased as follows: $\mu_{(D)}$

$>\mu_{(I^*)} > \mu_{(N)}$. Electropherograms showed that I* was stable in different ranges of pressure and temperature:

Pressure (kbar)	Active intermediate (I*)	Denatured state (D)
0.01 to 2	55 to 65 °C	>60 °C
3	50 to 60 °C	>60 °C
4	25 to 60 °C	>60 °C
4.5	no	>25 °C
5	no	>25 °C

Inactivation was irreversible. Mobility changes during inactivation was not due to dissociation of the tetramer into dimers or monomers. Indeed, electrophoretic mobility of I* and D did not correspond to mobility of the dimers and monomers. Unlike what was seen during the inactivation process, changes in the BuChE structure during post-inactivation were not observable by electrophoresis even after a relaxation time of 48 h. We hypothesize that the fine structural changes which occur during post-inactivation are very likely located in the active site gorge.

3.2 Kinetics of Inactivation and Post-Inactivation

The inactivation process of BuChE followed a biexponential model. At 25 °C, inactivation began above 1 kbar. Inactivation rate constants (k_1) below 4 kbar were $< 5\ 10^{-3}\ min^{-1}$. At 4 kbar, the rate was accelerated (k_1=1.5 $10^{-2}\ min^{-1}$). I* appeared at this pressure whatever the temperature. We hypothesize that formation of I* was responsible for acceleration of the inactivation process. Moderate pressures (from 1 to 3 kbar) had a protective effect against thermal denaturation [7]. Temperature alone or association of temperature and pressure > 3 kbar caused increase in inactivation rates. At 55 °C, 1 kbar, $k_1 \approx 0.1\ min^{-1}$ and 4 kbar, $k_1 \approx 0.2\ min^{-1}$.

Post-inactivation began at 1 kbar and 25 °C. Only N was detected on gels at this pressure and temperature. Therefore, we hypothesize that an unstable (post-inactivable) state (N') having a conformation close to that of N was formed. Furthermore, I*, detected on gels, is composed of a post-inactivable state (I') and a stable state (I). I' and I are in rapid equilibrium. The post-inactivation process appeared to follow the single-step complex first order model defined by two parameters [8]: $a = (1-\alpha') \exp(-k't) + \alpha'$. Where a is the ratio between the residual activity measured at different relaxation times and the residual activity measured 5 min after treatment ; t and k' are respectively the relaxation time and the post-inactivation rate constant ; α' corresponds to the sum of active states which are not involved in the post-inactivation process: $N_{(p,T)}$ and $I_{(p,T)}$. Thus, if a single unstable population post-inactivates, the process follows a mono-exponential model. k' increased with temperature and pressure. This indicates that N' and I' correspond to a continuum of species ($N'_1 ... N'_n$) and ($I'_1 ... I'_n$) that differ in stability. However, changes in k' was difficult to determine at pressures and temperatures where N' and I' were simultaneously present in different concentrations. When I' appeared, k'

decreased except at 3 kbar. This result suggests that I' underwent post-inactivation at a slower rate than N': $k'_4 < k'_2$.

4 Conclusions

During the denaturing process of BuChE induced by pressure and temperature (p, T), two phenomena were seen: inactivation and post-inactivation. These processes can be described by:

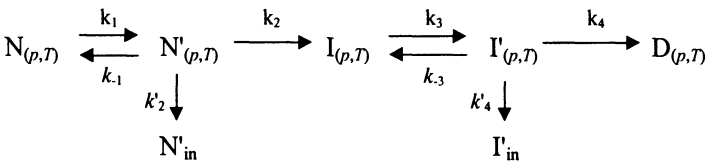

Where $N_{(p,T)}$ is the native state; $N'_{(p,T)}$ is a continuum of unstable (post-inactivable) intermediates which have a mobility similar to that of the native state; $N'_{(p,T)}$ post-inactivates to an inactive state N'_{in}; $I_{(p,T)}$ is a stable intermediate; $I'_{(p,T)}$ is a continuum of unstable intermediates; $D_{(p,T)}$ is the denatured state.

Post-inactivation is due to the formation of unstable conformational states ($N'_{(p,T)}$ and $I'_{(p,T)}$) in rapid equilibrium. This instability may result from hydration changes and/or subtle conformational changes occurring in the active site gorge of the enzyme.

References

[1] J. L. Sussman, M.Harel, F. Frolow, C. Oefner, A. Goldman, L.Toker, I. Silman, (1991), Science, 253, 872–879.
[2] P. Masson and C. Cléry, in Enzymes of the Cholinesterase Family, Ed by D. M.Quinn *et al.* Plenum Press, NY, (1995). 113–121.
[3] C. Cléry, F. Renault, P. Masson, (1995), FEBS Letters, 370, 212–214.
[4] C. Cléry, N. Bec, C. Balny, V. V. Mozhaev, P. Masson, (1995), Biochim. Biophys. Acta, 1253, 85–93.
[5] G. L. Ellman, K. D. Courtney, V. Andres, R. M. Featherstone, (1961) Biochem. Pharmacol., 7, 88–95.
[6] M. J. Karnovsky, L. Roots (1964) ; J. Histochem. Cytochem. 12: 219–221.
[7] A. Weingand-Ziadé, F. Renault, P. Masson, (1997), Biochim. Biophys. Acta, 1340, 245–252.
[8] A. Sadana, J. P. Henley, (1987), Biotechnol. Bioeng., 30, 717–723.

Combined Action of Temperature and Pressure on the Catalytic Activity of Wild-Type and D70G Mutant of Human Butyrylcholinesterase

A. Weingand-Ziadé, F. Renault and P. Masson

Centre de Recherches du Service de Santé des Armées, Unité d'Enzymologie, 24, avenue des Maquis du Grésivaudan, BP 87, 38702 La Tronche Cedex, France
101511.3606@compuserve.com

Abstract. The combined action of temperature and pressure on the catalytic activity of wild-type human butyrylcholinesterase (BuChE) and its D70G mutant were investigated. The D70 residue, located near the top of the active site gorge, is an important component of the peripheral anionic site of BuChE. Results showed a break in Arrhenius plots of wild-type BuChE (at about 22 °C) whatever the pressure, whereas no break was observed in Arrhenius plots of the D70G mutant. These results suggested a temperature-induced conformational change of the wild-type BuChE which does not exist in the D70G mutant. At 1 kbar, a transient state of wild-type BuChE, in which the substrate binding was reinforced, appeared but was not observed for the mutant. Hydration changes in the BuChE active site gorge could be involved in formation of this transient state. Results indicate that the D70 residue is involved in regulation of activity as a function of temperature and pressure.

1 Introduction

Acetylcholinesterase (AChE, EC 3.1.1.7) and butyrylcholinesterase (BuChE, EC 3.1.1.8) differ in substrate specificity and inhibitor sensitivity [1]. Since BuChE hydrolyses numerous esters, it has a pharmacological and toxicological importance [2]. The "atypical" variant of human BuChE has Gly in place of Asp 70 [3], and has a lower affinity for all positively charged substrates and positively charged inhibitors. It is now admitted that the D70 residue, located at the mouth of the active site gorge, 12 Å from the active site Ser 198, is an important component of the peripheral anionic site (PAS) of BuChE [4].

The kinetic behaviour of wild-type BuChE is complex: with positively charged substrates, wild-type BuChE displays activation at high substrate concentration [5], whereas the kinetic of the butyrylthiocholine (BuSCh) hydrolysis by the D70G mutant is Michaelian [4]. In addition, the temperature dependence of the hydrolysis rate of charged or uncharged substrates by wild-type BuChE does not follow the Arrhenius equation. The Arrhenius plot of BuSCh hydrolysis by wild-type BuChE

presents a break at a transition temperature of 18–20 °C in phosphate buffer (pH 7.0–7.4) [6], but no Arrhenius analysis of the D70G mutant had been performed until the present study.

In order to get insights into the temperature-dependent kinetic behaviour of human plasma BuChE and its D70G mutant, we undertook kinetic analysis of these enzymes under pressure as a function of temperature. This study allowed us to construct Arrhenius and Van't Hoff plots for the hydrolysis of BuSCh by BuChE and its D70G mutant. It was of interest to investigate the pressure dependence of the temperature at which the break occurs to get an insight into the origin of the break.

2 Materials & Methods

2.1 Enzyme Preparations

Human BuChE was highly purified from plasma as previously described [7]. The D70G mutant expressed in stably transfected human embryonal 293 kidney cells [4] was a gift from Pr O. Lockridge (U NMC, Omaha, NE, USA). The specific activity of the wild-type BuChE and the D70G mutant was 406 and 143 units.mg^{-1}, respectively, with BuSCh as substrate using the method of Ellman *et al.* [8] (1 unit hydrolyses 1 μmol of BuSCh per min at pH 7.0 and 25 °C).

2.2 Kinetic Measurements

Kinetic measurements were performed using the method of Ellman *et al.* [8] with BuSCh as substrate in 10 mM Tris pH 7.0. Although 10 mM Tris has a low buffer capacity at pH 7.0, the pH did not vary because the enzyme activity per assay was very low (0.0055 and 0.0090 unit/assay for the wild-type BuChE and its D70G mutant, respectively).

2.3 Determination of Catalytic Parameters

Kinetic data were plotted using the Lineweaver-Burk plot for Michaelian behaviour; K_m and V_{max} were determined by linear regression of the Michaelis-Menten equation. Activation energies, E_a, were determined from the slope of Arrhenius plots. The apparent heat of binding of substrate ΔH were calculated from the slope of the Van't Hoff plots.

3 Results & Discussion

3.1 Arrhenius Analysis of Wild-Type BuChE and D70G Mutant

The temperature dependence of the catalytic constant (k_{cat}) of wild-type BuChE did not follow the simple Arrhenius equation. At atmospheric pressure, the Arrhenius plot showed a break at a transition temperature (T_t) of 22 °C. This break shifted to higher temperatures with increasing pressure. The increase in T_t with pressure was linear with a slope dT_t/dP = 0.11 K/kbar. This value suggests a temperature-induced conformational change of the enzyme. The enzyme must exist in two different active forms on both sides of the break. The break may thus reflect a change in plasticity of the active site gorge around T_t.

The Arrhenius plot at atmospheric pressure of the D70G mutant was linear (results not shown), following the Arrhenius law. Under pressure, k_{cat} decreased with increasing pressure. Between 0.25 and 1 kbar, the curvature in Arrhenius plots may reflect changes in the rate of elementary steps, e.g. a change in the rate-limiting step. However, we cannot rule out that curvature may result from a conformational change due to the higher conformational flexibility of the mutant active site gorge. At higher pressures, 1.25 and 1.5 kbar, plots turned out to be linear, suggesting that k_{cat} was dependent either on a single rate constant or on a product of rate constants, and/or inverted rate constants.

3.2 Van't Hoff Analysis of Wild-Type BuChE and D70G Mutant

The pressure dependence of the "affinity" constant K_m of wild-type BuChE was not linear, showing a well between 0.75 and 1.5 kbar (results not shown). In the pressure range 0.001–0.75 kbar a slight increase in K_m was observed whatever the temperature. Above 0.75 kbar and up to 1 kbar a significant decrease in K_m was seen. Above 1 kbar, K_m progressively increased. At pressures lower than 0.75 kbar, the volume change accompanying the dissociation of the enzyme-substrate complex (ΔV) was slightly negative (–2 to –12 ml/mol between 10 and 35 °C), indicating that the affinity of the enzyme for BuSCh decreased moderately with increasing pressure. However, ΔV values must be considered as the algebraic sum of volume changes accompanying a sequence of events: enzyme-substrate interactions (ΔV_{int}), water structure changes around reactants (ΔV_w) and conformational change of the enzyme (ΔV_{conf}). Below 0.75 kbar, ΔV resulted mainly from ΔV_{int}. At intermediate pressures (0.75–1 kbar), since ΔV became strongly positive (+65 to +146 ml/mol), hydration of the binding site was decreased (water molecules were released in the bulk solvent). ΔV was dominated by the change in hydration of the active site gorge ΔV_w and to a lesser extent by the binding contribution ΔV_{int}. At pressures higher than 1 kbar, BuChE underwent the molten globule transition [9]. Thus, at p>1 kbar, hydration of the enzyme increased, showing an extended decrease in the volume because of electrostriction of water around charged groups and hydrophobic solvation of non-polar amino acid side chains.

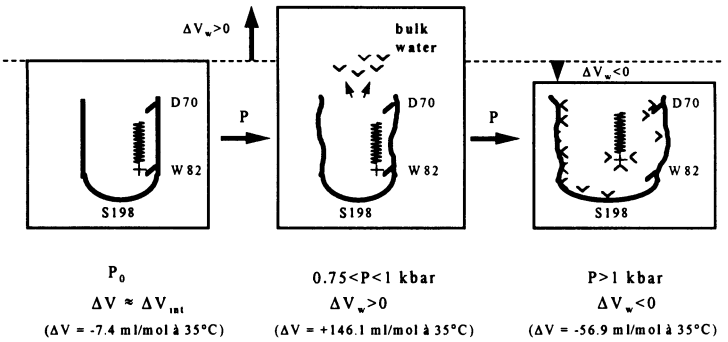

For the D70G mutant, the absence of an enzyme state, in which the substrate binding is strengthened for pressures ranging from 0.75 to 1.5 kbar, suggests that the D70 residue is involved in the hydration state of the BuChE active site gorge and plays a key role in its conformational stability.

4 Conclusions

Our results suggest that replacement of Aspartate 70 by a Glycine abolishes the temperature-induced conformational change observed in wild-type human BuChE. In the same way, the transient state that was seen at about 1 kbar for wild-type BuChE did not appear for the D70G mutant, indicating that the temperature dependence of the kinetic behaviour of the enzyme was different in both cases. Moreover, changes in hydration of the BuChE active site gorge may account for this transient state. The nature and the position of the D70 residue appear to be important for the conformational plasticity and the water/H-bond network dynamics of the enzyme as a function of temperature and pressure.

References

[1] Quinn, D.M. (1987); Chem. Rev. 87, 955–979.
[2] Lockridge, O. (1990); Pharmac. Ther. 47, 35–60.
[3] McGuire, M.C. *et al.* (1989); Proc. Natl. Acad. Sci. USA 86, 953–957.
[4] Masson, P., Froment, M.T., Bartels, C.F., Lockridge, O. (1996); Eur. J. Biochem. 235, 36–48.
[5] Eriksson, H., Augustinsson, K.B. (1979); Biochim. Biophys. Acta 567, 161–173.
[6] Masson, P., Balny, C. (1986); Biochim. Biophys. Acta 874, 90–98.
[7] Cléry, C., Bec, N., Balny, C., Mozhaev, V.V., Masson, P. (1995); Biochim. Biophys. Acta 1253, 85–93.
[8] Ellman, G.L., Courtney, K.D., Andres, V., Featherstone, R.M. (1961); Biochem. Pharmacol. 7, 88–95.
[9] Cléry, C., Renault, F., Masson, P. (1995); FEBS Letters 370, 212–214.

Pressure Activates Oligomeric Enzymes in Reversed Micelles by Stabilisation of Different Oligomeric Forms

N.L. Klyachko, P.A. Levashov, A.V. Levashov and C. Balny[1]

Department of Chemical Enzymology, Faculty of Chemistry, Moscow State University, 119899 Moscow, Russia
klyachko@enzyme.chem.msu.ru
[1]INSERM U 128, IFR 24, 1919 Route de Mende (CNRS), 34293 Montpellier cedex 5, France
balny@crbm.cnrs-mop.fr

Abstract. MDH, GPDH, and LDH were found to have differences in catalysis in aqueous solution and reversed micelles under pressure. Whereas all the enzymes and binary complexes between GPDH and LDH in water appeared to be almost insensitive to the pressure increase, the catalytic activity of MDH and complexes between GPDH and LDH were strongly dependent on pressure in reversed micelles.

1 Introduction

Recently, the use of hydrostatic pressure [1,2] has been combined with micellar enzymology for both increasing enzyme stability and modulating enzyme activity. Micellar enzymology is a promising approach to study the properties of enzymes revealing their tendencies to form superactive conformations and supramolecular structures [3, 4]. Most of the enzymes studied in the systems of reversed micelles in organic solvents exhibit a characteristic bell-shaped dependence of their catalytic activity on the surfactant hydration degree (w_0, molar ratio of water to surfactant, reflecting the size of a micelle). Maximal enzyme catalytic activity in reversed micelles is observed at a particular hydration degree where the size of the inner cavity corresponds to that of the entrapped protein. In the case of oligomeric enzymes the dependence of their catalytic activity on hydration degree represents a curve with several maxima; each optimum can be related to the functioning of one particular oligomeric form [5]. Our present study was carried out to reveal how pressure and micelles acting in co-operation can modulate the catalytic activity and/or stability of different forms of oligomeric enzymes.

2 Materials & Methods

Porcine heart malic dehydrogenase (MDH), rabbit muscle lactic and glyceraldehyde-3-phosphate dehydrogenases (LDH and GPDH) with specific activities 400, 95 and 470 units/mg, respectively, were from Sigma. Kinetics was carried out in a stopped-flow high-pressure apparatus [6]. MDH or LDH activity was measured as an oxalacetate or pyruvate, respectively, reduction with NADH; the GPDH catalytic activity was measured as a GAP oxidation with NAD^+ [7, 8].

3 Results & Discussion

3.1 Pressure Dependencies of MDH, GPDH and LDH in Aqueous Solution

The catalytic activity of MDH in aqueous solution does not change much in wide range of pressure applied (from 1 to 1000 bar), slightly decreasing when pressure is increased ($\Delta V^{\neq}_{app}$ is equal to 5 ml mol^{-1}). An even more pronounced negative slope ($\Delta V^{\neq}_{app}$ is equal to 45 ml mol^{-1}) was found in the case of pressure dependence of the catalytic activity of GPDH. In both cases pressure causes an enzyme inactivation starting from very low values (in the case of LDH noticeable inactivation starts from 600 bar). Neither was any difference found on the curve of GPDH catalytic activity when LDH in an excess was added to the system.

3.2 MDH, GPDH and LDH in Reversed Micelles at Different Pressures

MDH is a dimeric enzyme consisting of two equal subunits with molecular weight of 37 kDa each. Using reversed micelles as a medium, two maxima at w_0 12 and 17 were revealed on the dependence of the enzyme catalytic activity on hydration degree at atmospheric pressure that could be related to monomeric and dimeric forms of the enzyme functioning. The picture changes dramatically when the pressure increases. The one pronounced maximum appeared at w_0 = 14 and pressure of 300–500 bar (Fig. 1a). As seen, the difference between lowest and highest levels of the enzyme catalytic activity is about 10 times. Such a phenomenon can be attributed to the pressure effect on the enzyme molecule via micellar matrix structure. Our experiment in water can be an indication that pressure does not affect the enzyme structure directly.

What is the role of pressure? As indicated in our previous work [9], pressure can act the same way as glycerol does, i.e. rigidifying the matrix structure and leading to the enhancement of the enzyme activity and stability. At w_0 = 14, both monomeric and dimeric MDH particles could coexist in reversed micelles. Therefore, there are at least two ways in which pressure application can affect MDH in reversed micelles. The first possibility could be that pressure application leads to a shift of the equilibrium between monomeric and dimeric forms of MDH to a monomeric one by its stabilisation. The second possibility could be that

pressure stabilises a dimeric form of MDH in reversed micelles enduring (strengthening) protein-protein contacts and leading by this to a more compact form of the enzyme molecule existing in reversed micelles which appears then to be more sensitive to external effects. Discrimination between the two possibilities cannot then be made.

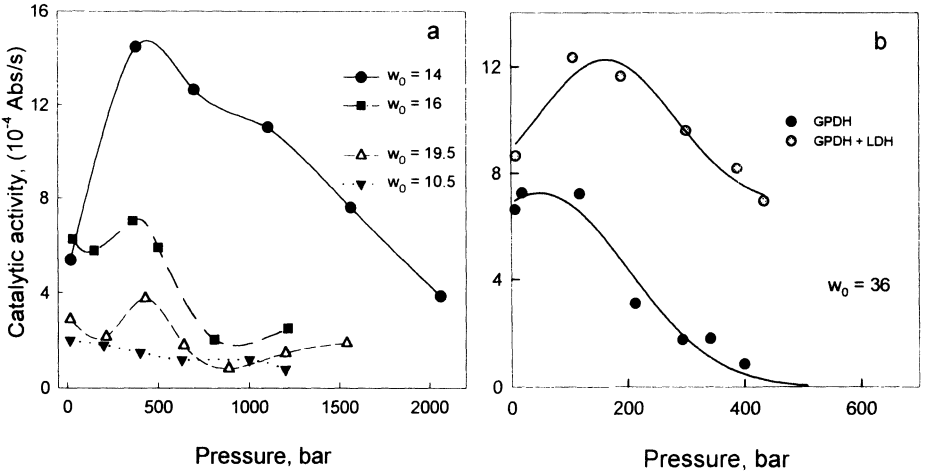

Fig. 1. Pressure dependencies of the catalytic activity of oligomeric enzymes in reversed micelles of AOT in iso-octane at different hydration degrees. a) MDH, b) GPDH in the presence and absence of LDH

As distinguished from MDH, both LDH and GPDH pressure dependencies of the enzyme catalytic activity in reversed micelles at w_0 10–30 have a monotonous character with negative slope upon pressure increasing. A slight difference in pressure dependence was observed for GPDH at high hydration degree. As seen in Fig. 1b, there is a narrow stable phase where the enzyme catalytic activity does not change while the pressure increases from 1 to 120 bar. Further pressure increase up to 400 bar leads to a profound decrease in the GPDH catalytic activity that drops more than 10 times. The phase transition occurs in the system at higher pressures followed by the turbidity increasing.

What was interesting for us to study in the case of GPDH and LDH is their work in a complex. Both enzymes are involved in the system of glycolysis and have a tendency to form complexes. Indeed, in reversed micelles, bi-enzymic complexes were found to exist. At atmospheric pressure, two maxima at w_0 21 and 36 were observed on the GPDH catalytic activity - hydration degree profile in the presence of LDH indicating two different particles functioning which were identified as GPDH-LDH monomers and GPDH dimer–LDH tetramers working in reversed micelles [10]. We studied the effect of pressure on the catalytic activity of GPDH in the presence of LDH in these conditions. A pronounced effect of GPDH activation upon pressure application is seen at w_0 = 36 (Fig. 1b). At this hydration degree where the complex between a GPDH dimer and a LDH tetramer can be formed in reversed micelles, the GPDH catalytic activity increases two times when pressure is increased up to 200 bar, after that decreases are always higher than that

in the absence of LDH. Whereas at 400 bar the GPDH catalytic activity decreases dramatically, the GPDH catalytic activity in the complex with LDH retains the initial level, i.e. being 10 times higher that that in the absence of LDH.

4 Conclusions

The work presented demonstrates for the first time the co-operative effect of reversed micelles and pressure application to MDH, GPDH, LDH, and complexes between the last two leading to a pronounced activation and stabilisation of enzymes and their particular heterooligomeric complexes (GPDH-LDH monomers and GPDH dimer – LDH tetramer) that cannot be realised in aqueous solution.

Acknowledgements: This work was supported in part by grants INSERM (PECO) and COST D10.

References

[1] Balny, C., Hayashi, R., Heremans, K. and Masson, P. (eds.) (1992); High Pressure and Biotechnology, Colloque INSERM vol. 224, J. Libbey, Montrouge.

[2] Mozhaev, V.V., Heremans, K., Frank, J., Masson, P. and Balny, C. (1996); High pressure effects on protein structure and function; Proteins: Struct. Func. Gen., 24, 81–91.

[3] Martinek, K., Klyachko, N.L., Kabanov, A.V., Khmelnitsky, Yu.L. and Levashov, A.V. (1989); Micellar enzymology: its relation to membranology; Biochim. Biophys. Acta, 981, 161–172.

[4] Tuena de Gomez-Puyou, M. and Gomez-Puyou, A. (1998); Enzymes in low water systems; Critical Rev. Biochem. Mol. Biol., 33, 53–89.

[5] Kabanov, A.V., Klyachko, N.L., Nametkin, S.N. and Levashov, A.V. (1991); Engineering of functional supramolecular complexes of proteins (enzymes) using reversed micelles as matrix microreactors, Prot. Eng., 4, 1009–1017.

[6] Balny, C., Saldana, J.-L. and Dahan, N. (1984); High pressure stopped-flow spectrometry at low temperatures; Anal. Biochem., 139, 178–189.

[7] Klyachko, N.L., Levashov, P.A., Levashov, A.V. and Balny, C. (1998); Pressure activates malic dehydrogenase in reversed micelles; FEBS Lett. (submitted).

[8] Levashov, P.A., Klyachko, N.L., Levashov, A.V. and Balny, C. (1998); Pressure stabilises complexes between D-glyceraldehyde-3-phosphate dehydrogenase and lactic dehydrogenase in reversed micelles; FEBS Lett. (submitted).

[9] Rariy, R.V., Bec, N., Klyachko, N.L., Levashov, A.V. and Balny, C. (1998); Thermobarostability of chymotrypsin in reversed micelles of aerosol OT in octane solvated by water-glycerol mixtures; Biotechnol. Bioeng., 57, 552–556.

[10] Levashov, A.V., Ugolnikova, A.V., Ivanov, M.V. and Klyachko, N.L. (1997); Formation of homo- and heterooligomeric supramolecular structures by D-glyceraldehyde-3-phosphate dehydrogenase and lactate dehydrogenase in reversed micelles of aerosol OT in octane; Biochem. Mol. Biol. Int., 42, 527–534.

Food Proteins

Proteolysis of Bovine β-Lactoglobulin and Chicken Egg Ovalbumin During Treatment at High Pressure

F. Bonomi[1], S. Iametti[1], C. Castagna[1], G.F. Dall'Aglio[2] and P.P. Rovere[2]

[1]Dipartimento di Scienze Molecolari Agroalimentari, University of Milan, Via Celoria 2, I-20133 Milan, Italy
[2]SSICA, Via Tanara 31, Parma, Italy
francesco.bonomi@unimi.it

Abstract. Bovine β-lactoglobulin and chicken egg ovalbumin were treated at 600 MPa for 10 min in the presence of proteases that had little if any activity on the folded, native proteins. Ovalbumin was pressure treated in the presence of 10% NaCl to minimize protein aggregation. With all proteases but thermolysin, that was inactivated by pressure, proteolysis was higher when the enzyme was added before the pressure treatment than when the enzyme was added to the pressure-treated protein. The nature of the products of the combined pressure/protease treatment depended on the balance between two concomitant reactions, i.e. protein aggregation and protein hydrolysis. Large peptides represented a significant fraction of the proteolytic products. Pressure alone reduced the β-lactoglobulin epitopes recognizability to 50% of that of the untreated protein (40% for ovalbumin). Corresponding values after pressure treatment in the presence of chymotrypsin were 23% for β-lactoglobulin and 10% for ovalbumin.

1 Introduction

Bovine β-lactoglobulin (BLG) and chicken egg ovalbumin (OVA) are widely used components of common foods, and are among the most common protein determinants of food intolerance in humans [1]. The approach currently used for reducing the number of sequential and conformational epitopes in these proteins relies on extensive proteolytic degradation. This procedure is often made difficult by the structural toughness of both proteins, that are accessible to many proteases only after heat or pH denaturation, a feature that has relevance also for their nutritional value [2, 3]. Heat denaturation of these proteins may result in a loss of their technological properties [4]. This latter drawback could be avoided when high pressure is used to replace heat as the denaturing agent, in conditions where the treatment generates transiently modified protein species without resulting in extensive and irreversible protein denaturation [5, 6]. In this work, we tested the susceptibility to different proteases of the conformers of both proteins that are transiently generated during pressure-induced denaturation. A preliminary charac-

terization of the products of the combined treatments was carried out as for their molecular properties and for their reactivity towards specific antibodies.

2 Materials & Methods

BLG (2.5 mg/ml) and OVA (2 mg/ml) in 50 mM phosphate, pH 7, were treated at 600 MPa for 10 min at 37 °C in a isostatic high-pressure generator (ABB Model QFP-6, ABB, Sweden), either in the presence or in the absence of proteases (trypsin, chymotrypsin, bromelain, thermolysin, all 1/20 of the treated protein on a weight basis). In control experiments, the same enzyme/protein mixtures were incubated for 10 min at 37 °C at atmospheric pressures. Proteolysis was measured in these latter conditions also on aliquots of the proteins that were pressure-treated in the absence of proteases. The extent of proteolysis was assessed quantitatively by RP-HPLC and SEC-HPLC, after arresting the proteolytic reaction with 0.1% TFA or 4 M urea, respectively. All OVA samples contained 10% NaCl to minimize aggregation upon pressurization [6]. Residual protease activity was detected with suitable substrates immediately after the pressure treatment. For immunochemical determinations, competitive ELISA tests were performed according to published procedures [6].

3 Results

As shown in Table 1, under the conditions used here, none of the tested proteases attacked untreated BLG to a significant extent. Proteases were active on pressure-treated BLG, but the highest proteolysis was observed when each protease was added to BLG solutions prior to subsequent pressure treatment of the protein mixture. The only exception was thermolysin, that was more active on pressure-treated BLG than when added prior to pressurization. This was due to inactivation of thermolysin by high pressure. Pressure inactivation was less pronounced for the other proteases, and trypsin showed the highest barotolerance.

As also shown in Table 1, bromelain and thermolysin gave quite limited proteolysis of untreated OVA, which was insensitive to the action of chymotrypsin and trypsin. Extensive proteolysis was observed when pressurizing mixtures of OVA and either intestinal protease, although with OVA the differences between the two experimental conditions used in our studies (i.e., addition of the enzyme before the pressure treatment or to a pressure-treated protein) were less pronounced than with BLG.

The molecular nature of the products of the combined pressure/proteolytic treatment was examined also by gel-permeation HPLC, as reported in Table 2. For either protein, the final outcome of the combined treatment apparently depended on the balance between two concomitant reactions, i.e. pressure-induced protein aggregation [5, 6] and protein hydrolysis, that were competing.

Table 1. Action of different proteases on OVA and BLG at ambient pressure, after treatment at 600 MPa, or when present during the pressure treatment itself [a]

Enzyme	Residual activity after pressure treatment, %[c]	Residual percent of intact protein[b]					
		BLG			OVA		
		ambient	after	during	ambient	after	during
trypsin	100	98	76	71	99	69	61
chymotrypsin	23	90	68	37	95	70	65
bromelain	88	100	71	38	84	75	70
thermolysin	11	100	70	89	86	65	68

[a]pressure treatments and incubation with enzymes were carried out for 10 min at 37 °C
[b]determined by RP-HPLC with detection at 220 nm
[c]determined on specific synthetic substrates immediately after pressure treatment

As reported in Table 2, SEC-HPLC showed that aggregates larger than the native proteins were a minimal fraction of the total protein when intestinal proteases were used in the course of pressure treatment, and that relatively large polypeptides represented a significant fraction of the hydrolytic products.

Table 2. Distribution of fractions of different molecular size in BLG and OVA following pressure treatment (HP) in the presence and in the absence of intestinal proteases[a]

Protein	Treatment	Amount of protein in fractions of different molecular size, % of total				
		aggregates	native-like	20–10 kDa	10–6 kDa	<6 kDa
BLG	none	10	90	-	-	-
	HP only	19	81	-	-	-
	HP + trypsin	0	4	28	51	17
	HP + chym.[b]	0	13	10	41	36
OVA	none	3	97	-	-	-
	HP only	21	79	-	-	-
	HP + trypsin	0	47	0	14	39
	HP + chym.[b]	7	45	0	12	36

[a]determined by SEC-HPLC in 50 mM phosphate, pH 6.8; detection at 220 nm
[b]chymotrypsin

As reported in Table 3, the protein unfolding induced by pressure treatment alone induced a decrease in the number of epitopes recognizable by specific antibodies on both BLG and OVA. By performing the pressure treatment in the presence of proteases, a further decrease in antibody recognition was observed. A comparison between the residual immunochemical reactivity figures and the proteolysis data obtained by RP-HPLC or by SEC-HPLC as listed in Tables 1 and 2 suggests that proteolytic action during pressure treatment may have removed some epitopic sites (with relatively low overall hydrolysis) in the case of OVA, but it was not so specific on recognizable epitopic sites in the case of BLG.

Table 3. Residual reactivity towards specific antibodies after treatment at 600 MPa for 10 min at 37 °C, in the absence or in the presence of proteases[a]

Protease present during the pressure treatment	Residual recognizability by specific antibodies, % of the untreated protein	
	BLG	OVA
none	56	40
trypsin	36	9
chymotrypsin	23	15

[a]determined by competititive ELISA

Work is in progress to assess the nature and the antigenicity of the hydrolysis products, and to find treatment conditions where residual immunochemical reactivity can be further reduced without extensive hydrolysis.

The preliminary data reported here indicate that this combination of treatments could be interesting for producing foods with improved digestibility and tolerance when eggs and whey proteins are among the ingredients.

Acknowledgements: Work supported by grants of the Italian Ministry for the University and Scientific and Technological Research (MURST, Rome, Italy; National Project "Biocatalisi e Bioconversioni").

References

[1] Tsukasa, M.; Ryo, N. Molecular structure and immunological properties of food allergens. *Trends Food Sci. Technol.* **1993,** *4,*289–293.

[2] Carbonaro, M., Bonomi, F., Iametti, S., Carnovale, E. Modification in disulfide reactivity induced by different pasteurization conditions of milk. *J. Food Science* **1996,** *61*, 495–499.

[3] Yoshinori, M. Laser light scattering study on the heat-induced ovalbumin aggregates related to its gelling property. *J. Agric. Food Chem.* **1996,** *44,* 2086–2090.

[4] Mine, Y. Recent advances in understanding of egg white protein functionality. *Trends in Food Science & Technology* **1995,** *6,* 225–230.

[5] Iametti, S., Transidico, P., Bonomi, F., Vecchio, G., Pittia, P., Rovere, P., Dall'Aglio, G. Molecular modifications of β-lactoglobulin upon exposure to high pressures. *J. Agric. Food Chem.* **1997,** *45*, 23–29.

[6] Iametti, S.; Donnizzelli, E.; Vecchio, G.; Rovere, P.; Gola, S.; Bonomi, F. Macroscopic and structural consequences of high-pressure treatment of ovalbumin solutions. *J. Agric. Food Chem.* **1998**, in press.

Pressure Stability of Lipoxygenase from Green Beans (*Phaseolus vulgaris* L.) at Subzero and Elevated Temperature

Indrawati, A. Van Loey, L. Ludikhuyze and M. Hendrickx

Department of Food and Microbial Technology, Laboratory of Food Technology, Katholieke Universiteit Leuven, Kardinaal Mercierlaan 92, B-3001 Heverlee, Belgium
Phone: 32-16-321572; Fax: 32-16-321960
Marc.Hendrickx @agr.kuleuven.ac.be
http://www.agr.kuleuven.ac.be/lmt/vdt/general/foodtech.htm

Abstract. Green beans LOX could be irreversibly inactivated in the entire p/T area studied (up to 7 kbar and –10 to 63 °C). The inactivation followed a first order reaction and could be accelerated by a p increase at constant T. The inactivation kinetic parameters were described as D, z and zp values.

1 Introduction

High pressure technology is currently investigated as an alternative to thermal processing in order to avoid quality degradation due to the thermal treatment. Since pressure depresses the melting point of water, food applications like pressure assisted freezing; pressure assisted thawing; non-frozen storage under pressure and modification of ice polyforms are possible [1]. Some kinetic studies have been carried out to investigate pressure stability of enzymes at moderate or elevated temperatures in enzymatic model systems [2, 3]. Unfortunately, little attention has been paid to enzyme inactivation in real food up to the subzero temperature area. The aim of this investigation was to study kinetic pressure effects (up to 7 kbar) on a food related enzyme, namely lipoxygenase (LOX) at subzero and elevated temperatures (–10 up to 63 °C) in green beans extract.

2 Materials & Methods

2.1 Green Beans Extract Preparation and Lipoxygenase Assay

Whole green beans were purchased from a local market (harvested in July 1997). The extract was obtained by squeezing the beans and subsequently centrifuging (25900 g; 4 °C; 15 min). The extract was stored under liquid nitrogen until use.

The enzyme activity was measured polarographically at 25 °C using linoleic acid as substrate and phosphate buffer (0.01 M; pH 6).

2.2 Pressure-Temperature (*p*/*T*) Treatment

A kinetic study of isobaric isothermal inactivation of LOX was performed in a themostated multivessel high pressure equipment (8 vessels, Resato, Roden, Holland). The extract was filled in flexible microcups (Elkay, 0.375 ml) without creating air bubbles and closed with parafilm. For pressure experiments at subzero temperature, the samples were wrapped in vacuumed polyethylene pockets to protect the extract solution from pressure medium contamination. Pressure was built up at a constant pressurization rate of 1 kbar/min. After an equilibrium time of 5 min to ensure achievement of the isobaric isothermal condition, a first vessel was decompressed and the residual enzyme activity of the sample in that vessel was measured and considered as A_0 (reference value). Afterwards, vessels were decompressed at predetermined time intervals.

2.3 Data Analysis

Since LOX inactivation followed a first order reaction (1) at all *p*/*T* combinations studied, the Thermal Death Time model could be used to describe the *p*/*T* inactivation, i.e. *D* value (decimal reduction time, in minute, 2.303/*k*, time needed to reduce the initial activity with 90%) and *z* value (the temperature sensitivity of *D* value, in °C, (2), temperature increase required to reduce the *D* value by one log unit). In an analogous way, the pressure sensitivity of the *D* value could be described as the *zp* value (in bar (3)).

$$\log(A) = \log(A_0) - \frac{k}{2.303} * t \,, \tag{1}$$

$$D = D_{\text{ref-}T} * 10^{\frac{T_{\text{ref}} - T}{z}} \,, \tag{2}$$

$$D = D_{\text{ref-}p} * 10^{\frac{p_{\text{ref}} - p}{zp}} \,. \tag{3}$$

3 Results & Discussion

Green beans LOX could be irreversibly inactivated by all treatments in the *p*/*T* domain (1 up to 7 kbar combined with −10 to 63 °C) studied. The inactivation followed a first order reaction either at subzero or at elevated temperature (Fig. 1).

Based on the estimated D values, an iso-D value contour diagram could be constructed as a function of pressure and temperature (Fig. 2).

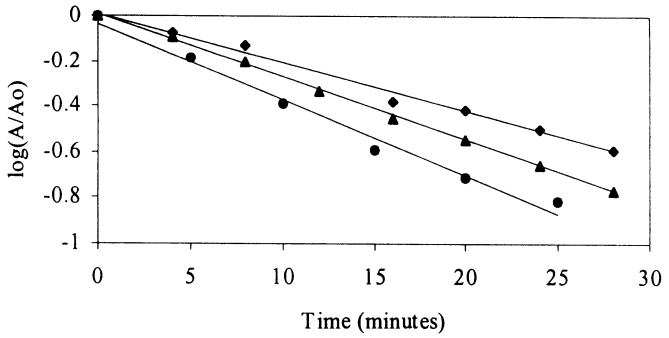

Fig. 1. Isobaric isothermal inactivation of green beans LOX at 6.5 kbar in the subzero and elevated temperature area (♦: –5 °C; ▲: 0 °C and ●: 40 °C)

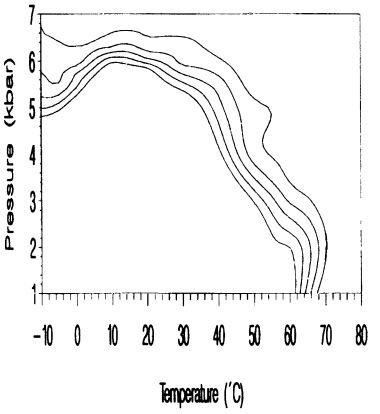

Fig. 2. An iso-D value contour diagram of green beans LOX inactivation as a function of pressure and temperature. The upper and lower lines indicate respectively a D value of 50 and of 150 min

At constant pressure above 5 kbar, the inactivation could be accelerated by increasing temperature above 20 °C or by decreasing temperature below 20 °C. It was observed that at elevated temperatures, the temperature dependence of the D values was increased by a pressure increase (Table 1).

In the entire p/T area investigated, increasing pressure at constant temperature enhanced the inactivation. By plotting the logarithm of D values as a function of pressure, the zp values could be estimated from the reciprocal value of the negative slope. It was noticed that the pressure sensitivity of D values was the highest at temperatures around 10–20 °C (Fig. 3).

Table 1. Temperature sensitivity of D values (°C) of green beans LOX inactivation at constant pressure

Pressure (kbar)	z-value (°C)	RSE (%)[a]	r^2
3	22.3	10.6	0.978
5	35.6	7.2	0.979
5.5	37.8	12.2	0.957
6	49.2	12.2	0.957

[a] residual standard error

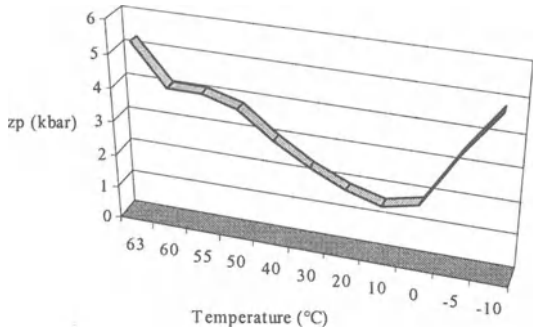

Fig. 3. Evolution of pressure dependency of D values of LOX inactivation in crude green beans extract as a function of temperature

4 Conclusions

Use of real food systems gives an advantage as to obtain a global view of pressure stability of an enzyme as influenced by its natural environment. Application of pressure combined with subzero temperature resulted in irreversible LOX inactivation, therefore, it could be interesting to be combined with food applications in subzero temperature such as freezing, thawing or non-frozen storage under pressure.

Acknowledgements: Our acknowledgements are addressed to Katholieke Universiteit Leuven, the Fund for Scientific Research-Flanders and the European Commission (FAIR-CT96-1175) for their financial support of this research.

References

[1] Kalichevsky *et al.* (1995), Trends Food Sci. Technol., 6, 253–259.
[2] Ludikhuyze *et al.* (1997), Biotechnol. Prog., 13, 532–538.
[3] Weemaes *et al.* (1998), Biotechnol. Bioeng. (in press).

Modeling Kinetics of Pressure-Temperature Inactivation of Enzymes: A Case Study on Soybean Lipoxygenase

L. Ludikhuyze, Indrawati, I. Van den Broeck, C. Weemaes and M. Hendrickx

Katholieke Universiteit Leuven, Department of Food and Microbial Technology, Laboratory of Food Technology, Kardinaal Mercierlaan 92, B-3001 Leuven, Belgium
Phone: 32-16-32.15.85; Fax: 32-16-32.19.60
Linda.Ludikhuyze@agr.kuleuven.ac.be

Abstract. Complete kinetic characterization of thermal (60–70 °C) and pressure-temperature (0.1–650 MPa; 10–64 °C) inactivation of soybean LOX was accomplished. Seemingly, LOX exerted maximal pressure stability at temperatures slightly higher than room temperature. In a final stage, a mathematical model adequately describing pressure-temperature inactivation of soybean LOX was developed, using the Eyring equation as starting point.

1 Introduction

In vegetable products, *especially in leguminosae*, lipoxygenase (LOX) is responsible for at least three detrimental effects [1]: (i) destruction of essential fatty acids, (ii) development of off-flavors and (iii) destruction of vitamins/pigments. Hence inactivation of LOX is pre-requisite to obtaining high-quality minimally processed vegetables. Hitherto blanching is pre-eminently the method to inactivate enzymes and to increase the shelf life of frozen vegetables. Nevertheless some disadvantages are linked to blanching, including loss of texture and nutritional quality, formation of a cooked taste, change in color and loss of soluble solids [2]. To overcome these problems, research for new non-thermal/combined processes has been stimulated. In this context, the potential of high pressure as an alternative to water blanching for inactivation of soybean LOX was kinetically investigated.

2 Materials & Methods

2.1 Enzyme and Activity Measurement

LOX from soybean (Sigma, L7395) was dissolved at a concentration of 0.4 mg/ml in a 0.01 M Tris HCl buffer at pH 9. The activity of the enzyme was measured spectrophotometrically at 234 nm (LKB, UV visible spectrophotometer, Biochrom

4060) using sodium linoleate as substrate. The absorption at 234 nm (25 °C) was recorded as a function of reaction time (3 min) and the activity was determined from the slope of the linear portion of the curve.

2.2 Isothermal and Isobaric-Isothermal Treatment

Isothermal treatments were performed in a thermostated water bath. Isobaric-isothermal treatments were performed in a high pressure equipment, consisting of 8 individual thermostated pressure vessels. After pre-set times, the samples were transferred from the hot water bath or the pressure vessels to a water bath at 25 °C and stored there until activity measurement (≈ 30 min).

2.3 Data Analysis

Kinetic studies allowed a model to be defined, describing quantitatively inactivation of soybean LOX. Both thermal and pressure-temperature inactivation could be accurately described by a first order kinetic model.

Temperature and pressure dependence of the inactivation rate constants could be determined by the equation of Arrhenius (1) and Eyring (2), respectively, where E_a is the activation energy (kJ/mol), R the universal gas constant (kJ/mol), V_a the activation volume (cm^3/mol), T the temperature (°C) and p the pressure (MPa)

$$k = k_{refT} \exp\left[\frac{-E_a}{R}\left(\frac{1}{(T+273)} - \frac{1}{(T_{ref}+273)}\right)\right], \quad (1)$$

$$k = k_{refp} \exp\left(\frac{-V_a}{R(T+273)}(p - p_{ref})\right). \quad (2)$$

The kinetic parameters (k, E_a, V_a) were calculated using a two-step linear regression approach on the linearized (logarithmic) data. Linear regression procedures were performed in the statistical software package SAS.

3 Results & Discussion

3.1 Isothermal and Isobaric-Isothermal Inactivation Kinetics

Isothermal inactivation of soybean LOX occurred in the temperature range 60 to 70 °C with k-values ranging from 2.02×10^{-2} to 15.5×10^{-2} min^{-1}. The activation energy value was calculated as 319.8±27.3 kJ/mol. Isobaric-isothermal inactivation was studied in the pressure range 0.1 to 650 MPa at temperatures between 10 and 64 °C. At constant temperature, k-values consistently increased as a function of pressure. At constant pressure, on the other hand, k-values firstly decreased to

reach a minimum value at temperatures between 30 and 40 °C and then increased again. Hence an antagonistic effect was noted at low temperature (T<40 °C) and high pressure (p>475 MPa). This effect became likewise apparent from a pressure-temperature kinetic diagram (Fig. 1), representing combinations of constant pressure and temperature characterized by the same inactivation rate constant.

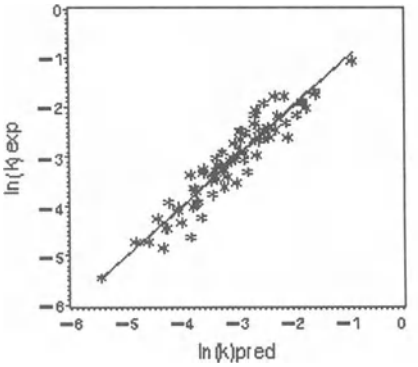

Fig. 1. p/T kinetic diagram for inactivation of soybean LOX

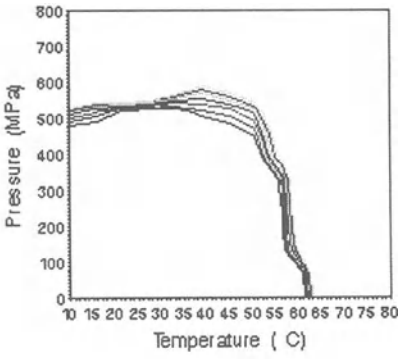

Fig. 2. Accuracy of fitting p/T inactivation of LOX using Eq. (5) and concomitant parameters

Activation volumes at different constant temperatures, calculated according to the Eyring equation, are presented in Table 1. This table clearly indicates the pressure dependence of the inactivation rate constants to be reduced at high temperature. The Arrhenius equation, on the other hand, was not valid over the entire temperature range. Hence activation energies were calculated for distinguished low and high temperature regions. Activation energy values were negative in the low temperature area, ranging from –53.9±3.1 kJ/mol at 525 MPa to –24.4±3.7 kJ/mol at 625 MPa. At high temperature, activation energy values were situated between 48.8±3.8 kJ/mol at 525 MPa and 11.5±3.4 kJ/mol at 575 MPa. In both temperature areas, thermal sensitivity was reduced at high pressure.

3.2 Modeling the Kinetics of Isobaric-Isothermal Inactivation of Soybean LOX

In a final stage it was endeavored to fit a mathematical model describing the combined pressure and temperature dependence of the inactivation rate constants to the entire data set. Since the Eyring equation (2) was valid in the entire experimental domain, this equation, in which k_{refp} and V_a are temperature dependent parameters, was used as starting point. Mathematical expressions (3) and (4) reflecting the temperature dependence of the latter parameters were fit on the data

$$V_a = a_1 T \exp(-b_1 T) \ , \tag{3}$$

$$\ln k_{refp} = a_2 T^2 + b_2 T + c_2 \ . \tag{4}$$

Implementation of these mathematical expressions into the general Eyring equation (2) yielded

$$\ln k = (a_2 T^2 + b_2 T + c_2) - \left(\frac{a_1 T \exp(-b_1 T)}{RT} (P - P_{ref}) \right) , \tag{5}$$

which was checked on its ability to predict isobaric-isothermal inactivation of soybean LOX. Kinetic parameter values, estimated using a non-linear regression procedure, are presented in Table 2 while the appropriateness of the proposed model and concomitant parameters in describing isobaric-isothermal inactivation of soybean LOX is shown in Fig. 2.

Table 1. Activation volumes for p/T inactivation of soybean LOX at ≠ constant T

T (°C)	V_a (cm^3/mol)
10	–62.6±3.1
15	–67.7±12.1
20	–66.5±2.8
25	–67.2±5.9
30	–67.9±7.5
35	–65.3±2.5
40	–48.9±4.4
45	–45.6±4.5
50	–22.7±3.3
55	–9.9±0.4
62	–8.6±1.4
64	–7.1±0.5

Table 2. Kinetic parameters for p/T inactivation of soybean LOX calculated according to Eq. (5)

Parameter	Estimated value
a_1	–15.6±1.4
b_1	(7.1±0.28)x10^{-2}
a_2	(2.66±0.27)x10^{-3}
b_2	(–1.39±0.18)x10^{-1}
c_2	–3.12±0.28
corrected r^2	0.991

Acknowledgements: This research has been supported by the National Fund for Scientific Research, the European Commission, the KULeuven Research Council and the Federal Office for Scientific, Technical and Agricultural Affairs.

References

[1] Whitaker, J.R. Lipoyxgenase. In Principles of enzymology for the food sciences; M. Dekker, New York, 1972, chapter 25, pp. 607–617.

[2] Williams, D.C. *et al.* Blanching of vegetables for freezing: which indicator enzyme to choose. Food Technology, 1986, 40(6), 130–140.

Effect of pH and Antibrowning Agents on the Pressure Stability of Avocado and Mushroom Polyphenoloxidase

C. Weemaes, L. Ludikhuyze, I. Van den Broeck and M. Hendrickx

Katholieke Universiteit Leuven, Department of Food and Microbial Technology, Laboratory of Food Technology, Kardinaal Mercierlaan 92, B-3001 Leuven, Belgium
Phone: 32-16-32.15.85; Fax: 32-16-32.19.60
Carla.Weemaes@agr.kuleuven.ac.be

Abstract. The effect of pH on the pressure stability of mushroom and avocado PPO was similar: pH reduction below 6.5–7 resulted in a reduced inactivation threshold pressure and an increased absolute value of the activation volume. The effect displayed by the antibrowning agents studied was dependent on the enzyme origin. Sensitisation of mushroom PPO was achieved by addition of 2.5 mM 4-hexylresorcinol. In case of avocado PPO, sensitisation towards pressure was most pronounced in the presence of EDTA.

1 Introduction

Polyphenoloxidase (PPO) is responsible for the browning of fruits and vegetables during post-harvest handling, processing and storage, and for discoloration of some fungi (*e.g.* mushroom). In the presence of oxygen, PPO catalyses the conversion of naturally occurring phenols into *o*-quinones, which subsequently polymerise to brown pigments. Apart from this colour deterioration, enzymatic browning results in the development of unpleasant flavours and a lowering of the nutritional value. Because of this decreased market value, control of enzymatic browning is very important to food manufacturing industries [1, 2]. Enzymatic browning prevention can be achieved by chemical and physical treatments, *i.e.* addition of antibrowning agents and inactivation treatments [3]. In the present article, the combined effect of chemical and physical (high pressure) treatments is investigated.

2 Materials & Methods

2.1 Enzyme and Activity Measurement

To investigate the effect of pH, commercial mushroom PPO (Sigma) and partially purified and lyophilised avocado PPO were dissolved in McIlvaine buffer (MB; pH 4–6.5) or 0.1 M phosphate buffer (PB; pH 6–8) at a concentration of respectively

0.08 and 3 mg lyophilised powder/ml. To investigate the effect of antibrowning agents, EDTA, NaCl, benzoic acid (BA), 4-hexylresorcinol (4-HR) or glutathione (GL) was added to the enzyme solutions [0.1 M PB, pH 6.5, 0.08 mg/ml for mushroom PPO; MB, pH 5, 0.5 mg/ml for avocado PPO]. In case of mushroom PPO, a fixed additive concentration of 5 mM was used, except for 4-HR (2.5 mM). In case of avocado PPO, an additive concentration that resulted in at least 20% activity reduction was selected, *i.e.* 10 mM EDTA, NaCl or BA, or 0.05 mM 4-HR or GL. The enzyme activity was measured spectrophotometrically (catechol as substrate).

2.2 Pressure Treatment

Isobaric treatments (at 25 °C) were performed in a multivessel high pressure apparatus (8 pressure vessels). After pre-set times (t), the samples were removed from the individual pressure vessels and transferred to ice water. After a storage period of 10–60 min, the residual enzyme activity was determined.

2.3 Data Analysis

Kinetic studies were performed to quantitatively describe the pressure inactivation of PPO. The pressure inactivation of mushroom PPO could, under all conditions studied, adequately be described by a first-order inactivation model. The pressure inactivation of avocado PPO appeared to display first-order kinetics in some conditions and showed fractional conversion behaviour in other conditions.

The pressure (p) dependence of the inactivation rate constants (k) could be expressed by the Eyring equation (1), where associated activation volume (V_a), k_{ref}, R and T respectively represent the k-value at a reference pressure (p_{ref}), the universal gas constant and the absolute temperature

$$k = k_{ref} \times \exp\left(\frac{-V_a(p - p_{ref})}{RT}\right). \quad (1)$$

3 Results & Discussion

3.1 Effect of pH on the Pressure Stability of PPO

At all pH values studied, the pressure inactivation (650–900 MPa) of mushroom PPO could accurately be described by a first-order kinetic model. Likewise, the pressure inactivation of avocado PPO (3 mg/ml; 650–900 MPa) at pH 5–8 appeared to follow first-order kinetics. At pH 4, on the other hand, fractional conversion behaviour was observed at 550–650 MPa. This particular kinetic

inactivation behaviour seemed to be due to a considerable difference in pressure stability of the two isozymes at this pH value. At pH 4, inactivation of the most pressure labile isozyme was noticeable at about 450 MPa. For inactivation of the more pressure stable isozyme at least 700 MPa was required. At pH 5–8, no difference in the pressure stability of the isozymes was noticed.

For both enzymes, the threshold inactivation pressure decreased with decreasing pH. The variation of the *k*-value with pressure is illustrated in Fig. 1, for both mushroom and avocado PPO. It seems that for both enzymes the absolute value of the activation volume decreased with increasing pH. The decrease was however much more pronounced in the case of mushroom PPO.

The increased pressure sensitivity of the enzyme when dissolved in acid media is interesting with regard to potential applications, since fruits and their derived products are mostly characterised by a low pH, and acid products are currently the most likely candidates for high pressure processing.

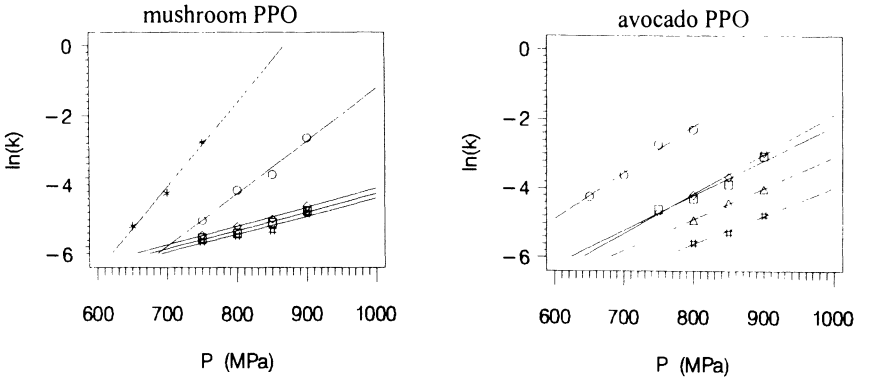

pH: (*) 4, MB; (O) 5, MB; (□) 6.5, MB; (◊) 6.5, PB; (#) 8, PB

pH: (O) 5, MB; (□) 6, MB; (◊) 6, PB; (#) 7, PB; (?) 8, PB

Fig. 1. Influence of pH on the pressure inactivation of mushroom and avocado PPO

3.2 Effect of Antibrowning Agents on the Pressure Inactivation Kinetics

In the presence of BA, EDTA, NaCl, 4-HR or GL, first-order inactivation kinetics of mushroom PPO were also observed. The presence of 4-HR resulted in a marked decrease of the threshold inactivation pressure for this enzyme. In the presence of this antibrowning agent, inactivation at pH 6.5 was observable at about 650 MPa. The presence of EDTA, on the other hand, resulted in a minor stabilisation of mushroom PPO. The pressure stability of the enzyme was not significantly altered by the other antibrowning agents tested. Only in the presence of 2.5 mM 4-HR, was the activation volume significantly changed.

Contrary to the inactivation at an enzyme concentration of 3 mg/ml, the inactivation of avocado PPO (pH 5) at a concentration of 0.5 mg/ml appeared to follow fractional conversion kinetics. The pressure sensitive isozyme could be inactivated by pressures exceeding 650 MPa, whereas inactivation of the more stable isozyme

necessitated about 825 MPa. Because of the pronounced stability of the latter isozyme, the effects of the selected antibrowning agents were only investigated for the most pressure sensitive isozyme. Addition of GL, BA or NaCl to the avocado PPO solution resulted in a stabilisation of the sensitive isozyme towards pressure (Fig. 2). Addition of EDTA resulted, on the other hand, in a considerable reduction of the pressure stability of the isozyme under consideration. The effect brought about by 4-HR was dependent on the pressure applied: at pressures below about 700 MPa a sensitising effect was observed, whereas at higher pressures the effect was stabilising. Only the presence of BA or 4-HR significantly altered the pressure dependence of the inactivation rate constants. Both in the case of BA and 4-HR, the activation volume was reduced by a factor 1.6.

Whereas the effect of pH on the pressure stability of avocado and mushroom PPO was comparable, it is clear that the pressure stability of the enzymes is distinctly affected by the antibrowning agents studied.

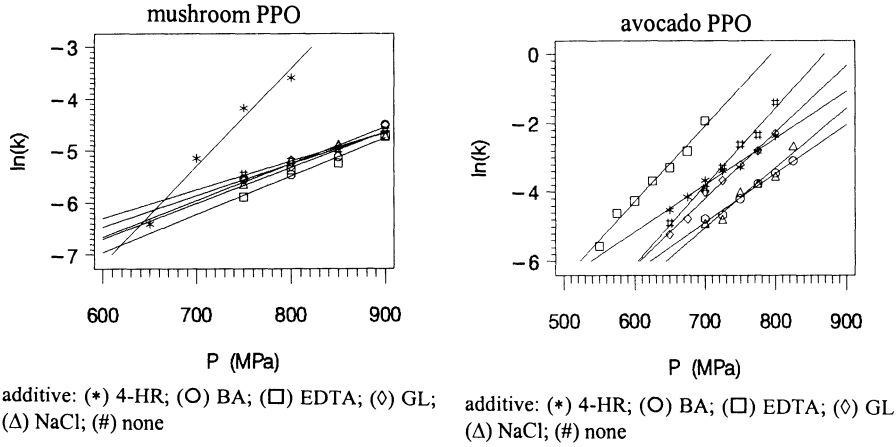

additive: (*) 4-HR; (O) BA; (□) EDTA; (◊) GL; (Δ) NaCl; (#) none

additive: (*) 4-HR; (O) BA; (□) EDTA; (◊) GL; (Δ) NaCl; (#) none

Fig. 2. Influence of antibrowning agents on the pressure stability of PPO

Acknowledgements: This research has been supported by the Flemish Institute for the Promotion of Scientific-Technological Research in Industry (IWT), the European Commission (project FAIR-CT96-1175), KULeuven Research Council (OT/94/19) and the Belgian Primeminister's Office of the Federal Office for Scientific, Technical and Agricultural Affairs (N0/01/010).

References

[1] Vámos-Vigyázó, L. (1981). Polyphenoloxidase and peroxidase in fruits and vegetables. Crit. Rev. Food Sci. Nutr. 5: 49–127.

[2] Whitaker, J.R.; Lee, C.Y. (1995). Recent advances in chemistry of enzymatic browning: an overview. In: Enzymatic browning and its prevention; Whitaker, J.R. and Lee, C.Y. American Chemical Society, Washington DC, pp. 2–7.

[3] McEvily, A.J.; Iyengar, R.; Otwell, W.S. (1992). Inhibition of enzymatic browning in foods and beverages. Crit. Rev. Food Sci. Nutr. 32: 253–273.

Thermal and Combined Pressure–Temperature Inactivation of Orange Pectinesterase: Influence of pH and Ca^{2+}-Ions

I. Van den Broeck, L.R. Ludikhuyze, A.M. Van Loey, C.A. Weemaes and M.H. Hendrickx

Laboratory of Food Technology, Department of Food and Microbial Technology, Faculty of Agricultural and Applied Biological Sciences, Katholieke Universiteit Leuven, Kardinaal Mercierlaan 92, B-3001 Heverlee, Belgium
Ilse.den@agr.Kuleuven.ac.be

Abstract. Inactivation of commercially available orange pectinesterase (PE) was investigated under isothermal and isothermal-isobaric conditions. In both cases, inactivation data could be accurately described by a fractional conversion model. The influence of pH and Ca^{2+}-concentration on the inactivation kinetics was studied. Acidification accelerated thermal as well as pressure-temperature inactivation. An increased Ca^{2+}-concentration caused sensitization to both temperature and pressure and increased the residual fraction of active PE after thermal treatment.

1 Introduction

Pectinesterase (PE) is an enzyme which is found in fruits and vegetables. It is bound by electrostatic interaction to the cell wall. Therefore, on juice extraction, it is technologically impossible to avoid contamination of the juice with this enzyme. In the cloudy juice, PE hydrolyses the pectin methyl esters of polygalacturonic acid transforming it gradually into low methoxy pectin or pectic acids. This de-esterification reduces juice viscosity and the low methoxy pectin formed complexes with calcium to form insoluble calcium flocculation resulting in cloud loss. These quality defects can be minimized by inactivating PE. Pasteurization is a conventional method used to inactivate PE. However, in recent years, there is growing consumer demand for high quality juices and fruit based products. This has led to the investigation of alternative, less severe methods to extend shelf life of juice products without the flavor and nutrient degradation which occur during thermal pasteurization. One of the most innovative technologies for processing of thermosensitive products is pressure treatment As its effect on food ingredients can be related to the fact that mainly noncovalent bonds are affected, food quality factors, such as nutrients, pigments and flavor remain mostly unchanged whereas microorganisms and enzymes are inactivated. However, sometimes very high

pressures are needed to inactivate bacterial spores and several enzymes. Therefore combination with other treatments, such as mild heating, is recommended.

Research has already been performed on the preservation of citrus fruit juices and the inactivation of orange PE by pressure [1]. Although some promising results were obtained, more information, mainly kinetic information, is indispensable in order to optimize the application of this new technology. Therefore, the main objective of the present study was to investigate the high pressure and/or temperature inactivation kinetics of orange PE. As several reports have already pointed out that PE is only partly inactivated by temperature and pressure, the influence of sensitizing factors such as pH and Ca^{2+}-ions was evaluated.

2 Materials & Methods

2.1 Pectinesterase and Activity Assay

Pectinesterase purified from orange peel was purchased as a lyophilized powder. The activity was determined titrimetrically. During hydrolysis at 22 °C, the pH was maintained at 7.0 by addition of 0.01 N NaOH using an automatic pH-stat titrator. The PE activity is proportional to the consumption rate of NaOH ($\Delta V_{NaOH}/\Delta t$).

2.2 Thermal and Pressure-Temperature Treatment

Isothermal treatment was performed in a water bath with temperature control. Orange PE solution, filled in capillary tubes, was immersed during pre-set times in the water bath at constant temperature.

Isobaric-isothermal treatment was conducted in a multivessel high pressure equipment (Resato, Holland). This pressure equipment allows combination of high pressure with temperatures between –20 and 100 °C. The samples, contained in flexible microtubes, are treated during pre-set times in the individual vessels of the pressure equipment.

2.3 Data Analysis

Inactivation of orange PE could be accurately described by a fractional conversion model (1). The temperature dependence of the inactivation rate constant, expressed by the activation energy (E_a), was calculated according to the Arrhenius law (2). The activation volume (V_a), indicating the pressure dependence of the inactivation rate constant, was calculated according to the theory of Eyring (3)

$$A_t = A_\infty + (A_0 - A_\infty)\exp(-kt)\,. \tag{1}$$

$$k = k_{\text{ref}} \times \exp\left[\frac{-E_a}{R}\left(\frac{1}{T} - \frac{1}{T_{\text{ref}}}\right)\right] \quad (2)$$

$$k = k_{\text{atm}} \times \exp\left[\frac{-V_a}{RT}\left(p - p_{\text{ref}}\right)\right] \quad (3)$$

3 Results & Discussion

3.1 Thermal Inactivation Kinetics

Model systems. After inactivating orange PE in water at temperatures up to 65 °C, a certain fraction remained active and hence the fractional conversion model was used to fit the inactivation data. The residual active fraction is independent of the temperature level in the temperature domain studied and is about 5% of the initial activity. This thermostable fraction can be completely inactivated by heating the sample for 1 min at 85 °C. Based on the estimated inactivation rate constants an activation energy of 327 kJ/mol was calculated.

Influence of pH. A citric acid buffer 5 mM, pH 3.7 (pH of commercially available orange juice) was used to study the influence of pH. Orange PE inactivates faster and at lower temperatures in citric acid buffer than in water, which means that orange PE is less thermostable in an acid medium. Moreover, the inactivation rate constant in citric acid buffer pH 3.7 is less temperature sensitive than the inactivation rate constant in water. Regarding the residual fraction of active PE, this fraction is obviously more temperature dependent in buffer than in water. A decrease in the residual fraction is observed with increasing temperature. This indicates that the residual fraction of active PE after treatment in a similar temperature domain is smaller in buffer than in water.

Influence of Ca^{2+}-ions. A 0.5 M, 1 M and 1.5 M $CaCl_2$-solution was used to study the influence of Ca^{2+}-ions. Ca^{2+}-ions decreased the thermal stability of PE. However, the temperature sensitivity of the *k*-value was not significantly influenced. Although orange PE was less thermostable in the presence of Ca^{2+}-ions, the percentage of residual PE after treatment was higher. Moreover, increasing the Ca^{2+}-concentration decreased the thermal stability of PE, lowered the inactivation temperature and resulted in a larger percentage of residual PE after treatment (respectively 24%, 28% – 36% for 0.5 M, 1 M and 1.5 M $CaCl_2$ solution). This fraction was clearly independent of the temperature level in the temperature domain studied.

3.2 Pressure-Temperature Inactivation Kinetics

Model systems. A synergistic effect of pressure and temperature was observed for the inactivation of orange PE in water; similar inactivation rate constants were obtained at lower temperatures if higher pressures were applied. Because no complete inactivation of the enzyme was attained after pressure treatment (6 to 9% of the original activity), it is assumed that PE isoenzymes with high heat resistance may also show pressure resistance. This residual fraction seemed to be independent of temperature and/or pressure in the pressure-temperature domain studied. From the estimated inactivation rate constants at elevated pressure and 25 °C an activation volume of –23 cm^3/mol was calculated.

Influence of pH. As for thermal treatment a citric acid buffer, pH 3.7, was used to study the influence of pH on combined pressure-temperature inactivation of orange PE. Pressures ranged from 400 to 600 MPa while temperatures from 18 to 28 °C were applied. A synergistic effect of pressure and temperature was observed and the inactivation rate was more enhanced in acid buffer than in water. Moreover, a decreased temperature sensitivity of the rate constant at elevated pressure was observed. The activation volume seemed to be independent of the temperature. Regarding the residual fraction of active PE after treatment, this fraction was of the same order of magnitude as for the inactivation in water.

Influence of Ca^{2+}-ions. An increased Ca^{2+}-concentration caused sensitization to combined pressure-temperature treatment. The residual fraction of active PE was independent of the pressure level and was not significantly different from the residual fraction obtained in the absence of Ca^{2+}-ions. Also the activation volume was not significantly influenced by addition of Ca^{2+}-ions.

References

[1] Ogawa, H.; Fukuhisa, K.; Kubo, Y.; Fukumoto, H. Pressure inactivation of yeasts, molds, and pectinesterase in satsuma mandarin juice: effects of juice concentration, pH, and organic acids, and comparison with heat sanitation. Agric. Biol. Chem., 54 (5), 1219–1225, 1990.

Properties of a Soluble Form of High-Pressure-Treated Egg Albumen

S. Iametti[1], E. Donnizzelli[1], P. Pittia[2], P.P. Rovere[3], N. Squarcina[3] and F. Bonomi[1]

[1]Dipartimento di Scienze Molecolari Agroalimentari, University of Milan, Via Celoria 2, I-20133 Milan, Italy
[2]Dipartimento di Scienze degli Alimenti, University of Udine, Via Marangoni 97, Udine, Italy
[3]SSICA, Via Tanara 31, Parma, Italy
stefania.iametti@unimi.it

Abstract. Addition of NaCl or sucrose to egg albumen prior to high-pressure treatment (up to 10 min at 800 MPa) prevented insolubilization or gel formation after pressure treatments of sufficient intensity for microbiological sanitation. As a consequence of protein unfolding, the treated albumen had increased viscosity, but retained its foaming and heat-gelling properties. The S-form of ovalbumin, whose presence is an index of egg aging, was not found in any of the pressure-treated samples, that also did not display evidence for covalent protein aggregation. Susceptibility of egg albumen proteins to hydrolysis by trypsin increased dramatically after pressure treatment, in particular when sucrose was used. Pressure treatment reduced recognition of ovalbumin by an anti-ovalbumin antiserum to 40% of that of untreated albumen. Most of the properties of the treated material, including the different effects of sucrose and NaCl, are explainable in terms of pressure-induced modifications of protein structure.

1 Introduction

Egg albumen represents an extensively used food ingredient, mostly because of its functional properties. The gelling, emulsifying, and foaming properties of fresh albumen are fundamental for making possible the production, and for assessing some sensorial properties (texture, flavor, etc.), of many foods. However, most of the functional properties of egg albumen are lost or modified after even the mildest heat treatments (such as pasteurization), that are normally used for the sanitation of egg components. Liquid egg white partially coagulates when treated at pressure >500 MPa [1], and strong self-supporting gels are formed at pressure higher than 600 MPa, but the hardness and the elastic modulus of the pressure-formed gels remain significantly lower than those of gels obtained by heat treatment [2]. Nevertheless, even in the presence of marked physical changes, the pressure-treated materials were reported to retain their natural flavor and nutritional value [3]. In this study we report on some modifications induced by pressure treatment

on albumen at pressure/time combinations that are relevant to food sanitation [4], in conditions where formation of gels was not observed, thus making the product suitable for direct replacement of fresh albumen.

2 Materials & Methods

Eggs were collected from a local market. High-pressure treatments were performed on bulk albumen separated from eggs, after gentle addition of 10% (w/w) sucrose or NaCl. Pressure treatment was carried out in water at a nominal temperature of 25 °C in a isostatic high-pressure generator ABB Model QFP-6 (ABB, Sweden). The sanitizing effects of high-pressure treatments were evaluated on whole eggs by means of a microbial challenge test. For assessing foaming properties, egg albumen was beaten for 3.5 min at 25 °C with a Philips Masterchef beater set at maximum speed. Foam density was measured by weight. Foam consistency was measured in triplicate assays by using a Stable Micro System texture analyzer equipped with a 2.5 kg detection cell. Heat-set gels from pressure-treated samples were prepared by heating at 90 °C for different times (10–60 min) in a water bath. Analysis of the strength of the gel was performed using an Instron Universal testing machine. ELISA tests were performed according to published procedures [5]. Susceptibility of albumen samples to tryptic hydrolysis was detected by incubation of 0.4 ml of diluted albumen samples (containing 1 mg/ml protein in 5 ml sodium phosphate buffer pH 6.8) with 0.5 mg of trypsin at 37 °C. The proteolytic reaction was stopped by adding 0.4 ml of 20% (w/v) trichloroacetic acid, followed by centrifugation at 13.000 × g for 15 min. The hydrolyzed substrate was expressed as the amount of tyrosine released in the supernatant, determined by using A_{280}= 1.25 for tyrosine.

3 Results

We found that addition of 7–10% (w/v) NaCl or sucrose to egg albumen prior to high-pressure treatment prevented insolubilization of protein and formation of gels after pressure treatments that were of sufficient intensity for microbiological sanitation, but were suitable (also in economic and practical terms) for application in the preparation of food ingredients. Treatments ranging from 5 min at 400 MPa to 10 min at 800 MPa were found to be of equal or better efficiency than pasteurization as well as for microbial count reduction in whole egg samples challenged before the treatment with common microbial contaminants of eggs (*Escherichia coli, Staphylococcus aureus, Streptococcus faecium).*

The pressure-treated soluble albumen had an increased viscosity, but retained almost completely the foaming and heat-gelling properties of untreated albumen, as shown in Table 1.

Table 1. Effects of high pressure treatment (600 MPa, 5 min, 25 °C) on the physical properties of egg albumen containing NaCl or sucrose, and of gels and foams obtained from treated and untreated albumen

Material or product	Property	10% Sucrose		10% NaCl	
		untreated	treated	untreated	treated
albumen	viscosity, Pa	0.04	0.41	0.02	0.14
heat-set gels	strength, N[a]	4.62	3.11	3.35	3.89
foams	A1[b], g × s	2267	1228	2615	1322
	A2[c], g × s	1326	872	1655	901
	consistency, A1/A2	1.71	1.41	1.58	1.47
	density, g/ml	0.26	0.31	0.25	0.18

[a]coagulated by heating for 30 min at 90 °C
[b]data refer to the measured area during probe penetration in foam (A1)
[c]data refer to the measured area during probe release from foam (A2)

The S-form of ovalbumin, an index of egg aging, was not detectable in any of the treated samples, that also did not display any evidence of covalent protein aggregation or of proteolytic degradation according to standard biochemical separation techniques (electrophoresis, and ion-exchange or size-exclusion HPLC).

Susceptibility of egg albumen to tryptic hydrolysis increased dramatically after pressure treatment, in a pressure-dependent fashion. As shown in Table 2, treatment in the presence of sucrose gave an increase in susceptibility to proteolysis larger than that observed after treatment in the presence of NaCl. As also given in Table 2, we found that recognizability of ovalbumin by anti-ovalbumin antisera in the treated albumen was reduced to about 40% of that of untreated albumen, irrespective of whether NaCl or sucrose were used during the pressure treatment.

Table 2. Effects of high pressure (600 MPa, 5 min) on some biochemical properties of egg albumen containing NaCl or sucrose

Property	10% Sucrose	10% NaCl
digestibility by trypsin[a]	1500	500
residual recognition by anti-ovalbumin antibodies[a]	39	42

[a]results are given as percent of untreated albumen and are the average of triplicate experiments

Under the same treatment conditions, loss of antibodies recognition and increase in proteolyzability by trypsin in pressure-treated albumen were identical to that measured when treating isolated ovoalbumin at relatively low protein concentration in phosphate buffer at pH 7.0 [5]. The absence of differences between the two systems is surprising when considering the high pH of albumen, and possible effects of other albumen proteins that could make ovalbumin in whole albumen less sensitive to pressure denaturation. Results of proteolysis studies

confirm the prominent role of ovalbumin in assessing the pressure-induced modifications of albumen.

The technological and health-related properties of the treated albumen make it interesting for direct use in the food industry (bakery, confectionery, dairy, etc.) as a suitable substitute for fresh, dried or pasteurized albumen. If current tests on products made by using the treated albumen show retention of the interesting features observed in this study, high-pressure treatment could become the elective treatment of egg-white based foods whenever increased digestibility – and, possibly, increased tolerance by sensitive individuals – is required.

Acknowledegments: Work supported in part by grants of the Italian Ministry for the University and Scientific and Technological Research (MURST, Rome, Italy, National Project "Biocatalisi e Bioconversioni").

References

[1] Messens, W.; Van Camp, J.; Huyghebaert, A. The use of high pressure to modify the functionality of food proteins. *Trends in Food Science & Technology* **1997,** *8,* 107–112.

[2] Okamoto, M.; Kawamura, Y.; Hayashi, R. Application of high pressure to food processing: textural comparison of pressure and heat-induced gels of food proteins. *Agric. Biol. Chem.* **1990,** *54,*183–189.

[3] Mine, Y. Recent advances in understanding of egg white protein functionality. *Trends in Food Science & Technology* **1995,** *6,* 225–230.

[4] Miglioli, L.; Gola, S.; Maggi, A.; Rovere, P.; Carpi, G.; Scaramuzza, N.; Dall'Aglio, G.F. Microbiological stabilization of low-acid food using a combined high-pressure temperature process. In *High pressure research in the biosciences and biotechnology;* Heremans, K., Ed., Leuven University Press, 1997,277–280.

[5] Iametti, S.; Donnizzelli, E.; Vecchio, G.; Rovere, P. R.; Gola, S.; Bonomi, F. Macroscopic and structural consequences of high-pressure treatment of ovalbumin solutions. *J. Agric. Food Chem.* **1998**, in press.

Nucleic Acids and Linear Polymers

DNA Supercoiling Under High Pressure

G-Q. Tang and S. Kunugi

Department of Polymer Science and Engineering, Kyoto Institute of Technology, Matsugasaki, Sakyo-ku, Kyoto 606-8585, Japan

Abstract. By using supercoiling assays including relaxing supercoiled/nicked DNA by wheat germ topoisomerase I and self-re-ligating linear DNA by T4 DNA ligase, effects of elevated pressure on the conformation of supercoiled DNA were addressed. The shifting behaviors of topoisomers resulting from supercoiling assays and shown by agarose gel electrophoresis indicated that elevated pressure shifted DNA supercoiling toward a more twisted state. Pressure-induced changes in DNA supercoiling have been quantified and are proposed to connect with pressure-induced perturbation of DNA conformation, probably *via* a channel of volume differences of supercoiled DNA corresponding to different superhelicities.

1 Introduction

DNA supercoiling and changes are of critical importance in various cellular processes such as gene replication, transcription and recombination, and chromosome segregation [1]. The extent of DNA supercoiling *in vivo* is mainly regulated by DNA topoisomerases (I and II), while many DNA-binding proteins and intercalated drugs play a balanced role. The tertiary structure of DNA is also sensitive to various environmental factors such as salt, temperature, and osmolarity [2–4]. Effects of environmental factors, drug or protein binding on DNA supercoiling in terms of the linking number (*Lk*), twisting number (*Tw*) and writhing number (*Wr*) can be monitored through the resulting changes in DNA topoisomer distribution through agarose gel electrophoresis.

Pressure is an important experimental variable which affects various biological processes involving some volume changes [5]. The secondary structure of DNA is stabilized by pressure elevations up to 200–300 MPa, largely owing to the enhancement of base stacking by increasing the pressure. Pressure-assisted changes in the higher-order structure of polynucleotides seemed to be only shown by the B-Z structural transition of poly[d(G-C)]$_2$ at a high level of pressure (600 MPa) and extremely high salt concentrations [6].

Here, supercoiling assays of supercoiled or linear DNA in the presence of wheat germ topo I or T4 DNA ligase were conducted in elevated pressures. It was found that the distribution of DNA topoisomers resulting from the reactions under

elevated pressure were modified such as moving down in gel electrophoresis, indicative of pressure effects on winding of the DNA helix.

2 Materials & Methods

Wheat germ DNA topo I was purchased from Promega (USA). T4 DNA ligase was purchased from Life Tech. (USA). Highly negative supercoiled pBR322 DNA was purchased from Boehringer Mannheim (FRG). Crystallized phenol was obtained from Wako Pure Chemicals (Osaka, Japan) and was equilibrated in 10 mM Tris-HCI (pH 8.0). Agarose S was obtained from Wako.

The relaxation reaction of DNA using wheat germ topo I was performed in a buffer of 50 mM Tris-HCI, pH 8.0, 50 mM NaCl, 5% glycerol in 20 °C. 5 U of topo I were used to relax 0.75 μg DNA in a total volume of 30 μl assay solution for 15 to 24 h. The relaxation reaction was stopped by phenol/chloroform extraction, and DNA was recovered by ethanol precipitation and re-suspended in a gel loading buffer (10 mM Tris-HCI, pH 8.0, 2 mM EDTA, 50% glycerol and 0.02% bromophenol blue).

Linear pBR322 DNA was obtained from a full cleavage of closed-circular DNA by restriction endonuclease EcoRI (Toyobo, Japan). The 20-hours recyclization reaction by T4 DNA ligase (1–2 Weiss units) was conducted at 20 °C in a buffer containing 50 mM Tris-HCl (pH 7.6), 10 mM $MgCl_2$, 1 mM ATP, 1 mM DTT, and 5% polyethylene glycol-8000.

The distributions of relaxation reactions were evaluated by 1% agarose gel electrophoresis with TBE buffer at room temperature (21–22 °C). When necessary, chloroquine was added in the TBE buffer (0.75 μg/ml). After electrophoresis, the gel was stained by 1.0 μg/ml ethimide bromide prior to being photographed under short wave UV-illuminance. The photos were analyzed using NIH Image 1.61 software.

All high pressure incubations were done in a pressure vessel (Yamamoto Suiatsu Co., Japan). Except for the pressure applied, all other conditions were the same as those applied for the control tests done at 0.1 MPa.

3 Results & Discussions

The relaxation reaction of pBR322 DNA catalyzed by wheat germ topo I or by T4 DNA ligase was found to be slowed by pressure elevation. Stopping the topoisomerization reaction of topoisomerase I conducted under elevated pressure prior to its completion, a mixture of partly relaxed DNA, intact supercoiled DNA and open-circle DNA was found, suggesting a mode of distributive relaxation as the leading mechanism of the enzyme in elevated pressure. Since topo I that individually experienced pre-incubations in atmospheric or high pressure displayed nearly identical abilities in relaxing negative supercoiled DNA at 0.1 MPa, the impact of pressure elevation on the structure of topo I may be either reversible or

negligible, and was not responsible for change in topoisomer distributions. Similar conclusions can be applied to T4 DNA ligase.

Effects of high pressure on the unwinding reactions of the negatively supercoiled pBR322 DNA to completion by topo I were evaluated by agarose gel electrophoresis at room temperature without or with additions of chloroquine. Gel electrophoresis results are exemplified in Fig. 1 A. It is shown that the resulting distribution patterns of DNA topoisomers were altered after the application of elevated pressure during the supercoiling assays. The products of the relaxation reactions deriving from reactions at elevated pressure migrated faster in the agarose gel than those deriving from reactions at 0.1 MPa, indicating an increase in DNA supercoiling to the positive direction. The presence of the DNA intercalative drug chloroquine in agarose gel electrophoresis in a low concentration selectively decreases the number of negative supercoiled DNA, while it increases the number of positive supercoiling DNA. One reason for the undistinguishable mobility of positive DNA topoisomers in agarose gel electrophoresis may be the concentration of chloroquine. Differences in the linking number of resulting relaxed forms of DNA as a function of pressure were measured by band-counting from a gel scan [3, 7]. Figure 2 displays the shifts in Gaussian centers of DNA topoisomer distributions [3, 7] following pressure elevations.

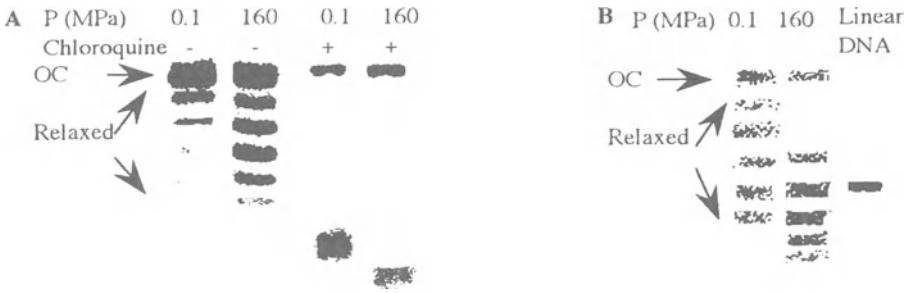

Fig. 1. Typical presentations of pressure effects on DNA supercoiling assays in the presence of (**A**) topo I or (**B**) T4 DNA ligase

We also performed the supercoiling assay by resealing linear or nicked pBR322 DNA in the presence of T4 DNA ligase to further address the effects of elevated pressure. Selected results of reactions separately carried out in atmospheric or under elevated pressures are shown in Fig. 1B. Similarily, the engagement of elevated pressure on the re-ligation reactions induced the altered distributions of DNA topoisomers.

Referring to an equation to express the twisting effects on DNA the helix [3], the winding effect of pressure on the DNA helix can be expressed as $\partial\theta/\partial p$ = (360°/l) $\partial(\Delta LK)/\partial p$, where θ is the angular degree of winding/unwinding DNA helix, p is pressure, 1 is the length of DNA (base pairs), and ΔLK is the linking number differences. The averaged extent of the increase in the winding of the DNA helix by pressure elevations at 20 °C was determined to be a 1.1×10^{-3}°/base/MPa

in the absence of Mg^{2+} in the reaction buffer, and 1.6×10^{-3}°/base/MPa in the presence of 10 mM Mg^{2+}, if a linear function was used. It is not clear whether this discrepancy in quantifying pressure effects was due to certain interactions between pressure
and the DNA binding of divalent ions or was just within the experimental

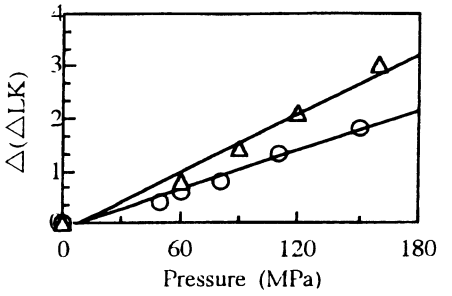

Fig. 2. Pressure dependence of changes in the Gaussian centers of topoisomer distributions as collected from supercoiling assays using topo I (O) or T4 DNA ligase (Δ)

fluctuations. For the helix of pBR322 DNA with 4361 base pairs, this implies a further winding by 4–6° under a stress of 1 MPa. Because the linking number of covalently closed-circular DNA remains unchanged unless the DNA experiences a breakage-resealing cycle, the increase in DNA supercoiling after the relaxation reaction incubated at elevated pressure was presumably achieved as a pressure-modified equilibrium of the population distributions of DNA conformations in thermal fluctuation [3, 7, 8]. Since exerting pressure effects in order to shift the system equilibrium requires the presence of volume differences, it is conceivable that a higher superhelicity of DNA, such as that found at elevated pressures, connects with a more compact and bent supercoiled structure. This is comparable to the results found in increased salt concentrations [8].

References

[1] Wang, J.C. (1996); Ann. Rev. Biochemistry. 65, 635–692.
[2] Anderson, P., and Bauer, W. (1978); Biochemistry. 17, 594–601.
[3] Depew, R.E., and Wang, J.C. (1975); Proc. Natl. Acad.Sci. USA. 72, 4275–4279.
[4] Lee, C-H., Mizusawa, H., and Kakefuda, T. (1981); Proc. Natl. Acad.Sci. USA. 78, 2838–2842.
[5] Kunugi, S. (1993); Prog. Polym. Sci. 18, 805–838.
[6] Krzyzaniak,A., Salanki, P., Jurcazk, J., and Barciszewski, J. (1991); FEBS. Lett. 279, 1–4.
[7] Pulleyblank, D., Shure, M., Tang, D., Vinograd, J., and Vosberg, H.-P. (1975); Proc. Natl. Acad. USA. 72, 4280–4284.
[8] Vologodskii, A.V., and Cozzarelli, N.R. (1994); Annu. Rev. Biophys. Biomol. Struct. 23, 609–643.

Pressure Effect on the Chain Shrinkage of Water Soluble Polymers Induced by Complexation with ANS

N. Tanaka[1], M. Takemura[1], T. Konno[2] and S. Kunugi[1]

[1]Department of Polymer Science and Engineering, Kyoto Institute of Technology, Sakyo, Kyoto 606-8585, Japan
[2]National Institute for Physiological Science, Myodaiji, Okazaki 444-8585, Japan
tanaka@ipc.kit.ac.jp

Abstract. The effects of pressure on the binding of a hydrophobic compound (8-anilino-1-naphthalenesulfonate, ANS) to polyvinylpyrrolidone (PVP) in aqueous solution were investigated by fluorescence titration at a pressure range of 0.1–400 MPa. An elevation in pressure induced the dissociation of ANS from an oligomer PVP (molecular weight < 6000), but enhanced its binding to a larger PVP molecule (MW > 10,000). SAXS measurements demonstrated that the ANS-binding to the high-MW PVP chain was coupled to the shrinkage of the chain. The volume change determined for a PVP with a molecular weight of 2000 was +4.3 ml/mol, and that determined for a PVP with a molecular weight of 10,000 was –73 ml/mol.

1 Introduction

The physical properties of water soluble polymer are widely investigated as a model for the globular protein [1]. Poly(N-vinyl-2-pyrrolidone) (PVP) is a typical water soluble synthetic polymer, and in aqueous solution, the coil dimension of PVP is reduced when it forms a complex with hydrophobic molecules [2]. In the present study, we investigated the pressure effect on the binding of a hydrophobic compound to PVP as a model system for protein folding. The effects of pressure on the binding of 8-anilino-1-naphthalenesulfonate (ANS) to PVP in aqueous solution were investigated by fluorescence titration at a pressure range of 0.1–400 MPa.

2 Materials & Methods

PVP samples were purchased from Aldrich (Milwaukee, USA) and purified by dialysis. The fluorescence titration of PVP (2mg/l) with ANS at elevated pressures was performed using high pressure cells possessing three optical windows manufactured by Teramecs Co. (Kyoto, Japan), combined with a Shimadzu RF5000 spectrofluorimeter (Kyoto, Japan) at 25 °C. The solution X-ray scattering

experiments on PVP were carried out with a solution scattering station (SAXS camera) installed at BL-10C, the Photon Factory, Tsukuba, Japan.

3 Results & Discussion

The binding of ANS to PVP of various molecular weights was monitored quantitatively by a fluorescence titration method. The fluorescence intensity of ANS is enhanced when it forms a complex with PVP in aqueous solution [2], because of the apolar microenvironment of the binding site. Thus, the fluorescence change in the titration of PVP with ANS is proportional to the concentration of ANS bound to PVP. The data were analyzed in order to create the Klotz plot given by the equation: The $1/n$ value, the number of pyrrolidone residues required to form an ANS-binding site, can be determined from the y-intercept of the plot, whereas the K_b value is determined from the inverse of the slope of the plots and the y-intercept. The Klotz plots for most PVP samples were linear, thus indicating that the binding of ANS to PVP was non-cooperative. The $1/n$ values for all of the PVP samples fell into almost the same range (a $1/n$ value of about 10). In the case of the oligomer, part of the chains are shorter than ten monomer units and should have no binding site leading to an increase of $1/n$. This might be the reason for the smaller K_b values of oligomers; for longer PVP chains K_b depended little on the size of the PVP molecule.

The ANS-titration experiments were carried out in a pressure range from 0.1 to 400 MPa. Figure 1 shows two plots of the average number of ANS molecules bound to a PVP molecule as a function of pressure. A comparison of the plots for PVP 2K ([ANS]=19.6 μM) with PVP 10K ([ANS]=21.3 μM) shows that whereas ANS binding to PVP 2K was suppressed by an increase in pressure, the binding to PVP10K was enhanced. Klotz analyses were performed for each PVP sample to yield estimates of the apparent K_b and n at various pressures The n value, i.e., the number of ANS binding sites on PVP, was independent of pressure.

We performed small-angle X-ray scattering analysis (SAXS) to directly observe the changes in the dimensions of PVP induced by ANS binding. Guinier plots of the SAXS data yield estimates for the radius of gyration (Rg), related to the size of the chain molecule. Both plots are linear in the low Q range (Guinier region), and the radii of gyration were estimated by linearly fitting the data points in this region. The Rg values of PVP 10K in the presence and absence of ANS were estimated to be 1.58 ± 0.7 (Å) and 24.4 ± 1.1 (Å), respectively. The results showed that the binding of ANS to PVP 10 K drastically reduced the expansion of the chain molecule. The Kratky plot of $I(Q)\cdot Q^2$ versus Q plot, is useful in describing the overall shape of the polymer chain molecule. In essence, the Kratky plot shows a clear peak for a globular conformation, but has a plateau shape and then increases monotonically for a flexible chain-like molecule. In the absence of ANS, the monotonically increasing Kratky pattern indicates that the PVP chain was in a flexible chain-like conformation. The addition of ANS drastically changed the

Kratky pattern for PVPs and the plot in this case increases sharply in the low Q range and exhibits a maximum at Q =1.7, corresponding to a globular shape for the PVP chain. The results from the Kratky plot, together with the estimates of Rg, demonstrated that the PVP molecule in water has a highly expanded flexible chain conformation, but has a restricted spatial distribution and a globular shape in the presence of ANS. The binding of ANS to PVP induced the shrinkage of PVP 10K, probably because of the high affinity of ANS to the hydrophobic core of the shrunken form of the PVP chain.

The most obvious evidence for the complexity of ANS-binding phenomena can be found in the difference in the pressure dependence of the apparent K_b between low-MW and high-MW PVP. A clue to the mechanism underlying this qualitative difference was provided by the SAXS data, which showed that the binding of ANS to the high-MW PVP was strongly coupled with a global shrinkage of the chain molecule. Accordingly, the fitting procedure applied to the data set for PVP 10K (ANS_0=21.3–44.4 μM) gave optimal estimates for (ΔG_b+ΔG_c) and (ΔV_b + ΔV_c). The resultant fitting parameters were (ΔG_b+ΔG_c) = –21.2 kJ/mol and (ΔV_b + ΔV_c) = –3.0 ml/mol. Assuming that the ΔV_b for PVP 10K were comparable to PVP 2K, then the ΔV_c for PVP 10K bound to ten ANS molecules should be about -73 ml/mol. This large negative ΔV_c value implies that the elevated pressure induces shrinkage of the ANS-bound PVP chain. It has generally been accepted that the PVP molecule contained both hydrogen bond donors are hydrophobic interactions [3].

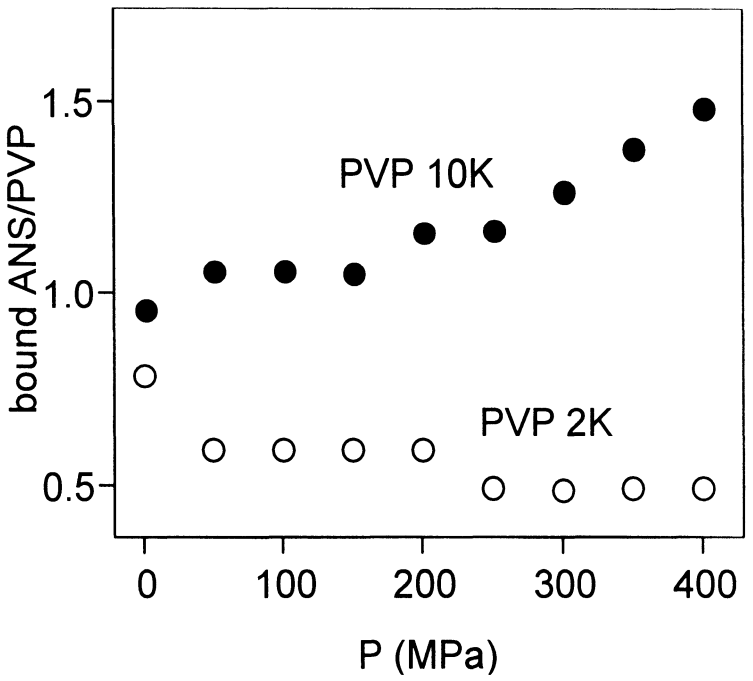

Fig. 1. The average number of ANS molecules bound to a PVP molecule as a function of the pressure p. O, PVP 2K ([ANS]=19.6 μM at 0.1 MPa); ●, PVP 10K ([ANS]=21.3 μM at 0.1 MPa)

The question arises as to which type of physical interaction was most responsible for the negative volume change during the chain shrinkage of PVP. Sun and King, in their study of the aggregation processes of PVP [3], have claimed that the formation of highly directional hydrogen bonds increases the volume of the system, whereas hydrophobic interactions tend to decrease the volume under high pressure. Their opinion on these hydrophobic interactions were probably based on the negativeΔV for the transfer of a small non-polar molecule from an aqueous to a liquid hydrocarbon environment under relatively high pressure (> 100 MPa). Following this line of thinking, the shrinkage of PVP enhanced by elevated pressure may be driven by hydrophobic interactions, which seems to be physically reasonable since the ANS-bound PVP has a large number of hydrophobic residues.

References

[1] Kunugi, S.; Takano, K.; Tanaka, N.; Suwa, K.; Akashi, M. (1997); Macromolecules, 30, 4499–4501.
[2] Kirsh, Y.E.; Soos, T.A.; Karaputadze, T.M. (1979); Eur. Polym. J., 15, 223–228.
[3] Sun, T.; King, Jr. H.E. (1996); Macromolecules, 29, 3175–3181.

Studies on the Mechanism of the Aminoacylation Reaction of Transfer Ribonucleic Acid at High Pressure

J. Barciszewski[1,2], P. Krzeminski[1,3], A. Wandel[1,3], J. Arabas[2], J. Jurczak[4] and S. Porowski[3]

[1]Institute of Bioorganic Chemistry of the Polish Academy of Sciences, Noskowskiego 12, 61 704 Poznan, Poland (e-mail: jbarcisz@ibch.poznan.pl), [2]High Pressure Research Center of the Polish Academy of Sciences, Sokolowska 13, 01-142 Warsaw, Poland, [3]Agriculture Academy, Wojska Polskiego 71, 60-625 Poznan and [4] Institute of Organic Chemistry of the Polish Academy of Sciences, Kasprzaka 44, 01-224 Warsaw, Poland

Abstract. We analyzed the effect of divalent cations such as magnesium and cobalt on the aminoacylation reaction at high pressure. Their increasing concentration inhibits its efficiency. Also the reaction is pH dependent. pH above 7 inhibits the reaction probably due to instability of the ester bond. Lead induced cleavage has been used to identify conformational changes of yeast $tRNA^{Phe}$ effected by high pressure. Low yield of a chain scission reaction is due to distortion of the spatial structure of tRNA where dihydrouridine and ribothymidine loops are separated from each other by a distance longer than in the native structure. Finally we showed that at 6 kbar coenzyme A can be aminoacylated with phenylalanine to form the thioester.

1 Introduction

Recently we have shown that transfer ribonucleic acid molecule specific for phenylalanine ($tRNA^{Phe}$) can be specifically aminoacylated to the 3' terminal adenosine at high pressure in the absence of specific aminoacyl-tRNA synthetase (AARS) and adenosine triphosphate (ATP). Aminoacyl-tRNA (AA-tRNA) synthesized at high pressure is fully biologically active and binds to ribosomes as well as participating in ribosomal synthesis of polyphenylalanine *in vitro* [1]. In the cell tRNA molecules are charged with their specific amino acids by AARS. This mechanism does not require specific binding of amino acids by their cognate tRNA molecules, because AARS recognizes information within the tRNA structure and, in some cases, that information does not include the anticodon triplet. Whether the synthetase does or does not contact the anticodon, the critical elements that determine aminoacylation efficiency and specificity are located in the tRNA acceptor stem. The relationship between the sequence and structure of the acceptor stem oligonucleotide and the attached amino acid constitutes an operational RNA code for amino acids that may have preceded the genetic code [2]. If so recognition of amino acids by tRNA at high pressure seems to be critical for the specificity of

the aminoacylation reaction because missaminoacylation occurs at very low level [1]. The aim of this study was to provide new data for the understanding of the mechanism of the aminoacylation reaction at high pressure. In this paper we analyzed the effect of divalent cations and pH on the reaction. We were interested to identify conformational changes which occur in tRNA molecules at high pressure and whether other naturally occurring compounds such as coenzyme A can be aminoacylated at high pressure.

2 Results & Discussion

The presence of divalent metal ions, in particular magnesium, is an absolute requirement for the formation of the active tRNA structure. Mg^{2+} ions change tRNA solution structure very efficiently. Also modified bases influence Mg^{2+} binding and affect global structure of each tRNA. For example, *Escherichia coli* $tRNA^{Thr}$ and $tRNA^{Phe}$ have optima of aminoacylation at 5 and 8 mM Mg^{2+}, respectively. Magnesium induces changes of Stokes radii of tRNA, which shrink drastically upon increasing the Mg^{2+} concentration up to 15 mM. The Rs value is reduced from 3.4 to 2.5 nm due to Mg induced phosphate group screening and loss of charges, which is accompanied by formation of new base pairs and increase of the base stacking. Cobalt ions have a less pronounced effect on tRNA structure but it is very similar in hydration properties. Increasing concentration (5, 10, 15 and 50 mM) of both cations inhibit phenylalanine-$tRNA^{Phe}$ formation at high pressure in the same way as enzymatic charging. We suggest that this is due to changes in the tertiary structure, and particularly in the pattern of hydration of the groove of tRNA. From a crystal structure analysis of a G-U pair containing RNA duplex, a water mediated interaction of the guanosine 2'-hydroxyl and 2-amino groups has

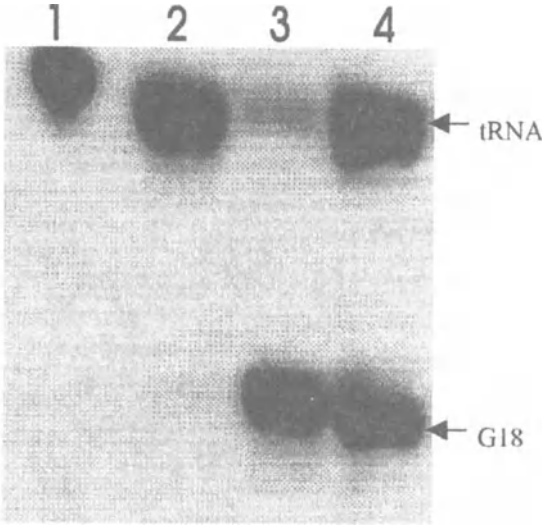

Fig. 1. Autoradiogram of lead induced cleavage of yeast 3'-end (^{32}P) labeled $tRNA^{Phe}$ from yeast in Tris-HCl buffer pH 7.2 containing 40 mM NaCl and 1 mM Pb^{2+}. Pascalization was done at 6 kbar at room temperature for 20 min. Lanes: 1. Control in the absence of Pb^{2+}. 2. Control for a time of achieving high pressure. 3. Hydrolysis at atmospheric pressure. 4. Hydrolysis at high pressure

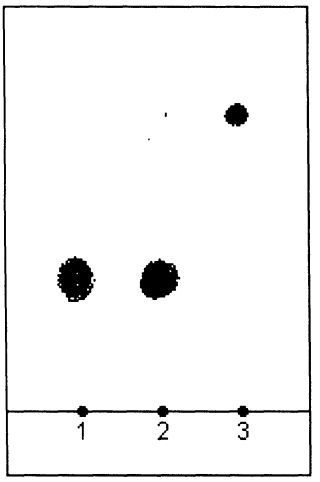

Fig. 2. Thin layer chromatography of amino-acylation reaction of CoA with [^{14}C] phenylalanine on silica gel. Plate was developed in: isopropyl alcohol-HCl-H_2O (70:15:15). The spots were scratched from the plate, dissolved in scintillation solvent and counted. Lanes: 1 Coenzyme A. 2 Phe+CoA at high pressure (6 kbar) for 12 h in IMID buffer. 3 radioactivity

been suggested but NMR spectra identified metal ion binding site in the vicinity of the G3-U70 base pair. Previously we have noticed that tRNAPhe exposed to high pressure changes its circular dichroism spectrum [1]. However it was difficult to describe them in molecular terms. We decided to probe the structure of tRNAPhe at high pressure with lead ions. It is known that Pb^{2+} ions in sub-milimolar concentrations cleave the internucleotide bond specifically between nucleosides D17 and G18 with additional minor cleavages after D16 and G15 [3]. The cleavage involves removal of the proton from the 2'OH of ribose 17 in the dihydrouridine loop by the Pb(II)-bound hydroxyl group fixed at U59C60 of the ribothymidine loop. At high pressure the cleavage reaction is inhibited in comparision wth the reaction done at ambient conditions (Fig.1). Lower intensity of the G18 band suggests that the strand scission is restricted, due to changes of the distance between Pb(OH) and the 2' OH group. This local movement is just a consequence of structural changes in dihydrouridine and ribothymidine loops of tRNAPhe already seen in the CD spectrum. It means that a high pressure induced conformation is similar to that acquired during interaction with aminoacyl-tRNA synthetase. For further understanding of the tRNA aminoacylation reaction, we have chosen another substrate, coenzyme A. It is a biologically important thiol, which participates in carboxyl group biosynthesis. At high pressure CoA-SH reacts with phenylalanine forming a thioester, phenylalanyl-S-CoA (Fig. 2). Recently it has been shown that synthesis of aminoacyl-S-CoA is also catalyzed by aminoacyl-tRNA synthetases [4].

From the obtained results we can conclude that at high pressure conformation of tRNA changes due to different hydration and structure of water. It is also evident that high pressure activates amino acids.

References

[1] Krzyzaniak, P. Salanski, J. Jurczak, Twardowski, T. and J. Barciszewski (1998); tRNA aminoacylated at high pressure is correct substrate for protein biosynthesis; Biochem. Mol. Biol. Int. 45, 489–500.

[2] Schimmel, P., Giege, R., Moras, D. and Yokoyama, S. (1993); An operational RNA code for amino acids and possible relationship to genetic code; Proc. Natl. Acad. Sci. USA 90, 8763–8768.

[3] Brown, R. S., Dewan, J. C. and Klug, A. (1985); Crystallographic and biochemical investigation of the lead(II)-catalyzed hydrolysis of yeast phenylalanine tRNA; Biochemistry 24, 4785–4801.

[4] Jakubowski, H. (1998) Aminoacylation of Coenzyme A and pantheithene by aminoacyl-tRNA synthetases: possible link between noncoded and coded peptide synthesis; Biochemistry 37, 5147 – 5133.

High Pressure Induced Gelation of Proteins and Polysaccharides

Formation of a Gel from β-Lactoglobulin Under Hydrostatic Pressure

C. Kanno, T-H. Mu, M. Ametani and N. Azuma

Utsunomiya University, Department of Applied Biochemistry, Utsunomiya 321-8505, Japan
Kanno@cc.utsunomiya-u.ac.jp

Abstract. The β-lactoglobulin (β-Lg) concentration required for inducing gelation was 10% at 800 MPa, 12% at 600 MPa and 18% at 400 MPa, but these gels were too soft for any measurement of their textural properties. The hardness and breaking stress of the gels from 14% β-Lg were both enhanced by increasing the pressure to 800 MPa, but not by increasing the pressurizing time. The microstructure of the β-Lg gel resembled a honeycomb in the alkaline pH region and coral in the acidic pH region. The secondary structure of soluble protein from the gel showed an almost unchanged α-helix, while the β-structure had disappeared, and random and β-turns had increased. The solubility of β-Lg was lower in a Tris-glycine-EDTA buffer at pH 8.0 than in the same buffer containing 0.5% SDS and 8 M urea. In the alkaline pH region, a high-molecular-weight aggregate in addition to a tetramer and dimer of β-Lg was detected, but not at pH 4. The SH content of gelled β-Lg was decreased by pressurization in the alkaline pH region. No gel was formed with more than 10 mM NEM under pressure. At pH 7 or more, the oxidation of SH and exchange of SH-SS in the β-Lg molecules were essential for the pressure-induced gelation.

1 Introduction

One of the functional properties of milk whey proteins is their gelation [1], which can be induced by means of heating or hydrostatic pressure. With industrial whey proteins, the protein concentration for inducing gelation, the rheological properties and the microstructure of gels induced from a whey protein isolate (WPI) were different from those of a why protein concentrate (WPC) at the same hydrostatic pressure [2]. β-Lactoglobulin (β-Lg) has previously been found to predominantly participate in pressure-induced denaturation [3–5] and gelation [6, 7], accounting for about 50% of the whey protein.

In order to clarify the gelation mechanism for whey proteins, we studied the conditions (pressure, pressurizing time, protein concentration, pH and *N*-ethylmaleimide (NEM)) required for gel formation from a β-Lg solution under hydrostatic pressure, and the rheological properties, protein solubility, electrophoretic properties, SH content, secondary structure, and microstructure of the pressure-induced β-Lg gels.

2 Materials & Methods

A β-Lg solution (10–18%, w/v) in 0.1 M Tris-HCl (pH 7.2) was pressurized in a Teflon tube (4 ml) at 200–800 MPa for 10 min at 30 °C with a hand-operated oil pressure apparatus. The resulting pressure-induced gels were homogenized in a 0.086 M Tris-0.09 M glycine-4 mM EDTA buffer at pH 8.0 (buffer A) or in the same buffer containing 8 M urea and 0.5% SDS (buffer B) and then centrifuged for 15 min at 20,000 × g [8]. The protein concentration in the supernatant was determined to evaluate the protein solubility. The hardness and breaking stress of the resulting gel were individually measured with a rheometer. Each gel was examined with a scanning electron microscope, after dehydration, drying, and coating. SDS-PAGE with or without 2-mercaptoethanol (2-ME) was performed. The SH groups were determined by the Ellman method [9]. The secondary structure was identified after diluting the soluble fraction in buffer A with a 50 mM phosphate buffer (pH 7.0). The water-holding capacity was also measured [10].

3 Results & Discussion

3.1 Effect of Pressure and Pressurizing Time

The β-Lg concentration required for inducing gelation was 14% at 400 MPa and 10% at 800 MPa, but these gels were too soft for any measurement of textural properties by a rheometer. A sufficiently firm gel was formed with 14% β-Lg at 600 MPa. The hardness and breaking stress of the sufficiently firm gels from 14% β-Lg were both enhanced by increasing the protein concentration and hydrostatic

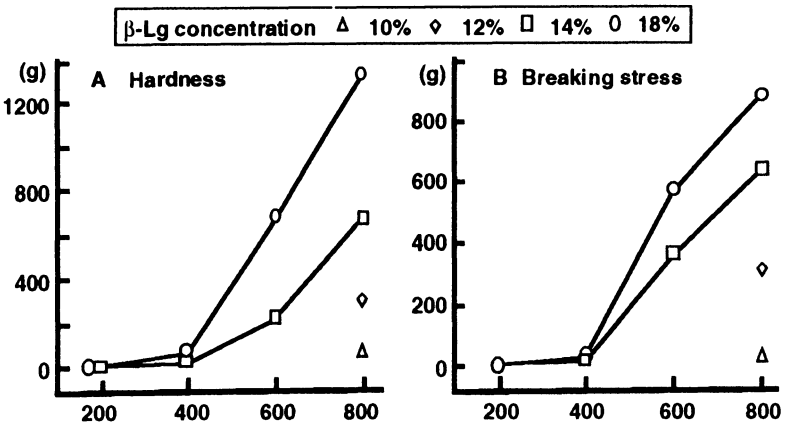

Fig. 1. Effect of pressure on the hardness (**A**) and breaking stress (**B**) of pressure-induced gels from different concentrations of β-Lg. β-Lg in 0.1 M Tris-HCl (pH 7.2) was pressurized for 10 min at the indicated pressure

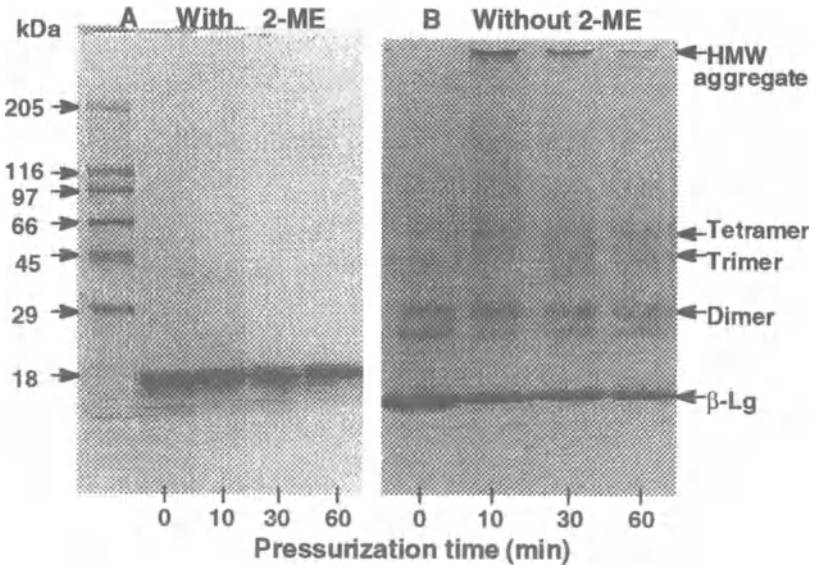

Fig. 2. SDS-PAGE patterns in the presence (**A**) and absence (**B**) of 2-ME of soluble protein in the pressure-induced gels from 14% β-Lg at 800 MPa. The protein soluble in a Tris-glycine-EDTA buffer (pH 8.0) was analyzed. Protein bands were detected with Coomassie brilliant blue R-250

pressure to 800 MPa (Fig. 1). The rheological properties of the gel from 14% β-Lg at 600 MPa were not influenced by increasing the pressurizing time. The protein solubility in buffer A or B decreased after 20 min with extended pressurizing time. The SH content decreased 10 min after pressurization, and remained at an almost constant level.

The microstructure of the β-Lg gel resembled a honeycomb in the neutral pH region and was not effected by pressurization time, but the pore size of the honeycomb was slightly enlarged by increasing time. The secondary structure of soluble protein from the gel after pressurization for 20 min at 800 MPa showed an almost unchanged α-helix, while the β-structure disappeared, and random and β-turns increased. β-Lg dissolved in buffer A was analyzed by SDS-PAGE with or without 2-ME (Fig. 2). With 2-ME, most β-Lg was detected as a monomer, whereas without 2-ME, a dimer, trimer, tetramer and high-molecular-weight (HMW) aggregate were detected in addition to the β-Lg monomer. HMW of β-Lg decreased with increasing pressurizing time, suggesting that the formed HMW aggregate was removed by centrifugation.

3.2 Effect of pH

The gels induced from 18% β-Lg at pH 4, 7 and 9 were milky in color at pH 4, translucent at pH 7, and transparent yellowish at pH 9. The hardness and breaking

In the alkaline pH range, such a hard gel was induced by intermolecular S-S bonding.

The microstructure of the β-Lg gel was like a honeycomb at pH 7 and 9, while being like coral at pH 4, as had been observed with WPI and WPC, respectively, at pH 7 [2]. The pores of the network structure of the gel formed at pH 9 were smaller than those at pH 7, suggesting that intermolecular S-S bonding had increased at pH 9. However, the water-holding capacity was unchanged between the gels from pH 7 and 9.

The protein solubility of the gels induced at pH 4, 7 and 9 under 700 MPa was 83, 65 and 38%, respectively, this solubility increasing in buffer B (81–88%). This result shows that pressure-induced gelation is caused by hydrophobic and hydrogen bonding, in addition to S-S linkage. SDS-PAGE without 2-ME showed that, at pH 7 and 9, an HMW aggregate in addition to a tetramer, trimer and dimer of β-Lg were detected, but not at pH 4. The SH content of gelled β-Lg was less at pH 7 and 9 than at pH 4.

3.3 Effect of NEM

NEM (1–14 mM) was added to 14% β-Lg and pressurized for 10 min at 800 MPa. No gel was formed with more than 10 mM NEM under hydrostatic pressure. The hardness of the gel induced from β-Lg containing 1–7 mM NEM was within the range of about 0.7 kg. Adding 10 mM NEM to β-Lg destroyed the gel microstructure. Increasing NEM (1–7 mM) increased the pore size, and blocking of the SH groups caused loosening of the network structure of the pressure-induced β-Lg gel.

At pH 7 or more, oxidation of the SH groups and exchange from SH to SS in the β-Lg molecules were essential for the pressure-induced gelation of β-Lg and to achieve a network structure like a honeycomb.

References

[1] Kinsella, J.E. and Whitehead, D.M. (1989); Adv. Food Nutr. Res., 33, 343–348.
[2] Kanno C. *et al.* (1998); J. Agric. Food Chem., 46, 417–424.
[3] Funtenberger. S. *et al.* (1995); Lebensm. -Wiss. u. Technol., 28, 410–418.
[4] Funtenberger, S. *et al.* (1997); J. Agric. Food Chem., 45, 912–921.
[5] Tanaka, N. *et al.* (1996); Int. J. Biol. Macromolec., 19, 63–68.
[6] Zasypkin, D.V. *et al.* (1996); Food Hydrocolloids, 10, 203–211.
[7] Dumay, E. *et al.* (1998); Lebensm. -Wiss. u. Technol., 31, 10–19.
[8] Shimada, K. and Cheftel, J.C. (1988); J. Agric. Food Chem., 36, 1018–1025.
[9] Ellman, G.L. (1959); Arch. Biochem. Biophys., 82, 70–77.
[10] Quguiner, C. *et al.* (1989); Int. J. Food Sci. Technol., 24, 601–612.

Hydration and Pressure–Temperature Phase Diagrams of Wheat Starch

J.P. Douzals[1], J.M. Perrier-Cornet[1], P. Gervais[1] and J.C. Coquille[*]

[1]ENSBANA 1, Esplanade Erasme, 21000 Dijon, France.
[*]ENESAD Bd O. de Serres, 21800 Quétigny, France
jp.douzals@enesad.fr

Abstract. Wheat starch suspensions (5% DM) were subjected to pressure (0.1 to 600 MPa) and/or temperature (–20 to 96 °C) during 15 min. Swelling index (s.i.) depended on starch hydration as a function of pressure or temperature level. *p-T* treatment improved starch hydration for low and high temperatures at the same pressure level. *p-T* denaturing conditions were found using DSC and loss of birefringence by the granules. The *p-T* phase diagram of starch was found to correspond to a pseudo ellipsoid curve. A 3D phase diagram of starch was proposed including pressure, temperature and initial moisture content.

1 Introduction

Previous studies showed that gelatinization of wheat starch is possible under pressure without heating [1, 2] and completely achieved at 600 MPa. The aim of this paper was to discuss pressure-temperature hydration and *p-T* phase diagrams of wheat starch in terms of thermodynamics as well as practical aspects.

2 Materials & Methods

Suspensions of commercial wheat starch (5% DM) were prepared in rubber bags (15 ml) and treated at the desired pressure and/or temperature during 15 min. Starch products were removed from the rubber bags and centrifuged at 2000 rpm during 2 min at 20 °C. Supernatants were removed and DM of pellets was determined in a dry air oven at 105 °C during 48 h. Precision in swelling index (s.i.) measurements was ±0.3 g $H_2O \cdot g^{-1}$DM.

DSC runs were performed using a Perkin Elmer DSC II apparatus with a heating rate of 10 °C·min^{-1}. Samples of about 40 mg were subjected to 20–120 °C. Melting enthalpy was manually determined. Results concerned three repetitions with a precision of ±0.5 J·g^{-1}DM. Starch melting was also estimated using an optical

microscope provided with polarizing filters and image analysis software. Images contained about 30 granules. Experiments were repeated three times.

3 Results & Discussion

Swelling index measured after thermal treatment is shown in Fig. 1. Swelling index was related to temperature and was about 9 g of water per g of DM at the melting temperature T_m (62 °C) given by DSC. Swelling index values attained to 20 g of water/g DM after treatment at 96 °C. Starch suspensions were subjected to pressure and results are given in Fig. 2. As shown in Fig. 2, the swelling index increased gradually with pressure and reached about 6.3 g water per g of DM at 600 MPa. DSC measurements showed complete gelatinization of wheat starch at 76 °C, 15 min as well as 600 MPa, 25 °C, 15 min with respective s.i. of 9.84 and 6.3 g of water per g of DM.

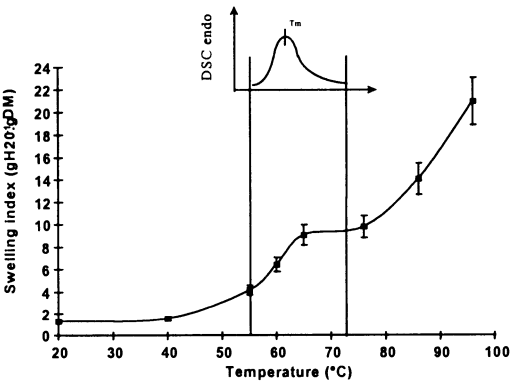

Fig. 1. Wheat starch swelling index vs. temperature after 15 min treatment. Upper curve shows DSC peak at the same temperature range. Initial DM was 5% and bars indicate the confidence interval of the mean

The hydration level of starch was different for an equivalent denaturing state when treated under pressure or temperature. Combined *p-T* treatments enhanced the starch swelling index in comparison with 25 °C for lower and higher temperatures at the same pressure level. (results not represented). However, according to previous results, such a *p-T* isohydration diagram of starch just showed equivalent conditions of hydration but did not correspond to a phase diagram given in Fig. 3.

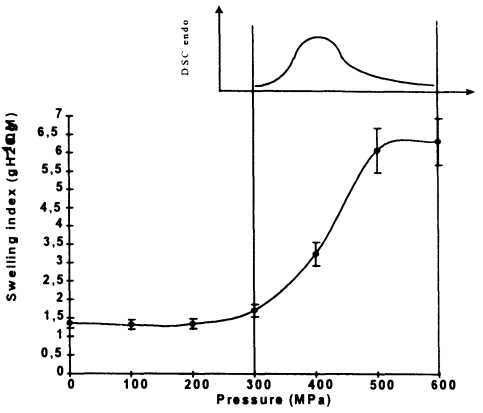

Fig. 2. Wheat starch swelling index vs. pressure after 15 min treatment. Upper curve was drawn from DSC results after pressurization. Initial DM was 5% and bars indicate the confidence interval of the mean at 95%

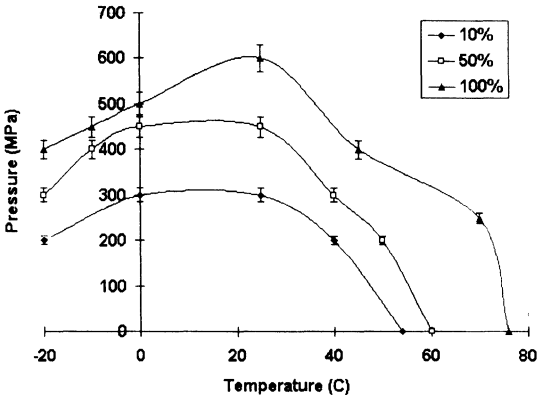

Fig. 3. *p-T* phase diagram of wheat starch as determined by DSC and loss of birefringence upon 5% DM suspensions. Percentages correspond to melted fraction and bars to the confidence interval of the mean at 95%

Referring to 25 °C, higher as well as lower temperatures enhanced starch gelatinization with a decrease in pressure of melting. Whatever the temperature, high pressures above 400 MPa involved starch melting with lower hydration (s.i.) than at higher temperature and lower pressure. This apparently better hydration efficiency under pressure may be explained by a plasticizer role of water especially visible when global volume is restricted.

When extending these results to very low moisture content at 0.1 MPa, starch melting is generally obtained at high temperatures (200–220 °C). As a liquid phase would occupy a greater volume than the solid phase due to a greater molecular

disorder, it is suggested that gelatinization of anhydrous starch might be impossible under pressure as shown in Fig. 4.

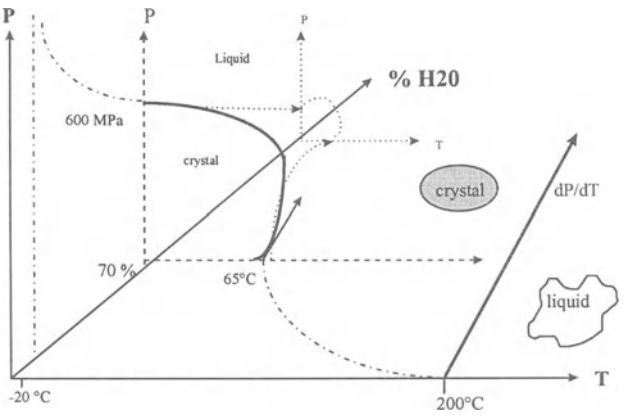

Fig. 4. Suggestion of *p-T* - MC phase diagram for starch

As shown in Fig. 4, because of a positive d*p*/d*T* slope, increasing pressure would avoid starch gelatinization at very low MC. With an increase in MC, starch gelatinization under pressure may occur with a significant decrease in melting temperature. Water starch linkages created under pressure involved volume reduction (plasticizing effect of water) with an inflexion of the d*p*/d*T* slope as already shown [1]. In excess water, this inflexion occurred at 200–250 MPa and 62–64 °C.

References

[1] A.H. Muhr and J.M.V. Blanshard, **1982**, *Carboh. Polym.*, 2, 61–74.
[2] J.P. Douzals, P.A. Marechal, P. Gervais and J.C. Coquille, **1996**, *J. Agric. Food Chem*, 44, 1403–1408.

Alterations of Calcium Alginate Gel Dispersions by High Pressure Treatment

M. Schwertfeger

Federal Dairy Research Centre, Hermann-Weigmann-Str.1, D-24103 Kiel
Phone: +49-431-609-2275; Fax: +49-431-609-2309
schwertfeger@bafm.de

Abstract. Calcium alginate gel dispersions were obtained by mixing solutions containing sodium alginate and calcium chloride, followed by homogenization and rinsing. Pressure treatment was performed at pressures up to 400 MPa. The properties of the products were characterized by texture analysis, measurement of electric conductivity and by light microscopy. The state of the samples under pressure was observed by a modified method of a falling ball [1]. By pressure treatment calcium alginate gel dispersions are transformed into homogeneous gels. The mechanical properties of the samples depend on the conditions of pressure treatment. Beyond a pressure of approximately 200 MPa the dispersions form a liquid with low yield stress and low viscosity. This phase transition is a fast process. Pressure treatments longer than 5 min have no visible effect on the formed gel. Pressures less than 200 MPa lead to an inhomogeneous product with a low gel strength.

1 Introduction

High pressure processing may be a powerful tool in food processing to obtain particular texture properties. In most studies the changes in protein-containing systems are characterized. Although other gel-forming substances, e.g. polysaccharides, play an important role as thickeners and gelling agents in food processing, little is known about the changes of their physicochemical properties caused by high pressure treatment [1, 2]. In this contribution the changes of some properties of calcium alginate gel known as non-thermoreversible caused by pressure treatment are displayed. Because of the low pressure needed for gel homogenization, pressurization of calcium alginate gel dispersions might be a way to obtain homogeneous, gelled food systems.

2 Materials & Methods

The calcium alginate gel dispersion was obtained by adding a solution of 1.98 g sodium alginate (Fluka) in 200 ml of water to a solution of 0.75 g calcium chloride in 500 ml of water under vigorous stirring followed by washing the gel particles by sieving and re-disperging in 300 ml of water (6 times). The dispersion was homogenized by mixing with a commercial household mixer and diluted to a final volume of 500 ml. Deionized water was used for all operations. The analysis of the gel according to standard methods [3] led to the following results: dry matter (102 °C) 0.37% , ash content (550 °C) 0.04_2% , calcium content 0.03_5% .

For high pressure experiments the samples were sealed in small flexible polyethylene bulbs. Compression and decompression was finished within 5 s. All experiments were performed at 25 °C. The changes in temperature due to adiabatic heating were neglected.

The mechanical properties of the gel were tested with a texture analyzer (Stable Micro Systems) equipped with a cylindrical probe (2 mm in diameter). The force was registered at a probe velocity of 1 mm/s. The electric conductivity was measured by placing the samples in a small cylindrical cell made of Perspex with electrodes of stainless steel and was registered as the ratio of the conductivity of the pressurized samples to the conductivity of the non-pressurized sample. The structure of the gels was studied by light microscopy. A small part of the gel was squeezed between a slide and a cover glass and was observed in phase contrast. The structure of the dispersion under high pressure was determined by placing a small steel ball on the top of the gel sample followed by measuring the distance of the falling ball after pressure treatment.

3 Results

The gel dispersion is an inhomogenous fluid with a high viscosity. After shearing and some hours of relaxation a small yield value is observed. After treatment at pressures less than 1.5 kbar no significant changes in gel strength (Figs. 1 and 2), electric conductivity (Fig. 3) and gel structure were observed.

Treatment at pressures around 1.5 kbar led to a product in which the gel particles began to get in closer contact. The formed product did not flow under its own weight. After treatment at pressures higher than 2 kbar a homogenous clear stiff gel was formed. The electrical conductivity and the gel strength rose with the pressure applied during the experiments.

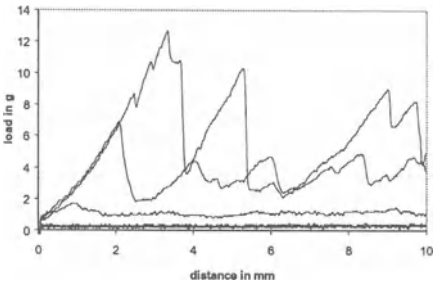

Fig. 1. Puncture test diagrams of high pressure treated calcium alginate gel dispersions. Samples treated for 5 min at 4, 3, 2, 1.5, 1 and 0.5 kbar and 1 bar (from top) at 25 °C

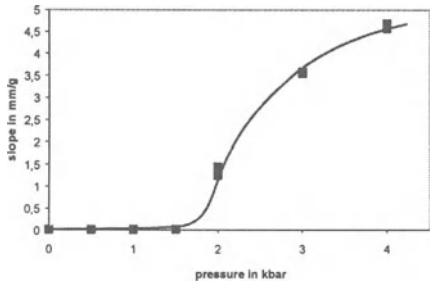

Fig. 2. Gel elasticity depending on the pressure applied during pressure treatment. The slopes are calculated at the first point of gel breakdown (first maxima of curves in Fig. 1.)

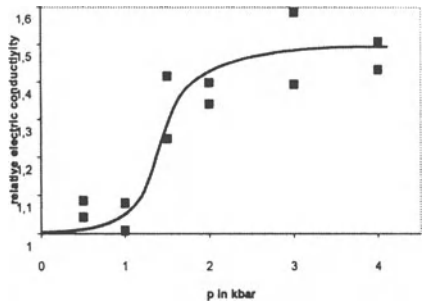

Fig. 3. Relative electrical conductivity of pressurized samples

Under high pressures beyond 2 kbar the gel changed its state and became a fluid with a low yield value; the steel ball fell down. Assuming Newtonian flow behaviour the viscosity could be calculated using Stoke's law obtaining a value

about $\eta < 8$ Pas. At all pressures the changes in gel structure was an instantaneous process, complete within about 1 min. The properties of the gels observed as gel strength and visible gel structure did not depend on the duration of pressurization (results not shown).

4 Discussion

By mixing solutions containing calcium ions and alginate ions a weak gel is formed by crosslinking the polymer chains with calcium ion bridges. Caused by rapid mixing in this gel the polymer molecules should be disordered and the gel should contain a large number of trains and loops.

These calcium-ion connections are not influenced by moderate pressures. Pressures higher than about 2 kbar lead to a rupture of these contacts caused by the smaller volume of water in the hydration sphere of calcium ions in the bulk phase connected by an increased number of charges of the carboxylic groups acting repulsive. The hydration sphere surrounding these groups should be decomposed under pressure caused by the smaller reaction volume of hydration of carboxylic ions compared to dissociation of water ($R\text{-}COOH \rightarrow R\text{-}COO^- + H^+$, $\Delta V \approx -14$ ml/mol, $H_2O \rightarrow H^+ + OH^-$, $\Delta V \approx -22$ ml/mol) [4]. Caused by this increase in repulsive forces the irregularly ordered polymer chains should transform into a slightly straighter conformation. The viscosity of the system should decrease under pressure caused by the repulsive forces and the straight conformation of the polymer molecules that prevent entangling of the chains.

By fast decompression the equilibrium of dissociation of the calcium alginate gel towards the free calcium ions and polymer ions is shifted rapidly backwards. The connections between the polymer chains are rebuilt whereas now the crosslinking starts from a homogenous system followed by formation of a homogenous gel in the whole bulb.

References

[1] Gekko, K. (1992); Effects of pressure on the sol-gel transition of food macromolecules, in: Heremanns, K. (ed.): High Pressure Research in the Biosciences and Biotechnology; Colloques Inserm, 224, 105–113.

[2] Gustin, D., Bera, F., Dumont de Chassart, Q., Mertens, B. (1992); Pectin Gelification under HHP: Gel Properties and Formation Mechanism, in: Heremanns, K. (ed.): High Pressure Research in the Biosciences and Biotechnology; Colloques Inserm, 224, 195–198.

[3] VDLUFA (ed.) (1996); Methodenbuch, 6. Ergänzungslieferung, VDLUFA-Verlag, Darmstadt.

[4] Asano, T., Le Noble, W. J. (1978); Activation and Reaction Volumes in Solution; Chem Rev, 78, 407–489.

Development of a Cream Caramel by High Hydrostatic Pressure at Low Temperature

E. Ponce, E. Beltrán, E. Sendra, M. Mor-Mur, B. Guamis and R. Pla*

Tecnologia dels Aliments, Ce.R.T.A. Facultat de Veterinària,
Universitat Autònoma de Barcelona, 08193 Bellaterra, Spain
Phone 34-93-5811446; Fax 34-93-5812006
ivppk@cc.uab.es

Abstract. Cream caramels are obtained with good functional properties by applying pressures of 450 MPa at –15 °C, but not at 50 °C.

1 Introduction

High hydrostatic pressure has been applied in foods for microbial inactivation [1]. Consumers are demanding in food: variety, new flavour experiences, easy handling, healthy products, absence of additives, long shelf-life and freshness. Integrating high pressure in productive processes can result in novel products [2]. Previous works of the authors and others [3, 4] have shown the gelation capacity of liquid whole egg under pressure conditions at moderate temperatures and, even, below 0 °C.

The aim of the present study was to develop a model cream caramel through high pressure and evaluate its functional properties compared with a traditional recipe.

2 Materials & Methods

Raw materials. Liquid whole egg (LWE): dry matter 22.9%; fat 9.7% and total nitrogen 2%. Milk: 14% rehydrated skim milk powder. Four mix formulations were tested:
(i) 70% milk, 20% LWE, 10% sugar
(ii) 52% milk, 40% LWE, 8% sugar
(iii) (i) plus 0.25% carrageenan and 0.08% locust bean gum
(iv) (ii) plus 0.25% carrageenan and 0.08% locust bean gum
High pressure processing. Combinations of pressure (450 MPa), temperature (–15 and 50 °C) and time (cycles of 30+30 and 60 min in a continuous process).
Heat induced gels. Cooked in a water bath at 80 °C for 30 min.

Water holding capacity (WHC). Centrifugation at high speed (12000 g) followed by removal of the exudate, and calculated by the following equation: 100-[((initial weight-final weight)/ moisture content)*100].
Confocal scanning laser microscopy (CSLM). Staining procedure and microscopic observations were done according to Ponce *et al.*[5].
Colour analysis. Hunterlab miniscan spectrophotometer 45°/0°. F_{cw} illuminate and 10° observer. L, a, b values and yellowness index were determined.

3 Results & Discussion

The results obtained after pressurization at 50 and −15 °C are presented in Table 1.

Table 1. Pressure (450 MPa) gelation of a model cream caramel at 50 and −15 °C

	50 °C	−15 °C
AD	-	-
AE	-	-
BD	-	+
BE	-	+
ADF	-	-
AEF	-	-
BDF	-	+
BEF	-	+

A: 20% liquid whole egg,70% milk, 10% sugar. B: 40% liquid whole egg, 52% milk, 8% sugar.
C: 85 °C for 30 min. D: 450 MPa for two cycles 30 min at −15 °C.
E: 450 MPa for 60 min at −15 °C. F: 0.25% carrageenan + 0.08% locust bean gum.

An important increase in the viscosity for all formulations studied was achieved at 50 °C for the cycles and continuous pressurizations, but no gelation was obtained. In the same way, at −15 °C, no gelation was reached in formulations with 20% LWE, however, compact gels were obtained doubling the LWE concentration (40%). Undoubtedly the protein content was a determinant factor in gelation under the pressurization conditions tested. All samples treated by heat gelified, all formulations with 20% LWE showed the characteristic texture and aspect of the cream caramel while those containing 40% LWE were excessively compact, elastic and less attractive. It is known that the locust bean gum has a good synergism with carrageenan enhancing the gel elasticity and force, with better water retention. Under pressure conditions these additives did not improve either the elasticity or the texture of the gels that, on the contrary, presented a heterogeneous and granular texture.

The WHC was always higher in samples with 40% LWE (Fig. 1). The presence of additives improved the WHC in all cases. Pressure gels showed a lower WHC than those formed by heat, specially those from samples with 20% LWE that also presented greater sineresis and juiciness.

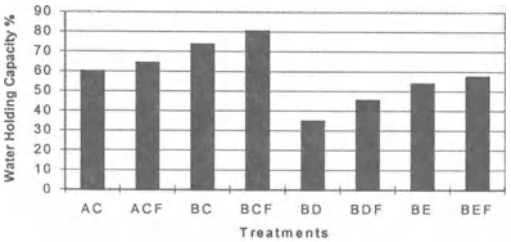

(A, B, C, D, E, F, see Table 1)

Fig. 1. Water holding capacity

Some of the differences detected in textural perception can be explained by observation of the samples through CSLM (Figs. 2a,b). Pressure gels did not display a similar gel forming behaviour compared to heat gels, differences in the internal structures are clearly revelled. Image (a) shows a more porous network, with larger irregular holes and smoother appearance in pressure gels, compared to heat gels (image (b)) with a very condensed and homogeneous network.

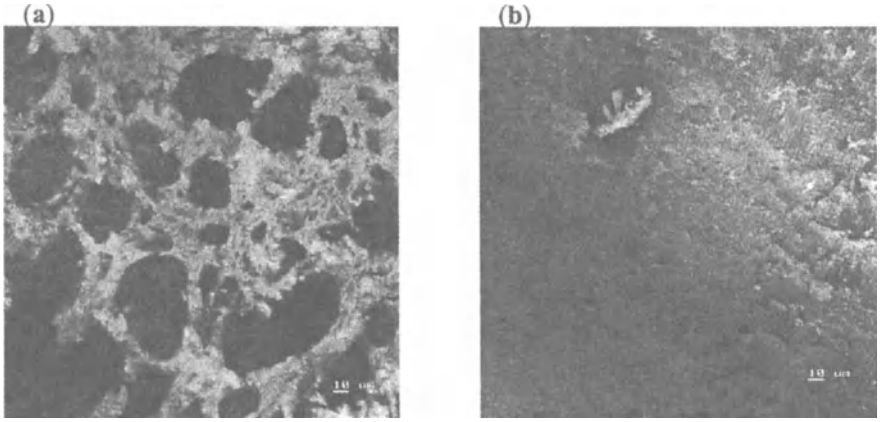

Fig. 2. (**a**) 40% LWE + 52% milk + 8% sugar 450 MPa for 60 min at −15 °C; (**b**) 40% LWE + 52% milk + 8% sugar 85 °C for 30 min

In relation to colour characteristics, higher milk proportion in the formulations gave a whiter mix before gelation (Table 2). Samples treated by heat presented higher whiteness and greater luminosity. Gels obtained by pressure showed less luminosity, though under visual perception they seemed more luminous and brilliant. These gels presented high sineresis, this fact could be related to the visual impression of greater luminosity and glossiness observed under fluorescent light.

Table 2. Colour parameters of mix formulations and pressure (450 MPa) and heat (80 °C/30 min) treated gels

	L	*a*	*b*	*Yi*	ΔE
A (mix control)	77.61	0.28	16.18	38.09	
AC	84.72	–0.26	17.09	36.50	7.18
AF (mix control)	79.70	1.22	16.21	36.96	
ACF	82.02	–0.60	17.79	39.32	3.39
B (mix control)	71.88	4.17	20.04	51.05	
BC	84.46	0.70	20.24	43.52	13.06
BE	53.28	5.40	16.41	56.80	18.98
BD	52.24	4.82	15.75	55.64	20.11
BF (mix control)	71.12	4.26	19.84	51.04	
BCF	82.61	0.83	21.53	47.39	12.11
BEF	52.92	6.14	17.17	59.79	18.49
BDF	53.47	5.52	16.16	55.71	18.07

(A, B, C, D, E, F, see Table 1)

4 Conclusions

Cream caramel can be obtained by specific pressure and time conditions at low temperatures (–15 °C). Gels obtained by pressure presented more important colour differences (ΔE) with respect to the control mix than heat induced gels. However, pressure cream caramels had a very fresh taste, higher juiciness and nicer flavour and colour. These functional properties together with its particular textural perception can be used to design new products and improve the existing ones, without addition of gelling agents and avoiding negative effects of heat treatments.

References

[1] Knorr, D. *et al.*, 1992. pp. 211–217. In C. Balny, R. Hayashi, K. Heremans, and P. Masson (Eds.), High pressure and biotechnology. Colloque INSERM/John Libbey Eurotext Ltd., London.

[2] Cheftel, J.C. 1992. Effects of high hydrostatic pressure on food constituents: an overview. pp. 195–209. In C. Balny, R. Hayashi, K. Heremans and P. Masson (Eds.), High pressure and biotechnology. Colloque INSERM/John Libbey Eurotext Ltd., London.

[3] Kanaya, H. *et al.*, 1992. Density variation in a heat and pressure-treated egg white during gel-to-glass-like transition. Jpn. J. Appl. Phys. 31, 3754–3758.

[4] Van Camp, J. and Huyghebaert, A. 1995. High pressure-induced gel formation of a whey protein and haemoglobin protein concentrate. Lebens-Wissen und Techn. 28, 111–117.

[5] Ponce, E. *et al.*, 1996. Texture and microstructure of egg gels formed under high hydrostatic presure at low temperature. In Proceedings of high pressure processing of food congress. Cologne, November 6–9.

Coagulation Under High Hydrostatic Pressure: Polymer Latices as a Model for Casein Dispersions

S. Ottow[1] and M. Schwertfeger[2]

[1]Institute of Inorganic Chemistry, University of Kiel, Olshausenstr. 40, D-24098 Kiel
Phone: +49-431-880-2404; Fax: +49-431-880-1608
shollricher@email.uni-kiel.de
[2]Federal Dairy Research Centre, Hermann-Weigmann-Str.1, D-24103 Kiel
Phone: +49-431-609-2275; Fax: +49-431-609-2309
schwertfeger@bafm.de

Abstract. The acidification of skim milk by glucono-δ-lactone (GDL) under high hydrostatic pressure leads to aggregate structures different from gels formed by acidification at ambient pressure. For a better explanation of the mechanism of acid coagulation carboxylated polystyrene latices were studied as a model system. A dispersion of carboxylated polystyrene particles was acidified by hydrolysis of GDL at 20 °C at pressures of 1 bar and 2 kbar, respectively. Colloidal stability, pH and aggregate structure as a function of time and initial concentration of GDL were observed.Under high pressure coagulates were formed at low initial concentrations of GDL and short durations of pressure treatment. After a short time of pressurization small floccules were formed. Longer durations of pressure treatment led to aggregate structures similar to a cobweb depending on initial concentration of GDL. It was observed that during acidification at ambient pressure the mobility and the streaming potential of the dispersions decreased whereas the charge of the particles remained negative during the observed reaction time. Coagulation at ambient pressure needed higher concentrations of GDL and longer reaction times. All aggregates had a strong tendency to form closer structures under very low shear stress. A mechanism of colloidal stability of the latex particles based on the structure of water surrounding the carboxylic groups at the surface of the particles is proposed.

1 Introduction

The influence of high hydrostatic pressures on foods has been studied extensively in recent years to develop a new method of food preservation. However from the point of view of a colloid chemist, high pressure is a more interesting tool for obtaining unknown changes of properties of various systems, e.g. gel formation and aggregate structures.

Whereas the gel formation of protein-containing systems has been studied widely, little is known about the influence on particle aggregation [1]. For a better

understanding of the processes which occur during high-pressure acidification of milk proteins the behaviour of polystyrene latices as a well known, pH sensitive model system was studied.

2 Materials & Methods

In the experiments a carboxylated polystyrene latex dispersion was used. The dispersion was purified by centrifugation after preparation and was characterized as follows: average particle diameter (d_{32}): 200 nm, surface charge 2.3 C/g, average charge density 197 A^2/charge, dry matter 3.42 mg/ml.

For acidification glucono-δ-lactone (GDL; Jungbunzlauer) was used. All operations were performed using deionized water.

Pressure experiments were carried out by mixing 1 ml of the latex dispersion with 1 ml of the freshly prepared solution of GDL immediately before pressurization at 2 kbar and 20 °C.

3 Results

The pH was measured using pH indicator sticks (Merck) after visual examination of the samples (Fig. 1). In the diagrams, the coagulated samples are marked. At the beginning of the reaction, the changes in pH were significant. After 20 min, they were minimal. The pressurized samples had a lower pH compared to the non-pressurized ones.

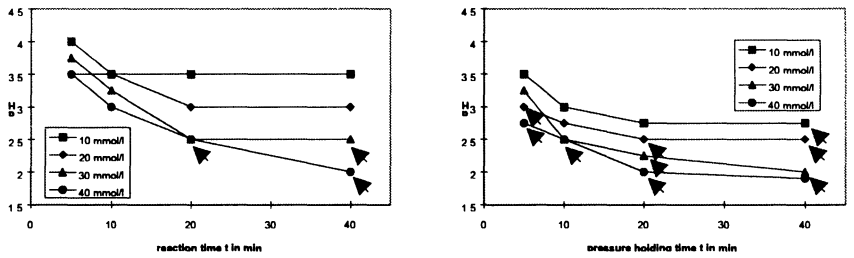

Fig. 1. Changes in pH by hydrolysis of GDL at various initial concentrations and reaction times at pressures of 1 bar (left) and 2 kbar (right)

Colloidal Stability. The critical coagulation concentration (ck) was determined after various times of pressurization at pressures of 1 bar and 2 kbar. The coagulated samples are indicated as black symbols (Fig. 2).

At ambient pressure, the samples only coagulated at high concentrations and after long reaction times. Pressure treatment caused coagulation within shorter time and at lower concentration of GDL. Samples which were stable when examined

visually were coagulated by shaking. Already formed floccules agglomerated to large-sized aggregates under minimal shearing.

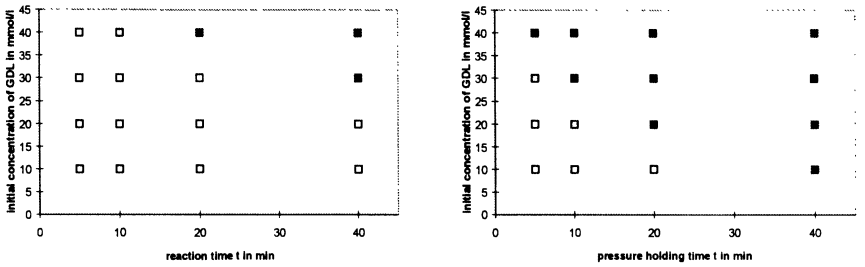

Fig. 2. Colloidal stability of latex dispersions depending on reaction times and initial concentration of GDL at pressures of 1 bar (left) and 2 kbar (right). White symbols indicate stable dispersions, coagulate samples are marked as black symbols

Streaming Potential (PCD). In a Particle Charge Detector (PCD; Mütek) 2.5 ml of water were added to 5 ml of the latex dispersion. After reaching the equilibrium 2.5 ml of a 0.2 M solution of GDL were added. The streaming potential was registered as a function of reaction time. Initially the dispersion had a large negative signal of about –750 mV. After adding GDL the streaming potential suddenly reaches –570 mV and increases slowly towards –270 mV within 35 min under shearing (results not shown).

Electrophoretic Mobilities. 100 µl of the dispersion were mixed with solutions of GDL of different concentrations. The electrophoretic mobilities were measured after various reaction times (Brookhaven Zeta Plus). The mobility of the particles decreased with the reaction time. At an initial concentration of GDL, the mobility is high and approximately constant within the observed time. At initial concentrations of 20 up to 40 mmol/l the mobility is independent of reaction time but smaller compared to a concentration of 10 mmol/l (results not shown).

Aggregate Structure. A drop of each sample was observed and photographed in a light microscope without using a cover slide in dark field illumination. Short reaction times lead to small floccules, longer times (about 40 min) lead to large network-like structures. With increasing concentration of GDL the dimension of the coagulates became larger. Structure and dimension of the aggregates depend also on the reaction time.

4 Discussion

The carboxylic groups located on the latex surface are strongly hydrated [2]. Thus it is possible that the hydration sphere surrounding the carboxylic groups contributes to colloidal stability. The stabilization mechanism of the latex dispersions might have an electrostatic and a steric part, caused by the hydration sphere. The surface potential decreases in acidic pH, caused by hydrolysis of GDL. The formed aggregates contain charges acting repulsive so that a slow coagulation seems to be possible and leads to network-like structures. Under similar conditions, latex dispersions do not coagulate when diluted to a lower particle concentration (1+4 v/v). The competing hydration of the carboxylic groups and of the ions in the bulk phase further contributes to destabilization.

The colloidal stability seems to be determined by the formation of an undisturbed hydration sphere around the particles.

Under high pressure, processes with a negative reaction volume are preferred. At pressures beyond 1.5 kbar the hydration sphere around casein particles is destroyed [3] and the water molecules tend to move into the bulk phase indicated by the smaller reaction volume of the dissociation of a carboxylic group (R-COOH $\rightarrow$ R-COO^- + H^+) of about –14 ml/mol compared to the reaction volume of the dissociation of free water ($H_2O \rightarrow H^+ + OH^-$) of about –22 ml/mol [4]. Also the hydrolysis reaction of GDL under pressure is accelerated [1] and the pH shifts faster compared to ambient pressure.

Under high pressure, obviously competing processes of hydration occur: hydration of the carboxylic groups on the particle surface and hydration of protons and OH-groups of the gluconic acid anion. The decomposition of the hydration sphere around the particles has a larger (negative) reaction volume compared to the ionization of the carboxylic groups and is therefore preferred.

It can be summarized that under high pressure the hydration sphere is weakened, the pH drops faster compared to ambient pressure and the particles have a smaller surface potential, insufficient for colloidal stability. The particles coagulate and the residual charge causes the formation of network-like structures.

References

[1] Schwertfeger, M., Buchheim, W. (1998); Acidification of milk by glucono-δ-lactone under high pressure; in Isaacs, N. S. (ed.): High Pressure Food Science, Bioscience and Chemistry, Royal Society of Chemistry, Cambridge.

[2] Ottow, S. (1998); Thesis; Universität Kiel, in preparation.

[3] Ohmiya, K., Kajino, T., Shimizu, S., Gekko, K. (1989); Effect of pressure on the association states of enzyme treated caseins; Agric Biol Chem, 53, 1–7.

[4] Asano, T., Le Noble, W. J. (1978); Activation and reaction volumes in solution; Chem Rev, 78, 407–489.

Pressure Induced Swelling Kinetics of Starch Granules

J. Snauwaert and K. Heremans

Katholieke Universiteit Leuven, Department of Chemistry, Leuven, Belgium
johan.snauwaert@fys.kuleuven.ac.be

Abstract. Pressure driven hydration of starch induces microstructural changes in the granules which finally result in the formation of a gel. The initial structural changes due to hydration produce a swelling of the potato starch granules which has been monitored *in situ* by optical microscopy in the diamond anvil cell. The rate constant of this swelling process increases with increasing pressure and the associated activation volume is -18 cm^3/mol. The swelling rate constant is independent of the surface-volume ratio of the granules.

1 Introduction

Starch granules are the major carbohydrate storage reserve of plants and are insoluble in water at normal temperature and pressure conditions. This mechanical stability arises from the chemical structure and arrangement of amylose and amylopectin within the granules. The smectic phases in which amorphous amylose and crystalline amylopectin are organised into alternating radial layers are responsible for their birefringence effect [1]. Gelatinisation of starch is a process in which the highly oriented structure is disintegrated by pressure or temperature due to the uptake of water. The pressure driven hydration of starch induces microstructural changes in the granule which finally result in the formation of a gel and the loss of their birefringence.

Here, we have studied the initial structural changes due to the pressure induced hydration. This hydration produces a swelling of the potato starch granules which has been monitored *in situ* by optical microscopy in the diamond anvil cell. The kinetics of the pressure dependent swelling process was investigated at different pressures.

2 Materials & Methods

The potato starch was kindly supplied by Dr. K. Autio from VTT Technical Research Centre of Finland, Biotechnology and Food Research. A 5% aqueous starch suspension was mounted in the 75 μm thick stainless steel gasket of a diamond anvil cell (Diacell Products, Leicester, UK) in the presence of ruby and

in situ microscopic observations were registrated under pressure at room temperature (25 °C). The pressure was determined by measuring the shift of the ruby fluorescence with a Spex Raman spectrometer. The *in situ* observations were recorded on video, digitised and analysed by an image processor. To prevent starch sedimentation the viscosity of the solution was increased by solubilising a portion of starch by heating. A 2% presolution was obtained by boiling starch during 15 min under continuous stirring. This 2% presolution was used for the manufacture of a 5% starch suspension.

3 Results

To study the microstructural changes induced by hydrostatic pressure we recorded the swelling of potato starch granules on video at different pressures. The digitised images were analysed and the individual granule volume was calculated using the estimated lengths of the major and minor axes of the best fitting ellipse. A clear individual pressure response could be noticed at different pressures under the microscope. Only a small fraction of the granules started swelling at pressures around 600 MPa. The number of swelling granules enhanced with increasing pressure and at 800 MPa all granules were involved in a swelling process. The first optical indication of granule swelling was given by a change in the refractive index of the hilum of the granule. Once the process has started, it cannot be stopped and a complete disintegration follows. This swelling process can only be stopped by reducing the pressure below the initial gelatinisation pressure. The dynamic volume increase could be fitted by a first order reaction for each granule.

The dispersion of the rate constants of the individual granules which exhibit an exponential growth at a particular pressure is rather small and independent of the granule size (Fig. 1). The associated volume change calculated from the average rate constant is -18 cm^3/mol.

During the initial swelling process the characteristic birefringence of the granules remained unchanged until a certain threshold level was reached. The pressure induced failing of the birefringence is shape dependent. Elliptical granules appear to have a much lower swelling threshold than spherical granules. The disruption of the 'Maltese crosses' under polarised light starts at a volume increase of 8% for medium ($\pm$ 50 μm) elliptical granules.

We also investigated the infrared spectrum of the individual swollen granules in an aqueous solution by infrared microspectroscopy. These stable swollen granules were obtained by reducing the pressure, as mentioned earlier. Unfortunately, the infrared spectrum of the undamaged but swollen potato starch granules is dramatically influenced by the dominating water band. This is in contrast to previous reports [2, 3] where the granules were squashed in the diamond anvil cell by which the water content is largely reduced. In this way we could not obtain any valuable infrared information of the swelling process.

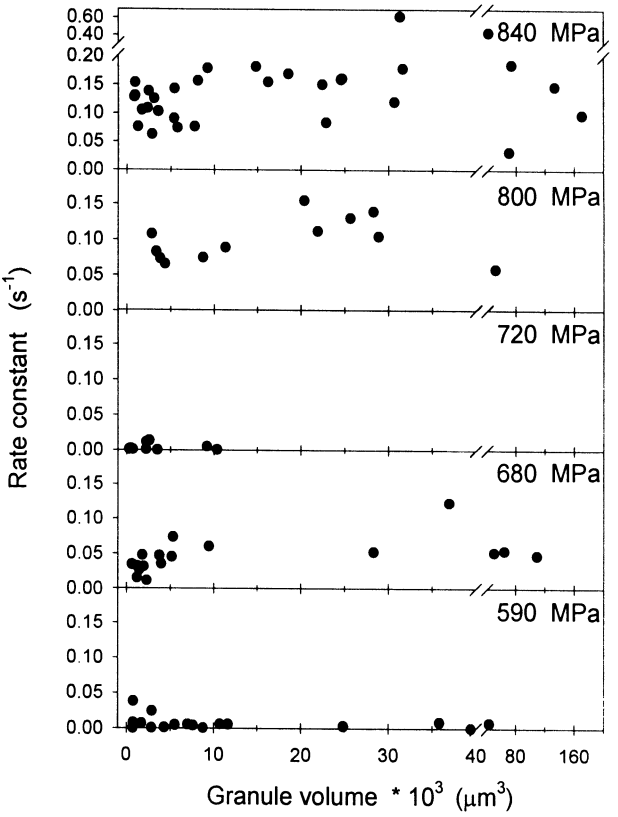

Fig. 1. Swelling rate constant as a function of the granule volume at different pressures

4 Discussion & Conclusions

The high pressure induced gelatinisation of starch involves a specific process in which water plays an essential role. Other solvents or additives, such as glycerol and sucrose, increase the gelatinisation onset temperature [4]. Alcohols are unable to produce starch gels even at much higher pressures. Potato starch granules which have been dried in an oven for 12 h at 120 °C and suspended in pure ethanol did not gelatinise at very high pressure. Even at 3 GPa when the ethanol became solid, the granules did not swell at all (unpublished observations). This adds support to the view that water structure changes with pressure. The onset of swelling can be seen first at the hilum, which is considered to be less organised than the rest of the granule. The initial swelling process of the potato starch granules seems to be a first order process. It has been postulated that differences in size and shape of the individual starch granules may lead to non-uniform swelling [5]. Our results indicate that the swelling rate constant is not related to the size and shape of the granules. This indicates that the water uptake is independent of the surface-volume

ratio of the granules. The fact that only the hilum of the granule changes dramatically at the onset of swelling indicates that its water permeability is different from the rest of the granule surface, so that the water influx occurs mainly through the hilum. The associated activation volume (–18 cm^3/mol) corresponds to the molar volume of water. The volume change is of the same order but opposite sign as previously estimated for temperature induced starch gelatinisation [6]. The opposite sign is in accordance with the elliptic phase diagram of protein denaturation [7].

The vanishing of the birefringence is related to the hydration of the amylopectin crystalline layers which leads to the disruption or 'melting' of the smectic phase. Symmetry arrangements could explain the lower swelling threshold observed in elliptical granules than in spherical granules.

Acknowledgements: This research is supported by EU project FAIR-CT-96-1175.

References

[1] Waigh, T. A., Hopkinson, I., Donald, A. M., Butler, M. F., Heidelbach,F. and Riekel C. (1997); Analysis of the native structure of starch granules with X-ray microfocus diffraction; Macromolecules, 30, 3813–3820.

[2] Rubens, P., Goossens, K. and Heremans, K (1997); Pressure induced gelatinisation of different starch types; High Pressure Research in the Biosciences and Biotechnology, Heremans, K. (Ed.). Leuven University Press, Leuven , Belgium, 191–194.

[3] Snauwaert, J., Rubens, P., Vermeulen, G., Hennau, F. and Heremans, K. (1997); *In situ* microscopic observations of pressure induced gelatinisation of starch in the diamond anvil cell; 35th EHPRG Meeting on High Pressure Food Science, Bioscience and Chemistry, University of Reading (UK), September 7–11.

[4] van Soest, J. J. G., Bezemer, R. C., de Wit, D., Vliegenthart, J. F. G. (1996); Influence of glycerol on the melting of potato starch; Industrial Crops and Products, 5, 1–9.

[5] Aguilera, J. M. and Baffico, P. (1997); Structure-mechanical properties of heat-induced whey protein/cassava starch gels; J. Food Science, 62, 1048–1066.

[6] Thevelein, J. M., Van Assche, J. A., Gerlsma, S. Y. and Heremans, K.(1981); Gelatinisation temperature of starch, as influenced by high pressure; Carbohydr.Res., 93, 304–307.

[7] Smeller, L. and Heremans, K. (1997);Some thermodynamic and kinetic consequences of the phase diagram of protein denaturation; High Pressure Research in the Biosciences and Biotechnology, Heremans, K. (Ed.). Leuven University Press, Leuven, Belgium, 55–58.

Carrageenan Gelification Under High Hydrostatic Pressure: Preparation and Processing of Solutions and Analysis of Gels Obtained

B. Steyer, F. Béra, C. Massaux, M. Sindic, Ch. Blecker and C. Deroanne

Unité de Technologie des Industries Agro-Alimentaires, Faculté Universitaire des Sciences Agronomiques, 2 Passage des Déportés, B-5030 Gembloux, Belgique
steyer.b@fsagx.ac.be

Abstract. The effects of high hydrostatic pressure (200, 400 MPa) and temperature (20, 40 and 60 °C) on the ι-carrageenan gelification were studied. The H.H.P. carrageenan gels were compared with those obtained by heat treatment at the same temperature and atmospheric pressure. Gels obtained under high pressure showed a maximum of hardness at 200 MPa for 120 min at 60 °C and a minimum at 400 MPa for 60 min at 40 °C. Results indicated that the textural properties of ι-carrageenan gels can be adapted by H.H.P. treatment parameters (pressure, pressurisation time and temperature).

1 Introduction

Carrageenans, highly sulphated polysaccharides extracted from red seaweeds, are widely used as functional ingredients in the food industry. Gelification and thickening are their two main functional properties which contribute significantly to the sensorial and textural characteristics of different foods [1]. When heated at high temperature (>70 °C), ι-carrageenan exists in solution as random coils but on cooling and in the presence of neutral salts, such as KCl, thermoreversible gels are formed [2].

High hydrostatic pressure processing is already used for diverse macromolecular transformations. It can be employed to change food structure, in particular to obtain weak or strong gels [3]. From studies on the effect of high pressure on the sol-gel transformations of some gelling agents (gelatin, *O*-methylcellulose), Suzuki e*t al.* have suggested that high pressure prompts gel formation of gelatin, but retards that of *O*-methylcellulose [4].

Gekko studied the sol-gel transitions of carrageenans by the determination of the melting pressure of the gels (obtained by thermal treatment) at various temperatures [5], but no detailed study of pressure-effect on the formation of carrageenan gel has been reported. The present work describes different attempts

of gelification under high pressure at 200 and 400 MPa at three temperatures (20, 40 and 60 °C). The texture profile analysis was performed on obtained gels.

2 Materials & Methods

The ι-carrageenan sample (Satiagel CT52) extracted from *Euchema spinosum* (Rhodophyceae) was supplied by SKW Biosystems Benelux (Bruxelles, Belgium) in the K^+ salt form and was used without further purification.

The ι-carrageenan solution (3%, w/w) was prepared by sprinkling under high-speed stirring, dry hydrocolloids in a 0.5% KCl (analytical grade) solution, at room temperature.

100 ml of this solution were poured into plugged flasks and subjected to high pressure treatment using an EPSint high pressure apparatus (Temse, Belgium). Pressure treatments were 200 and 400 MPa for 30, 60 or 120 min at temperatures of 20, 40 and 60 °C. Blanks were made at the same temperature and atmospheric pressure. All treatments were repeated at least three times.

After treatments, samples were kept at 8 °C for one night and then carefully taken out of the flask and cut in a disc of desired height (50 × 18 mm). Gelified structures were characterised by SMS texturometer (TA-XT2) following a Texture Profile Analysis (TPA) procedure.

3 Results & Discussion

A 3% solution of ι-carrageenan was submitted for 30, 60 and 120 min to atmospheric pressure and to 200 and 400 MPa under the following temperatures: 20, 40 and 60 °C.

At 20 °C, no gel was formed. Under these conditions, all samples (pressurized and non-pressurized) formed highly viscous solutions. At this temperature, high pressure cannot induce the formation of a structured gel.

Gels having enough firmness for texture measurements were formed at 40 and 60 °C under atmospheric pressure but also at 200 and 400 MPa. Three textural parameters from the TPA procedure were particularly observed: hardness, cohesiveness and springiness.

Tables 1 and 2 summarize the textural properties of gels formed at 40 and 60 °C, respectively.

All gels formed at 40 °C under high pressure were less hard, less cohesive and less springy than gels formed at the same temperature at atmospheric pressure. Moreover, at this temperature, the hardness of gels decreased with the applied pressure. A minimal hardness was obtained at 400 MPa for 60 min of pressurization.

Table 1. Textural properties of heat and pressure-induced gels of ι-carrageenan treated at 40 °C

Conditions for gel formation		Gels of ι-carrageenan (Satiagel CT52) 3% w/w		
Pressure (MPa)	Time (min)	Hardness (N)	Cohesiveness (-)	Springiness (-)
0.1[a]	60	2.06 (0.08)	0.75 (0.01)	0.93 (0.01)
	120	2.29 (0.20)	0.76 (0.01)	0.93 (0.04)
200[b]	30	1.95 (0.07)	0.57 (0.09)	0.89 (0.00)
	60	1.66 (0.06)	0.64 (0.05)	0.85 (0.02)
	120	1.67 (0.05)	0.60 (0.01)	0.87 (0.04)
400[b]	30	1.43 (0.07)	0.60 (0.11)	0.78 (0.04)
	60	1.11 (0.06)	0.50 (0.05)	0.80 (0.03)
	120	1.51 (0.06)	0.48 (0.05)	0.84 (0.01)

Numbers in parentheses represent standard deviation of the mean.

[a]Heated at atmospheric pressure in a water bath at 40 °C. [b]Pressurized at 40 °C.

Table 2. Textural properties of heat and pressure-induced gels of ι-carrageenan treated at 60 °C

Conditions for gel formation		Gels of ι-carrageenan (Satiagel CT52) 3% w/w		
Pressure (MPa)	Time (min)	Hardness (N)	Cohesiveness (-)	Springiness (-)
0.1[a]	60	3.06 (0.31)	0.75 (0.01)	0.97 (0.01)
	120	3.49 (0.20)	0.76 (0.01)	0.93 (0.04)
200[b]	30	2.49 (0.65)	0.77 (0.01)	0.90 (0.01)
	60	3.82 (0.26)	0.72 (0.01)	0.94 (0.00)
	120	4.09 (0.60)	0.71 (0.02)	0.88 (0.06)
400[b]	30	3.25 (0.67)	0.73 (0.02)	0.90 (0.07)
	60	3.10 (0.40)	0.71 (0.02)	0.92 (0.04)
	120	3.07 (0.20)	0.74 (0.01)	0.88 (0.08)

Numbers in parentheses represent standard deviation of the mean.

[a]Heated at atmospheric pressure in a water bath at 60 °C. [b]Pressurized at 60 °C.

Contrary to 40 °C, at 60 °C, high pressure seemed to have little or no effect on cohesiveness and springiness. A treatment under 200 MPa seemed to increase the gel hardness in comparison with the treatment at atmospheric pressure.

At each pressure, the gel hardness increased with the temperature. The carrageenan gels obtained under H.H.P. exhibited different textural properties than those obtained at atmospheric pressure. For instance, in our results, the hardness showed a minimum at 400 MPa for 60 min at 40 °C and the maximal value of this parameter was obtained at 200 MPa for 120 min at 60 °C.

It seems that ι-carrageenan gelification strongly depends on the time-temperature-pressure parameters. On the one hand, the texture can be less firm under high pressure. The pressurization reduces the textural properties. Gekko has shown that high hydrostatic pressure can destabilize gels. An intermolecular

hydrogen bond formation should accompany a reduction of water of hydration, leading to an increase in the volume of the system [5]. Thus, following Le Chatelier 's law, this phenomenon is disadvantaged by an increase of pressure and so destabilizes the gel. On the other hand, the texture can be firmer under high pressure. The intermolecular hydrogen bonds were probably mediated through the bridging water molecules in cross-linking junctions as demonstrated by Gekko for gelatin gels [5].

Further experiments are needed to better understand the gelification process and reasons for the different pressure-time-temperature dependency observed with this carrageenan. From a practical point of view, the textural properties of ι-carrageenan gels can be adapted by H.H.P. treatment parameters (pressure, pressurization time and temperature).

Acknowledgements: This research was supported by the Ministère de la Région wallonne, en application du Programme de Formation d'Impulsion à la Recherche scientifique et technologique.

References

[1] Société Satia (1986); Utilisation des hydrocolloïdes dans les applications alimentaires; Propriétés fonctionnelles des polysaccharides, Eds M. Colonna et M. Thibault, 143–186.

[2] Lynch, M.G., Mulvihill, D.M. (1996); Rheology of ι-carrageenan gels containing caseins; Food Hydrocolloids, 10, 151–157.

[3] Fernandes, P.B., Raemy, A. (1996); High pressure treatment of whey protein/ polysaccharide systems; High pressure and biotechnology, Eds R. Hayashi and C. Balny, 337–342.

[4] Suzuki, K., Taniguchi, Y., Enomoto, T. (1972); The effect of pressure on the sol-gel transformations of macromolecules; Bull. Chem. Soc. Jpn., 45, 336–338

[5] Gekko, K. (1992); Effects of pressure on the sol-gel transition of food molecules; High pressure and biotechnology, Eds. C. Balny *et al.*, 224, 105–113.

Microscopic and Rheological Characterization of High Pressure Treated Starch Dispersions

M. Stolt and K. Autio

VTT Biotechnology and Food Research, P.O. Box 1500, FIN-02044 VTT, Finland
Martina.Stolt@vtt.fi

Abstract. The structure of four different high pressure treated aqueous starch dispersions (starch concentration ~10%) was studied by rheological techniques and light microscopy. The rheological properties of the pressure and heat treated samples were compared. Waxy maize and potato starch formed gels under pressure. The rheological properties of these gels differed from the properties of heat induced gels. Barley starch showed some swelling of granules, but no gel formation after the pressurization. No major structural changes were observed for the amylomaize starch dispersion after pressurization at 900 MPa and 30 °C.

1 Introduction

Aqueous starch dispersions can be gelatinized at room temperature under high pressure [1–6]. The pressure needed for gel formation depends, however, considerably on the origin of the starch, starch concentration, temperature and duration of pressure treatment. In this study, the pressure induced changes of dispersions of four different native starches were investigated using light microscopy and rheological techniques.

2 Materials & Methods

Samples of waxy maize, amylomaize, potato and barley starch were prepared using a method where the bulk of native starch was suspended in a 2% heat gelatinized starch paste [7]. This was done in order to reduce the sedimentation of starch during the pressure treatment. For the samples of waxy maize, amylomaize and barley starch, waxy maize starch was used for the heat gelatinized paste, and for the potato starch samples potato starch was used. The concentration of native starch in the heat gelatinized paste was 8.2% for the waxy maize, amylomaize and potato starch dispersions, and 10% for the barley starch dispersion.

Small plastic pouches filled with starch dispersion were pressure treated at 600–900 MPa in a multivessel high pressure unit (Resato International B.V., The

Netherlands) for different time periods. The cylindrical vessels have an internal diameter of 25 mm and they are 85 mm high. The rate of pressure build-up was 10 MPa/min up to 100 MPa and 20 MPa/min from 100 MPa upwards. The vessels were tempered at 30 °C, but the temperature increased 10 °C at maximum during pressure build-up due to adiabatic heating. By pressure treatment time is meant the time the samples were kept at constant pressure. The samples were analyzed immediately after the treatment.

Heat treatment was carried out by heating the plastic pouch containing the sample in a 90 °C water bath for 30 min. The sample was analyzed the following day.

Rheological measurements were performed at 25 °C by a Bohlin VOR rheometer (Bohlin Reologi Ab, Sweden). For fluid-like samples concentric cylinders were used as measuring system. The diameter of the bob was 14 mm. For gelled samples a cone/plate measuring system, with a diameter of 30 mm and a cone angle of 5°, was used.

The sample was loaded into the measuring system and allowed to rest for 10 min. A strain sweep test was performed using the oscillatory mode of the rheometer. The strain was gradually increased from 0.000206 to 0.206 in 40 logarithmic steps. A frequency of 1 Hz was used. The storage and loss modulus and the phase angle were recorded as functions of applied strain.

The viscosity of fluid-like samples was measured at an increasing shear rate from 18.5 to 184 s^{-1}, followed by a decreasing shear from 184 to 18.5 s^{-1}. The total shearing time was 170 s. Due to the thixotropic nature of the samples, the shearing loop was repeated five times, with a 30 s interval between the measurements, until no or only slight thixotropy was observed.

A drop of a the fluid-like sample was smeared onto an object glass, iodine stained with Lugol's solution and examined under a light microscope (Olympus Vanox T, Japan). The birefringence of unstained smear samples was studied under polarized light. Of the gelled samples, embedded sections were prepared. They were examined similarly to the smears.

3 Results & Discussion

Waxy maize starch formed a weak gel during a 10 min pressure treatment at 600 MPa. The storage modulus of the gel was almost five times higher than the storage modulus of the corresponding heat gelatinized sample and the phase angle was considerably lower (Table 1). The gel formation of the pressurized sample was microscopically discovered to be related to the swelling and disintegration of the starch granules and loss of birefringence (Fig. 1). A colloidal type of gel network was observed.

Table 1. The storage modulus (G') and the phase angle (δ) for the pressure and heat treated samples (ND=not detected)

Starch type	Pressure treated				Heat treated	
	Pressure (MPa)	Time (min)	G' (Pa)	δ (°)	G' (Pa)	δ (°)
Waxy maize	600	10	70	18	15	29
Amylomaize	900	50	ND	ND	ND	ND
Potato	750	30	3540	3	330	6
Barley	600	50	ND	ND	1560	6

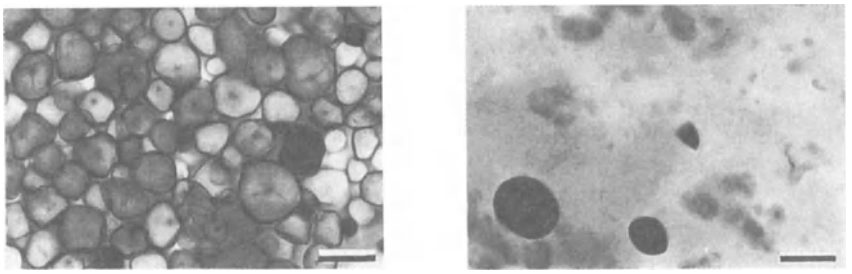

Fig. 1. Micrographs of untreated (left) and pressure treated (right) waxy maize starch (bar=20 μm)

For amylomaize starch, slight swelling of starch granules was observed after a 50 min pressure treatment at 900 MPa. The starch granules were still birefringent after this treatment, and no major change in viscosity was detected.

Potato starch formed a very rigid gel during a 30 min pressure treatment at 750 MPa. The storage modulus of the pressure induced gel was about ten times higher than the storage modulus of the corresponding heat induced gel (Table 1). During the pressure treatment, loss of birefringence and swelling of granules was observed.

Barley starch did not form a gel during a 50 min pressure treatment at 600 MPa, but the viscosity of the dispersion increased slightly. Microscopic examination showed some swelling of granules (Fig. 2) and a complete loss of birefringence. By heat treatment a rigid gel was formed (Table 1).

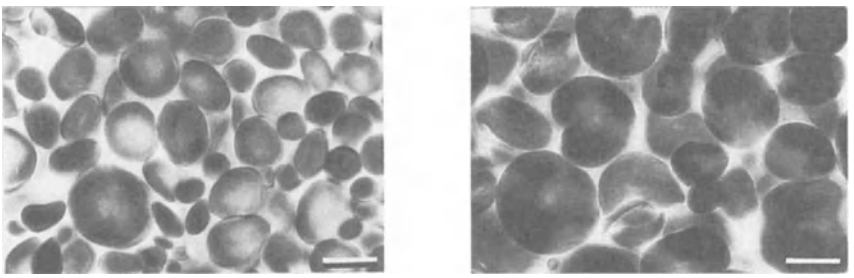

Fig. 2. Micrographs of untreated (left) and pressure treated (right) barley starch (bar=20 μm)

4 Conclusions

Waxy maize and potato starch formed gels under pressure. The pressure induced gels were in both cases stronger than the corresponding heat induced gels. For amylomaize no major structural changes were detected. Barley starch did not form a gel during pressurization, but some swelling of granules and a complete loss of birefringence was observed.

Acknowledgements: This research has been financially supported by the European Union (Project FAIR-CT96-1175).

References

[1] Muhr, A.H. and Blanshard, J. M. V. (1982); Effect of hydrostatic pressure on starch gelatinisation; Carbohydrate Polymers, 2, 61–74.
[2] Muhr, A.H., Wetton, R. E. and Blanshard, J. M. V. (1982); Effect of hydrostatic pressure on starch gelatinisation, as determined by DTA; Carbohydrate Polymers, 2, 91–102.
[3] Hibi, Y., Matsumoto, T. and Hagiwara, S. (1993); Effect of high pressure on the crystalline structure of various starch granules; Cereal Chemistry, 70, 671–676.
[4] Douzals, J.P., Marechal, P. A., Coquille, J. C. and Gervais, P. (1996); Microscopic study of starch gelatinization under high hydrostatic pressure; Journal of Agricultural and Food Chemistry, 44, 1403–1408.
[5] Stute, R., Klingler, R. W., Boguslawski, S., Eshtiaghi, M. N. and Knorr, D. (1996); Effects of high pressure treatment on starches; Starch/Stärke, 48, 399–408.
[6] Rubens, P., Goossens, K. and Heremans, K. (1997); Pressure induced gelatinisation of different starch types: A FTIR study; In: High Pressure Research in the Biosciences and Biotechnology, ed. K. Heremans, Leuven University Press, Belgium, pp. 191–194.
[7] Conde-Petit, B. and Escher, F. (1994); Influence of starch-lipid complexation on the aging behavior of high concentration starch gels; Starch/Stärke, 46, 172–177.

Chemical Reactions of Food Constituents at High Pressure

Chemical Reactions of Food Components Under High Hydrostatic Pressure

B. Tauscher

Institute of Chemistry and Biology, Federal Reserch Centre for Nutrition,
Haid-u.-Neu-Str. 9, D-76131 Karlsruhe, Germany
Bernhard.Tauscher@bfe.uni-karlsruhe.de

Abstract. Food pasteurized by hydrostatic high pressure have already been marketed in Japan. There is great interest in this method also in Europe and USA. Temperature and pressure are the essential parameters influencing the state of substances including foods. While the influence of temperature on food has been extensively investigated, effects of pressure, also in combination with temperature, are attracting increasing scientific attention now. Processes and reactions in food governed by Le Chatelier's principle are of special interest; they include chemical reactions of both low- and macromolecular compounds. Examples of pressure affected reactions are presented.

1 Introduction

High-pressure application is a promising technique for the preservation and processing of food. Food pasteurized by hydrostatic high pressure have already been marketed in Japan. There is great interest in this method also in Europe and USA. Advantages compared to thermal processing, such as better retention of colour, taste, and nutrients are explained by the failure of pressure to break covalent bonds. However, pressure as a thermodynamic factor similar to temperature is known to influence chemical equilibria and reaction rates according to the Le Chartelier principle, allowing covalent bond ruptures as a consequence of chemical reactions which are associated with reductions in volume [1].

Examples of pressure induced reactions are autoxidation of unsaturated and saturated fatty acids [2]; Diels–Alder reaction between vitamins K 1–3 and myrcene [3]; formation of Diels–Alder products by coenzyme Q0 and myrcene [3]; solvolytic degradation of allyl- and benzylisothiocyanate; stability of vitamin A, B and C under different conditions; solvolytic etherification of vitamin A acetate; degradation of dipeptide esters [4]; formation of volatiles and chlorophyll degradation.

In experiments under different pressures and temperatures we have in rare cases found very drastic pressure effects within minutes under conditions of commercial pressure application. In most cases, however, no effects have been observed.

2 Examples of Pressure Induced Reactions

2.1 Cyclization Reactions of Food Components

Cycloadditions – giving rise to two new bonds – according to dipolar or concerted mechanism are accompanied by strong volume contraction in the transition state and accelerated by pressure [5]. We studied Diels–Alder reactions of food ingredients, cyclization fo squalene and formation of 2,5-dioxo-piperazine from aspartame.

Squalene is a C30 carbon present e.g. in olive and rice oil. Squalene and its 2,3-epoxide are important precursors of polycyclic hydrocarbons. In an enzymic reaction squalene yields, in a series of concerted cyclization reactions from the all-chair conformation, a five-chain condensed ring system which subsequently, in a concerted Wagner–Meerwein cascade of rearrangements, stabilizes as fern-8-ene. Ring formation is associated with five new bonds emerging.

We studied a 10% (v) solution of squalene in ethanol/n-hexane = 1:1 (v/v) at 650 MPa and 70 °C for up to 24 h at pH 1, pH 2 and pH 3. At pH 1, but not at higher pH, plenty of reaction products were detected. They remain being elucidated.

Prenylquinones as important carriers in the electron transport chain are ubiquitous. In the mitochondria of mammals ubiquinone (coenzyme Q) is responsible, in plants plastoquinone. In Diels–Alder-reactions quinones may act as dienophiles. We studied the reaction of coenzyme Q0 with myrcene at 650 MPa and 70 °C.

A Diels–Alder reaction between co-enzyme Q0 and myrcene may give rise to serveral isomeric compounds. Reaction products of co-enzyme Q0 and myrcene at 650 MPa, 0.1 MPa and 70 °C were separated by HPLC. A large quantity of products (isomers) is present as soon as after few minutes of pressure exposure (650 MPa, 70 °C).

The vitamin K group includes vitamin K1 present in green plants, vitamins K2 from bacteria, and synthetic vitamin K3. Vitamin K1 is a precursor of the posttranslational carboxylation of specific glutamate residues to γ-carboxyglutamate in many proteins involved in blood clotting.

The Diels–Alder reaction between vitamin K3 and myrcene under high hydrostatic pressure was shown only recently [6]. Vitamin K1, too, reacts with myrcene when exposed to pressure and elevated temperature; two products are formed.

The reaction products of vitamin K1 and myrcene at 650 MPa, 0.1 MPa and 70 °C were separated by HPLC. After about 8.9 min cis-vitamin K1 appeared, its trans-isomer after 9.8 min. At a ration of 12:88. 'Meta' and 'para' isomeric Diels–Alder products appeared after 8.3 and 9.4 min, resp. After three hours of pressure exposure minor quantities of the products have formed, while after 15 min no products were detected.

The influence of pressure on the formation of the cyclization product of the dipeptide Aspartame as a model reaction was investigated in a grape juice matrix.

Aspartame has been shown to be highly sensitive to pressure e.g. in Milk [4]. 1-2 mmol/l solutions of L-aspartyl-L-phenylalanine methylester (=Aspartame, Nutrasweet) in 0.05 mol/l Tris/HCI buffer, pH 7, and in commercial grape juice were treated at 700 MPa for 3, 10 and 30 minutes. Aspartame was very unstable in Tris buffer, but nearly unaffected in grape juice under the same conditions. Degradation products were L-aspartyl-L-phenylalanine and cis-3,6-dioxo-5-(phenylmethyl)-2S-piperazine acetic acid (diketopiperazine, DKP, the acceptable daily intake (ADI) value of DKP is one tenth of that of Aspartame) and aspartyl-phenylalanine. Pressure treatment of fruit of acid pH will not lead to significant formation of cyclization products from Aspartame like peptides.

2.2 Stability of Vitamins to High Hydrostatic Pressure

The stability of vitamins under high pressure conditions is of particular interest. As model systems solutions of ca. 1000 mg/l ascorbic acid in 0.1 mol/l sodium acetate buffer, pH 3.5–4, plus 10% sucrose were used [7]. Three variants were studied: complete exclusion of oxygen by evacuation and rinsing with nitrogen, oxygen saturation, and solutions exposed to air. The samples were filled into teflon bottles (10 ml) and exposed to 0.1, 300, 450 and 650 MPa for 10, 20 and 40 min at 40, 60 and 75 °C and examined by the L-ascorbic acid colour test of Boehringer Mannheim (Germany) (No. 409 677) with extended incubation time. In all model solutions with normal exposition to air vitamin C losses were greater under pressure (maximally 45% after 40 min treatment at 600 MPa and 75 °C). In oxygen free solutions loss of Vitamin C was slowed down as expected. With 10% sucrose a protective effect against degradation of vitamin C due to hydrostatic pressure was observed.

The influence of combined pressure and temperature on retionol, dissolved in a 100% ethanolic solution, was investigated at four pressure levels (0.1, 200, 400 and 600 MPa) and four temperature levels (25, 40, 60 and 75 °C). At all temperatures studied, pressure up to 400–600 MPa was required to induce significant destruction of retinol. Vitamin A acetate in 100% ethanolic solution was studied at the same pressure levels but at higher temperatures (60, 70, 80 and 90 °C). The degradation of vitamin A acetate became more pronounced with increasing temperature and pressure. At the highest temperature, complete degradation was observed after 2–16 minutes treatment, depending on the pressure applied.

Instead of the expected Diels–Alder-adducts, two retinylethyl ethers were identifed as reaction products. A plausible mechanism including formation of the retinyl cation is suggested. The mechanism was decribed by C.K. Ingold [9].

2.3 Influence of High Pressure on Isothiocyanates

Isothiocyanates are important for human health and for the sensory quality (pungency) of some vegetable produce. They are formed from glucosinolates in an enzymatic reaction corresponding to the Lossen degradation of hydroxamic acids.

They may enter into further reactions, e.g. solvolysis to form thiocarbamates and thiocarbamic acids. These reaction products can enter into further hydrolysis forming amines.

Allyl and benzyl isothiocyanate in aqueous ethanolic solution were treated at 25, 40, 60 and 70 °C at atmospheric and elevated pressure (600 MPa). Reaction times were 30, 60, 90 and 120 minutes. A more detailed study was performed for the allyl isothiocyanate, including shorter reaction times and four different pressure levels (0.1, 200, 400 and 600 MPa). In all cases, high pressure increased the extent of degradation. Moreover, in the case of the allyl isothiocyanate, a strong change in flavour of the reaction mixtures treated under pressure was recognised.

In the case of benzyl isothiocyanate, a small quantity of a white solid reaction product 1,3-dibenzylthiourea was isolated. This suggests the intermediate formation of benzylamine.

References

[1] Tauscher B. (1995); Pasteurization of Food by Hydrostatic High Pressure: Chemical Aspects; Z Lebensm Unters Forsch, 200, 3–13.

[2] Kowalski E., Ludwig H. and Tauscher B. (1996); Behaviour of organic compounds in food under high pressure: lipid peroxidation; In: High pressure Bioscience and Biotechnology; Hayashi R. and Balny C. (Eds); Progress in Biotechnology 13, 473–479.

[3] Grupe C., Marx H., Kübel J., Ludwig H. and Tauscher B. (1997); Cyclization reactions of food compounds to hydrostatic high pressure; In: High pressure research in Bioscience and Biotechnology; Heremans K. (Ed.), 339–342.

[4] Butz P., Garcia-Fernandez A., Fister H. and Tauscher B. (1997); Influence of High Hydrostatic Pressure on Aspartame: Instability at Neutral pH; J. Agric. Food Chem., 45 302–303.

[5] Scheeren J.W. (1989); In: Jurczak J. and Baranowski B. (Eds); High pressure chemical synthesis. Elsevier, Amsterdam Oxford New York Tokyo, 168–209.

[6] Ludwig H., Marx H. and Tauscher B. (1994); Diels–Alder Reactions of Food-Relevant Compounds under High Pressure Conditions; High pressure Research Group, Proceedings of the XXXII Annual Meeting, Brno, Czech Republic, 199–202.

[7] Taoukis P.S., Panagiotidis P., Stoforos N.G., Butz P., Fister H. and Tauscher B. (1998); Kinetic of Vitamin C Degradation Under High Pressure-Moderate Temperature Processing in Moedel Systems and Fruit Juices; In: High Pressure Food Science, Bioscience and Chemistry; Isaacs N.S (Ed.); The Royal Society of Chemistry, Cambridge, United Kingdom, 310–316.

[8] Kübel J., Ludwig H., Tauscher B. (1997); Influence of UHP on Vitamin A acetate Content; In: High Pressure Research in the Biosciences and Biotechnology; Heremans K. (Ed.); Leuven University Press, Leuven, Belgium, 331–334.

[9] Ingold C.K. (1969); Structure and Mechanism in Organic Chemistry, 2nd ed.; Cornell University Press. Ithaca, New York.

[10] Grupe C., Ludwig H. and Tauscher B. (1998); The Effect of High Pressure on the Degradation of Isothiocyanates; In: High Pressure Food Science, Bioscience and chemistry, Isaacs N.S. (Ed.); The Royal Society of Chemistry, Cambridge, United Kingdom, 125–129.

The Influence of High Pressure on the Autoxidation of Major Unsaturated Fatty Acid Constituents of Milk

P. Butz, B. Zielinski, H. Ludwig and B. Tauscher

Federal Research Centre for Nutrition, Institute of Chemistry and Biology, Engesserstr. 20, D-76131 Karlsruhe, Germany
Peter.Butz@bfe.uni-karlsruhe.de

Abstract. The influence of high pressure on the autoxidation of oleic and linoleic acid methyl esters was investigated as it seems to be the model system closest to the problem. The reaction was studied at 0.1, 100, 350 and 600 MPa at 40 °C. Treatment times were 1, 2, 3, 5 and 20 h. Gas chromatographic data of the decrease of oleic acid methyl ester, taken as a measure for the degree of autoxidation, showed no influence of pressure. The autoxidation of linoleic acid methy lester was accelerated by pressures from 350 MPa as shown by gas chromatographic data of the decrease of the educt as well as by the increase of primary oxidation products measured by HPLC or by the increase in UV-absorption at 234 nm. The primary oxidation products were separated by reversed phase HPLC: no effect of pressure on the distribution of isomers was found.

1 Introduction

Of the milk lipids 95% are triacylglycerols; the major unsaturated fatty acids of milk fat are oleic acid (18:1 or 9-octadeconic acid; 25% by weight) and linoleic acid (18:2 or 9,12-octadeconic acid; 2.1% by weight). It is generally agreed that autoxidation is the main reaction involved in oxidative deterioration of lipids leading to food spoilage. The matter of concern are sensorial unpleasant carbonyls formed from the reaction of molecular oxygen with unsaturated C_{18}-chains (which may have already been liberated from acyllipids by the action of lipases present in milk and dairy products). As the autoxidation of lipids is a rather complex process investigations in less complex model systems are required to study the influence of pressure. In this work the influence of high pressure on the autoxidation of oleic and linoleic acid methyl esters was investigated as it seems to be the model system closest to the problem.

2 Materials & Methods

High Pressure Treatment. Experiments were conducted in a high pressure device consisting of a series of thermostated micro-autoclaves (ID 16 mm, ca. 10 ml) connected by valves [1]. Pressure was generated manually using a hand pump in combination with a pressure intensifier. The pressure transmitting medium was water. Due to adiabatic heating an initial temperature rise is to be expected on pressurizing (about 3 °C per 100 MPa). Measurements in the autoclave by a high pressure thermocouple indicated temperature changes of not more than 4 °C at maximum pressure due to rapid heat exchange with the vessel walls and the relatively slow manual pressure build-up. The initial temperature was usually restored after 1 to 2 min.

Preparation of Samples. 110 µl of linoleic acid methyl ester or oleic acid methyl ester (Sigma) were pipetted under nitrogen into a laminated plastic pouche (outside polyethyleneterephthalate copolymer 8 µm, middle aluminium 7 µm, inside LDPE 75 µm) and heat sealed. With a syringe 15 ml of oxygen (=0.66 mmol) were injected into the sample and the bag sealed again. Temperature controls were identical samples in pressureless autoclaves, after treatment all samples were stored until analysis at –18 °C.

HPLC. The separation of the primary oxidation products of linoleic acid methyl ester was done by reversed phase HPLC on a HD-SIL-C8, 125 × 4.6 mm column, with a HD-SIL-C8, 10 × 4.6 mm precolumn at a flow rate of 1 ml per minute. The liquid phase was acetonitrile/water from 50:50 up to 90:10. The injection volume was 20 µl at a sample start concentration of about 4.42 mg/ml in acetonitrile. Detection was at 215 nm (carbonyl group) and at 234 nm (conjugated diene).

Gas Chromatography. The decrease of the methyl ester of linoleic acid and oleic acid after pressure treatment was monitored directly by gas chromatography using an internal standard (palmitic acid methyl ester, 2.123 mg/ml). GC conditions were: DB1 column (J+W, 0.25 µm, 0.32 mm, 30 m, polydimethylsiloxane); FID at 200 °C; injector 200 °C; 200 °C isothermal; pressure 0.1 MPa, split 1:33, carrier gas helium.

UV-Spectrometry. The content in conjugated dienes may be taken as a measure of increasing oxidation. The absorption maximum for conjugated dienes is at 234 nm. 5 µl of the oxidized linoleic acid methyl ester were dissolved in 5 ml of 80% ethanol and measured in 1 cm quartz cuvettes at 234 nm.

3 Results & Discussion

Figure 1 shows the change in concentration of linoleic acid methyl ester after different times of treatment at 0.1, 100, 350 and 600 MPa and 40 °C. A clear decrease with time is seen leading to about a residual 64% after 20 h treatment at 600 MPa. This result is qualitatively similar to the autoxidation of linolenic acid methyl ester under the same conditions [2]. Interestingly the autoxidation of linolenic acid methyl ester was retarded by rising pressures and strongest under normal pressure.

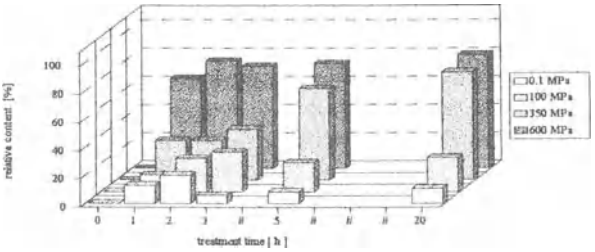

Fig. 1. Autoxidation of linolenic acid methyl ester. Change in concentration after different times of pressure treatment at 40 °C

With linoleic acid methyl ester the opposite seems to be the case. While at normal pressure and 100 MPa only marginal changes are found, the methyl ester decreases to about 70% at 350 MPa under the given conditions. Gas chromatographic data of the decrease of oleic acid methyl ester, taken as a measure for the degree of autoxidation, showed no influence of pressure (data not shown). The autoxidation of linoleic acid methyl ester was accelerated by pressures from 350 MPa as shown by gas chromatographic data of the decrease of the educt (Fig. 1) as well as by the increase of primary oxidation products measured by HPLC (Fig. 2) or by the increase in UV-absorption at 234 nm (Fig. 3). The primary oxidation products were separated by reversde phase HPLC: no effect of pressure on the distribution of isomers was found.

It is concluded that pressure treatment does not affect the main unsaturated lipid constituent of milk (oleic acid). There is no effect on oleic acid. The oxidation of linoleic acid is accelerated by pressure, but the effects are small (ca. 10% loss) at application times below 1 h. There are no new oxidation products (compared to thermal treatment). Complementary investigations in dairy product matrices seem advisable.

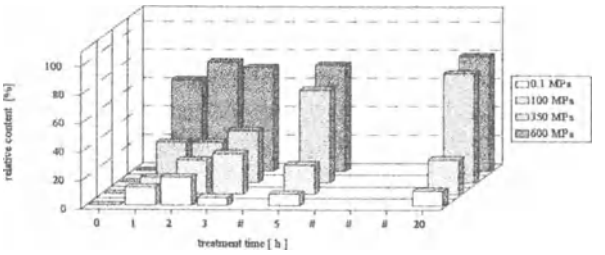

Fig. 2. Primary autoxidation products of linolenic acid methyl ester after different treatments at 40 °C. Relative content from RP-HPLC peak areas

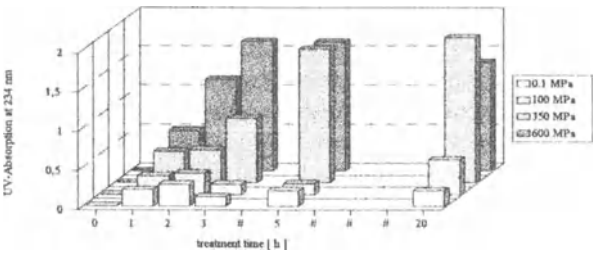

Fig. 3. Primary autoxidation products of linolenic acid methyl ester after different treatments at 40 °C. Relative content from UV-absorption at 234 nm

*Acknowledgements:*This work has been sponsored by the Commission of the European Union under contract No. FAIR CT96-1113.

References

[1] Butz, P., Koller, W.D., Tauscher, B. & Wolf, S. (1994); Ultra-high pressure processing of onions: Chemical and sensory changes; Lebensm.-Wiss. und -Technol., 27, 463–467.

[2] Tauscher, B. (1995); Review: Pasteurization of food by hydrostatic high pressure: chemical aspects. Z. Lebensm. Unters. Forsch. 200, 3–13.

Unexpected Solvolysis of Vitamin A Acetate Under High Pressure Conditions

J. Kübel[1,2], H. Ludwig[2] and B. Tauscher[1]

[1]Institute of Chemistry and Biology, Federal Research Centre for Nutrition, Engesserstr. 20, D-76131 Karlsruhe, Germany
[2]Institute of Pharmaceutical Technology, Universität of Heidelberg, INF 346, D-69120 Heidelberg, Germany
Phone: +49-(0)721-6625 116; Fax: +49-(0)721-6625 167
Bernhard.Tauscher@bfe.uni-karlsruhe.de

Abstract. Vitamin A acetate was tested for its changes under high pressure. In model solutions of vitamin A acetate in ethanol a Diels-Alder reaction was expected. Instead two ethyl ethers of vitamin A were obtained. Both the all-E-retinylethylether and the 13-Z-retinylethylether are formed via the retinyl-cation as intermediate. The mechanism for such etherifications was well described by C. K. Ingold [5].

1 Introduction

After having been discussed as an alternative method for preservation of food and pharmaceutical products, high pressure treatment of food has become the subject of intensified research in recent years [1]. Though it inactivates enzymes and contaminating microorganisms it is believed not to change valuable food components, such as vitamins and sensory quality. Chemical aspects, however, have been paid little attention so far, even though Henri Louis Le Chatelier had described the effect of external force (i.e. pressure) on a system in equilibrium state about one hundred years ago. Moreover, the influence of pressure on chemical reactions is very well known. Recently, the impact of high hydrostatic pressure on food by chemical changes was shown [2].

Vitamin A is a food component of high physiological importance. A dimer of the vitamin A alcohol, kitol, which is formed according to the Diels-Alder reaction mechanism has been described [3]. As the Diels-Alder reaction is very sensitive to pressure (activation and reaction volumes up to $-45\ cm^3/mol$) and is a thermally allowed pericyclic reaction, this dimer may also emerge under high pressure conditions.

Previous experiments revealed a greater loss of vitamin A acetate in model solutions at high pressure, giving rise to four product fractions detected by HPLC analysis [4]. Here the two main products of the reaction are presented and a plausible mechanism of their formation is proposed.

2 Materials & Methods

Because the results of the experiments using vitamin A alcohol were not reproducible, all-E-vitamin A acetate (Merck; oily concentrate for biochemical purpose) was used for the high pressure experiments. Solutions of vitamin A acetate (concentration: $2 \cdot 10^{-2}$ mol/l) in absolute ethanol were filled into air-tight bags (trilaminate of PEt/Al/LDPE) and heat sealed. The samples were cooled to -18 °C before pressure treatment. This was to avoid too much adiabatic heating during the build-up of pressure. The pressure maximum was reached quickly (about 1 min).

The reaction conditions were 650 MPa / 70 °C / 10 h to get 100% degradation of the vitamin A acetate.

Samples were analysed by HPLC (Knauer Nucleosil 50-5, 250 mm × 4.6 mm) using n-hexane/ethyl acetate (90/10, v/v); detection was done by absorption at 325 nm. The structures of the products were identified by NMR (Bruker Spectrospin drx 500) and IR spectroscopy (Bruker IFS66-FT-IR) and mass spectrometry (Finnigan MAT 90) (Fig. 1).

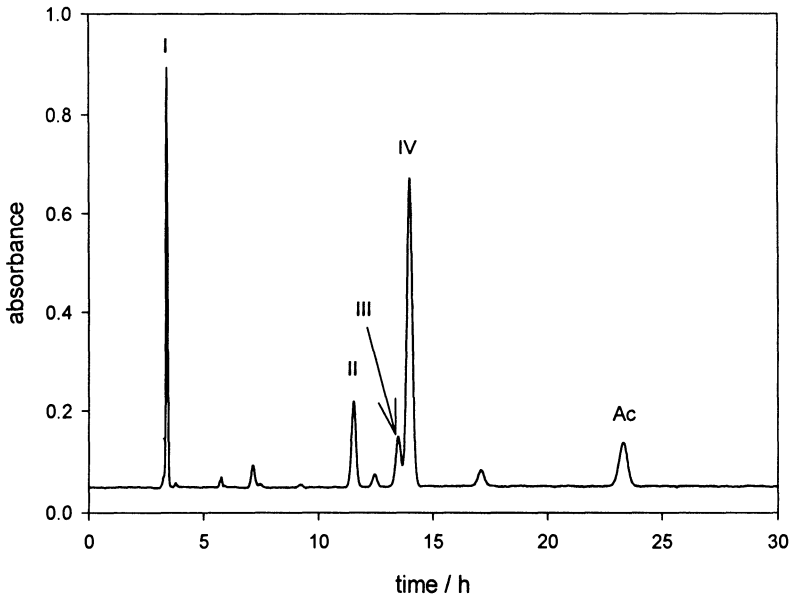

Fig. 1. Chromatogram of vitamin A acetate after treatment with 650 MPa at 70 °C for 4 h; I–IV: reaction products, Ac: all-E-vitamin A acetate

3 Results & Discussion

The ^{13}C-NMR spectra of both main products did not have a peak characteristic of a carbon atom of a carbonyl group, and their IR spectra did not show a carbonyl band either. The high resolution mass spectrum yielded a molecular weight of $C_{22}H_{34}O$ in both cases.

The ^{1}H-NMR spectrum of product II, however, was very similar to that of the all-E-vitamin A acetate; the $COCH_3$ group only was missing. Instead an ethyl group attached to a heteroatom appeared.

The ^{1}H-NMR spectrum of product I differed from product II mainly in the area of the olefinic protons. The peak of the proton at C^{12} underwent the greatest change of resonance frequency.

The two main products were thus the ethers of vitamin A. The main product appeared to be the all-E-retinylethylether, while the second one was the 13-Z-retinylethylether (Fig. 2).

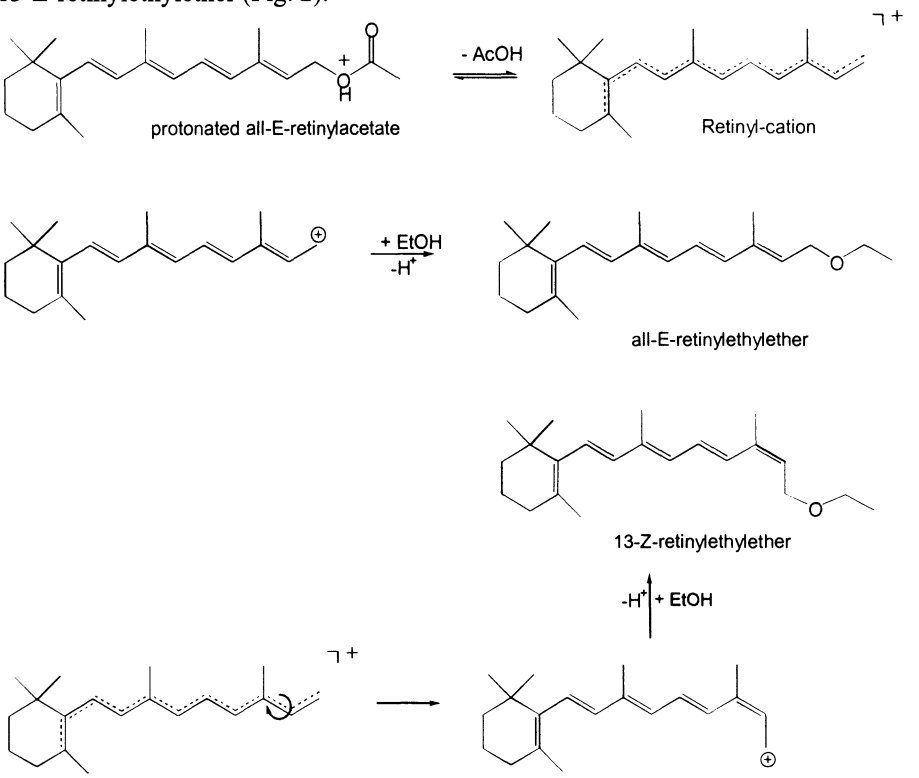

Fig. 2. The supposed reaction mechanism

The first step of the reaction mechanism is an acid catalysed ester cleavage that retains the bond connecting the carbonyl carbon atom with the oxygen atom of the

alcohol leading to the retinyl-cation as a leaving group. Protons result from a self-dissociation of ethanol under pressure. The retinyl-cation is stabilised by resonance leading to a certain lifetime. Hence the cation is able to undergo isomerization forming sterically unhindered Z-isomers of the cation.

Eventually the cation electrophilically attacks a lone pair of the oxygen of the solvent ethanol to give the ethers after loss of a proton. The reaction was allowed also in methanol and yielded the corresponding methyl ethers of vitamin A. This confirmed the mechanism pathway proposed.

However, no kitol analogue dimer of the vitamin A acetate has been identified so far under these reaction conditions.

The described mechanism of ester cleavage was investigated by Ingold [5] and is called $A_{Al}1$, but has not yet been described at high pressure conditions.

In fact, a unimolecular cleavage like that of vitamin A acetate should be retarded at high pressure. However, one product of this step is acetic acid which, of course, will dissociate even more readily at high pressure conditions leading to a negative reaction volume due to electrostriction. This is the driving force for the reaction to take place.

References

[1] Hayashi, R.; Application of High Pressure to Food Processing and Preservation: Philosophy and Development, in: Engineering and Food (Spieß, W.E.L. and Schubert, H., eds.), Vol. 2 (1989) p. 815.

[2] Tauscher, B.; Z. Lebensm. Unters. Forsch. 200 (1995) p. 3.

[3] Burger, B. V. *et al.*; Chem. Comm. (1965) 588; [b] Burger, B.V. *et al.*; J. Chem. Soc. Perkin Trans I (1973) 590.

[4] Kübel, J. *et al.*; Influence of UHP on vitamin A content, in: High Pressure in the Bioscience and Biotechnology (Heremans, K., ed.), Leuven University Press (1997) p. 331.

[5] Ingold, C.K.; Structure and Mechanism in Organic Chemistry, 2nded., Cornell University Press, Ithaca, New York, 1969.

High Pressure Processing of Foods and Food Related Materials

The Relevance of Kinetic Data in High Pressure Food Processing

M. Hendrickx, S. Denys, Indrawati, L. Ludikhuyze, I. Van den Broeck and C. Weemaes

Katholieke Universiteit Leuven, Department of Food and Microbial Technology, Laboratory of Food Technology, Kardinaal Mercierlaan 92, B-3001 Leuven, Belgium
Phone: 32-16-32.15.85; Fax: 32-16-32.19.60
Marc.Hendrickx@agr.kuleuven.ac.be

Abstract. High pressure is an emerging technology with high potential as a new unit operation in food preservation and processing. The most likely applications will be in combination processes, especially with moderate temperature elevation. However, there are a number of scientific, technological and industrial difficulties to be overcome in order to successfully apply HP/T processes to foods, both from a legislative point of view and from optimal quality and consumer acceptability requirements. To overcome these difficulties, a scientific kinetic basis for design, evaluation and optimization of HP/T processes is indispensable.

1 Introduction

The general objective of the EU-project FAIR-CT96-1175 ("Combined high pressure thermal treatment of foods: a kinetic approach to food safety and quality") is therefore to develop a scientific food engineering basis, enabling industrial application of this new technology in a justified way. The objective will be reached through implementation of eight research tasks. Firstly detailed kinetic studies will be performed on different safety and quality aspects including inactivation of food quality related enzymes (task 1), inactivation of microorganisms (task 2), changes in food structure (task 3) and changes in nutritional and sensorial quality aspects (task 4). In each task an increasing order of complexity in the composition of the medium (from simple model systems over complex model systems to real food products) will be considered. Based on the kinetic information gathered, concepts for quantitative process impact evaluation (task 5) will be formulated. Hence these will be the basis for evaluation of process impact uniformity and repeatability (task 6), shelf life studies (task 7) and process optimization (task 8).

2 Methodology

The kinetics of a reaction describe its progress in time. How the reaction progresses as a function of time is expressed by mathematical models such as a first order kinetic model (1) or a fractional conversion model (2), where A is e.g. the enzyme activity, k the inactivation rate constant (min^{-1}) and t the time (min).

$$A_t = A_0 \exp(-kt) \tag{1}$$

$$A_t = A_\infty + (A_0 - A_\infty)\exp(-kt) \tag{2}$$

The rate of the inactivation reaction will be expressed in the values of the kinetic parameters, estimated by applying one of these models to an experimental data set. Temperature and pressure dependence of the time dependent parameters (inactivation rate constants) will be evaluated according to the Arrhenius (3) and Eyring (4) equation, respectively, where E_a is the activation energy (kJ/mol), V_a the activation volume (cm^3/mol), R the universal gas constant (kJ/mol,K), T the temperature (K) and p the pressure (MPa).

$$k = k_{\text{ref}T} \exp\left[\frac{-E_a}{R}\left(\frac{1}{T} - \frac{1}{T_{\text{ref}}}\right)\right] \tag{3}$$

$$k = k_{\text{ref}P} \exp\left[\frac{-V_a}{RT}(P - P_{\text{ref}})\right] \tag{4}$$

In this paper, merely the results on enzyme inactivation kinetics are discussed. The enzyme samples are submitted to HP/T conditions during pre-set times and afterwards enzyme activity is measured. Possible reactivation is taken into account to ensure that only the irreversible inactivation reaction is registered.

3 Results & Discussion

The food quality related enzymes focused on in this paper are polyphenoloxidase (PPO), the activity of which results in enzymatic browning of damaged fruits, vegetables and fungi, lipoxygenase (LOX) which induces off-flavors and the destruction of essential fatty acids in vegetables, especially in *Leguminosae* and pectinmethylesterase (PME), which is responsible for cloud destabilization of (orange) juices, gelation of concentrates and consistency loss of (tomato) products.

3.1 Polyphenoloxidase

Initially, thermal inactivation (50–60 °C) at atmospheric pressure and pressure inactivation (900 MPa) at room temperature of commercial mushroom PPO have

been kinetically studied. Besides the influence of pH and several anti-browning agents such as benzoic acid, EDTA, glutathione, sodium chloride and 4-hexylresorcinol on the inactivation, the kinetics have been investigated [1]. In a second phase, complete kinetic characterization of inactivation of PPO extracted from avocado has been established in the pressure range of 0.1 to 900 MPa at temperatures between 25 and 77.5 °C. Pressure-temperature inactivation could be accurately described by a first order kinetic model and *k*-values were determined for about 110 combinations of constant pressure and temperature. Using these data, a pressure-temperature kinetic diagram was constructed (Fig. 1), from which an antagonistic effect of low pressure and high temperature could be derived, i.e. application of low pressure protects the enzyme against thermal inactivation. Further, a mathematical model (5) was developed describing adequately the combined pressure-temperature dependence of the inactivation rate constants, using the Arrhenius equation as starting point [2].

$$\ln k = (aP^3 + bP^2 + cP + d) - \left[\frac{E_{a0}\exp(-nP)}{R}\left(\frac{1}{T} - \frac{1}{T_{ref}}\right)\right] \quad (5)$$

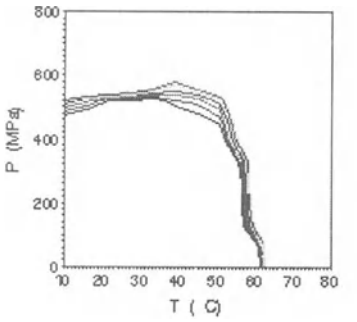

Fig. 1. *p/T* kinetic diagram for inactivation of avocado PPO

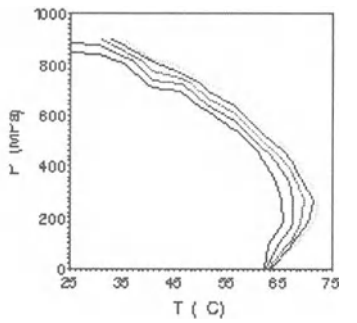

Fig. 2. *p/T* kinetic diagram for inactivation of soybean LOX

3.2 Lipoxygenase

Thermal inactivation of soybean LOX proceeded in the temperature range of 60 to 70 °C while pressure-temperature inactivation occurred in the pressure range of 0.1 to 650 MPa, at temperatures between 10 and 64 °C. Both thermal and pressure-temperature inactivation could be accurately described by a first order kinetic model. *k*-Values for about 60 combinations of constant pressure and temperature were calculated and used for the construction of a pressure-temperature kinetic diagram (Fig. 2). As opposed to PPO, an antagonistic effect was found at low temperature and high pressure. Seemingly, soybean LOX is most pressure stable at temperatures slightly higher than room temperature. Because the Arrhenius equation was not valid in the entire temperature region, it was endeavored to fit a mathematical model describing the combined pressure-temperature inactivation of

soybean LOX (6), using the Eyring equation as starting point. Subsequently, this mathematical model was validated under dynamic pressure-temperature conditions, including pulsated pressure treatments [3].

$$\ln k = (aT^2 + bT + c) - \left(\frac{V_{a0} T \exp(-nT)}{RT} (P - P_{ref}) \right) \quad (6)$$

3.3 Pectinmethylesterase

Pressure-temperature inactivation of PME from oranges has been studied in the pressure range 0.1 to 900 MPa at temperatures between 20 and 65 °C. Inactivation could be accurately described by a fractional conversion model. As for PPO, an antagonistic effect of low pressure and high temperature was observed. However, a kinetic model describing the combined pressure-temperature inactivation of orange PME has not yet been proposed. Tomato PME, on the other hand, was much more pressure stable and its inactivation followed first order kinetics. Besides some case studies have been performed concerning the influence of pH and Ca^{2+} ions. Tomato PME was less pressure stable in the presence of Ca^{2+} ions or in citric acid buffer (pH 3.5–4.5) than in water. At temperatures where the enzyme inactivates at atmospheric pressure, an antagonistic effect of pressure and temperature was noted, i.e. inactivation was slower at elevated pressure than at atmospheric pressure. This antagonistic effect was less pronounced in citric acid buffer or in the presence of Ca^{2+} ions than in water. At low pressures and elevated temperature where no inactivation occurs, activation of tomato PME was observed. This pressure induced activation of tomato PME was enhanced in the presence of Ca^{2+} ions.

Acknowledgements: The European Commission supported this work (project FAIR-CT96-1175).

References

[1] Weemaes, C., De Cordt, S., Ludikhuyze, L., Van den Broeck, I., Hendrickx, M. and Tobback, P. 1997. Influence of pH, benzoic acid, EDTA and glutathione on the pressure and/or temperature inactivation kinetics of mushroom polyphenoloxidase. Biotechnology Progress, 13, 25–32.

[2] Weemaes, C., Ludikhuyze, L., Van den Broeck, I. and Hendrickx, M. 1998. Kinetics of combined pressure-temperature inactivation of avocado polyphenoloxidase. Biotechnology and Bioengineering, in press.

[3] Ludikhuyze, L., Indrawati, Van den Broeck, I., Weemaes, C. and Hendrickx, M. 1998. The effect of combined pressure and temperature on soybean lipoxygenase: II. Modeling inactivation kinetics under static and dynamic conditions. Accepted for publication in Journal of Agricultural and Food Chemistry.

Modeling Conductive Heat Transfer and Process Uniformity During Batch High-Pressure Processing of Foods

S. Denys, L.R. Ludikhuyze, A.M. Van Loey and M.E. Hendrickx

Laboratory of Food Technology, Department of Food and Microbial Technology, Faculty of Agricultural and Applied Biological Sciences, Katholieke Universiteit Leuven, Kardinaal Mercierlaan, 92, B-3001 Heverlee, Belgium
Siegfried.Denys@agr.KULeuven.ac.be

Abstract. A numerical model for predicting conductive heat transfer during batch High Hydrostatic Pressure (HHP) processing of foods was developed and was tested for a food simulator (agar gel). Different types of HHP processes were simulated. Good agreement between experimental and predicted temperature profiles was observed. The model provides a very useful tool to evaluate batch HHP processes in terms of uniformity of any heat- and/or pressure-related effect. This is illustrated for inactivation of *Bacillus subtilis* α-amylase (BSA).

1 Introduction

The Pascal principle (pressure is transmitted uniformly and immediately through the pressure transferring medium) yields a great advantage to HHP as compared to thermal processing [1]. However, a pressure increase or decrease is associated with a proportional temperature change of the vessel's contents, proportionate to the thermal expansion coefficient and the specific volume of the product, and inversely proportionate to its specific heat according to [2]. The non-uniform temperature distribution, resulting from transfer of heat -generated at pressure build-up- will lead to a non-uniform distribution of the desired effect (inactivation of micro-organisms, enzymes, etc.) within the product. The present work suggests taking into account the non-uniform temperature distribution which appears during the process to assure that the objective of the process has been accomplished everywhere within the food product. A numerical approach is suggested.

2 Materials & Methods

'Conventional' HHP processes, HHP processes with gradual, step by step compression and decompression, and pressure cycling HHP processes were carried

out with agar gel (3% agar in distilled water). Thermal properties of this substance are close to those of water. A warm isostatic press (SO. 5-7422-0, Engineered Pressure Systems International, Belgium) with a maximum operating pressure of 600 MPa and a volume of 590 ml was used. A cylindrical sample holder was used with maximum radial dimensions as allowed by the dimensions of the internal room of the high-pressure vessel, in order to minimize the impact of (convective and conductive) heat transfer in the high-pressure medium layer between the sample holder and the inner wall of the vessel.

3 Heat Transfer Model

A numerical solution for a conductive heating finite cylinder was chosen to simulate heat transfer. An 'over-all' heat transfer coefficient at the surface of the cylinder was considered to account for heat transfer through the wall of the sample holder and through the thin layer of high-pressure medium situated between the sample holder and the inner wall of the high-pressure vessel. The pressure dependency of the thermal conductivity of water as observed by Bridgman [3] was implemented. The 'volumetric' specific heat of water was derived from the pressure dependency of the density of water, as described in [4]. For heat transfer within the high-pressure medium, thermal properties were provided by the distributor (Resato, Roden, the Netherlands).

To calculate temperature changes of the product, corresponding to periods of pressure increase or decrease, an equation for adiabatic temperature increase or decrease [2] was used. A term representing internal heat generation or internal 'heat reduction' during pressure build-up or pressure release, respectively, was incorporated in the numerical scheme. This allows handling non-adiabatic conditions due to loss of heat through the wall of the high-pressure vessel. The thermal expansion coefficient of the product was determined at different conditions of pressure and temperature, by means of experiments, whereby the temperature increase corresponding to a pressure increase was measured. The obtained pressure-temperature dependency of α_{TP} was incorporated in the method as a numerical parameter.

To evaluate HHP processes in terms of effect uniformity, pressure-temperature inactivation kinetics of an enzymatic model system based on BSA (15 mg/ml in 0.01 M Tris-HCl at pH 8.6) were implemented. These inactivation kinetics were determined under isobaric-isothermal conditions [5], and were validated under more realistic, dynamic process conditions [6]. By integration in the numerical scheme, the activity retention could be evaluated at any point in time.

4 Results & Discussion

Typical experimental time-temperature profiles for a 'conventional' batch HHP process of agar gel at 348 MPa are shown in Fig. 1. Using the appropriate initial conditions and the occurring boundary conditions (compression time, applied pressure), temperature profiles for three positions corresponding to the locations of the thermocouples in the processed product were generated for every HHP process and are also shown in the figure (full lines). The best fit was obtained when the 'over-all' surface heat transfer coefficient h was estimated 300 W/m^2 °C. Varying this value had no impact on the temperature increase (due to pressure build-up) in the central region of the product, as calculated by the model, but mainly influences the nature of the calculated temperature profile at the border of the product. Good agreement of experimental and predicted temperature profiles was obtained. Analogous results were obtained for the more complex HHP processes (results not shown).

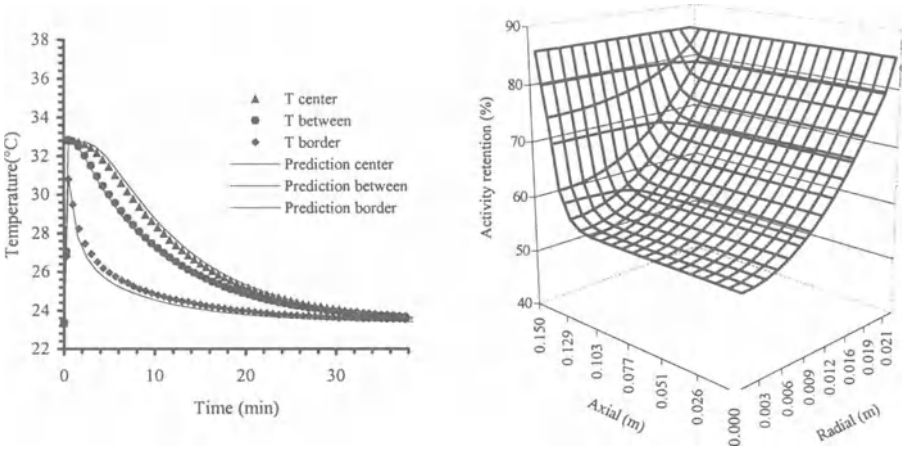

Fig. 1. Experimental and simulated time-temperature profiles for a 'conventional' batch HHP process (348 MPa), and a typical spatial distribution in the high-pressure vessel for inactivation of BSA, as calculated by the model

4.1 Effect Uniformity

Figure 1 also illustrates the typical spatial distribution –as calculated by the model– of the inactivation of the enzymatic model system BSA, resulting from a virtual 'conventional' batch HHP process of agar gel. The conditions of this 'virtual'

process were: initial temperature 20 °C; compression time 30 seconds; applied pressure 600 MPa; holding time 15 min.

5 Conclusions

The proposed numerical model could accurately describe conductive heat transfer during batch HHP processing of 3% agar gel. The use of a pressure- and temperature-dependent thermal expansion coefficient α_{TP} enables the model to predict temperature changes caused by compression and decompression. Obviously, experiments with other materials should be performed in order to further test the proposed method. The model is proposed as a very useful tool to evaluate batch HHP processes in terms of (uniformity of) any heat- and/or pressure-related effect.

References

[1] Knorr, D. (1993); Effects of high-hydrostatic-pressure processes on food safety and quality; Trends Food Sci. Technol., 4, 370–375.

[2] Zemansky, M.W. (1957); In Heat and Thermodynamics; McGraw-Hill Book Company, New York, 248–253.

[3] Bridgman, P.W. (1923); The thermal conductivity of liquids under pressure; Proc. Am. Acad. Arts Sci., 59, 141–169.

[4] Bridgman, P.W. (1912); Water, in the liquid and five solid forms, under pressure; Proc. Am. Acad. Arts Sci., 13, 439–558.

[5] Ludikhuyze, L.R., De Cordt, S.V., Weemaes, C.A., Herremans, C.H., Van Impe, J.F., Hendrickx, M.E. and Tobback, P.P. (1997); Kinetics for isobaric-isothermal inactivation of *Bacillus subtilis* α-amylase; Biotechnol. Progr., 13, 532–538.

[6] Ludikhuyze, L.R., Van den Broeck, I., Weemaes, C.A. and Hendrickx, M.E. (1997); Kinetic parameters for pressure-temperature inactivation of *Bacillus subtilis* α-amylase under dynamic conditions; Biotechnol. Progr., 13, 617–623.

Comparative Studies Concerning the Digestibility of Raw, Heated and High-Pressure-Treated Foods in Young Pigs and *In Vitro*

H. Schöberl[1], W. Ruß[1], R. Meyer-Pittroff[1], F.X. Roth[2] and M. Kirchgessner[2]

Technische Universität München-Weihenstephan
[1]Lehrstuhl für Energie- und Umwelttechnik der Lebensmittelindustrie
[2]Institut für Ernährungsphysiologie
85350 Freising-Weihenstephan, Germany
Phone: +49-(0)8161-714362; Fax: +49-(0)8161-714415
scho@eul.blm.tu-muenchen.de

Abstract. The aim of this research was to show the influence of the high-pressure treatment on the digestibility of food-stuffs. Test methods used were feeding trials and *in vitro* digestibility tests. Feeding trials using pigs showed no changes in the digestibility of the individual nutrient fractions of high-pressure-treated food-stuffs as compared to fresh goods. The nutritional value of the proteins also remained unchanged. Differences could be seen in heat-treated food-stuffs. The digestibility as well as the nutritional value of the proteins decreased significantly by the treatment. NFE, fats and crude fibre showed no changes. The *in vitro* digestibility trials showed different results to the feeding trials. No significant differences between the high-pressure-treated and the untreated samples of pork could be seen, whereas the pressure-treated samples of the soybeans had a better digestibility than the untreated.

1 Introduction

The digestibility of food stuffs, and the degree to which they can be metabolised, are dependent upon several factors, one of which is the method in which they have been prepared. The effect of a high-pressure treatment on the digestibility of food stuffs is largely unknown. Hayashi *et al.* [1] have reported an increase in the digestibility of high-pressure-treated chicken egg-white and egg-yolk *in vitro*.

The aim of this research is to determine the influence of the various methods of treatment on the digestibility of food stuffs. The methods applied for testing were feeding trials on young pigs and *in vitro* digestibility tests.

2 Materials & Methods

2.1 Feeding Trials

Feed was manufactured from various foods based upon the nutritional requirements of pigs. The main components were potatoes (30%), carrots (19%), meat (8.2%), peas (8%) and vegetable oil (5%). For hygienic reasons, and to facilitate the acceptance of the food by the pigs, the food could not be produced from purely untreated ingredients. The meat and a part of the potatoes were therefore boiled. The content of native proteins and nitrogen-free extract (NFE) made up 25 and 33%, respectively, of the nutrient content in the dry matter.

The feed was subjected to three different treatment methods. One part was treated at a pressure of 500 MPa for 10 min at 20 °C and a further part was heat-treated at 121 °C for 20 min. The third portion remained untreated. These three feed batches were used in feeding trials for four weeks with nine pigs, which had a live mass of 50 – 60 kg. The pigs were kept in metabolism cages, which enabled a separate collection of faeces and urine.

The pigs were split into three groups of three, each group getting the different feed batches for two weeks. The groups were switched after the two weeks, thus enabling the testing of each feed batch on six pigs.

The faeces and the urine were removed daily for one week after the first week, to allow for adaptation to the feed. The faeces were freeze-dried. To determine the nitrogen balance the feed, the faeces and the urine were examined for nitrogen content.

For the determination of the digestibility of the nutrients the feed and the excreted faeces of the animals were examined for proteins, fat, crude fibre and NFE content.

The digestibility can be calculated as a quotient of the nutrient contents in the faeces and in the feed

$$\text{Digestibility} = 1 - \left(\frac{\text{Nutrient excreation [g/d]}}{\text{Nutrient intake [g/d]}} \right) \times 100 \cdot$$

2.2 *In Vitro* Digestibility Trials

For controlling the results gained in the trials on the animals *in vitro* digestibility trials with high-protein food were conducted.

The digestibility of the proteins was examined using a pepsin-hydrochloric acid solution. The sample meat was lean pork from the upper leg and soybeans. The sample materials were finely mixed with a conventional household blender and subjected to the following treatment methods:

300 MPa, 10 min holding time, 20 °C, pressure-build-up time of 200 MPa /min;
500 MPa, 10 min holding time, 20 °C, pressure-build-up time of 200 MPa/min;
700 MPa, 10 min holding time, 20 °C, pressure-build-up time of 200 MPa/min;
100 °C, 10 min;
121 °C, 20 min;
untreated.

One gram of every sample was then suspended in a pepsin-hydrochloric acid solution (25 mg pepsin 0.7 FIP-U/mg /l 0.1n HCl) and treated for 24 h in a shaking bath at 37 °C. After treatment the solution was filtered (Schleicher and Schüll 597.5), the filter remains dried and subjected to a Kjehldahl nitrogen analysis.

3 Results & Discussion

3.1 Animal Trials

The various treatment methods showed no significant changes in the digestibility as far as fat, crude fibre and NFE were concerned. The proteins in the untreated and the high-pressure-treated batches also showed no significant changes in digestibility. Significant changes only appeared in the digestibility of the proteins in the heat-treated feed batch. The protein-digestibility in this case was around 10% lower than in the other two batches (Table 1).

Table 1. Digestibility of the individual nutrient fractions in dependence of the treatment method (untreated; high-pressure-treated at 500 MPa, pressure holding time 10 min, 20 °C; heat-treated at 121 °C, 20 min). The ± values indicate the standard deviations

Nutrient fraction	Digestibility [%]		
	Untreated	High-pressure-treated	Heated
Protein	87.1^{a} ±0.9	88.2^{a}±1.0	80.5^{b}±2.1
Fat	89.6±1.4	89.0±2.2	90.1±1.7
crude fibre	65.0±4.0	63.3±4.1	67.2±1.9
NFE	94.8±0.2	94.7±0.4	94.5±0.2

[a), b)] means statistically significantly different

Conclusions about the effect on digestibility of the proteins could be obtained using the nitrogen balance data. In particular the nitrogen retention in % of the nitrogen intake and the nitrogen retention in % of the digestible nitrogen are important indicators of the nutritive value of the proteins.

According to the nitrogen balance of the animals, the differences in the protein utilisation become even greater (Table 2). The nitrogen retention in the animals is only 45.4% of the nitrogen consumed when the heat-treated material was given. In comparison it makes 58.6% in the food treated under high pressures, and 57.9% in the untreated food.

Table 2. Nitrogen balance in dependence on the treatment method (untreated; high-pressure-treated at 500 MPa, pressure holding time 10 min, 20 °C; heat-treated at 121 °C, 20 min). The ± values indicate the standard deviations

	Untreated	Heated	High-pressure-treated
N-retention in % of the N-intake	57.9^{a}±4.2	45.4^{b}±3.9	58.6^{a}±3.9
N-retention in % of the digestible nitrogen	66.4^{a}±4.1	56.3^{b}±4.0	66.5^{a}±4.5

[a), b)] means statistically significantly different

If the N-retention in % of the digestible nitrogen is regarded a similar relationship can be seen. The value of the protein as a nutrient is not changed through the high-pressure treatment. In the heat-treated feed the protein retains only 85% of the value observed in the untreated and high-pressure-treated feed.

3.2 *In Vitro* Digestibility Trials

The results of the *in vitro* digestibility trials were different from the feeding trials. No significant differences between the high-pressure-treated, the 100 °C treated and the untreated samples of pork could be seen. The protein digestibility in the 121 °C treated meat samples was lower than the others. The pressure-treated samples of the soybeans had a better digestibility than the untreated. The heated samples (100 °C) of soybeans were less digestible than the untreated or the high-pressure treated samples (Table 3).

Table 3. Protein digestibility of pork and soybeans, in dependence of the treatment method, by pepsin in % (untreated; high-pressure-treated at 300 MPa, 500 MPa, 700 MPa, pressure holding time 10 min, 20 °C; heat-treated at 121 °C, 20 min; heat-treated at 100 °C, 10 min)

Food	Digestibility [%]					
	Untreated	300 MPa	500 MPa	700 MPa	Heated 100 °C	Heated 121 °C
Pork	93.4	94.9	96.7	94.6	93.0	67.9
Soybeans	73.0	74.9	80.0	84.7	65.6	n.n.

4 Conclusions

Feeding trials using pigs showed no changes in the digestibility of the individual nutrient fractions of high-pressure-treated food-stuffs as compared to fresh goods. The nutritional value of the proteins also remained unchanged. There were differences between the feeding trials and the *in vitro* trials. No significant differences between the high-pressure-treated, the 100 °C treated and the untreated samples of pork could be seen. The protein digestibility in the 121 °C treated meat samples was lower than the others.

The pressure-treated samples of the soybeans had a better digestibility than the untreated. The heated samples (100 °C) of soybeans were less digestible than the untreated or the high-pressure-treated samples.

Acknowledgements: This research was supported by "Bayerischer Forschungsverbund Abfallforschung und Reststoffverwertung" (BayFORREST).

References

[1] Hayashi, R.; Kawamura, Y.; Nakasa, T.; Okinaka, O.; Application of High Pressure to Food Processing: Pressurization of Egg White and Yolk, and Properties of Gels Formed. Agric. Biol. Chem. 53, 1989, 2935–2939.

High Pressure Processed Apple Desserts. Microbiological and Physicochemical Properties

M. Fonberg-Broczek[1,3], E. Kostrzewa[2], D. Zdziennicka[2], K. Karlowski[3], B. Windyga[3], H. Sciezynska[3], K. Górecka[3], A. Grochowska[3], B. Urbanek-Karlowska[3], J. Arabas[1], J. Szczepek[1] and S. Porowski[1]

[1]High Pressure Research Centre, Polish Academy of Sciences,
Sokolowska 29/37, 01-142 Warsaw, Poland
Phone: +48 22 632 70 55; Fax: +48 3912 0331
equipment@unipress.waw.pl
[2]Institute of Agricultural and Food Biotechnology,
Rakowiecka 36, 02-532 Warsaw, Poland
[3]National Institute of Hygiene, Chocimska 24, 00-791 Warsaw, Poland

Abstract. This paper describes studies of the microbiological quality and physicochemical properties of high pressure processed apple desserts. The desserts were produced from fresh apples of excellent quality. After removing useless parts, the fruits were washed, crumbled by cutting and then mixed with pectin acid and sugar or Aspartame at room temperature. Individual portions of dessert were packed in commercial polystyrene packages of 100 or 200 ml and heat sealed with thin aluminium foil cover. Pressure treatment of the desserts was performed at a pressure of 300 MPa, at temperatures 20 °C or 50 °C, in 10 min. Pressurization was conducted using high pressure food processor 1.5 l, 700 MPa developed in the High Pressure Center. Microbiological and physicochemical investigations of the pressure processed desserts were carried out directly after pressurization and after 3 months refrigerator storage. The following parameters were determined: soluble solids, (°Brix at 20 °C), total titrable acidity (g citric acid/100 g f.u.), pH, degradation index (Di) using Fuleki method, Aspartame content and ascorbic acid content. The instrumental colour values L, a, b and dominating wave length were measured with a Minolta Chroma Meter CR200. The appearance, colour, smell, taste and consistency of the desserts were evaluated by a six person trained panel using 5-point quality scores. The products were characterized by good microbiological parameters, slightly gelatinous consistency of fruit jelly, almost natural colour, fresh fruit aroma and a taste better than that of traditional fruit desserts.

1 Introduction

The extent of inactivation of microorganisms achieved at particular pressure depends on a number of interacting factors including not only pressure level and duration, processing temperature, microbial species but also substrate composition

of products. From this point of view the safety of products requires careful investigations. On the other hand very important are investigations of changes in significant factors that determine the acceptability of food products: colour, flavor, consistency and taste, caused by pressure treatment and occurring during storage period of high pressure preserved products.

In our preliminary work [1–3], we have described microbiological and physicochemical properties of high pressure processed strawberry desserts sweetened with Aspartame.

The aim of our new experimental work presented in this paper was concerned with optimization of the UHP process and assessment of the quality of apple desserts sweetened with sugar and/or Aspartame, preserved by the UHP method as compared to pasteurization.

2 Materials & Methods

The desserts were prepared from apples, variety Champion - high quality fruit with greenish-pale pulp, resistant to change of colour with characteristic pear-apple flavour, sweeteners - sugar and/or Aspartame, pectin and citric acid.

Preparation of desserts: washed and peeled apples after removal of useless parts were crumbled by cutting to small pieces and mixed with the dry contents previously dissolved in water. Two of the samples were packed at the ambient temperature and the other two were heated to 75 °C. One part of the desserts was preserved by pasteurization which was conducted at a temperature of 85 °C during 15 min. Desserts prepared for UHP treatment were packed in commercial polystyrene packages (vol. 100 to 250 ml) and heat sealed with thin aluminium foil cover. Desserts prepared for pasteurization were packed in glass jars (vol. to 200 ml) with twist-off covers.

The parameters of the process are summarized in Table 1. High pressure treatment was conducted in a high pressure food processor piston-cylinder type vessel with inner diameter of 110 mm volume of 1.5 l and maximum pressure of 700 MPa [4] equipped with internal heat exchanger. Distilled water was used as pressure transmitting medium.

Quality studies of the products were performed before pressure processing (after thermal preprocessing), directly after pressure processing and after 3 months storage at +3 to +5 °C.

The investigation incorporated:

1. Measurement of 4 physicochemical parameters: pH, soluble solids °Brix at 20 °C, total titrable acidity (g citric acid/100 g f.w.), Aspartame content.
2. Determination of the instrumental colour values L*, a*, b* and dominating wave length - using Minolta Chroma Meter CR 200.
3. Evaluations of appearance, colour, smell, taste and consistency performed by a trained panel (six persons) using 5-point quality scores.
4. Microbiological investigation was performed according to ISO methods.

Table 1. Composition of apple desserts and parameters of thermal preprocessing and pressurization of apple desserts

Sample number	Components of desserts (water to 100%) (%)				Temp. of prepro-cessing (°C)	Parameters of high pressure treatment		
	Apples	Sweeteners		Pectin		Temp (°C)	Time (min)	UHP (MPa)
		Sugar	Aspartame					
J-1	60	12	-	0,8	20	20	10	400
J-2	70	-	0,06	0,8	20	20	10	400
J-3	60	12	-	0,8	75	50	10	400
J-4	70	-	0,06	0,8	75	50	10	400

3 Results

Composition of apple desserts and parameters of thermal preprocessing and UHP treatment are detailed in Table 1. Samples of desserts were prepared by four different methods.

Physicochemical characteristics of these desserts: pH, soluble solid and total acidity, measured directly after high pressure treatment and after 3 months of storage, did not change when compared to the initial samples and the same results were observed for pasteurized samples. Aspartame content decreased by about 9–12% directly after UHP treatment and by 30% after 3 months of storage. In the pasteurized samples Aspartame content lowered from 18 to 24% directly after pasteurization.

The results of the sensorial tests of the apple desserts preserved by high pressure and pasteurization showed that the UHP treated samples had much higher quality than pasteurized samples when evaluated directly after treatment as well as after 3 months of storage. Colour parameters were measured instrumentally in two chosen, visually different dessert samples. The intensity of colour (L) of the investigated samples decreased in both groups: after UHP treatment and after pasteurization. In the samples subjected to high pressure the value of the component "–a" (colour: green) decreased in all of the samples after 3 months storage, however in the pasteurized sample (J-1) it changed from –2.15 to +0.14, which caused change of colour from green to red. In the UHP samples the value of component "+b" (colour yellow) decreased over time, and in the pasteurized samples it decreased directly after the process but increased after 3 months. The differences in the values "–a" and "+b" are explicit when light greenish-pale UHP desserts are compared to the yellow-brown colour of pasteurized desserts. The colour of UHP desserts also had

a better mark when evaluated by a trained panel (six persons) using 5-point quality scores.

The microbiological investigation showed good microbiological quality of high pressure processed apple desserts. The quality was in accordance with Polish standards for fruit products.

4 Conclusions

1. Ultra High Pressure (UHP) treatment of apple desserts at 400 MPa, 50 °C temperature during 10 min guarantees production of safe products with high quality sensorial parameters.
2. Apple desserts preserved with UHP were characterised by a much higher quality than the pasteurized desserts.

Acknowledgements: This research was supported by National Committee of Scientific Research Grant No P06G 005 10/1996-1997.

References

[1] Fonberg-Broczek, M., Arabas, J., Górecka, K., Grochowska, A., Karlowski, K., Kostrzewa, E., Szczepek, J., Sciezynska, H., Windyga, B., Zdziennicka, D., Zurkowska-Beta, J., Porowski, S., High-pressure processed apple and strawberry desserts, XXXVth Meeting of European High Pressure Research Group, Reading, September 7 to 11,1997.

[2] Fonberg-Broczek, M., Arabas, J., Górecka, K., Grochowska, A., Karlowski K., Kostrzewa, E., Szczepek, J., Sciezynska, H., Windyga, B., Witczak, Z., Zdziennicka, D., Zurkowska-Beta, J., Porowski, S., Quality studies of high pressure processed fruit products - preliminary results, Third Main Meeting, COPERNICUS PROGRAMME, Concerted Action CIPA-CT94-0195, Leuven, October 24 to 25, 1997.

[3] Fonberg-Broczek, M., Arabas, J., Kostrzewa, E., Reps, A., Szczawinski, J., Szczepek, J., Windyga, B., Porowski, S., High Pressure Treatment of Fruit, Meat and Cheese Products - Equipment, Methods and Results; to be published in Processing of Foods: Quality, Optimization and Process Assessment, CRC Press LLC.

[4] Szczepek J., Arabas, J., Experimental technique for high pressure investigation in chemistry, biology and food science, in High Pressure Research in Bioscience and Biotechnology, Proc. XXXIVth Meeting of the European High Pressure Research Group, Heremans, K. Ed. Leuven University Press, 1997, 471.

The Role of Polysaccharides and Metal Ions in the Cell Walls in the Pressure-Induced Hardening of Root Vegetables

M. Kasai, K. Hatae and A. Shimada

Ochanomizu University, School of Human Life and Environmental Science, 2-1-1, Otsuka, Bunkyo-ku, Tokyo 112-8610, Japan
kasai@cc.ocha.ac.jp

Abstract. The hardening of Japanese radish was brought about by standing after pressurization without a change of the water content. A decrease was observed in the concentratons of the calcium and potassium ions of hemicelluloses I and II during standing. There were no significant changes in the polysaccharide fractions with pressurization or standing. A small decrease in hemicellulose I and a small increase in hemicellulose II were observed with increasing standing time. The tissue pH decreased and alkali-insoluble proteins increased after pressure treatment as well as standing after pressure release.

1 Introduction

Plant foods such as vegetables and fruits can be hardened by preheating around 60 °C [1] and by storage. The hardening caused by these methods is important for controlling the hardness in cooking. It is said that the main cause of the hardening is demethylation of pectins followed by the formation of bridge bonds between divalent metal ions and pectins [1]. On the other hand, some factors other than pectins have been presumed. The mechanism of the hardening is not yet elucidated. In previous work [2], we have shown that vegetables can be hardened by pressure treatment without heat or chemical additives. These features are advantageous for a mechanistic study of the hardening. In this study, we focus on the role of cell wall components in pressure-induced hardening.

In our previous work on fractionated pectins [2], we confirmed the deesterification of pectins and an increase in the pectin components which are bound to divalent metal ions. However, these changes are confined to short standing times. During hardening at a longer standing time, some factors other than pectins have been considered to be involved. In order to elucidate the hardening mechanism, the interactions between cell wall components should be considered.

2 Materials & Methods

The middle parts of Japanese radish used as samples were cut into cubes of 1 × 1 × 1 cm. The samples were packed with a vaccum sealer and pressurized at 400 MPa and room temperature for 10 min with a high-pressure equipment (R7K-3-10-5, Yamamoto Suiatsu Co., Ltd.). After the pressure release, the samples were left at 20 °C for 0–24 h. The hardness of pressurized samples was measured by a texturometer (GTX-2, Zenken Co., Ltd.). AIS (70% alcohol-insoluble solid) of ca. 1.0 g was fractionated into four portions. These fractions were pectic substances and hemicellulose I and II, and cellulose. Fractions were extracted using 0.5% ammonium oxalate, 5% NaOH, respectively. Each extract was dialyzed and concentrated. The residue of the 17.5% NaOH extraction was cellulose. The metal ion contents of each polysaccharide fraction were determined by atomic absorption spectrophotometry (AA-660, Shimadzu Co., Ltd.). A 15 g sample was homogenized in 45 ml of ice-cooled deionized water, the pH was measured using a pH meter. A 15 g sample was mixed with 45 ml of 10% NaOH under ice-cooled conditions and treated in the same manner. From the precipitate, alkali-insoluble protein was determined by the Kjeldahl method.

3 Results & Discussion

3.1 Degree of Hardening Induced by Pressure

First of all, we examined how the pressure-induced hardening is caused by pressurization and standing. As shown in Table 1, the effect of pressure pretreatment that initially increases and then levels off is observed both before and after cooking. The water content changes little during standing (data are not shown), so that the hardening is brought about by some factors other than water.

Table 1. Variation of hardness (N) of pressurized Japanese radish with standing

	Standing time (h)					
	0	2	7	16	24	non-pressurized
before cooking	37.2	43.8	43.0	42.6	43.0	28.4
after cooking	26.7	32.2	36.9	41.3	40.1	12.4

3.2 Effect of Metal Ions

It has been suggested that the pressure-induced hardening has something to do with the calcium ions which are liberated from the water-soluble pectin fraction [2]. Here we have studied this in more detail by separating the cell wall components into four fractions. As shown in Table 2, significant changes are observed only for the potassium and calcium ions in hemicellulose II and the calcium ions in

hemicellulose I. Although it is generally accepted that interactions of divalent metal ions with the polysaccharides play a role in controlling the hardness, the concentration of calcium ions in hemicelluloses are unexpectedly decreased. It is suggested that the calcium and potassium ions are transferred from the hemicellulose to some other components such as proteins that are likely to be negatively charged, and that, in consequence, the coupling between hemicellulose and cellulose becomes stronger. As shown in Table 2, with increasing standing time a small increase in hemicellulose I which is weakly hydrogen bonded to cellulose was observed as was a small increase in hemicellulose II which is strongly hydrogen bonded.

Table 2. Variations of metal ion contents and polysaccharides in each fraction with standing

	Standing time (h)					
	0	2	7	16	24	non-pressurized
Potassium ions (mg/g of each fraction)						
pectin	26.6	25.6	26.0	26.1	27.6	24.7
hemicellulose I	13.1	13.6	14.2	15.5	18.3	14.2
hemicellulose II	42.7	39.2	37.4	30.9	33.9	49.4
cellulose	0.02	0.02	0.02	0.04	0.01	0.01
Calcium ions						
pectin	4.9	5.2	5.4	5.6	6.0	4.9
hemicellulose I	8.8	7.7	7.2	6.8	6.8	9.1
hemicellulose II	4.3	3.9	3.8	3.1	3.4	4.7
cellulose	0.1	0.1	0.2	0.1	0.1	0.01
Magnesium ions						
pectin	4.2	3.6	3.7	3.8	4.1	4.0
hemicellulose I	0.5	0.6	0.5	0.5	0.6	0.6
hemicellulose II	0.9	0.8	0.9	0.6	0.7	1.0
cellulose	0.01	0.01	0.01	0.01	0.01	0.01
Polysaccharides (g/100 g of sample)						
pectin	0.55	0.57	0.57	0.59	0.57	0.55
hemicellulose I	0.28	0.26	0.26	0.25	0.22	0.26
hemicellulose II	0.15	0.15	0.14	0.18	0.18	0.14
cellulose	0.32	0.33	0.34	0.33	0.32	0.32

3.3 Effect of Calcium and Magnesium Ions on the Hardness

Next, we examined how the effect of divalent metal ions on the hardness varies with standing. For this purpose, we removed the metal ions from the pressurized sample with chelating agents such as EGTA and EDTA; the calcium ions can be selectively removed by EGTA and almost all divalent metal ions can be removed by EDTA.

As shown in Table 3, the difference in the hardness between the non-chelated and calcium ions chelated samples becomes small with standing. This may be

interpreted in the following way: (1) the combination of the calcium ions and some components takes place during a short standing time and induces hardening, and (2) the role of the calcium ions in the pressure-induced hardening is not direct during a long standing time, probably through interactions among the components without the calcium ions. The interactions can be promoted by a decrease of calcium ion concentration in hemicelluloses.When almost all the divalent metal ions (mainly calcium and magnesium in Japanese radish) are removed, on the other hand, the hardness of the pressurized samples decreases drastically and remains invariant with standing. This indicates that the magnesium ions do not affect the time dependence of the pressure-induced hardening although they greatly influence the vegetable hardness.

Table 3. Hardness (N) of pressurized Japanese radish after chelating treatment

Treatment	Standing time (h)				
	0	2	7	16	24
A. non-chelated	37.2	45.6	43.0	43.3	42.0
B. EGTA	25.1	34.9	36.9	37.1	39.7
C. EDTA	1.9	2.7	2.6	2.4	2.4

3.4 Variations of Tissue pH and Protein Solubility

The tissue pH and the protein solubility are the remaining factors that may influence the pressure-induced hardening. The tissue pH is decreased by the pressure treatment and standing and the alkali-insoluble protein is increased slightly by the pressure treatment and increased more up to 2 h standing (Table 4). The decrease of the tissue pH is mainly due to the demethylation of pectins followed by the production of the acid form. Although the tissue pH seems to play a role in the hardening, it is uncertain whether it is dominant or not.

Table 4. Variation of tissue pH and alkali-insoluble proteins (%) of pressurized Japanese radish with standing time

	Standing time (h)					
	0	2	7	16	24	non- pressurized
tissue pH	5.9	5.7	5.5	5.5	5.6	6.3
alkali-insoluble proteins	3.5	5.7	4.9	5.8	5.6	2.8

References

[1] Bartolome, L.G. and Hoff, E. (1972) Firming of potatoes: Biochemical effects of preheating., J. Agric. Food Chem., **20**, 266–270.

[2] Kasai, M., Okamoto, N., Hatae, K., and Shimada, A. (1997) Role of calcium and magnesium ions in the hardening of pressure-treated root vegetables., J. Agric. Food Chem., **45**, 599–603.

Influence of High Pressure on Protein–Polysaccharide Interactions

V.B. Galazka*[1], D.D.S. Smith[2], D.A. Ledward[3] and E. Dickinson[1]

[1]Procter Department of Food Science, University of Leeds, Leeds LS2 9JT, UK
[2]BBSRC Institute of Food Research, Earley Gate, Reading RG6 2EF, UK
[3]Department of Food Science and Technology, University of Reading, Whiteknights, P.O. Box 226, Reading RG6 6AP, UK
V.B.Galazka@afnovell.reading.ac.uk

Abstract. Probe spectrofluorimetry data for bovine serum albumin (BSA) show a reduction in protein surface hydrophobicity in the presence of dextran sulphate (DS), ι-carrageenan (ι-CAR) or κ-carrageenan (κ-CAR) (2.5:1 weight ratio) and after high pressure treatment. Size exclusion chromatography studies for BSA in the presence of polysaccharide indicate electrostatic protein–polysaccharide interactions at low ionic strength and neutral pH, which become much stronger at pH 6.5 but disappear in 0.1 M NaCl. These interactions become considerably stronger after pressure treatment (600 MPa) at low ionic strength. It appears that stronger complex(es) formed during pressurization are not simply due to the induced change in pH during treatment and the strength of complexation is related to the charge density on the polysaccharide (DS > ι-CAR > κ-CAR) [1,2]. Complexation of BSA with DS appears to protect the protein against pressure-induced aggregation at low ionic strength.

1 Introduction

Proteins and polysaccharides are present together in a wide range of food products. The desired characteristics in food products such as structure, stability and textural attributes may be achieved by mixing two (or more) polysaccharides or proteins. Depending on the strength and nature of mixed biopolymer interactions the functional properties of proteins may be changed.

Recent studies have reported [3] that the strength of interaction between ι-CAR or κ-CAR with BSA increases as the pH is decreased from pH 7 towards pH 6. The destabilization of oil-in-water emulsions containing BSA + anionic sulphated polysaccharides by flocculation and creaming appears to be related to the density of the sulphate group on the polysaccharide (DS > ι-CAR > κ-CAR) [2, 3].

2 Materials & Methods

BSA (globulin-free lyophilized powder, ≥99% purity, product A-7638, lot. 16H9314) and DS were purchased from Sigma Chemical Co. The food grade carrageenans were kindly donated by Systems Bio Industries (Carentan, France). Solutions of these proteins (5 mg/ml) with and without polysaccharide (2 mg/ml) were prepared in HPLC grade water and the pH adjusted to 7 or 8 by addition of 0.05 M HCl or 0.05 M NaOH [1, 2]. Imidazole buffer (20 mM) was used for experiments performed at pH 6.5. Samples were pressurized as described previously [1]. Changes in surface hydrophobicity were estimated by reaction with 1-anilinonaphthalene-8-sulphonate (ANS) [1], thermal stability by differential scanning calorimetry (DSC) [1], and size exclusion chromatography was used to assess the molecular sizes of protein aggregates, protein–polysaccharide complex(es) [1].

3 Results

The effect of pressure treatment at 600 MPa for 20 min on the various structural parameters are compared in Table 1.

Table 1. Properties of BSA in the absence and presence of DS, κ-CAR or ι-CAR (2.5:1 weight ratio) at low ionic strength and neutral pH for untreated and treated (600 MPa for 20 min) samples

Sample	S_0 (absorbance units/ mol of ANS) (0.17–16 μM BSA)	T_m (°C) 5 mg/ml	ΔH (kcal/mol) 5 mg/ml
BSA (untreated)	275	70.5	1.8×10^5
BSA (treated)	126	70.5	1.0×10^5
BSA + κ-CAR (untreated)	148	69.0	1.4×10^5
BSA + κ-CAR (treated)	85	69.9	0.7×10^5
BSA + ι-CAR (untreated)	67	68.5	1.3×10^5
BSA + ι-CAR (treated)	35	69.5	0.3×10^5
BSA + DS (untreated)	27	52.6	0.2×10^5
BSA + DS (treated)	20	46.9	0.2×10^5
Polysaccharide alone (treated)	0	0	0

It is seen that pressurization causes a reduction of surface hydrophobicity and a major loss of tertiary structure for pure BSA which is in line with the previous work of Galazka *et al.* [1, 2] and Hayakawa *et al.* [4]. Addition of the sulphated polysaccharides greatly reduces the protein hydrophobicity (S_0) (DS > ι-CAR > κ-CAR) and, furthermore, in all cases, S_0 for the pressure processed biopolymer mixtures is lower than for the untreated mixture at the same weight ratio. Since ANS does not bind to the polysaccharide alone, it is assumed that the decrease in S_0 is attributed to electrostatic repulsion between the two negatively charged mole-

cules and/or blocking of ANS to the BSA binding sites arising from electrostatic protein–polysaccharide complexation. Our DSC data indicates that strong complex(es) are formed between BSA + DS such that pressure treatment has little additional effect. In the case of ι-CAR or κ-CAR, weak complex(es) are formed between the protein + carrageenan so that pressure treatment causes further denaturation of BSA.

Size exclusion chromatography data [1] at pH 7 for BSA alone indicate that protein–protein complexation induced by pressurization is due to polymerization by –S–S– bridging. Figure 1 presents size exclusion chromatography profiles for the mixed system BSA + ι-CAR (2.5:1 weight ratio) at pH 6.5, 7.0 and 8.0 in the absence of NaCl. Chromatogram (a) for the untreated mixture and chromatogram (d) for the treated mixture at pH 8 correspond to dimerized BSA with no evidence of protein–polysaccharide complexation. We note that stronger complex(es) are formed during/after high pressure treatment (Fig. 1e,f) and with decreases in pH (Fig. 1b,c). The presence of 0.02 M NaCl induces reversible dissociation of most of the complexed BSA to its monomeric form, which is consistent with the complex being held together by electrostatic interactions.

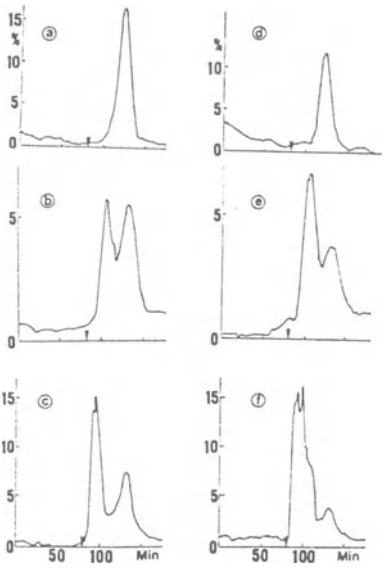

Fig. 1. Size exclusion chromatograms of untreated and pressure treated (600 MPa) BSA + ι-CAR in the absence of NaCl. Chromatogram (**a**) untreated pH 8; (**b**) untreated pH 7; (**c**) untreated pH 6.5; (**d**) treated pH 8; (**e**) treated pH 7; (**f**) treated pH 6.5. From [2]

Under similar experimental conditions, the replacement of ι-CAR with κ-CAR (Fig. 2) gives weaker protein–polysaccharide complex(es), which also strengthen after pressure treatment and/or reduction in pH. In systems containing DS instead of the carrageenans (not shown) at low ionic strength very strong electrostatic complexation occurs both in the native and pressure treated form. Additions of

0.1 M NaCl to the native mixture dissociates the complex to the BSA monomeric form, whereas in the pressure treated mixture we see a complex system of peaks which is indicative of the presence of both monomeric and oligomeric proteins, as well as some residual BSA–DS complex.

Recent surface tension measurements by Dickinson and Pawlowsky [3] and Galazka *et al.* [5] have shown that the strength of protein–polysaccharide interactions are clearly sensitive to pH and high pressure treatment.

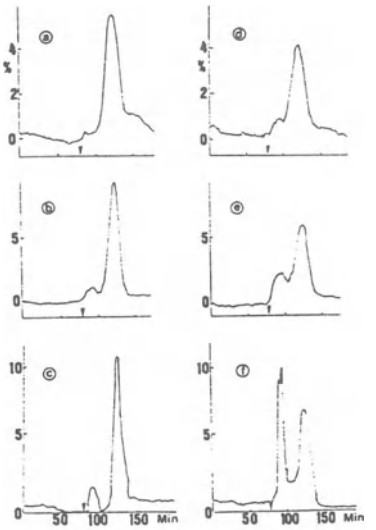

Fig. 2. Size exclusion chromatograms of untreated and pressure treated (600 MPa) BSA + κ-CAR in the absence of NaCl. Chromatogram (**a**) untreated pH 8; (**b**) untreated pH 7; (**c**) untreated pH 6.5; (**d**) treated pH 8; (**e**) treated pH 7; (**f**) treated pH 6.5. From [2]

References

[1] Galazka, V., Ledward, D., Sumner, I. and Dickinson, E. (1997); Influence of high pressure on bovine serum albumin and its complex with dextran sulfate; J. Agric. Food Chem., 45, 3465–3471.

[2] Galazka, V., Smith, D., Ledward, D. and Dickinson, E. (1998); Complexes of bovine serum albumin with sulphated polysaccharides: effects of pH, ionic strength and high pressure treatment; Food Chem. in press.

[3] Dickinson, E. and Pawlowsky, K. (1997); Influence of κ-carrageenan on the properties of a protein-stabilized emulsion; Food Hydrocolloids; in press.

[4] Hayakawa, I., Linko, Y.-Y. and Linko, P. (1996); Mechanism of high pressure denaturation of proteins; Lebensm.-Wiss. Technol; 29, 756–762.

[5] Galazka, V., Smith, D., Dickinson, E. and Ledward, D. (1998); Effect of high pressure on protein–polysaccharide complexes in 'Food Emulsions and Foams'; (ed. Dickinson, E. and Rodríguez Patino, J.); Royal Society of Chemistry; in press.

High Hydrostatic Pressure for Preservation of Salted Tarts: Quiche Lorraine

C. Tonello[1] and L. Voignier[1,2]

[1]Hautes Pressions Technologies, Chemin des Romains, F-55000 Bar le Duc, France
Phone: +33 (0)3 29 77 24 25; Fax: +33 (0)3 29 77 25 26
hptech@club-internet.fr
[2]EPL-AGRO, Technopôle Philippe de Vilmorin, F-55006 Bar le Duc cedex, France

Abstract. Shelf-life (at 4 °C) of vacuum-packed quiche lorraine, which was of 3 weeks without high pressure treatment, was increased from 12 weeks to more than 15 weeks after pressurisation at 400, 500 or 600 MPa for 5 min at room temperature. Shelf-life of untreated gas-packed (50% N_2 / 50% CO_2) quiches was of 5 weeks against at least 14 weeks after pressurisation at 400 or 500 MPa. Sensorial analysis showed no significant difference between untreated and pressurised gas-packed quiches. There were differences of taste for vacuum-packed quiches which were certainly due to not well controlled amounts of salt in both types of quiches.

1 Introduction

French consumption of salted tarts has increased regularly at about 20% a year since the 1990s to reach 5400 tons in 1997. The percentage of frozen salted tarts decreased in benefit of the fresh tarts which are sold ready-cooked and ready-to-make.

We could not find any published examples of pressurised products such as tarts. So, we decided to study the influence of high hydrostatic pressure on one type of salted tart: quiche lorraine. This product is a traditional French dish which has a fragile heterogeneous structure and a short shelf-life (between 6 and 21 d) at 4–8 °C, depending on the preparation. During this study, we evaluated the sensory quality and the microflora evolution of ready-cooked quiches packed under gas or vacuum-packed.

2 Materials & Methods

Quiche lorraines were prepared according to the labelled recipe in the Unité Agro-alimentaire of EPL-AGRO. Components (in weight) were 36.4% of pastry (19.6% of flour, 10.9% of lard, 5.5% of water and 0.4% of salt), 36.4% of sauce (24.5% of

milk, 3.5% of dairy cream, 8% of egg, and 0.4% of salt and pepper) and 27.2% of strips of bacon. They were vacuum-packed or gas-packed under a mix of 50% of CO_2 and 50% of N_2 (v/v) after cooking in an oven at 165 °C during 15 min then 180 °C during 15 min. The total solids content of quiches was 58.5% and the pH was 6.1.

Packed quiche lorraines were treated in Hautes Pressions Technologies industrial pilot plant the day of preparation. The chamber consists of a 50 dm^3 capacity vessel. High pressure was applied through a hydraulic pump which pressurised water (up to 700 MPa) at 125 MPa per minute.

Total microflora, lactic acid bacteria, yeasts and moulds, coliforms and sulfito-reducing anaerobe populations were evaluated after treatment by classical microbiological techniques during several weeks of storage at 4 °C. Sensory quality of quiches was evaluated by an hedonic test.

3 Results & Discussion

The effects of high pressure treatments, between 400 MPa to 600 MPa during 5 min at room temperature, seem not to be very significant on the microorganism content, when evaluated one day after pressurisation, because microbial contamination of untreated quiche was very low. Differences appeared during the storage between untreated quiches and quiches pressurised in different conditions in the both packagings. Coliforms and sulfito-reducing anaerobe populations could not be detected in untreated or in pressurised samples even after several months at refrigerated temperature.

3.1 Vacuum-Packed Quiches

Shelf-life of vacuum-packed quiches, evaluated according to French safety standards, was extended from 3 weeks without treatment to 12 weeks after a pressurisation at 400 MPa for 5 min, and to more than 15 weeks after a 500 MPa or a 600 MPa treatment. Total microflora and lactic acid bacteria were stabilised during all the experimental period only when quiches were pressurised at 500 or 600 MPa (Fig. 1).

Sensory comparison between untreated products stored 4 d and 500 MPa treated products stored 55 d was done by 28 persons who graded quiches between 1 (very bad) to 9 (very good). Results analysed by a Wilcoxon test (non-parametric test) showed there was no significant difference between untreated and pressurised quiches as far as aspect and texture were concerned (Table 1). On the other hand, feeling in mouth, taste and general effect were significantly different ($p=0.05$). This was attributed to the taste of salt. It was undoubtedly a technical problem due to the comparison of two different batches of quiches where salt content was not well controlled enough. But unfortunately this problem did not allow us to exclude a real effect of pressurisation on taste.

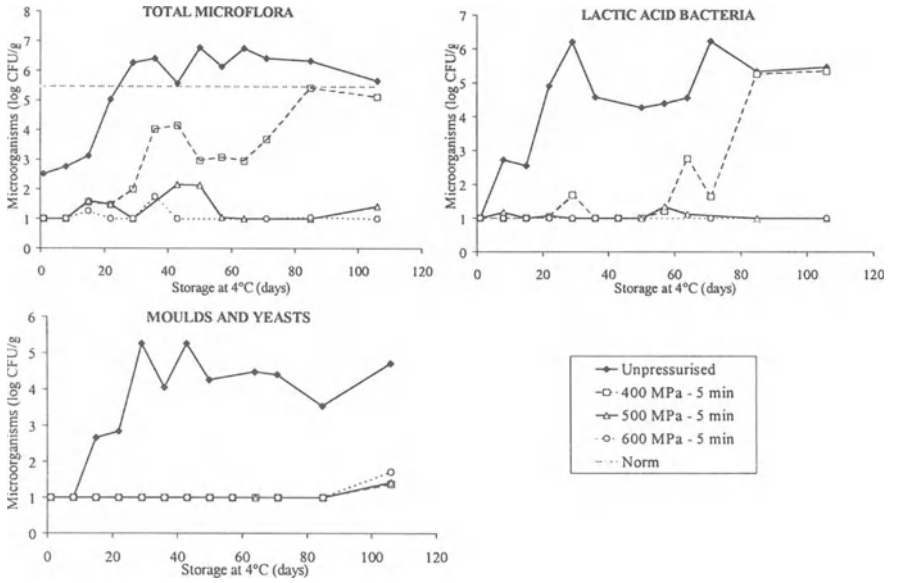

Fig. 1. Microorganisms evolution in vacuum-packed quiches

Table 1. Sensory analysis results of vacuum-packed quiches (U: untreated, P: pressurised)

	Aspect		Texture		Taste		Feeling in mouth		General effect	
	U	P	U	P	U	P	U	P	U	P
Mean	4.9	5.3	5.3	5.0	5.8	4.9	5.5	4.7	5.6	4.9
Standard deviation	1.8	1.6	2.1	1.5	1.8	1.5	1.9	1.9	1.8	1.5
Difference (p=0.05)	Non sign.		Non sign.		Significant		Significant		Significant	

3.2 Gas-Packed Quiches

Untreated gas-packed quiches had a shelf-life of about 5 weeks but microflora evolution of untreated ones was less regular than those that were vacuum-packed (Fig. 2). Pressure treatments at 400 MPa or 500 MPa allowed microbial populations to be stabilised at less than 10^3 CFU/g for at least 14 weeks of storage at 4 °C.

Sensory analysis were done by 15 persons who compared one day aged unpressurised quiches versus 500 MPa treated quiches stored 43 d at 4 °C. Results analysed by a Friedman test (non-parametric) showed that there was no difference between the two types of quiches for the 5 descriptors (Table 2).

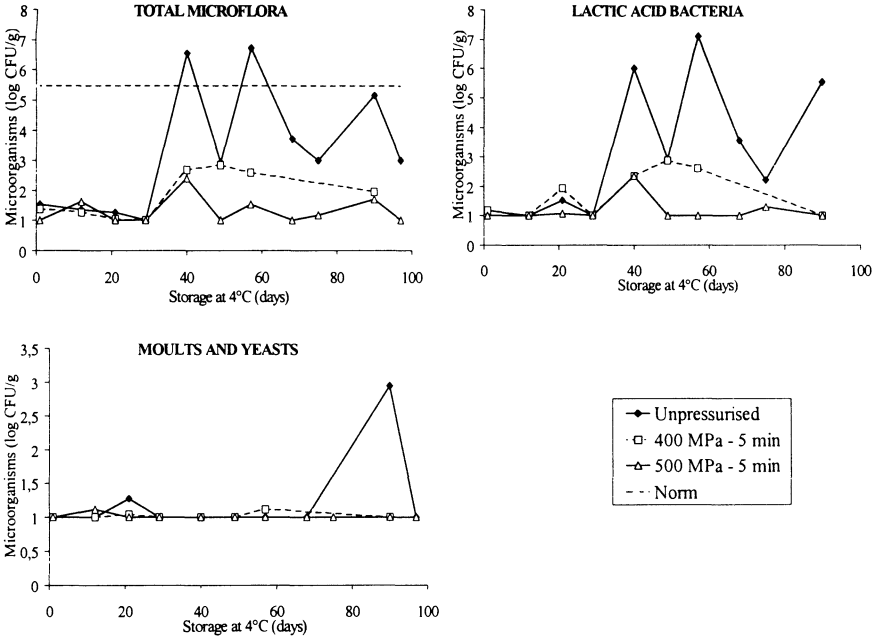

Fig. 2. Microflora evolution of gas-packed quiches

Table 2. Sensory analysis results of gas-packed quiches (U: untreated, P: pressurised)

	Aspect		Texture		Taste		Feeling in mouth		General effect	
	U	P	U	P	U	P	U	P	U	P
Mean	5.7	4.9	4.9	4.9	4.9	4.3	5.8	4.4	5.9	4.4
Standard deviation	2.1	2.1	1.7	1.8	1.7	1.9	1.8	2.1	2.1	1.9
Difference (p=0.05)	Non sign.		Non sign.		Non sign.		Non sign.		Non sign.	

4 Conclusions

Fragile texture and multilayer products such as quiche lorraine could be successfully treated by high pressure. Shelf-lives at 4 °C were multiplied by 3 or 4 at least, without important sensory modifications. Even vacuum-packed products are generally well adapted to pressurisation; better results were obtained with gas-packed samples.

Effects of High Pressure on Textural Characteristics of Cod (*Gadus morhua*) Muscle

K. Angsupanich and D.A. Ledward

University of Reading, Department of Food Science & Technology, PO Box 226, Whiteknights Rd., Reading RG6 6AP, UK
Phone: +44-(0)118-9318715; Fax: +44-(0)118-9310080
D.A.Ledward@afnovell.reading.ac.uk

Abstract. Comparison of the effects of pressure and heat on cod muscle showed marked differences in their effects on texture. Chewiness, gumminess and hardness of samples treated at 400 and 600 MPa increased significantly ($p<0.05$) when compared to the fresh and to samples treated at 200 or 800 MPa. In contrast to pressure treatment heat treatment was shown to lead to a significant ($p<0.05$) decrease in chewiness, gumminess and hardness. However both pressure and heat treatment has only a small effect on the springiness of samples. Furthermore, pressure treated samples (400 MPa) are harder than cooked (50 °C) ones ($p<0.01$). However cooking pressure treated caused the hardness to decrease to values similar to those found on cooking alone. It is suggested that while heat treatment gives rise to structures which are primarily stabilised by disulphide bonds and hydrophobic interactions, pressure involved myosin gels are stabilised by hydrogen and disulphide bonds.

1 Introduction

The use of high pressure on meat and seafood products to both preserve them and modify their eating and functional properties is of increasing interest. The pressure induced gelation and denaturation of the structural proteins of muscle has been studied [1]. Pressure and heat treated systems differ in the mode of protein unfolding and subsequent aggregation [2] and this may affect the textural quality. The aim of this study is to determine the effects of pressure on the textural characteristics of cod muscle and compare them to those of heated samples.

2 Materials & Methods

Texture Profile Analysis (TPA) was carried out with a Stable Micro System (version 3.7G). Untreated and treated (pressure at 200–800 MPa, 20 min; heat at 40–80 °C, 10 min; cooked (50 °C) then pressure (400 MPa) treatment and pressure

then cooked treatment) cod samples (2×2×1.5 cm) were compressed to 50% of their original height or strain using a cylindrical shaped piston 38 mm in diameter, speed of 2 mm/s. The texture profile was determined from these curves. All experiments were performed in triplicate. Two-way analysis of variance was carried out for statistical analysis using the Statistical Analysis System (SAS), SAS Institute Inc., Cary North, Carolina. Differences between means were analysed by a LSD range test at a significance level of $p \leq 0.05$.

3 Results

Figures 1a shows that an increase in temperature had no significant ($p \leq 0.05$) effect on the springiness and cohesiveness of the cod fillets, but there was a significant decrease in gumminess, hardness and chewiness when heated to 50 °C. The decrease may be due to the thermal dissociation of muscle protein and the enzymatic hydrolysis of muscle protein [3]. Furthermore, the texturial characteristics correlate, to some extent, with the moisture content of the samples which decreases with increased temperature [4].

As with temperature the effect of pressure on both cohesiveness and springiness (Fig. 1b) was small while hardness, gumminess and chewiness of samples treated at 400 and 600 MPa increased significantly when compared to the fresh samples and samples treated at 200 MPa. However, the values decreased after treatment at 800 MPa.

When the textural properties of heat and pressure treated fish fillets are compared, it is seen that the gumminess, hardness and chewiness of heated samples decrease as temperature increases to 50 °C, presumably due to myosin denaturation (and collagen), since actin and many sarcoplasmic proteins do not denature below 50 °C [5]. Decreases in gumminess, hardness and chewiness were not found on increasing pressure to 200 MPa, even though myosin readily denatures [6], presumably reflecting the difference in the nature of the gel networks formed. For samples subjected to 800 MPa, the properties decreased slightly when compared with samples treated at 400–600 MPa. The decreases might be due to the decreasing moisture content in the muscle seen after treatment at 600 and 800 MPa.

Figure 2b shows the different treatments have little effect on cohesiveness and springiness. It is seen there is no significant difference ($p \leq 0.05$) in gumminess, hardness and chewiness between the cooked and cooked then pressure treated samples (Fig. 2a), while, as found previously, the pressure treated sample is much gummier, harder and chewier than the others. However when the pressure treated sample was heated to 50 °C, the values decreased to a value similar to that found for the cooked samples. These observations further suggest that thermally labile hydrogen bonds help stabilise the pressure set gel. The rationale to explain these results is as follows: on pressure treatment at 400 MPa a predominantly hydrogen bonded network is set up which readily melts at 50 °C allowing some disulphide

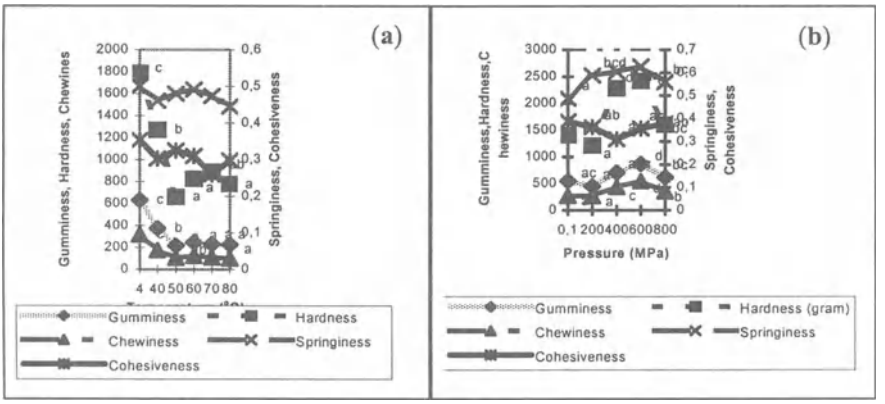

Fig. 1. The effect of temperature (40–80 °C for 10 min, (**a**))and pressure (200–800 MPa for 20 min, (**b**)) on the gumminess, hardness, chewiness, springiness and cohesiveness of cod muscle. All values are the means of 24 determinations (8 determinations on each of 3 fish). Values with the same subscripts are not significantly different ($p \leq 0.01$)

bonds and numerous hydrophobic interactions to form and set up a heat set gel. However the gel network formed by heat at 50 °C will be stabilised by disulphide bonds and hydrophobic interactions and although the hydrophobic interactions will break and reform during and following pressure treatment there will be little, if any, scope for additional hydrogen bond stabilisation to occur.

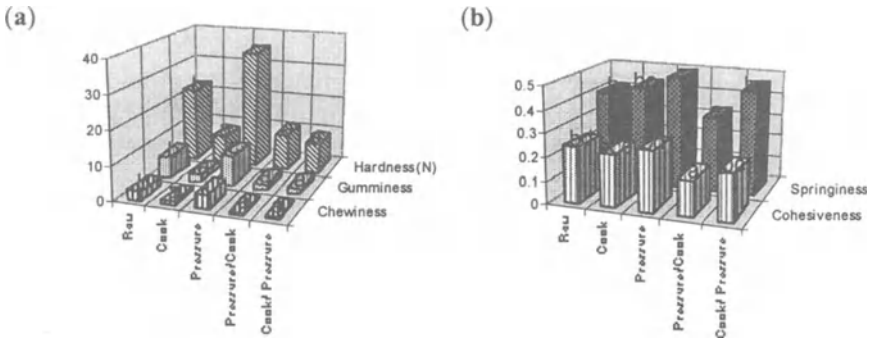

Fig. 2. The effect of pressure (400 MPa) or temperature (50 °C) or a sequential combination of both treatments on the gumminess (**a**), hardness (**a**), chewiness (**a**) cohesiveness (**b**) and springiness (**b**) of cod muscle. All values are the means of 15 determinations (5 determinations on each of 3 fish). Bars with the same subscripts are not significantly different ($p \leq 0.01$)

4 Conclusions

The characteristic pressure treated texture is different to that seen in both raw and cooked fish being harder, gummier and chewier than the cooked product. This would appear to be primarily due to the different response of the myofibrillar proteins to heat and pressure. This suggests that pressure induces a different structure to the heated system, since thermally labile hydrogen bonds are largely unaffected by pressure while hydrophobic interactions, stabilised by heat, are vulnerable to pressure [2]. It is suggested that hydrogen bonded structures must contribute to the structures of the pressure treated samples. Heat treatment gives rise to structures which are primarily stabilised by disulphide bonds [7] and hydrophobic interactions and leads to different textural characteristics.

Acknowledgements: We thank The Royal Thai Government for the financial support of this study.

References

[1] Cheftel, J.C. & Culioli, J. (1997). *J. Meat Sci.*, **46**, 211–236.
[2] Galazka, V.B. & Ledward, D.A. (1997). High pressure effects on biopolymers. In *Food macromolecules*, 2nd edition, ed. J.R. Mitchell & D.A. Ledward. Elsevier Applied Science, Oxford, UK.
[3] Deng, J.C. (1981). *J. Food Sci.*, **46**, 62–65.
[4] Lanier, T.C., Lin, T.S., Hamann, D.D. & Thomas, F.B. (1981). *J. Food Sci.*, **46**, 1643–1615.
[5] Davies, J.R., Bardsley, R.G., Ledward, D.A., & Poulter, R.G. (1988). *J. Sci. Food Agric.*, **43**, 60–68.
[6] Angsupanich, K.; Ledward, D.A.. *Food Chem.* **1998**, (in press).
[7] Lee, H. & Lanier, T.C. (1995). *J. Muscle Foods*, **6**, 125–138.

Influence of High Isostatic Pressure on Muscle of Octopus (*Octopus vulgaris*)

J.L. Hurtado, P. Montero and A.J. Borderías

Instituto del Frío(CSIC), Ciudad Universitaria, Madrid 28040, Spain
jborderias@if.csic.es

Abstract. Octopus was pressurized at 200, 300 and 400 MPa for 15 min at 7 and 40 °C; and at 400 MPa continuously and in three 5 min cycles at 7 and 40 °C. Microbiological analyses, shear strength and proteolytic activity were analyzed. The high pressure treatments reduced the microbial load, especially when it was applied cyclically at 40 °C, and caused a change of predominant flora. Proteolytic activity clearly decreased when pressures of over 200 MPa and shear strength increased in pressurized samples irrespective of the pressure and temperature levels.

1 Introduction

Muscle of octopus (*Octopus vulgaris*) has a short life in chilled storage because of its high proteolytic activity [1], which is around 25 times greater than in gadoids and 3 times greater than in squid (unpublished data). Because of this there is a high rate of non-protein nitrogen production, and this favours bacterial growth.

A number of papers have been published on the use of high isostatic pressure in food processing [2–4], and specifically on fish [5]. Cheftel [4] reported that given the pressure-resistant effects of some food constituents and the strong resistance of some strains, research ought to be directed at processes combining high pressure and other processes such as the application of moderate temperatures

Ashie *et al.* [6] and Ashie and Simpson [7] studied the softening of fish when pressurized at 200 and 300 MPa and attributed this to rupturing of the network of connective tissue that surrounds the muscle fibres, breaking of the A band and disintegration of the sarcomere. Other studies on warm-blooded animals have also reported tenderizing under high pressure, probably due to breaking of the myofibrillar structure, conversion of F-actin to G-actin and breaking of cell organules with consequent flushing of lysosome enzymes [8].

The object of this work was to observe the behaviour of microorganisms, proteolytic activity and shear strength of octopus muscle under high isostatic pressure at 7 and 40 °C, with pressure applied either cyclically (oscillatory pressure) or continuously.

2 Materials & Methods

Raw Material and Treatments. Octopus (*Octopus vulgaris*) was harvested off the coast of Pontevedra (Spain) and transported in ice to our laboratory in Madrid, within 12 h post-harvest. The animals were cleaned and the arms were collected. They were then vacuum packed for subsequent high-pressure treatment. Samples were pressurized in a hydrostatic pressure device (Gec Alsthom ACB 900 HP, Type ACIP mo 665, Nantes, France.). Two experiments were performed. One was at 200, 300 and 400 MPa for 15 min at 7 and 40 °C. The other consisted of pressurizing at 400 MPa continuously and in three 5 min cycles at 7 and 40 °C.

Methods. For microbiological analyses, samples were prepared by homogenizing 10 g of octopus arm with 90 ml of peptone (Adsa-Micro) in a Stomacher 400 (Seward) homogenizer. A series of decimal dilutions was then made from this. The following counts were performed: total viable microorganisms on samples seeded on Plate Count Agar (PCA, Oxoid) and incubated at 30 °C for 3 d.; total enterobacteria seeded on VRBG (Oxoid) and incubated at 37 °C for 18 h; lactic bacteria, on MRS plates incubated at 30 °C for between 3 and 5 d; counts of *Staphylococcus aureus* were performed on Baird-Parker Agar plates incubated for 48 h. In all cases the counts were expressed as the log of colony forming units per gram (cfu/g). The Gram test was carried out using the KOH method of Gregersen [9]. Shear strength was determined on an Instron universal texturometer with an adapted Kramer cell. For measurement, slices of octopus arm were cut approximately 2 mm thick. At least three measurements were made per lot at a speed of 100 mm/min using a crosshead that exerted a maximum of 5 kN. Results were expressed as N/g of sample. For proteolytic activity analysis, octopus muscle was homogenized in a ratio of 1:5 (w/v) with a solution of 0.15 M NaCl in an Omnimixer homogenizer (Model 17106) for 2 min, setting 7 in a bath containing water and ice. It was then filtered through a damp gauze. A 6 ml aliquot of the filtrate was then incubated in a Unitronic model S 320-100 water bath (J.P. Selecta) at 40 °C for 1 h. The enzymatic reaction was halted by adding 10% trichloroacetic acid (TCA) at 4 °C and a ratio of 1:2. The mixture was incubated at 4 °C for 15 min to allow unhydrolyzed proteins to precipitate, followed by 15 min centrifugation at 6100 × g in a Beckman centrifuge (model J2-MC rotor JA-20) at 4 °C. TCA-soluble oligopeptides in the supernatant were analyzed by the Lowry test [10]. Activity was expressed as nmols of Tyr/h/g.

3 Results & Discussion

Total viable counts (TVC) decreased under high pressure, especially at 400 MPa. It was also found that the influence of temperature on reduction of microorganisms was minimal. Yasui and Samejima [11] reported reductions of one or two log colony forming units per gram (cfu/g) in the total viable counts of tuna and squid

pressurized at 450 MPa and 25 °C. On the other hand, Shigehisa *et al.* [12] found reductions of six log numbers in several kinds of bacteria and fungi, although in this case the study was conducted on a culture rather than a muscle substrate. Carballo *et al.* [13] reported reductions of over two log numbers in meat hamburgers pressurized at 300 MPa at room temperature for 20 min. The microbial load is reduced when pressure is applied cyclically, especially at 40 °C. Other authors have reached the same conclusion, for example in pasteurization of pineapple juice [14] or even in *Bacillus stearothermophilus* spores [15]. There was a drastic reduction in enterobacteria at lower levels at all of the experimental pressures. Similar results have been reported by Carballo *et al.* [13] in meat hamburgers pressurized at 300 MPa. However, no differences were found between sample pressurized cyclically and samples pressurized continuously. Significant numbers of *Staphylococcus aureus* were not found. Under high pressure there was a sharp reduction in Gram-negative bacteria and a very slight reduction in lactic bacteria (Gram-positive), which caused a change of predominant flora.

Proteolytic activity clearly decreased when pressures of over 200 MPa were reached. This activity decreased still further under pressurization at 40 °C rather than 7 °C. Cyclic pressurizing did not improve these results. Cheftel [4] reported that the behaviour of enzymes subjected to high pressure can be contradictory. While in some cases the protein becomes denatured, and hence the enzyme is deactivated, in others high pressure induces rupturing of cell organules, so that the enzymes are flushed into the medium and activated. Shoji and Saekı [16] in turn concluded that pressurizing of fish muscle deactivates the enzymes involved in the breakdown of ATP. Ohshima *et al.* [5] reported that the enzymes involved in the breakdown of phospholipids in fish muscle are deactivated by high pressure.

Shear strength increased in pressurized samples irrespective of the pressure and temperature levels. Also, there was no difference between cyclically and continuously pressurized samples. These results are not in agreement with findings reported by Ashie *et al.* [6] and Ashie and Simpson [7], which showed softening of the muscle in the species *Panatomus saltatis* when pressurized at 200 and 300 MPa; this was attributed to physical changes in the muscle structure, particularly perimysial and epimysial breaking of the network of connective tissue that surrounds the muscle fibres. Other authors [8,17] working on warm-blooded animals have also concluded that high pressure softens meat. They offer a variety of explanations, for instance rupturing of lysosome corpuscles, conversion of F-actin to G-actin and breaking of the myofibrillar structure. In the present case no explanation was found for the absence of softening, although this could have been due to the fact that cephalopods have a high percentage of connective tissue arranged in a particular way, which could be maintained especially by the formation of hydrogen bridges after pressurization. Moreover, Fernández Martín *et al.* [18] indicate that pressurizing modifies the calorimetric profile (DSC) of myosin and actin in the muscle of mammals, which could be related to the softening found in these muscles. On the other hand Fernández Martín *et al.* [19] report that pressurization of fish muscle protects myosin and alters the calorimetric profile of actin, which in cephalopods could contribute to the absence of softening after pressurization.

4 Conclusions

The high pressure treatments applied to octopus muscle reduced the Gram-negative microbial load and the proteolytic activity but did not soften the muscle.

Acknowledgements: This study was supported by funds from projects ALI97-0759 and 06G/053/96.

References

[1] Tanikawa, E.; Motohiro, T. and Fujii, T. 1970. Preservation and control of freshness in marine products. Chap.12. Kosei, Tokyo.
[2] Hoover, D.G.; Metrick, C.; Papineau, A.M.; Farkas, D.F. and Knorr, D. 1989. Food Technology.43(3):99–107.
[3] Knorr, D.1992. In: New methods of food preservation.pp 159–175. Gould G.W.(ed).Blackie Acad. & Professional. London.
[4] Cheftel, J.C.1995. Food Science and Technology International. 1: 75–90.
[5] Oshima, T.; Ushio, H. and Koizumi, C. 1993. Trends in Food Science and Technology. Nov(4):370–374.
[6] Ashie, I.N. and Ramaswamy, H.S. 1997. Journal of Muscle Foods. 8:13–32.
[7] Ashie, I.N.A. and Simpson, B.K. 1998. Journal of Muscle Foods. 9:193–199.
[8] Johnston, D.E. 1992. In "The chemistry of muscle-based foods." (Ledward, D.A., Johnston, D.E. and Knight,M.K. Eds). The Royal Society of Chemistry. p 298.
[9] Gregersen, T. 1978. Eur. J. Appl. Microbiol. 5, 123–127.
[10] Lowry, O.H.; Rosebrough, N.J.; Farr, A.L. and Randall, R.J. 1951. J. Biol. Chem. 193:265–275.
[11] Yasui, T. and Samejima, K. 1985. New Food Ind. 27(5):76–82.
[12] Shigehisa, T.; Ohmori, T.; Saito, A.; Taji, S. and Hayashi, R. 1991. Intl. J. Food Microbiol. 12:207–216.
[13] Carballo, J.; Fernández, P.; Carrascosa, A.V.; Solas, M.T. and Jiménez Colmenero, F. 1997. Journal of Food Protection. 60(1):48–53.
[14] Alemán, G.D.; Ting, E.Y.; Mordre, S.C.; Hawes, A.C.O.; Walker, M.; Farkas, D.F. and Torres J.A. 1996. J. Food Science. 61(2): 388–390.
[15] Hayakawa, I.; Kanno, T.; Yoshiyama, K. and Fujio, Y. 1994. J. Food Science. 59(1):164–167.
[16] Shoji, T. and Saeki, H. 1989. Use of high pressure in food. pp. 75–87. (Hayashi, R. ed.) San-ei Publ. Kyoto, Japan.
[17] Beilken, S.L.; Macfarlane, J.J. and Jones, P.N. 1990. J. Food Science. 55(1):15–19.
[18] Fernández-Martín, F.; Fernández, P.; Carballo, J. and Jiménez Colmenero, F. 1997. J. Agric. Food Chem. 45:4440–4445.
[19] Fernández-Martín, F.; Pérez-Mateos, M. and Montero, P. 1998. J. Agric. Food Chem. 46(8):3257–3264.

Effect of a High Pressure Treatment on the Texture and Enzyme Activities of Selected Vegetables

S. Crelier, M.-C. Robert and M.-A. Juillerat

Nestlé Research Centre, P.O. Box 44, CH-1000 Lausanne 26, Switzerland
simon.crelier@chlsnr.nestrd.ch

Abstract. The impact of HHPT on tomatoes, carrots, potatoes and broccoli was investigated regarding enzyme activities as well as mechanical texture alteration. Pectin methylesterase, polygalacturonase and peroxidase were affected at pressures above 500 MPa. Extensive tissue damage occurred however already at 200 MPa, leading to a dramatic softening and liquid exudation during cutting/compression tests. As a consequence of tissue disruption, potatoes and carrots also turned brown very quickly. Tomato juice viscosity, on the other hand, was durably increased by HHPT.

1 Introduction

Food quality related enzymes, among others, can be partially or totally inactivated by a High Hydrostatic Pressure Treatment (HHPT) [1]. The use of such a technique could therefore be suggested to suppress texture-degrading activities and hence help preserve thickness, viscosity or "crunchiness" in fresh vegetable food products. On the other hand, HHPT is also likely to affect the structure of the product in a mechanical way, and the present study is aimed at evaluating the global impact of HHPT on four vegetable systems: tomato (*Lycopersicon esculentum*), carrot (*Daucus carota*), potato (*Solanum tuberosum*) and broccoli (*Brassica broccolis*). Mechanical characteristics of vegetable tissues were evaluated before and after treatment, the same being done with a selection of enzyme activities.

2 Materials & Methods

Fresh vegetables were purchased from local markets. They were processed whole, crushed or as a liquid extract. The samples (placed in a polypropylene pouch) were treated in a 0.8 l, batch-type thermostated HP machine from ABB, Västerås (Sweden). The *treatment duration* was fixed at 15 min.

Mechanical characteristics were measured on a TA+Di texture analyser from Stable Micro Systems, Godalming (GB). *Cutting experiments* were performed on a

horizontal 18 mm diam. cylindrical sample, and *compression tests* on a vertical cylinder (28 mm high, 18 mm diam.). *Dynamic viscosity* of tomato juice was measured over storage time at 22 °C using a Brookfield type LV viscometer with spindle N°2 at 50 rpm.

Pectin Methylesterase assay (PME, E.C. 3.1.1.11): dosage rate of 0.01 N NaOH at constant pH 7.5 during hydrolysis of 0.5% pectin at 25 °C.

Polygalacturonase assay (PG, E.C. 3.2.1.15): appearance of reducing ends upon cleavage of 2% sodium polygalacturonate (45 °C, pH 5.0). Derived from [2].

Peroxidase assay (POX, E.C. 1.11.1.7): appearance of tetraguaiacol monitored at 470 nm (25 °C, pH 7.0).

3 Results

Fresh Tomatoes were crushed and the juice degassed before processing. Residual PME, PG and POX activities were measured and compared with a control, untreated sample. The results are given in Table 1, along with values for viscosity and WF_{plt}, the *weight fraction of pellet obtained by centrifugation* of a juice sample (3000 g, 20 min). The results clearly show that PME and POX are not affected by pressures up to 500 MPa, even at 60 °C. PG, on the other hand, is completely inactivated at 500 MPa/60 °C.

Table 1. Global impact of HHPT on tomato juice

p/T [MPa/°C]	PME [U/ml]	PG [U/ml]	POX [U/ml]	Viscosity [mPa·s]	WF_{plt} [%]
0.1/20	34.1	2.36	0.447	200	24.5
250/30	36.3	2.08	0.453	220	30.5
250/60	36.2	2.44	0.449	126	20.1
500/30	32.2	0.35	0.436	260	30.5
500/60	34.8	<0.05	0.191	176	29.3

Most striking is the *immediate effect* of HHPT on the juice water retention (increase in WF_{plt}) and viscosity. HHPT leads to a swelling of the vegetable tissues, which makes the juice thicker. This effect could still be observed after a 13 weeks storage time at 22 °C, as shown on Fig. 1. Pressure and temperature have antagonistic effects regarding juice thickening, the best results being obtained at 500 MPa/30 °C. The magnitude of these mechanical effects *was greatly reduced when using previously frozen tomatoes.*

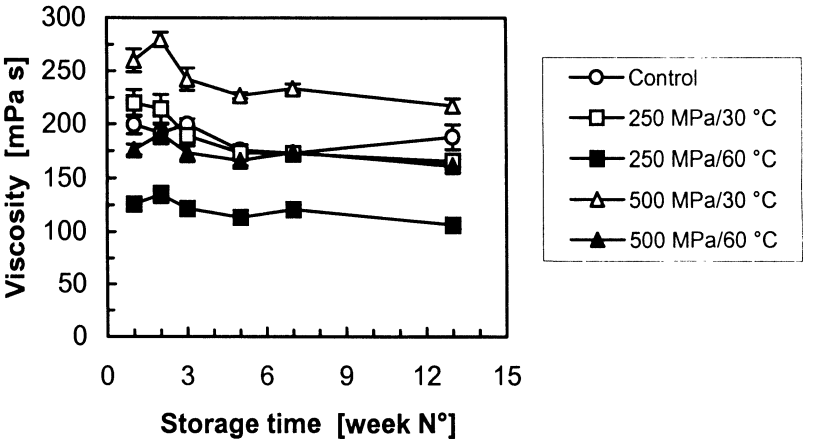

Fig. 1. Viscosity of HHPT-treated tomato juice stored at 22 °C

Carrots were processed whole and unpeeled. No apparent effect on compressibility and POX activity could be observed at 125 MPa. Above this pressure the vegetable became *soft and soggy*, all changes which were reflected in the cutting and compression tests. The *roots exuded liquid and turned brown* very quickly after the treatment, indicating residual polyphenoloxidase (PPO) activity and important tissue damage (data not shown).

Potatoes were processed whole and unpeeled as well. Again, no effect of HHPT was observed at low pressures, as shown on Fig. 2 (compression test) where the softening of the tuber leads to curves with a much lower slope above 125 MPa. Potatoes also turned brown very rapidly after the treatment.

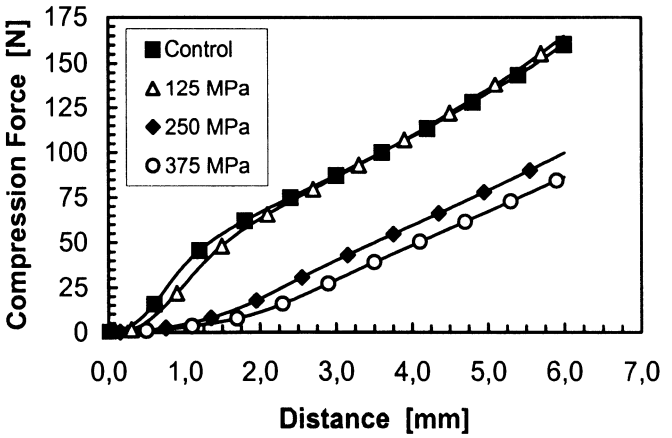

Fig. 2. Compression test for a vertical potato cylinder

Broccoli flowers were processed in a water-filled pouch. A dramatic softening of the vegetable again ensued. No colour change was however observed in this case.

4 Conclusion

As already reported [3,4], fresh tomato juice is thickened by HHPT. This durable effect is maximum at high p / low T. It is however lost when using frozen and thawed tomatoes.

Vegetables treated above 125 MPa become immediately soft, spongy and exude liquid upon compression. They have lost their crunchy state. Carrots and potatoes turned dark very quickly after treatments above 125 MPa, due to residual PPO activity and tissue disruption. Pressures above 500 MPa are required to significantly inactivate (texture-degrading) enzymes. The degree of POX inactivation did not vary much with the type of sample (crushed or whole vegetable, liquid extract).

These pressure values are clearly incompatible with the HHPT treatment of fresh vegetable pieces for food consumption. HHPT could however be advantageously used for the treatment of crushed products (fruit and tomato juice, carrot puree, guacamole).

Acknowledgements: Support from Swiss OFES (contract N° 95.0895) is gratefully acknowledged.

References

[1] Seyderhelm I. *et al.* (1996); J. Food Sci. 61 (2), 308–310.
[2] Pressey R. *et al.* (1971); J. Food Sci. 36, 1070–1073.
[3] Poretta S. *et al.* (1995); Food Chem. 52, 35–41.
[4] Rovere P. *et al.* (1996); Industria Conserve 71,. 473–483.

Release of Iron from Beef, Liver, Soya Flour and Spinach on High Pressure Treatment

A.B. Defaye and D.A. Ledward

Department of Food Science and Technology, The University of Reading, Reading RG6 6AP, UK

Abstract. Pressure treatment at 600 MPa for 20 minutes led to a significant increase in the soluble iron content of liver but no change in the soluble iron content of soya flour and spinach. In beef muscle soluble iron decreased due to precipitation of haemoprotein and in isolated haemoglobin no loss of haem iron was found. High pressure induced catalysis of lipid oxidation in meat may relate to release of soluble iron from non-haem complexes

1 Introduction

Cheah and Ledward found in meat subjected to high pressure an increase in rate of lipid oxidation on subsequent air storage.They suggested this was due to the release of free iron from one or other of the complexes present. This study investigates the release of soluble iron from a variety of iron rich foods following heat or high pressure treatment: Beef, Liver, Soya flour and Spinach were studied. The iron in these foods exists in different forms .Mainly as heme in beef, as hemosidrin and ferritin in liver, as oxalates or phytates in spinach and soya flour. We also investigated the effect of high pressure treatment on the free iron content in hemoglobin.

2 Materials & Methods

All food samples were from a local supermarket. After blending with an equal weight of water, 25 g of sample were put in a plastic bag and pressure or heat treated at 600 MPa for 20 min or 100 °C for 10 min. After centrifugation at 3000 g, and filtration the samples were freeze dried and resolublised to the appropriate concentration for the determination of the soluble iron content by atomic absorption spectroscopy, after wet digestion. For the hemoglobin study the technique described in the literature [2] was used.

3 Results & Discussions

Pressure and heat treatment of beef caused a decrease in the soluble iron content by 50 and 67%, respectively (Table 1). The main constituents of soluble iron in beef is diffusate iron, heme and ferritin iron. The denaturation of the hemoproteins and perhaps ferritin will result in the formation of insoluble aggregates which will explain for the decrease in soluble iron after treatment. The break up of the protein coat surrounding the cluster of hydrous ferric oxide in ferritin is probably responsible for some of the 50% increase in the soluble iron content in liver on pressure treatment. Heat treatment of liver produced a gel making estimates of soluble iron content difficult.

Pressure treatment was found to have no significant effect on the soluble iron content in both spinach and soya flour. This is not surprising as the iron is strongly bound in the phytates and oxalates although heat treatment caused a small increase in soluble iron in spinach ($p<0.05$).

In the hemoglobin study the free iron contents in the control and pressure treated solutions were 0.6036 ± 0.03 and 0.6308 ± 0.01 ppm, respectively, indicating that pressure treatment has no significant effect on the free iron content associated with this protein ($p< 0.05$) from hemoglobin.

Table 1. The soluble iron content (ppm) in beef, pig's liver, spinach and soya flour after pressure, 600 MPa/20 min or heat treatment 100 °C/10 min. All values are the means of ± SD of five replicates

Sample		Treatment	
	Control	Pressure	Heat
Beef	3.0±0.06	1.76±0.11	0.99±0.29
Spinach	1.22±0.09	1.22±0.08	1.48±0.16
Pig's liver	49.1±1.9	78±3.5	-
Soya flour	2.65±0.27	2.79±0.07	2.95±0.25

4 Conclusions

There is no evidence to support the suggestion that the increase in the rate of lipid oxidation in pressure treated meat is due to the release of free iron from hemoproteins but release from other iron complexes (ferritin and perhaps heamosidrin) is likely.

References

[1] Cheah and Ledward. 1996. High Pressure effects on Lipid oxidation in minced Pork. *Meat Science*. Vol.43, No 2, 123–134.

[2] Johannes Everse (ed).1984 *Methods in Enzymology*. Hemoglobins Part B. Vol. 231, 505–509.

The Effects of Hydrostatic High Pressure on the Brewing Process and Beer

S. Fischer, H. Schöberl, W. Ruß and R. Meyer-Pittroff

Technische Universität München, Lehrstuhl für Energie- und Umwelttechnik der Lebensmittelindustrie, 85350 Freising-Weihenstephan, Germany
fisc@eul.blm.tu-muenchen.de

Abstract. New methods for increasing the stability of products, other than pasteurisation, are often applied in the manufacture of non-alcoholic drinks. Quite promising results have been achieved here using high-pressure treatment. Since the increasing of the stability without affecting the flavour of the product is also of interest to breweries, the effects of high pressures on beer were to be examined. From this initial starting point further possibilities for applying high-pressure treatments arose. Due to this, the research was expanded to include the entire brewing process. This paper can be seen as a screening of the possible areas of use for high-pressure treatments in breweries. Chemical-technical analyses of high-pressure treated mash, wort and beer were conducted. The high-pressure treatment gave rise to changes in the protein-fractions, the viscosity and the saccharification of the mash. The solubility of the bittering substances and the isomerisation of the α-acids in the wort were also influenced. The high-pressure treatment of the beer led to a considerable reduction of the hazing potential.

1 Introduction

The high-pressure treatment presents several significant advantages as compared to the thermal processes. The formation of Maillard products is reduced [1], and experiments with high-pressure treated lemon juice led to significantly better taste-test results after a three-month storage period than was the case with thermally treated samples [2]. The reaction of the enzymes to the high-pressure treatment is the most significant aspect of the treatments' effect on the mashing process, since the selectivity of the enzymes can be changed, or the enzymes themselves can be activated or inactivated. Mash and wort ingredients such as carbohydrates and proteins go through structural changes [3]. By using high pressures micro-organisms are inactivated, the pressure required for inactivation being dependent upon the type of microorganism [4]. The microbiological stability is thus guaranteed, for which reason the research was expanded to include colloidal stability, since this lays the foundations for the stabilisation of beer.

2 Materials & Methods

High-pressure treated mash, wort and beer samples, as well as the corresponding untreated comparative samples, were subjected to the relevant chemical-technical analyses set up by MEBAK (Mitteleuropäische Brautechnische Analysen-kommission) [5].

The high-pressure treatment occurred at 300, 500 and 700 MPa for 5 min in each case. The pressure build-up and decrease rates were set at 200 MPa/min.

The high-pressure treatment of the mash occurred at 20 °C in PE bags. The treated bags were subjected to a congress-mashing process.

Some trials were additionally applied to mashes treated to 50% under high pressures.

For the trials on the wort, a defined amount of hop pellets was added to unhopped wort and treated under high pressures in PE bags again. One sample was kept at 700 MPa for 30 min. Two further samples were boiled at atmospheric pressure for 30 and 60 min, respectively.

For the research into the influence of the high-pressure treatment on beer a pale lager was filled into PEN bottles. As a comparison one sample was pasteurised for 20 min in a water bath at 60 °C.

3 Results & Discussion

The high-pressure treatment has a strong influence on the relevant enzyme-substrate systems of the mash. The protein fractions of the mash were heavily altered by the high-pressure treatment. As Fig. 1 shows, the dissolved-protein content rises, as do those of high- and low-molecular nitrogen. The endopeptidases have the greatest influence on the rising dissolved-protein content. An activation of the endopeptidases or an expansion of their specifity could thus be present, or alterations of the substrates might be so great that they are dissolved much more readily. When original unsoluble protein fractions are taken into consideration this does not seem entirely implausible. The increase in the high-molecular nitrogen is quite probably attributable to the same causes. But attention must be paid to the interactions between the different fractions. The dipeptidase-low molecular-nitrogen-fraction system is inhibited, since the FAN content sinks despite the high availability of the former. The content of coagulable nitrogen rises to 500 MPa and falls again after this point. Fraction proceeds quite well. The viscosity decreases with rising pressures. The partially treated samples showed a much lower decrease. The viscosity is mainly attributable to the breakdown of the gums, and thereby the β-glucanases and the β-glucan-solubilase. The saccharification of the mash could not be ensured anymore after 500 MPa. At 300 MPa it was reached marginally sooner than in the untreated sample. The final attenuation sank with a pressure increase, which could be expected due to the lack of saccharification and the lower FAN content. No changes could be determined in the extract and pH-value.

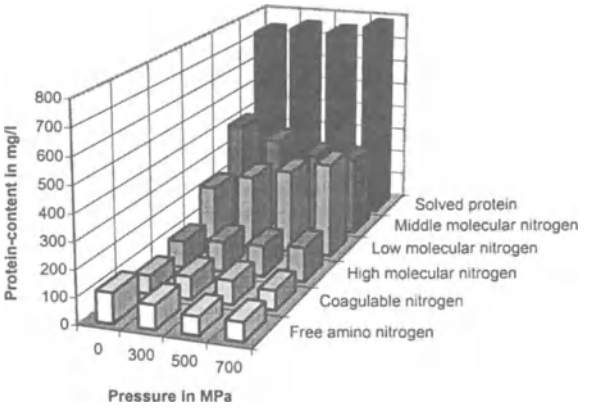

Fig. 1. Protein fractions in mg/l, in dependence on pressure in MPa

The high-pressure treatment of the wort (Table 1) shows that the boiled samples achieve the best solution of hop ingredients, this dependence on the good stirring effect while boiling. The isomerisation shows good results at 700 MPa and 30 min, a significant time dependence is recognizable

Table 1. Bitterness units in BU and α- and iso-α-acids in mg/l in dependence on the pressure in MPa

	0 MPa	300 MPa, 5 min	500 MPa, 5 min	700 MPa, 5 min	700 MPa, 30 min	30 min boiling	60 min boiling
Bitterness units	79	90	99	97	98	157	164
α-Acids	143	123	134	126	90	76	50
Iso-α-Acids	0	2	2	21	51	87	119

The high-pressure treatment of the beer showed no significant changes with respect to colour, foam stability and the spectrum of aromatic compounds. Haziness and the potential for hazing were influenced quite significantly however. Table 2 shows the relation of the haziness and the hazing potential.

The haziness increased to pressures of over 300 MPa. This increase is due to the falling-out of proteins, and possibly carbohydrates as well. The hazing potential sank to such a degree due to the high-pressure treatment that even the values for the pasteurised samples lay higher. This was especially surprising with the sample treated at 500 MPa, since it had shown a higher initial haziness.

Table 2. Turbidity and potential for the arising of turbidity in EBC dependence on the pressure in MPa

	0 MPa	Pasteurized	300 MPa	500 MPa	700 MPa
Turbidity	1,0	1,0	0,9	2,0	13,4
Potential for the arising of turbidity	32.5	24.7	22.7	22.6	----

4 Conclusions

The influence of high pressures on the individual areas of the beer preparation should be evaluated separately. The influence upon the mash and the wort treatment can only be applied with great difficulty. One should not forget however that the high-pressure treatment creates possibilities which could lead to an optimisation of the composition of the mash. The isomerisation of the α-acids can also be positively influenced. The area with the best possibilities at the moment remains the stabilisation with high pressures. The lowering of the hazing potential with an unchanging haziness lets the implementation of high pressures seem sensible, especially since this effect occurs in the relatively low-pressure range of approximately 300 – 400 MPa, simplifying the application.

Acknowledgements: This research was supported by "Wissenschaftsförderung der deutschen Brauwirtschaft e.V.".

References

[1] Tamaoka,T., Itoh, N.: High pressure effect on Maillard reaction. Agric. Biol. Chem., 55 (1991)8, 2071 – 2074.
[2] Ogiwara, H., Fukuhisa, K., Fukumoto, H.: High Pressure and Biotechnology, 269 - 278, John Libbey Eurotext, 1992.
[3] Cheftel, J.C., High Pressure and Biotechnology, 195–209, John Libbey Eurotext,1992.
[4] Ludwig, H., Bieler, C., Hallbauer, K., Scigalla, W.: High Pressure and Biotechnology, John Libbey Eurotext, 25–32, 1992.
[5] MEBAK: Brautechnische Analysenmethoden Band I + II, Eigenverlag, Weihenstephan, 1997.

A Comparison Between UHP Hydrostatic Exposure and UHP Discharge Production Methods

E. Ting, S. Tremoulet, J. Hopkins and R. Many

Flow International Corporation, 23500 64th Ave South, Kent, Washington, 98032 USA
Eyt@aol.com

Abstract. The differences between ultrahigh-pressure (UHP) hydrostatic exposure and UHP discharge are discussed. UHP hydrostatic exposure in excess of 1000 MPa is being used to inactivate microorganisms as well as induce texture changes to foods without thermal degradation or product shear. Direct UHP discharge at pressures up to 400 MPa can be used to homogenize and treat foods by combining hydrostatic pressure exposure effects with high shear rate and elevated temperature during discharge. The magnitude of adiabatic heating during hydrostatic exposure and the magnitude of discharge heating are calculated and measured for some foods. Maximum temperature achieved is significantly less for UHP hydrostatic exposure than for discharge methods. The production energy requirement for hydrostatic exposure is also significantly less than that for discharge methods.

1 Introduction

Ultrahigh-pressure (UHP) offers food companies an expanded avenue for high quality production. A number of different methods are evolving for UHP food production. The two major high-pressure methods are direct discharge of product and static hydrostatic exposure of product.

Traditionally, high pressure has been used in the food industry mostly for homogenization. Using a high-pressure pump, the product is increased in pressure and then allowed to discharge through a very narrow gap. Extremely high velocities are created along with cavitation which shear solid particles or liquid globules into much smaller units to improve the stability of many food dispersions. Homogenization pressures up to 40,000 psi have been in commercial use. High product velocity, high shear, and a resultant increase in product temperature characterize the direct discharge method. The method is illustrated in Fig. 1.

If during the above process the product pressure is simply increased, held and then lowered without product discharge, the product would not experience velocity, shear, homogenization, or product temperature increase. Depending on the magnitude of this hydrostatic pressure, various other desirable effects can be achieved.

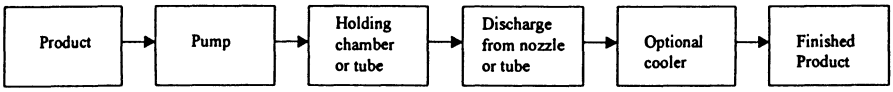

Fig. 1. Direct discharge of product under pressure

Typically with hydrostatic exposure at pressures below 100 MPa, no major microbiological effects are observed in the product. However, at pressures less than 100 MPa, some physical effects such as syrup infusion are achieved on foods. For foods with significant air content, densification due to air displacement may also take place. At higher hydrostatic pressure, certain microorganisms such as bacteria, fungi, parasites, and viruses can be inactivated while not degrading vitamins, nutrition, or taste of fresh or recently prepared foods. Pressure can inactivate food pathogens or spoilage microorganisms to increase food safety and shelf life in essentially fresh unprocessed products without the use of chemical preservatives, heat, or irradiation. At even higher pressures, typically in excess of 700 MPa, enzymes can also be inactivated. UHP exposure can also be used to produce desirable texture changes in certain food types. Protein and certain starches can experience a rheology change after UHP exposure. The hydrostatic exposure method is essentially a batch method since discrete quantities of products are dealt with at a single time. Nevertheless, when multiple chambers are used, semicontinuous output can be achieved. The hydrostatic exposure method is illustrated in Fig. 2.

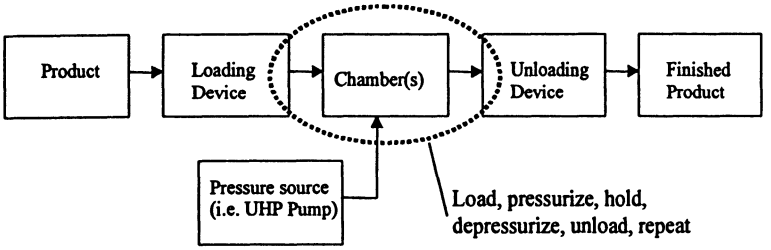

Fig. 2. Hydrostatic exposure of product to pressure

2 Compressibility of Water

The work performed in generating pressure is based upon the fact that most foods are water based and are compressible under pressure. The extent of water compressibility was measured by Bridgman [1]. His data can be fitted to an equation for water compression as shown (1) and used for calculating energy associated with compression. Bridgman's original data at 22 °C are shown in Fig. 3 along with the fitted compressibility curve:

$$\frac{V_0}{V} = \frac{\rho}{\rho_O} = \left(1 + \frac{P}{L}\right)^c \quad . \tag{1}$$

Where

ρ = density
V = volume
L, c = material constants

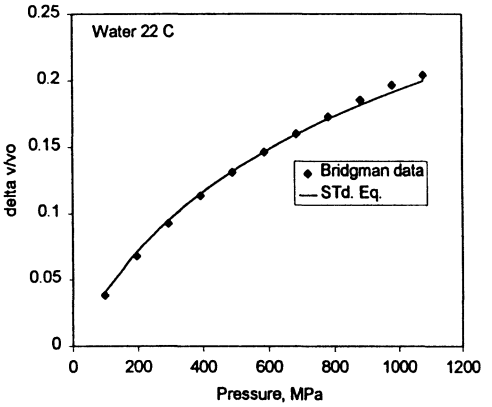

Fig. 3. Water compression data obtained by Bridgman

3 Pressurized Discharge

A major feature of direct discharge is the conversion of pressure energy into velocity, shear and heat upon discharge. This will result in product homogenization and thermal modification. These changes may be desirable for certain products and undesirable for other products. When direct discharge is combined with a residency time of sufficient duration to produce microbiological and enzyme effects, additional benefits can be realized. The temperature rise associated with direct discharge can be mitigated by continuous cooling or staged cooling as illustrated in Fig. 2. For example, the use of a long small diameter tube can create a continuous pressure drop over a distance and thus allow the introduction of cooling to limit product temperature rise. The amount of power dissipated by pressurized discharge can be calculated using Eq. (1) and:

$$E = PV_P + \int_{V_o}^{V_p} P_v dV = V_0 \rho_0 C_p \Delta T \tag{2}$$

where
E = energy dissipation
p = pressure
V_0 = volume at ambient pressure
V_p = volume at pressure
ρ_0 = density at ambient pressure
Cp = specific heat
ΔT = change in temperature

The integral term contained in Eq. (2) represents the energy due to product compression. If a constant Cp value is assumed, then solving numerically, the approximate change in temperature can be calculated. At pressures greater than 400 MPa, the discharged liquid will likely exceed the boiling point unless cooling is added. The result for water is shown in Fig. 4.

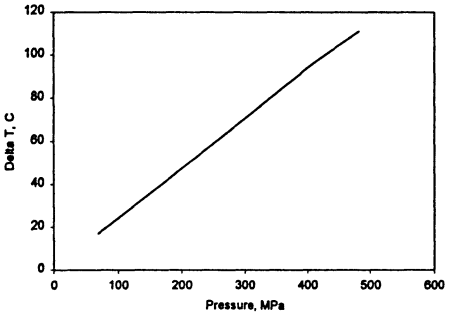

Fig. 4. Temperature change in water due to pressurized discharge

The generation of heat may be desirable for certain products but it also increases the energy required for the process. If active cooling of the discharge is implemented to reduce temperature increase, then the amount of energy use will be higher. The cooling energy used will be at least equal to the energy of discharge. Cooling cycle inefficiencies will further increase energy consumption. At higher pressures, the amount of energy needed makes this method only attractive for high value added products. The amount of power used to discharge water at a flow rate of 1 l/min is shown in Fig. 5.

At higher pressures, the combination of direct discharge with a dwell time under pressure can create synergistic effects based upon hydrostatic exposure effects. This hybrid between homogenization and hydrostatic exposure can incorporate a pressure energy recovery method, thus separating the discharge temperature effects from the hydrostatic pressure effects. Once the complexity of the recovery device has been mastered, equipment life in theory can be improved because the holding tube or vessel does not experience alternating pressures.

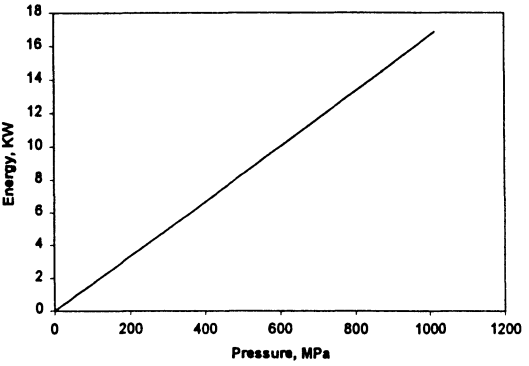

Fig. 5. Power needed to discharge water at 1 liter per minute

4 Hydrostatic Exposure

A main feature of the hydrostatic exposure method is the absence of shear, homogenization and product heating. The only temperature effect achieved with hydrostatic exposure is a temporary temperature change as a result of adiabatic heating during product compression. The magnitude of this change is low and does not result in any thermal degradation. For example, orange juice compressed to 413 MPa experiences a temperature change of approximately 10 °C. Upon decompression, this equal amount of heat is instantly removed due to adiabatic cooling. Product exiting from the chamber is at essentially the same temperature as when it entered. Measured temperature changes due to adiabatic compression are shown in Fig. 6 for a number of food products.

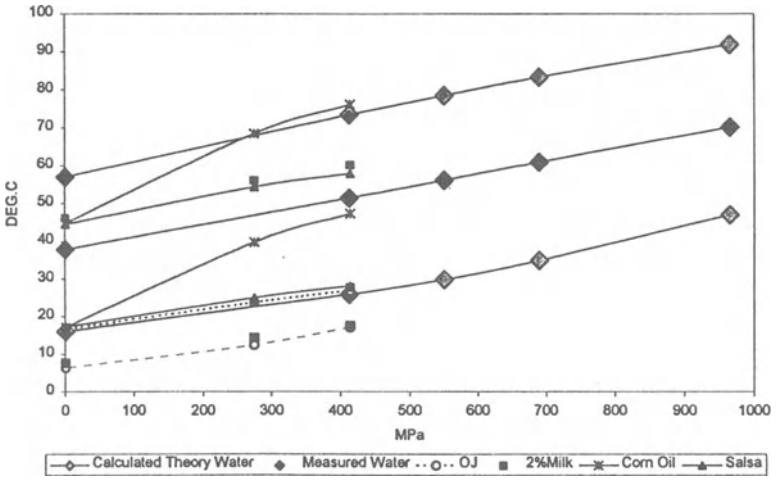

Fig. 6. Measured and calculated adiabatic temperature increase for water and selected foods. Initial product temperature is shown by zero pressure point

Sometimes at the start-up of room temperature operation, a lower product exit temperature can be observed. This is typically associated with a non-steady-state thermal condition. Heat transfer from the product to the chamber under compression can effectively mimic a refrigeration cycle and lower the heat energy content of the product. Thus under non-steady-state conditions, upon decompression, adiabatic cooling can produce a lower than initial product temperature.

The measured product data in Fig. 6 were obtained using a chromel-alumel thermocouple immersed into approximately 2 l of product. The products were subjected to direct compression within an isolator and pressure was obtained from an external intensifier pump (Flow International, Model 7X-100). Target pressure was achieved in less than 5 s. This is sufficiently fast to simulate a true adiabatic condition. Thermocouple error due to pressure is anticipated to be no greater than approximately 0.4 °C at 400 MPa [2]. Figure 6 plots the theoretical temperature change due to adiabatic compression using water thermodynamic data. These values were obtained by using tabulated thermodynamic data. This method of calculation is more precise than those based on water compression as in (1). Under adiabatic compression or expansion, isentropic behavior was assumed and the PVT values determined at constant entropy. As expected, most foods behaved water-like and showed a parallel behavior to water. Due to the complex nature of food products, their thermodynamic data are not available at this time. The exceptions to water-like behavior are associated with substances high in oils. Corn oil showed a significant deviation from water-like behavior. The more complex structure of oils resulted in much greater compression as well as a greater change in compressibility as a function of pressure than water. Combined with the lower specific heat of oils as compared to water, oil unquestionably shows a significantly higher adiabatic temperature increase than water or most water-like foods.

When oils are used as the hydrostatic media in high-pressure chambers to prevent equipment corrosion, an inadvertent side effect is the heating of the food due to heat transfer from the much hotter oil to the cooler product while under pressure. This can be a significant source of experimental error particularly when the oil to product ratio is high.

The energy required for hydrostatic exposure is significantly less than that required for pressurized discharge. The energy expended for compression is directly related to the degree of product compressibility. High forces or high stresses do not necessitate high-energy usage. For example, an infinitely incompressible product would require no energy for compression. The calculated energy needed to compress water to pressure is shown in Fig. 7. The exact energy will depend on additional factors such as machine inefficiencies. However, the general magnitude of this energy use is comparable to the energy used in conventional food production operations and lower than that of high-pressure discharge. The amount of energy used in compression is typically an order of magnitude less than that used in heating the liquid to boiling. Future equipment will incorporate pressure energy recovery and further reduce energy use for UHP production.

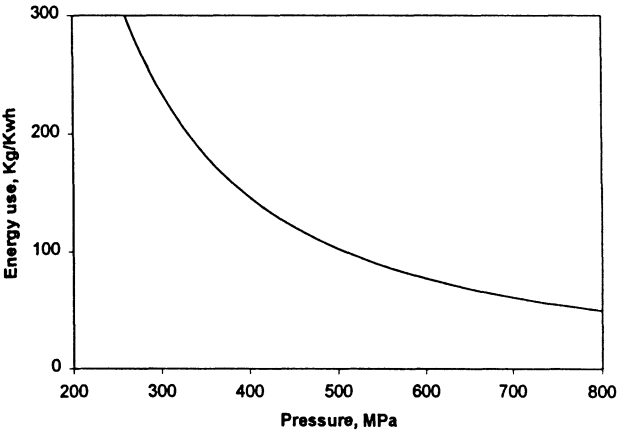

Fig. 7. Energy needed to compress water and water-like foods to high pressure

5 Conclusions

Pressurized discharge and hydrostatic exposure are each unique methods of UHP production. High shear and high energy usage limits direct discharge to lower operating pressures and homogeneous products. Discharge above approximately 400 MPa will likely cause boiling temperatures to be achieved. Hydrostatic exposure is not limited to any maximum pressure and is characterized by low energy use. Hydrostatic exposure can be used on homogeneous liquids to mostly solid products. Adiabatic heating is low for foods comprised mostly of water. As a thermodynamic effect, adiabatic heating is very reproducible when no additional unknowns, such as an oil based hydrostatic media, are introduced.

References

[1] P.W. Bridgman; Proc. of the American Academy of Arts and Sciences, Vol. XLVII, No. 13, Jan. 1912.

[2] V.M. Cheng; Applied Physics Letters, 26, 6–7, 1975.

Pascalisation of Delicatessen

C. Tonello[1], S. Kesenne[1,2] and M. Waechter[1,2]

[1]Hautes Pressions Technologies, Chemin des Romains, F-55000 Bar le Duc, France
Phone: +33 (0)3 29 77 24 25; Fax: +33 (0)3 29 77 25 26
hptech@club-internet.fr
[2]EPL-AGRO, Technopôle Philippe de Vilmorin, F-55006 Bar le Duc cedex, France

Abstract. Natural microflora of sausages, chicken liver mousse and rillettes were enumerated after high pressure treatments at room temperature and after different times of storage. The evolution of the total microflora of sausages stored at 25 °C after treatments at 400 MPa and 500 MPa for 10 min was similar to untreated sausages. Shelf-life of the chicken liver mousse, refrigerated after a pressurisation at 400 MPa during 10 min, was extended to 2 months and longer with a 500 MPa treatment. Coliform development was stopped in rillettes pressurised 30 min at 400 MPa and stored 14 d at refrigerated temperature, but a 500 MPa treatment was required to inhibit total microflora growing during this storage period.

1 Introduction

High hydrostatic pressure technology has different interests in meat products: tenderisation, gelation, thawing, salt penetration and sterilisation at less than 100 °C [1–3]. But the main application is "pascalisation" which is the pressure inactivation at room or cold temperature of microorganisms causing spoilage or foodborne disease [4].

Sliced delicatessen treated by high pressure is still commercialised in Asia and in Europe. A raw pork ham (Fuji Chiku), with a low salt content, was tested on the Japanese market in 1997 [5, 6]. In 1998, an industrial equipment (with a 320 dm^3 vessel for a maximal pressure of 400 MPa) was specially built for pascalisation of cooked ham (Espuña) in Spain.

During this applied study, we have worked on high pressure treatment effects on microbial stabilisation and sensorial quality of sausages, chicken liver mousse and rillettes (potted mince made from pork).

2 Materials & Methods

The three different products were treated in Hautes Pressions Technologies industrial pilot plant. The chamber consists of a 50 dm^3 capacity vessel. High

pressure was applied through an hydraulic pump which pressurised water (up to 700 MPa) at 125 MPa per minute. All pressurisations were done at room temperature.

Sausages and chicken liver mousses were bought in the shops. The first were vacuum-packed and the second were gas-packed. They were pressurised in their commercial packagings. Rillettes were prepared at the Unité Agro-alimentaire of EPL-AGRO, vacuum-packed and stored between 4 °C and 6 °C during 7 d before pressurisation.

The total microflora was enumerated after distribution of 1 ml of sample in two Petri dishes containing PCA medium (BIOKAR) and incubation at 30 °C for 3 d. VRBL medium (BIOKAR) was used to estimate coliforms after an incubation of 24 h at 37 °C.

The sensory analysis of the rillettes was done with a triangular test (two identical samples and one different) on 25 persons.

3 Results & Discussion

3.1 Sausages

Although there was an apparent total inactivation of the total microflora of sausages, just after treatment at 400 MPa and 500 MPa during 10 min, all samples had a bad microbiological quality already after 7 d of storage at 25 °C (Fig. 1).

The high pressure treatment applied was not sufficient to allow product storage at room temperature.

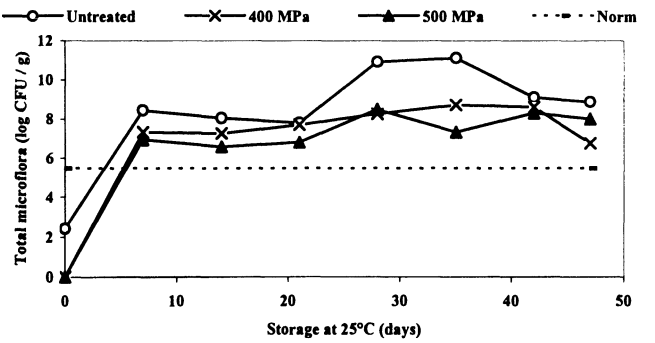

Fig. 1. Evolution of total microflora of sausages vacuum-packed after treatment during 10 min at room temperature

3.2 Mousse of Chicken Livers

The total microflora of chicken liver mousse was consequently reduced after pressurisation at 400 MPa or 500 MPa during 10 min, despite a high microbiological contamination of samples (Fig. 2).

Shelf-life (at 4 °C) was extended to more than 60 d for 400 MPa treated mousse and to more than 75 d with a 500 MPa pressurisation. There was a texture modification (less foaming) but no change of taste and smell.

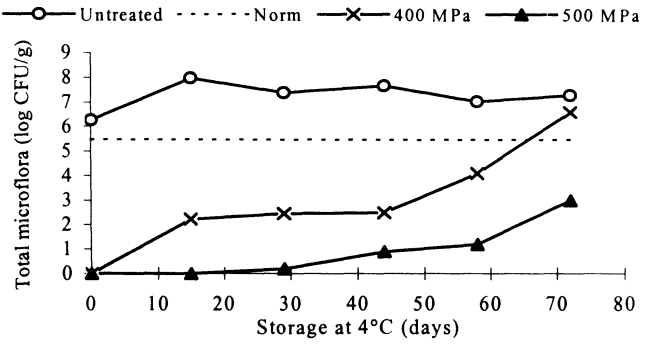

Fig. 2. Evolution of chicken liver mousse total microflora after 10 min treatments at room temperature

3.3 Rillettes

High pressure treatments between 300 MPa and 500 MPa applied during 30 min at room temperature on rillettes allowed a decrease in microbial contamination (Fig. 3). A 500 MPa pressure was required to stabilize total microflora for at least 14 d when products were stored at 4 °C. Pressure at 400 MPa and 500 MPa avoided coliform multiplication during the storage (Table 1).

The sensory analysis showed that there was no significant difference between untreated and pressurised rillettes.

Table 1. Rillettes coliform content (CFU/g) just after pressurisation and after 14 d of storage at 4 °C

	Just after pressurisation	After 14 d of storage
Untreated	<5	>750
300 MPa	<5	>750
400 MPa	<5	<5
500 MPa	<5	<5

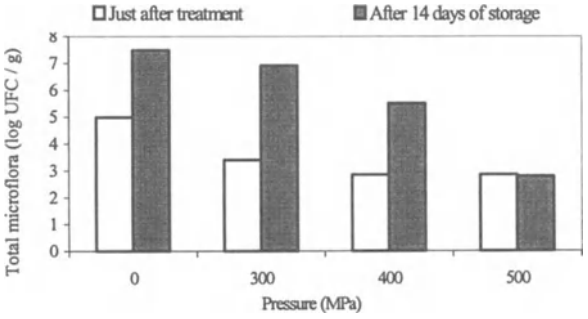

Fig. 3. Total microflora of rillettes treated 30 min at room temperature

4 Conclusions

The high pressure treatments applied were not sufficient to allow product storage at room temperature. On the other hand, other products, stored at 4 °C after treatment, showed good results.

This technology is very interesting for delicatessen stored at chilled temperature to increase shelf-lives. It allows a better microbiological quality to be obtained and less logistical constraints without important modification of sensory quality.

References

[1] Hayashi R. (1989); Application of high pressure to food processing and preservation: philosophy and development; Engineering and Food., Ed: Spiess and Schubert. Elsevier Applied Science, England, 2, 815–826.

[2] Hayashi H. (1992); Utilization of pressure in addition to temperature in food science and technology; High Pressure and Biotechnology, Eds: Balny, Hayashi, Heremans and Masson, Colloque INSERM 224, John Libbey Eurotext Ltd, London, 224, 185-192.

[3] Cheftel J.C. and Culioli J. (1997); Effects of high pressure on meat: a review; Meat Science, 46, 211–236.

[4] Shigehisa T., Ohmori T., Saito T. and Hayashi R. (1991); Effects of high hydrostatic pressure on characteristics of pork slurries and inactivation of microorganisms associated with meat and meat products; International Journal of Food Microbiology, 12, 207–216.

[5] Nose M., Yamagishi S. and Hattori M. (1992); Development of a processing system of meat and meat products by introducing high pressure treament; High Pressure and Biotechnology, Eds: Balny, Hayashi, Heremans and Masson, Colloque INSERM 224, John Libbey Eurotext Ltd, London, 224, 321–323.

[6] Cheftel J.C. (1998); Commercial pressurised food in Japan; High Pressure Food Science, Bioscience and Chemistry, Eds. Isaacs, the Royal Society of Chemistry, Cambridge, 506–507.

Effect of High Pressure Treatment on Lipoxygenase Activity in Cherry Tomatoes

R. Tangwongchai, D.A. Ledward and J.M. Ames

Department of Food Science and Technology, The University of Reading, Whiteknights, Reading, RG6 6AP, UK
Phone:+44-(0)118-9318715; Fax:+44-(0)118-9310080
D.A.Ledward@afnovell.reading.ac.uk

Abstract. Lipoxygenase (EC 1.13.11.12) plays an important role in the genesis of flavour and aroma compounds in plant products as it catalyses the oxidation of polyunsaturated fatty acids containing *cis,cis*-1,4-pentadiene units. It is also important as it has the ability to form free radicals which can degrade such compounds as vitamins, proteins and lipids. Ripe intact cherry tomatoes were subjected to pressures of 200, 300, 400 and 600 MPa for 10 min at ambient temperature (ca. 20 °C). The lipoxygenase activity was determined by spectophotometry [1]. The tomatoes were cut into small pieces, then blended for 1 min and the headspace volatile compounds were analysed by gas chromatography-mass spectrometry. Pressurisation at 200 and 300 MPa for 10 min did not significantly affect the lipoxygenase activity, while a pressure of 400 MPa for 10 min caused a significant decrease in its activity. Treatment at 600 MPa led to complete and irreversible loss of activity. Compared to unpressurised tomatoes, treatment at 600 MPa gave significantly reduced levels of hexanal, *cis*-3-hexenal and *trans*-2-hexenal, which are important contributors to 'fresh' flavour in tomato.

1 Introduction

Lipoxygenase (LOX) or lipoxidase (EC 1.13.11.12) plays an important role in the generation of flavour and aroma compounds in plant products as it catalyses the oxidation of polyunsaturated fatty acids containing *cis,cis*-1,4-pentadiene units. It is also important as it has the ability to form free radicals which can degrade compounds such as certain vitamins, proteins and lipids. The purpose of this study was to investigate the effect of high pressure treatment on the LOX activity and the resulting changes in the volatile compounds produced due to inhibition of the enzyme.

2 Materials & Methods

Ripe intact cherry tomatoes were put into heat-sealed polyethylene bags and subjected to pressures of 0.1 (atmospheric), 200, 300, 400 and 600 MPa for 10 min at ambient temperature (ca. 20 °C) in the Stansted High Pressure Rig.

Enzyme Extraction: Whole cherry tomatoes were cut and homogenised with double their volume of 0.1 M phosphate buffer, pH 6.5, containing 1 mM EDTA and 0.1% (w/v) TritonX-100. The suspension was filtered through a double layer of cheesecloth and centrifuged at 20000 g for 40 min at 5 °C. The supernatant was diluted with 0.1 M phosphate buffer (1:1) before determining the enzyme activity.

LOX assay: The lipoxygenase activity was determined by spectophotometry at 234 nm [1].

Analysis of Volatile Compounds: Tomatoes (25 g) were cut into small pieces, blended for 1 min and the headspace volatiles were collected on a Tenax trap by purging with nitrogen gas. 1,2-Dichlorobenzene was injected in the trap as an internal standard. The compounds were thermally desorbed on to a GC column (BPX-5) and analysed by gas chromatrography-mass spectrometry (GC-MS). Peaks were identified from their retention indices and mass spectra. Quantitative analysis was based on peak area integration of the GC-MS chromatogram.

3 Results & Discussion

Lipoxygenase Activity. When the whole fruits were subjected to pressures of 200–600 MPa for 10 min, the enzyme activity was significantly decreased at 400 MPa and the enzyme was completely inactivated at 600 MPa (Fig. 1).

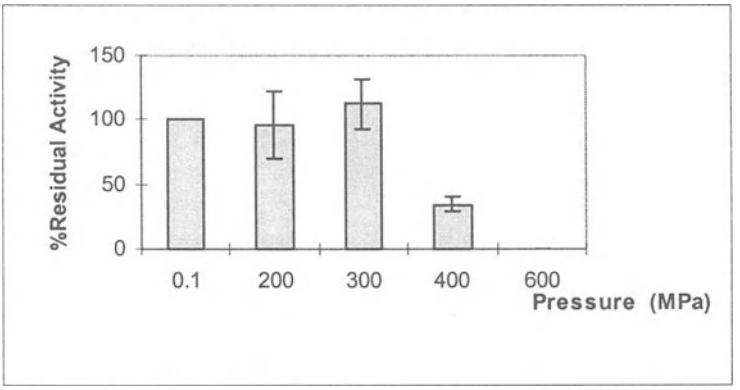

Fig. 1. The effect of high pressure treatment on the crude extract LOX activity from whole cherry tomatoes

Volatile Compounds. The volatile compounds found in tomatoes which were untreated or pressure treated at 600 MPa for 10 min gave different GC profiles. Significant differences were seen for hexanal + *cis*-3-hexenal (peak 5) and *trans*-2-hexenal (peak 8) (Fig. 2). Some of volatiles in the chromatogram are listed in Table 1.

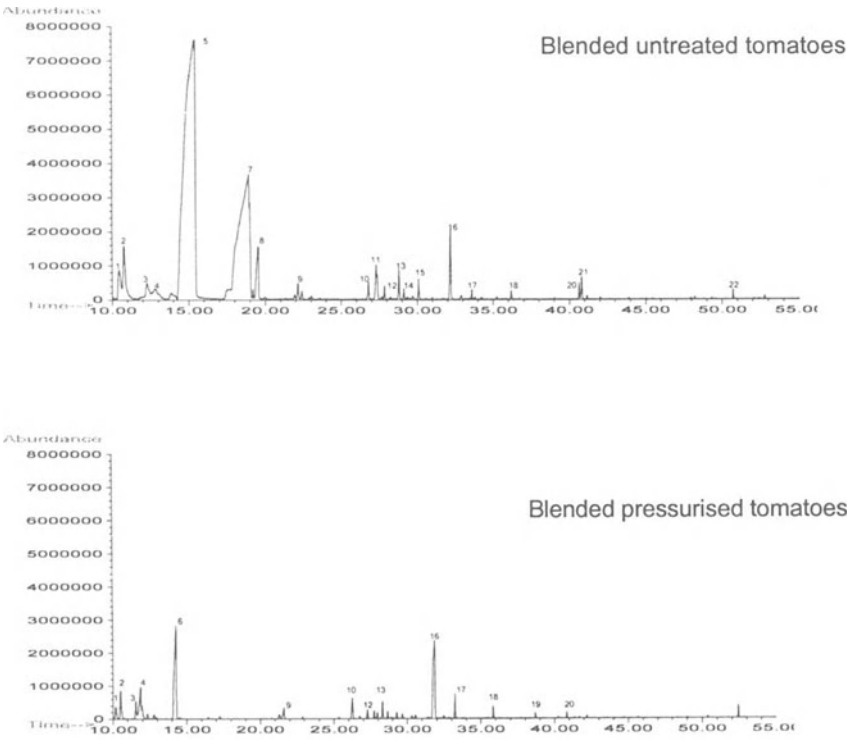

Fig. 2. The GC-MS chromatograms of blended untreated and pressurised tomatoes at 600 MPa for 10 min. Peak 16 is internal standard

4 Conclusions

LOX activity is markedly decreased following pressurisation at 400 MPa for 10 min and is completely removed after treatment at 600 MPa for 10 min. Pressurisation at 600 MPa for 10 min mainly results in the absence of hexanal, *cis*-3-hexenal and *trans*-2-hexenal, which are important volatile compounds of 'fresh' tomato flavour. These compounds are formed largely by lipoxygenase degradation of linoleic and linolenic acids.

Table 1. Major volatile compounds in fresh and pressurised tomatoes

Peak	Compounds	Concentration (ng/25 g wet wt)[1]	
		Fresh	Pressurised
1	1-Penten-3-one	94[a]	62[b]
2	Pentanal	85	154
3	Dimethyl disulfide	57	45
4	2-Methyl-1-butanol	43[b]	98[a]
5	Hexanal+*cis*-3-hexenal	3242	nd[2]
6	Hexenal	nd	492
7	*trans*-2-Hexenal	1267[a]	9[b]
8	1-Hexanol	110[a]	2[b]
9	Heptanal	20	21
10	*cis*-2-Heptenal	6	nd
11	Benzaldehyde	34[a]	12[b]
12	Dimethyl trisulfide	10[b]	21[a]
13	6-Methyl-5-hepten-2-one	30	59
14	2-Pentyl furan	8	13
15	Octanal	16	9
16	1,2-Dichlorobenzene (internal standard)		
17	*trans*-2-Octenal	7[b]	35[a]
18	Nonanal	12	22
19	*trans*-2-Nonenal	3[b]	10[a]
20	*cis*-4-Decanal	11	nd
21	Methyl salicylate	34[a]	2[b]
22	*trans*-6,10-Dimethyl-5,9-undecadien-2-one	7[a]	3[b]

[1]the different superscript means significant differences between fresh and pressurised sample (by Wilcox's test)

[2]not detected

Acknowledgements: This study was supported by a grant of The Royal Thai Government.

References

[1] Ben-Aziz A., Grossman S., Ascarelli I. and Budowski P. 1970. *Analytical Biochem.* **34**, 88–100.

Effects of High Hydrostatic Pressure on the Aromatic Compounds of Strawberry "Coulis"

Y. Lambert[1,2], G. Demazeau[1], A. Largeteau[1] and J.-M. Bouvier[2]

[1]Ecole Nationale Supérieure de Chimie et de Physique de Bordeaux,
Interface Hautes Pressions, Avenue Pey Berland, BP 108, 33400 Talence, France
Phone: +33 5 56 84 27 37; Fax: +33 5 56 84 27 10
lambert@chimsol.icmcb.u-bordeaux.fr
[2]CLEXTRAL, Z.I de Chazeau, BP 10, 42 700 Firminy, France

Abstract. The aromatic volatile compounds of high pressure treated strawberry "coulis" (*Fragaria ananassa* Gariguette) were analyzed by capillary gas chromatography-mass spectrometry (GC-MS) and compared with aromatic volatile compounds of raw strawberry and heat-treated strawberry "coulis". Contrary to sterilized samples, no significant changes of all the aromatic volatile compounds were observed between untreated and high pressure treated strawberry "coulis".

1 Introduction

High pressure processes preserve flavor, food product taste but also natural properties of biological products [1]. The aim of this study has been to evaluate the aromatic composition of a strawberry "coulis" after it has undergone a high pressure processing treatment. «Gariguette» strawberries were chosen because they are rich in aromas and have an excellent flavor. The analysis of the aromatic volatile compounds was undertaken by Capillary Gas Chromatography linked with Mass Spectrometry (GC-MS). Finally the same evaluation was carried out on sterilized "coulis" (120 °C, 20 min) and the results of aromatic volatile compounds compared with raw and pressurized "coulis". A qualitative evaluation of the aromatic chromatograms of the various coulis was firstly realized by isolating peaks of aromatic volatile compounds. Secondly, a quantitative approach has been accomplished by evaluating concentrations of the volatile compounds.

2 Materials & Methods

2.1 Sample Preparation

Strawberries were washed with distilled water. "Coulis" were prepared from ground «*Garriguette du Périgord*» strawberries in order to obtain their juice, while solid particles were removed. The samples were thermo-sealed in plastic bags (CRYOVAC-NOP-120, Soplaril, France).

2.2 High Pressure Treatment

Samples were hydrostatically pressurized in a 3 l sample compartment, by means of an hyperbar experimental apparatus, designed to attain a maximum pressure of 800 MPa , constructed by *NFM-Technologies* (Le Creusot, France), *FRAMATOME* (Paris, France), and marketed by *CLEXTRAL* (Firminy, France). The pressures used were 200 and 500 MPa, for 20 min, at 20 °C and with a pressure climbing rate of 375 MPa per minute.

2.3 Sterilization

The samples were sterilized in a water-steam vertical autoclave, Apave model, 40×70 type, for 20 min and 120 °C.

2.4 Isolation and Concentration of the Volatiles

Triplicate samples of strawberry "coulis" were treated. A fixed amount (149.7±5.94 g) was suspended in 100 ml of organic-free water and homogenized. The solution was extracted three times by stirring with dichloromethane previously purified by distillation. After each extraction the slurries were centrifuged for 30 min (at 5031×*g*) to recover the organic extract. The extract was concentrated to 500 µl using Kuderna-Danish columns.

2.5 Gas Chromatography-Mass Spectrometry (GC-MS)

Chromatographic peaks were identified by GC-MS using a Hewlet Packard MSD5970 quadrupole mass spectrometer coupled with a Hewlet Packard HP5890 gas chromatograph equipped with a splitless-split injector port and a Free Fatty Acid Phase (FFAP) (30 m × 0.32 mm) column. Tridecane, used as internal standard, was introduced into the slurries before extraction at a concentration of 1 mg•kg^{-1} fruit [2].

3 Results & Discussion

Chromatograms of fresh, high pressure treated at 200 MPa and 500 MPa and sterilized strawberry "coulis" are presented (cf. Figs. 1–4).

With these chromatograms, 14 aromatic volatile were isolated and are listed in Table 1.

There exists no profile difference between chromatograms of fresh and pressurized strawberry "coulis" (cf. Figs. 1–3). No new aromatic peaks are created and non disappear, the only change is in the concentration of volatile compounds (Table 1). However, the chromatogram of sterilized "coulis" is modified. As appears from Fig. 4, many chromatographic differences exist. New aromatic peaks are created which are characteristic of heat products (Table 1).

The concentrations only give an idea of the overall global aromatic intensity. Indeed, there does not seem to be a simple relationship between the total concentration of volatile compounds and their sensory appreciation [3].

On the basis of these results it is probable that high pressure treatment of fresh aromatics fruits will become a most useful method for food processing.

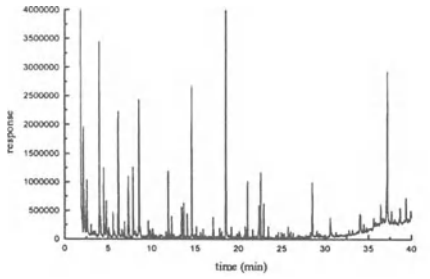

Fig. 1. Chromatogram of fresh strawberry "coulis"

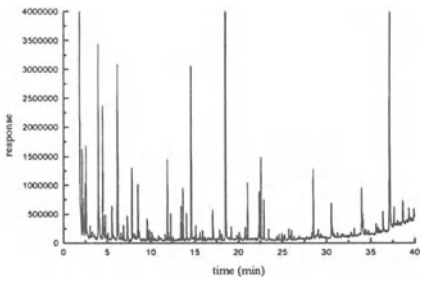

Fig. 2. Chromatogram of strawberry "coulis" after H.P. treatment (200 MPa, 20 min, 20 °C)

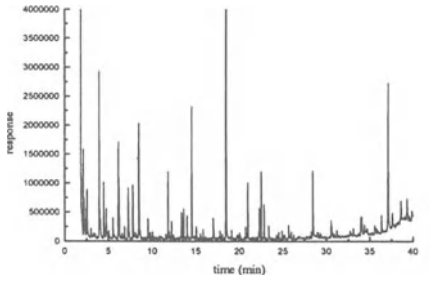

Fig. 3. Chromatogram of strawberry "coulis" after H.P. treatment (500 MPa, 20 min, 20 °C)

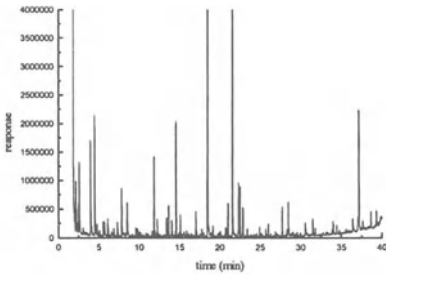

Fig. 4. Chromatogram of strawberry "coulis" after sterilization (0.1 MPa, 20 min, 120 °C)

Table 1. Concentrations (μg/kg) for volatile compounds of strawberry coulis after treatment. (HP: 20 min at 20 °C). *, **, *** Significance respectively at 10%, 5% and 1% probability level; NS = not significant for $p<0.05$. Student t-test

Components	Retention time [min]	Not treated	200 MPa	500 MPa	Sterilized
ethyl butanoate	2.136	340.42	221.60^{***}	350.25^{NS}	333.66^{NS}
hexanal	2.561	257.20	319.38^{*}	267.58^{*}	582.87^{***}
methyl hexanoate	3.976	839.11	623.92^{**}	840.48^{NS}	775.43^{NS}
ethyl hexanoate	4.777	184.51	87.85^{*}	194.16^{NS}	69.16^{**}
hexanol	7.306	477.50	148.29^{***}	450.04^{NS}	265.05^{***}
furfural	10.12	39.67	43.81^{NS}	41.66^{NS}	56.28^{NS}
linalol	11.908	290.82	256.53^{NS}	303.26^{NS}	670.70^{***}
methyl-2-propanoic acid	12.255	84.31	82.52^{NS}	77.01^{NS}	171.80^{***}
geraniol	18.71	–	–	–	98.79
benzene methanol	19.198	57.61	56.92^{NS}	54.24^{NS}	114.77^{***}
unknown (heat)	21.65	–	–	–	3704.24
furaneol	22.398	169.60	187.87^{NS}	168.47^{NS}	508.89^{***}
nerolidol	22.594	242.67	244.63^{NS}	295.91^{**}	401.38^{***}
γ-decalactone	28.526	270.29	245.19^{NS}	331.32^{NS}	393.22^{**}

4 Conclusions

To conclude, high pressure processing appears to be an appropriate process to treat food products with high aromatic characteristics. It guarantees a sanitation of the product [1] while preserving the majority of the aromatic constituentt of the product at pressures commonly used in the food industry.

References

[1] Hayashi R., Use of high pressure in bioscience and in biotechnology, High Pressure Bioscience and Biotechnology, 1995, vol 13, pp.1–7 Ed.: Elsevier Applied Science.

[2] Gunther-Douillard C., Etude des composés volatils de l'arôme de différentes variétés de fraises, Thèse de Doctorat, Université de Paris-Sud, 1988, pp.1–207.

[3] Douillard C., Guichard E., Comparison by multidimensional analysis of concentrations of volatile compounds in fourteen frozen strawberry varieties, Sci. Aliments, 1989, 9, 61–83.

Milk and Milk Products

Proteolysis and Viscoelastic Properties of High Pressure Treated Gouda Cheese

W. Messens, J. Arevalo, K. Dewettinck and A. Huyghebaert

University of Ghent, Faculty of Agricultural and Applied Biological Sciences, Department of Food Technology and Nutrition, Coupure Links 653, B-9000 Ghent, Belgium
Winy.Messens@rug.ac.be

Abstract. The proteolysis and viscoelastic properties of high pressure treated Gouda cheese were studied during ripening (0–42 d) using pressures from 50 to 400 MPa and holding times from 20 to 100 min. The proteolysis by chymosin and plasmin, and the proteinase/peptidase system of the starter, were not influenced by pressure treatment of Gouda cheese. By pressure treatment, the cheese got less rigid, less solid-like, more viscoelastic and had less resistance to flow at longer times. However, after 42 d of ripening, no significant differences could still be observed between pressurised and unpressurised Gouda cheese.

1 Introduction

Gouda cheese is ripened for a period of 1 to 20 months to develop flavour and texture characteristics. The considerable inventory cost incurred in ripening has stimulated interest in accelerated ripening [1].

High pressure (HP) treatment of Cheddar cheese could reduce the ripening time from 6 months to 3 d [2] and lead to a continuous microstructure and lower microbial counts [3]. Also, HP brining of Gouda cheese at 300 MPa leads to destabilisation of the paracasein micel structure [4].

2 Materials & Methods

Samples with a cylindrical shape (7 cm height, 4 cm diameter) taken from a non-brined Gouda cheese block with a close structure curd (48+) (Belgomilk C.V., Moortslede, Belgium) were salted for 6 h at 14 °C by immersion in brine (19.5% NaCl) resulting in a salt content of the cheese cylinders of 1.94%.

Three days after brining, the cylinders were pressure treated according to a central composite design varying three factors (Table 1). Also, at each ripening time, unpressurised cheese was simultaneously analysed.

Table 1. Levels of examined factors

Factor	−1	0	+1
Pressure (MPa)	50	225	400
Holding time (min)	20	60	100
Ripening time (d)	0	21	42

The pH of a mixture of grated cheese and distilled water (1:1) was measured. Grated cheese was weighed into pre-weighed dishes containing about 20 g of pre-dried sand, and dried to constant weight at 105 °C for moisture determination. Also, a suspension of 20 g of grated cheese and 40 g of distilled water was incubated for 1 h at 40 °C, set at pH 4.6 and centrifuged (3000×*g*; 20 min; 5 °C). The solidified fat was removed and the supernatant was filtered to determine pH 4.6-soluble nitrogen (pH 4.6-SN) and 5% phosphotungstic acid soluble nitrogen (PTA-SN) in the filtrate. Nitrogen was determined by the Kjeldahl method. The amount of free amino acids (FAA) in the water soluble extract was determined by the Cd-ninhydrin method [5]. SDS-PAGE was applied for the separation of the polypeptide fraction not soluble at pH 4.6 (pellet) [6].

Slices of 5 mm were studied at 14 °C on a Bohlin controlled stress (CVO) rheometer using serrated plates with a diameter of 2.5 and a gap setting of 4.5 mm. Oscillation experiments were performed in the linear viscoelastic region at 1 Hz and at a strain level of 1% [7]. During the creep measurements, an instantaneous stress of 300 Pa was applied to the sample for 120 s, after which the resulting sample deformation was followed for 120 s [8].

3 Results & Discussion

3.1 pH and Water

From 225 MPa onwards, HP treatment gave rise to a significant higher pH. The difference between the pH of pressure treated and unpressure treated cheese at a certain ripening time is expressed as a pH-shift. Increasing pressure and holding time leads to an increase in the pH-shift. The increase in pH-shift levels off at higher pressures, while it is more pronounced at higher holding times. Pressure intensity and holding time had no effect on the water content of Gouda cheese, while ripening time had: as cheese aged, the water content decreased from 37.57 at 0 d of ripening to 36.39 g/100 g cheese at 42 d of ripening.

3.2 Proteolysis

The concentration of pH 4.6-SN/TN was not influenced by pressure or holding time. During ripening, the pH 4.6-SN increased rapidly during the first 21 d of ripening and more slowly from 21 to 42 d.

By analysing the pH 4.6-insoluble nitrogen, it was observed that no consistent differences in electrophoretic patterns were observed between cheeses that were pressurised and those that were not. Since proteolysis in cheese at the level detectable by SDS-PAGE is almost entirely a consequence of the action of chymosin and plasmin [1], it seems that the action of these enzymes is not influenced by HP treatment. Also, chymosin and plasmin are the principal proteolytic agents responsible for the production of pH 4.6-SN [9]. Hence, the amount of pH 4.6-SN was not influenced by pressure.

A linear increase in PTA-SN/TN and FAA was observed over the whole ripening period studied. The PTA-SN/TN and FAA were not influenced by pressure intensity or holding time. Hence, the proteinase, peptidase system of the starter [9] was not influenced by HP treatment of Gouda cheese.

3.3 Rheology

At each condition, the storage modulus (G', Pa) was larger than the loss modulus (G", Pa) indicating a more solid-like structure. There is a trend for a decrease in G' and G" with pressure. Possibly, rupture of some non-covalent interactions within the protein network takes place by HP treatment [10]. However, tgdelta (G"/G') of pressurised samples was higher implying that HP treated Gouda cheese has a less elastic-like behaviour compared to unpressurised Gouda cheese. No effect of holding time was noticed on G', G" or tgdelta. No significant difference in G', G" and tgdelta can still be observed between pressurised and unpressurised Gouda cheese after 42 d of ripening.

At 0 d ripening, both creep and recovery compliance values of unpressurised cheese were smaller than those of pressurised cheese (Fig. 1), which indicates a greater degree of deformation for the latter. The more solid-like nature of unpressurised cheese samples is stressed by the smaller slope of the creep compliance or flow curve.

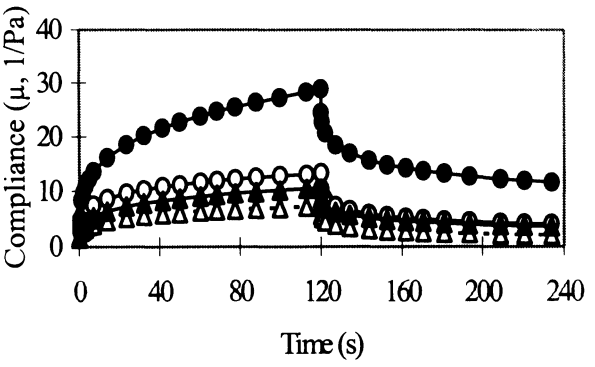

Fig. 1. Creep/recovery curves at 0 (circles) and 42 (triangles) d of ripening for pressurised (400 MPa, filled sybols) and unpressurised (open symbols) Gouda cheese

The flow curves of the cheeses were fitted by a model consisting of 2 Kelvin elements connected in series with a spring and a dashpot element [8]. It was derived that the rigidity of pressure treated samples is less (higher instantaneous compliance). Also, by pressure treatment, the cheese gets less solid-like (higher retarded compliance of the first and second Voight element). In addition, pressure treated cheese has less resistance to flow at longer times (smaller Newtonian viscosity). At 42 d of ripening, however, no significant differences could still be observed between pressure treated and non-pressure treated cheese.

4 Conclusions

The ripening time of Gouda cheese cannot be reduced by the use of HP between 50 and 400 MPa for 20 to 100 min. By contrast, the viscoelastic properties of Gouda cheese treated at 400 MPa differ significantly to those that were not treated. As the ripening proceeds, however, no differences can still be observed.

Acknowledgements: Financial support of IWT (grant 951263) and FAIR-CT-96-1113 is acknowledged.

References

[1] Folkertsma, B. *et al.* (1996); Accelerated ripening of Cheddar cheese at elevated temperatures. International Dairy Journal, 6, 1117–1134.
[2] Yokoyama, H. *et al.* (1992); Method for accelerating cheese ripening; European Patent Application EP 0469857 A1.
[3] Torres-Mora, M.A. *et al.* (1996); Early microstructure changes in Cheddar cheese and the effects of high pressure curd processing. Book of Abstracts of Institute of Food Technologists Annual Meeting. New Orleans, USA, 9.
[4] Messens, W. *et al.* (in press); High pressure brining of Gouda cheese and its effect on the cheese serum; Lebensmittel-wissenschaft und -technologie.
[5] Folkertsma, B. and Fox, P.F. (1992); Use of the Cd-ninhydrin reagent to assess proteolysis in cheese during ripening; Journal of Dairy Research, 59, 217–224.
[6] Dewettinck, K. *et al.* (1997); Comparison of SDS-PAGE profiles of four Belgian cheeses by multivariate statistics; Lait, 77, 77–89.
[7] Dewettinck, K. *et al.* (in press); Dynamic rheological properties of Gouda cheese as influenced by age and position; Milchwissenschaft.
[8] Ma, L. *et al.* (1996); Viscoelastic properties of reduced-fat and full-fat Cheddar cheeses; Journal of Food Science, 61, 821–823.
[9] McSweeney, P.L.H. and Fox, P.F. (1997); Chemical methods for the characterization of proteolysis in cheese during ripening; Lait, 77, 41–77.
[10] Messens, W. *et al.* (1997); The use of high pressure to modify the functionality of food proteins; Trends in Food Science and Technology, 4, 107–112.

Reaction Kinetics of Ultra-High Pressure Treatment of Milk

B. Rademacher[1], J. Hinrichs[1], R. Mayr[2] and H.G. Kessler[1]

Technische Universität München, Dairy and Food Research Centre Weihenstephan,
[1]Institute of Food Process Engineering, Weihenstephaner Berg 1
[2]Institute of Microbiology, Weihenstephaner Berg 3, D-85354 Freising, Germany
rademacher@charly.lmvt.blm.tu-muenchen.de

Abstract. Pressure-induced changes in milk, i.e. the extension of shelf-life, the inactivation of pathogenic bacteria, the denaturation of whey proteins and the inactivation of milk enzymes, are examined at 20 °C and described kinetically. The results allow an improvement in the process conditions of pressure treatment of milk considering the specific product requirements.

1 Introduction

High pressure treatment of milk has the potential to inactivate microorganisms and enzymes and to modify the functional properties of macromolecular food constituents like proteins. In analogy to heat-induced changes kinetic data are the basis for improving process conditions of pressure treatment. So the aim of the examinations is to characterize the pressure-induced inactivation of enzymes and microorganisms as well as protein denaturation and to determine kinetic data.

2 Materials & Methods

Experiments concerning shelf-life and enzyme inactivation were carried out with one-day-old raw milk. The end of shelf-life was set when the pH dropped below 6.5 or sensory changes were detected. Inactivation of alkaline phosphatase and γ-glutamyltransferase was analyzed by photometric [1] and fluorometric [2] methods, respectively. The effect of pressure on the survival of vegetative pathogens was analyzed in UHT-milk (3.5% fat). Strains used were *Escherichia coli* O157:H7 NCTC 12079, *Listeria monocytogenes* NCTC 11994 and *L. monocytogenes* Scott A. Denaturation of whey proteins was examined in pasteurized skim milk. The remaining content of native whey protein fractions was measured by HPLC after precipitation of the milk at pH 4.6 [3]. All samples were pressure treated in an equipment consisting of ten pressure vessels with a volume of 32 ml each. Pressure increase and release rates were kept constantly at

200 MPa/min. The temperature of pressure treatment was set to 20 °C in all experiments. The maximum rise of temperature due to increase of pressure was 25 °C and temperature balance was almost reached within 5 min. A holding time of 0 min means that the pressure was built-up to the desired level and released immediately.

3 Results

3.1 Shelf-Life of Pressure Treated Raw Milk

Figure 1 summarizes the results of several shelf-life experiments after different UHP-treatments. Presuming that pasteurized and cooled milk normally has a shelf-life of about 10 d at 10 °C, the line gives pressure/time combinations which must be applied to fulfill this requirement. Reasonable holding times are obtained if pressures from 400 to 600 MPa are applied at room temperature. At the end of shelf-life a total plate count of approx. 10^6 to 10^7 per ml was observed.

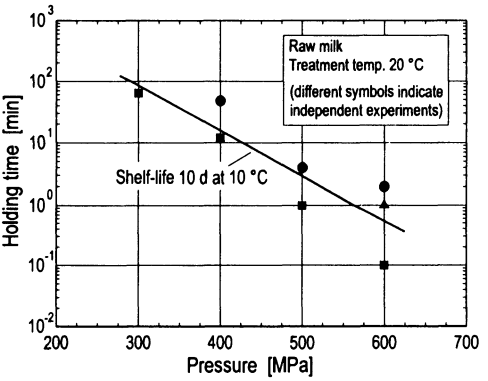

Fig. 1. Line of equal shelf-life of pressure treated raw milk (10 d at 10 °C)

3.2 Inactivation of Pathogenic Bacteria

It is known that the pressure resistance of different species from the same genus and even of different strains from the same species or in different substrates may vary considerably [4]. Therefore it is necessary to determine the inactivation of pathogens by pressure treating the pathogenic strains in the original food matrix. *E. coli* O157:H7 was treated with pressures from 500 to 600 MPa in UHT-milk at a temperature of 20 °C. In the logarithmic plot of concentration against time a linear behaviour was observed. Applying the concept of 7 log-units inactivation [5], a treatment of at least 600 MPa and 20 min should be applied for the destruction of *E. coli* O157:H7 in milk. Compared to *Escherichia coli* the *Listeria* strains tested

are less pressure resistant. A reduction of 7 log-units can be obtained with 500 MPa within 30 min for both strains. The inactivation of *L. monocytogenes* NCTC 11994 can be described by a first order reaction whereas the inactivation curves of strain Scott A were not linear [6].

3.3 Denaturation of Whey Proteins

The structural qualities of milk products are mainly determined by the functional properties of the milk proteins, especially the different fractions of whey proteins. In the case of β-lactoglobulin A the denaturation behaviour is shown in Fig. 2. The higher the pressure the lower is the measured amount of native β-lg A at a comparable holding time. In any case, only a small amount of native protein was detected at the end of the holding time of 20 min. The reaction may be described by a reaction order of 2.0 for the genetic variants A and B, which do not differ significantly in their denaturation behaviour. Compared to lactoglobulin the denaturation of α-lactalbumin requires higher pressures. The content of α-la remains nearly unchanged at pressures of 400 to 500 MPa during the examined holding time of 20 min. At 600 MPa a time dependent decrease becomes visible and at 700 MPa a 50% denaturation can be achieved within 20 min.

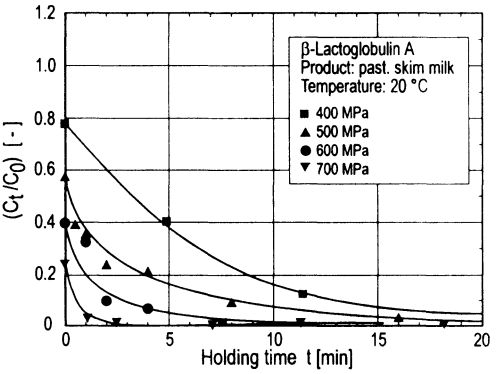

Fig. 2. Denaturation of β-lactoglobulin A in pasteurized skim milk

3.4 Inactivation of Milk Enzymes

Enzymes, namely the alkaline phosphatase and γ-glutamyltransferase, which are naturally present in raw milk, could act as internal process markers, if the inactivation kinetics of these enyzmes are close to the inactivation of pathogens by pressure. The inactivation of γ-glutamyltransferase as influenced by pressure and time is given in Fig. 3. Inactivation starts at pressures above 400 MPa and follows a first order reaction. An activation volume of $\Delta V^{\#} = -44$ ml/mol was calculated. The alkaline phosphatase is more stable against pressure. A complete destruction of the enzyme, which means a residual activity of less than 0.1%, can only be

achieved with pressures above 700 MPa. The inactivation can be described by a first order reaction as well. An $\Delta V^{\#}$ of –34 ml/mol was estimated.

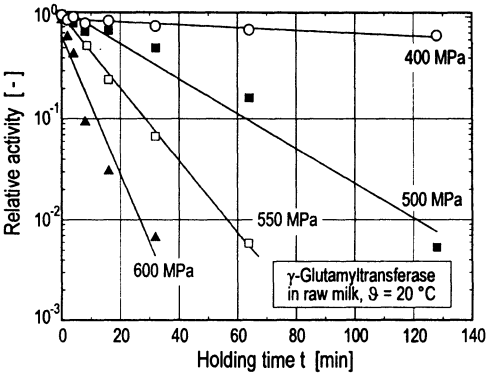

Fig. 3. Inactivation of γ-glutamyltransferase in raw milk

4 Conclusions

Concerning the microbiological safety of milk, *p*/*T*-combinations, which would lead to a shelf-life of 10 d at 10 °C, do not fulfill the requirements of 7 log-units destruction of the investigated pathogens when pressure treated at 20 °C. Furthermore a 7 log-units destruction of these pathogens cannot be obtained without denaturation of β-lactoglobulin. Regarding quality control the kinetics of denaturation of γ-glutamyltransferase and α-lactalbumin are sufficiently close to the inactivation of *L. monocytogenes* strains NCTC 11994 and Scott A and *E. coli* O157:H7 NCTC 12079 to provide a useful marker for the destruction of these organisms.

Acknowledgements: This research project is supported by the FEI (Forschungskreis der Ernährungsindustrie e. V., Bonn), the AiF and the Ministry of Economics. Project No.: 11392N.

References

[1] Zehetner, G., Bareuther, G., Henle, T. and Klostermeyer, H. (1995); Z. Lebensm. Unters. Forsch., 201, 336–338.
[2] Rocco, R.M. (1990); J. Food Protection, 53, 588–591.
[3] Hinrichs, J., Rademacher, B. and Kessler, H.G. (1996); Milchwissenschaft, 51, 504–509.
[4] Patterson, M.F., Quinn, M., Simpson, R. and Gilmour, A. (1995); J. Food Protection, 58, 524–529.
[5] Angelotti, R. (1978); Federal Register, 43, 30791–30793.
[6] Rademacher, B., Mayr, R., Pfeiffer, B. Scherer, S. and Kessler, H.G.; Manuscript in preparation.

Effect of High Pressure on Yoghurt

A. Reps, I. Warminska-Radyko and F. Dajnowiec

University of Agriculture and Technology, Olsztyn, Poland
Department of Food Technology, Institute of Food Biotechnology,
Heweliusza 1 str. Olsztyn Kortowo 10-718, Poland
marecki@art.olsztyn.pl

Abstract. The effect of high pressure on yoghurt microflora was studied. It was found that pressure of 400 MPa (15 min) and higher inactivated completely *Lactobacillus delbruecki* sp. *Bulgaricus*, being present in the composition of yoghurt's microflora. *Streptococcus salivarius* sp. *Thermophilus* (SST) is resistant to the pressurization. The degree of SST inactivation is dependent on the strain. During the storage of yoghurt after the pressurization, a decrease in the SST count was observed. Yoghurt pressurized under 400 MPa and higher was not subjected to further acidification during 3-week storage at 1 and 20 °C.

1 Introduction

The methods of preservation employed so-far may cause many unfavourable changes in foodstuffs that may lower their nutritive value.

At present, after solving many technical problems, there is a real possibility that high pressure can be employed in preservation of food [1, 5, 8].

The effect of high pressure on the microorganisms that are present in milk and dairy products varies very much. Yeast and moulds are least resistant to the pressure, the degree of bacterial inactivation is differentiated whereas the spores are resistant to the pressure's effect.

It was found that the pressure was able to change the metabolism of lactic acid bacteria and could inhibit their acidifying activity [6, 7].

The process of acidification of milk subjected to the effect of high pressure was considerably longer in spite of the fact that a significant number of lactic acid bacteria remained in the milk [2–4].

In Japan a world leader in the practical application of high pressure, yoghurt preserved by the method of high pressure is found on the market [9].

The aim of the studies undertaken was to determine the effect of high pressure on the bacteria that are present in the composition of yoghurt, and to state whether the complete inactivation of bacteria was necessary to preserve yoghurt.

2 Materials & Methods

Yoghurts were manufactured with the use of commercial lyophilised cultures CRhodia (France), containing *L. delbruecki* sp. *Bulgaricus* (LDB) and *S. salivarius* sp. *Thermophilus* (SST).

The yoghurt was filled into sterile Teflon vials and subjected to pressure treatment in hydraulic pressure device (Liquid vessel LV/30/16) manufactured by Unipressequipment, Division, Warszawa, Poland. The process was conducted at an ambient temperature. The compression and decompression time was fixed at 2 and 0.5 min, respectively.

The yoghurts (I and II), manufactured with the use of cultures from two different batches, were subjected to the pressure treatment for 15 min in the range of 200–1000 MPa at intervals of 200 MPa.

Yoghurt was pressurized under 400 MPa for 15, 30 and 45 min and under fluctuating pressure for 3×5, 3×10 and 3×15 min.

Before and after the pressure treatment and after one-, two-, and three-week storage (at temperature of 1 °C and 20 °C), pH of yoghurts was measured and LBD and SST count was determined. The ability of acidifying milk by the microflora of yoghurts, being stored for 3 weeks at 1 °C and 20 °C after pressurization, was examined.

Yoghurt was subjected to the pressure treatment of 400 MPa for 60, 90, 120 and 180 min. Before and after the pressurization and after 24-h storage at 1 °C and 20 °C, LBD and SST count in yoghurt, was determined.

The effect of high pressure on the selected *S. salivarius* sp. *Thermophilus* strains, was studied. For the experiment, lyophilised strains T040 and T060 from RChodia collection, Biolacta-Texel and T7, T72, T79, T149 and T150 from the collection of Institute of Food Biotechnology Olsztyn, were used.

The strains were animated and activated by three times repeated passages on a sterile skimmed milk till the formation of curd. The strains were pressurized under 400 MPa for 30 min and then the SST count before and after the pressure treatment and after 24-h storage at 1 °C and 20 °C was determined.

3 Results

During the pressurization of yoghurt (I) it was observed that LDB was slightly resistant to the pressure treatment and during 15-min pressurization under 200 MPa, the complete inactivation of these bacteria was found.

A big resistance of SST to high pressure was stated. The pressure of 200 MPa reduced a number of the above mentioned bacteria in yoghurt (1.8×10^9) by one order of size. Under the pressure of 400 MPa, any reduction of bacteria amounted to 5 orders of size, nevertheless the remaining level of bacteria in yoghurt was 5.4×10^4. After the pressurization at 1000 MPa, the bacterial count remained at the level of 1.2×10^3.

During the one-, two- and three-week storage of yoghurt after pressurization at temperatures of 1 and 20 °C, the decrease of SST, in contrast to the control sample, was found. At a temperature of 20 °C, the decrease in the SST count ran somewhat quicker.

Acidity of the contol (non-pressurized) yoghurt during its storage at 20 °C was lowered from pH 4.7 to 3.8. In comparison with the above, acidity of yoghurt after pressurization in 200 MPa and storage at 20 °C was lowered from 4.73 to 4.33.

Acidity of yoghurt after pressure treatment of 400, 600, 800 and 1000 MPa during the storage was unchanged.

The obtained results indicate that SST, as present in the composition of yoghurt, is resistant to pressurization, however the remaining bacteria did not show any acidifying activity.

The successive yoghurt (II) was manufactured with the use of culture from another batch. In the mentioned yoghurt, the survival of LDB under 200 MPa was as much as 64%. The complete inactivation of LDB in yoghurt was found after pressurization in 400 MPa.

SST in yoghurt II was more resistant to the effect of pressure than in yoghurt I. The pressure of 1000 MPa reduced the SST count by 2 orders of size whereas in yoghurt I – by 6 orders of size. During the storage of yoghurt, quick reduction of the SST number was observed. After one week of storage of yoghurt, pressurized in 600, 800 and 1000 MPa, any absence of SST was not stated.

From the conducted studies, it resulted that the pressure of 400 MPa could be suitable in preservation of yoghurt.

It was interesting to note how the time and pulsating pressure affected the microflora of yoghurt. The mentioned yoghurt was subjected to pressurization of 400 MPa for 15, 30, 45, 3×5, 3×10 and 3×15 min. The obtained results confirmed that under the above mentioned conditions, LDB was completely inactivated. The level of SST was little reduced, maximum by one order of size.

The pulsating pressure inactivated LDB in yoghurt to a smaller degree than the constant pressure.

During three-week storage, a decrease of the LDB count in yoghurt was found. The decrease in bacterial number proceeded more intensively. Acidity of yoghurt stored for 3 weeks at temperatures of 1 and 20 °C was not changed while in unpressurized yoghurt, acidity was increased from pH 4.68 to 4.49 (1 °C) and 3.95 (20 °C).

Prolongation of the time of yoghurt's pressurization under 400 MPa up to 60, 120 and 180 min caused considerably higher reduction of SST. The initial number of bacteria, i.e. 1.7×10^9, was reduced after 120 min to 4.2×10^4 and after 180 min to 9.9×10^3. During 24-h storage, higher reduction of SST was observed at temperature of 20 °C.

The degree of SST survival, as affected by the pressure of 400 MPa/30 min, was dependent on the strain and varied from 0.004% to 38.63%. It should be mentioned, however, that due to the higher number of bacteria in milk before pressurization, many living SST organisms remained in milk (7.6×10^4 – 1.7×10^8).

It was observed that during 24-h storage at 1 and 20 °C, after pressurization, the SST number was decreased and in the case of 20 °C, the bacterial number was considerably more intensive.

Four strains from the ones examined after pressurization acidified milk considerably more slowly and three strains lost their milk-acidifying ability all together. The obtained results suggest that for manufacture of yoghurt which is to be preserved by the method of high pressures, we should use SST strains, which are sensitive to the high pressures.

The conducted studies showed that there was a possibility of preserving yoghurt by the method of high pressures. The pressure of 400 MPa and higher applied for 15 min inactivated completely LDB contained in yoghurt whereas SST was resistant to the effect of the pressure but lost its acidifying ability and its level was quickly lowered during the storage of yoghurt at 1 as well as at 20 °C. Thus, to preserve yoghurt, the complete inactivation of microflora is not necessary.

References

[1] Cheftel J.C. 1995. Review:High pressure, microbial inactivation and food preservation. Food Sci.Technol. International. 1,75–90.

[2] Farr D., 1990. High pressure technology in the food industry. Trends Food Sci. Technol., 1(1), 14–15.

[3] Johnston D.E., Austin B.A., Murphy R.J. 1992. Effects of high hydrostatic pressure on milk. Milchwiss. 47, 760–763.

[4] Kolakowski P., Reps A., Dajnowiec F., Babuchowski A. 1997. Effect of high pressure on some properties of cow's milk. Med. Fac. Landbouww. Univ. Gent. 62/4a, 1373–1377.

[5] Knorr D. 1998. Advantages, possibilities and challenges of high pressure application in food processing. In The properties of water in food. Ed. D.S. Reid. Pub. Blackie Academic and Professional, 419–438.

[6] Miyakowa H., Anjitsu K., Shibashi N., Shimamura S. 1994. Effects of pressure on enzyme activites of *Lactobacillus helveticus* LHE-511. Biosci. Biotech. Biochem. 58, 606–607.

[7] Maciejska A., Kolakowski P., Kornacki K., Reps A., Arabas J., Fonberg-Broczek M. 1997. The effect of high pressure on selected strains of lactic acid bacteria. III Int. Meeting Process optimalization and minimal processing of food. Leuven/Belgium.

[8] N.N. 1997. High hydrostatic pressure food processing. In Nonthermal preservation of food. Ed. G.V. Barbosa-Canovas *et al.* M. Dekker Inc. New York, 9–53.

[9] Tanaka T., Hatanaka K. 1992. Application of hydrostatic pressure to yoghurt to prevent its after acidification. Nippon Shokahin Kogyo Gakkaishi, 39, 173–177.

Influence of Pressurization on Goat Milk and Cheese Composition and Yield

A.J. Trujillo, C. Royo, V. Ferragut and B. Guamis

Unitat de Tecnologia dels Aliments, Centre Especial de Recerca en Tecnologia dels Aliments (CeRTA), Facultat de Veterinària, Universitat Autònoma de Barcelona, 08193 Bellaterra, Spain
ivpp56@cc.uab.es

Abstract. Fresh goat cheese was made from pasteurized (72 °C, 15 s) or HP-treated milk (500 MPa, 15 min, 20 °C). Microbiological quality (i.e. mesophilic aerobic bacteria and enterobacteria) of pressurized milk was comparable to pasteurized milk. Pasteurized and HP-treated milks had different pHs and non-casein nitrogen. During the curd formation, the pH fell faster in pasteurized milk than in HP-treated milk and there was a slightly larger amount of milk fat separated from the curd whey in HP-treated milk. HP treatment reduced the level of whey expelled from the curd making the whey removal process more difficult, and so the time involved in the cheesemaking was increased. The cheese made from HP-treated milk had higher levels of moisture and salt, but a slightly lower fat content than pasteurized milk. Additional retention of whey protein and, especially, the greater moisture led to improvements in cheese yield from HP-treated milk.

1 Introduction

Heat treatment is the technology process most frequently applied to milk. The heat treatment most often used for cheesemaking is pasteurization. The main goal of milk pasteurization for cheesemaking is the elimination of pathogens which can be present in milk. Recently, new technologies such as high hydrostatic pressures (HP) are being applied to the conservation of foods. The changes in milk (relevant to cheesemaking) induced by HP treatment are numerous [1]. One of the most important effects of HP on milk is whey protein aggregation [2]. Aggregated whey protein is retained in curd when HP-treated milk is renneted increasing yield. Optimal conditions of HP treatment of milk could be found for cheesemaking. In general HP treatments with pressures of 400 MPa can produce raw milk with a shelf life similar to that of pasteurized milk [3]. That means, HP treatment provides a reduction in microbial counts while no effects on flavor and few modifications on gelling properties, native milk enzymes and nutrients are found. These characteristics may allow the production of raw milk cheeses, including fresh cheese, by means of HP-treated milk with improved performance.

There is little information about the effects of HP treatment of milk on cheese production, composition and yield. The purposes of this study were to compare the physicochemical characteristics of milk (pasteurized and pressurized), its ability to produce fresh goat cheese and its yielding capacities.

2 Materials & Methods

2.1 Milk Treatment and Cheese Manufacture

Six laboratory-scale cheesemaking standard productions (uncooked pressed goat cheese) were made (3 for each group). Previously, milk was heated to 72 °C for 15 s or pressurized at 500 MPa at 20 °C for 15 min.

2.2 Milk and Whey Analysis

Milk samples were collected from Murciano-Granadina goats. All analyses were performed by standard procedures (IDF-FIL) in duplicate on each treatment (pasteurized or pressurized), for pH, total solids (TS) and fat (F), total nitrogen (TN), non-protein nitrogen (NPN) and non-casein nitrogen (NCN). Percentage of nitrogens was multiplied by 6.38 to give the milk protein equivalents.

Total aerobic microoganisms and enterobacteria counts in raw, pasteurized and HP-treated milks were determined using standard media (PCA: Plate Count Agar and VRBG: Violet Red Bile Glucose, respectively) according to standard methods [4].

2.3 Cheese Analysis

The following analyses were performed on 24 h old cheese: pH, TS, F (Van Gulik method) and TN. Salt was determined by chloride analysis (Corning 926 salt analyzer). Cheese yield (CY) for each vat of cheese was calculated as kilograms of cheese per 100 kilograms of milk.

3 Results & Discussion

HP treatment produced milk with microbiological quality similar to that of pasteurized milk (Table 1).

Because analysis of milk was performed after pasteurization or pressurization, some changes in milks composition resulting from the technological processes were observed (Table 2).

Table 1. Microbiological counts of milks as cfu/ml

Milk	Media	
	PCA	VRBG
Raw	256,670[a]	820
Pasteurized	17,520	<1[b]
Pressurized	20,670	<1[b]

[a]Arithmetic mean of three replicates
[b]Colonies not observed

Table 2. Composition of milk used for cheesemaking

Variables[1]	Pasteurized Milk	Pressurized Milk
pH	6.54 (0.08)[2b]	6.66 (0.09)[a]
TS (g/kg)	138.08 (6.37)[a]	141.43 (3.18)[a]
F (g/kg)	51.16 (2.56)[a]	52.00 (3.46)[a]
TP (g/kg)	32.23 (1.86)[a]	32.51 (0.98)[a]
NPN (g/kg)	0.48 (0.01)[a]	0.50 (0.03)[a]
NCN (g/kg)	7.79 (0.52)[a]	6.46 (0.65)[b]

[1]TS: total solids, F: fat, TP: true protein, NPN: non-protein nitrogen, NCN: non-casein nitrogen
[2]Means and standard deviation
[ab]Means with the same superscripts in the same row do not differ at P<0.05

Table 3 shows milk and curd acidification. The differences in pH during curd acidification indicate a more rapid rate of acid development by the starter in pasteurized milk than in HP-treated milk.

Table 3. Acidification during cheesemaking and whey composition

Variables[1]	Pasteurized Milk	Pressurized Milk
Acification (pH)		
Milk	6.54 (0.08)[2b]	6.66 (0.09)[a]
Milk + starter	6.39 (0.01)[b]	6.47 (0.05)[a]
At wheying off	6.38 (0.01)[b]	6.42 (0.07)[a]
	6.28 (0.08)[b]	6.37 (0.13)[a]
	5.76 (0.33)[b]	6.07 (0.25)[a]
At pressing		
At salting	7.33 (0.41)[a]	7.44 (0.34)[a]
Whey composition	0.96 (0.24)[b]	1.09 (0.21)[a]
TS (%)	1.44 (0.04)[a]	1.18 (0.04)[b]
F (%)		
TN (g/kg)		

[1]TS: total solids, F: fat, TN: total nitrogen
[2]Means and standard deviation
[ab]Means with the same superscripts in the same row do not differ at P<0.05

The composition of whey collected during cheesemaking from pasteurized and HP-treated milks is shown in Table 3. As expected a decrease of TN in whey from cheesemaking from HP-treated milk and a slightly higher percentage of F compared to the whey from pasteurized milk were observed.

The cheese made from HP-treated milk had higher levels of moisture and salt, but a slightly lower fat content than pasteurized milk. Additional retention of whey protein and, especially, the greater moisture led to improvements in cheese yield from HP-treated milk (Table 4).

Table 4. Cheese composition at 24 h and cheese yield

Variables[1]	Pasteurized Milk	Pressurized Milk
PH	5.14 (0.14)[2b]	5.4 (0.21)[a]
TS (%)	45.98 (2.71)[a]	42.64 (2.36)[b]
TN (%)	2.49 (0.04)[a]	2.41 (0.15)[a]
F (%)	26.17 (1.89)[a]	24.5 (3.12)[b]
NaCl (%)	1.35 (0.22)[b]	1.92 (0.25)[a]
CY (%)	18.69 (0.74)[b]	19.62 (0.33)[a]

[1]TS: total solids, F: fat, TN: total nitrogen, CY: cheese yield
[2]Means and standard deviation
[ab]Means with the same superscripts in the same row do not differ at $P<0.05$

Acknowledgements: This study has been financially supported by the CE-FAIR-CT-95-1113 Project "High pressure treatment of liquids, foods and derived products". A longer version of this work has been submitted to the Milchwissenschaft journal for publication.

References

[1] Trujillo, A.J., Ferragut, V., Gervilla, R., Capellas, M., Guamis, B. (1997); Recent Research Developments in Agricultural and Food Chemistry, 1, 137-159, Research Signpost, Trivandrum, India.

[2] Felipe, X., Capellas, M., Law, A.J.R. (1997); Comparison of the effects of high-pressure treatments and heat pasteurization on the whey protein in goat's milk; J. Agric. Food Chem., 45, 627–631.

[3] Mussa, D.M., Ramaswamy, H.S. (1997); Ultra high pressure pasteurization of milk: kinetics of microbial destruction and changes in physico-chemical characteristics; Lebensm.-Wiss. u.-Technol., 30, 551–557.

[4] ICMSF. (1983); Microorganismos de los alimentos. Técnicas de análisis microbiológicos, Acribia Ed., Zaragoza, Spain.

Maturation Profiles of Goat Cheese Produced from High Pressure Treated Milk

A.J. Trujillo, C. Royo, V. Ferragut and B. Guamis

Unitat de Tecnologia dels Aliments, Centre Especial de Recerca en Tecnologia dels Aliments (CeRTA), Facultat de Veterinària, Universitat Autònoma de Barcelona, 08193 Bellaterra, Spain
ivpp56@cc.uab.es

Abstract. Goat cheese was made from pasteurized (72 °C, 15 s) or HP-treated milk (500 MPa, 5 min, 20 °C). The pasteurized and HP-treated milk cheeses were found to be very similar in terms of sensory quality, electrophoretic profiles and nitrogen fractions (water and trichloroacetic acid soluble nitrogens). The HP-treated milk cheeses had higher pH and moisture content, they matured more quickly, as determined by the formation of total free amino acids, and they developed a strong flavor.

1 Introduction

In general cheese made from raw milk tends to develop a stronger flavour and generally ripens more quickly than cheese made from pasteurized milk. Changes in cheesemilk caused by pasteurization include denaturation of some indigenous enzymes, slight denaturation of whey proteins and their interaction with casein and destruction of the thermolabile indigenous microflora including non-stater lactic acid bacteria (NSLAB). It seems likely that NSLAB plays an important role in the biochemistry of cheese ripening [1–3].

Hydrostatic high pressure (HP) processing is a nonthermal food processing method that is being looked upon with interest since the nutritional and sensory qualities of foods such as flavor and color are generally not adversely affected. The ability of HP treatment to provide a reduction in microbial counts in milk, while no adverse effects are produced [4], could allow the production of raw milk cheeses by means of HP-treated milk. Thus, it appears important to know the consequences and possible implications of HP treatment of milk on the ripening process, and ultimately on the sensory characteristic of the cheeses.

2 Materials & Methods

2.1 Cheese Manufacture

Goat cheeses were manufactured in 25-l vats according to a standard protocol (uncooked pressed goat cheese) from pasteurized (72 °C, 15 s) or HP-treated milk (500 MPa, 15 min, 20 °C). Cheesemaking was performed in triplicate. Samples were taken at 1, 15, 30 and 45 d of ripening.

2.2 Compositional Analysis

A sample of each cheese was taken and analyzed by standard procedures (IDF-FIL) in duplicate for total solids (TS), fat (F; Van Gulik method) and total nitrogen (TN). The pH of a cheese/distilled water (1:1) slurry was measured. Salt was determined by chloride analysis (Corning 926 salt analyzer).

2.3 Assessment of Proteolysis

Proteolysis was monitored thoughout ripening by measuring levels of water-soluble nitrogen at pH 4.6 (WSN) as described by Kuchroo and Fox [5] and 12% trichloroacetic acid soluble nitrogen (TSN) using the macro-Kjeldahl method. The liberation of free amino acids was determined on the water extract by the cadmium-ninhydrin method of Folkertsma and Fox [6].

2.4 Sensory Assessment

At 45 d of ripening cheeses were graded by a trained taste panel consisting of seven judges on a 0–8 (0-poorest: 8-best) scale considering four attributes (appearance, flavor and aroma, texture, and overall quality).

3 Results & Discussion

Figure 1 shows the pH evolution during ripening. In general pasteurized milk cheeses had lower pHs than HP-treated milk cheeses. Pasteurized milk cheeses (45 d) presented higher TS (665.0–692.0 g/kg) and lower salt (up to 6.81%) than HP-treated milk cheeses (649.7–678.9 g/kg and up to 7.73%, respectively).

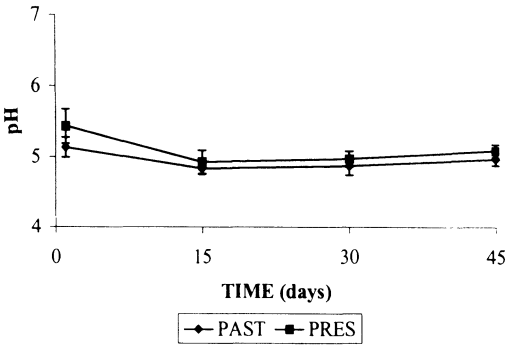

Fig. 1. pH evolution throughout ripening in goat cheeses made from pasteurized and pressure-treated milk

It appears that pressure treatment of milk leads to higher final pH values in cheese and a greater moisture retention that could be due to the incorporation of whey protein which modifies the properties of the resultant gel during cheese-making. In general, in both cheeses the WSN contents increased with age due to hydrolysis of the casein (approximately 6 to 31% for all cheeses). Similarly, the proportion of TSN which represents peptides and amino acids (although not necessarily the same peptides as WSN), also increased (from 2 to 24%). Both nitrogen fractions were higher in the cheeses made from pasteurized than HP-treated milk cheeses in all the stages of the ripening and equilibrium was reached at 45 d of maturation.

Analysis of the water-soluble extracts of the cheeses by the cadmium-ninhydrin method (which is highly sensitive for free amino acids), surprisingly showed that the HP-treated milk cheeses contained considerably higher concentrations throughout ripening (Fig. 2).

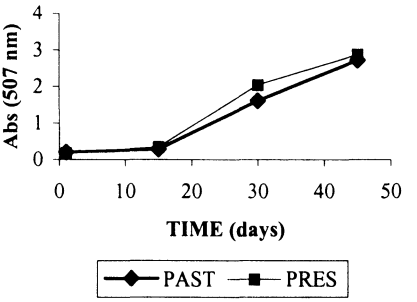

Fig. 2. Formation of total free amino acids throughout ripening in goat cheeses made from pasteurized and pressure-treated milk

The scores for appearance, aroma and flavor, texture and overall acceptability are listed in Table 1. After 45 d of ripening the ranking was similar for both

cheeses, although the HP-treated milk cheeses were considered more flavored than pasteurized milk cheeses by the judges. These results are in agreement with the high level in free amino acids of HP-treated milk cheeses.

Table 1. Grades for quality of goat cheese made from pasteurized and pressure-treated milks. *Mean and standard deviation of scores by a seven member taste panel at 45 d

ATTRIBUTE	CHEESE	
	PAST	PRES
Appearance	4 (1.29)*	5 (1.34)
Aroma	5 (1.46)	5 (0.76)
Flavour	5 (1.53)	6 (0.95)
Texture	5 (1.07)	5 (1.46)
Overall quality	5 (1.40)	5 (0.90)

These differences in respect to free amino acids and sensory characteristics indicated a higher extent of proteolysis in the HP-treated milk cheeses which could be attributed 1) to the destruction of native milk enzymes present in HP-treated milk, 2) to the residual microflora (NSLAB) after the technological treatments (heat or pressure resistances), and 3) the physicochemical alterations of milk due to treatments which resulted in different whey protein contents incorporated in curd and different moisture and salt contents in cheese.

Acknowledgements: This study has been financially supported by the CE-FAIR-CT-95-1113 Project "High pressure treatment of liquids, foods and derived products".

References

[1] Bouton, Y., Grappin, R. (1995); Comparaison de la qualité de fromages à pâte pressée cuite fabriqués à partir de lait cru ou microfiltré; Lait, 75, 31–44.

[2] Grappin, R., Beuvier, E. (1997); Possible implications of milk pasteurization on the manufacture and sensory quality of ripened cheese; Int. Dairy J., 7, 751–761.

[3] McSweeney, P.L.H., Fox, P.F., Lucey, J.A., Jordan, K.N., Cogan, T.M. (1993); Contribution of the indigenous microflora to the maturation of Cheddar cheese; Int. Dairy J., 3, 613–634.

[4] Trujillo, A.J., Ferragut, V., Gervilla, R., CapellaS, M., Guamis, B. (1997); Recent Research Developments in Agricultural and Food Chemistry, 1, 137–159, Research Signpost, Trivandrum, India.

[5] Kuchroo, C.N., Fox, P.F. (1982); Soluble nitrogen in Cheddar cheese: comparison of extraction procedures; Milchwissenschaft, 37, 331–335.

[6] Folkertsma, B., Fox, P.F. (1992); Use of the Cd-ninhydrin reagent to assess proteolysis in cheese during ripening; J. Dairy Res.; 59, 217–224.

Goat's Milk Cheese Accelerated Ripening. Compositional Indexes

E. Sendra, J. Saldo and B. Guamis*

Tecnologia dels Aliments, C.e.R.T.A., Facultat de Veterinària,
Universitat Autònoma de Barcelona, 08193 Bellaterra, Spain
Phone 34-935811446; Fax: 34-935812006
IVPP57@CC.UAB.ES

Abstract. Cheese ripening is carried out by application of 50 MPa for three days. The results are compared with those obained by conventional processes.

1 Introduction

Cheese ripening acceleration is of great interest for the dairy industry and according to a patent application it can be achieved through high hydrostatic pressure (HHP) (10–250 MPa) [4]. Previous studies from our group [3] applied HHP (350–500 MPa) for microbial inactivation in fresh goat's milk cheese preservation with success. HHP application for goat's milk cheese ripening acceleration is being undertaken in the project: FAIR CT96:1113 by our group. The aim of the present study was to test mild HHP conditions on a semi-hard goat's milk cheese and evaluate its effects on composition and proteolysis.

2 Materials & Methods

Cheese manufacture:

1. Goat's milk pasteurization (72 °C, 15 min)
2. Added: starter, rennet and calcium chloride
3. Coagulation: 30 °C approx. 45 min
4. Cut and reheat (8 to 10 mm cubes)
5. Whey removal and drainage
6. Molded (yielding 250 g units)
7. Pressed: 0.5 kg/cm^2 for 4 h
8. Brine salted for 45 min
9. Regular ripening conditions are 14 °C and 88% relative humidity. Superficial mould growth is expected in this type of cheese as it is ripened without packaging.

Experimental groups: Immediately after salting in brine three groups were established:

1. Control group: brought to ripening
2. Temperature group cheese: packaged and kept at 25 °C for 72 h
3. High pressure cheese: packaged and pressurized

Cheese packaging: cheeses for pressurization treatment and temperature incubation were vacuum packaged in barrier film (low water and oxygen permeability).

High pressure treatment: 50 MPa at 25 °C for 72 h. Treatments were applied to cheese after 1 d of pre-ageing.

Evaluated parameters in the present study are: dry matter content [7], fat [2], ash [1], pH [8], total nitrogen content [6], proteolysis: nitrogen soluble at pH 4.6 and nitrogen soluble in trichloroacetic acid 12% (nTCA) [9], counts of aerobic mesofilic microorganisms [5].

3 Results & Discussion

3.1 I Experiment

Sampling:

- 1 d after salting: **initial** cheese
- 3 d later when all the groups had been subjected to the described treatment conditions:
  - **final**: 4 d aged cheese,
  - **T**: 1 d aged cheese + 3 d incubation at 25 °C,
  - **HP**: 1 d aged cheese + 3 d 50 MPa 25 °C

Average composition of cheese was: ash 4.87±0.11, fat 56.5±2.9% and total nitrogen 5.13±0.18% in dry matter. No differences in pH, fat content and total nitrogen in dry matter basis were observed within groups (Table 1).

Table 1. Dry matter and pH values

	Initial	Final	T	HP
Dry matter	47.99±0.32	49.06±0.67	48.70±1.18	48.09±0.36
pH	5.11	5.13	5.07	4.96

HP and T cheese retained higher moisture than final because of the packaging, water retention tended to be higher in pressurized cheese.

pH values were within a narrow range whereas HP values tended to be lower, maybe due to the higher rate of lactose degradation under the treatment conditions.

Nitrogen fraction values are presented in Fig. 1. Proteolysis increased slightly due to both temperature incubation and pressurization, but the effect of pressure was higher than temperature itself.

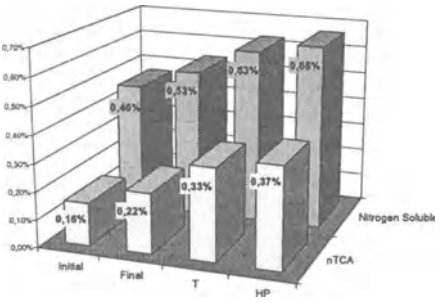

Fig. 1. Nitrogen fractions (all values in dry matter basis)

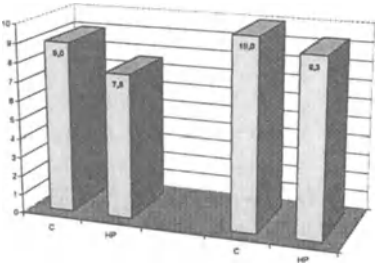

Fig. 2. Microbial counts (log CFU)

Right after the treatment microbial counts notably decreased and so we decided to evaluate microbial populations in both samples (final and HP) 6 days later, and there was a partial recovery of the microbial population in few days. This is probably because there was not really cellular death, some of the microorganisms were probably sublethally injured by pressure and it took them some time to recover (Fig. 2).

3.2 II Experiment

In order to evaluate if there was an influence of ageing time prior to the treatment a second expiriment was planned, where only pH and nitrogen fractions were evaluated. Cheeses were pressurized after 4 d pre-ageing with 50 MPa at 25 °C for 72 h and samples were named as follows:

C: control cheese 4 d ageing; **T**: cheese 4 d aged + 3 d incubated at 25 °C;
HP: cheese 4 d aged + 3 d under pressure.

4 Results

Nitrogen fraction results are presented; incubation at 25 °C by itself did not originate changes in nitrogen fraction content, and it may be related to pre-ageing time when the treatment was carried out (different dry matter and nitrogen soluble contents at pH 4.6) (Fig. 3). pH did not suffer changes under the studied conditions and was within the range 5.16–5.20 for all groups.

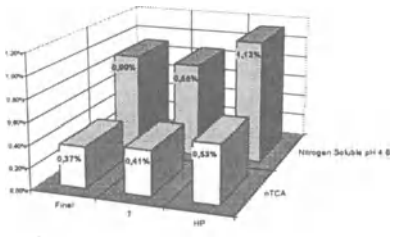

Fig. 3. Nitrogen fractions (all values in dry matter basis)

5 Conclusions

HP groups presented a slight increase in N soluble pH 4.6 and higher increase in N soluble 12% TCA than the other groups. Temperature control cheese showed slightly higher values for nitrogen fractions than control, but the pressure effect was more dramatic than the temperature itself.

Microbial counts decreased by 1.5 log units. The release of microbial enzymes together with the presumable enzyme-substrate interaction enhancement due to pressure application could explain the proteolysis increase in pressurized cheese, much higher than that observed in the temperature control group only due to more suitable conditions for microbial growth.

Acknowledgements: With the support of a grant by the Comissionat per a Universitats i Recerca de la Generalitat de Catalunya.

References

[1] Association of Official Analytical Chemist. 1990. Official Methods of Analysis 15th ed. AOAC, Washington, DC.

[2] British Standards Institution. 1955. Gerber method for the determination of fat in milk and milk products. British Standard, No. 696. BSI, London, United Kingdom.

[3] Capellas, M. *et al.* 1996. Populations of aerobic mesophils and inoculated *Escherichia coli* during storage of fresh goat's milk cheese treated with high pressure. J. Food Protect. 59 (6): 582–587.

[4] Fuji Oil Company, Limited (1992) Method for accelerating cheese ripening. *European Patent Application number 91306976.1*

[5] International Commission on Microbiological Specifications for Foods. Microorganismos de los Alimentos. Técnicas de análisis microbiológicos. Vol. I 1983. Ed. Acribia, Zaragoza.

[6] International Dairy Federation. 1964. Determination of the casein content of milk, IDF Standard No. 29. Int. Dairy Fed. Brussels, Belgium.

[7] International Dairy Ferderation, Norme 4A:1982. Fromages et fromages fondus. Determination de l'extrait sec total (provisoire).

[8] Marth E. H. 1978. Standard methods for the examination of dairy products. 14th ed.. American Public Health Association. Washington, DC.

[9] McSweeney PLH, Fox PF (1997) Chemical methods for the characterization of proteolysis in cheese during ripening. Lait77, 41–76.

Pressure Temperature Phase Diagrams of Some Fat Containing Foodstuffs: Milk Cream, Milk Fat

P.D. Sanz, A.D. Molina-García, J.A. Carrasco and F. Fernández-Martín

Instituto del Frío (CSIC), Ciudad Universitaria, E-28040, Madrid, Spain
psanz@if.csic.es

Abstract. The knowledge of the thermotropic and barotropic behaviour of food components is of high interest in many fields related to food technology. Milk fat products, being mixtures of many different lipids and non-lipidic substances, show a complex thermal behaviour, depending on the physical history of the sample [1, 2]. Many studies dwell on the thermal behaviour of both milk fat and cream at atmospheric or higher pressures [e.g. 3, 4]. As a part of a wider scope study on the effects of high pressures on milk fat-based products, some determinations have been carried out of the phase changes which take place in samples of cream and milk extracted fat.

1 Introduction

An important part of the work carried out at our laboratory centres around the characterisation of processes (involving food products) related to the employment of hydrostatic pressure (HP) in the temperature regions around the freezing point [e.g. 5, 6]. We have become interested in finding out about the phase changes which take place in cream and dairy fat at different pressures and temperatures, by our simple current experimental design: a pressure vessel externally thermostated, with two thermocouples. Despite the crudeness of this design, some data of interest can be obtained.

2 Materials & Methods

An HP equipment, from ACB GEC Alsthon (Nantes, France) was employed: a 2.3 l hydrostatic pressure vessel thermostated by an externally circulating fluid (regulated at an external bath). Although the pressure attainable is 500 MPa, we have only worked up to around 200 MPa. Two thermocouples allow the determination of temperature at two points inside the vessel. Temperature data and pressure –measured by a gauge– are collected quasi-continuously (every 3 s) by a data-logger interfaced to a personal computer.

Temperature scans were performed from a starting point at 5 °C, heating up to 80 °C and cooling back to 5 °C, or cooling down to –20 °C and heating back to 5 °C. The scan speed, not directly controllable, varies from 1 °/min to 0.001 °/min. Pressure was maintained constant during the process. Alternatively, to avoid the sharp compression-decompression cycle effects on temperature, pressure was set and the vessel was sealed, allowing it to fluctuate freely with temperature.

Temperature readings were plotted against time and temperature and, once discarded effects likely due to fluctuations in pressure or bath temperature or to initial lack of thermal equilibrium, thermal changes that could be related to phase changes were identified (e.g., Fig. 1).

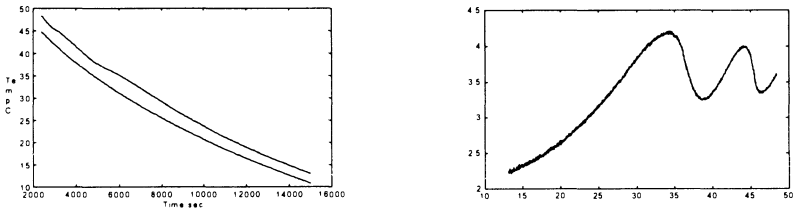

Fig. 1. Examples of thermocouple readings (temperature in °C vs. time in s) for the differential sample set-up (left), and subtraction of the same two signals, showing two thermal effects on a milk fat sample (as temperature increment vs. temperature in °C), right

Milk cream was obtained from a local producer (CLESA, Madrid, Spain) with no homogenisation or thermal treatment, at 37% fat content. Samples were kept at 2.5 °C and employed in short or treated 1 min at 60 °C, for longer delays.

Milk fat was extracted from this cream by either: i) A mechanical method: churning at room temperature, washing the resulting butter with distilled water till clear wash and melted filtering on anhydrous calcium chloride to remove most of the water. ii) An organic solvent extraction: extraction with diethyl ether/petroleum ether after treatment with ammonia and ethanol.

Two sample set-ups were tested: i) bulk: a pressure-tight container (around 25 g of sample), with a thermocouple in its centre, the other thermocouple recording the pressurising liquid (water or ethylene glycol/water) temperature, and ii) differential: two 2 g containers placed at symmetrical positions inside the vessel, each one with a thermocouple in its centre, one being filled with the sample and the other with distilled water, as a reference.

3 Results

Both milk fat extracts behaved in an indistinguishable way in our experiments. The DSC thermogram at atmospheric pressure (Fig. 2, left) shows a gradual transition extending from –40 to nearly 0 °C, a sharp endotherm (10–13 °C), a second sharp endotherm at 20–21 °C (sometimes associated with a subsequent crystallisation

exotherm), and a further extended transition from 30 to 40 °C. The heat involved in each transition varies depending on the thermal history of the sample.

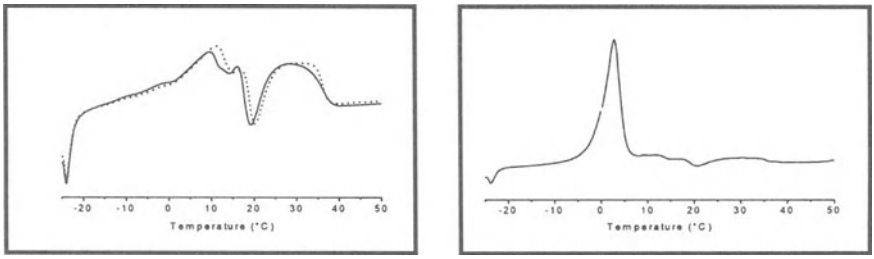

Fig. 2. Left: DSC heating scans of milk fat (continuous line, solvent extracted; dots, churning extracted). Right: DSC heating scan of cream. In both cases, ordinate axis in heat arbitrary units

Employing our HP apparatus the only heat effect that we can detect with any precision corresponds most likely the two mentioned sharp transitions (Fig. 3, left). They evolve strongly with pressure increasing dramatically its temperature in the interval studied (as expected, because melting of fat generally involves a volume increase).

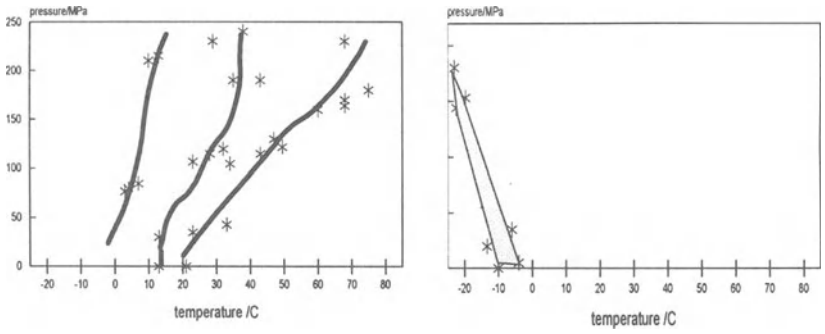

Fig. 3. Left: Milk fat phase diagram: stars correspond to thermal effects detected and lines separate likely borders between phase regions. Right: Cream phase diagram: the shadowed area covers the region between melting and freezing points

Cream samples showed the DSC thermogram (at atmospheric pressure) of Fig. 2 (right). It consists of several heat effects of which the endothermic water melting is the main one. Other thermal transitions are similar to those observed in milk fat, but proportionally reduced in heat effect.

When checked on our HP apparatus, only the main peak, corresponding to water melting and freezing, was obtained, being displaced by pressure in a similar way to the freezing point of pure water (Fig. 3, right), decreasing with increasing pressure. Other transitions are too small in heat effect to be detected by us.

4 Discussion

The results presented here reflect the difficulty in obtaining data related to phase changes which take place inside a HP vessel, with the described experimental set-up. A temperature sensor will only allow the appreciation of changes in temperature due to the sample heat exchange associated with a phase transition. Most of the heat is lost and most of the conditions are out of our control. The speed of heat diffusion, for example, depends on the conductivity of fluid, sample container and sample itself. Or the temperature scanning speed, not linearly controllable.

Currently we are working on several approaches to deal with these problems. Some improve the temperature and pressure scans, by contributing to make them more regular and less bumpy, or more constant, if that is desired. An other line implies the use of a quasi-adiabatic cell where a thermal signal can be taken as more reliable. Lastly, the introduction of alternative sensors for detecting phase change, relying on properties other than temperature, could be of great utility.

Acknowledgements: This research was supported from the "Plan Nacional de Investigación Científica y Desarrollo Tecnológico" of Spain by the ALI97-0759 Project.

References

[1] Banks, W.(1991); Bulletin of the IDF, 260, chaps. 1, 4.
[2] Kleyn, D.H. (1992); Food Technology, Jan 1992, 118.
[3] Buchheim, W. and Prokopek, D. (1992); Dtsch. Milchwirstsch, 43, 1374.
[4] Buchheim, W. and Frede, E. (1996); DMZ-Lebensmitt. Milchwirtschaft, 117, 228.
[5] Sanz, P.D., Solas, M., Otero, L., de Elvira, C., Carrasco J.A. and Molina-García, A.D. (1998); Polish Journal of Food and Nutrition Sciences (in press).
[6] Sanz, P.D., Otero, L., de Elvira, C. and Carrasco, J.A.(1997); International Journal of Refrigeration, 20, 301.

Freezing and Thawing Under High Pressure

Pressure Assisted Thawing of Potato Cylinders

O. Schlüter, S. George, V. Heinz and D. Knorr

Department of Food Biotechnology and Food Process Engineering,
Berlin University of Technology, Königin Luise Str. 22, D-14195 Berlin, Germany
Phone: +49 30 314 71250; Fax: +49 30 832 7663
FOODTECH@mailszrz.zrz.tu-berlin.de

Abstract. Water as the major constituent of most food materials undergoes phase transition in a way which can be influenced by increased hydrostatic pressure. Besides a depression of the melting point a reduction of the required latent heat can be observed. Therefore, in a range up to 200 MPa thawing times of pure water were markedly reduced without an increase of the surrounding temperature. Plant tissue like potato cylinders showed a similar behaviour. Using a multi-thermocouple and a finite difference method, thawing times at different pressure levels can be predicted.

1 Introduction

Freezing of food provides a safe and convenient way of shelf life extension without negative effects on the nutritional quality, but before further treatments a thawing of the frozen food is necessary. The convective and conductive thawing methods (air and/or water flow) with which however a process duration of several hours must be accepted are in common use.

Thawing with the aid of microwaves indeed offers at high-cost an abridged process duration, but is however skin depth limited, and there exists the danger of partial product overheating. In addition to parameters like product geometry, the flow rate of the surrounding fluid and the thermophysical properties, the

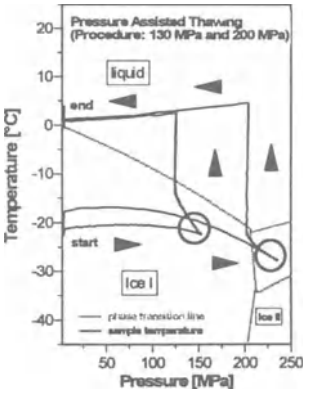

Fig. 1. Pressure assisted thawing at 130 and 200 MPa figured in the phase diagram of water [1]. The range of phase transition is marked by circles

temperature difference (product - environment) has a significant influence on the rate of the phase transition in the case of the convective and conductive thawing methods. Water as the major constituent of most food materials undergoes phase transition in a way which can be influenced by increased hydrostatic pressure (Fig. 1). Besides a depression of the melting point a reduction of the required latent heat can be observed. Therefore, in a range up to 200 MPa thawing times of pure water were markedly reduced without an increase of the surrounding temperature. Plant tissue like potato cylinders showed a similar behaviour.

2 Materials & Methods

2.1 Experimental Setup

Equally sized cylinders (dia: 32 mm, length: 50 mm) cut from potatoes were initially frozen at –35 °C. Using a multi-thermocouple (Fig. 2) the temperature field of the sample was measured during thawing on different pressure levels.

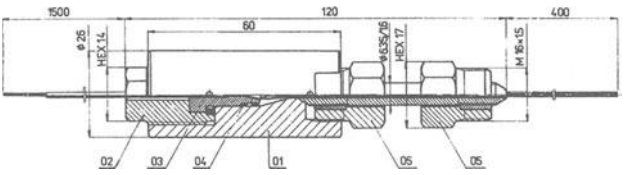

Fig. 2. Section of the multi-thermocouple high pressure cell (UNIPRESS; Warszawa). 1: cell body; 2: plug screw; 3: plug with 7 thermocouples; 4: seals; 5: HP 1/4 connector

The high pressure vessel had an inner diameter of 55 mm (Fig. 3). The temperature was controlled externally by flexible tubes fixed on the outer surface and connected to a cryostat. The temperature and the pressure were recorded digitally.

2.2 Thawing Time Prediction

Experimental thawing curves (Fig. 4) were recalculated by a finite difference method [3].

Radial symmetrical one dimensional heat conduction was assumed to describe correctly the situation inside the middle part of an extended potato cylinder (Fig. 5).

Additionally, a heat balance was implemented at each volume element to adjust the time dependent temperature field. Convective heat transfer at the surface was calculated by using a transfer coefficient of k=110 W/m² K. The moving freezing front was modelled by introducing temperature dependent apparent specific heat c_p

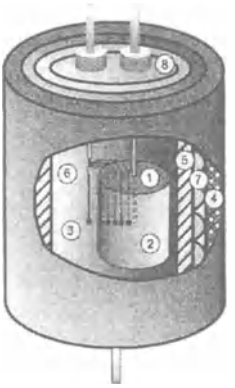

Fig. 3. Schematic drawing of the experimental arrangement. 1: potato cylinder; 2: thermocouple (Pt 100); 3: multi-thermocouple; 4: insulation; 5: pressure vessel; 6: pressure medium (20% ethanol / 80% glycol, v/v); 7: cooling tubes; 8: upper seal

and thermal conductivity λ in the vicinity of the freezing point into the heat balances of the finite difference scheme. Data for temperature dependent c_p and λ of potato tissue are available elsewhere in the literature [2].

$$\lambda(T, p_i) = p_3 + p_0 \left[1 - \exp\left(\frac{-T + p_4}{p_1} \right)^{p_2} \right] \tag{1}$$

In this paper, continuous functions of temperature were used to model empirically the behaviour of either c_p or λ below the temperature level of the pressure dependent freezing point. In the case of λ the cumulative Weibull [4] distribution was used. Equation 1 is used together with the parameters in Table 1 to predict λ (Fig. 6) within the finite difference algorithm if the local temperature drops below the freezing point. An approximation of the apparent heat capacity c_p (Fig. 7) can be obtained using the density Weibull distribution (2) together with the parameters listed in Table 2.

$$c_p(T, Q_i) = Q_3 + \left\{ Q_0 \left(\frac{T - Q_5}{Q_1} \right)^{Q_2} \frac{Q_2}{T - Q_5} \exp\left[-\left(\frac{T - Q_5}{Q_1} \right)^{Q_2} \right] \right\} \tag{2}$$

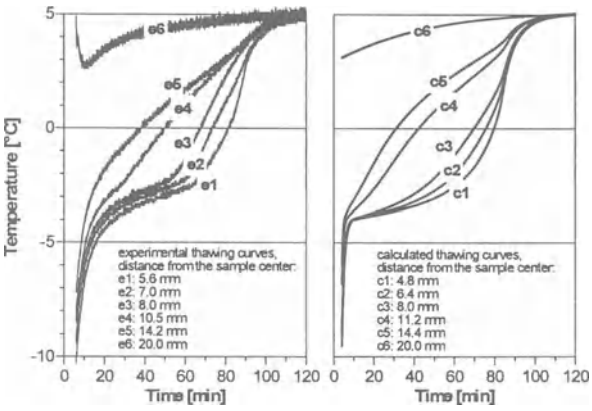

Fig. 4. Determined thawing curves using a multi-thermocouple and re-calculated thawing curves for thawing at ambient pressure

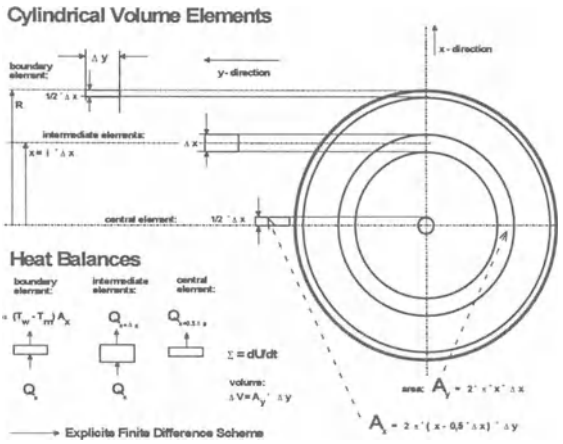

Fig. 5. Schematic view of the radial, one-dimensional heat balancing at the different volume elements within the cylindrical sample

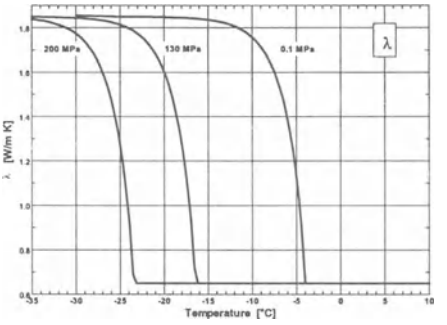

Fig. 6. Thermal conductivity λ as a function of temperature on different pressure levels (0.1; 130 and 200 MPa). The cumulative Weibull distribution (1) together with the parameters listed in Table 1 was used for prediction of λ

Table 1. Parameters of the cumulative Weibull distribution used to predict the temperature dependent thermal conductivity λ

Parameter	Denotation	Value		
		0.1 MPa	130 MPa	200 MPa
P_0	Left asymptote	1.2	1.2	1.2
P_1	Scale parameter	2.1	2.1	2.1
P_2	Shape parameter	0.9	0.9	0.9
P_3	λ (if $T > T$(freezing))	0.65	0.65	0.65
P_4	Freezing temp.	–3.5	–16.5	–23.5

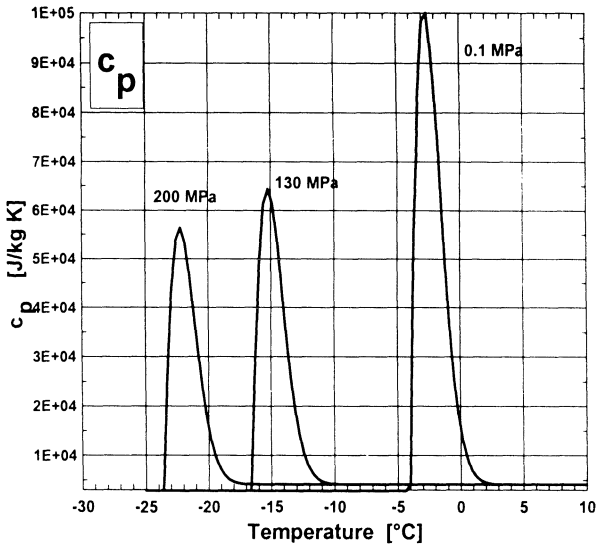

Fig. 7. Apparent specific heat c_p as a function of temperature on different pressure levels (0.1; 130 and 200 MPa). The density Weibull distribution (2) together with the parameters listed in Table 2 was used for prediction of c_p

Table 2. Parameters of the density Weibull distribution used to predict the temperature dependent apparent specific heat c_p

Parameter	Denotation	Value		
		0.1 MPa	130 MPa	200 MPa
Q_0	Peak parameter	$2.4*10^5$	$1.5*10^5$	$1.3*10^5$
Q_1	Scale parameter	2.0	2.0	2.0
Q_2	Shape parameter	1.8	1.8	1.8
Q_3	c_p (if T >T(freezing))	$4.1*10^3$	$4.1*10^3$	$4.1*10^3$
Q_4	Left asymptote	$2.8*10^3$	$2.8*10^3$	$2.8*10^3$
Q_5	Freezing temp.	−3.5	−16.5	−23.5

3 Results

At constant temperature of the pressure vessel the thawing times at different pressure levels were markedly reduced compared to control process at ambient condition. At 130 MPa the central element of the potato cylinder with 32 mm diameter reached the unfrozen state 35 min earlier than the control. Re-calculation of the obtained experimental temperature profiles (Fig. 8) was possible by modeling temperature dependent changes in specific heat using the Weibull distributional function. The integrated peaks of the apparent specific heat fit closely to the latent heat which is reported for water [1].

Similar to water the latent heat of potato tissue can be reduced by increasing the pressure. At 200 MPa the required heat for thawing is reduced by 35% to 182 kJ/kg.

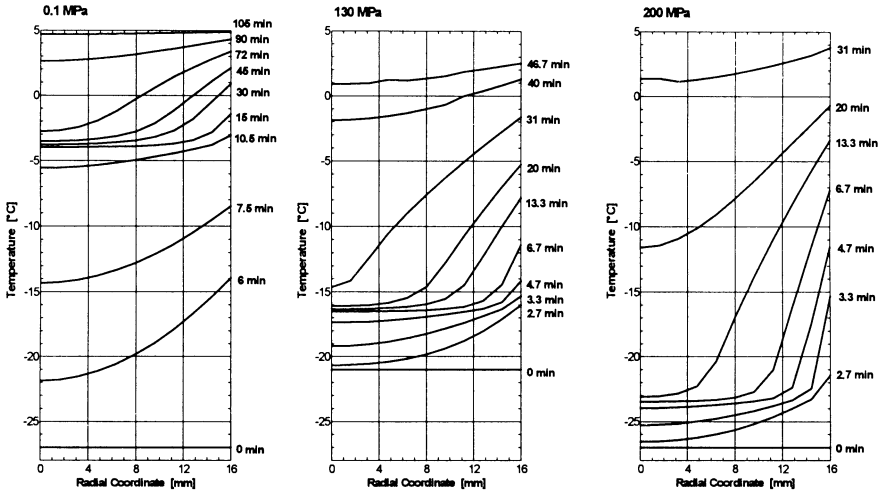

Fig. 8. Thawing time prediction by re-calculated temperature profiles at different pressure levels (0.1, 130 and 200 MPa)

Acknowledgements: Parts of this work have been supported by the German Research Foundation (DFG-Kn 260/6-1). S. George was supported by a sandwich program of the German Academic Exchange Service (DAAD).

References

[1] Bridgman, P.W. (1912) Water in the liquid and five solid forms under pressure. Proc. Am. Acad. Arts Sci. **47**: 441–558.

[2] Cleland, A.C. and Earle, R.L. (1984) Assessment of freezing time prediction methods. J. Food Sci. **49**: 1034–1042.

[3] Marek, R. and Götz, W. (1995) Numerische Lösung von partiellen Differentialgleichungen mit finiten Differenzen, Moreno-Verlag, Buchenloe.

[4] Weibull, W. (1951) A statistical distribution function of wide applicability, J. Appl. Mech. **18**: 293–297.

Thermal Behaviour of the High-Pressure-Assisted Freezing Process and Its Effect on the Quality of Large Foodstuffs

P.D. Sanz , L. Otero, J.A. Carrasco, C. de Elvira, M. Guerra and A.D. Molina-García

Instituto del Frío (CSIC), Ciudad Universitaria, 28040 Madrid, Spain
psanz@if.csic.es

Abstract. Many different aspects are involved in a complete characterisation of the high-pressure-assisted freezing (HPAF) process. Final microstructure and temporal variation of temperature are considered in this work which employs semitendinous beef muscle and agar gel as experimental samples. The process of freezing by a conventional method generally ends with nucleation of exclusively extracellular ice, intracellular ice nucleation taking place only when a large heat gradient is applied. In the case of a HPAF process, a global nucleation is obtained in the whole sample volume. These effects are observed in the sample microstructure by scanning electron microscopy. Besides, the thermal behaviour of each process is different, as is evident from the different shape of the temperature vs. time freezing curves obtained with a food model.

1 Introduction

Commercial applications of high pressure treatments to food products require previous studies on the effect of this new technology in topics such as organoleptic properties, microbiology [1], packaging related [2], etc. Classical food freezing at atmospheric pressure is a well-known process from the sanitary, qualitative and economical points of view. Both sanitary and quality aspects depend largely on the final temperature reached at the centre of the product [3] and on the freezing rate of the process. Economical aspects are related to a good knowledge of the process (equipment design and optimisation, right process cost evaluation, etc).

In order to look deeply into the high-pressure-assisted freezing (HPAF) process, mathematical and physical modelling tasks as well as corresponding validation experiments must be carried out. With reference to the former, several models which consider the behaviour of intervening state thermodynamical variables, the instantaneous amount of produced ice [4], etc. are being developed at present. In the latter, there is a lack of experiments in parallel with physical models and foods highlighting similarities and distinctions between HPAF and conventional freezing techniques which allow progress in the new process optimisation. The aim of this

work is to compare the behaviour of a large beef muscle and that of a model substance when both are frozen via a conventional technique or by HPAF. Food microstructure quality and model thermal aspects are analysed.

2 Materials & Methods

The high pressure device employed consists of a 2.3 l vessel manufactured by ACB GEL ALSTHON able to work up to 500 MPa and to be thermostated at temperatures over –30 °C. Cu-Constantan thermocouples for sample temperature measurement, and a pressure gauge are connected to a computer. Atmospheric pressure freezing was also carried out inside the high pressure vessel. The tested products were agar gel of 99% water content and beef semitendinous muscle.

Setting up alike boundary and initial conditions in both freezing processes and in order to analyse their thermal behaviour, different temperatures have been employed. Additionally, SEM microscopy has been used to determine the damages to the microstructure of the beef muscle frozen by HPAF and conventional freezing techniques.

3 Results & Discussion

When large volume products are frozen with conventional techniques, substantial thermal gradients arise inside the product and as a consequence the final structure differs among regions placed at different radii. Actually, when analysing the structure of a conventionally frozen foodstuff, a strong dependence on the way the process has been carried out and especially on the freezing rate is observed. In the case of freezing beef muscles, even in the best of the cases, the process will generally end with nucleation of exclusively extracellular ice. If high nucleation rates are applied (e.g. by cryogenic methods), intracellular nucleations can be achieved but ice nucleii always would be more likely to appear at the surface rather than in the centre of a large frozen foodstuff and that is so because heat is preferentially removed by the system from surface areas [5].

As has been established in a previous work [4], in a HPAF process, the sample is subjected to nearly 200 MPa and then cooled down to approximately –20 °C; then pressure is released and further cooling completes the freezing operation. A global nucleation takes place in the whole volume of the sample with pressure release (characterised by a large instantaneous heat release). In this way, a semitendinous beef muscle was frozen. An area which includes the centre of the product is shown in Fig. 1, where the presence of small ice crystals inside the cells can be observed. This phenomenon appears to be related to the high subcooling effect achieved throughout the sample (not limited to the surface). The existence of these intracellular crystals agrees well with the large amount of instantaneous ice

observed after an adiabatic expansion in this region of pressure and temperature [4]. An effect of the global ice formation is to avoid the exit of large amounts of water from cells, reducing, so, the damage caused by dehydration, as well as by the large-sized extracellular ice crystals. When the microstructure of large frozen food products is analysed by microscopy, it is seen that conventional freezing at atmospheric pressure causes structural damage to the centre of samples, while with the use of HPAF they appear considerably reduced.

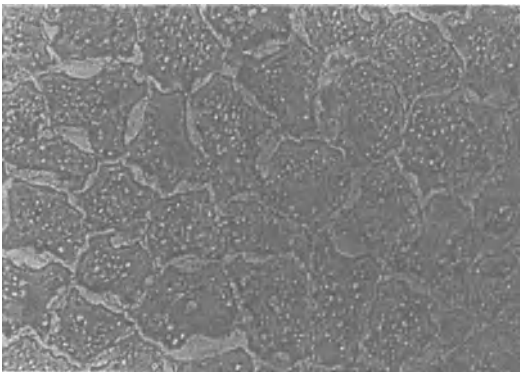

Fig. 1. Centre of a *semitendinous* beef muscle frozen by using HPAF

In order to further our knowledge of HPAF, several experiments with a model substance (agar gel) have been carried out comparing thermal aspects involved in the process with those corresponding to an atmospheric pressure freezing process, in the same container and under similar conditions. Figure 2 presents the temperature variation with time for both processes, the phase change in the former being faster than in the latter. Again, it is shown that both freezing processes take place in different ways because heat transfer mechanisms work in each case differently. Nevertheless, this fact and others related should be considered in depth in future works.

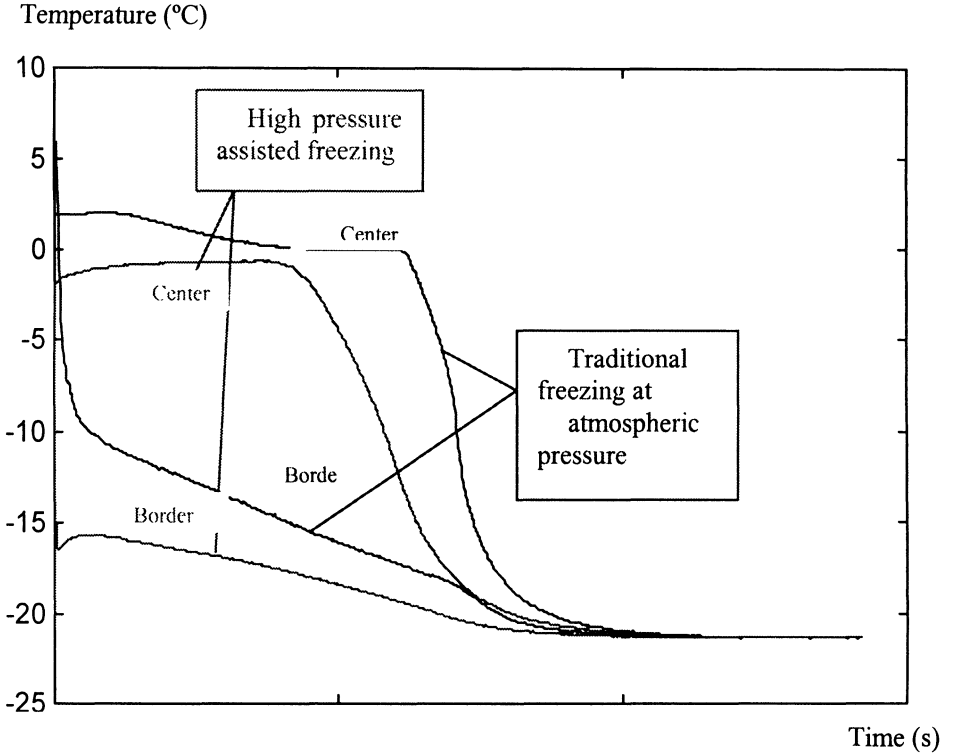

Fig. 2. Agar gel: after HPAF and after freezing at atmospheric pressure

Acknowledgements: This research was supported from the "Plan Nacional de Investigación Científica y Desarrollo Tecnológico" of Spain by the ALI97-0759 Project.

References

[1] Arroyo, G., Sanz, P.D. & Préstamo, G., *J. App. Bacteriol.*, **82**, 735–742, 1997.
[2] Fradin, J.F., le Bail, A., Sanz, P.D. & Molina-García, A.D., *Food Sci. Tech. Int.* In press.
[3] Elvira, C.de, Sanz, P.D. & Carrasco, J.A., *J. Food Engin.*, **29**, 257–268, 1996.
[4] Sanz, P.D., Otero, L., de Elvira, C. & Carrasco, J.A., *Int. J. Refrig.*, **20**, 301–307,1997.
[5] Otero, L., Martino, M.N., Sanz, P.D. & Zaritzky, N.E., *Scanning*, **19**, 241–242, 1997.

High Hydrostatic Pressure Freezing and Thawing of Pork Meat: Quality Preservation, Processing Times and High Pressure Treatment Advantages

C. Massaux, F. Béra, B. Steyer, M. Sindic and C. Deroanne

Faculté Universitaire des Sciences Agronomiques de Gembloux, Unité de Technologie des Industries Agro-Alimentaires, Passage des Déportés, 2, B-5030 Gembloux, Belgium
Massaux.c@fsagx.ac.be

Abstract. High hydrostatic pressures (50, 100 and 200 MPa) are applied during freezing-thawing processes of pork meat. HHP freezing-thawing is then compared to classical freezing-thawing. Physicochemical parameters of meat samples (thawing loss, tenderness, color, centrifugal drip, ...) are measured to characterize the meat quality. Freezing and thawing times accurately measured are also compared. Finally, proportions of instantly frozen water (during freezing process) and instantly thawed ice (during thawing process) are calculated by means of energetic equations. The measurements indicate that freezing-thawing under a pressure of 100 MPa is the most interesting process for pork meat. No exudate is measured, thawing time is reduced, discoloration and toughening of meat are slight.

1 Introduction

Classical freezing and thawing cause changes in texture and cooking properties of foods, probably due to destruction of membrane structure and/or concentration changes in solutes [1]. Developments in new methods of freezing and thawing of foods are required in food industries.

Effects of high pressure on the solid/liquid phase diagram of water open the way to new applications in food technology. The property of water to remain in the liquid state down to about –22 °C at pressures up to 210 MPa [2], allows the rapid freezing and thawing of foods through pressure applications. Freezing and thawing rates are of great importance with regard to final quality of meat [3] and processing times.

2 Materials & Methods

The *Longissimus dorsi* muscles of pork are divided into three equal parts and vacuum-packaged in polyethylene bags. A third is frozen and thawed under high pressure (50,

100 or 200 MPa) and put in the meanwhile in a freezer at –20 °C, a third is frozen at –20 °C during 5 d and a third (control) is cooled at +10 °C during 24 h. A first study has evaluated the effects of a 50 and a 100 MPa freezing-thawing and a second study, the effects of a 200 MPa treatment. Dry matter was determined by the official method (AFNOR 1976, NF V 04–401) and centrifugal drip by weight after centrifugation 30 min. at 42.700 g. Thawing and cooking losses were determined by weight difference before and after treatment. Total loss was calculated by adding of thawing and cooking losses. Color of raw meat was characterized by C.I.E. values (L*, a*, b*) with a spectrocolorimeter Miniscan XE (Hunterlab). Changes in textural properties of cooked meat were evaluated by a Warner-Bratzler test with a texturometer SMS.TA-XT2.

Freezing and thawing times were accurately measured with 3 K-thermocouples placed in the high pressure vessel: the first indicated the pressure liquid temperature, the second was located against the meat sample and the third was put in the meat by means of a system of packing gland.

Freezing treatment under HHP: after cooling of the HHP vessel at a negative temperature, the meat was placed in the vessel and the pressure was immediately increased. When the meat temperature was sufficiently low, the pressure was released, inducing the pressure-shift-freezing.

Thawing treatment under pressure: the frozen meat was placed in the HHP vessel stabilized at a positive temperature. The pressure was then increased, facilitating rapid thawing. When the meat temperature was positive, the pressure was released. The freezing and thawing processes at atmospheric pressure were realized by water immersion (–15 °C or +10 °C).

3 Results

3.1 Quality Preservation

The different parameters measured to characterize the meat quality are presented in Table 1.

Table 1. Physicochemical characterization of control samples (unfrozen), classically frozen samples and HHP frozen samples

Samples	Thawing loss (%)	Cooking loss (%)	Total loss (%)	Centrifugal drip (%)	Hardness Maximal peak (N)	Dry matter (%)	Color L* (lightness)	a* (redness)	b* (yellowness)
Pork1 / Control	3.5[a]	27 6	30 2	27 9	35 3 ± 4 1	25 0	55 5 ± 1 8	6 0 ± 0.3	15 7 ± 0 4
Pork1 / Classical	12 9	28 1	37.4	25 6	35 6 ± 6 1	25 8	56 4 ± 3 0	5 8 ± 1 4	16.4 ± 0 4
Pork1 / HHP 200	2 9	33 0	34 9	38.6	50 0 ± 8 9	24.9	73 8 ± 0.7	4.1 ± 0.1	17 0 ± 0.2
Pork2 / Control	3 0[a]	24 4	26 7	24 2	29 1 ± 3 2	26 2	53 7 ± 1 4	6 8 ± 1.0	14 6 ± 0 6
Pork2 / Classical	9 1	23 8	30.8	21 6	19 1 ± 2.0	27 5	55.0 ± 0 8	7 7 ± 1 1	17 3 ± 0 1
Pork2 / HHP 50	6 3	25 7	30 4	25 8	29 5 ± 3 8	26 4	56 6 ± 0 8	7 5 ± 1 2	16 7 ± 0 1
Pork2 / HHP 100	3.1	25 8	28 1	28 1	25 7 ± 3.2	26 5	65.3 ± 1 6	6.9 ± 1.1	17 5 ± 0 5
Measurements count by sample	1	1	-	2	10	2	4	4	4

[a] drip loss generated by the vacuum-packing

Results show that high pressure freezing-thawing of pork meat is likely to reduce thawing loss. Cooking loss increases slightly with HHP treatment but total loss is less than the exudate obtained by classical freezing-thawing. Centrifugal drip increases with applied pressure. Dry matter squares with the thawing loss: a higher thawing loss involves a higher dry matter. Discoloration and toughening of meat are observed and increase with the working pressure.

3.2 Proportions of Instantly Frozen Water or Thawed Ice

The proportions of instantly frozen water (during freezing process) and instantly thawed ice (during thawing process) are calculated by means of energetic equations based on the specific heat and latent heat of meat and on the temperatures measured during the pressurization. These temperatures and the calculated solid/liquid proportions are presented in Table 2.

Table 2. Temperatures measured during freezing and thawing processes and calculated proportions of instantly frozen water and thawed ice

	Freezing			Thawing		
Pressure (MPa)	T° before the pressure release (°C)	T° after the pressure release (°C)	instantly frozen water (%)	T° before the pressurization (°C)	T° after the pressurization (°C)	instantly thawed ice (%)
50	-6	-1,6	6,7	-7,5	-10	2,5
100	-11	-1,6	14,3	-7	-14	7,2
200	-12	-1,6	15,8	-8	-26,4	20,4

We notice all the calculated proportions increase with applied pressure. This observation is directly in relation with the solid/liquid phase diagram of water which shows that water remains in the liquid state down to about –22 °C at pressures up to 210 MPa [2]. During the freezing process, a higher pressure (limited to 200 MPa) allows a greater cooling, induces a steeper rise of temperature at the pressure release and enables a larger amount of water to be frozen instantly. During the thawing process, a 200 MPa pressure involves a steeper drop of temperature at the pressurization, enabling a larger amount of ice to be thawed instantly.

3.3 Processing Times

Table 3 shows the freezing and thawing times measured at atmospheric pressure and under different pressures.

In this table, we observe the time of the freezing or thawing taking place under pressure is in direct relation with applied pressure: the more the pressure is high, the more the process time is reduced.

Concerning the total time of freezing, working under pressure is longer than at atmospheric pressure. This can be explained by the poor heat transfers between sample and pressure medium, which are necessary to complete the meat freezing.

We also notice there is nearly no time difference between the 100 and the 200 MPa treatment. The total time of the thawing process decreases with the higher pressures. This observation agrees with the calculated proportions of instantly thawed ice: higher pressures thaw instantly a larger amount of ice and then decrease the time process.

Table 3. Freezing time and thawing time of pork meat as a function of applied pressure and sample weight

		Freezing		Thawing	
Pressure (MPa)	**Sample weight (g)**	Pressure release and freezing plateau	Total time (+10°C to -3°C)	Pressurization and thawing plateau	Total time (-8°C to +6°C)
0	350	1h45'	1h50'	2h45'	3h11'
50	330	1h43'	3h47'	2h02'	2h27'
100	340	1h18'	3h02'	1h29'	1h58'
200	350	1h08'	3h08'	47'	2h05'

4 Conclusions

The most interesting method of pork meat freezing-thawing seems to be the process under a pressure of 100 MPa. No exudate is measured, thawing time is reduced, discoloration and toughness of meat are slight. The major advantages of high pressure treatment in freezing and thawing processes are reduced drip loss and lowered processing times.

Acknowledgements: The authors wish to acknowledge 'Region Wallonne, Direction Generale des Technologies, de la Recherche et de l'Energie' for financial support.

References

[1] Bevilacqua, A., Zaritzky, N.E. and Calvelo, A. (1979); Histological measurements of ice in frozen beef, J. Food Technol., 4, 237–251.

[2] Lüdeman, H.D. (1992); Water and aqueous solutions under high pressure, High pressure and biotechnology, Eds Balny C. and al., colloque INSERM, 224, 371–379.

[3] George, R.M. (1993); Freezing processes used in the food industry, Trends in Food Science & Technology, 4, 134–138.

Pressure-Assisted Freezing of Pork Muscle Meat vs. Ordinary Freezing: Protein Denaturation

F. Fernández-Martín, P.D. Sanz and L. Otero

Instituto del Frio (CSIC), Ciudad Universitaria, E-28040 Madrid, Spain
fermarfer@if.csic.es

Abstract. Pork muscle meat was subjected to high pressure/temperature combinations with and without water freezing by appropriate decompression. Processing effects on the proteins were assessed by differential scanning calorimetry (DSC). Denaturation was full for actin and very severe for the other muscle proteins. Connective tissue proteins remained practically unaltered. Pressure-assisted freezing was certainly disadvantageous with respect to conventional freezing.

1 Introduction

There is an increasing general interest in applying high-pressure technologies to food processing. Pressurization of meat products has been used with different aims; muscle systems, for instance, have been pressure processed for the purpose of tenderizing either pre- or post-rigor meat. One of the major fields of application, however, seems to be the combination of hydrostatic pressures and subzero temperatures as alternative methods to freezing and frozen storage for food preservation.

The main aim of this work concerns the unfolding effects that pressurization at subzero temperatures, with or without water freezing, may produce on the proteins of muscle meat. Samples frozen by conventional methods will be used as reference. The quality of the pressure-processed meats will be evaluated by textural measurements.

2 Materials & Methods

2.1 Meat Samples

Pieces ~20 cm length from pork *M. longissimus dorsi* were obtained from a local market, cut into smaller portions (~5 cm) and vacuum-sealed in flexible

polyethylene bags. Intramuscular connective sheets were trimmed from the meat pieces to be also processed.

2.2 Pressure/Temperature Treatments

A pilot machine HP900 model (GEC ALSTHOM, France) was used. It essentially consists of a cylindrical vessel of ~2.5 l filled with an ethylene glycol/water mixture as pressure-transmitter and cooling media (external recirculating thermostat system). The evolution of pressure and temperature were recorded during processing by a computer program. Process parameters were 210 MPa and –21 °C, which correspond to a monophasic domain of supercooled water close to the ice I boundary in the water phase diagram. Samples were transferred to the vessel at the processing temperature and then pressurized. The samples in the middle zone lasted ~2.5 h to get the target temperature. The samples were then heated at ambient temperature before depressurizing to avoid any risk from freezing, the total pressurization step lasting ~3 h (P/NF). Alternatively, other samples were adiabatically expanded at atmospheric pressure while being at –21 °C to get ice I crystallization throughout the sample (P/F). The processed samples were stored overnight in a refrigerator (4–7 °C) until analysis.

2.3 Conventional Freezing

Freezing was also carried out at high cooling rates by means of an air blast freezing tunnel (Frigoscandia 010) working at –40 °C with a velocity of air of 5.5 m/s. Once the geometric center of the meat pieces showed constant temperature, they were kept there 30 min as holding time, the whole process lasting ~3 h. The frozen samples (F) were stored like the above ones before analysis.

2.4 Differential Scanning Calorimetry (DSC)

Thermal denaturation of the muscle proteins was studied by means of a Perkin-Elmer DSC7 differential scanning calorimeter previously calibrated. Small pieces of meat, free from visible traces of fat and connective tissue, were capsulated into aluminum pans and hermetically sealed to avoid vaporization losses. At least 6 samples of about 15–20 mg (±0.002 mg by an electronic balance Perkin-Elmer AD4) were used per product category. The samples were scanned at 10 °C/min over the temperature range 20–90 °C under dry nitrogen purge of 30 cc/min. Water content of each individual sample (pinhole in the capsule lid) was determined by desiccation at 105 °C. Averages temperatures (T, °C) and enthalpies of thermal denaturation ΔH, J/g_{dm} (referred to dry matter content hereinafter) are given within 0.5 and 6%, respectively.

2.5 Mechanical Tests

A Universal Testing Machine Instrom 1140 was used to obtain force-deformation curves. Samples (8–10) were sheared perpendicularly to the myofibres direction at 50 kg load and 40 cm/min crosshead speed. Cylindrical samples 1.5 cm ∅ were sheared in a Warner-Bratzler cell. A cylindrical 0.5 cm ∅ stainless steel plunger with round end was used for penetrometry.

3 Results & Discussion

Figure 1 shows typical DSC traces of the processed muscle meats normalized to dry matter content. Raw, untreated meat (R) exhibited the three main endothermic regions (myosin, sarcoplasmic proteins and collagen, and actin, respectively) with a total denaturation enthalpy of ~14.1, which compared well with bibliographic data. Conventional freezing (F) at high cooling rate and low temperature supposed very small changes with respect to the original R data (13.8). Pressurization at –21 °C resulted in a big protein denaturation: actin practically disappeared and myosin and sarcoplasmic proteins were highly reduced in the DSC trace (5.1). Freezing by fast decompression following the pressurization step produced relatively important additional unfolding effects (4.1). In contrast, collagen was very stable to any kind of pressurization (due to its hydrogen-bonded structure) and freezing, either single or in combination.

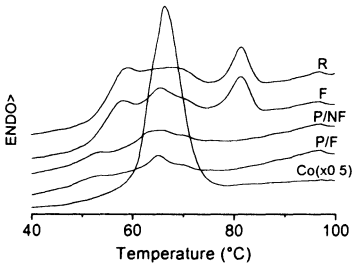

Fig. 1. Normalized (dry matter) DSC curves of muscle meat samples: R, untreated; F, frozen; P/NF, pressurized-non-frozen; P/F, pressure-assisted frozen; Co(×0.5), pressure-assisted frozen connective tissue (half ordinate scale sensitivity)

Obviously, these DSC data corresponded to the thermal denaturation (in the calorimeter scan) of the "native-like" protein fraction of the processed sample overcoming the respective treatment. Then, the lower the DSC figure obtained the higher the denaturing character of the corresponding process. In this respect, DSC data were coherent with results previously reported on pork meat batters [1] and blue whiting mince [2] subjected to pressure/heat combinations. Antagonistic effects were detected there: pressure (interdependently with temperature) caused

protein denaturation at non-denaturing temperatures but preserved protein from subsequent thermal denaturation at thermal unfolding conditions.

Figure 2 shows the breaking force F_{max} (N) for Warner-Blatzler (WB) and penetrometry (P) tests. WB data on raw R and air frozen F samples were significantly higher than data corresponding to pressurized meats P/NF and P/F. Penetration data showed, however, an inverted pattern since samples R and F were softer than pressurized meats, P/NF being in turn significantly softer than pressure-assisted frozen P/F. Intact stromal proteins, mainly collagen, may mask the effects derived from (pressure induced) protein denaturation and microstructural changes in the myofibres (TEM is in progress). In this respect it seems that penetrometry would be more convenient concerning protein denaturation.

In summary, hydrostatic pressurization at subzero temperatures of muscle meat (protein systems, in general), either with or without pressure-assisted freezing, was certainly a very disadvantageous kind of process with respect to conventional freezing.

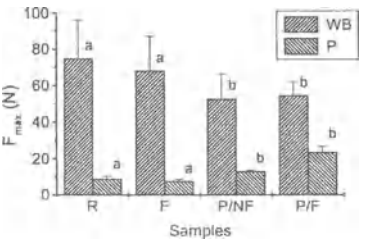

Fig. 2. Breaking force F_{max} (N) and s.d. for Warner-Blatzler (WB) and penetrometry (P) tests on muscle meat samples: R, untreated; F, frozen; P/NF, pressurized-non-frozen; P/F, pressure-assisted frozen. Different letters indicate significant ($P<0.05$) differences

References

[1] Fernández-Martín, F., Fernández, P., Carballo, J., Jiménez Colmenero, F. (1997); Pressure-heat combinations on pork meat batters: Protein thermal behavior and product rheological properties; J. Food Agric. Chem., 45, 4440–4445.

[2] Fernández-Martín, F., Pérez-Mateos, M., Montero, P. (1998); Pressure-heat combinations on blue whiting (*Micromesistius poutassou*) mince: Thermal and mechanical properties; J. Food Agric. Chem., 46, 3257–3264.

Texture and Structure of High-Pressure-Frozen Food Gels

M. Fuchigami and A. Teramoto

Okayama Prefectural University, Faculty of Health and Welfare Science, Dept. of Nutritional Science, 111 Kuboki, Soja, Okayama 719-1197, Japan
fuchigam@fhw.oka-pu.ac.jp

Abstract. To determine the effect of high-pressure-freezing on quality, agar, carrageenan and gelatin gels with 0, 5, 10, 20% sucrose were frozen at 100–700 MPa at ca. –20 °C then thawed at atmospheric pressure. Texture and structure of gels frozen at 200–400 MPa improved in comparison to gels frozen at 0.1 MPa (frozen in freezers at –20 °C, –30 °C or –80 °C) or 100, 600 and 700 MPa, but differed from the original gel. As the concentration of sucrose increased, appearance, texture and structure of gels improved. Gels were also thawed at high pressure, then pressure was reduced. Texture of gels frozen at 200–400 MPa was the same as the original gel. This indicated that phase transitions (ice VI → ice V → ice III → liquid → ice I) occurred during reduction of pressure at –20 °C. Thus high-pressure freezing-thawing at 200–400 MPa was effective on the improvement in quality of frozen gel.

1 Introduction

With food gels of high water content (e.g. tofu, konjac, agar), damage to structures through freezing is extensive and the texture after thawing becomes unacceptable. Such gels frozen at atmospheric pressure (0.1 MPa) do not recover their gel phase when thawed. During phase transition from water to ices, ice I expands in volume, but high pressure ices (ice II – ice IX) do not [1,2]. If the high density property of high pressure ices is applied to frozen food gels, damage of gels may be retained. Thus, tofu has been discussed previously [3,4]. The results were as follows: high-pressure-freezing at 200, 340 and 400 MPa appeared to be effective in improving both the texture and structure of frozen tofu. The objective of this study was to research the effects of high pressure and sucrose on the improvements in texture and structure of frozen food gels (agar, carrageenan and gelatin) containing a lot of water.

2 Materials & Methods

1.5% agar gel, carrageenan gel (0.8% locust bean gum added to 0.7% kappa-carrageenan) and 5% gelatin gel {with 0%, 5%, 10% or 20% sucrose (w/w)} were used. Seven pieces (15 mm dia and 10 mm thick) of gels were sealed in polyethylene bags. Four packs of samples with various concentrations of sucrose were put into a pressure vessel (6 cm inside dia and 20 cm high) previously kept at ca. –20 °C, and immediately pressurized for 45 min at 100 MPa (ice I), 200 MPa (liquid phase), 340 MPa (ice III), 400, 500, 600 MPa (ice V) or 700 MPa (ice VI) using a high pressure food processor (Dr. Chef, Kobe Steel Ltd.). After reduction of pressure, gels were stored for 1 d at –30 °C then thawed at 20 °C (gelatin: 15 °C). After the amount of syneresis was measured, the rupture stress and strain of gels were measured by a creepmeter (Rheoner, RE-33005, Yamaden Ltd.). The structure was observed with a cryo-scanning electron microscope (S–4500, Hitachi Ltd.) and the ice pore size of frozen gels was measured using software for image analysis (Mac-scope, Mitani Ltd.). They were compared with the unfrozen gels, pressurized gels, gels frozen in freezers (–20 °C, –30 °C or –80 °C) at 0.1 MPa or gels frozen-thawed at high pressure.

3 Results

3.1 Texture and Structure of Gels High-Pressure-Frozen-then-Thawed at Atmospheric Pressure

Pressurization at 15–20 °C did not affect visual appearance, texture and structure of gels. However, in agar gel frozen at 0.1, 100, 600 and 700 MPa, appearance, texture (stress-strain curves) and structure differed greatly from the original gel due to syneresis (Figs. 1 and 2). The pore size of gel without sucrose was large while the gel network contracted slightly. Therefore, the final rupture stress and strain increased. On the other hand, appearance of agar gel without sucrose, frozen at 200–400 MPa, was the same as the original gel. Although stress decreased and strain increased, they were more similar to the original gel than gel frozen at 0.1, 100, 600 and 700 MPa. The ice crystals in agar gel frozen at 200–400 MPa were smaller than in the agar gel frozen at 0.1, 100, 600 and 700 MPa. When agar gel was frozen at 200–400 MPa, texture and structure of frozen gel improved compared to gel frozen at atmospheric pressure, but differed from the original gel. These results suggest that ice I might be formed during reduction of pressure or during storage of gel in a freezer. Thus, the quality of agar gel becomes worse due to volume expansion by the formation of ice I.

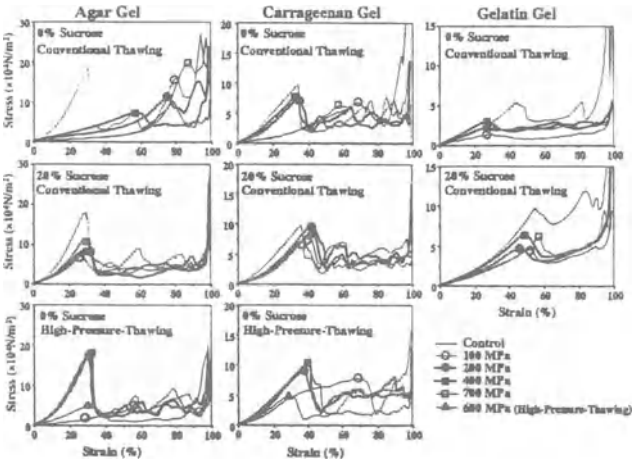

Fig. 1. Stress-strain curves of high-pressure-frozen gels

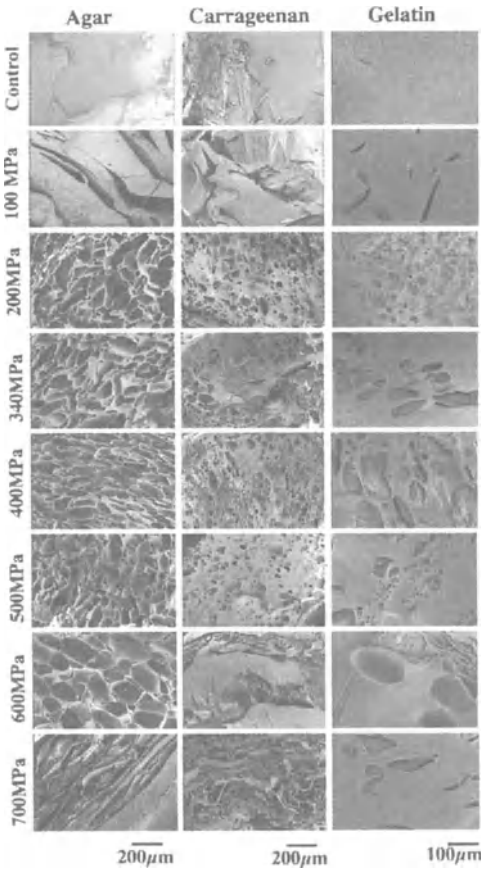

Fig. 2. Cryo-scanning electron micrographs of agar gel high-pressure-frozen-then-thawed at atmospheric pressure

When carrageenan gel was frozen at 200–500 MPa (gelatin gel was frozen at 200–700 MPa), the quality of frozen gels improved compared to gels frozen at 0.1 and 100 MPa (ice I). With an increase of sucrose, appearance, texture and structure of all gels improved significantly. The freeze-thaw tolerance of carrageenan and gelatin gels was better than that of agar gel.

3.2 Texture and Structure of Gels High-Pressure-Frozen-then-Thawed at High Pressure

To determine the phase transition of ices during reduction of pressure, high-pressure-frozen gels were thawed at the same high pressure after which pressure was reduced. Texture and structure of gels frozen at 200–400 MPa were the same as the original gels (Figs. 1 and 3). This indicates that phase transitions (ice VI → ice V → ice III → liquid → ice I) occurred during reduction of pressure at –20 °C, or during storage in the freezer. Thus high-pressure freezing-thawing at 200–400 MPa appears effectively to improve the quality of frozen gels.

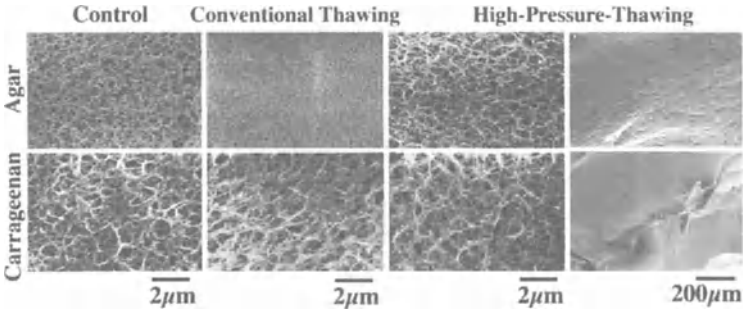

Fig. 3. Effect of thawing methods on minute structure of network of high-pressure-frozen gels without sucrose

References

[1] Fletcher, N. H. (1970); The chemical physics of ice, Cambridge University Press, London.
[2] Hobbs, P. V. (1974); Ice physics, Oxford University Press, London.
[3] Fuchigami, M. and Teramoto, A. (1997); Structural and textural changes in kinu-tofu due to high-pressure-freezing; J. Food Sci., 62, 828–832 & 837.
[4] Fuchigami, M., Teramoto, A and Ogawa, N. (1998); Structural and textural quality of kinu-tofu frozen-then-thawed at high-pressure; J. Food Sci., 63, in press.

High Hydrostatic Pressure Effects on Freezing and Thawing Processes of Pork Meat

C. Massaux, F. Béra, B. Steyer, M. Sindic and C. Deroanne

Faculté Universitaire des Sciences Agronomiques de Gembloux, Unité de Technologie des Industries Agro-Alimentaires, Passage des Déportés 2, B-5030 Gembloux, Belgium
Massaux.c@fsagx.ac.be

Abstract. Effects of high hydrostatic pressures (50, 100 and 200 MPa) are studied to evaluate the HHP interests in the freezing and thawing processes of pork meat. The results show thawing loss is clearly reduced by freezing-thawing under HHP. Among the studied procedures, the pressure of 100 MPa is the most interesting freezing-thawing for pork meat: there is no exudate, except the one induced by the vacuum-packing, and only slight discoloration and toughness of meat.

1 Introduction

High hydrostatic pressure (HHP) has interesting effects on the solid/liquid phase diagram of water. Water can remain in the liquid state down to about –22 °C at pressures up to 210 MPa [1]. This property allows rapid freezing and thawing of foods through pressure applications. During freezing, use of high pressure facilitates supercooling, and promotes uniform and rapid ice nucleation throughout the sample on pressure release, producing smaller ice crystals. Inversely, pressurization of frozen foods allows rapid thawing of a part of the ice. The pressurized sample is then heated to supply the heat of fusion of the part which is still solid and also to prevent recrystallization on depressurization [2]. This rapid thawing could limit mass transfers from cells, responsible for drip loss during classical thawing. Deuchi and Hayashi observed that high pressure thawing of beef results in reduced drip. However, higher pressures than 50 MPa cause denaturation of proteins resulting in whitening of meat [3].

The aim of the present research is to evaluate the HHP interests to improve the quality of frozen pork meat.

2 Materials & Methods

The *Longissimus dorsi* muscles of pork (24×6×6 cm), divided into three equal parts, are vacuum-packaged in polyethylene bags. A third is frozen and thawed under a same

high pressure (50, 100 or 200 MPa) and stored in the meanwhile at –20 °C, a third is directly placed in a freezer at –20 °C during 5 d and a third is maintained at +10 °C during 24 h in a cold room and used as a control. A first study has evaluated the effects of a 50 and a 100 MPa freezing-thawing and a second study, the effects of a 200 MPa treatment. Dry matter was determined by the official method (AFNOR 1976, NF V 04-401) and centrifugal drip by weight after centrifugation 30 min at 42,700 g. Thawing and cooking losses were determined by weight difference before and after treatment. Total loss was calculated by addition of thawing and cooking losses. Color of raw meat was characterized by C.I.E. values (L*, a*, b*) with a spectrocolorimeter Miniscan XE (Hunterlab). Changes in textural properties of cooked meat were evaluated by a Warner-Bratzler test with a texturometer SMS.TA-XT2.

3 Results

Figure 1 displays the different exudate (1 measure by sample) and the dry matter (mean of two measures) for each meat sample. We observe in this figure that thawing loss is clearly reduced by freezing-thawing under HHP. Treatments under 100 and 200 MPa display the same exudate than the one observed with unfrozen control samples. Cooking loss seems to be slightly increased by HHP treatment but total loss is less than the exudate obtained by classical freezing-thawing. By comparison with the classical freezing-thawing process, the 50 MPa treatment decreases slightly the thawing loss but does not reduce the cooking and total losses. Dry matter squares with the thawing loss: a smaller dry matter is in relation with a smaller thawing loss.

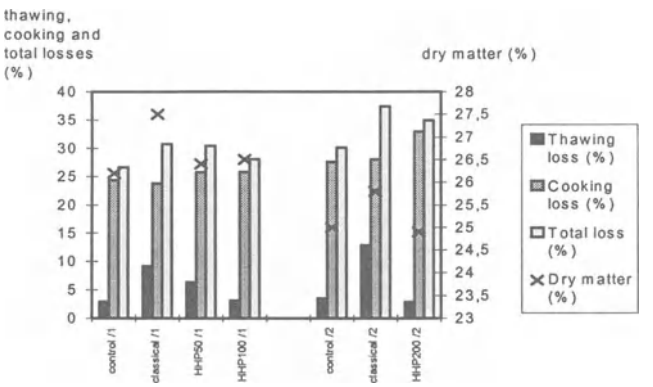

Fig. 1. Thawing loss, cooking loss, total loss and dry matter measured on control samples, classically frozen samples and HHP frozen samples

Figure 2 shows the centrifugal drip measured on each sample. The presented results are the mean of two measurements. We notice in this figure that centrifugal drip increases with applied pressure and is lower with unfrozen controls and

classically frozen samples. A high centrifugal drip is equivalent to a small water hold capacity and is probably worse for the meat quality.

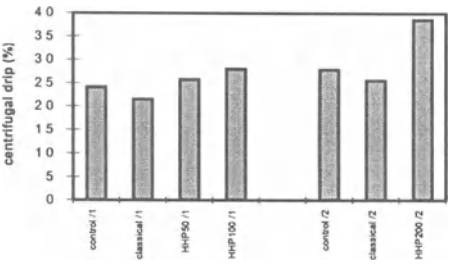

Fig. 2. Centrifugal drip measured on control samples, classically frozen samples and HHP frozen samples

Figure 3 presents the mean of ten hardness measurements realized on each meat sample. We see in this figure that textural properties are not really affected by a 50 or 100 MPa treatment but hardness of meat is clearly increased by a pressure of 200 MPa applied during freezing and thawing.

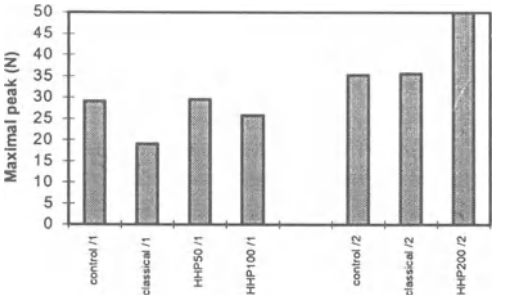

Fig. 3. Hardness measured on control samples, classically frozen samples and HHP frozen samples

Figure 4 displays the different parameters characterizing the color of meat samples (mean of 4 measures by parameters). We observe in this figure that the color of controls and classically frozen samples are similar. The pressurized meat displays a discoloration increasing with applied pressure. The meat whitening is characterized by a higher L* parameter and a lower a* parameter; b* parameter is equal for all samples.

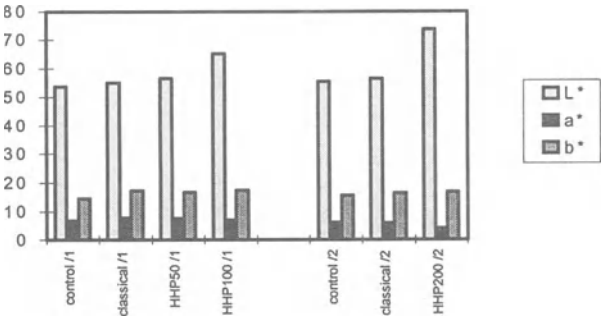

Fig. 4. L*, a*, b* values measured on control samples, classically frozen samples and HHP frozen samples

4 Conclusions

Among the studied procedures, the freezing-thawing process under a pressure of 100 MPa seems to be an interesting treatment for pork meat: there is no exudate, except the one induced by the vacuum-packing, and only slight discoloration and toughness of meat.

Acknowledgements: We thank 'Region Wallonne, Direction Generale des Technologies, de la Recherche et de l'Energie' for financing this research.

References

[1] Lüdemann, H.D. (1992); Water and aqueous solutions under high pressure, High pressure and biotechnology, Eds Balny C. *et al.*, colloque INSERM, 224, 371–379.

[2] Kalichevsky, M.T., Knorr, D. and Lillford, P.J. (1995); Potential food applications of high-pressure effects on ice-water transitions, Trends in Food Science & Technology, 6, 253–259.

[3] Deuchi, T. and Hayashi, R. (1992); High pressure treatments at subzero temperature: application to preservation, rapid freezing and rapid thawing of foods, High pressure and biotechnology, Eds Balny C. *et al.*, colloque INSERM, 224, 353–355.

Application of High Pressurization to Fish Meat: The Ultrastructural Changes and Nucleotide in Frozen Carp Muscle Under High Pressure Thawing

K. Yoshioka[1], A. Yamada[1], T. Maki[2], C. Yoshimoto[2] and T. Yamamoto[3]

[1]Department of Food and Nutrition, Faculty of Home Economics, Nakamura Gakuen University, Befu, Jonan-ku, Fukuoka, Japan
[2]Department of Research and Development, Ichiban Foods Co., Ltd,. Ikawa, Iizuka, Fukuoka, Japan
[3]Department of Nutrition Morphology, Graduate School of Health and Nutrition Sciences, Nakamura Gakuen University, Fukuoka, Japan

Abstract. Frozen carp muscle was thawed under high pressure and the ultrastructural changes and the nucleotide contents were compared with those thawed by running water. In high pressure thawing, each myofibril became loose but the sarcoplasm between myofibrils, the sarcoplasmic reticulum and the membranous structure were all well preserved. In running water thawing, the sarcoplasm between myofibrils was observed to expand and the membranous structures either disappeared or were vacuolated.

1 Introduction

High pressure is transmitted equally and instantaneously to the center of ice crystals. The thawing process of frozen fish muscles thawed under high pressure proceeds differently from that under atmospheric pressure, that is, the ice phase is considered to be transferred instantly into the liquid phase [1]. In this study, frozen carp muscles were thawed by exposure to high pressure and/or running water, and then were observed with an electron microscope. The physicochemical properties and ultrastructural changes of these muscles were also examined to evaluate the thawing procedure.

2 Materials & Methods

Live carp (*Cyprinus carpio*, 500–600 g average body weight) were purchased, killed by a blow to the head and instantly stored in the round at –25 °C for 30 d. The frozen carp were put into polyethylene bags, and then thawed by high pressure at 100 and 200 MPa for 10 min by a food pressurizing testing machine (Mitsubishi Heavy Industries MFP-7000) and by running water at 15–17 °C for 45–50 min. For

the electron microscopic observation each sample was filleted and small pieces were cut from the dorsal part of the sample. They were then fixed in half-strength Kalnovsky fixative buffered with 0.1 M phosphate at pH 7.4, followed by post-fixation with 1.0% osmium tetroxide. After dehydration in graded ethanol, they were then embedded in Epon 812. Ultrathin sections were cut, stained with uranyl acetate and lead, and observed using a transmission electron microscope (JEM 1200 II X). The physical properties of the filleted samples were examined for their breaking strength test, creep test, and the color difference (ΔE). In addition, the contents of inosinic acid monophosphate (IMP) from the frozen-thawed muscles were determined by high performance liquid chromatography (HPLC).

3 Results & Discussion

The changes in the ultrastructure of frozen-thawed carp muscles were observed under an electron microscope and compared with those of skeletal muscle fiber of fresh carp. The individual myofibrils of fresh carp muscle were regularly arranged and each myofibril measured about 1 micron in diameter. The Z-, I-, A-, M-, and H-bands could be clearly identified. In the center of the A-band, H-bands were observed and the H-bands were somewhat light. A sarcoplasmic reticulum and T-tubules were also observed in the sarcoplasm between myofibrils (Fig. 1). In electron micrographs of the muscle fibers at 200 MPa, the myofibrillar structures were found to be preserved but showed a rather loose appearance and the M-bands almost disappeared. A striation pattern was seen but the Z-bands were not clearly discernible. Some of the sarcoplasmic reticulum between myofibrils became vacuolated and the membranous structures also lost their structural organization. Based on these findings, high pressurization was thus thought to affect the protein of carp muscle [2]. To investigate the effect of high pressurization on thawing, carp fillet samples were also subjected to 100 MPa. In the same manner as after 200 MPa, the arrangement of myofibrillar filaments became loose and the M-band was seen unclearly and the Z-band was also somewhat vague. Thin filaments in the I-band were clearly observed and the sarcoplasm between myofibrils was comparatively well preserved, in which the membranous structure and sarcoplasmic reticulum were present (Fig. 2). While viewing the carp muscle fibers at l00 MPa under high magnification, irregular shaped vacuoles were observed in the sarcoplasm between myofibrils, which was considered to be affected by ice crystal formation (Fig. 3).

On the other hand, regarding the carp muscle fibers subjected to running water thawing, the myofibrillar structure was found to be mostly normally preserved. However, the sarcoplasm between myofibrils was found to have expanded, in which some of membranous structures disappeared and the mitochondria aggregated and lost their normal structures.

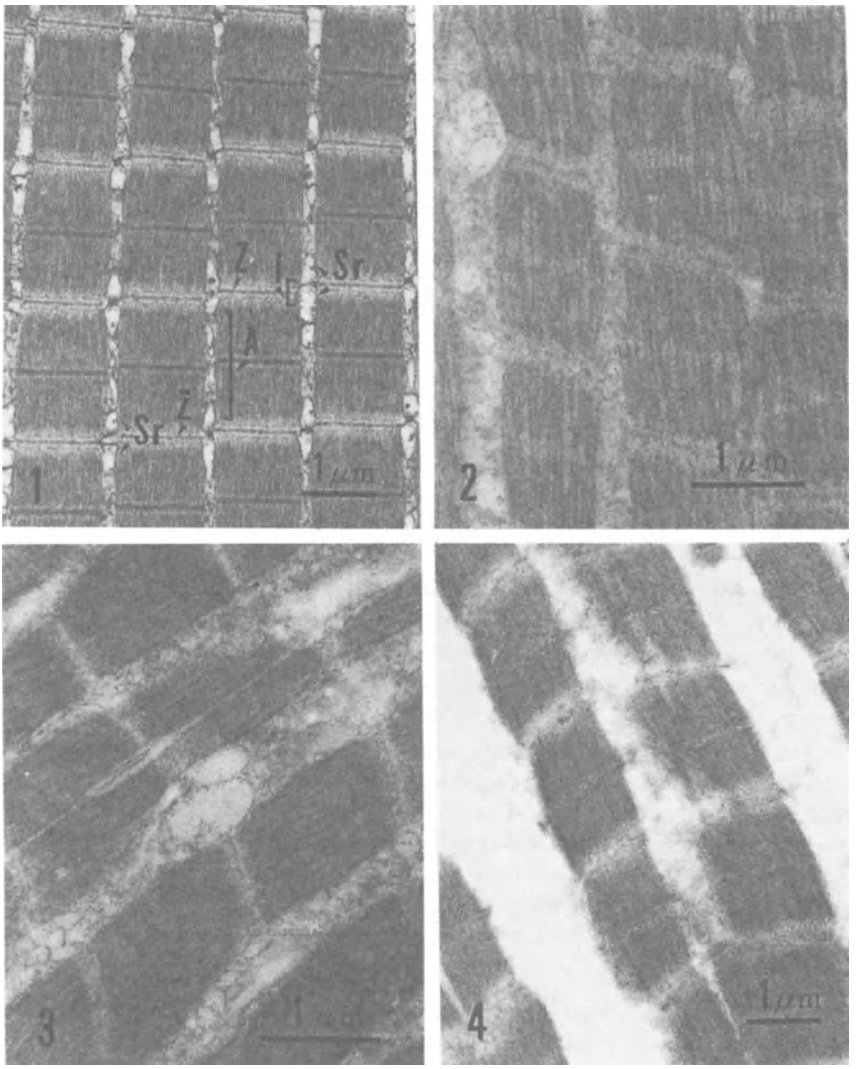

Fig. 1. A longitudinal section of skeletal muscle fibers of fresh carp. It shows individual myofibrils arranging regularly. The A-(A), I- (I) and Z(Z)-bands can be clearly seen.
Sr: sarcoplasmic reticulum

Fig. 2. A longitudinal section of carp muscle thawed at 100 MPa. A banding pattern of myofibrils is well preserved, though myofibrillar structure becomes loose

Fig. 3. A longitudinal section of carp muscle thawed at 100 MPa. Large vacuoles are seen in the sercoplasm between myofibrils which seemed to be produced by ice crystal formation

Fig. 4. A longitudinal section of carp muscle thawed by running water. The myofibrillar structure observed mostly normally preserved, but the sarcoplasm between myofibrils is found to have expanded and appears to be washed-out. The sarcoplasmic reticulum appeares to be vesicular in part

The sarcoplasmic reticulum appeared to be vesicular in part (Fig. 4). Under high magnification, the sarcoplasm between myofibrils were observed to noticeably expand and the membranous components disappeared, thus suggesting freezing and thawing to have influenced the muscle fibers.

To summarize these results, high pressure thawing affected the myofibrillar structure while each filament became loosely arranged and the banding pattern of myofibrils became unclear; however, the sarcoplasm between myofibrils remained well preserved Some sarcoplasmic reticulum were observed to be vacuolated. In comparison to the findings at 200 MPa, the membranous structure at 100 MPa was found to be less affected. In running water thawing, though myofibrillar structures were also relatively well preserved, the sarcoplasm between myofibrils expanded in which the sarcoplasmic reticulum became vacuolated and other membranous structure disappeared. All of those findings together represent the characteristics of carp muscles after the running water thawing.

Regarding the changes in physical properties, carp muscles under high pressure thawing demonstrated a high degree of viscoelasticity, compared with that observed under running water thawing [3]. The color difference (ΔE) in the flesh color also showed little difference between the muscles thawed under 100 MPa and those thawed under running water and both findings were also quite similar to those of fresh carp muscle. Furthermore the IMP content of frozen-thawed carp muscle decreased compared with that of the fresh muscle but the content of IMP was not so different in amount between high pressure thawing and running water thawing.

Based on the above findings, high pressure thawing and running water thawing of frozen carp muscles produced the ultrastractural changes of individual thawings, respectively. Such characteristics are considered to influence both the physical properties as well as the taste of fish muscle. These findings thus suggest that high pressure thawing at between 100 MPa and 150 MPa (under 200 MPa) results in preserving the good quality of fish meat.

References

[1] Deuchi, T. and Hayashi, R. (1992); High pressure treatment at subzero temperature: application to preservation, rapid freezing and rapid thawing of foods; (eds. Balny, C., Hayashi, R , *et al.* High Pressure Biotechnology), 224, 353–355. John Libbey Eurotext.

[2] Yoshioka, K. and Yamamoto T. (1998); Changes of ultrastructure and the physical properties of carp muscle by high pressurization; Fisheries Science, 64(1), 89–94.

[3] Yoshioka, K., Yamada, A., and Maki, T. (1996); Application of high pressurization to fish meat: Changes in the physical properties of carp skeletal muscle resulting from high pressure thawing; (eds. Hayashi, R. and Balny, C. High Pressure Bioscience and Biotechnology) ,13 , 369–374. Elsevier Science B.V.

New Experimental Methods, Applications and Equipment

A New Application of Moderate Hydrostatic Pressure for Efficient Detection of Living Yeast by Flow Cytometry

F. Abe and K. Horikoshi

The DEEP-STAR Group, Japan Marine Science and Technology Center, 2-15 Natsushima-cho, Yokosuka 237-0061, Japan
abef@jamstec.go.jp

Abstract. Application of non-lethal levels of hydrostatic pressure (30–50 MPa) was found to increase intracellular accumulation of carboxyfluorescein or carboxydichlorofluorescein 5- to 10-fold in the yeast *Saccharomyces cerevisiae*. This observation was confirmed by analysis of individual labeled cells by flow cytometry. Pre-incubation of cells at 30 MPa also induced dye accumulation at atmospheric pressure, indicating that hydrolysis activity of the prefluorochrome was induced by elevated hydrostatic pressure.

1 Introduction

There is an increasing demand for precise and rapid detection of microorganisms in foods or natural samples. Colony counting is a traditional method to enumerate viable cell numbers in a sample, but is time consuming and takes a few days. Flow cytometry combined with fluorescent staining is a relatively new and promising method for analysis of microorganisms [1]. Fluorescein diacetate (FDA) and its derivatives, such as carboxyfluorescein diacetate (CFDA) or carboxydichlorofluorescein diacetate (CDCFDA), are non-fluorescent molecules that defuse into cells and are hydrolyzed by intracellular non-specific esterases to give fluorescent products [2]. The fluorescent products can be accumulated only in those cells that have intact cell membranes, therefore, dead cells with leaky membranes are not stained. However the fluorescence intensity of labeled cells varies considerably among strains, probably because of differences in intracellular esterase activities. This may cause inaccuracy in detection of yeast cells in heterogeneous populations by flow cytometry. Recently, I have found that accumulation of CF or CDCF was facilitated by non-lethal levels of hydrostatic pressure. In this study, the effect of hydrostatic pressure on fluorescence staining of living yeasts with CDCFDA was analyzed, which may contribute to the efficient detection of microorganisms by flow cytometry.

2 Materials & Methods

Cells of *Saccharomyces cerevisiae* were grown in YPD (1% yeast extract, 2% bactopeptone, 2% D-glucose) broth at 24 °C. Cells ($2–4\times10^7$ cells/ml) were incubated with 10 μM CDCFDA in YPD containing 50 mM citric acid (pH 5.0), under hydrostatic pressures. After application of hydrostatic pressure for 1 h, the cells were washed and suspended in MB buffer (100 mM Mes/Bis-tris, pH 5.0). Fluorescence of the labeled cells (AU; arbitrary units) emitted at 535 nm with excitation at 485 nm was recorded as {F(labeled cells)-F(non-labeled cells)} per 10^7 cells.

Cells were incubated with 10 μM CDCFDA under several hydrostatic pressures for 1 h. After decompression, the labeled cells were washed twice with distilled water and resuspended with MB buffer. Cells were analyzed using the Bryte-HS Flow Cytometry System (Bio-Rad) at atmospheric pressure.

3 Results

Figure 1A shows the variability of CDCF-staining with different strains. Two strains, the sake yeast IFO2347 (strongly labeled strain) and IFO10159 (weakly labeled strain, which is less readily detectable by flow cytometry), were used in the following analysis. In IFO10159, total fluorescence intensity of CDCF-labeled cells (24.8 AU per 10^7 cells) was only 2.5-fold greater than non-labeled cells (9.9 AU per 10^7 cells). Application of hydrostatic pressure markedly promoted the accumulation of CDCF in both IFO 2347 and IFO10159, peaking at 30 and 50 MPa, respectively (Fig. 1B). Although there are no data to explain that the levels of enhancement would have a significant impact on detection limits in natural samples, application of moderate hydrostatic pressure could be potentially a new procedure for detection of living yeasts.

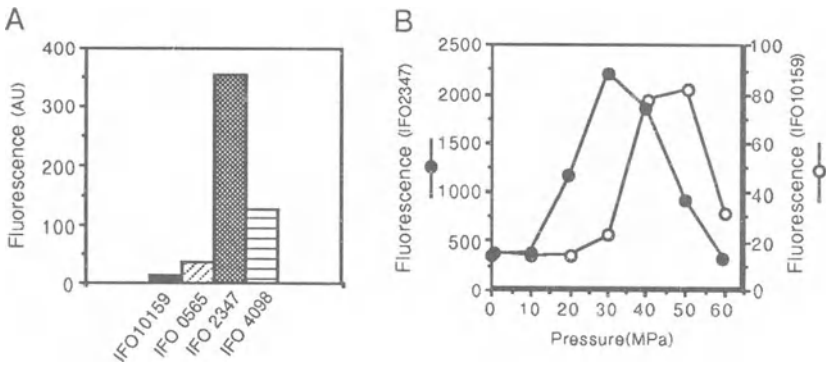

Fig. 1. **(A)** Variability of fluorescent staining with different strains. **(B)** Pressure-induced accumulation of CDCF in IFO2347 and IFO10159

Hydrostatic pressure above 40 MPa markedly inhibited cell growth; however, cell survival determined as relative CFU was not considerably affected by application of hydrostatic pressure for 1 h [3]. Therefore, it is evident that hydrostatic pressure can enhance CDCF-staining in the absence of cell proliferation or significant loss of viability, as necessary for precise determination of viable cell number in a sample.

Figure 2A shows the histograms of populations of IFO2347 cells labeled with CDCFDA under several hydrostatic pressures. When the cells were labeled at atmospheric pressure, the peak and mean fluorescence of labeled cells were 23 and 26 AU, respectively (Fig. 2A, 0.1 MPa). When the cells were subjected to a pressure of 30 MPa for 1 h, the accumulation of CDCF increased 4- to 6-fold. The peak and mean fluorescence were 92 and 162 AU, respectively (Fig. 2A, 30 MPa). However, staining was not enhanced at a pressure of 60 MPa (Fig. 2A, 60 MPa). Similar results were obtained with IFO10159 [4]. These results of flow cytometry analysis are mostly consistent with the results obtained by ordinary fluorescence analysis shown in Fig. 1B.

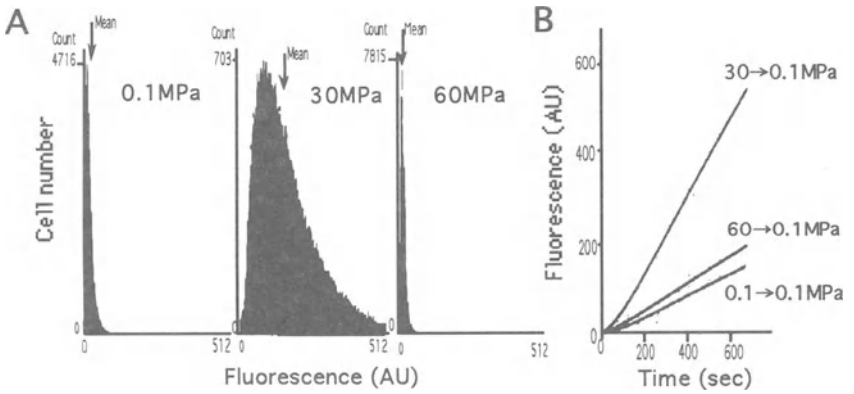

Fig. 2. (**A**) Histograms of populations of CDCF-labeled cells. (**B**) The effect of hydrostatic pressure on hydrolysis of CDCFDA in IFO2347. Cells were pre-incubated at 0.1, 30 or 60 MPa for 1 h, subsequently 50 μM CDCFDA was added

Cells were preincubated at several hydrostatic pressures for 1 h in YPD (pH 5.0), and subsequently the hydrolysis activity was measured at atmospheric pressure. Figure 2B shows the changes in fluorescence emission after addition of 50 μM CDCFDA to the pressure-adapted cells. The cells adapted to 30 MPa hydrolyzed CDCFDA at a rate approximately three times greater than that observed in the case of cells adapted to 0.1 MPa or 60 MPa. These results indicate that preincubation of the cells at 30 MPa induced CDCFDA-hydrolysis activity, and it was maintained after decompression.

4 Discussion

In a preliminary experiment, hydrolysis of CFDA and CDCFDA in both MB buffer and cell extract is simply facilitated by elevated hydrostatic pressure, which means the chemical reaction of dye hydrolysis accompanies negative volume changes ($\Delta V^{++}<0$). Preincubation of cells at a pressure of 30 MPa promoted the accumulation of CDCF, suggesting that hydrostatic pressure may (i) induce the synthesis of esterases, (ii) promote the hydrolytic activity of esterases, (iii) promote the passive diffusion of prefluorochrome CDCFDA through the cell membrane, or (iv) stimulate glucose metabolism required for dye hydrolysis at 30 MPa, because the metabolism has a role in the process [4]. We have reported that an increase in hydrostatic pressure to 40–60 MPa promotes the acidification of vacuoles [3, 5]. Such an increase in hydrostatic pressure also induces acidification of the cytoplasm (unpublished data). It is likely that a reduction of vacuolar pH by 0.2–0.3 might affect the activity of some esterases. It would be worthwhile analyzing the effect of moderate hydrostatic pressure to fluorescent staining in other yeast species or bacteria. Although the precise course of the induction pathway is still unclear, these findings may contribute to improved methods of analysis by flow cytometry, and reveal the necessity of investigating intracellular metabolic events in living organisms under hydrostatic pressure.

References

[1] Davey, H., and Kell, D.B. (1996); Flow cytometry and cell sorting of heterogeneous microbial populations: the importance of single-cell analyses; Microbiol. Rev. 60, 641–696.

[2] Breeuwer, P., Drocourt, J.-L., Bunschoten, N., Zwietering, M.H., Rombouts, F.M., and Abee, T. (1995); Characterization of uptake and hydrolysis of fluorescein diacetate and carboxyfluorescein diacetate by intracellular esterases in *Saccharomyces cerevisiae*, which result in accumulation of fluorescent product; Appl. Environ. Microbiol. 61, 1614–1619.

[3] Abe, F., and Horikoshi, K. (1995); Hydrostatic pressure promotes the acidification of vacuoles in *Saccharomyces cerevisiae*; FEMS Microbiol. Lett. 130, 307–312.

[4] Abe, F. (1998); Hydrostatic pressure enhances vital staining with carboxyfluorescein or carboxydichlorofluorescein in *Saccharomyces cerevisiae*: Efficient detection of labeled yeast by flow cytometry; Appl. Environ. Microbiol. 64, 1139–1142.

[5] Abe, F., and Horikoshi, K. (1997); Vacuolar acidification in *Saccharomyces cerevisiae* induced by elevated hydrostatic pressure is transient and is mediated by vacuolar H^+-ATPase; Extremophiles 1, 89–93.

In Situ Viscosity Measurement During the Ultra High Pressure Treatment of Fluid Food Systems

P. Först and A. Delgado

Lehrstuhl für Fluidmechanik und Prozessautomation, Weihenstephaner Steig 23, D-85350 Freising
foerst@lfp.blm.tu-muenchen.de

Abstract. Two techniques to measure the viscosity of fluid food samples during the ultra high pressure treatment have been developed and validated for different kinds of liquids at ambient pressure and elevated pressure up to 7000 bar. First measurements for different model liquids were carried out and the effects of pressure and temperature on the viscosity were studied and compared with literature data.

1 Introduction

The presented work deals with *in situ* viscosity measurement techniques for the investigation of basic physical or chemical processes during the ultra high pressure treatment of fluid food systems, which are not yet well understood. High hydrostatic pressure may induce molecular structural changes of the different food ingredients, see e.g. [1]. There are no measurement devices suitable for fluid food ingredients available for this pressure range. The maximum pressure applied is 7,000 bar. Up to now only pressure viscosity data for lubricants [2], water and some organic liquids [3, 4], but not for food ingredients are available in literature.

2 Experimental Setup

Inductive Method (IM). This technique refers to a rolling ball method as described in [5] but with a variable inclination angle. The proportional control factor between sphere velocity and viscosity was found by calibration with viscosity standards at ambient pressure.

For the measurements the pressurised tube is disconnected from the manual pump (2) and mounted on a positioning device (1). The tube is kept at constant temperature by a water jacket connected to a thermostat. The moving sphere in the high pressure tubing is detected by an inductive method, i.e. a small voltage peak is produced when the sphere made from steel passes one of two pickup-coils

integrated in an oscillatory circuit surrounding the high pressure tube. The signal is filtered and amplified and triggers a multi-counter (Fig. 1).

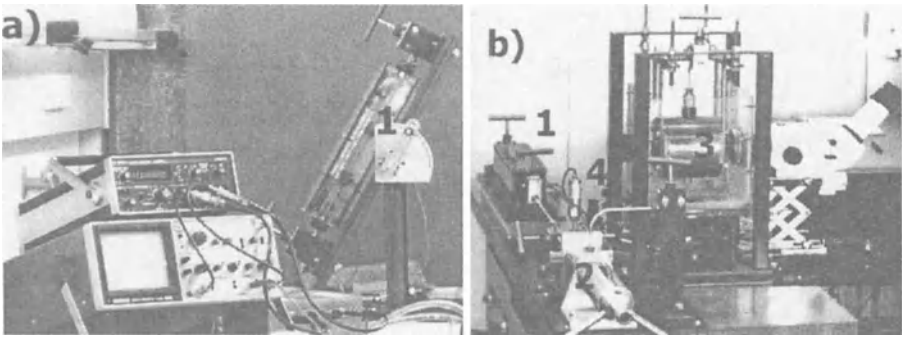

Fig. 1. (**a**) Measurement setup for the inductive method. (**b**) Manual pump (2) for both methods with inductive tube (1), optical cell (3) for the optical method and pressure transducer (4)

Optical Method (OM). Small glass microspheres (diameter 50 μm) are injected at the top of the optical cell at ambient pressure. The sedimentation behaviour of the microspheres is observed through the optical window of the high pressure cell by a light microscope (Zeiss, Jena) after the pressure is raised. As yet the time is measured by a stop watch. The viscosity can be calculated from the settling velocity according to Stokes law and so absolute viscosity values are obtained. Exact knowledge of the density difference is required either by literature or by separate accurate measurements. The diameter ratio of sphere to inside diameter of the optical cell is less than 3.5×10^{-3}. For this reason wall effects are negligible. The optical method is only applicable for transparent fluids.

3 Comparison of Methods

Some test measurements for water and sucrose solution were made to compare the results of both methods and to find out measurement uncertainties. Additionally the results were compared with high pressure literature data [3, 4] for water. The accuracy at ambient pressure was good for both methods (<2% relative error). At high pressure the measurement uncertainty is increased for the following reasons:

- Pressure expansion of tube (IM)
- Compressibility of sphere and fluid (both methods).

The compressibilities of the spheres are very small, therefore the change in diameter can be neglected (rel. error <0.5%). The change in solid density is more pronounced and produces a maximum additional error of ca. 1.5% (for glass at 7000 bar). The fluid density data are extracted from literature [6] for water, from product information sheets (Wacker Chemie, Burghausen) for polydimethysiloxane and measured for sucrose solution by compression tests.

The pressure expansion of the tube (IM) produces a slight change of inside diameter of 0.6% at maximum pressure. Unfortunately the proportional control factor depends strongly on the annular gap between sphere and tube. As the function is known [5] and the expansion of the gap dependent on the internal pressure can be calculated [7] the pressure dependence of the proportional control factor can be determined. If this correction is made the results of both methods are in good agreement. Figure 2 shows the results for water and sucrose solution (40% w/w) and literature data for water.

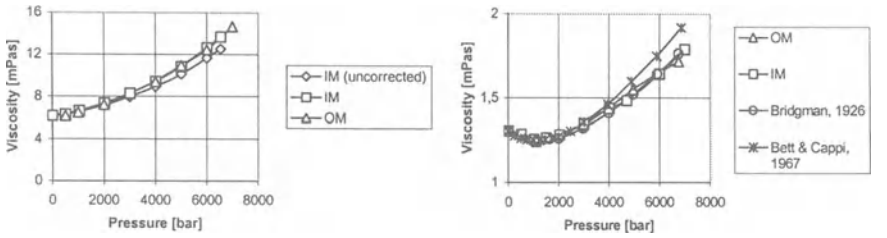

Fig. 2. Comparison of both methods and literature data for (**a**) sucrose solution (40% w/w, 20 °C) and (**b**) distilled water (10 °C)

4 Results & Discussion

For both measurement devices it is possible to determine the viscosity as a function of pressure and temperature within a error margin of 5% even at maximum pressure. The additional error at elevated pressures is mainly due to uncertainties in pressure-density data for the fluids. Both systems are easy to handle. To test the systems with regard to their applicability for fluid food systems the following model fluids were used: polydimethylsiloxane (AK10) as a nonpolar fluid and both water (W) and sucrose solutions (SS) of different concentrations as polar fluids. The influence of pressure and temperature on the viscosity is shown in Fig. 3.

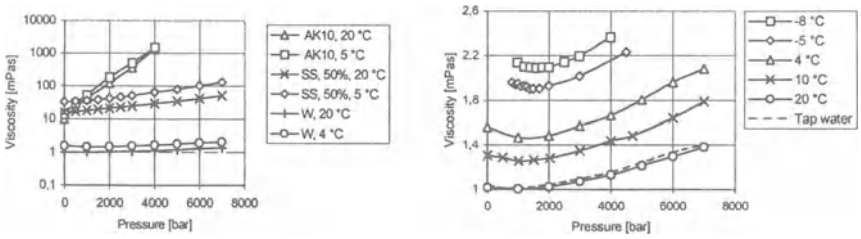

Fig. 3. The influence of pressure and temperature on the viscosity for (**a**) different liquids and (**b**) distilled water as well as tap water (20 °C , not visible due to the small deviation of less than 2.5%)

Figure 3a shows the applicability of the systems in a wide viscosity range as the pressure viscosity behaviour is strongly dependent on the kind of liquid. The viscosity of polydimethysiloxane shows a much more pronounced pressure dependence than water or sucrose solution.

Figure 3b shows viscosity measurements of distilled water at different temperatures in the range of –8 °C to 20 °C.[1] This plot shows that - in contrast to the other fluids studied - the viscosity decreases for low pressures and only increases at higher pressures. The position of the minimum viscosity value is shifted towards lower pressures if the temperature is raised. The total effect of pressure on the viscosity is small in the pressure range regarded here. For 20 °C a measurement for filtrated tap water was carried out to see if a difference between distilled water and tap water could be detected. The measuring device (IM) was sensitive enough to detect the small difference.

There is a need for more measurements to interpret the strongly different manner in which fluids with different molecular structures behave and to set up a model to predict the pressure viscosity behaviour. For the investigated liquids besides water an exponential viscosity pressure function is found to adequately describe the behaviour for higher pressures, but for low pressures (<1000 bar) this function does not seem to be valid.

For the used setup the viscosity of water is situated at the lower end of the measurement range. The viscosity range can be further extended in both directions by adjusting the diameter and density of the sphere (both methods) and the inner diameter and inclination angle of the tube (IM) to approximately 10^4 Pas. Additionally, fluid density data can be determined with the used setup by a double measurement set with spheres of different densities.

References

[1] Johnston, D.E.: High Pressure. In: Johnston, D.E.; Ledward, D.A.; Knight, M.K. (eds): The Chemistry of Muscle Based Foods. Cambridge: Royal Society of Chemistry, 1992, 298–307.

[2] Larsson, P.O.; Jonsson, U.: A New High Pressure Viscometer. Tribologia 16 (1997), 31–48.

[3] Bridgman, P.W.: The Effect of Pressure on the Viscosity of forty-three Pure Liquids. Am. Acad. Arts Sci 61 (1926), 57–99.

[4] Bett, K.E.; Cappi, J.B.: Effect of Pressure on the Viscosity of Water. Nature 207 (1965), 620–621.

[5] Hoeppler, F.: Der exzentrische Fall von Kugeln in Hohlzylindern mit Flüssigkeiten oder Gasen. Z. Tech. Physik 14 (1933), 165–169.

[6] Saul, A.; Wagner, W.: A fundamental equation for water covering the range from the melting line to 1273 K at pressures up to 25000 MPa. J. Phys. Chem. Ref. Data 18 (1989), 1537–1564.

[7] Buchter, H.H.: Apparate und Armaturen der Chemischen Hochdrucktechnik. Berlin, Heidelberg, New York: Springer-Verlag, 1967.

[1] Water remains fluid at sub-zero temperatures for the investigated pressure range here.

Sample Preparation for Molecular Diagnostics by Pressure Cycling

J.A. Laugharn, Jr.[1], F. Tao, L. Sciaba-Lentz, D.W. Bradley and R.A. Hess

[1]BMA Laboratories, Inc., and BioSeq, Inc., 25 Olympia Avenue, Unit F, Woburn, MA 01801-6307, USA
jlaugharn@bmalabs.com

Abstract. The utility of pressure-assisted cell lysis was studied to demonstrate the potential usage of high pressure in the first steps of sample preparation for *in vitro* molecular diagnostics. Pressure cycling between liquid and solid phase provided sufficient lysis of yeast, a model system of difficult-to-lyse biological material. A DNA yield of 32% was achieved by one cycle of pressure changing from 200 MPa for 5 min to atmospheric pressure at –5 °C versus 10% at 15 °C. Multiple pressure cycles improved the DNA yield. The DNA and RNA obtained from pressure lysed cells were suitable for molecular diagnostic analysis. This novel lysis process is easy, fast, efficient, scalable, economical and automatable for high-throughput sample analysis.

1 Introduction

Sample preparation of DNA, RNA and proteins, from biological materials for *in vitro* molecular diagnostic analysis of cancer and infectious disease is problematic and costly [1]. Sample and specimen preparation for cancer and infectious disease analysis is performed on diverse types of biological fluids, (e.g. plasma, sputum, broncioalveolar lavage) and biological tissues (e.g. solid tumor material). In addition, numerous cellular components and diverse targets (e.g., DNA, RNA and protein) may need to be monitored simultaneously. Here, we demonstrate that pressure is useful to lyse difficult cells and recover DNA by pressure cycling.

Saccharomyces cerevisiae (yeast) was chosen as a model system of a biological material that is difficult to lyse. To evaluate the factors that influence the lysis, we varied pressure and temperature, as well as buffer components and additions of lysing enzymes, glass beads, and ribonuclease inhibitors. Constant and pulsing pressure were evaluated. The effectiveness of the lysis methods was determined by DNA/RNA qualitative and quantitative analysis.

Pressure-assisted freezing-thawing method can be useful in cell lysis, and in addition, it has the potential to achieve multiple purposes, such as, preservation of enzymatic activity of proteins and RNA integrity, as well as inactivation of contaminant microorganisms [2, 3].

2 Materials & Methods

The custom-built pressure instrument used in this study, BaroCycler™ (Bioseq Inc.), requires less than 10 s to reach the desired pressure level and the sample is easily accessible in less than 5 s. Pressure was transmitted via ethylene glycol/water to samples sealed in 250 µl micro-centrifuge tubes. The temperature of the sample chamber was controlled by a circulating water bath.

Yeast (Sigma, MO, USA) was cultured overnight in YPD medium, and counted using a hemacytometer. 10^6 to 10^8 cells were first pelleted at 10,000 rpm for 1 min and washed with phosphate buffered saline (PBS, pH 7.4) and the supernatant was removed. Cells were resuspended for pressurization in either 250 µl of a bentonite[1] solution (1% bentonite in PBS, pH 6) or 270 µl of detergent lysis buffer (2% Triton X 100, 1% SDS, 100 mM NaCl, 10 mM Tris-Cl, pH 8, 1 mM EDTA). Samples were stored frozen at –70 °C prior to pressurization.

After pressure treatments, each sample was briefly vortexed, and centrifuged at 10,000 rpm for 1 min. The supernatant was collected and nucleic acids were extracted by PCI (phenol/chloroform/isoamyl alcohol, 25:24:1), followed by ethanol precipitation. The sample was resuspended in TE buffer (10 mM Tris, 1 mM EDTA, pH 7.5).

Prior to the quantitative assays, samples were treated with RNase cocktail (Ambion, Inc., TX, USA) to remove RNA at room temperature for 30 min. Quantitative assay was conducted using a PicoGreen DNA assay (Molecular Probes, WA, USA) by measuring the fluorescence intensity (λ_{ex}=490 nm, λ_{em}=530 nm).

The positive control of the yeast lysis experiments was obtained by following a glass bead yeast lysis protocol [5]. Yeast cells were washed with PBS and resuspended in 270 µl detergent lysis buffer. The sample was vortexed for 3 min in the presence of 500 µl PCI and 100 mg acid washed glass beads. Supernatant was collected after centrifugation at 12,000 rpm for 5 min. The quality of the nucleic acid samples were then assayed by agarose gel electrophoresis or the PicoGreen assay.

3 Results

The pressure effects were studied under various temperatures. Pressure was also cycled so that liquid/solid phase changes occur during the lysing process.

3.1 Constant Pressure Treatments at Various Temperatures

Yeast samples in the bentonite solution were treated at temperatures of 25, 48 and 86 °C, and various pressure levels ranging from 170 to 540 MPa, for 4 min comprising a 2 min incubation at atmospheric pressure and 2 min incubation at 250 MPa.

[1] Bentonite (Aldrich, WI, USA) is a clay which is known to inhibit ribonucleases.

Agarose gel electrophoresis showed that there were pressure-induced increases in yeast lysis at 25 °C in the pressure range tested. At higher temperature, 48 and 86 °C, more lysis occurred at all pressure levels. A positive pressure effect was observed at 25 and 48 °C, but less at 86 °C, because lysis occurred without applying pressure at this high temperature.

A temperature profile of yeast lysis under cryobaric condition is shown in Fig. 1a. Detergent lysis buffer was used. The percentage of DNA yield was obtained by comparing the fluorescence intensity of the pressurized sample and that of the positive control in the PicoGreen assay. It shows that close to 40% DNA was released from one pressure cycle. Relatively high DNA yields were obtained at sub-zero temperatures, suggesting that cycling between liquid and solid phases or compression of ice crystals may contribute to the lysing process.

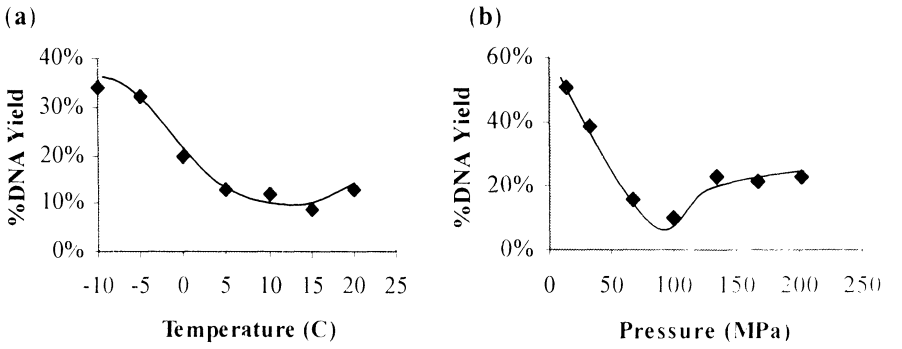

Fig. 1. %Yield of yeast genomic DNA from one pressure cycle (5 min at 200 MPa, 5 min at 1 atm) (**a**) at various temperatures and (**b**) various pressures at –5 °C

3.2 Pressure Profile at Sub-Zero Temperatures

Figure 1b shows two mechanisms of the pressure lysis. Between 100 and 200 MPa, at –5 °C, the increase of DNA yield could be due to the pressure-induced phase change. The higher yield at 200 MPa may be contributed by the freeze-thaw and pressure. Note, at –5 °C, the thawing occurs at close to 50 MPa [4]. Surprisingly, it was also observed that high DNA yields were also obtained at 14 MPa and 34 MPa. This may be caused by shearing due to rearrangement of ice crystals in respect to pressure. Microscopic explanation needs further investigation.

3.3 Phase Cycling Enhanced Yeast Cell Lysis

The cryobaric yeast lysis was found to be cycle-dependent and high efficiency was obtained after multiple cycles of pressure-driven phase changes (Fig. 2a). The agarose gel (Fig. 2b) shows that the quality of the DNA from the cryobaric process was identical to the positive control.

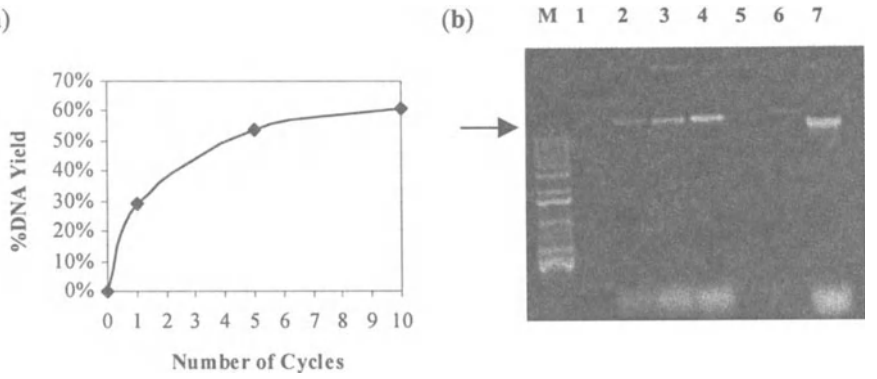

Fig. 2. Yeast lysis with various number of cycles (1 min at 250 MPa and 1 min at 1 atm) (**a**) at –5 °C. An agarose gel stained by SyberGreen (Molecular Probes) (**b**) shows the same DNA samples as in (**a**). Arrow indicates the position of the yeast genomic DNA. Lane 1, sample had no pressure treatment (0 cycle, 20 min at room temperature); Lane 2–4, 1, 5 and 10 cycles; Lane 5, yeast resuspended in distilled water, room temperature for 20 min; Lane 6, atmospheric pressure freeze-thaw once; Lane 7, glass bead method, a positive control

4 Conclusions

Similar amounts of genomic DNA, and total RNA were detected in the supernatant of pressurized cell suspensions compared to the positive, glass-bead lysed control. Cell lysis was much less in samples that had been manually temperature cycled between –70 °C and 25 °C at ambient pressure (our negative controls in the demonstrated experiments), than the ones that were pressurized at –5 °C.

In our laboratory, using high pressure lysis of various biological materials, such as plant leaf, mammalian cells, microbes, and bacteria, we have successfully performed molecular biology analysis using pressure treated samples, such as, DNA sequencing, RT-PCR, PCR, mammalian cell transfection and restriction digestion (data not shown). Since this process occurs at sub-zero temperatures, this technique may be beneficial for some temperature and/or chemical-sensitive sample preparation processes, such as proteomics and forensic science.

References

[1] Persing, D.H. *et al.*; (1993) Diagnostic Moleucular Microbiology; ASM, DC, USA.
[2] Shigehisa, T. *et al.*; (1996); High Pressure Bios. Biotech.; Hayashi & Balny (Eds) 273–278.
[3] Ferrão-Gozales, A. *et al.*; (1997); High Pressure Research Bios. Biotech.; Heremans (Ed); 95–98.
[4] Denys, S.; ibid; 351–354.
[5] Rose, M.D. *et al.*; (1990); Methods in Yeast Genetics: a Laboratory Course Manual; Cold Spring Harbor Laboratory Press, NY, USA.

An *In Situ* Technique To Visualize Temperature and Velocity Fields in Liquid Biotechnical Substances at High Pressure

M. Pehl and A. Delgado

Lehrstuhl für Fluidmechanik und Prozeßautomation, Technische Universität München, D-85350 Freising, Germany
pehl@lfp.blm.tu-muenchen.de

Abstract. A first application of encapsulated thermochromic liquid crystals (TLCs) for the visualization of temperature and velocity fields in pressurized liquids has been studied experimentally. By means of a tempered high pressure optical cell, investigations have been carried out over wide temperature ranges and at pressures up to p=700 MPa. Two parameters were observed and analyzed during pressurization: the inhomogeneous temperature fields and concurrently occuring velocity fields. The motion of the test liquid is composed of forced and natural convection. The results illustrate that TLCs provide a suitable means of investigating thermodynamic fluid processes under high pressure. As such, the visualization of temperature and velocity fields using TLCs can be a key technique for the study of physicochemical phenomena occuring in high pressure applications.

1 Introduction

In high pressure applications an increase of the substance temperature is caused by pressurization. In the case of inhomogeneous temperatures, thermal convection may also take place. Furthermore, forced convection occurs during pressurization as a result of the incoming flow into the vessel generated by the diminishing specific volume. Both convection and gradients of temperature can be of considerable importance during high pressure investigations because they affect heat and mass transfer which, in turn, affect biological and physicochemical processes. Hence, the need for knowledge of these fields is often emphasized but as of yet no adequate measuring technique has been available.

For these reasons a technique to detect temperature and velocity fields in liquids at high pressure is being developed. The technique is based on the temperature sensitivity of the selective reflection of light from the liquid crystal particles. Simultaneously, the particles are used as tracers to visualize the flow field. This in situ technique permits a detailed study of temperature and velocity fields of high pressure applications.

2 Materials & Methods

The liquid crystal measuring technique provides an efficient total field method to examine the thermodynamic fluid processes in flow fields at normal pressure, e. g. [1–3]. The technique is based on the selective reflection shown by cholesteric liquid crystals when they are illuminated with white light. The molecules have a helical structure whereby the axial spacing of its turns (pitch) and reflected wavelengths depend on the temperature, see also [4]. Selectively reflected wavelengths of unsealed liquid crystalline substances at high pressures up to 300 MPa were observed by Pollmann and Wiege [5] but a measuring technique as developed in the present study is not described in literature.

The experiments are performed by using a tempered pressure cell with four sapphire windows (∅=6 mm) as shown schematically in Fig. 1. The cell volume (2 ml) is illuminated by a sheet of white light. Right angled to the incident light sheet the field is recorded by a fixed 3-chip RGB-camera.

In this study, six types of TLCs were used and each type had a different detectable temperature range and temperature resolution. TLCs with a starting-temperature (temperature at the beginning of red colour) between –30 and +30 °C and a bandwidth (temperature difference between the red and blue colours) between 0.7 and 10 °C were used. In order to disperse the oily liquid crystal particles in the distilled water sealed TLCs (∅=10–150 μm) from the manufacturer Hallcrest (UK) were used.

The TLCs are encapsulated in a transparent polysaccharide. In this first feasibility study the colours were estimated visually by eye.

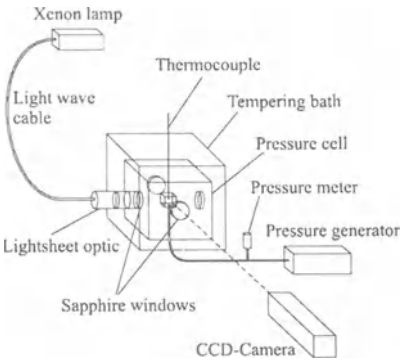

Fig. 1. Scheme of the experimental setup

3 Results

The isochromics of TLCs with a starting-temperature of 10 °C and a bandwidth of 1 °C are shown in the diagram of temperature vs. pressure in Fig. 2. The data was recorded as follows: the cell was tempered and a thermal equilibrium was attained,

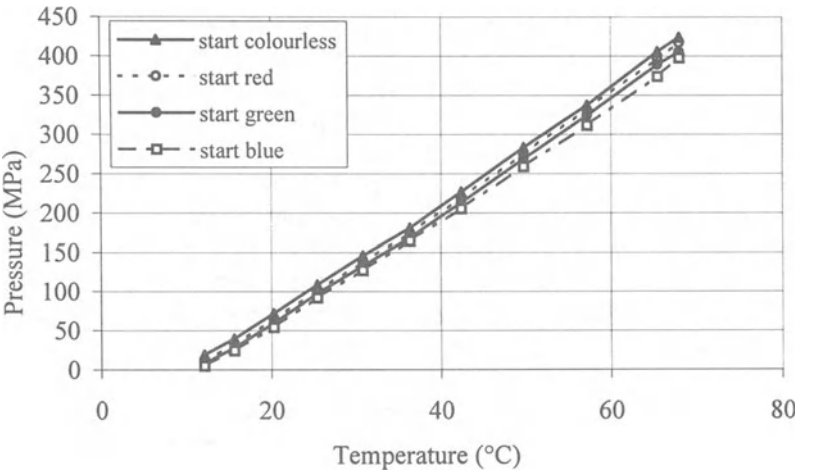

Fig. 2. Isochromics in the diagram of temperature vs. pressure, TLC- type BM/R10C1W/S-40

the liquid was pressurized to the beginning of a given colour and the thermal equilibrium was awaited again, and finally the pressure was accurately adjusted again to the beginning of the given colour and the data was recorded. In Fig. 2 the isochromics have been found to show a near linear dependence.

It can be concluded that an increase in pressure causes an increase of the helical pitch whereas an increase in temperature causes an opposite effect.

In addition to the measurements described above other samples of TLCs were tested. Using TLCs with lower starting-temperatures (down to –30 °C) the results showed that the "working scope" can be shifted to higher pressures while keeping the temperature constant. In all cases, an enlargement of the bandwidth with respect to pressure was found. However, a temperature resolution of about 0.5 °C can also be attained at high pressures. When large bandwidth TLCs were used at high pressures it became increasingly difficult to estimate the beginning of a given colour and the isochromics drift from a linear relationship. However, consecutive tests showed a relative standard deviation of <1.1%, except for the blue isochromics (this was caused by the indistinctable colour variation change from violet to blue that cannot be observed with the naked eye).

The developed measuring technique has already been proven because temperature gradients and their respective colour patterns have been found in water using TLC particles at pressures up to 7000 bar. Small TLCs ($\varnothing \approx$ 10–20 μm) were used to visualize flow fields in water and aqueous solutions because the force of their mass becomes negligible. In order to see the velocity fields and to estimate the time of decay in the test chamber small TLC particles were dispersed in distilled water. Under different boundary conditions (pressurizing time, temperature, and level of pressure) a mean velocity was calculated from the average of the highest velocities in the four areas of the velocity field (Fig. 3), whereby the direction of

the convection was not considered. When the liquid is pressurized fast the mean velocity is high because of the forced convection. Moreover, Fig. 3 shows that for all different boundary conditions a decay time of about 200 s was found. As shown in Fig. 3 a good heat and mass transfer is given for times <50 s.

Finally, it can be concluded that gradients of temperature and velocity are caused by pressurization. This new aspect must be taken into consideration because heat and mass transfer depend strongly on the temperature and velocity field. The experimental results found have shown the suitability of the measuring technique developed here. In future studies, we are going to automatize the technique by means of an image analyzing system in order to achieve higher resolution and reproductibility of temperature and velocity data.

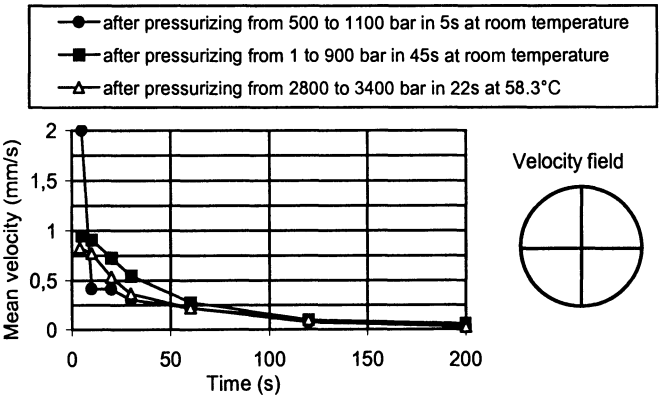

Fig. 3. Mean velocity in water after pressurizing, TLC-type BM/R10C1W/S-40

Acknowledgements: The authors would like to acknowledge the financial support for this work provided by the "Bund der Freunde der Technischen Universität München e. V.".

References

[1] Wozniak K., Wozniak G., Siekmann J. (1996); Non-Isothermal Flow Diagnostics Using Microencapsulated Cholesteric Particles; Applied Sci. Research 56: 145–156.

[2] Treuner M., Delgado A., Rath H., Duda U., Szymczyk J., Siekmann J. (1992); Experimental investigation of thermal Marangoni-convection in large-sized drops; Proc. of the 4th international symposium on experimental methods for microgravity materials science research, 2.–5. March 1992, San Diego, California, USA: 115–120.

[3] Duda U., Pehl M., Siekmann J. (1997); Plateau-Experimente zur Untersuchung der thermokapillaren Konvektion; Forsch. Ingenieurwesen 63: 52–63.

[4] Chandrasekhar S. (1992): Liquid crystals, 2nd ed., Cambridge: University Press.

[5] Pollmann P., Wiege B. (1987); Helix inversion of cholesteric liquid crystals at high pressure. Selective light reflection measurements on binary mixtures up to 3000 bar and 130 °C. Mol. Cryst. Liq. Cryst. 150b: 375–386.

Transport Phenomena in Foods Under High Hydrostatic Pressure

Y. Lambert[1,2], G. Demazeau[1], A. Largeteau[1] and J.-M. Bouvier[2]

[1]Ecole Nationale Supérieure de Chimie et de Physique de Bordeaux,
Interface Hautes Pressions, Avenue Pey Berland, BP 108, 33400 Talence, France
phone: +33 5 56 84 27 37 ; fax: +33 5 56 84 27 10
lambert@chimsol.icmcb.u-bordeaux.fr
[2]CLEXTRAL, Z.I de Chazeau, BP 10, 42 700 Firminy, France

Abstract. The effect of high hydrostatic pressure treatments on the mass transport and diffusion of sugar (sucrose) in apple cuts has been evaluated. Experiments have shown how high pressure increases the mass transport effect. With an increase in the sugar content of the foodstuff and a consequent reduction in the water content some foods could be stabilized by high pressure. The effects of pressure between 200 and 800 MPa, time from 2 to 120 min, temperature between 4 and 40 °C and the sugar concentration of the solute have all been studied.

1 Introduction

The diffusion-impregnation procedure relies on the food solid, either whole or cut into pieces, being immersed in a solution that contains a high solution of the solutes (generally sugar or salts) and/or flavors. The application of high pressure then induces the transfer of the solute or the flavors from the immersion fluid to the solid [1]. The result is a fixing, or impregnation, of a proportion of the solute in the foodstuff. It is accompanied to a lesser degree by a reduction in the water content of the solid or its solutes. An objective is to minimize the loss of any solutes from the food solid but a reduction in the water content of the foodstuff is an advantage since that would enhance the conservation of the product. An especially interesting feature of the process is that it can allow the transfer of a variety of agents into the foodstuff (conserving agents, textural additives, natural or artificial aromas, color agents, etc.) and can favor the desorption of a part of the water in the foodstuff thus permitting a better conservation [2]. It has been suggested that high pressures could be used in the preliminary stages of food preparation [3,4].

The variables in this diffusion/impregnation process are: the treatment pressure, the duration of the treatment, the temperature, the composition of the immersion fluid and the concentration of the solute and size and shape of samples.

2 Materials & Methods

2.1 Preparation of Samples

The investigations all used the same variety of apple, the 'Granny Smith', that was obtained from normal retail outlets. These apples are all calibrated (Table 1).

Table 1. Characteristics of the Granny Smith apples used in the investigations

Characteristics	Average and range for representative sample of Granny Smith apples
Mass	216.4 g (±7.1 g)
Volume	227.9 cm^3 (±18.2 cm^3)
*Water content	82.44% (±0.32%)
*Sugar content	12.8% (±1.25%)

The cut pieces of apple were prepared from peeled whole apples, washed in water and manually cut into cubes with sides of from 2.5 to 3 cm. The pieces were then dropped into syrup (water and sucrose mixture). The average weight of cube sample was 170.1 g (± 16.1 g) and the volume of syrup used for each sample cube was 250 cm^3. The samples were thermo-sealed in plastic bags (CRYOVAC-NOP-120, Soplaril, France). Before and after pressurization the samples were stored at 4 °C.

2.1.1 Water Content. The water content of each of the apple samples before and after the high pressure treatment was measured with a humidity analyzer (MA 30 Sartorius, France). Each measure was repeated 4 times.

2.1.2 Sugar Content. Sugar content in each sample of apple cut before and after the high pressure treatment was measured with Enzymatic Bioanalysis Food Analysis, Sucrose/D-Glucose/D-Fructose, Boehinger Manheim Cat No 716260. Each measure was repeated 4 times.

2.1.3 High Pressure. Treatment. The samples were pressurized in the experimental prototype Hyperbar designed by FRAMATOME and NFM-Technology. Its useful volume is 3 l it can work at pressures from 0 to 800 MPa and its temperature range is from –20 to +80 °C. The maximum rate of increase in pressure is 500 MPa per minute.

3 Results & Discussion

The high-pressure treatment results in the penetration and impregnation of sucrose in the apple pieces that are immersed in syrup (cf. Fig. 1). Sugar gain in the apple (see (1)) increases by 60% at 200 MPa and 80% at 800 MPa. Sugar content of fresh apple is 12.8%, after high pressure treatment at 200 MPa it is 20.7%.

$$\text{sugar gain} = \frac{(\text{sugar content of apple after treatment - sugar content of apple before treatment})}{\text{sugar content of apple before treatment}} \times 100 \quad (1)$$

The distribution of sugar in the apple is uniform. Values differ by only 2% between the center and the outside surface of the apple.

For the reference sample (3 d at atmospheric pressure in sucrose solution at 30% and 20 °C) distribution is uniform only if the time of immersion is over 3 d. Amount of sugar in the apple increases by 60% (cf. Fig. 1). Sugar content of the reference sample after 3 d is 19.4%.

Sugar gain of the apple at increasing pressures is accompanied by the transfer of water to the surrounding solution. Dilution factor (see (2)) increases with increase in pressure. After treatments at 200 MPa and 800 MPa, sugar content of the solution are respectively 26% and 24.5%.

$$\text{dilution factor} = \frac{(\text{sugar content of solution before treatment})}{\text{sugar content of solution after treatment}} \quad (2)$$

Sugar concentration and water desorption reach a plateau, or saturation level, at a certain pressure: no increase in sugar concentration exists beyond 600 MPa (cf. Fig. 1). There is only a 20% gain in sugar concentration for an increase in pressure from 200 MPa to 800 MPa.

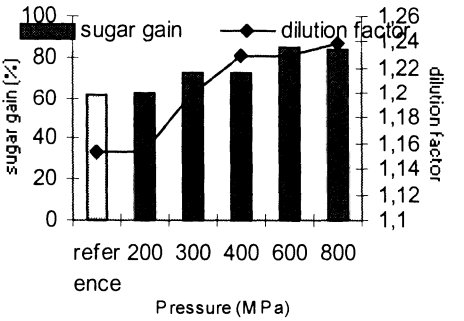

Fig. 1. Effect of pressure (10 min, 20 °C) on sugar gain of apple and dilution factor of solution in sucrose solution (30%)

A high-pressure treatment at 400 MPa for 2 min allows an increase in the sugar content of apple. Sugar gain in the apple increases by 23% for 2 min and 83.4% for 60 or 120 min (cf. Fig. 2). Large gains are possible in sugar concentration with increase in time.

There is a limit to sugar increase reached at 60 min. After 60 min at 400 MPa sugar content in apple is saturated. Indeed sugar content of apple is 22.2% when sugar content of solution is 24.4%. The difference of concentration between apple and solution decreases after 60 min so there is no gradient.

However uniform distribution of sugar in the apple always exists, even with short times (2 min).

Water desorption of apple and dilution factor of solution increase for an increase in time (cf. Fig. 2). Water loss does not seem to be limited by a long time of treatment. Dilution factor increases between 60 min and 120 min, sugar content of the solution decreases from 24.5% to 24%. Increasing time of treatment causes a dehydration of the foodstuff.

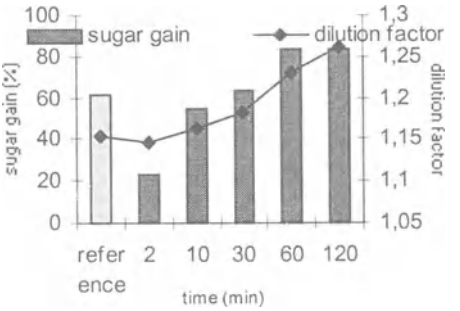

Fig. 2. Effect of time of pressurization (400 MPa, 20 °C) on sugar gain of apple and dilution factor of solution in sucrose solution (30%)

Time seems to be more significant than pressure for the diffusion/impregnation process. There is 60% more sugar in apple after 60 min compared to that after 2 min and only 20% more sugar in apple at 800 MPa or 600 MPa compared to at 200 MPa (cf. Figs. 1 and 2).

Increasing the temperature of treatment increases the viscosity of sucrose solution [11] but temperature changes have very little effect on the sugar increase in the foodstuff (cf. Fig. 3). Sugar content of fresh apple is 12.8%, after treatments at 4 °C and 40 °C, sugar content of the apple are gained respectively of 7.7% and 7.85%. Sugar gain in the apple increases by 56.5% for a high-pressure treatment at 4 °C and 64% at 40 °C (cf. Fig. 3).

Temperature changes have very little effect on the rate of water desorption from the foodstuff. Dilution factor is not modified (cf. Fig. 3), it changes from 1.18 at 4 °C to 1.19 at 40 °C. Degree Brix of the solution is 25.4 after treatment at 4 °C and 25.2 after pressurization at 40 °C.

The two-way mass transfer of sugar from solution to foodstuff and of water from foodstuff to solution is favored by an increase in the sucrose concentration of the solution (cf. Fig. 4). There is a disproportionate gain in the sugar content of the foodstuff for a given increase in the sucrose concentration of the solution: a sugar gain of 2.9% with solution at 15° brix compared to a sugar gain of 106.5% with

solution at 50° brix. Consequently it is possible to multiply sugar content in apple by two with a syrup at 50° brix. The water desorption of the foodstuff is proportional to the sugar concentration of the solution. Increasing concentration of solution, dilution factor is increased (cf. Fig. 4). Degree Brix of the sucrose solutions (15° and 50°) are respectively decreased to 14.6° and 38.6° after high pressure treatment at 400 MPa for 10 min at 20 °C.

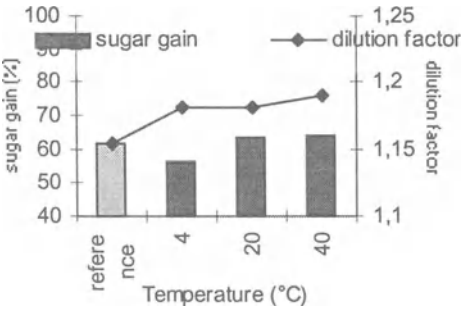

Fig. 3. Effect of temperature (400 MPa, 10 min) on sugar gain of apple and dilution factor of solution in sucrose solution (30%)

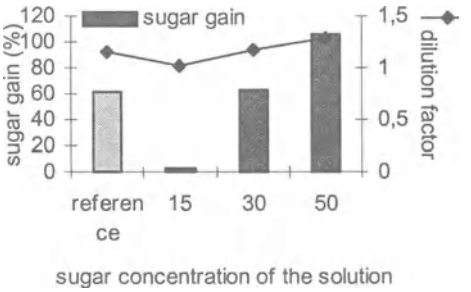

Fig. 4. Effect of sugar concentration of solution on sugar gain of apple and dilution factor of solution (400 MPa, 10 min, 20 °C)

As shown in Figs. 1–4 a high-pressure treatment at 400 MPa for 10 min at 20 °C in sucrose solution at 30% gives the same results of sugar impregnation that reference (3 d at atmospheric pressure in sucrose solution at 30% and 20 °C).

4 Conclusions

These experimental results have shown, with apple and sugar solution, only time and concentration of solution seem to have a significant effect on the diffusion/impregnation process under high pressure. But other parameters might be more significant as you change the characters of the foodstuff and the solute.

It would be very interesting to be able to create a mathematical model of the diffusion process under high pressure. In particular, it would be very useful to correlate and to evaluate diffusivity of Fick's law with pressure.

References

[1] Tonello C., Kesenne S., Muterel C., Jolibert F., Augmentation de la durée de conservation de produits à base de fruits traites sous hautes pressions hydrostatiques, Proceeding Agoral 97, 1997, pp. 477–482. Ed.: Lavoisier tec&doc, Paris.

[2] Raoult-Wack A.L., Les procédés de déshydratation-imprégnation par immersion dans des solutions concentrées, Thèse de doctorat, Université de Montpellier II, 1991.

[3] Knorr D., Advantages opportunities and challenges of high hydrostatic pressure application to food systems, High Pressure Bioscience and Biotechnology, 1996, pp.279–287. Ed.: Hayashi R., Balny C., Elsevier, Amsterdam.

[4] Bohuon P., Deshydratation-Impregnation par immersion en solutions ternaires: etude des transports d'eau et de solutés sur gel et produits d'orgine animale, Thèse de doctorat, Université de Montpellier II, 1995.

Engineering Solutions for Research, Pilot and Production High Pressure

M. Freeman

Stansted Fluid Power Ltd., 70 Bentfield Road, Stansted, Essex CM24 8HT, UK
Mark_Freeman@SFP-4-hp.demon.co.uk. http://www.sfp-4-hp.demon.co.uk

Abstract. The design and manufacture of high pressure equipment and systems is an evolving technology and this paper examines the considerations for high pressure systems for research, pilot and production for bioscience, biotechnology and food processing. Factors affecting the design of research and pilot systems will be discussed along with equipment solutions, particular reference being made to recent developments in in-line processing by high hydrostatic pressure and high pressure homogenisation.

1 Introduction

High pressure equipment and systems have been established for many industrial and research applications for a number of years to pressures in the range of 200 to 400 MPa. However, with the application of high pressure to bioscience, biotechnology and food processing there has been a requirement to work at increased pressures up to 1000 MPa. Stansted Fluid Power Ltd. has been involved in high pressure equipment and systems design and manufacture for nearly thirty years and has been working with the bioscience and biotechnology applications for most of this period. As a result of this work the company has developed equipment and systems especially to meet the requirements of the market. Having established a range of user friendly systems for researchers, internal and customer driven developments continue to evolve quality engineering solutions for pilot and production systems.

2 Research Systems

The essential feature of a research system should be its ability to simulate all possible process conditions as precisely as possible. Research systems must therefore in most instances demonstrate more control and process flexibility than the eventual pilot and production systems that may be developed from experiments and studies conducted on them.

It is an all too common experience to find that research systems have been poorly defined or implemented so that the research work it limited by the performance of the experimental systems. At Stansted Fluid Power Ltd. the aim is to develop systems that meet or exceed the requirements of the experimental program for which they are intended (Fig. 1). For high pressure bioscience and biotechnology there are three essential parameters that must be controlled: pressure, temperature and residence time; in addition there is a need to control pressure and temperature ramp rates to fully model a process.

It is important that all aspects of future scale up are considered and the limitations of experimental equipment understood and accounted for in scale up plans. If an industrial process will achieve pressure in a short time i.e. <15 s it is essential that the experimental simulations have also simulated this so that factors associated with pressure ramp rate can be evaluated. An easily overlooked, but important, consideration is the effect of relative thermal mass and heat transfer for the product and pressure chamber. While primary parameters can generally be simulated, the small scale of most research systems compared with production plant will mean that heat transfer within the systems is significantly different. This must be considered and evaluated if heat transfer or temperature control is important to process, as would be vital in a "pressure shift freezing" application.

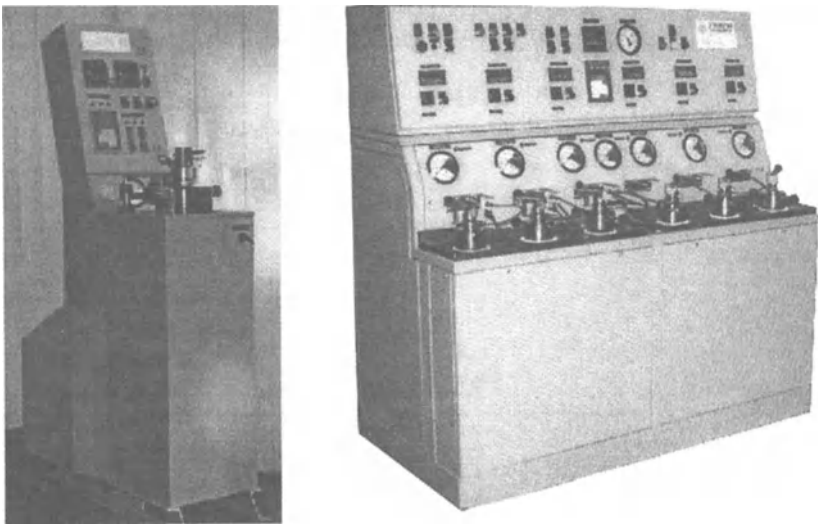

Fig. 1. Examples of laboratory systems for high hydrostatic pressure research. The left hand photograph shows a small 330 ml × 900 MPa general purpose research system, the right hand figure shows a multiple vessel kinetics study system for Unilever Research, Vlaardingen laboratory. This system has six 30 ml chambers and may be pressurised 0–900 MPa in <2 s. The system also allows independent temperature control of each chamber, ramp rate control on pressurisation and decompression and has a computer controlled interface

3 Pilot & Production Systems

Pilot and production systems must provide the facility to perform processes dictated by the results of experimental studies; as such these system are usually designed for a specific task and Stansted Fluid Power Ltd. offer customised solutions for particular processing requirements (Fig. 2). However, while pilot and production systems do not generally need to perform to the extremes that are demanded of experimental systems, these systems present their own demands on equipment manufacturers. As processes near commercial implementation new design considerations not normally associated with high pressure equipment, but required for the food processing industry, must be taken into account. These new considerations are primarily associated with cleanliness of equipment. In systems where batch treatment of containerised products are processed the requirements do not generally require significant new engineering and cleaning routines as the products are not in contact with the equipment only packaging/containers. Where "in-line" treatment is involved there are many challenges that must be overcome to produce a system that meets industrial processing requirements. It is often the case that the practices of good high pressure design do not fit in well with normal food processing equipment practices and can necessitate some compromise and/or novel design to produce suitable systems.

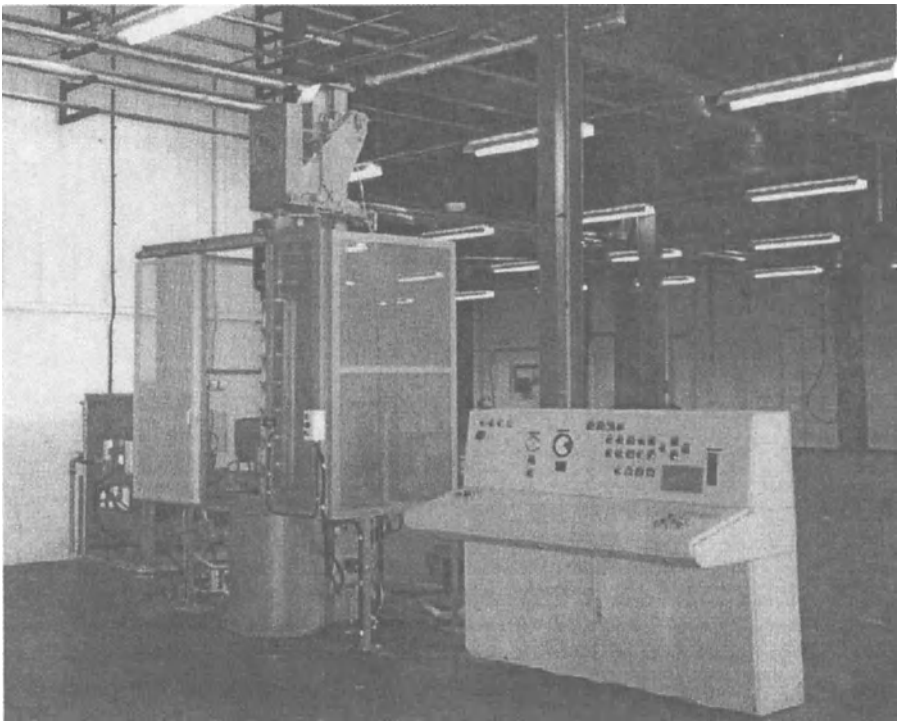

Fig. 2. Example of pilot scale production equipment

4 High Pressure Homogenisation

Stansted Fluid Power Ltd. has been involved with high pressure homogenisation and cell rupture systems since the early 1970s when with the National Institute of Medical Research in London a continuous flow high pressure system was developed. Subsequent evolution has created a large range of systems for applications in bioscience, biotechnology and food industries. Recent interest in utilising high pressure homogenisation as a preservation technique has lead to new developments to meet the requirements of this application. The technique utilises the heavy shear generated by high pressure homogenisation, generally in the 150 to 300 MPa range, to mortally damage spoilage organisms. The process has the advantages over high hydrostatic pressure of being a continuous treatment and not requiring pressure vessels, which are the major cost items on these systems. As a pasteurisation method with potential to be developed for sterilisation it is essential that all product is treated under the appropriate conditions. Traditional plunger pumps and intensifier systems typically have large pressure fluctuations during the pump cycle, which potentially allows a proportion of the product to pass through the system inadequately processed. In addition, at pressures above 100 MPa plunger pumps may become unreliable. To overcome these problems Stansted Fluid Power Ltd. has developed an intensifier based pumping system in which, by synchronised overlapped operation of two long stroke hydraulically driven intensifiers, the pressure pulse is virtually eliminated (Fig. 3). Furthermore, slow cycling of the intensifiers reduces wear and fatigue to produce robust and reliable solutions.

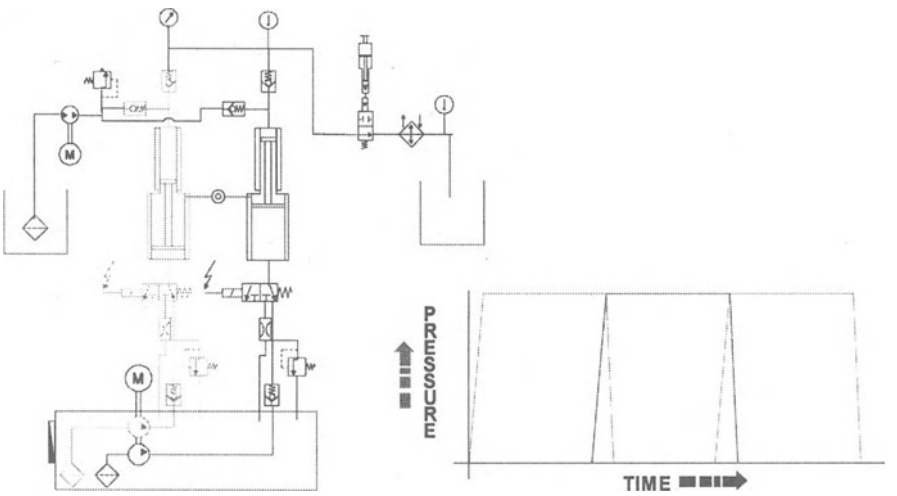

Fig. 3. Simplified schematic of twin synchronised intensifier system with pressure vs. time graph for the system illustrating smooth delivery

High Pressure and Preservatives for Cosmetics – New Data and First Practical Experiences

T. Vardag[1], R. Schmidt[2] and M. Jager[2]

[1]Uhde Hochdrucktechik GmbH, Buschmuehlenstraße 20, 58093 Hagen, Germany
VardagT@uht.krupp.com
[2]Nutrinova GmbH, Industriepark Hoechst, 65926 Frankfurt, Germany
SchmidtR@msmnutri.hoechst.com

Abstract. Current changes in consumer attitude towards cosmetic products as well as additional regulatory requirements have prompted cosmetics producers to look more carefully at ingredients with regard to their safety and environmental impact. One consequence has been the replacement of some previously used preservatives by "gentle" alternatives. In the past, we have reported on a technology combining the application of potassium sorbate with a high pressure treatment allowing the production of microbiologically safe cosmetic products, without the need for more aggressive preservatives. In this concept the action of the high pressure treatment leads to a significant reduction in the initial microbial counts while a "gentle" preservative ensures the required in-use protection and makes high pressure technology more cost efficient. In order to verify if potassium sorbate provides the required protection against recontamination during use, consumer tests have been performed to simulate "real life" conditions. First results indicate that, following a high pressure treatment, potassium sorbate at 0.3% is sufficient to protect an o/w-creme packaged in a jar and used every day in a typical environment.

1 High Pressure Treatment and Preservatives for Product Decontamination

1.1 Stability and Antimicrobial Effectiveness of Preservatives in Combination with High Pressure

In our previous work on this subject [1] we reported that high pressure treatments at 500 to 6000 bar do not affect the stability of sodium benzoate or potassium sorbate. This was seen as a prerequisite for using these preservatives together with a high pressure process. We concluded that these preservatives are principally suitable to provide product protection following high pressure treatment.

The high pressure treatment of the samples for the stability trials and the in-use testing have been performed in a 4 l Uhde pilot plant designed for pressures up to 6000 bar (Fig. 1).

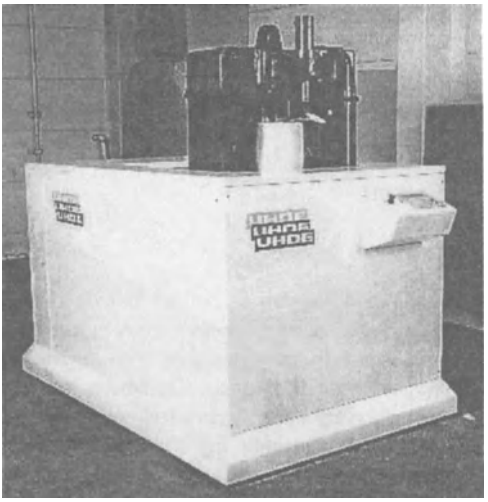

Fig. 1. Uhde pilot plant

1.2 Synergistic Effects Between High Pressure Treatment and Potassium Sorbate

It has also been shown that high pressure treatment and potassium sorbate act synergistically in reducing microbial counts of previously contaminated samples [2]. While in some cases high pressure treatment under the conditions applied was not sufficient to inactivate all microorganisms, the same treatment in the presence of potassium sorbate resulted in lower residual CFU. These inactivation trials have been run in an o/w-creme and an o/w-skin milk.

1.3 Kinetic Studies on Inactivation of *Staphylococcus aureus*

Staphylococcus aureus was shown to be the most resistant of all test organisms to high pressure. Therefore it was chosen for kinetic studies to evaluate process characteristics in more detail. All other microorganisms were completely inactivated at 4000 bar and 30 min holding time at room temperature. No growth occurred in these samples after a subsequent storage period of 1 year.

1.3.1 Synergistic Effect of High Pressure Treatment and Potassium Sorbate. When a citrate buffer of pH 5.7 contaminated with approx. 10^7 CFU/ml of *St. aureus* was exposed to pressure at 4000 bar and 25 °C the rate of inactivation was increased in the presence of 0.3% potassium sorbate (Fig. 2). This synergism indicates enhanced efficiency of the process and therefore allows it to be run more economically.

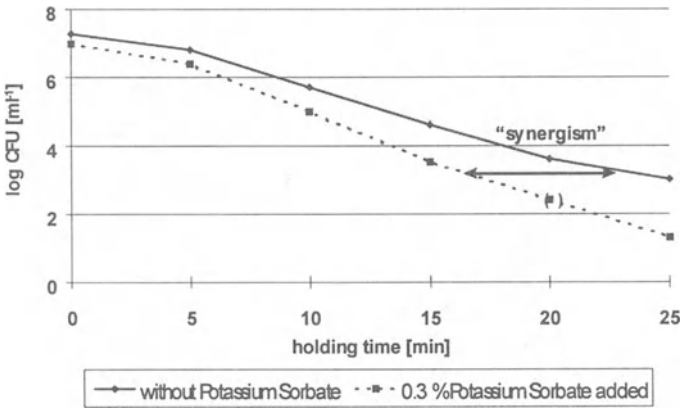

Fig. 2. Synergistic effect of high pressure and potassium sorbate on the inactivation of *St. aureus*

1.3.2 Effects of Modified Process Parameters. Many cosmetic matrices cannot be heated to pasteurisation temperatures due to limited heat stability of ingredients. However, most cosmetic products tolerate temperatures of approx. 40 °C.

It has been reported in the literature that increased temperatures accelerate the inactivation of microorganisms under high pressure conditions. Therefore the next step was to examine the process efficiency at elevated temperature.

Increasing the process temperature results in significantly shorter decimal reduction times. Table 1 indicates that a high pressure treatment at 40 °C results in the same degree of decontamination in about half the time as compared to 25 °C.

Table 1. Decimal reduction times of *St. aureus* at 25 and 40 °C

	Unpreserved samples	Potassium sorbate preserved samples
25 °C	13.7 min	10.5 min
40 °C	5.9 min	5.4 min

Temperature, pressure holding time and the period of storage between addition of preservative and pressure treatment all seem to play an important role for the outcome. Additionally it could be worthwhile to check the influence of different levels of preservative on the observed synergism. In the case of potassium sorbate

the pH especially should be varied, to facilitate an optimum efficiency in combination with high pressure.

2 High Pressure Treatment and Preservatives – In-Use and Challenge Testing

High pressure treatment with or without added preservatives can only guarantee the initial microbiological quality of a product. As in-use contamination has to be expected for almost any cosmetic product, incorporation of an effective preservative system will be necessary. Only for "one-use-products" in very small packaging units may high pressure treatment without preservatives be feasible.

To verify the preservative efficiency of 0.3% potassium sorbate in our test product under more realistic conditions (o/w-creme as described above), we conducted an in-use study over a period of 3 months. Each tester received three jars of the pressure treated product and was asked to place them in a typical environment (e.g. bathroom shelf) and to use them once daily (dipping a finger into the jars to take out a small amount of product). After 1 week, 4 weeks and 3 months samples were collected and analysed for contamination.

Results indicate that preservation with 0.3% potassium sorbate in this leave-on product was adequate to protect it for an in-use period of three months. Only one of the controls which had not been in-use was contaminated. It should be noted that these in-use tests were successful although the pH of the formulation was around pH 6, which is at the high end of the suitable range for the action of sorbate [3].

Taking into account the principle of "as little as possible, as much as necessary" the combination of high pressure to ensure a faultless initial hygienic status and potassium sorbate to provide the required in-use protection appear to be adequate for an o/w product that is comparatively difficult to preserve.

Acknowledgements: The authors thank Prof. H. Ludwig and his team at the University of Heidelberg for performing the microbiological studies and Mrs. R. Steube for assistance in the laboratory.

References

[1] Vardag, T., Jager, M. (1996) *Combined Methods for preserving foods and cosmetics*, Food Marketing & Technology, October 1996, pp. 58–65.

[2] Vardag, T., Jager, M.(1996) *High pressure treatment and preservatives*, Conference Proceedings Preservatech 1996, pp.33–40, Ziolkowsky Verlag f. chem. Industrie, Augsburg.

[3] Lueck, E., Jager, M. (1997) *Antimicrobial food additives*, 2nd ed., Springer Verlag, Berlin, Heidelberg, New York.

New Technique for Kinetic Studies of Pressure-Temperature Induced Changes of Biological Materials

J. Arabas[1], J. Szczepek[1], L. Dmowski[1], V. Heinz[2] and M. Fonberg-Broczek[1]

[1]High Pressure Research Center UNIPRESS, Polish Academy of Sciences,
29/37 Sokolowska St., PL-01-142 Warsaw, Poland
Phone: +48 22 632 23 93; Fax: +48 22 632 42 18
equipment@unipress.waw.pl
[2]Department of Food Biotechnology and Process Engineering, Berlin University of Technology, 22 Königin-Luise St., D-14195 Berlin, Germany
Phone: +49 30 31 471441; Fax: +49 308327 663
hein1331@mailszrz.zrz.tu-berlin.de

Abstract. In this paper a high pressure technique for kinetic experiments of biological materials is described. The technique is applicable to a multivessel as well as to a single vessel system. This technique allows the measurement of pressure and temperature to which samples are subjected and to keep homogenous temperature during pressurisation as well as to respond quickly to temperature overshoots caused by adiabatic heating-cooling during pressure build-up and release. Relevant exemplary kinetic data are presented.

1 Introduction

High pressure kinetic experiments of biological materials can be carried out using two different systems: single vessel and multivessel. In both systems temperature should be homogenous in the entire sample volume. In addition temperature should be quickly equilibrated after pressure build-up and release. These conditions are hardly secured in existing multivessel equipment in which pressure vessels are characterized by a relatively big volume (8 – 20 ml) and thermal capacity, and usually provided with heating/cooling jackets through which temperature controlled fluid is circulated. For effective control of static and dynamic process conditions a high capability pressure-temperature measuring system is very essential. Both parameters should be measured by sensors subjected to the same conditions as the sample. From the available reports on kinetic investigations of biological materials it is known that only temperature is measured inside each vessel (in the direct vicinity of the sample) but pressure is evaluated from sensors built-in to a pressure generating system. This leads to significant errors in kinetic studies. The new technique described in this paper is devoid of the above-mentioned shortcoming.

2 Materials & Methods

A small, cylindrical vessel, made of high strength beryllium copper alloy is placed in a bath or in a freezer. The lower plug is provided with a capillary connector and two electrical feeds-through for a resistance pressure gauge [1], the upper plug is provided with a thermocouple. A sample is closed in a flexible ampoule placed inside the vessel in the vicinity of the pressure gauge and thermocouple. The pressure transmitting medium used is non-polar liquid, for example, a mixture of hexane and pentane, extraction naphtha or silicon oil. Manganin sensor was chosen as a pressure gauge with regards to its resistance to mechanical damage during normal operation and maintenance. Its pressure coefficient was $\alpha=1/R_0\times dR/dp=2.34\times10^{-2}$/GPa at 25 °C. Instantaneous values of pressure were computed taking into account temperature dependence of the pressure coefficient $\alpha(T)$ and zero-pressure resistance $R_0(T)$ [2].

3 Results

We applied the described new technique in the High Pressure Multivessel Apparatus U111 (Fig. 1a) constructed in the High Pressure Research Center (UNIPRESS) for Berlin University of Technology (TUBER). The compact multivessel apparatus is provided with five 2 ml volume, 700 MPa pressure vessels (Fig. 1b) which are placed in the cooling-heating thermostat suitable for working at temperatures –40 to +100 °C. Each vessel is equipped with the Unipress manganin pressure gauge and 1 mm diameter sheathed thermocouple type K. The gauges are linked to a high accuracy digital multimeter system. The apparatus allows pressure build-up in the range of 1 to 20 MPa/s and pressure release ranging 1 to 100 MPa/s. Quick response to temperature overshoots caused by adiabatic heating-cooling makes it possible to carry out short lasting pressure treatments. The multivessel apparatus based on the described technique allowed TUBER to get new kinetic data at a sub-zero temperature range as well as at elevated temperatures under pressure up to 700 MPa. Figure 2 shows examples of such experiments. The measuring capability of the multivessel apparatus enables it also to be applied to other studies of biological materials, for example, high pressure assisted thawing and freezing (Fig. 3).

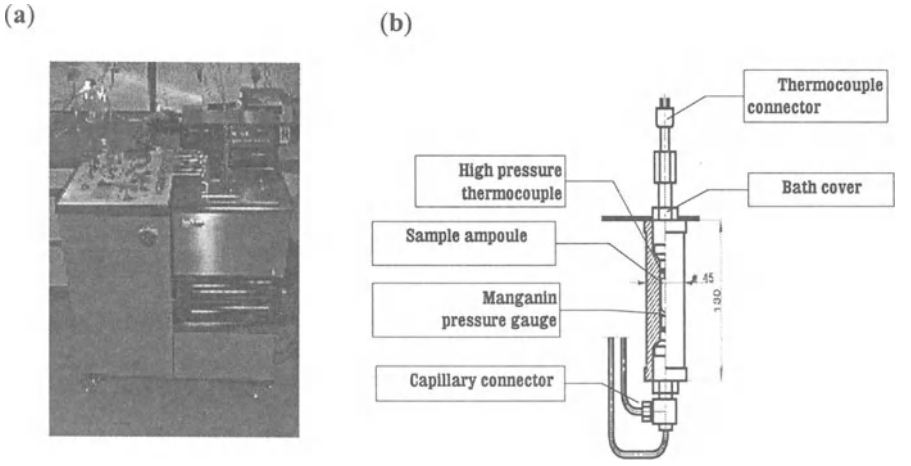

Fig. 1. Multivessel apparatus U111 for kinetics studies (**a**) view of the apparatus, (**b**) cross section of high pressure vessel

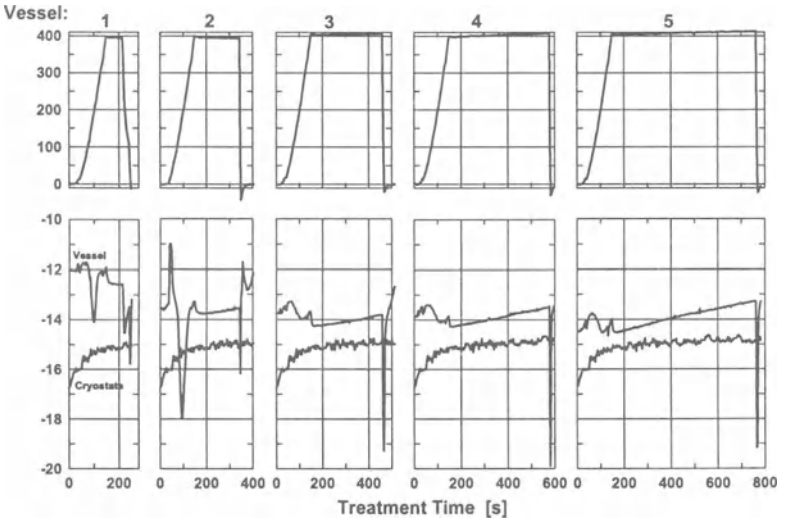

Fig. 2. Kinetic high pressure experiment within the sub-zero temperature range. The heat of compression is quickly equilibrated due to the small dimensions of the vessels. The temperature difference between the interior of the vessels and the medium in the cryostat was controlled in order to maintain constant sample temperature [3]

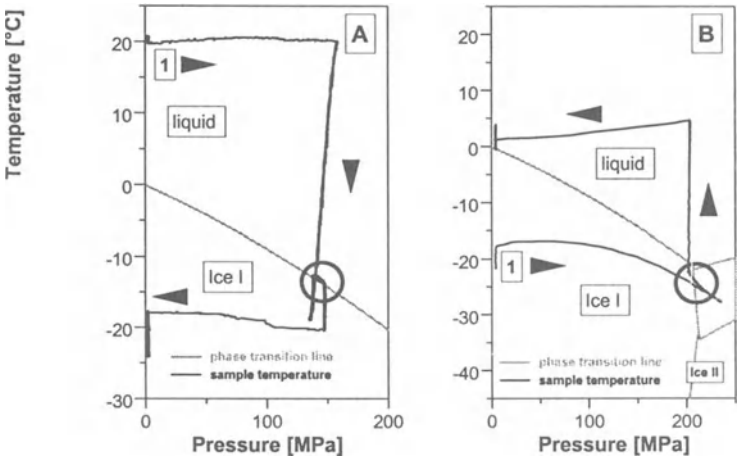

Fig. 3. Determination of phase transition temperatures in plant tissue (potato cylinders; diameter: 6 mm) during freezing (**A**) and thawing (**B**) [3]

4 Conclusions

The fact that the pressure sensor is placed in the vicinity of the investigated sample and that the temperature dependence of the pressure coefficient is taken into account, allows the computation of reliable instantaneous values of pressure applied to the sample. The small dimensions of the vessels plunged into the cryostat bath allows kinetics studies even at relatively short times. The described technique proved to be a versatile and effective tool for studies of pressure-temperature induced changes of biological materials.

Acknowledgements are made to the EC Copernicus Programme - Process Optimization and Minimal Processing of Foods, Contract CIPA - CT 0195 for support for collaboration.

References

[1] J. Szczepek, J. Arabas, High Pressure Research in the Biosciences and Biotechnology, K. Heremans (Ed.), Leuven University Press, Leuven, Belgium, 1997, pp. 471–474.
[2] L.H. Dmowski, E. Litwin-Staszewska, to be published in Meas. Sci. Technol.
[3] TU-Berlin, unpublished data.

High-Pressure Apparatus for Investigation of Biological Systems

A. Antanovich and Yu. Sadkov

Russian Academy of Sciences, Institute for High Pressure Physics, 142092 Troitsk, Moscow region, Russia
antanov@ns.hppi.troitsk.ru

Abstract. Two high pressure apparatuses for investigation of biological systems rated at 1000 and 2000 MPa are described.

1 Introduction

A number of investigations of beef qualitative indicators under high pressure were carried out in the Institute for High Pressure Physics in cooperation with the Academy of Applied Biotechnology in 1990–1993. Two high pressure apparatuses rated at 500 and 1000 MPa were developed for these investigations. The second of them is shown in Fig. 1. It consists of a two-layer high pressure cylinder (1), removable bottom (2) with "knife" seal (3), piston assembly (4), upper support (5) and mobile plunger (6).

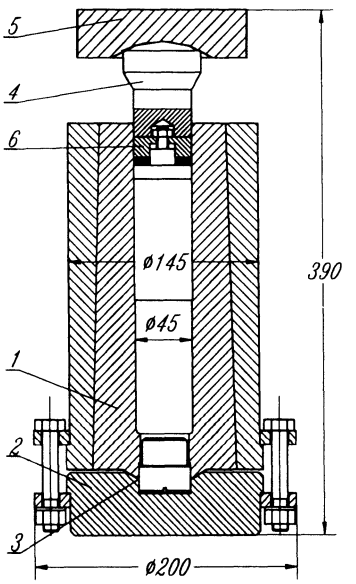

Fig 1. High pressure apparatus rated at 1000 MPa

The results of investigations conducted displayed in particular that:

1. The treatment of beef with a pressure of 300 MPa ensures the destruction of pathogenic microflora, including *E. coli, Salmonella,* as well as bacteria of the *Proteus* group. With the pressure increase the microbial contamination of beef diminishes.
2. The degree of product readiness for use, corresponding to its readiness at the traditional treatment of meat raw material, is attained in the static regime of loading at a pressure of 700 MPa. The application of cyclic loading makes it possible to lower the treatment pressure value to 200 MPa.

At present the work on the study of high pressure effects on biological objects are resumed in the Institute. In order to widen the high pressure range, a high pressure apparatus (hydrostat), rated at up to 2000 MPa and 80 °C, was developed and manufactured. This apparatus will constitute the subject of the present communication.

2 Materials & Methods

The apparatus design is presented in Fig. 2. The hydrostat proper consists of a container (1), mobile (2) and fixed (3) plungers (pistons) with seals (4) and internal resistance heater (5).

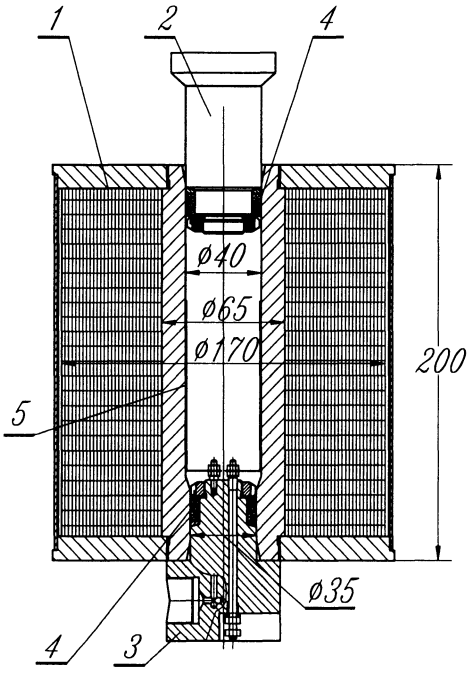

Fig. 2. High pressure apparatus rated at 2000 MPa

The container comprises a core, bandage and restricting flanges. The core is manufactured from corrosion-resistant steel of the martensite class. Its heat treatment ensures the yield strength σ_T=1100 MPa at a sufficiently high plasticity ($\delta \cong 12\%$). The flanges from crude corrosion-resistant steel are screwed on the core on both its ends and restrict the space during winding of the power bandage. Prior to the coupling of flanges with the core a thin coat of epoxide resin is applied on the core thread. This ensures a rigid coupling between the flange and the core after the hardening of the resin. The power bandage is made from high-strength steel ribbon (σ_B=1900 MPa, σ_T=1300 MPa) with a cross-section 5×0.8 mm, wound on the core between the flanges. The bandage consists of 70 layers, the first two-thirds of which are wound with a force of 4000 kN, ensuring a stress in the ribbon during its winding equal to 1000 MPa, while the last one-third of the layers is wound with a force of 3000 kN, ensuring a stress in the ribbon 750 MPa. The external bandage layer is "broached" with 6 bands from soft steel (thickness 0.4 mm), equally spaced along the periphery, which prevent the ribbon from unwinding due to accidental damage. On its outside the bandage is covered with a protective casing. The required ribbon tension during its winding is provided by a specially developed complex of equipment, based on two powerful slow-speed direct current electrical motors (N=10 kW), working in the regime of electrical deceleration. The voltage control on their winding ensures the required braking moment on motor shafts and hence the necessary ribbon tension. A special device maintains it. After the bandage winding, final processing of the internal core channel, including grinding and lapping of the seal seats, is accomplished. The rated internal pressure in the container constitutes 2000 MPa at 10^4 cycles of loading and unloading.

The internal surface of container core is step-shaped: the working chamber itself is 40 mm in diameter, while in the lower fixed plunger seat the diameter is 35 mm. This configuration of the container internal surface prevents relative displacement of the container and the fixed plunger during the working pressure release. If the surface of the container is smooth, it will go up the lower plunger due to friction in the seal of the upper mobile plunger. The step-shaped surface ensures a reliable pressing of the container against the fixed plungers as long as the container is pressurized. The mobile and fixed plungers are manufactured, as the container core, from corrosion-resistant steel, heat-treated up to σ_T=1300–1500 MPa. Both of the plungers are equipped with the sealing polyurethane or rubber rings of the V-shaped cross-section and antiextrusion bronze rings. The durability of the fixed plunger seal even with the rubber rings at a pressure of ~1000 MPa constitutes a few tens of cycles. The durability of the mobile plunger seal is much lower: the rubber rings at a pressure exceeding 1000 MPa have to be replaced for each loading cycle.

The resistance heater made from sheet steel with a high electrical resistance, rolled up into a cylinder 40 mm in diameter, is mounted on the fixed plunger. The heater is electrically insulated from the container with sheets of micanite (thickness 0.1 mm) wrapping the heater on its external and internal surfaces. The total thickness of the heater with the insulation does not exceed 0.5 mm. The electrical current is supplied through a steel quenched lead 4 mm in diameter, located in the

lower fixed plunger and insulated from it. The lead sealing in the plunger is accomplished in the form of a cone with an angle of 6°. A micanite gasket is placed between the cone recess in the plunger and the cone on the lead. The cone seal is tightened by a nut on the plunger side. The second lead for the electrical current supply to the heater is the plunger itself. The temperature control is accomplished using a thermocouple, fastened to the heater insulation by thermoresistant varnish. The pressure control is accomplished using a manganin transducer, positioned on the working end of the fixed plunger. The measuring leads from the thermocouple and manganin transducer are passed through the filled with epoxide resin hole in a special cone 3 mm in diameter, made in the fixed plunger.

Distilled water serves as a pressure-transmitting working medium. The pressure in the container is generated during the mobile plunger motion under a hydraulic press action. The working stroke of the mobile plunger depends on the investigated object porosity and does not exceed 60 mm. At present, the working chamber of the container is depressurized with the use of a special screw extractor. It is supposed that in future this operation will be performed by means of an additional hydraulic pump, which during its return stroke will feed the working liquid into the container through a special channel in the lower fixed plunger.

3 Results

At present the described high pressure apparatus has been manufactured and is being subjected to laboratory tests.

A Procedure for Minimizing Temperature Overshoots During Pressure Build-up and Release in Kinetic Experiments

J. Arabas[1], T. Sotani[2], S. Asada[3] and H. Kubota[2]

[1]High Pressure Research Center UNIPRESS, Polish Academy of Sciences,
29/37 Sokolowska St., 01-142 Warsaw, Poland
phone: +48 22 632 23 93; fax: +48 22 632 42 18
equipment@unipress.waw.pl
[2]Department of Chemical Science and Engineering,
Faculty of Engineering, Kobe University
Rokkodai, Nada-ku, Kobe 657, Japan
Phone: +81 78 803 1153; Fax: +81 78 803 1171
hkubota@appchem.chme.kobe-u.ac.jp, sotani@appchem.chme.kobe-u.ac.jp
[3]Department of Home Economics, Konan Women's University,
6-2-23 Morikita-cho, Higashinada-ku, Kobe 658-0001, Japan
Phone: +81 78 413 0391; Fax: +81 78 412-7177
asada@konan-wu.ac.jp

Abstract. In this paper a single vessel system for high pressure - low temperature kinetic experiments installed at Kobe University, Konan Women's University, Japan, on the basis of a new high pressure vessel developed in the High Pressure Research Center, Poland, is outlined. A study of temperature distribution inside the vessel during treatment is described. A large temperature gradient, mostly due to adiabatic heating/cooling, can lead to serious errors in defining experimental conditions in kinetic experiments. In order to minimize the temperature overshoots during pressure build-up and release, we applied a procedure of vessel temperature control which allows us to maintain simple temperature at almost constant level during experiment.

1 Introduction

High pressure kinetic experiments of biological materials are carried out using pressure systems equipped with thick-wall pressure vessels. The vessel is usually cooled using two different systems: external cooler or heat exchanger built-in into an inner layer of the compound cylinder vessel [1,2]. In the first case, the entire vessel is immersed into a bath, cryostat, refrigerating chamber or the vessel is equipped with an external jacket coupled to a circulating bath or cooler. Such a system is easy to build and is applied especially for monolithic vessels but is characterized by a long time-constant of temperature stabilization. The second

system is technologically more complicated and more expensive but its time-constant is lower. However, in both systems it is difficult to quickly equilibrate temperature changes. The procedure described in this paper allows the temperature overshoots to be minimized.

2 Materials & Methods

High pressure set-up consists of: vessel equipped with thermostating jacket coupled to an external circulating bath, high pressure pump with releasing valve (Fig. 1). We propose a procedure consisting of pre-cooling the pressure medium before pressure build-up and heating the vessel before pressure release. It is possible to find experimentally the time lag between the change of bath temperature and the response of the sample temperature. During pressure build-up and release the temperature overshoots can be compensated by proper setting of the circulating medium temperature. It is necessary to set the temperature of the bath to a lower value for pressure build-up and to a higher value for pressure release.

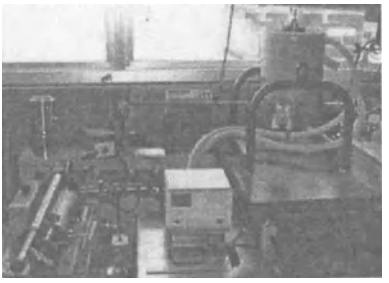

Fig. 1. Single vessel system for high pressure - low temperature kinetic experiments installed at Kobe University, Konan Women's University, Japan

3 Results

We applied the described procedure for carrying out kinetic experiments using the set-up based on the multifunction high pressure vessel built in the High Pressure Research Center (UNIPRESS) for the Konan Women's University and Kobe University. The 50 ml volume, 700 MPa pressure vessel is made entirely of stainless steel UGINE®4542 (ASTM 630). The vessel is equipped with an external jacket suitable to work with circulating cooling/heating thermostat ranging –40 to +50 °C. The lower plug of the vessel is provided with a sheathed thermocouple. The gauging point of the thermocouple is located in the middle of the vessel. The pressure transmitting medium used is a mixture of water and methanol. The vessel is thermostated using the Haake F6-C50 refrigerated circulator. Pressure is

generated by the high pressure manual pump Hikari 10000 bar and measured by a strain pressure transducer. Figure 2 shows the charts of pressure and temperature versus time without application of the described procedure. For a 200 MPa pressure cycle the temperature deviations can be about 8 °C, both for pressure build-up and release. Figure 3 shows that the time lag between the change of bath temperature and the response of the sample temperature is about 7 min. Taking into account this value of lag, it is possible to reduce the temperature overshoot even down to 1 °C (Fig. 4).

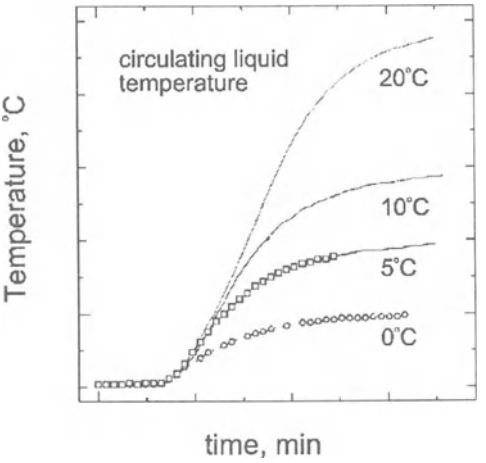

Fig. 2. Temperature change of the sample after resetting the circulating liquid temperature

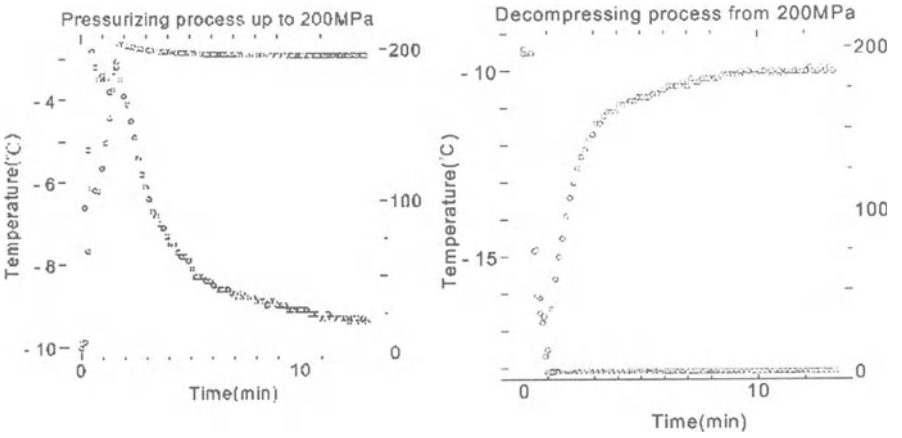

Fig. 3. Temperature overshoots during (*left*) pressure build-up and (*right*) release

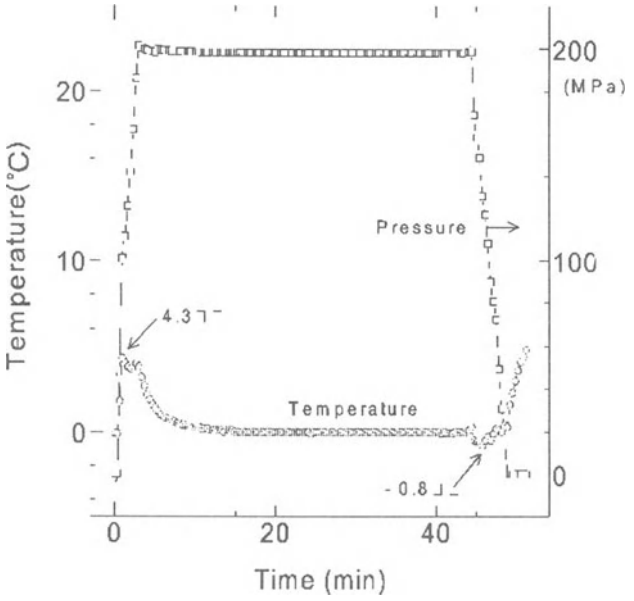

Fig. 4. Pressurizing process according to the described procedure

4 Conclusions

The results indicate that applying the procedure we could minimize the temperature overshoots remarkably. However, a rate of pressure build-up and release is limited.

Acknowledgement is made for the funding of this work to the Japan Society for the Promotion of Science under the auspices of the Bilateral Exchange Programs with the Polish Academy of Sciences.

References

[1] J.Szczepek, J.Arabas, High Pressure Research in the Biosciences and Biotechnology, K. Heremans (Ed.), Leuven University Press, Leuven, Belgium, 1997, pp. 471–474.

[2] T.Sotani, H.Kubota, A.Sakata, 14 ECTP Proceedings, Lyon, France, 16–19 Sept. 1996, to be published in High Temperatures - High Pressures, 1998, vol. 30.

Whole Organisms and Human Cells, Deep Diving

Reversibility of High Pressure Effects in Isolated Adult Murine Skeletal Muscle Fibres Tested at Pressures up to 600 Bar and a Temperature of +4 °C

K.R. Kress, O. Friedrich, H. Ludwig[1] and R.H.A. Fink

University of Heidelberg, II. Institute of Physiology, INF 326, D-69120 Heidelberg, Germany
Fink@novsrv1.pio.uni-heidelberg.de
[1]University of Heidelberg, Institute of Pharmaceutical Technology and Biopharmacy, Section Physical Chemistry, INF 346, D-69120 Heidelberg, Germany
Horst.Ludwig@urz.uni-heidelberg.de

Abstract. We investigated the reversibility of high-pressure induced effects in differentiated murine skeletal muscle fibres after a 3 h pressure application. Applied pressure ranged from 100 bar up to 600 bar. Force and stiffness measurements were used to test functional intactness of the contractile filaments and the two microelectrode voltage clamp technique to test the integrity of the cell membrane. Our results showed that up to 200 bar all investigated parameters were virtually unchanged from those of untreated fibres. For higher pressures sudden changes in all parameters were observed which led to partial loss of mechanical function and loss of membrane current kinetics. For pressures higher than 300 bar all fibres were damaged in Ringer's solution whereas some fibres were still intact in hypertonic Ringer's solution up to 500 bar.

1 Introduction

Application of high pressure and simultaneous cooling are commonly used effective procedures to preserve biological samples. However, differentiated cells and tissues like those of the skeletal muscle are very fragile and in general destroyed by high pressure or cooling below 0 °C. As it would be very useful to extend the combined high pressure and cryopreservation to differentiated cells and tissue, we have tested the functional intactness of single skeletal muscle cells by applying cell physiological techniques to measure membrane excitability and contraction as sensitive parameters of cell integrity after reversible exposure to high pressure application.

2 Materials & Methods

Fast-twitch muscles (Mm. lumbricales of *Xenopus laevis* and M. extensor digitorum longus (edl) and Mm. interossei of adult *BALB/c mice* (20 weeks old)) were dissected and transferred into an autoclave at +4 °C for high pressure application, edl fibres in paraffin oil and interossei fibres in Ringer's solution (mM: NaCl 136; KCl 4; $CaCl_2$ 2; $Mg(CH_3COO)_2$ 1; HEPES 5). Additionally, for pressures higher than 200 bar hypertonic solutions (200 mM glucose added to Ringer's solution) were tested with calcium mainly replaced by magnesium. Hydrostatic pressure was slowly increased (2 bar/min from 0 to 60 bar and 6 bar/min from 60 bar to the maximum pressure) at constant temperature and maintained at the chosen test pressure for approximately 3 h. Applied pressure ranged from 100 bar to 600 bar. After 3 h of high pressure application pressure was slowly decreased to atmospheric pressure. From the muscles single edl fibres with a diameter of approximately 60 µm were mechanically isolated for force and stiffness recordings at an ionic strength of 150 mM [1] while short interossei fibres were enzymatically isolated with collagenase treatment for membrane conductance measurement with the two microelectrode voltage clamp technique [2].

3 Results

In a first set of experiments performed on frog fibres, we found that for pressures up to 200 bar there was almost no morphological change visible while for higher pressures nearly all cells were damaged. In the additionally tested 200 mM hypertonic solution some percent of the fibres were still intact after a 500 bar pressure application of 10 min duration. At higher pressures all fibres were damaged. The hypertonic solution in which calcium was mainly replaced by magnesium showed no improvement. Therefore, we decided to investigate more closely the pressure range from atmospheric pressure up to 250 bar in order to quantify the onset of the high-pressure induced changes.

Mechanical effects up to 250 bar. We investigated Ca-activation and stiffness because Ca-activation of the troponin-tropomyosin complex is the central process of force development. Stiffness is a measure of the interaction of the contractile proteins myosin and actin and Fig. 1 shows results of force and stiffness measurements performed on fibres after treatment with various pressures for 3 h. Stiffness of relaxed fibres (1A), force development (1B) and its activation kinetics (1C). The time to maximum force approximated by an exponential time course (for $t=\tau$ the 66% value) was plotted against pressure. They were similar up to 200 bar, whereas for higher pressures dramatic changes were observed leading to increased stiffness and reduced and prolonged force development. pCa-force-relation (1D) was unchanged up to 200 bar and shifted towards lower pCa-values for pressures beyond.

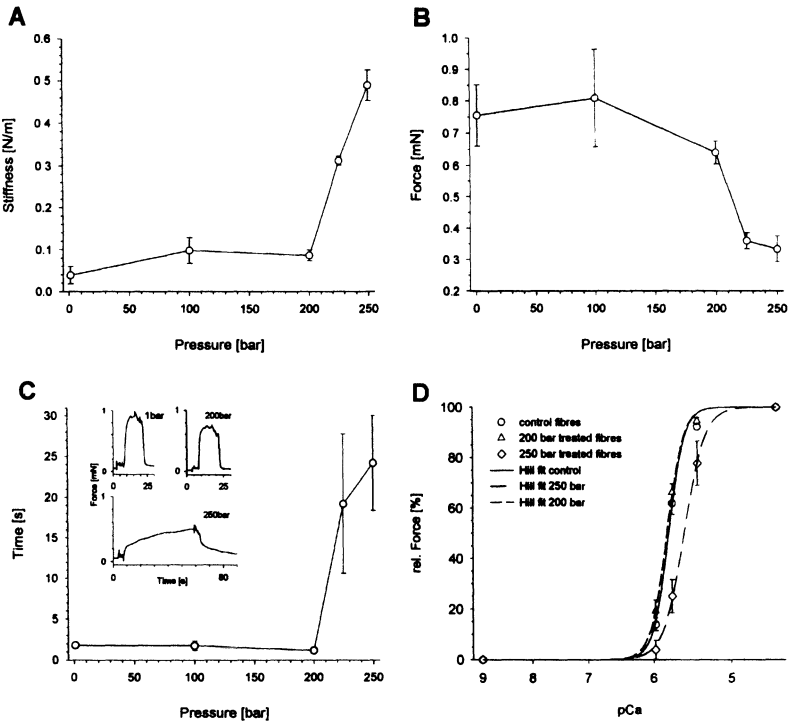

Fig. 1. Mechanical characteristics of high-pressure treated skinned fibres. (**A**), Stiffness of relaxed fibres. (**B**), Maximum force of Ca-activation. (**C**), Activation of force-development by Ca-activation (66% of maximum force). Inset: representative force transients. (**D**), pCa-force relation

Membrane effects up to 250 bar. We measured the resting potential and sodium and potassium currents to prove the intactness of the lipid bilayer cell membrane and its Na- and K-channel proteins. Figure 2 shows results of sodium and potassium currents from voltage clamp recordings of fibres treated with various pressures. Resting potential of single fibres showed moderate decline up to 200 bar and markedly less negative potentials for higher pressures. Na- and K-currents at 100 bar and 200 bar (Fig. 2C) were similar to those of untreated fibres (Fig. 2A), whereas for higher pressures (250 bar, Fig. 2D) no currents could any longer be elicited.

4 Discussion

We carried out high pressure application to muscle fibres to test for reversibility of pressure induced changes regarding mechanical and electrical properties of differentiated cells. We found that up to 200 bar the investigated parameters were comparable to untreated fibres. For higher pressures sudden changes were detected

which (i) led to partial loss of mechanical function and (ii) loss of membrane currents. The underlying molecular mechanisms have to be understood and prevented before an effective combined high-pressure cryopreservation of intact differentiated cells can be contemplated. In this context, it is also of great interest to analyze the mechanisms of high pressure adaptation of biological species in the deep sea [3].

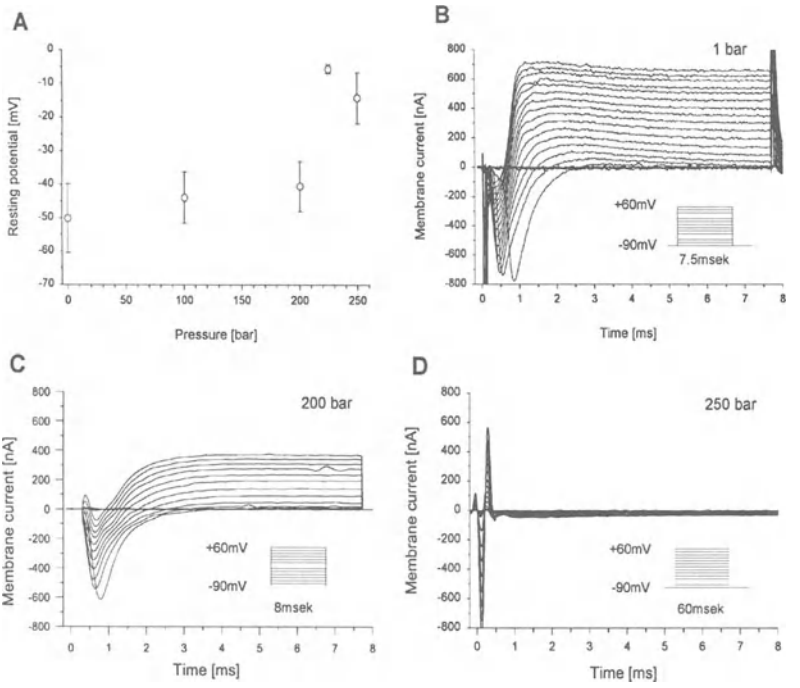

Fig. 2. Membrane properties of high-pressure treated fibres. (**A**), Resting potentials of single fibres. (**B**),(**C**),(**D**), Sodium and potassium currents at atmospheric pressure (1 bar), 200 bar and 250 bar, respectively

References

[1] Veigel, C., Maydell, R.D. von, Kress, K.R., Molloy, J.E., Fink, R.H.A. (1998); The effect of ionic strength on kinetics of rigor development in skinned fast-twitch skeletal muscle fibres; Pflügers Arch. 435, 753–761.

[2] Friedrich, O., Ehmer, T., Fink, R.H.A. (1998); Calcium currents during contraction and shortening in enzymatically isolated murine skeletal muscle fibres; J. Physiol. Submitted.

[3] Somero, G.N. (1992); Adaptations to high hydrostatic pressure; Annual. Rev. Physiol. 54, 557–77.

The Influence of Water Dissolved Argon and Nitrogen on Hydra (*Hydra attenuata*) Budding Activity Under Normal Ambient Pressure

A.G. Belyaev, B.N. Pavlov and S.V. Buravkov[1]

State Scientific Centre of Russian Federation-Institute for Biomedical Problems,
76a Khoroshevskoye shosse, 123007 Moscow, Russia
Phone: +7-(095)-1956329; Fax: +7-(095)-1952063
[1]Space Biomedical Centre for Training and Research
buravkova@mmcc.ibmp.rssi.ru
http://www.ibmp.rssi.ru

Abstract. The water environment, saturated with a hypoxic oxygen-argon mixture, has a high stimulating effect on hydra (*Hydra attenuata*) budding in comparison with a water environment saturated with air. The stimulating effect was not only increasing the amount of young buds, but reducing the bud development period in comparison with control groups. A water environment saturated with a hypoxic oxygen-nitrogen mixture has a low stimulating effect on hydra budding.

1 Introduction

The effect of neutral gases, such as helium, nitrogen and argon, was studied in numerous animal species, belonging to various classes [1, 3–5].

Water animals, such as Coelenterata, can serve as an object to study neutral gases influence. Taking into account that Coelenterata perform breathing with all their body surface, we can suppose that a change in the gas composition of the water environment can have a rather fast effect on their physiology.

Hydra is a classic object of biological studies (Fig. 1). Budding is a normal way of hydra reproduction. Budding activity depends upon numerous factors, such as temperature, chemical composition of the water environment [2].

Fig. 1. Hydra

The aim of this work was to demonstrate the effect of a water environment saturated with hypoxic 15% oxygen-argon mixture (15% OxArM) in comparison with the effect of a water environment saturated with hypoxic 15% oxygen-nitrogen mixture (15% OxNM) and with normal conditions of breeding (normal ambient pressure and room temperature) as a control of hydra budding activity.

2 Materials & Methods

A long-years cultivated pure line of *Hydra attenuata* was taken for the experiments. Adult hydras were placed in plastic Petri dishes, filled with studied water environments. All hydra specimens were of the same size and held no buds at the start of the experiment. Two series of the experiments (6 d each) were performed. In each series of the experiments, ten samples containing 15 hydra specimens in each sample were taken.

In the first series of the experiments, hydras were placed in a water environment containing 15% oxygen-argon mixture. In the second series, hydras were placed in water, which had been saturated with 15% oxygen-nitrogen mixture. In both series, budding activity was compared with a control group, in which the water environment was saturated with air. After each 2 d had been counted, buds appeared.

Water environments were saturated with studied gas mixtures under the pressure of 200 mmHg. At the beginning of the experiments, calculated concentrations of dissolved gases were as listed in Table 1:

Table 1. Calculated concentrations of dissolved gases

Water environment saturated with 15% OxArM	Water environment saturated with 15% OxNM	Water environment saturated with air
Oxygen –4.2 sm^3/l	Oxygen –4.2 sm^3/l	Oxygen –6.4 sm^3/l
Argon –28.6 sm^3/l	Nitrogen –17.0 sm^3/l	Nitrogen –15.8 sm^3/l

All experiments were carried out under normal ambient pressure and a temperature of 20 °C.

3 Results & Discussion

A water environment saturated with hypoxic oxygen-argon mixture strongly stimulates hydra budding in comparison with water saturated with hypoxic oxygen-nitrogen mixture and with the control group. The stimulation concerned not only the number of emerging buds, but also the time of bud formation and development decreased in comparison with control groups. On the second day buds that had emerged in argon mixture groups appeared to be maturer than in control groups.

The total number of hydra specimens in an oxygen-argon environment 1.5 times exceeded the number in control groups.

In addition, we can suppose that argon slows budding inhibition caused by increasing hydra density in dishes.

The water environment saturated with an oxygen-nitrogen mixture has a weak, statistically non-significant stimulating effect, causing hydra reaction to non-favorable factor of hypoxia. Obtained data are illustrated in the following plots.

The total number of hydra specimens (buds and free-living specimens) is shown in Fig. 2.

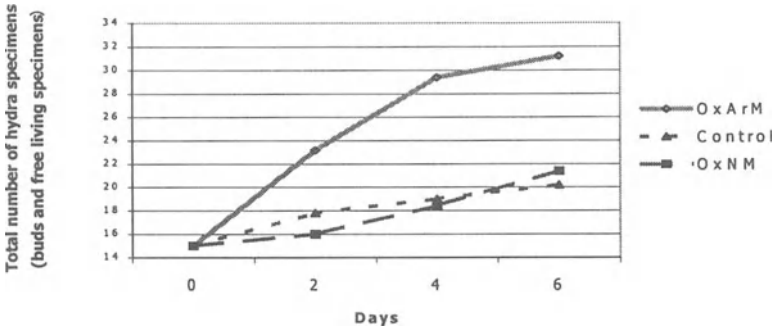

Fig. 2. Total number of hydra specimens

It can be seen that numbers evenly increase in all groups. The number in groups placed into an oxygen-argon environment strongly differs from the number of control groups, increasing it 1.5 times. The number in groups, placed into an oxygen-nitrogen mixture practically does not differ from the number in control groups.

As seen in Fig. 3, budding activity in argon groups 1.5–2 times increased on 3–4 d compared with other groups.

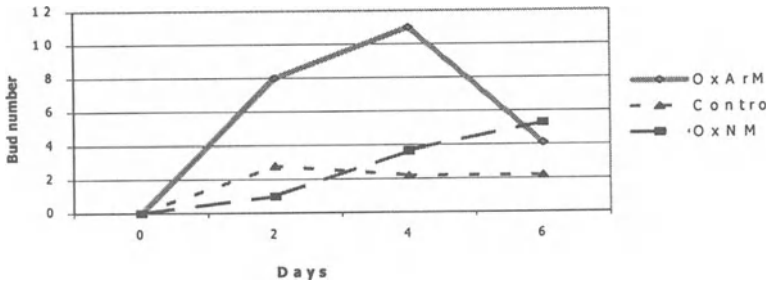

Fig. 3 Budding activity in the different groups

In Fig. 4, we can see that the number of free-living specimens in an argon environment exceeded the number in nitrogen and control groups by 1.5 times to the end of experiment.

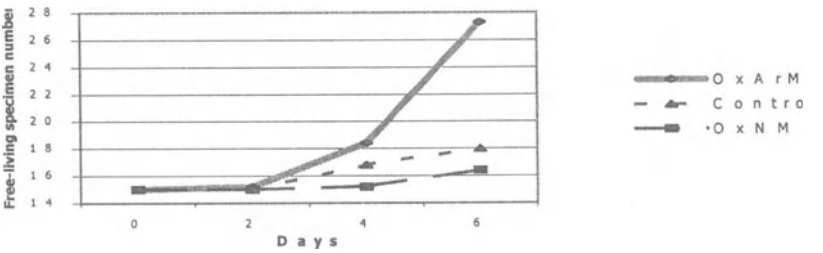

Fig. 4. Number of free-living specimens in the different groups

The analyses show that hydra specimens placed in a water environment saturated with a 15% oxygen-argon mixture are able to produce more buds than hydra specimens placed into normal water. This did not occur in hydras placed in a water environment saturated with a 15% hypoxic oxygen-nitrogen mixture.

The significance of the obtained results was estimated with statistical methods.

Taking into account the small sizes of samples, the small differences between bud numbers in different samples, and the permanent changes of factors, effecting the budding in the experiments, statistical analysis of budding appeared to be difficult.

This statistical analysis aimed to estimate the significance of argon presence and of hypoxia factor.

To estimate the significance of these factors an examination was made of the total number of hydras (buds and free-living specimens) difference in hypoxic environments, saturated with OxArM, OxNM and in control.

Data were tested with Wilcoxon matched pairs test (Tables 2–4).

Table 2. Estimation of water environment saturated with 15% hypoxic OxArM, influence on budding activity in comparison with control. H_0 – samples do not differ

	Valid N	T	Z	p-level
OxArM & Control	10	0.00	2.803060	0.005065

The analysis showed that H_0 is rejected. Total numbers of specimens differs significantly (p-level = 0.005065). Saturation of water with 15% hypoxic OxArM significantly influenced the budding activity.

Table 3. Estimation of hypoxia factor influence on hydra budding activity in the comparison with control groups. H_0 – samples do not differ

	Valid N	T	Z	p-level
OxNM & Control	10	7.500000	1.777047	0.075570

The analysis showed that H_0 is **not** rejected. Total numbers of specimens does not differ significantly. Thus, it is statistically proved that the hypoxia factor does not have a significant influence on the budding activity of hydras placed in a water environment saturated with 15% hypoxic OxNM.

Table 4. Estimation of argon influence on budding activity of total number of specimens at the end of experiment in groups with OxArM and OxNM are to be compared. H_0 – samples do not differ

	Valid N	T	Z	p-level
OxArM & OxNM	10	0.00	2.665570	0.007690

This analysis showed that H_0 is rejected. The data, showing the absolute value of the whole specimens number, significantly differ from each other. Thus, it is statistically shown that the presence of argon influences the budding activity.

It is statistically proved that argon is the factor, influencing the budding activity of the hydras.

The changes in the gas composition of the water environment influence not only the budding activity, but the behavior of the hydras as well. The analysis of the hydra's behavior in both parts of the experiments shows that the water environment, saturated with 15% hypoxic oxygen-nitrogen mixture inhibits the motility and irritability of the specimens. The water environment saturated with the 15% hypoxic oxygen-argon mixture does not influence the motility and irritability of hydras.

Thus, the presence of dissolved high-concentrated argon in the water environment is the significant factor causing a budding stimulation under normal temperature and ambient pressure. The hypoxic factor delays the forming and development of the buds in the first days, causing a shock reaction.

References

[1] Cook, S.F., 1950. The Effect of Helium and Argon on Metabolism and Metamorphosis. J. Cell. and Comp. Physiol., 36: 115–127.
[2] Kanaev, I.I., 1952. Hydra. M. – L.: AS USSR.
[3] Lazarev, N. 1941. Biological actions of gases under pressure; Leningrad, VMMA.
[4] Maio, D.A. and. Neville, J.R, 1966. Aerospace Med. 37: 290.
[5] Schreiner, H.R., 1968. General Biological Effects of the Helium-Xenon Series of Elements. Union Carbide Corporation, Linde Division Research Laboratory, Tonawanda, New York Federation Proceedings Vol. 27, No. 3.

The Effects of Oxygen-Argon Gaseous Mixtures on Humans Under Long-Term Hyperbaric Condition

B.N. Pavlov, S.V. Buravkov[1], P.E. Soldatov, A.V. Vdovin and N.V. Deviatova

State Scientific Centre of Russian Federation-Institute for Biomedical Problems,
76a Khoroshevskoye shosse, 123007 Moscow, Russia
Phone: +7-(095)-1956329; Fax: +7-(095)-1952063
[1]Space Biomedical Center for Training and Research
buravkova@mmcc.ibmp.rssi.ru
http://www.ibmp.rssi.ru

Abstract. The goal of the present investigation was to estimate the human performance and adaptation of physiological systems during long-term exposure in argon-nitrogen-oxygen atmosphere. Four male volunteers participated in simulated diving to 10 m performed in the diving complex "GVK-250". The subjects were exposed during 7 d to the following gas mixture (in partial pressures): oxygen - 0.2±0.005 kg/cm^2, nitrogen - 0.8±0.01 kg/cm^2 and argon - 1.0±0.01 kg/cm^2. The volunteers performed physical and mental work in order to study mechanisms of cardiovascular, respiratory and nervous systems regulation under physical activity. We found no modifications of normal physiological characteristics of central nervous, cardiovascular, respiratory systems' tests and in results of urine biochemical tests. Blood biochemical measurements did not show significant differences from control levels except shifts in lipid metabolism which are often observed during long-term simulated deep diving. Positive effects in adaptation to hypoxic condition were revealed under argon gas mixture exposure. Under hyperbaric pressure a workload of 100 Wt, the volunteers performed this work 62% higher in 15% argon-oxygen mixture than in 15% nitrox. We conclude that argon could be assumed as a physiologically active gas actively participating in redox-reactions and causing increased resistance of the organisms to hypoxic hypoxia.

1 Introduction

First investigations on behavioural reactions of mice under high pressures of oxygen-argon mixtures compared with oxygen-nitrogen mixtures were studied by N.V. Lazarev in 1936–1941 [1]. Argon was found to be more a narcotic gas compared with nitrogen on animals' and human organisms and therefore it could not be used in diving practice.

Later more detailed investigations of behavioural and physiological effects of oxygen-argon and oxygen-nitrogen mixtures under 5 MPa were performed on

several species of animals (mice, rabbits and dogs) [2]. The main animals' behavioural reactions and electrophysiological data both under argon and nitrogen were the same in principal. However, the first shifts in data were revealed at lower pressures and motional excitation was less marked at the first stage of compression under argon. These results corresponded with data of other investigators on different objects [3–5].

According to the literature no human investigations of long-term diving imitation in argon atmosphere have been performed both in Russia and other countries. Only a few papers on studies of narcotic effects of argon during short-term diving experiments appeared [6,7]. Investigations of Marshall and Fenn [8] revealed decreased evoked potentials of frogs under 20% oxygen-argon mixture breathing at 0.4 and 0.6 MPa.

Therefore we studied the long-term effects of oxygen-argon gaseous mixtures on human performance, organism resistance to hypoxic hypoxia during 7 d human experiments.

2 Materials & Methods

All experimental procedures were carried out in a specially designed hyperbaric pressure chamber "GVK-250" which permits long-term pressure exposures of humans up to 2.5 MPa. This diving complex "GVK-250" consists of a 3-part pressure chamber with a total chamber volume of 30 m^3. This complex has all the systems needed for long-term saturation exposures up to 6 humans during 3 months in different gas mixtures breathing. 4 male volunteers participated in simulated diving to 10 m.

The subjects were exposed during 7 d to the following gas mixture (in partial pressures): oxygen - 0.2±0.005 kg/cm^2, nitrogen - 0.8±0.01 kg/cm^2 and argon - 1.0±0.01 kg/cm^2. Hypoxic breathing gas mixtures consisted of 0.15±0.01 kg/cm^2 instead of 0.2±0.005 kg/cm^2. The volunteers performed physical and mental work in order to study mechanisms of cardiovascular, respiratory and nervous systems regulation under physical activity.

Biochemical analysis of urine, measurements of EEG, mental and physical working performance, dynamic tremors, chronoreflexometry, oxyhemometry and ECG were performed before experimental procedure (background), under high pressure condition, during (3 d) and after decompression (2 d). Oxygen and carbon dioxide concentrations were permanently monitored using special chromatography which allowed us to measure correctly the concentration of oxygen in oxygen-nitrogen-argon mixtures.

3 Results & Discussion

This study revealed that long-term exposure (7 d) of humans in normoxic oxygen-nitrogen-argon environment is safe because no changes in human investigations of central nervous system, cardiovascular and lung systems and clinical analysis of urine were revealed during the experiment. All measured data did not exceed normal physiological range.

EEG showed a different degree of sedative effects of the argon breathing mixture on all volunteers. Regular α-rhythms slightly increased on the 2nd day. On the 3rd day appearance of single τ- rhythms with 50 mkV amplitude was marked. Δ-waves and β-activity also appeared on EEG's but had no changes under pressure. Application of hypoxic 15% oxygen-argon mixture during 30–40 min at normal ambient pressure led to increasing of EEG-oscillations in a range of α-rhythm frequencies. The effects of oxygen-argon mixtures at increased barometric pressure were the same as at normal pressure except that changes were more marked. Visual estimation of EEG showed that their changes were caused more likely by specific action of argon under high pressure rather than by the effects of hypoxic event development in the central nervous system in conditions of hypoxic oxygen-argon mixture breathing. During all 7-days exposure no signs of central nervous system dysfunction or disturbances of regulatory mechanisms in rhythmic activity generation on EEG have been revealed.

A study of mental working performance showed some decrease in numbers of solved examples and decrease in number of mistakes. This was more remarkable under oxygen-nitrogen breathing. Under hypoxic condition at high pressure of oxygen-nitrogen mixtures some increasing speed of counting (number of solved examples in 2 min) occurred (from 81.68 to 84.87), although the numbers of mistakes increased by 1.5 times (from 3.62 to 5.56) compared with normoxic hyperbaric condition and by 1.85 times - with normal ambient pressure.

Data under breathing with hypoxic oxygen-argon mixture did not change significantly from results given under normoxic hyperbaric oxygen-nitrogen-argon mixture. Some slowness in counting speed (from 81.68 to 77.31) and insignificant increase of mistakes' numbers were revealed. Given facts corresponds with the data obtained by Zalzman *et al.* [2] who revealed no euphoria when applying hyperbaric oxygen-argon mixtures and the hypothesis of nitrogen and argon actions under high pressure on different structures of the central nervous system.

The volume of performed physical work, which was estimated using ergometer at 100 Wt workload, under normoxic hyperbaric oxygen-nitrogen-argon mixture increased compared with normal ambient pressure to 193% in mean (from 4008 to 11755 kgm), pulse was less, decrease of minute blood volume and increase of pulse pressure were observed. When using hypoxic oxygen-nitrogen mixtures under high pressure the increase of performed work volume to 65% (from 4008 to 6625 kgm) was revealed with a significant increase of minute blood volume and particularly pulse pressure compared with ambient pressure. This means that increasing working performance could be realised though increasing workload on the cardiovascular system.

Breathing with a hypoxic hyperbaric oxygen-argon mixture led to insignificant decrease of physical work volume (from 4008 to 3975 kgm), some pulse increase, decrease of minute blood volume and increase of pulse pressure compared with air ambient pressure. Comparing obtained results of physical work performance and volunteers' hemodynamics under hypoxic oxygen-argon mixture with the results under air breathing one may draw a conclusion that physiological action of hypoxic oxygen-argon mixture under high pressure provides positive adaptation of organism to hypoxia.

Investigation of the cardiovascular system of volunteers breathing with oxygen-nitrogen-argon mixture under high pressure revealed that values of arterial pressures of all participants decreased from 115–120/75–80 to 105–110/65–75 mm Hg with exposure time. Three volunteers showed decrease of heart rate during long-term hyperbaric exposure. This bradicardia could probably be caused by organism saturation by the inert gas argon or by development of adaptation to work on the ergometer. Detailed examination of the ECG revealed R-wave splitting on 3–4 d of normoxic hyperbaric exposure at all participants. Breathing with hypoxic oxygen-nitrogen-argon mixture under high pressure led to sinus arrhythmia, changes in start and end phases of ECG. Sometimes the P-wave consisted of two phases. This process could be explained by atrium depolarisation. Described changes usually occurred after physical workloads in recovery periods and therefore could be explained by an adaptation process to new the environment or as a reaction of the cardiovascular system to hypoxia or functional workloads.

Therefore our investigations of cardiovascular, pulmonary, nervous systems under normoxic and hypoxic hyperbaric oxygen-nitrogen-argon mixtures indicated that presence of argon in breathing mixtures caused a positive effect on organism adaptation to hypoxia. However the given results did not allow us to investigate all underlying mechanisms because during workloads volunteers were subjected to the processes of multiple saturation-desaturations which could have an influence on the results. Further experiments on long-term exposure under hypoxic hyperbaric condition will allow us to estimate the role of argon in adaptation processes.

References

[1] Lazarev, N. (1941); Biological actions of gases under pressure; Leningrad, VMMA.
[2] Zalzman, G. *et al.* (1979); The basics of hyperbaric physiology; Leningrad, Medicine.
[3] Behnke, A. and Jahrbrough, O. (1939); Respiratory resistance, oil-water solubility and mental effects of argon compared with helium and nitrogen; Amer. J. Physiol., 126, 409–415.
[4] Bennett, P. and Dossett, A. (1973); EEG activity of rats compared by inert gases to 700 feet and oxygen-helium to 4000 feet; Aerospace Med., 44, 239–244.
[5] Carpenter, F. (1954); Anaesthetic action of inert and nonreactive gases on intact animals and isolated tissues; Amer. J. Physiol., 178, 505–509.
[6] Fowler, B. and Ackles, K. (1972); Narcotic effects in man breathing 80–20 argon-oxygen and air conditions; Aerospace Med., 43, 11.
[7] Langley, T. and Hamilton, R. (1975); Somatic-evoked brain responses as indicators of adaptation to nitrogen narcosis; Aviat. Space and Environ. Med., 46, 147–151.
[8] Marshall, J. and Fenn, W. (1950); The narcotic effects of nitrogen and argon on central nervous system of frogs; Amer. J. Physiol., 163, 733–740.

Flow Cytometric Testing of Blood Platelet Activation in Diving

R. Olszanski

Department of Underwater Medicine, Military Medical Academy, Gdynia, Poland

Abstract. We tested variants of diving (short air diving and saturated diving) employing flow cytometry to assess the risks of decompression sickness. In short air diving we measured the percentage of microplatelets and platelet aggregates and platelet neutrophil aggregates. We observed a significant increase in the platelets bearing the CD62P molecule which is a typical symptom of platelet activation. In saturated diving we observed a marked increase in the percentage of activated platelets bearing CD62P molecules and an enhanced number of microplatelets in the blood of divers in the air group. In both groups of divers we observed some changes in the platelet system however compression and decompression in nitrox atmosphere seems to be less harmful to the platelets. Evaluation of the platelets may become a primary element in determining the risk of decompression sickness.

1 Introduction

The problems of saturated diving, even in shallow depths, have not been solved yet and the solution to these problems is very important as this opens the way to deep diving.

In the phase of decompression divers may suffer from the effects of inert gas supersaturation. The result of this may be the appearance of gas bubbles (so called "silent bubbles") in the blood vessels. Evaluation of haemostasis may become a primary element for determining the risk of decompression sickness (DCS).

DCS is a life-threatening illness affecting divers. Inert gas supersaturation during decompression results in the formation of gas bubbles leading to gas emboli and the activation of coagulation cascade. The surface of the "silent bubbles" act as an activator of the "Hageman factor".

Platelets are involved both in prothrombotic and in proinflammatory processes, therefore the increased activation of platelets is potentially hazardous and may form a very important part of the DCS clinical picture. There is a very high variability in the susceptibility to DCS among candidates for training to be professional divers. We suggested testing of platelets activation markers as a tool in estimating individual susceptibility to DCS.

Flow cytometry has been recognized as the most useful and sensitive method of clinical testing and monitoring changes in the platelets system. We hypothesize that the activation of platelets during decompression corresponds to the risk of DCS, and consequently the aim of our studies was testing changes in platelet activation markers in divers subjected to diving [2, 3].

2 Materials & Methods

We tested various types of diving, employing flow cytometry to evaluate the risk of decompression sickness as follows:

Air Diving. 30 professional male divers were submitted to hyperbaric exposures 0.6 MPa corresponding to a depth of 60 m, for 35 min (plateau phase). The total decompression time was 3 h 7 min using the Polish Navy tables for air.

Air and Nitrox Saturated Diving. In a group of nineteen professional male divers - nine were subjected to saturated compression at 4 ata for 76 h in nitrox atmosphere, and ten to compression at 2.8 ata for 90 h in air atmosphere.

None of the divers tested had taken Aspirin or any other drug that could effect platelets function during a period of 14 d immediately prior to the tests.

Immediately before and 30 min after decompression 0.1 ml blood samples were taken from a cubital vein to EDTA Vacutainers and to test tubes with a 1% paraformaldehyde solution. We used mouse monoclonal antibodies (mAb), anti-human platelet glycoprotein (GP) IIIa and IIb (two parts of the fibrinogen receptor-CD61 and CD41) labelled with fluorescein isothiocyanate (CD61-FITC), anti-human GP Ib alfa (a part of the receptor for the von Willebrand factor - CD42b) labelled with phycoerythrin (PE) from DAKO A/S (Denmark) and anti-human platelet PADGEM (platelet activation-dependent granule external membrane) protein - CD62P - activation marker for platelets active in release reaction - labelled with PE from Becton-Dickinson (Mountain View, CA).

We tested the percentage of platelets bearing chosen membrane glycoproteins using mAb CD42b, CD61, (DAKO A/S Denmark), and CD62P Becton Dickinson (Mountain View, CA), the expression of these molecules on platelets in paraformaldehyde fixed blood samples, the percentage of microplatelets, and the platelet-neutrophil aggregates. The molecule expression reflects the density of the molecules on the platelet surface and is presented as a mean of the fluorescence intensity (MFI).

Flow cytometer FACScan hardware and Lysis II software (Becton Dickinson) were employed in platelet testing, and a double staining procedure for the examination of platelets in whole blood was applied and Cell-Dyn 3500 apparatus (ABBOT) was used for platelets testing.

Statistical analysis of the tested parameters before and after the compression was done applying a paired T-test. The U Manna-Whitney test was used for the

analysis of the differences between divers and the comparative group. The probability value $p<0.05$ was considered significant [1].

The exposures were carried out at the Department of Diving Gear and Underwater Work Technology, at the Naval Academy in Gdynia, Poland and the Department of Hyperbaric Medicine and Sea Rescue, at the Institute of Maritime and Tropical Medicine in Gdynia, Poland.

3 Results

Air Diving. We measured the percentage of microplatelets and platelet aggregates and platelet-neutrophil aggregates. We observed a significant increase in the percentage of platelets bearing the CD62P molecule which is a typical symptom of platelet activation and releasing reaction: increase from 3 ± 2.3% before air exposure to 5.9 ± 2.4 after air decompression compared to 0.9 ± 1.2 controls.

A marked increase was noted in the percentage in platelets forming aggregates with neutrophils from 3.7 ± 1.5% to 10.7 ± 4.4% which is probably the result of simultaneous activation of neutrophils in the blood. Platelet aggregates were unexpectedly diminished from 12 ± 2.1 to 7.2 ± 2.3 after air decompression. Changes in other molecules expression were not significant [3].

Air and Nitrox Saturated Diving. We observed a significant increase in the number of leukocytes and neutrophils after compression in the Nitrox group, and a marked drop in the platelet count in the Air group. In both groups we observed a marked increase in the percentage of activated platelets bearing CD62P molecules and an enhanced number of microplatelets in the blood of divers in the Air group. In both groups of divers we observed some changes in the platelets system but nevertheless compression and decompression in a nitrox atmosphere seems to be less harmful for the platelets [2].

4 Discussion

An important role in the process of saturation and desaturation of the body is played by perfusion of the tissues. In the case of unsatisfactory decompression it gets disturbed and it is extremely difficult to assess to what extent the perfusion is affected by the gas induced by incorrect decompression. This produces symptoms of decompression sickness.

So far the examinations of haemostasis in divers has focused on the evaluation of blood platelets after hyperbaric exposures [2, 3].

Obtained results prove the activation of platelets in divers subjected to air diving. However an increase in the number of platelets bearing CD62P molecules was the most significant change noted after diving. CD62P expression on platelets is a morphological marker of release reaction, which results in the secretion of

many prothrombotic substances to blood. Therefore, the more evident increase in the percentage of platelets bearing PADGEM is a direct sign of the platelets release reaction due to microbubble formation in blood.

An insignificant drop in the platelet count and a marked increase in the number of microplatelets suggest the destruction of some platelets.

5 Conclusions

1. Evaluation of the blood platelet functions may be one of the fundamental elements indicating the level of risk of decompression sickness in divers.
2. Flow cytometry testing of the blood platelets activation may be a sensitive indicator of DCS threatening.

References

[1] Baj, Z. Application of flow cytometry in blood platelets testing. Centr Europ. J. Immunol. 21, suppl 3: 119–127, 1996.

[2] Olszanski, R., Baj, Z., Buczynski, A., Konarski, M., Klos, R., Skrzynski, S., Zeman, K Evaluation of decompression sickness risk in saturated air and nitrox dives judged on the basic of changes in haemostasis. Proc. of 23 rd EUBS Congess 1997, 91–95.

[3] Olszanski, R., Sicko, Z., Baj, Z., Czestochowska, E., Konarski, M., Kot, J., Radziwon, P., Raszeja-Specht, Winnicka, A. Effect of saturated air and nitrox diving on selected parameters of haemostasis. Bull.Inst.Marit.Trop.Med.Gdynia, 1997, 48 /1–4/, 75–82.

Some Peculiarities of Human Microflora in Oxygen-Argon Hyperbaric Gaseous Media

Z.O. Soloviova, V.K. Ilyin, B.N. Pavlov, P.E. Soldatov and A.M. Nosovsky

Russian Federation State Scientific Center - Institute for Biomedical Problems,
Khoroshevskoye shosse 76a, 123007 Moscow , Russia
Phone: 007-095-1956509; Fax: 007-095-1952253

Abstract. The paper concerns peculiarities of the human microflora state in different argon-containing media. It is assumed that argon media provide active impact on colonial properties of tested microbes. Also, evidence is listed that suggests activity of human aerobic microflora (including conventional pathogens) in hyperbaric habitats with argon media.

1 Introduction

At present, development of the World Ocean Shelf is impossible without sojourn of humans under water. By that, one of the basic effective factors, which provides influence on human organism is high pressure. Realization of practical problems is provided by use of deep diving chambers. It is known that the hyperbaric media create conditions for human microbiocenosis modifications to the negative side. This mainly concerns activation of gramnegative microflora and suppression of grampositive commensales taking part in saturation period [1,2]. It has been shown that the activity of pathogenic features of human microflora in specific conditions of deep-sea barochambers can lead to infectious diseases manifesting. This results in breakdowns of deep-sea works, that bring about large economic damage. This can also be applied to caisson works by building of subway lines. Big deep-sea works were realized with use of oxygen-helium hyperbaric media. At present, problems of modification of hyperbaric media composition are being examined for optimisation of the physiological state of humans in hyperbaric conditions. For this purpose research of oxygen-argon hyperbaric gaseous media influences on physiological activity of humans has been realized. As the result of research performed at the Institute for Biomedical Problems with participation of humans [3], facts were obtained about the positive role of argon for adaptation of human organisms for lasting hypoxic hypoxia. The purpose of our investigations was to evaluate microbiocenosis of the human high respiratory tract and external ear duct in oxygen-argon hyperbaric respiratory mixtures.

The objectives of the studies:

- to evaluate peculiarities of quantitative contamination of the tested biotopes of humans by microorganisms, which refer to different tinctorial groups (grampositive, gramnegative);
- to evaluate modifications of antibiotic susceptibility of human microflora in oxygen-argon hyperbaric gaseous media.

2 Materials & Methods

We have investigated microflora of mucus envelopes of the high respiratory tract, and the skin cover of the external ear duct of 8 volunteers who participated in two simulation dives under pressures of 0.12 MPa and 0.4 MPa (short-term dives). Duration of experiments: 7 and 4 d accordingly, the samples were taken by sterile cotton swab at baseline period, at the end of isopression and at the end of decompression. Control: one simulation dive in oxygen-nitrogen hyperbaric gaseous media under pressure of 0.6 MPa (short-term dive). The inoculation was performed onto the following media: Endo, Sabouraud, Mannitol salt agar, 5% blood agar.

The following microbial groups were taken into consideration: general amount of aerobes, grampositive cocci, gramnegative rods, yeasts.

The microbial cultures isolated within the experiment were tested on their susceptibility to antibiotics of different chemical groups: tetracyclins, macrolydes, semisynthetic penicillins, aminoglycosides, chloramphenicol.

3 Results

On the basis of comparable analysis, obtained in oxygen-argon and oxygen-nitrogen hyperbaric gaseous media, it is difficult to reveal any tendencies in quantitative changes of grampositive and gramnegative components of microflora in tested biotopes. Meanwhile it must be taken into consideration that the contamination level of grampositive microflora exceeded limits traditionally applied by us as optimal ($\geq 1–9\times10^3$ cfu/swab), which in fact was less expressed in short-term experiments (unlike in oxygen-nitrogen mixture) and very much expressed in long-term saturation in oxygen-argon hyperbaric gaseous media. In cases when grampositive components achieved lower values, an increase in the gramnegative component was revealed (Figs. 1–3).

Thus human microbiocenosis in oxygen-argon hyperbaric gaseous media may be qualified as non-satisfactory, which circumstance states the necessity for use of effective measures for correction of human microbiocenosis in oxygen-argon hyperbaric media.

In a comparison of multiple antibiotic resistance of microbial cultures isolated from humans in oxygen-nitrogen and oxygen-argon hyperbaric gaseous media the

quantitative increasing of strains resistant to four or and more antibiotics was revealed in the latter. However in oxygen-argon hyperbaric gaseous media this took part together with quantitative decrease of sensitive strains, unlike in oxygen-nitrogen hyperbaric gaseous media, where quantitative increasing of microorganisms sensitive to antibiotics took part within the entire period of the experiment. The factors of tested gaseous media probably did not render influence on antibiotic susceptibility, since this influence was not reflected by modification of resistance to peculiar antibiotics. Therefore, we may presume that in oxygen-argon hyperbaric gaseous media other antibiotic resistant factors are activated which do not depend on peculiarities of chemical groups of antibiotics, which are extrachromosomal genetic factors of bacteria, e.g. plasmids and transposons determining resistance to antibiotics, for which oxygen-nitrogen media provides limiting impact. Thus, modification of multiresistance index in oxygen-argon hyperbaric gaseous media must be examined as a probable spreading of antibiotic resistant plasmids [4].

The obtained results on human microflora peculiarities in oxygen-argon hyperbaric gaseous media conditions provide a base for further detailed research in this direction.

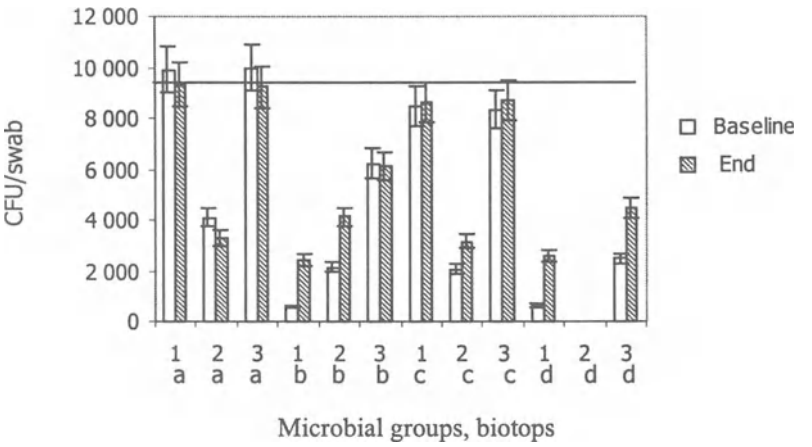

Fig. 1. Dynamics of quantitative contents of grampositive cocci (1), gramnegative rods (2) and total aerobes (3) in left (a) and right (b) external ear, nasal (c) and throat (d) mucus envelopes of volunteers during short-term experiment in oxygen-nitrogen hyperbaric media

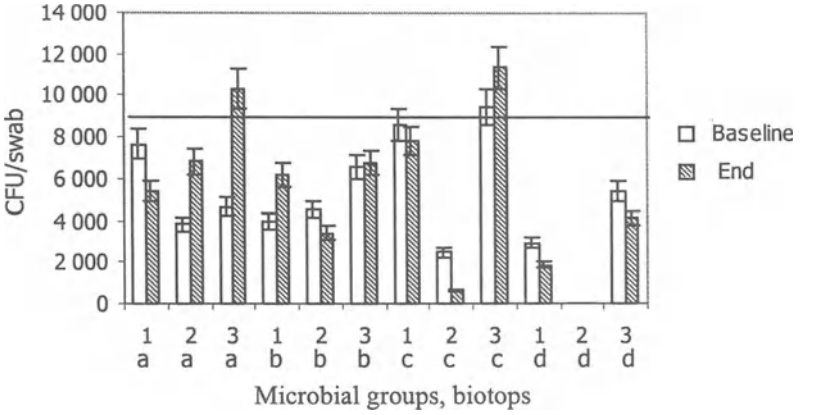

Fig. 2. Dynamics of quantitative contents of grampositive cocci (1), gramnegative rods (2) and total aerobes (3) in left (a) and right (b) external ear, nasal (c) and throat (d) mucus envelopes of volunteers during short-term experiment in oxygen-argon hyperbaric media

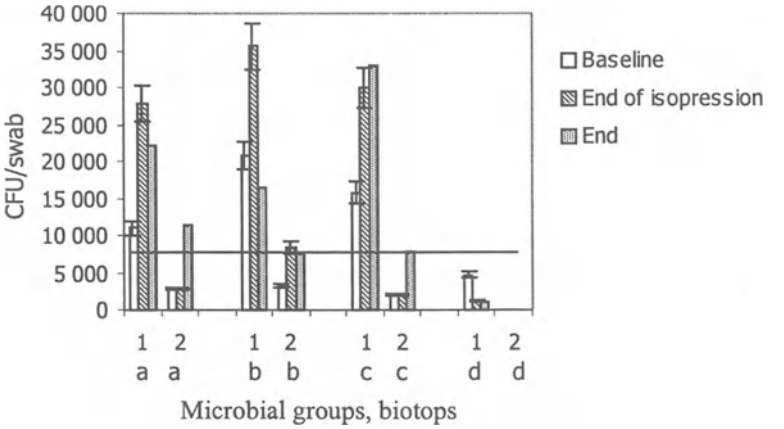

Fig. 3. Dynamics of quantitative contents of grampositive cocci (1), gramnegative rods (2) in left (a) and right (b) external ear, nasal (c) and throat (d) mucus envelopes of volunteers during long-term experiment in oxygen-argon hyperbaric media

References

[1] Victorov A.N., Ilyin V.K., Policarpov N.A. *et al.* Microbial aspects of habitable deep diving complexes exploration. (1992); Undersea Biomedical Research, 6, 23–28.

[2] New antibacterial strategies. (1990); Proc. Int. Symp.Brockett Hall, p.9–12.

[3] Pavlov B.N., Grigoriev A.L., Smolin V.V., Komordin I.P. Hyperoxic, normoxic and hypooxic oxygen–argon gaseous mixtures influence on humans under different barometric pressures and respiration times. (1997); VTH International Meeting on High Pressure, Biology, St. Peterburg, p.9.

[4] K.E. Sanderson, Genetic relatedness in the family Enterobacteriaceae. (1976); Ann. Rev. Microbial, v.30, p.327–349.

The Basic Principles of Deep Divers Anti-Infection Safety

V.K. Ilyin[1], A.N. Viktorov[1], D.O. Meshkov[1], B.N. Pavlov[1], S.I. Klimarev, L.V. Starkova, K.G. Apostolidi[2], Ju.M. Jarin[2], A.I. Volozhin[3], E.A. Andreeva[1] and Z.O. Soloviova[1]

[1]Russian Federation State Scientific Center - Institute for Biomedical Problems, Khoroshevskoye shosse 76a, 123007 Moscow, Russia
Phone: 007-095-1956509; Fax: 007-095-1952253
[2]Moscow Medical Academy
[3]Moscow Medical Stomatology Institute

Abstract. The paper concerns the problem of elaboration of infection safety program for deep diving. Based on the database of the peculiarities of microflora under deep diving conditions the authors propose a new approach to infection prophylaxis using ecologically compatible means in combination with effective disinfection of the environment.

1 Introduction

The microbial status of hyperbaric habitats is considered to be unsatisfactory. The basic factor of infection risk in deep diving is a syndrome of colonial resistance decrease, the linear development of which depends on duration of isopression. The weakening of human colonial resistance in deep diving conditions is accompanied and complicated by development of certain niches in the barochamber environment which allow pathogens to develop and exist for a long period of time, including the very deep diving and intermediate period. Besides, the high pressure factor provides a selective impact on conventional pathogenic human microflora, mainly on gramnegative aerobic rods and suppress commensale microflora development (mainly - grampositive rods and cocci). Linear increasing of conventionally pathogenic share of human microflora creates conditions for exo- and endogenous infection [1, 2].

2 Materials & Methods

We have investigated the microbial status of 74 deep divers who participated in 13 deep dives (heliox, depth 100–350 m, duration 20–45 d). Based on the obtained results we have tested newly elaborated means and methods (immobilized

enzymes, probiotics, physiotherapy, disinfectants in 3 hyperbaric saturation experiments with participation of volunteers (5–20 atm, heliox, duration 7–20 d)). The methods of investigations – microbiological and clinical.

3 Results & Discussion

The process of quantitative and special contents of human microflora in hyperbaric habitats differ from those in normobaric ones. In normobaric habitats the balance of microflora is disturbed periodically due to microbial exchange between isolated individuals of residential and "guest" groups. During a certain period of time, peculiar for each individual, the balance is restored. There are no special factors of normobaric confined habitat to provide evidence direct or indirect selection of any microbial group [1, 3]. Under hyperbaric conditions the development of disbiotic changes is linearly dependent on the duration of hyperbaric isopression and has a certain tendency to recover the microbial balance in the period of decompression. The data on the influence of hyperbaria on biological activity of microbes stress two types of processes which clarify the nature of modifications of quantitative and special content of microflora in hyperbaric media, i.e. suppression of aggressive enzymes production, increase of cell division time for grampositive microbes, and selection of baroresistant strains with high productivity of aggression and defense enzymes - gramnegative rods.

Electron microscopy data suggest deep structural changes in the cells of both the microbial groups. The main difference between them is the size (thickness) of the cell wall, which significantly increased in grampositive cocci and remained the same in gramnegative ones. Probably, under similar energy resources, in hyperbaric conditions the grampositive cells need to spend more energy on cell building needs (proteins, peptidoglycane, mureine etc.) than they do under normal conditions, and than gramnegative cells do under normal and high pressure. This circumstance may be followed by deviations in generation time of different tinctorial groups of microbes and lack of enzyme productivity of grampositive microbes. As a result, grampositive commensales are gradually replaced by gramnegative conventional pathogens in human biotopes under hyperbaric conditions. The latter are highly productive and produce larger amounts of aggression enzymes - exonuclease, hemolysine, phosphatase - than under normal pressure and, therefore, are very active in hyperbaric media. In addition, high resistance of one of the most serious infectious agents in deep diving - *Pseudomonas aeruginosa* - allow the latter to persist in the life support system objects for a very long period of time. The principles of creation of infection safety of deep diving must not be based on the traditional scheme of epidemic process, which include source of infection, ways of transmission and sensitive organism, since infectious agents develop niches of settling in a barochamber environment. These niches "surround" divers and interact with them directly, without any interfaces. The main niche is the water supply system (WSS), where *Pseudomonas*

aeruginosa is accumulated to an epidemiologically significant level and then contaminate human organisms while washing. All attempts to decontaminate the WSS physically or chemically have yet failed to result positively due to the specificity of its contamination by *Pseudomonas aeruginosa*. The latter forms a protective glycocalex film on the internal surface of the tubes. Therefore the only prospective possibility is to use systems which allow to filtrate or act in other ways to decontaminate water on terminal patterns of the WSS. The experiments and in-vitro studies suggest electromagnetic EHF fields to be effective. They effect complete elimination of vital cells from a concentration 1×10^6 CFU/ml within 4 s. We consider this way to be the only effective and harmless method of water decontamination. Its application together with sanitary treatment of surfaces inside the barochamber with the aid of disinfectants using quaternary ammonia and chlorine-containing preparates - separately or in combination - should allow the achievement of microbial safety of barochambers environment [6]. The practical implementation of these measures is the problem of time, because meanwhile existing means for sanitary treatment of barochamber environments (UV, hydrogen peroxide) are not satisfactory. The other direction to be elaborated, bearing in mind peculiarities of human microflora "behavior" under high pressure - is to create unselective and ecologically compatible ways for prophylaxis of infections of deep divers. The basic means for infectious therapy are antibiotics. Meanwhile data of antibiotic susceptibility of human microflora in confined habitats suggest passive accumulation of R-plasmids on strains, capable of spread in confined objects. In this process may be involved also genetic determinants of pathogenicity. This way the formation of nosocomial strains is released even without selective activity of antibiotic assumption. This process takes place in any confined habitat and is recently followed by "malignisation of microflora" (spreading of pathogenic determinants on commensale microflora)[5, 8]. In hyperbaric conditions the formation of polyresistant strains is more intensive. As was shown by in vitro studies, the R-plasmids' transfer frequency is increased in high pressure. The plasmids under high pressure have higher segregation stability then those under normal pressure.

Taking into consideration all of the above, it is necessary to focus concrete measures of divers infectious safety on prophylaxis and treatment of syndrome of colonial resistance decrease using ecologically compatible means which suggest strengthening of natural colonizing barriers [7]: commensale microflora; epitelium of skin and mucouse envelopes; immunity.

The effective means of prophylaxis and treatment of external otites is Dalcex-Trypsin (trypsin immobilized on dialdehydcellulose as a powder, elaborated in the Institute for textile materials). Using Dalcex-Tripsin the external ear ducts were not subjected to inflammation during the iso/decompresssion period. Moreover, normal commensale microflora remained at very high levels within all the period of compression. During this period the epitelial wall and the tympanum remained non-inflamed in all the experimental period. The activity of the ceruminal glands remained constantly healthy.

For prophylaxis of divers disbacteriosis (as the manifesting form of syndrome of colonial resistance decrease) the most effective is assumption of probiotics - lactobacterinum and bifidumbacterinum. Lactobacterinum is more active versus gramnegative pathogens in many biotopes including the high respiratory tract [4]. This is of much importance taking into consideration the possibility for translocation of conventional pathogens to the other biotopes and development of opportunistic infections (incl. otitis media). The effect of Lactobacilli to inhibit R-plasmids spreading is capable of control of the formation of nosocomial strains in hyperbaric habitats.

Also it seems to be beneficial to use principles of physiotherapy to control human microflora in deep diving. The effective application of xenon UV radiator "Jakhont-F" for current prophylaxis of inflammation of covering tissues and mucous envelopes of the external ear and the high respiratory tract. Its application can be rather effective before and after saturation, especially in short-term diving.

The third way for prophylaxis of infections in deep diving is stimulation of natural immunity. Investigations of vitamin-stimulating macrophage activity have successfully been performed.

These are the main categories of means and measures for prophylaxis of colonial resistance decrease of deep divers.

References

[1] Victorov A.N. *et al.* Microbial aspects of habitable deep diving complexes exploration. (1992); Undersea Biomedical Research.6, 23–28.

[2] Victorov A.N. *et al.* The problems of microbial safety in regenerative life support systems exploration. (1994); Acta Astronautica. V.35, N9–11, pp 573–576.

[3] Victorov A.N. *et al.* The characteristics of interaction between normal and conventionally pathogenic human microflora in different types of closed objects. (1994); 45 Congress of International Astronautic Federation (abstr.) Jerusalem, Israel.

[4] Ilyin V.K. *et al.* Space crew members microbial flora in spaceflight and prospective approaches to its ecological control. (1996); Proceedings 6th European Symposium on life sciences research in space Trondheim, Norway, 16–20 June, ESA SP–390. pp. 229–233.

[5] Ilyin V.K. R-plasmids spread in habitable closed objects and its ecological control (1996); 31 COSPAR Scientific Assembly. Birmingham, UK, Book of Abstracts, p. 226.

[6] Klimarev S.I. *et al.* Microwave steriliser of potable water in stream. (1998); 981539 SAE technical papers series. Mat. 28th Int.Conf. on Env. Systems. Danvers MS, July 13–16.

[7] Victorov A.N. *et al.* Deep divers colonial resistance decrease syndrome and its prevention. (1997); In "High Pressure Biology and Medicine. Papers presented at the 5th meeting on High Pressure Biology. S.-Petersburg, Russia. Pp. 218–224.

[8] Ilyin V.K. *et al.* Korniushenkova Cultural, Biochemical, Genetic, Ultrastructural Microbial Characteristics under High Pressure. (1997); In "High Pressure Biology and Medicine. Papers presented at the 5th meeting on High Pressure Biology. S.-Petersburg, Russia. Pp.115–120.

Effects of Thiol-Reactive Reagents on Hemolysis Under Hydrostatic Pressure of Human Erythrocytes

T. Yamaguchi and S. Terada

Department of Chemistry, Faculty of Science, Fukuoka University, Jonan-ku, Fukuoka 814-0180, Japan
takeo@ssat.fukuoka-u.ac.jp

Abstract. The relation between high-pressure (200 MPa)-induced hemolysis and spectrin tetramer-dimer equilibrium was examined by using human erythrocytes treated with SH-reactive reagents such as iodoacetamide (IAA), N-ethylmaleimide (NEM), diamide, and *p*-chloromercuribenzoate (PCMB). The concentration profile of hemolysis at 200 MPa of IAA-treated erythrocytes showed a maximum curve. Similar behaviors were observed in NEM- or diamide-treated erythrocytes. In the case of PCMB, the values of hemolysis at 200 MPa increased monotonically. On the other hand, the concentration of spectrin dimers increased largely with increasing the concentration of IAA and NEM, but remained at low values in PCMB. These results suggest that hemolytic properties at 200 MPa in erythrocytes treated with SH-reactive reagents are not associated with the tetramer-dimer equilibrium of spectrin.

1 Introduction

When human erythrocytes are exposed to high pressure, hemolysis [1] and vesiculation [2] start to occur at about 130 MPa. The degree of hemolysis and vesiculation increases gradually at higher pressures. In such hemolyzed cells, parts of spectrin are detached from the membrane [3]. Spectrin is a cytoskeletal protein. Spectrin heterodimers self-associate in a head-to-head fashion to form tetramers [4]. The spectrin tetramer-dimer equilibrium is affected by several factors such as temperature, salts, and chemical reagents. In the native membrane, most of the spectrin are tetramers and play an important role in the maintenance of the membrane mechanical stability. We have demonstrated that the hemolytic properties of human erythrocytes under high pressure provide useful information on the membrane structure [1–3]. Thus, it is of interest to examine how the membrane stability under high pressure is modulated by the dissociation to spectrin dimers. Here, using SH-reactive reagents, we describe the relation between high-pressure-induced hemolysis and the spectrin tetramer-dimer equilibrium.

2 Materials & Methods

2.1 Materials

Compounds were obtained from the following sources; iodoacetamide (IAA) and N-ethylmaleimide (NEM), Wako Pure Chemicals; diamide, Sigma; *p*-chloromercuribenzoate (PCMB), Nacalai Tesque. All other chemicals were of reagent grade.

2.2 Treatment of Erythrocytes with SH-Reactive Reagents

Human blood that was drawn in citrate/mannitol/adenine/phosphate solution was obtained from the Fukuoka Red Cross Blood Center. The blood was centrifuged at 750 × g for 10 min at 4 °C. The plasma and buffy coat were removed carefully. The erythrocytes were washed three times in phosphate-buffered saline (PBS, 10 mM sodium phosphate, 150 mM NaCl, pH 7.4). For chemical modifications of erythrocytes, the red cells suspended at a 20% hematocrit in PBS were incubated for 30 min at 37 °C with SH-reactive reagents such as IAA (1–200 mM), NEM (0.5–2 mM), diamide (0.5–2 mM), and PCMB (10–100 μM). After incubation, the erythrocytes were washed three times in chilled PBS.

2.3 Hemolysis

Intact erythrocytes and chemically modified ones were subjected to a high pressure, as described previously [3]. Briefly, 3 ml of the erythrocyte suspension (0.3% hematocrit) in PBS was inserted into a syringe-type cell and set in the pressure bomb. The samples were compressed at a rate of 20 MPa/min, incubated for 30 min at 200 MPa and 37 °C, and then decompressed up to atmospheric pressure at a rate of 40 MPa/min. The erythrocyte suspension was centrifuged at 750 × g for 10 min at 35 °C. The concentration of hemoglobin in the supernatant was estimated from the absorbance at 542 nm. One hundred percent hemolysis was carried out by adding 10 μl of 5% Triton X-100 into the suspension.

2.4 Nondenaturing Polyacrylamide Gel Electrophoresis of Spectrin Oligomers

Ghost membranes were prepared from chemically modified erythrocytes, according to the method of Dodge *et al.* [5]. To extract cytoskeletal proteins from the membranes, one volume of the ghosts was mixed with one volume of 0.1 mM EDTA, 0.1 mM PMSF, pH 8.0, and incubated overnight at 0 °C. After incubation, the ghost suspension was centrifuged at 42,000 × g for 30 min at 4 °C. The supernatant was used for nondenaturing polyacrylamide gel electrophoresis. The electrophoresis was carried out using 2.5% acrylamide gel. Gels were stained with

Coomassie Blue and the bands of spectrin tetramers and dimers were analyzed using an Advantic DM-303 scanning densitometer.

3 Results

Figure 1 shows the relationship between the hemolysis at 200 MPa and the spectrin tetramer-dimer equilibrium in IAA-treated erythrocytes.

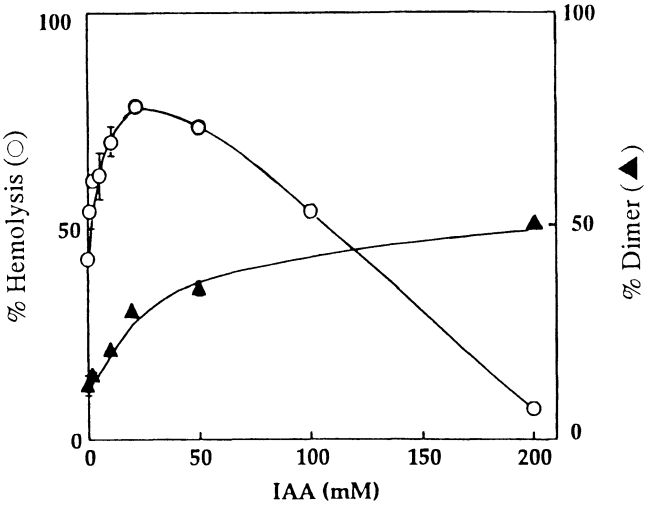

Fig. 1. Relationship between hemolysis at 200 MPa and spectrin dimer in IAA-treated erythrocytes

The values of hemolysis at 200 MPa increased up to 20 mM of IAA and then decreased at higher concentrations. On the other hand, the equilibrium of spectrin shifted gradually to dimers with increasing the concentration of IAA. Similar results were obtained in NEM-treated erythrocytes (Table 1). When the erythrocytes are treated with diamide, spectrin is mainly cross-linked and oligomers of spectrin are formed [1, 3]. The hemolytic properties of such diamide-treated erythrocytes were similar to those of IAA-, or NEM-treated cells. Additionally, the effect of PCMB on hemolysis at 200 MPa was examined. The erythrocytes treated with 100 μM PCMB were hemolyzed completely under high pressure. However, spectrin tetramer-dimer equilibrium remained almost constant.

Table 1. Relationship between hemolysis at 200 MPa and spectrin tetramer-dimer equilibium in erythrocytes treated with SH-reactive reagents

Reagent	Equilibrium (%)		% Hemolysis
	Dimer	Tetramer	
None	12.7 ± 3.7	87.3 ± 3.7	45.9 ± 7.6
2 mM NEM	72.4 ± 3.1	27.6 ± 3.1	33.7 ± 3.4
2 mM diamide	40.9 ± 6.0	59.1 ± 6.0	38.0
100 μM PCMB	22.5 ± 1.2	77.5 ± 1.2	97.3 ± 2.4

4 Discussion

High-pressure-induced hemolysis is sensitive to the chemical modifications [1] and enzymatic digestion [6] of membrane proteins. In the present work, we have shown that the membrane stability of human erythrocytes at 200 MPa is modulated by chemical modifications of membrane SH groups. The values of hemolysis at 200 MPa of IAA- or NEM-treated erythrocytes increase upon mild modification of membrane SH groups and then decrease upon further modification. Such a decrease of hemolysis at 200 MPa may be associated with the reorganization of membrane proteins in chemically modified erythrocytes [7]. Data of spin labeling demonstrate that such a reorganization occurs above 30 °C [7]. In diamide-treated erythrocytes, spectrins are intra- and intermolecularly cross-linked. The hemolytic properties at 200 MPa of such red cells are similar to those of IAA- or NEM-treated cells. It seems likely that the shift to spectrin dimer makes the membrane structure more unstable. So, it is interesting to examine the effect of SH-reactive reagents on spectrin tetramer-dimer equilibrium. The rate of spectrin dimer increases in these SH-modified cells. Thus, the tetramer-dimer equilibrium of spectrin is incapable of explaining the hemolytic properties at 200 MPa of SH-modified erythrocytes. This idea is also supported by the results from PCMB-treated erythrocytes.

Interestingly, the hemolysis at 200 MPa of PCMB-treated erythrocytes is enhanced monotonically. Mercurials such as PCMB and $HgCl_2$ react with water channels and inhibit the water transport [8]. Further experiments are necessary to determine whether the membrane fragility under high pressure of PCMB-treated erythrocytes is associated with the inhibition of water channels.

References

[1] Kitajima, H. *et al.* (1990); Hemolysis of human erythrocytes under hydrostatic pressure is suppressed by cross-linking of membrane proteins; J. Biochem., 108, 1057–1062.

[2] Yamaguchi, T. *et al.* (1991); Vesiculation induced by hydrostatic pressure in human erythrocytes; J. Biochem., 110, 355–359.

[3] Yamaguchi, T. *et al.* (1989); Effects of temperature and pH on hemoglobin release from hydrostatic pressure-treated erythrocytes; J. Biochem., 106,1080–1085.

[4] Ungewickell, E. and Gratzer, W. (1978); Self-association of human spectrin: A thermodynamic and kinetic study; Eur. J. Biochem., 88, 379–385

[5] Dodge, J.T. *et al.* (1963); The preparation and chemical characteristics of hemoglobin-free ghosts of human erythrocytes; Arch. Biochem. Biophys., 100, 119–130.

[6] Yamaguchi, T. *et al.* (1993); Hemolytic properties under hydrostatic pressure of neuraminidase- or protease-treated human erythrocytes; J. Biochem., 114, 576–581.

[7] Yamaguchi, T. *et al.* (1994); Effects of chemical modification of membrane thiol groups on hemolysis of human erythrocytes under hydrostatic pressure; Biochim. Biophys. Acta, 1195, 205–210.

[8] Knepper, M.A. (1994); The aquaporin family of molecular water channels; Proc. Natl. Acad. Sci.USA, 91, 6255–6258.

Author Index

Springer and the environment

At Springer we firmly believe that an international science publisher has a special obligation to the environment, and our corporate policies consistently reflect this conviction.

We also expect our business partners – paper mills, printers, packaging manufacturers, etc. – to commit themselves to using materials and production processes that do not harm the environment. The paper in this book is made from low- or no-chlorine pulp and is acid free, in conformance with international standards for paper permanency.

Springer